Science and Technology Facilities Council

UK XFEL Science Case

Science and Technology Facilities Council

Science and Technology Facilities Council
Polaris House
North Star Avenue
Swindon
SN2 1SZ

stfc.ukri.org

Contents

8. Opportunities for UK Industry, Society and Defence

8.1. Addressing national strategic priorities
8.2. Properties of shocked materials for engineering and defence
8.3. Nucleation, solidification and crystallization in soft-matter
8.4. Dynamic processes in additive manufacturing, combustion, laser machining and photolithography
8.5. Gamma sources application in nuclear security and materials in nuclear industry
8.6. Industrial inspirations from deeper insights into biology: pharma to clean energy
8.7. Overall economic context

9. UK Facility Requirements and Options Analysis

9.1. Facility X-ray requirements: photon energy, bandwidth, pulse duration, repetition rate and pulse energy
9.2. Facility general requirements: laser & THz fields, high energy and high-power lasers, electrons, detectors, data, sample delivery, preparation labs and user support facilities, skills training pipeline
9.3 Options analysis:
A. Build a unique UK XFEL optimised for new capability
B. Build a UK XFEL providing capacity well beyond 10 years
C. Invest more in dedicated UK facilities at existing XFELs
D. Increase investment to support users in exploiting existing opportunities (e.g. long term grant funding schemes, CDTs, "UK XFEL Institute")
E. Dedicated R & D effort towards a future XFEL ("test facility")
F. Extend activities of existing Life and Physical Sciences Hubs

Appendices

Appendix 1: An outline of a technical solution

Introduction
Key parameters for facility design
Other key features
Concept outline 1: Superconducting accelerator
Concept outline 2: Hybrid accelerator
Concept outline 3: Normal conducting accelerator

Appendix 2: Complementarity of techniques

A2.1 Cryo-Electron Microscopy (Cryo-EM), Tomography (cryo-ET), and Diffraction (cryo-ED)
A2.2 Ultrafast electron diffraction (UED)

Appendix 3: Complementary technologies

A3.1 Complementary pulsed X-ray technologies
A3.2 Plasma and laser wakefield acceleration
A3.3 High harmonic sources

Appendix 4: Community engagement and authorship

Workshops and community engagement events
Authorship of 1st draft of Science Case

1. UK XFEL Science Case – Executive Summary

An advanced X-ray free electron laser facility in the UK would create major new opportunities across the sciences and in technology, help to answer pressing scientific questions, and contribute to solving societal challenges of major importance. The facility would boost physical, chemical, material and life sciences, and would generate wide-ranging interdisciplinary advances. We can foresee it having an impact in advancing technology, healthcare, frontiers of knowledge, net zero commitments and economic strengths. Moreover, the facility would prove a vital element in developing a world-leading science and innovations "moonshot" for the nation, positioning the UK for global leadership in attaining carbon neutrality and sustainability.

Ultrafast X-rays from free electron lasers (FELs) allow us to image the workings of matter at all relevant scales of both space and time. In common with neutron, synchrotron X-ray sources and electron microscopy, X-ray FELs, or XFELs, can establish the static structure of matter at the atomic scale; however,. XFELs are unique in that they also allow us to follow the myriad types of structural dynamics that are essential to understanding the workings of matter at the quantum scale, at their natural timescales of attosecond – nanosecond. They are transformative in enabling the understanding and control of matter at the quantum *spatial* and *temporal* scales.

Intense X-ray pulses also open new windows into the understanding of light and matter in the universe, making possible a range of new opportunities, such as: probing properties of matter in solar and planetary interiors; understanding the coupling between photons (X-rays and γ-rays) and massive particles such as electrons, protons and nuclei; and new tests of quantum gravity and the Standard Model.

High brightness X-rays can be used to develop new technologies based upon photolithography with nanometre resolution. The energetic electron beam from the linear accelerator required to drive the X-ray laser can be used directly to perform fundamental physics investigations, drive the world's brightest *γ* ray source, and advance new accelerator technology.

Examples of big scientific questions that an advanced XFEL will be able to answer include:

- How do materials behave at the high pressures of planetary cores?
- How do enzyme-catalysed reactions occur in a living cell?
- Can we control states in quantum materials (e.g. superconductivity) with light?
- How do molecular machines efficiently cross energy barriers to drive biological processes?
- How X-rays propagate in the cores of stars?
- How do liquids, like water, change and fluctuate at the nanoscopic scale?
- Can we exploit quantum mechanics in solar technologies?
- Can intense X-ray pulses be used for advanced semiconductor chip manufacturing?

As well as underpinning a vast array of science, the capability delivered by XFEL will also be critical in the advancement of emerging technologies with great potential importance, including:

- Developing fast data storage
- Controlling quantum materials (e.g. new superconductors)
- Optimising novel quantum sensors and quantum elements for information processing
- Advancing light harvesting, solar biofuels, and energy storage technologies
- Discovering advanced drugs and antibiotics
- Facilitating sustainable chemistry
- Delivering advanced materials for use in defence, industry and nuclear energy

In this Science Case we explain these far-reaching science and technology opportunities, and further sketch an ambitious facility of realistic scale that would deliver this science. The outline design incorporates a range of unique features, in terms of X-ray characteristics, auxiliary targets and light sources, that will ensure such a facility remains a leading part of international light source provision for the next 50 years. We summarise how construction a UK XFEL facility would create an economic and industrial stimulus both regionally and nationally, forming an essential part of a science infrastructure landscape that ensures a vibrant, high technology environment, and helping to build and retain cutting-edge skills in the UK work force.

The international landscape of X-ray sources - synchrotron and XFEL - has seen rapid advances in the last decade. XFELs are now established in the USA, Germany, Switzerland, Italy, Japan, South Korea and China, with multiple sources being planned at other locations. Similar growth has been seen with high brightness synchrotrons and, with Diamond Light Source II, it is hoped that the UK can maintain a strong presence in that technology and its application to increase understanding of the static structure of matter.

X-ray FELs are increasingly being seen as indispensable to the development of new technologies where the quantum scale structural dynamics of matter must be understood and exploited. A primary driver for the Linac Coherent Light Source (LCLS) II in the USA has been its fundamental contribution to the Department of Energy's mission, most critically in Basic Energy Sciences but also in National Security Science, and the missions of other major agencies within the USA, including the National Institutes of Health (NIH) and the National Science Foundation (NSF). Similarly, the other international XFELs are seen as making essential contributions to science and to future economic and national strength. It is clear that most major industrial nations are moving towards securing their own XFEL capability, in recognition of their growing importance to current and future science and technology developments.

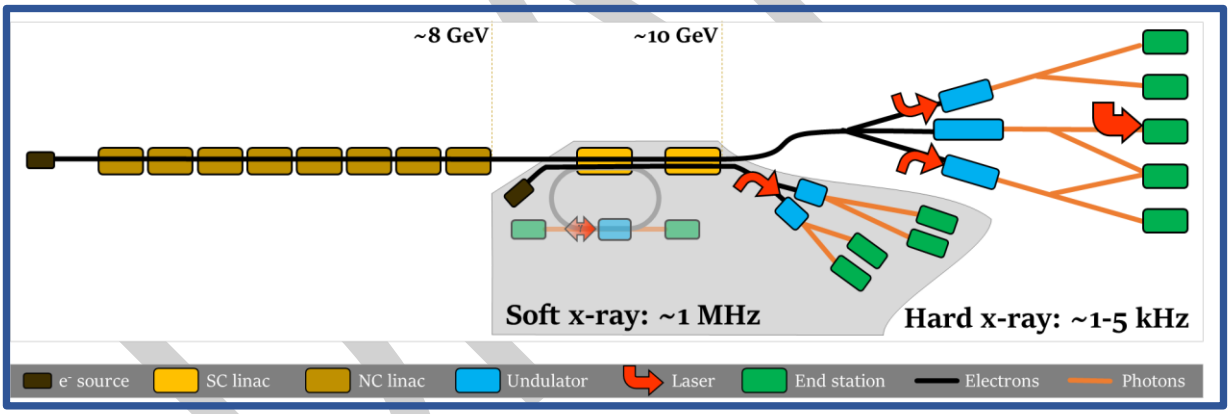

An outline design of one potential configuration to deliver the science discussed in this case

A UK XFEL can be a world leading facility in many respects. We can especially ensure the highest quality and most versatile X-ray specifications, by moving beyond conventional X-ray generation schemes and exploiting developments in laser seeding, attosecond operation, and high brightness modes, to approach transform limited X-ray pulses of high spectral purity and brightness, and unprecedented temporal resolution. High repetition rate in the soft X-ray range, and moderately high repetition rate over the hard X-ray range, is a powerful combination that is one option we consider and this would be world-leading and cost effective. Access to the most advanced radiation sources (terahertz (THz), laser and high harmonic generation (HHG)), and relativistic electron (from laser wakefield acceleration (LWFA)) and other charged particle beams at the interaction point, will allow for a wide range of unique experiments. Direct use of the high-quality relativistic electron beam can be used to advance accelerator science (e.g. plasma wakefield accelerators) and for a gamma source brighter than any in the world, with substantial benefits to nuclear science and UK industry. Detector and sample delivery of the highest calibre will be developed alongside the light sources to provide best-in-the-world performance, with world-leading data handling and data science developments available to support the most advanced analysis.

To allow the facility to deliver the fullest range of the potential science and technology, ease of accessibility for users and for new user communities is a critically important issue. In part, this can be addressed by designing appropriate technical configurations of instruments, end stations and data systems into the facility from the outset. The possibility of conducting experiments solely via user supplied samples, without on-site users, will be developed in scientific areas that are currently at an advanced level of technical maturity, such as serial nano-crystallography and some time-resolved chemical dynamics studies. This approach can significantly boost throughput, and deliver a big reduction in the threshold to access. The second part of the solution to lowering barriers to access will lie with improving training and support for new users, in order to develop, and widely propagate, the required expertise to use the facility effectively. Work on this should start now, building on the actions already undertaken by the Life and Physical Sciences Hubs at Harwell. Related actions, such as establishing dedicated Centres for Doctoral Training across a variety of science areas, should be undertaken with urgency. These measures are important to ensure readiness in the UK for an eventual facility, but equally will allow UK science to fully exploit the existing international XFEL opportunities.

The UK enjoys membership of the European XFEL and must continue as a full member of this organisation, albeit as one voice of many, as this facility is likely to remain one of the worlds' premier XFELs for decades. In the longer term, the planned UK XFEL would deliver new capability complementary to the European XFEL. UK engagement with European science is likely to be maintained, but not substantially grow, over the coming decades. Clearly, we are now having to rethink strategies for protecting our best interests across a wide range of science and technology capabilities as geopolitical alignments evolve.

A major advantage of building a national XFEL capability of international class is that it will ensure UK access to that capability, whilst being a strong incentive to partners for continuing engagement and reciprocity. The direct national economic benefits of constructing and hosting a large scientific infrastructure in one's own country is well documented. Further benefits lie in opportunities for greatly expanding the national skills base in the UK workforce, from PhDs and engineers, to technicians and apprentices. A UK XFEL would boost skills in areas critical to the economy, such as advanced electronics and control systems, optics, hardware and software for handling unprecedented data volumes, precision engineering and advanced manufacturing. The importance to future key sovereign and industrial capabilities, only available if we have full control on all decisions, must be at the core of decision making. Without a UK XFEL programme there is high risk of lost science and technology opportunities and, worse still, of a loss of skills in academia and industry and an accelerated brain drain. Building an XFEL is an essential part in a national strategy that ensures we remain a technology maker, and do not become a technology taker.

We should compare the current situation to that of the New Light Source (NLS) project in 2008-10, where high technical risks (*will XFELs work*?) and scientific risks (*will XFELs make a significant scientific impact*?) were seen. This encouraged a risk averse strategy, and led the UK to do nothing at the time. Now the situation is reversed. Today, the technical and scientific risks are looking low: these machines *work* and they *produce copious quantities of great science*. A 'do nothing' or a 'do little' strategy is now riskiest (as we discuss in section 8) and could severely damage national competitiveness, technology and sovereign capability, and scientific standing. The more ambitious the machine, the lower the future risks to UK science and technology.

2. Introduction

This draft UK XFEL Science Case has been developed over the past nine months through a wide community consultation, a series of seven workshops, and extensive analysis and discussion. Whilst much of the material has been prepared by the core science team and staff from STFC's RAL/Diamond and Daresbury sites (as listed **Appendix 4**), there has also been extensive input from many scientists around the country and overseas, for which we are immensely grateful. This input is reflected in the author list.

This draft Science Case contains an analysis of the societal challenges and scientific opportunities that can be addressed by a unique UK XFEL. These opportunities exist across a broad range of disciplines: physics and X-ray photonics; matter at extreme conditions; quantum and nanomaterials; chemical dynamics and energy; life sciences; and applications in industry, medicine and defence. All of these opportunities are discussed in their respective sections (**3 – 8**). In **Section 9**, we examine the technical capabilities required to capture these opportunities, and how the integration with other capabilities in the UK landscape will be vital, and also present and analyse a range of options to deliver this science. A series of Appendices present outline designs of machines that can satisfy all, or a large part, of the science demand (**Appendix 1**), the broader developing methodological landscape (**Appendix 2**), and assessments of synergies with other technologies (**Appendix 3**).

We begin in this section with an introduction to the science and technology that underlies the draft Science Case. We start with a primer on XFEL sources and a broadbrush overview of the science opportunities; we then introduce the powerful time-resolved methods, such as X-ray spectroscopy and scattering, that are enabled by an XFEL; and we present a brief survey of existing XFELs and discuss the exciting new capabilities that could form part of an adventurous UK XFEL and that would enhance this existing landscape.

2.1 Overview of the impact of X-ray FELs on science

X-ray free electron lasers (XFELs) have led to transformative developments in light source science over the last decade, and are now an established method for generating light with unique characteristics, i.e. short wavelength light pulses with durations in the range 100 fs to 0.1 fs. XFELs are unique tools that are finding growing applications in science, technology and medicine, and are proving extraordinary in enabling things not possible before, and changing what is perceived possible. In addition to the numerous rich scientific applications have already been achieved, new methods and approaches are being spawned in many areas. The broader societal impact of XFELs is not yet fully realised, with the further discoveries they enable still expanding, but, after only ten years, the potential is already well demonstrated.

The mechanism of X-ray free electron laser radiation has its origins in the formation of self-modulation in a relativistic electron beam as it radiates in an undulator (**Figure 2.1**). In an X-ray FEL, high quality relativistic (3 – 15 GeV) electron bunches of low emittance are required, necessitating the use of large-scale, high-performance linear electron accelerators. On entering the alternating polarity magnetic field structure of the undulator, the electrons begin to radiate and, critically, there is a back reaction of the radiation upon the electrons in the bunch. Passage through a sufficient length of undulators leads to a regular structuring of the electron density in the bunch, the consequence of which is coherent, high brightness X-ray radiation. This process, termed Self-Amplified Spontaneous Emission[1] [2] (SASE), is the dominant principle of operation of free electron lasers in the X-ray region.

Lasing in the vacuum ultra-violet range via this method was achieved at the Deutsches Elektronen-Synchrotron (DESY) in Hamburg, and this machine began operating as the FLASH user facility from 2005 with extension into the soft X-ray range [3]. The Linac Coherent Light Source (LCLS) at the SLAC National Accelerator Laboratory in California first lased in the X-ray range in April 2009[4], heralding a new dawn in X-ray science. In the relatively short time since then, there have been numerous demonstrations of important new science (as discussed in this case) and five new X-ray facilities have begun operation around the world.

Other concepts are now being explored to extend the capabilities of X-ray lasers, including the consideration of oscillator-based lasing, as first envisioned by John Madey[5] (the inventor of the FEL concept). Laser preconditioning of the electron bunch (*seeding*) before it enters the undulator has proved effective at greatly improving the coherence properties and stability of the output, with this approach successfully demonstrated in the soft X-ray range at the FERMI facility[6] in Italy. Lasing on a very short, single SASE spike, leading to near transform limited operation, has also been developed through manipulation of the phase space of the incoming electron bunch, with the first demonstration of attosecond time domain pulses[7] at LCLS within this last year. With the capabilities of these light sources developing so rapidly, we are heading into the next generation of X-ray FELs with far greater control of the X-ray pulses, and it is these opportunities that the UK XFEL is poised to develop.

The properties of light from free electron lasers are dramatically different from those of storage rings and conventional lasers. Storage ring synchrotron radiation has enormous spectral coverage and can deliver a high photon fluence (photons per second) up to hard X-rays (10s of keV), which has allowed these sources to be the dominant tool for crystallography, X-ray spectroscopy and many other areas of X-ray science for the last four decades. These sources do, however, have low peak brightness, especially if a narrow spectral bandwidth or a short pulse is selected. With advanced pulse slicing, they can provide sub-picosecond temporal resolution, but only with a tiny flux, which severely limits the utility for measuring rapid changes. Conventional lasers have advanced hugely in recent years and can produce extremely short pulses (~5 fs) at very high brightness, but these capabilities are limited to a restricted spectral range (0.5 - 5 eV). With High harmonic generation (HHG) the accessible range can be extended, but the low intrinsic conversion efficiency ($< 10^{-6}$ in the extreme ultraviolet (XUV) and $< 10^{-8}$ in the SXR) is a severe restriction to fully exploiting incisive X-ray techniques, like X-ray spectroscopy at atomic edges, and atomic position resolution by X-ray diffraction.

SASE free electron lasers deliver coherent radiation across an exceptional spectral range (< 10 eV to multiple-keV), with narrow bandwidth (~0.1% of photon energy) and very energetic (millijoule) short pulses (~10 fs duration), and therefore with exceptional brightness (10^{12} photons per pulse). A FEL undulator produces a very bright pulse at the fundamental frequency, but also bright pulses at three- and five-times that frequency (the harmonics), with the photon number dropping by a factor of around 100 at each harmonic step. This is a vastly wider spectral range than that covered by conventional lasers, and the pulses are typically a hundred thousand times shorter and millions of times brighter than those that a storage ring can provide. XFELs are having a revolutionary impact on the science we do with light, potentially as far-reaching an impact as those created by the laser and synchrotron radiation. The main science driver for X-ray FELs is the access to the structural dynamics of matter at the quantum scale that no other light source can deliver (see **Box 2.1**).

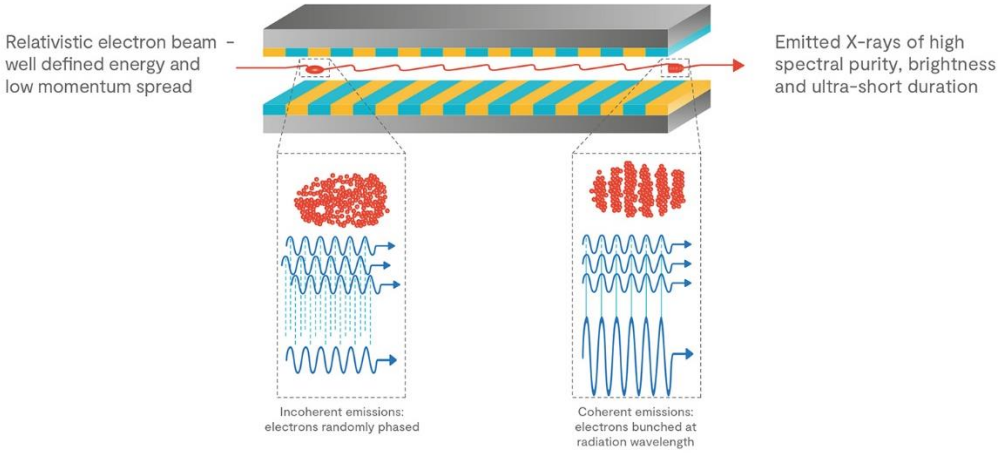

Figure 2.1: Principle of operation of a SASE X-ray Free Electron Laser (After McNeil)

In the decade since their first operation numerous applications of X-ray FELS have been demonstrated. It is impossible detail everything in this introduction but we cover many examples through this Science Case, and there are several recent reviews and special issues that offer a detailed and up-to-date survey [8 9]. Here, we offer a sample of recent significant results that serve to illustrate the impact of X-ray FELs across multiple scientific disciplines: these topics are discussed further in Sections 3 – 8 of this Science Case.

The opportunities afforded by XFELs for pump-probe studies, typically with an ultrafast laser IR/visible/UV pump pulse and an X-ray probe, have had a great impact on chemical dynamics. Recent liquid and gas phase chemistry studies have improved our understanding of chemical dynamics of relevance to catalysis[10 11], where X-ray emission spectroscopy has proved a decisive method in resolving research questions. Combining X-ray diffraction and X-ray emission from molecules of interest in biochemistry is also proving very promising, with some recent work by Kern et al [12] leading to new insights on the photosystem II complex photocycle. Further opportunities in time-resolved resonant inelastic X-ray scattering (RIXS) and X-ray emission spectroscopy (XES) will be enabled by the high repetition rate XFELs that are now becoming operational. Much opportunity has also been enabled in physics, where pump-probe methods have allowed the interrogation and study of dynamics in states only transiently accessible, for example, for high pressure shocks, hot dense matter, matter dressed by lasers and matter in extreme electric and magnetic fields. Recent examples for matter at extreme conditions include probing shock compression of materials[13] and probing laser generated dense matter [14]. Optical and THz field dressing of quantum materials probed by XFEL pulses is leading to the discovery of hidden phases of significance to high T_c superconductivity and other functional properties[15 16].

In life sciences, an important early scientific breakthrough with FLASH, the XUV FEL at Hamburg, which has operated since 2005, was the coherent diffractive single shot imaging of biological and non-biological structures led by Hajdu and Chapman. These same ideas have been implemented at LCLS, and promising results are emerging on imaging non-periodic, non-reproducible structures and nanocrystals utilising the single shot coherent detection imaging (CDI) methodology. In the future, there is potential for such a technique to provide nanoscopic imaging of biological assemblies and molecular machines within the necessary time resolution and under operating conditions (i.e. living cell temperatures) may prove of great importance. A recent ground-breaking study has shown the possibility of using the snap-shot imaging capability of an XFEL to study rare, but functionally critical, conformational changes in a virus[17]. It has, however, been in the sphere of serial nano-crystallography that XFELs have had the largest impact in life sciences so far, opening up the study of otherwise inaccessible proteins (such as membrane proteins that frequently cannot be made to form macroscopic crystals), and also allowing structures to be studied free of radiation damage and potential cryo-artefacts. Recent examples include investigations of light harvesting in photosystem II[18], and studies of the protein that is a critical agent in sleeping sickness[19] and of the machinery of neuronal molecular transport [20]. Although not yet competing with the rate of protein structures deposited in the data banks by synchrotron studies the opportunity to solve structures not otherwise tractable makes XFEL-based crystallography very valuable to structural biology. Moreover, XFELs bring the unique possibility of studying the structural dynamics of light-activated proteins, something that has not been possible before, as illustrated in Pande et al [21] which resolved the structural dynamics occurring in the photo-excited cis/trans isomerization induced in the photo-active yellow protein.

These are a few examples from a rapidly growing body of scientific literature all enabled by XFELs. Although these achievements are already impressive, we should keep in mind that XFEL light sources have only been available for just over a decade. Much development has taken place and much more must be anticipated as the newer and upgraded facilities start to operate. There remains enormous, as yet untapped, scientific and technological potential for these light sources. In the sections that follow, these topics are considered in greater detail and emerging opportunities across a wide range of science are highlighted and discussed.

Box 2.1: XFELs provide unique access to the structure and dynamics of matter at the quantum scale: nanometre spatial and ultrafast temporal scales

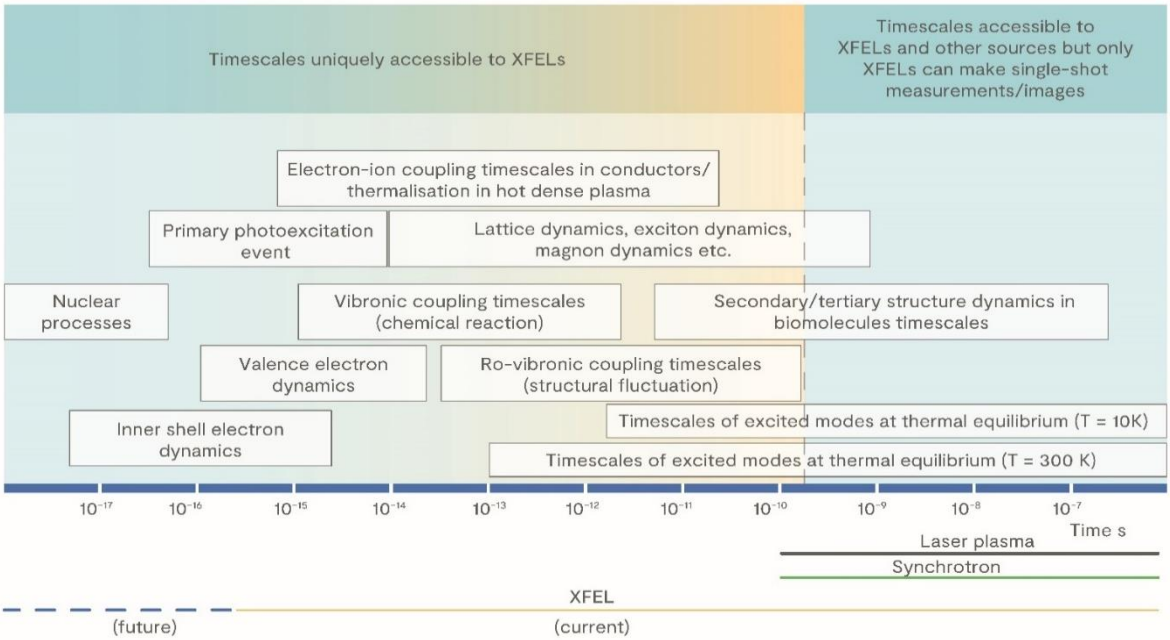

Ultrafast X-rays from free electron lasers allow us to image the workings of matter at all relevant scales of both space and time. XFELs, in common with neutron, synchrotron X-ray sources and electron microscopy, can establish the static structure of matter at the atomic scale. XFELs, however, are unique in that they also allow us to follow, at their natural timescales of attosecond – nanosecond, the myriad structural dynamics that are essential to understanding the workings of matter at the quantum scale. They are transformative in enabling the understanding and control of matter at the quantum spatial and temporal scales.

2.2 Time and space resolved measurement with an XFEL

The combination of time-resolved X-ray scattering and X-ray spectroscopy provided by XFELs has proved transformative. These methods enable measurements, resolved in space and time, at the fundamental quantum scales of systems relevant to physics, chemistry, material and life sciences.

2.2.1 X-ray structural and electronic probes

The short wavelengths of X-ray photons, and the short de Broglie wavelengths of electrons and neutrons of appropriate energy, permit diffraction imaging of the structure of matter at the atomic spatial scale. In contrast to the case for neutrons and electrons, with X-rays it is also possible to interrogate the electronic states of matter through various types of spectroscopy, and this has been the key to elucidating both the electronic and geometric structure of materials, molecules and biomolecules. The frontier challenge is also to measure the dynamics of these electronic and geometric properties, which at the nanoscopic/quantum scale are typically very fast (attosecond – nanosecond) [see

Box 2.1]. Such time-resolved measurements require very short duration X-ray probes, to enable this structural information to be sampled at a sufficiently high temporal resolution. X-ray pulses from XFELs are routinely generated with 10 fs or shorter duration, with sub-femtosecond modes now available, which match to this task. In this Section, we briefly overview the classes of time-resolved X-ray probing techniques that are available and then discuss the types of measurements that are currently being made (see **Box 2.2**).

2.2.2 Time-resolved X-ray scattering

X-rays may interact with matter via either elastic or inelastic scattering (the latter is discussed with X-ray spectroscopy in **Section 2.2.3**). The elastic scattering signal is dominated by Thomson (Compton) scattering from the large number of electrons localised to the atomic sites. If the scattering is from a periodic structure (see **Figure 2.2)**, such as a crystal lattice, constructive interference between the scattered X-ray waves leads to strong peaks at certain angles (Bragg peaks)[22], which give the reciprocal space information from which the lattice structure can be readily retrieved. Through serial exposures, high brightness X-rays, such as those available from an XFEL, enable the lattice structure of nanocrystals to be retrieved with atomic resolution. This has proven of significant value, as many proteins can only be crystallized to form nanoscopic, rather than macroscopic, crystals [23].

Even in a non-periodic structure, the X-ray scattering signal for spatially coherent X-rays can give a complex diffraction pattern from which the structure can be retrieved using powerful algorithms, which numerically solve the phase problem by applying various physical constraints in an iterative retrieval procedure [24] [25]. This coherent diffraction imaging (CDI) procedure is well suited to the high brightness coherent X-rays from XFELs, and the concept of “diffract-before-destroy” for imaging non-periodic structures has been used to gain nanometre resolution in a variety of biological [26]and non-biological [27] nanoscale structures, although not atomic resolution so far. The possibilities for static nanoscale imaging of single particles by CDI are being actively pursued at all of the XFELs currently in operation and progress is regularly being reported (see sections 3.4 and 7.5).

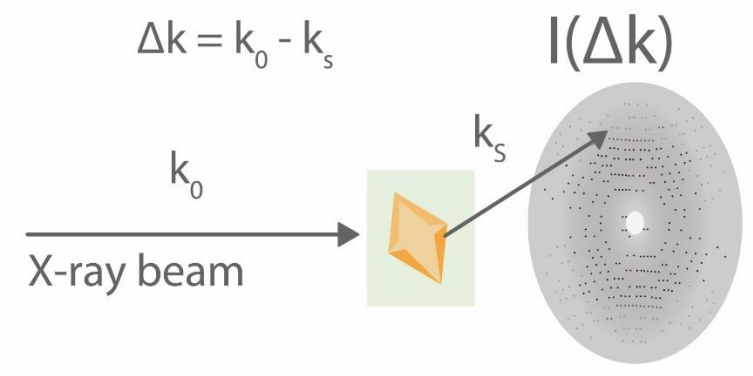

Figure 2.2: X-ray scattering, from either a crystal or a non-periodic object

The X-ray pulses from XFELs have a very short duration, as well as a very high brightness; consequently, if they are applied time synchronized with another interaction that can initiate structural change, then time-resolved X-ray diffraction becomes possible. Such a scenario is termed a pump-probe measurement, with temporal information being gained by repeating the measurement over the appropriate range of pump-probe delays. A large number of recent experiments illustrating this possibility have been carried out at the LCLS and SACLA (SPring-8 Angstrom Compact free-electron LAser in Japan) XFELs. The X-ray brightness is high enough even to capture structural changes in an ensemble of gas phase small molecules[28], and pump-probe measurements of laser activated molecular dynamics have revealed photochemical structural changes that occur over a few hundreds of femtoseconds. Structural changes of much larger photoactive protein molecules, in a nanocrystalline form, have also been captured in a number of cases[21]. Optical and terahertz fields can be used to induce non-equilibrium phases in strongly correlated quantum condensed phase materials with new emergent properties, and these have been captured by time-resolved X-ray diffraction[16]. Recently, progress has been made on short electron pulse generation for ultrafast electron diffraction (UED)[29 30 31], although accessing the sub-10 fs temporal range remains challenging and UED returns no information upon the electronic states. The synergy of XFEL and UED techniques is discussed in Appendix 2.1.

For time-resolved studies, unless picosecond resolution is sufficient, technical effort must be applied to establish the relative timing of X-ray and optical pulses. In the LCLS (the first X-ray FEL), there was an intrinsic temporal jitter of up to several hundred femtoseconds; in the newer facilities, this has been reduced through the development of a number of so called "time-tools" [32 33] that can sort the pulse timing to a fidelity of better than 10 fs. Future machines with lower intrinsic jitter and higher resolution time-tools are under development[34 35]; these are anticipated for widespread use that will improve the achievable resolution to better than 1 femtosecond. This timing technology is also vital for the time-resolved X-ray spectroscopy techniques discussed in **Section 2.2.3** below.

2.2.3 Time-resolved X-ray spectroscopy

Inelastic X-ray interactions can be enormously powerful, and their measurement via various channels forms the basis of several well-established X-ray spectroscopy techniques (see **Figure 2.3**): X-ray photoelectron spectroscopy; Auger electron spectroscopy; X-ray absorption spectroscopy; and X-ray photoemission spectroscopies, such as resonant inelastic X-ray scattering (RIXS). With XFEL pulses, these X-ray spectroscopy tools can be made time-resolved, with temporal resolution in the femtosecond and, in the near future, even the sub-femtosecond range.

Photoelectron emission results when an X-ray photon is absorbed by the target and a bound electron is excited to the continuum from a valence states inner shell states. If X-rays of well-defined energy are used, the energy analysis of the photoelectrons emitted from the valence and inner shells gives direct information on the binding energies of these states. Angularly resolved measurements of the photoelectrons can give additional detailed information on state symmetries. This technique has been widely exploited to investigate the chemical state of materials and, in this form, is often termed

Electron Spectroscopy for Chemical Analysis (ESCA), following pioneering developments by Siegbahn[36] that led to his Nobel Prize in Physics in 1981.

Ionisation of an inner shell electron can lead to an unstable electronic hole, which can undergo decay through electron-electron correlation with the emission of further Auger electrons[37]. Auger electrons carry information on the energy levels of the involved ionic forms and are used for probing electronic structure of surfaces in the context of electron microscopy. It has been shown possible to track mechanisms of radiation damage in biomolecules[38] using time-resolved X-ray Auger and absorption spectroscopy probing of optically excited molecules at an XFEL. Streaking in a laser field of atomic photoelectrons and Auger electrons has been used to resolve temporal delays in emissions from different states, with as little as a few tens of attosecond difference[39].

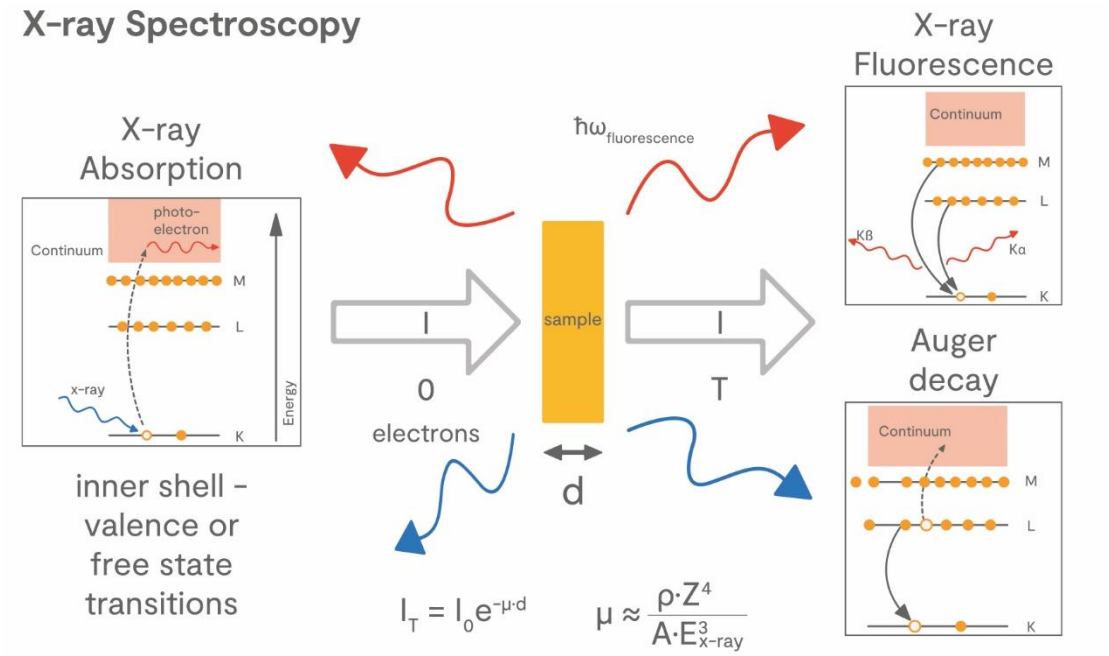

Figure 2.3: X-ray spectroscopy

Resonant ionisation close to an absorption edge of a particular atom, corresponding to a transition from an inner shell state to an unoccupied valence or low-lying continuum state, is a powerful way to learn about the electronic structure in the vicinity of that atom. The cross-section for photo-absorption at different X-ray energies can be determined from absorption or electron yield measurements in a condensed phase or gaseous system, and can reveal the details of the unoccupied and partially occupied valence and low continuum states near the ionisation threshold. This method of X-ray absorption near edge structure (XANES) is widely used to establish critical local electronic structure information[40]. Further into the continuum, the absorption modulations are termed extended X-ray absorption fine structure (EXAFS) and have been used for many years to establish local bond lengths around a specific atomic site[41]. Time-resolved X-ray absorption and RIXS using XFELs have now become proven techniques for photochemistry studies[10].

X-ray photon emission measurement methods are now being used in time-resolved mode using XFELs. For example, with RIXS, a core excited intermediate state relaxes to one or other of the neutral valence states by emission of a photon, and the energy and direction (momentum transfer) of the emitted photons are measured using an angularly resolving X-ray spectrometer. In the language of non-linear optics, this process is termed spontaneous Raman emission (in contrast to the stimulated Raman processes discussed in **Section 2.2.4**). The energy levels of the occupied and partially occupied states can be registered from this signal, as well as the existence of the low energy collective excitation modes and their momenta. This provides a powerful way to probe low energy (eV to meV) excitation modes in a condensed phase material. Time-resolved RIXS studies have proved valuable in elucidating the nature of excitations in photoexcited correlated materials[42] .

2.2.4 Non-linear X-ray spectroscopy

In so much as RIXS and other photon in/photon out methods using spontaneous emission are two-photon in nature, they can be regarded as examples of a non-linear X-ray interaction. The spontaneous emission is, however, into unoccupied field modes and so is not controlled by the applied X-ray fields. High brightness X-ray sources provide new opportunities for controlled non-linear X-ray processes. One example is stimulated X-ray Raman demonstrated by Rohringer et al[43 44].

High brightness, high repetition rate XFELs open the possibility of non-linear X-ray spectroscopy with entirely new capabilities. An early proposal in this direction is the possibility of impulsive X-ray electronic Raman creating and probing atomically localised valence electronic excitation, and so tracking ultrafast electronic coupling through a molecule even on attosecond timescales [45]. Another new concept is for non-linear X-ray diffraction involving a two-photon, optical and X-ray photon, scattering into an X-ray mode that can be heterodyne detected against an applied X-ray field in the same mode. This method is predicted to have the potential to image the charge density evolution of excited electronic states[46]. Experimental prospects for exploitation of non-linear X-ray spectroscopy are discussed in *Section 3.3*.

2.2.5 Measurement modes with XFELs

To date, the majority of studies conducted at XFELs have fitted into the categories of measurements of structural dynamics, properties of transient state, or nano-crystallography. As repetition rates increase and the X-ray properties become more controlled, it is likely that classes of measurement based around coherent diffraction imaging, and studying fluctuations with X-ray correlation spectroscopy, time-resolved pair distribution functions and mapping out conformational trajectories, will become more important. The current state of the art is captured in **Box 2.2**.

Box 2.2: Current modes of measurement being used at X-ray FELs

Access to structural dynamics: Dynamical phenomena can be probed after laser excitation on a time scale down to femtoseconds thus covering electronic dynamics, lattice dynamics and chemical bonds breaking/forming.
"Orbital-specific mapping of the ligand exchange dynamics of $Fe(CO)_5$ in solution" ***Nature*** 520, 78 (2015)

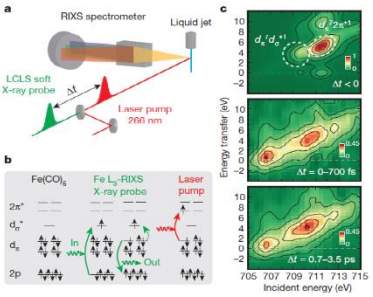

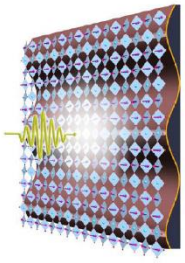

Access to transient states: Matter can be probed under only transiently attainable conditions of extreme pressure, high E & B fields, laser dressing and high energy density.
(Image from Andrea Cavalleri group MPSD Hamburg)

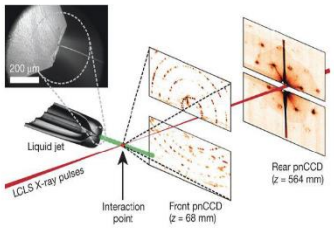

New modes of crystallography & nanoscopic imaging: For seeing the nanoscopic arrangements relevant to nanotechnology and life-sciences free from radiation damage and adverse effects of sample preparation. (Nature 470, 73 (2011))

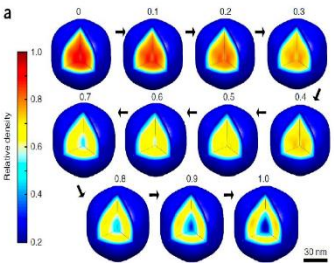

Capturing rare events: In physical, chemical and biological systems critical processes can proceed through brief rare events (e.g. barrier crossings) arising from intrinsic fluctuations.
Nature Methods, 14, 877 (2017)

2.3 Survey of Existing Facilities and Capabilities

For the next decade at least, the UK will remain reliant on the international XFEL facilities in Germany, the USA, Japan, Switzerland, Italy, South Korea and China. To develop a future UK XFEL facility with unique capability, it is essential to plan this in the context of these existing facilities. Here we briefly review their capabilities.

Now, and in the coming decades, the key frontier for a broad range of important scientific and technological disciplines will develop into the quantum realm, i.e. in a domain requiring measurement and understanding on ultra-small length scales, simultaneously with associated ultra-fast time scales. Accessing this domain, which is crucial for new knowledge, discovery and technological progress, is only possible with an XFEL that provides structural and electronic dynamics insight at the quantum scale.

Recognising this, there are currently five XFELs operating in the world, all in G7 countries, with several others under construction, notably in Asia. These few machines are already having significant global scientific impact, with almost half their scientific output in high impact journals. It is a signpost to the future, in much the same way that decades ago, early synchrotrons, lasers, electron microscopy etc. signalled new multi-disciplinary tools that we take for granted today.

Table 2.1: Summary of existing XFELs (March 2020)

Facility (Year of First Operation)	Max Photon Energy (keV)	Beam Energy (GeV)	Pulses/s	Bunch Charge (nC)	Facility Length (km)	RF Technology
FLASH (2005)	0.3	1.2	27000	1	0.32	SC
LCLS-I (2009)	11	13.6	120	0.25	1.7	NC
SACLA (2011)	15	8.5	60	0.2	0.8	NC
FERMI (2011)	0.3	1.5	50	0.5	0.5	NC
European XFEL (2017)	25	17.5	27000	1	3.4	SC
SwissFEL (2017)	12	5.8	100	0.2	0.7	NC
PAL XFEL (2017)	12	10	60	0.2	1	NC
LCLS-II (2021)	5	4	10^6	0.1	4	SC
	25	15	120	0.125	4	NC
HE UPGRADE	12	8	10^6	0.1	4	SC
SHINE (2025)	25	8	10^6	0.1	3.1	SC

Table 2.1 lists the main parameters of short-wavelength FEL facilities in order of their coming online, and includes two facilities which are under construction and will be online in the next five years. The colour coding relates to the RF technology – superconducting (SC) or normal conducting (NC). The first facility to offer short-wavelength FEL light to users was the pioneering FLASH in 2005, recently upgraded to FLASH-II by including gap tunable undulators. FLASH was originally constructed as an SC linac test facility and the technological advances it produced were critical to the design and success of the European XFEL. The first hard X-ray facility was LCLS-I, which started operations in 2009 and has since been joined by facilities in Japan, the EU, Switzerland and South Korea.

SC technology permits a higher pulse repetition rate than NC. European XFEL (in common with FLASH) operates in a pulsed mode, where the RF cavities are switched on and off 10 times per second. This limits the total number of FEL pulses per second and is not favoured by some users. When LCLS-II comes online from 2022 it will operate in a continuous wave (CW) mode, generating evenly spaced pulses at 1 MHz and photon energies up to 5 keV. For higher photon energies, the beam will be accelerated up to 15 GeV using the existing NC linac sections, so the FEL output will be limited to 120 Hz. The high-energy (HE) upgrade to LCLS-II will add extra SC linac sections to allow 1 MHz operation at 8 GeV with expected photon energy 12 keV. Finally, the SHINE facility is under construction in a tunnel underneath Shanghai and is expected to be operational by 2025. This is also driven by an 8 GeV SC accelerator and will produce 1 MHz FEL pulses at energies up to 25 keV.

It should be noted that the accelerating gradients available from SC cavities are significantly less than those available from NC cavities – this is the reason that although LCLS-I and European XFEL have similar beam energies, European XFEL is twice as long. Another trend revealed by the table is that the required beam energy to produce hard X-ray photons has reduced over time. This is due to advances in undulator technology, such as narrow-gap in-vacuum devices or superconducting devices, which mean that shorter periods with stronger on-axis fields are now available.

All the operational machines listed have large international user communities, built up in the decade since they first began operating. UK users have been very actively involved in science at FLASH, LCLS and SACLA for over a decade (see **Figure 2.4**). User communities have rapidly grown around FERMI, European XFEL, and PAL-XFEL, and are starting to turn attention to Swiss-FEL. The UK user community is currently relatively small, compared to the synchrotron user community and, critically to the UK XFEL, user communities in Germany, USA and other countries hosting these facilities. The UK community is, however, growing steadily, aided by initiatives such as the Life and Physical Sciences Hubs at Diamond and the CLF, respectively, and the new capabilities being offered as these international facilities evolve. It is vital for the strength of UK science across a wide range of areas that we do everything possible to grow this community substantially, otherwise we face losing our standing compared to the competition in key areas of frontier science and advanced technology.

Figure 2.4: Aerial views of operating X-ray FELs: LCLS, USA (top left) started operating in 2009; SACLA, Japan (top right) operating since 2012; Swiss FEL, Switzerland (bottom left) operating since 2018; European XFEL, Germany (bottom right) operating since 2018

2.4 Potential XFEL developments leading to new capability

In barely a decade since the first XFEL, remarkable progress has been made in adding new capabilities to this technology. Seeding and self-seeding have improved spectral brightness, attosecond pulses have significantly enhanced temporal resolution, and two-colour modes have facilitated new pump-probe experiments. Furthermore, the progress to-date represents only the very early stages in XFEL development – a host of new capabilities are being developed that would be incorporated into a UK XFEL. Building a new facility offers the opportunity to integrate the most exciting emerging features in an optimal way.

The first light from a free electron laser in the X-ray range was observed just 11 years ago (March 2009). The intervening decade has not only seen the construction of some half dozen machines around the world, but also enormous advances in the ability to simulate and implement new X-ray modes that are constantly advancing the scientific reach made possible by XFELs. These capabilities offer for example: two-colour, two pulse X-rays; variable polarization states; high spectral purity X-rays; higher brightness X-rays; and sub-femtosecond X-ray pulses. Existing facilities are often constrained by site and machine design factors, making it hard to offer all of these newer options. A UK XFEL, starting from a clean slate, could therefore leapfrog the existing facilities and would be superbly positioned to implement all of these advances, and to add to them other emerging capabilities. Many of these new capabilities go beyond SASE by manipulating the electron bunch (e.g. pre-modulation of density or controlled emittance spoiling) prior to it entering the undulator. Although all these modes are underpinned by access to an excellent electron beam driver, they are ultimately controlled by the operating modes of the undulator and so, by using a versatile undulator design, all can be made available at a single facility if properly configured. We briefly review a sample of these possibilities within this section.

2.4.1 High repetition rate laser seeding

One area with exceptionally high potential for a UK XFEL is to extend the range of seeding[6] (introduced in **Section 2.1**) to much higher repetition rates and to higher photon energy. Seeding greatly improves the coherence properties and stability of the output. The FERMI facility in Italy has demonstrated seeding up to ~400 eV at a repetition rate of ~100 Hz. In a recent demonstration[47], two external lasers were used to precisely tailor the longitudinal phase space in the electron bunch before it entered the undulator. A UK XFEL could operate with a thousand times as many seeded pulses per second by utilising superconducting linear acceleration with high repetition rate (~100 kHz) lasers – both areas of UK expertise. In combination with high repetition rate sample delivery and detectors, the massively enhanced data acquisition rate would greatly speed up existing experimental techniques. In addition, this would also open up entirely new classes of experiment due to the excellent X-ray coherence and stability, for example in: X-ray emission spectroscopy[10] of dilute samples; X-ray angularly resolved photoelectron spectroscopy using the high repetition-rate to gain sufficient signal in the low space-charge limit; and transient grating measurements[48] of transport rates at sub-nanometre scales in materials. Furthermore, using the latest non-linear optical laser technology (see **Section 9.2.1**) to generate the appropriate seeding would extend the range over which seeding operates to reach higher photon energies (> 1 keV), thereby extending the benefits to new areas of science by spanning an important range of critical absorption edges in carbon, nitrogen, oxygen and metals.

2.4.2 High spectral purity X-rays

Laser seeding is anticipated to be less effective above 1 keV, but alternative technologies are being developed to improve coherence and stability at the higher photon energies. A useful figure of merit related to coherence is the relative spectral bandwidth, with lower values indicating a higher degree of spectral purity. While existing XFELs typically operate with bandwidth between 1×10^{-3} for the default SASE mode and 2×10^{-4} for self-seeding (already introduced), new techniques are expected to far surpass this performance. Double self-seeding, employing two monochromatisation stages within

the FEL, has the potential to achieve bandwidths ~7×10^{-5}. High-Brightness SASE (HB-SASE), a scheme developed by UK FEL physicists, could achieve a bandwidth of ~2×10^{-5}, and will be tested at soft X-ray at SwissFEL in 2021. Its use of magnetic delay chicanes rather than optics could prove more flexible to different energies and higher repetition rates.

The method that promises the highest spectral purity is the XFELO (X-ray FEL Oscillator), which uses a low gain FEL enclosed in an optical cavity comprising diamond crystal Bragg mirrors with a geometry allowing a tunability of a few percent. Bandwidths of ~1×10^{-7} are anticipated, with modest pulse energies but exceptional shot-to-shot stability. Experiments to address the challenging cavity alignment tolerances are planned at LCLS-II. Such a scheme is, however, only possible on an accelerator with a repetition rate of around 1 MHz or higher, below which optical cavity lengths become unfeasibly large. A facility with high repetition beam at lower energy only (e.g. 2 GeV) could employ an oscillator FEL at EUV wavelength, to provide good stability and spectral purity, and potentially provide seed pulses for an XFEL.

Another potential possibility is to seed directly at hard X-ray wavelengths. A potential seed source is under development at Arizona State University. With this source, a compact low energy accelerator transforms a transverse electron diffraction pattern into a coherent longitudinal electron bunching, into which a laser pulse is counter-propagated to produce a pulse of coherent hard X-rays with sufficient power to act as a seed for a longer XFEL amplifier. Experiments are currently underway and the results will be of interest.

2.4.3 Higher pulse energy

Pulses of high spectral purity, produced via any of the methods above, can be further amplified very efficiently by extending the FEL undulator beyond the normal saturation point, while tapering down the field strength to keep the FEL pulse in resonance with the decreasing electron bunch energy. It is expected that increases in pulse energy of 1 - 2 orders of magnitude can be achieved using this tapering technique, with a simultaneous damping of the shot-to-shot fluctuations to a few percent. For example, by using low charge, highly compressed electron bunches in combination with self-seeding/ HB-SASE and post-saturation tapering it is anticipated that few-femtosecond, nearly transform-limited pulses, with > mJ pulse energies and few-percent shot-to-shot stability, could be produced.

2.4.4 Attosecond pulses

The recent demonstration of ~400 attosecond duration pulses at the LCLS facility (2018)[7] is a particularly significant development, and is a feature that would be a major focus of a new UK XFEL facility. The LCLS study reports one- and two-colour attosecond pulse generation over the photon energy range 500 eV - 1 keV, but it is anticipated that the same method will work through to the hard X-ray range. The study of dynamics on ultrafast timescales is one of the defining features of XFELs, and is made possible by the ultrashort duration of the XFEL pulses. Moreover, the large coherent bandwidth (5 – 8 eV in the pulses generated so far) is a key resource for future multi-dimensional, non-linear X-ray spectroscopies. A number of demonstration experiments have already been carried out at LCLS using the attosecond X-rays, e.g. measuring relative photo-electron emission delays for ionisation from different states of a molecule, and demonstrating impulsive electronic X-ray Raman excitation.

The techniques demonstrated to-date all effectively ‘slice’ the electron bunch in order to generate a short X-ray pulse. This slicing has been done using the self-field generated in a wiggler section, with the phase space manipulated in a chicane before entering the undulator. The possibility of using lasers instead of the self-field is also attractive, because, as the function of the laser is to slice rather than to seed, it could be performed at any photon energy, and would increase control and improve synchronisation to external sources. The pulses at higher photon energy would also be significantly shorter to access even faster time-scales.

2.4.5 High average power

As well as high pulse energy, high average power from the X-rays and from the electron beam would open up unprecedented opportunities. The potential of XFELs in direct industrial processing, for example for photolithography at soft X-ray wavelengths to achieve deep sub-nanometre feature resolutions, is a little explored area, so far. Interest in this from companies in the semiconductor chip sector was registered in our information gathering exercise, but it is clear that, even for a test facility to prove the concepts, an exceptionally high repetition rate (multi-MHz) will be required. Adding a return loop or an energy recovery configured accelerator section at the front end (perhaps up to 1 GeV) could be used for such a purpose, before the bunches to be accelerated to a higher energy pass through a conventional linac section (see **Appendix 1**). This would also create opportunities for direct science access to a GeV range electron beam at a high repetition rate. An additional potential benefit of this is the construction of an ultra-high average brightness gamma source based upon inverse Compton scattering (discussed in **Sections 3 and 8**). Opportunities to develop a high repetition rate electron acceleration test facility will also be provided by the development of the relativistic high brightness linac required to drive the X-ray laser.

2.4.6 Combining X-rays with other advanced capability

Beyond the potential for advanced X-ray modes sketched above, an enormous extension of science reach can be accomplished by combining other advanced capability at the X-ray interaction point. Ultrafast lasers, used with the X-rays in pump-probe configuration, are a mainstay of time-resolved XFEL research. Hitherto the laser photon energy ranges on offer at XFELs, and their pulse duration, have typically been rather limited due to practicalities and budgetary issues. In a machine designed to optimise these capabilities from scratch, the full range of pulse compressed laser/non-linear optical sources spanning from < 100 nm to 10 μm can be used for science (see **Section 9.2.1**), and with a repetition rate commensurate with experimental demands. By developing synchronised electron gun technology (in the 1 – 10 MeV energy range) at a number of end-stations, new opportunities in THz and electron-initiated biology, chemistry and physics, will become possible (see **Section 9.2.3**). A state-of-the-art, high rep-rate, high power laser — essential for science in the area of X-ray non-linear interactions (see **Section 3**) and matter at extreme conditions research (see **Section 4**) — will also be able to launch synchronised energetic electrons or ions/protons into the sample at the interaction point, permitting a wide range of new experiments for material science, defence and astrophysical applications.

2.4.7 Conclusion

Only a few of the possibilities for unique capability in a UK XFEL are covered above. It is also expected that advanced undulators (e.g. superconducting) and ultra-low emittance electron sources will **extend photon energy reach** for a given electron beam energy, as well as facilitating higher energy per pulse. Harmonic lasing will increase intensity at higher photon energies, too. In addition to combining X-rays with other advanced capabilities, **the two-**colour **(or multi-colour) FEL capability could be greatly enhanced** in a facility designed for this purpose, with broader ranges of temporal and spectral separation. Advances are anticipated in the control of pulse structures beyond that already described, to include **control of polarisation, orbital angular momentum and carrier-envelope phase**. It is expected that **facility capacity can be increased**, e.g. following the approach of using fast-kickers demonstrated at European XFEL, and advanced controls incorporating machine learning will enable more **rapid optimisation and restoration of setups**. In short, there are clear and numerous opportunities for world-leading capabilities, which can be customised to meet the needs of UK science.

[1] A.M. Kondratenko and E.L.Saldin "Generation of coherent radiation by a relativistic electron beam in an ondulator" Particle Accelerators, 10, 207 (1980)

[2] R. Bonifacio, C. Pellegrini and L.M. Narducci, "Collective instabilities and high-gain regime in a free electron laser", Opt.Comm. 50, 373 (1984) DOI: 10.1016/0030-4018(84)90105-6

[3] W. Ackermann et al, "Operation of a Free Electron Laser in the Wavelength Range from the Extreme Ultraviolet to the Water Window", Nature Photonics **1**, 336-342 (2007) DOI: 10.1038/nphoton.2007.76

[4] P. Emma et al, "First lasing and operation of an angstrom free electron laser", Nature Photonics, 4, 64 (2010) DOI: 10.1038/NPHOTON.2010.176

[5] J. Madey, "Stimulated emission of bremsstrahlung in a periodic magnetic field", J.Applied Physics, 42 1906 (1971) DOI: 10.1063/1.1660466

[6] E. Allaria et al, "Highly coherent and stable pulses from the FERMI seeded free-electron laser in the extreme ultraviolet", Nature Photonics, 6, 699 (2012) DOI: 10.1038/NPHOTON.2012.233

[7] J. Duris et al, "Tunable isolated attosecond X-ray pulses with gigawatt peak power from a free-electron laser", Nature Photonics, 14, 30 (2020) DOI: 10.1038/s41566-019-0549-5

[8] E. Seddon et al, "Short-wavelength free-electron laser sources and science" Rep.Prog.Physics. 80, 115901 (2017) DOI: 10.1088/1361-6633/aa7cca

Phil.Trans A, 377 Theme issue "The measurement of ultrafast electronic and structural dynamics with X-rays" ed. J.P. Marangos (2017) DOI: 10.1098/rsta.2017.0481

[10] Ph. Wernet et al, "Orbital-specific mapping of the ligand exchange dynamics of $Fe(CO)_5$ in solution" *Nature* 520, 78 (2015) DOI: 10.1038/nature14296

[11] W. Zhang et al, "Tracking excited-state charge and spin dynamics in iron coordination complexes" *Nature* 509, 345 (2014) DOI: 10.1038/nature13252

[12] J. Kern et al, "Structures of the intermediates of Kok's photosynthetic water oxidation clock", Nature, 563, 421 (2018) DOI: 10.1038/s41586-018-0681-2

[13] M.G. Gorman et al, "Direct observation of melting in shock compressed bismuth with fs X-ray diffraction *PRL* 115, 095701 (2015) DOI: 10.1103/PhysRevLett.115.095701

[14] L.B. Fletcher et al, "Ultra-bright X-ray laser scattering for dynamic warm dense matter physics" *Nature Phot.* 10, 1038 (2015) DOI: 10.1038/nphoton.2015.4

[15] M. Först et al, "Melting of charge stripes in vibrationally driven…..", *PRL* 112, 157002 (2014) DOI: 10.1103/PhysRevLett.112.157002

[16] R. Mankowski et al, "Nonlinear lattice dynamics as a basis for enhanced superconductivity in $YBa_2Cu_3O_{6.5}$" *Nature* 516, 71 (2014) DOI: 10.1038/nature13875

[17] A. Hosseinizadeh et al, "Conformational landscape of a virus by single-particle X-ray scattering" *Nature Methods*, 14, 877 (2017) DOI: 10.1038/nmeth.4395

[18] C. Kupitz et al, "Serial time resolved crystallography of photosystem II using a femtosecond X-ray laser", *Nature* 513, 261 (2014) DOI: 10.1038/nature13453

[19] L. Redecke et al, "Natively inhibited Trypanosoma brucei cathepsin B structure determined by using an X-ray laser" *Science* 339, 227 (2013) DOI: 10.1126/science.1229663

[20] Q. Zhou et al "Architecture of the synaptotagmin-SNARE machinery for neuronal exocytosis" *Nature* 525, 62 (2015) DOI: 10.1038/nature14975

[21] K.Pande et al, "Femtosecond structural dynamics drives the trans/cis isomerization in photoactive yellow protein" *Science,* 352, 725 (2016) DOI: 10.1126/science.aad5081

[22] W.H. Bragg and W.L. Bragg, "The reflexion of x-rays by crystals", Proc.R.Soc.Lond.A. 88, 428-38 (1913) DOI: 10.1098/rspa.1913.0040

[23] H.N. Chapman, et al, "Femtosecond X-ray protein nanocrystallography", Nature, 470, 73 (2011) DOI:10.1038/nature09750

[24] D. Sayre, "Some implications of a theorem due to Shannon", Acta. Crystallogr., 5 843-843 (1952) DOI: 10.1107/S0365110X52002276

[25] J. Miao et al, "Extending the methodology of X-ray crystallography to allow imaging of micrometre-sized non-crystalline specimens", Nature, 400, 342 (1999)

[26] M.M. Siebert et al, "Single mimivirus particles intercepted and imaged with an X-ray laser", Nature, 470, 78-81 (2011) DOI: 10.1038/nature09748

[27] J.N. Clark et al, "Ultrafast three-dimensional imaging of lattice dynamics in individual gold nanocrystals", Science, 341, 6141 (2013) DOI: 10.1126/science.1236034

[28] J.M. Glownia et al, "Self-referenced coherent diffraction X-ray movie of Angstrom and femtosecond-scale atomic motion", Phys.Rev.Lett., 117, 153003 (2016) DOI: 10.1103/PhysRevLett.117.153003

[29] T. Ishikawa et al, "Direct observation of collective modes coupled to molecular orbital-driven charge transfer", Science 350, 1501 (2015) DOI: 10.1126/science.aab3480

[30] M.Z. Mo, et al. "Heterogeneous to homogeneous melting transition visualized with ultrafast electron diffraction". Science, 360, 1451 (2018) DOI: 10.1126/science.aar2058

[31] J. Yang, et al, "Imaging CF_3I conical intersection and photodissociation dynamics with ultrafast electron dynamics", Science, 361, 6397 (2018) DOI: 10.1126/science.aat0049

[32] M. Harmand et al, "Achieving few-femtosecond time-sorting at hard X-ray free-electron lasers". Nature Photonics 7 (3), 215-218 (2013) DOI: 10.1038/nphoton.2013.11

[33] M.R. Bionta et al, "Spectral encoding method for measuring the relative arrival time between x-ray/optical pulses", Review of Scientific Instruments, 85, 083116 (2014) DOI: 10.1063/1.4893657

[34] N. Hartmann et al, "Attosecond time-energy structure of X-ray free-electron laser pulses", Nature Photonics, 12, 215–220 (2018) DOI: 10.1038/s41566-018-0107-6

[35] Y. Ding et al, "Femtosecond X-ray pulse temporal characterization in free-electron lasers using a transverse deflector", Phys. Rev. Accel. Beams 14, 120701 (2011) DOI: 10.1103/PhysRevSTAB.14.120701

[36] K. Siegbahn et al, "ESCA: Atomic, Molecular and Solid State Structure Studied by means of Electron Spectroscopy", Published by Royal Society of Sciences of Uppsala (1967)

[37] L. Meitner, "Uber die Entstehung der β-Strahl-Spektren radioaktiver Substanzen", Zeitschrift fur Physik 9: 131-144 (1922)

[38] T.J.A. Wolf et al, "Probing ultrafast $\pi\pi^*$ /$n\pi^*$ internal conversion in organic chromophores via K-edge resonant

absorption", Nature Communications 8, 29 (2017) DOI: 10.1038/s41467-017-00069-7

[39] M. Drescher et al, "Time-resolved atomic inner-shell spectroscopy", Nature volume 419, pages 803–807 (2002) DOI: 10.1038/nature01143

[40] J. Stöhr, "NEXAFS Spectroscopy", Springer Series in Surface Science 25 (1992) DOI: 10.1007/978-3-662-02853-7

[41] J.J. Rehr and R.C. Albers, "Theoretical approaches to X-ray absorption fine structure", Rev. Mod. Phys. 72 621 (2000) DOI: 10.1103/RevModPhys.72.621

[42] M.M. Dean et al, "Ultrafast energy- and momentum-resolved dynamics of magnetic correlations in the photo-doped Mott insulator Sr_2IrO_4", Nature Materials, 15, 601 (2016) DOI: 10.1038/nmat4641

[43] N. Weninger et al, "Stimulated electronic X-ray Raman scattering", Phys.Rev.Lett., 111, 233902 (2013) DOI: 10.1103/PhysRevLett.111.233902

[44] T. Kroll et al, "Stimulated X-ray electronic spectroscopy in transition metal complexes", Phys.Rev.Lett., 120, 133203 (2018) DOI: 10.1103/PhysRevLett.120.133203

[45] J.D. Biggs et al, "Watching energy transfer in metalloporphyrin heterodimers using stimulated X-ray Raman spectroscopy", PNAS, 110, 15597 (2013) DOI: 10.1073/pnas.1308604110

[46] J.R. Rouxel et al, "X-ray sum frequency diffraction for direct imaging of ultrafast electron dynamics", Phys.Rev.Lett., 120, 243902 (2018) DOI: 10.1103/PhysRevLett.120.243902

[47] P.R. Ribic et al, "Coherent soft X-ray pulses from an echo-enabled harmonic generation free-electron laser", Nat.Phot. 13, 555 (2019) DOI: 10.1038/s41566-019-0427-1

[48] F. Bencivenga et al, "Nanoscale transient gratings excited and probed by extreme ultraviolet femtosecond pulses", Science Advances, 5, eaaw 5805 (2019) DOI: 10.1126/sciadv.aaw5805

3. Science Opportunities in Physics and X-ray Photonics

Physics and exploration of new physical principles and methods has been a major driver in the development of light source applications to science. From X-ray diffraction to the broad range of X-ray spectroscopy, the initial steps required the elucidation of physical principles, refinement of the measurement and analysis methods and development of new instrumentation in which physics played a primary role. Given the unique new X-ray properties on offer from next generation XFELs , for instance ultrashort pulses, large coherent bandwidth and ultra-high brightness, it is imperative that the physics and X-ray photonics of their interaction with matter is fully explored, not only because of the basic physics interest in its own right, but also in order to spur the development of new measurement methods and applications for future X-ray science. Moreover, these unique X-ray characteristics provide opportunities for fundamental physics experiments and tests. This section deals with a range of these opportunities with an emphasis on looking forward to exciting new frontiers.

First in **Section 3.1**, we examine the basic interaction of intense X-rays with matter and the opportunity this affords in chemical physics and solving basic questions of energy and charge transfer following photoexcitation. This has application to understanding the dynamics of radiation damage of biomolecules, probing and controlling chirality and of new probes for ultrafast quantum coherent phenomena. Next in **Section 3.2** we examine new opportunities in X-ray scattering that go beyond the conventional approaches of elastic non-resonant scattering and employ new concepts by exploiting higher order photon correlation functions, quantum imaging concepts, inelastic scattering and signatures of electronic coherence in scattering. In **Section 3.3** the we examine the new opportunities unlocked by attosecond domain X-ray pulses that are now available. This includes the ultrafast probing of electronic coherence in new pump-probe X-ray spectroscopies and the possibilities to exploit the large coherent bandwidth to develop new classes of non-linear X-ray spectroscopy with potential to fully follow the propagation in space and time and decoherence pathways of electronic superposition states in matter. In **Section 3.4** we look at the potential opened by using high repetition-rate coherent diffraction imaging and related methods, along with advanced data sorting algorithms, to track the trajectory of molecular conformational change through the complex energy landscapes typical of biological and liquid systems. In **Section 3.5** we turn to tests of fundamental X-ray interaction physics looking at non-linear QED physics and potential for tests of the Standard Model using X-rays of extreme brightness in a facility offering a high repetition rate in-order to capture rare events. Finally, in **Section 3.6** we look at the potential to directly use the high quality relativistic electron beam that drives the XFEL to investigate new approaches in future accelerator and light source physics and to drive the world's brightest gamma ray source.

3.1 Frontiers in ultrafast chemical physics

Incisive ultrafast X-ray probing provides unprecedented insight into how energy and charge is transferred within and between molecules in processes such as photoexcitation or X-ray ionisation, following external stimulation. Taking inspiration from non-linear optical spectroscopy techniques, and implementing them in the X-ray regime, will enable dynamic probing of electronic properties and how they couple to molecular structure. These techniques will prove key in finding answers to questions such as how DNA responds to ionising radiation and how to control photophysical processes at the quantum level.

3.1.1 Introduction

Light interactions with molecules were essential to the development of the conditions that made possible life on Earth. Irradiation of interstellar media created the molecular building blocks of life, while absorption and conversion of solar energy continues to sustain the processes that allow complex life to thrive. Light interactions are also critical for studying molecules during chemical reactions and biological processes, illuminating the structure and dynamics of reactants, catalysts and products as they evolve in time.

Conversion of light energy into molecular potential energy is initiated by the displacement of electrons in the molecule by an electromagnetic field. Coupling of electronic states results in charge oscillations, or electron wavepackets, which occur on extremely fast (attosecond) timescales. Understanding and/or controlling how this charge is subsequently transferred and coupled to the molecular structure is key to determining how this energy is used to break or form bonds.

Photochemical processes are found in natural systems, such as those that govern vision,[1] vitamin D production,[2] photosynthesis,[3] UV photo-protection of DNA bases,[4] and the magnetic "vision" of migrating birds.[5] The charge transfer at the heart of these processes is equally relevant in determining the function of catalysts and batteries, and combustion and corrosion/degradation processes, such that these are optimised for particular applications. Questions remain about how electromagnetic energy is converted into chemical or electrical energy via coupling of the electronic motion into the molecular framework, with the experimental and theoretical tools available today unable to provide comprehensive answers.

Chemistry has predominantly relied upon an adiabatic description of chemical processes, where any atomic motion results in an almost instantaneous rearrangement of the electrons that "glue" the atoms together via bonds. In most situations, this assumption, known as the Born-Oppenheimer (BO) approximation, is reasonable, as the electrons are lighter and therefore move faster than the atoms. Following absorption of a photon, however, the potential energy surface of the excited electronic state has points or seams, called conical intersections, which cross with other electronic states. Near these intersections, as the separation of the electronic states becomes smaller, electron wavepacket motion slows down to the point where it becomes similar in magnitude to the motion of the atoms, and the BO approximation breaks down. This non-BO behaviour becomes more prevalent as the complexity and number of degrees of freedom of the molecules increases.

Theoretical simulations of molecules at conical intersections are extremely difficult to model, as the electronic and atomic motion cannot be de-coupled. With current models and computing power, this complex behaviour cannot be described accurately, even for simple molecules, without significant approximation. Likewise, experimental methods currently lack the tools and observables that can broadly probe the motion of the system through a conical intersection.

3.1.2 New X-ray spectroscopy techniques

A range of ultrafast X-ray spectroscopy techniques has been developed at X-ray FELs to exploit site-selective absorption by inner shell electrons in molecules. For example, X-ray near edge absorption spectroscopy, X-ray fluorescence spectroscopy, resonant inelastic X-ray scattering, and X-ray angle resolved photoelectron spectroscopy have been used as sensitive probes of chemical states and electronic structure. The advent of beamlines producing circularly polarised X-rays[6] has also enabled the chiral and magnetic properties of molecules and materials to be probed.

The high brightness and ultrafast pulse capability of a free electron laser will revolutionise X-ray spectroscopy by bringing it into the non-linear regime, facilitating the study of dynamical chemical processes with unprecedented time and spatial resolution. Non-linear spectroscopy, based on various absorption, fluorescence, wave mixing, and Raman schemes, has already been exploited in the optical domain to reveal details of the inter- and intra-molecular processes that govern transient chemical dynamics. Translating these techniques into the X-ray regime will enable electronic-nuclear couplings to be probed with atomic specificity, unravelling the behaviour at conical intersections and determining how charge and energy flows across and between molecules.[7,8]

A range of X-ray spectroscopy techniques, coupled with optical techniques and X-ray diffraction imaging, can be combined in multi-pulse schemes to stimulate, observe, and even control chemical dynamics. This provides a powerful toolbox to answer some fundamental questions, such as how DNA reacts to ionising radiation[9] so that the mechanisms for cancer induction are understood and new ways of enhancing radiotherapy outcomes can be developed. For example, exciting new research has shown that high dose rate radiotherapy, which can be simulated in FEL experiments, is less toxic to healthy cells compared to cancer cells[10].

Box 3.1 illustrates how an X-ray FEL could be used to study the effects of radiation on isolated or solvated DNA in extraordinary detail. Different pulsed radiation sources (electrons, ions, X-rays) would initiate an interaction. The ionisation process and initial charge migration proceeds on an attosecond timescale, but, after as little as a few femtoseconds the electron motion couples to the molecular structure: this determines the ultimate destination of the charge, weakening or breaking bonds and transferring energy within the molecule or to its surroundings, on timescales from femtoseconds to microseconds. The electronic and nuclear coupling could be tracked over these timescales using new non-linear spectroscopies and ultrafast diffraction available with X-ray FEL pulses, in combination with synchronized optical lasers.

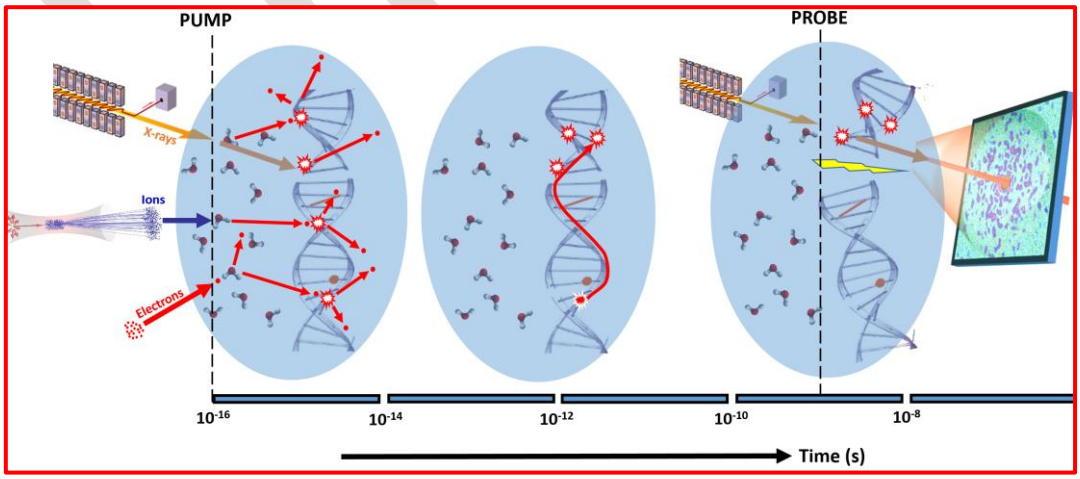

Box 3.1. *Ionization of DNA and its surroundings is initiated by a short burst of radiation (electrons, ions or X-rays). Charge is transferred on attosecond to picoseond timescales, ultimately causing bond cleavage and damage to the DNA. These steps can be probed at different times by XFEL pulses with linear and non-linear X-ray spectroscopies or ultrafast diffraction imaging.*

3.1.3 Chiral X-ray probes

One of the most intriguing scientific questions is why the molecular building blocks of life on Earth, such as amino acids and sugars, exist predominantly with 'one handedness'. This reflection asymmetry in molecules was termed *chirality* by Kelvin, and the mirror images are known as *enantiomers*. As a consequence of this homochirality, the action of most biological processes depends critically on the handedness of receptors, enzymes, and drugs. Currently, the only way of identifying enantiomers is through interaction with another chiral object of known handedness. While circularly polarised light has long been exploited to help reveal structural asymmetries in molecules, the small differences in the interaction with the opposite enantiomers limits the ability of light to identify and control molecular chirality. These chiroptical effects are weak because, from a molecule's perspective, the electric field's spiral rotation is much longer than the dimensions of the molecule itself, i.e. it is not present in the dipole approximation. Chiral differentiation relies on magnetic dipole interactions, which are orders of magnitude weaker, such that differences in the excitation rates of left- and right-handed enantiomers (circular dichroism) is typically <0.1%. However, as the wavelength of the light shortens and the chiral electric dipole interaction becomes stronger, X-ray FEL pulses open up the possibility of probing the chirality of molecules and the magnetic properties of nanostructures on ultrafast timescales.

Recent discoveries have shown that asymmetries of 10% or more can be present in photoelectron angular distributions via electric dipole transitions to the continuum. [11,12,13] This photoelectron circular dichroism (PECD) originates from the interaction of the outgoing electron with the chiral potential of the molecule, with the electron being preferentially scattered parallel or anti-parallel to the light direction. This behaviour has been shown to be present for photoionisation of valence and inner shell electrons[14], and in the single photon, multiphoton, and tunnelling ionisation regimes[15]. PECD therefore has the potential to become a universal sensitive observable for chiral dynamics.

Other developments have revealed that optical pulses can have more exotic configurations of their spin and orbital angular momentum. Pulses can now be produced where the local chirality changes rapidly in space and time, e.g. pulses with polarisations that map out all of the Poincaré sphere across the wavefront[16] or that have sub-cycle changes in the electric field rotation[17].

CHIRAL INDUCTION AND ULTRAFAST REVERSAL IN THE PLANAR MOLECULE FORMAMIDE

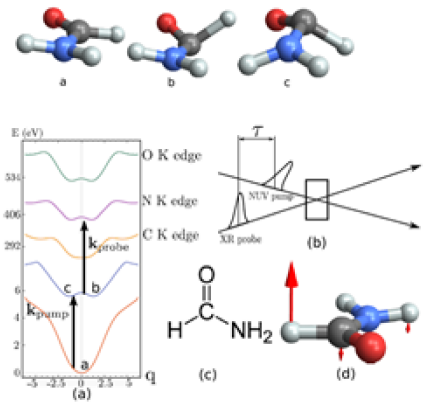

The formamide molecule is excited into a state which oscillates between two opposite chiral configurations. This transient chirality could be probed by circular dichroism in X-ray absorption or photionization. Such a flagship experiment offers a first step on the road to exploiting light to control the creation and/or separation of specific enantiomers.

Figure 3.1: Potential for inducing, probing and controlling chirality

There are already proposals to implement some of these schemes for XFEL undulators.[18] Future developments will see pulses produced with electric fields that trace out 3D patterns in space, enabling

strong, direct coupling of the electric field to the chiral properties of the molecules via electric dipole interactions[19].

Combining optical and XFEL pulses of this nature will offer an unprecedented way of sensitively probing global and local changes in the symmetry of molecules on sub-optical cycle timescales. These fields have the potential to induce chirality in achiral molecules and control the handedness of the products of chemical reactions.

In the *flagship experiment*, a chiral UV pulse projects the planar molecule formamide[20] from its achiral ground state (a) into an excited state with an initially chiral configuration (b). This creates a vibrational wavepacket in which the molecule flips between enantiomeric states (b,c) with a period of 100 fs. This chiral induction and ultrafast reversal could be observed with an X-ray FEL pulse through the circular dichroism in the absorption spectrum, or the asymmetry in photoelectron angular distributions. This could transform future pharmaceutical and agrochemical production of enantiomerically pure products, facilitating the selective pharmacological and species targeting required to reduce health and environmental side effects. Ultimately, better understanding of light-induced chiral induction and amplification could provide critical insight into the physical and chemical processes that led to homochirality in life.

3.1.4 Molecules in intense X-ray fields

The high brightness of X-ray FEL pulses presents opportunities to perform diffraction imaging of single molecules. At intensities of up to 10^{20} Wcm^{-2}, however, is it possible to obtain scattering data from an unperturbed molecule before it is inevitably destroyed by the pulse? Conversely, could complementary structural information be derived from the resulting fragmentation dynamics? To answer these questions requires a fundamental understanding of how complex molecules couple to intense X-ray fields.

One would expect the molecules to attain high ionization states before they explode through coulomb repulsion of the multiply-charged fragments, as with intense optical laser pulses; however, for X-rays, sequential single photon ionization of inner shell electrons is prevalent. If a heavy atom is present in the molecules, the X-ray field efficiently ionises its inner shell electrons. Within a few femtoseconds, Auger processes ionize outer electrons while re-filling the inner shell holes. This results in sequential photoionization-Auger events, generating an even higher charge state of the atom.[21] This charge has been found to quickly distribute around the molecule, via processes such as inter-coulombic decay (ICD), so that further absorption and ionization of X-ray photons takes place. These mechanisms produce a charge state of the molecule which is higher than could be obtained for the atom by itself.[22]

This dramatic and ultrafast shift in electrons within the molecule means that it suffers radiation damage, since the initial electron distribution is altered substantially. Additionally, on timescales as short as 10 fs, Coulomb repulsion is already pushing the atoms from their equilibrium positions. This has consequences for XFEL diffraction imaging of single molecules, and these effects need to be considered to enable correct interpretation of scattering patterns.

These processes have been observed in atoms and small molecules,[23] and very recently in fullerene,[24] but much more complex molecules need to be studied in order to see how electronic coupling behaves over greater spatial extents. Fragmentation patterns of complex molecules can themselves yield important structural information and can reveal details of how biological structures are damaged by ionizing radiation. Coulomb explosion imaging (CEI) has been established using intense optical pulses, with the momentum vectors of the fragment ions used to recreate the molecular structure,[25] and has already been applied to obtain the absolute configuration of some simple chiral molecules.[26] The higher charge states that can be reached by XFEL pulses will improve the resolution of the molecular reconstruction obtained from CEI. Molecular models are also being developed to include the initial vibration motion of the atoms and the subsequent nuclear dynamics,[27] giving multi-pulse schemes the potential to generate high resolution, ultrafast molecular movies of atomic motion in the molecule. The ability to observe fast proton migration within molecules is particularly important, as this migration drives many chemical processes, but cannot been seen with X-ray diffraction techniques that rely on scattering from electrons.

These developments will depend upon the continued development of multi-hit detector technology[28] and correlation mapping,[29] to enable the complex fragmentation patterns generated from large molecules to be interpreted meaningfully. For instance, co-variance mapping has been recently been used to study the fragmentation patterns of trapped peptide ions, enabling detailed information on amino acid sequences and chemical modifications to be obtained.[30] Similar schemes could be highly valuable for studying how biological molecules suffer radiation damage following irradiation with ionizing particles.

3.2 New concepts in scattering

Structure is the basis for our comprehension of the many properties of matter. XFELs will enable us to determine dynamic changes in structure, leading to much deeper understanding of function on the nanoscale. By combining ultrafast X-ray scattering with new ideas from e.g. quantum optics and scattering physics, we anticipate that even disordered or fragile samples will be accessible for study, that the phase problem will be circumvented, and that electron dynamics and coherent transport phenomena will be imaged.

3.2.1 Introduction

X-ray scattering has shaped our understanding of the structure of matter. The iconic renderings of the DNA double-helix structure,[31] the structure of globular proteins,[32] and the atomic structure of crystalline matter,[33] constitute early breakthroughs that were awarded Nobel prizes. The number of known structures is growing exponentially[34] (see also Section7 *Life Sciences*), reflecting the growing importance of structure-function relationships in many branches of modern science. This success notwithstanding, significant limitations and therefore opportunities, remain.

The large-photon flux and coherence of XFELs, combined with cutting-edge ideas from *e.g*. quantum optics, may enable forms of single-particle imaging[35] that circumvent the requirement of crystalline targets and allow molecules to be observed in their natural state, avoiding potential distortion due to the crystalline environment. The importance of sampling a whole range of thermodynamic states is also discussed in Section 3.4. Furthermore, greater information might be extracted for delicate, fragile, or disordered materials that are challenging or impossible to study with the technologies available today. Perhaps most revolutionary, concepts are advanced that may overcome the *phase problem*, arguably the most defining challenge for all forms of x-ray imaging.

The short pulse duration at XFELs could have even greater impact. The absence of dynamics from the structure-function dogma reflects that current imaging methods provide static, time-averaged images. The ability to determine short-lived and transient structures may transform the development of future nanoscale technologies and bring greater understanding to all aspects of structural science. For instance, by measuring time-resolved sequences of molecular structures on a femtosecond timescale, the motion of atoms in a molecule following the interaction with light can be revealed, with great impact on our understanding of energy and charge transport and reactivity in photoactive molecules, which could be exploited in areas such as quantum technologies, photonics, and molecular electronics.

These new opportunities come alongside new and exciting physics. Imaging techniques such as ghost imaging exploit ideas from quantum optics and involve the detection of photons that never interact with the sample, with the quantum version of ghost imaging going one step further by using entangled photons. Likewise, ultrafast measurements with hard x-rays may transgress current distinctions between structural dynamics and spectroscopy and provide insights into the fundamental nature of the combined motions of electrons and nuclei that cannot be achieved by other means. Finally, theoretical predictions indicate that, for sufficient time-resolution and coherence, new quantum interference phenomena in scattering will appear, carrying unique information about ultrafast electron dynamics and transient coherences in material systems.

3.2.2 New imaging techniques

Correlated X-ray scattering, or fluctuation X-ray scattering, detects momentum-transfer correlations between two or more photons scattered by the same molecule, making it possible to determine structure in the absence or short- or long-range order. The concept, advanced in the late 1970s,[36,37] remained largely undeveloped until the emergence XFELs, which finally provided sufficient photon fluence and pulse durations shorter than rotational diffusion times. In 2009, it was demonstrated at LCLS that angular correlations can determine the local structure in colloidal glasses[38] . Though these are disordered, it was shown that locally the molecules arrange into icosahedral shapes, and that these shapes change structure over time. With currently existing XFELs, the signal to noise ratio is still

insufficient to determine the structure of particles as complex as proteins, but with further improvements in photon fluence, the technology may attain this goal. Apart from studies in native environments, the method could also become instrumental in single-particle imaging, where it could overcome the issue of unknown sample orientations[39].

Ghost imaging originates in quantum optics[40] and exploits the observation of photon correlations. These protocols have been extended to classical light[41,42], making them relevant also to non-seeded XFEL sources. The immediate advantage of ghost imaging is that the radiation dose absorbed by a fragile sample can be lowered dramatically[43]. The approach also offers distinct improvements in resolution, signal to noise, and, under specific circumstances, greater efficiency in data collection[44]. At optical wavelengths, it has been demonstrated that ghost imaging can provide special performance when parametric down-conversion is phase-matched to give non-degenerate signal and idler wavelengths[45]. This allows an object to be illuminated at one wavelength and the spatial information recorded at another, perhaps where the imaging detector is more sensitive or less noisy. Ghost tomography schemes have been proposed that aim at atomic resolution of complex targets[46], and analogous ideas have been put forward that exploit the random time-structure of SASE pulses to achieve pump-probe resolution of dynamics without actual time-delay scans[47]. An interesting opportunity at future high-flux XFELs is quantum ghost imaging via parametric down-conversion of X-ray photons, allowing one photon of an entangled pair to be diffracted off a sample and detected in coincidence with its twin[48]. By scanning the photon that did not interact with the target, the phase information imprinted in the state of the field can be detected, which could yield real-space images that avoid the phase problem altogether (see breakout Box 3.2).

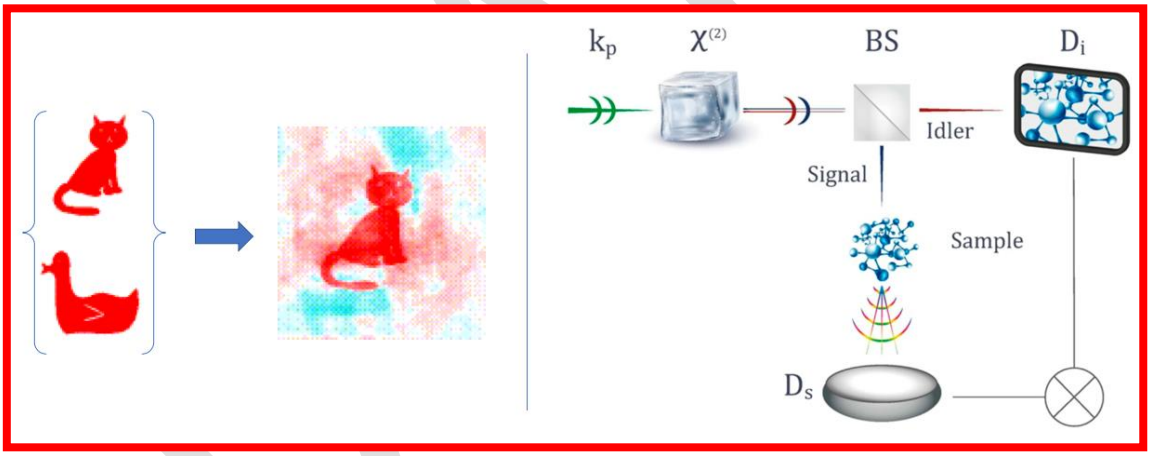

Box 3.2 Current imaging techniques measure the amplitudes and not the phases. The importance of this so-called phase problem is illustrated on the left. If we combine the phases for the cat with the amplitudes for the duck, the resulting image looks more like a cat than the duck (http://www.ysbl.york.ac.uk/~cowtan/fourier/fourier.html). Ideas from quantum optics, e.g. ghost imaging or incoherent diffraction may overcome this problem. On the right, a proposed quantum diffraction setup is shown that would be capable of measuring phase.[48]

Another exciting technique that originates in ideas originally put forward by Hanbury Brown and Twiss is incoherent diffractive imaging[49,50,51], which exploits higher-order correlations between fluorescence emission from different atoms to retrieve structural information. This approach may provide striking advantages such as element specificity and opportunities for phasing in a manner analogous to anomalous dispersion when performed in conjunction with coherent diffraction[50]. Since the cross section for incoherent fluorescence emission is higher than for elastic scattering, incoherent diffraction can produce stronger signals than standard coherent diffraction and detect higher momentum transfer thanks to the uniform angular distribution of fluorescence emission. The cumulative result is a

potential for rapid structure determination that requires a significantly smaller number of observations to fill the full 3D Fourier space than conventional method[50], and sub-Abbe resolution may be achieved if higher than second order correlations are exploited.[49,52] The concept has recently been demonstrated at the FLASH XFEL using a patterned mask,[51] as shown in Fig. 3.2.1. Similarly to the other techniques discussed in this section, incoherent diffractive imaging requires the extreme brilliance and high pulse repetition rate of new XFEL sources. It also requires pulse durations shorter than the radiative lifetime of fluorescence (e.g. 2.6 fs for the Kα fluorescence in Fe atoms). A striking prospective application could be ultra-high resolution of yet unresolved structural changes in metal clusters in Photosystem II, which are essential for the manner in which water is oxidised during photosynthesis.

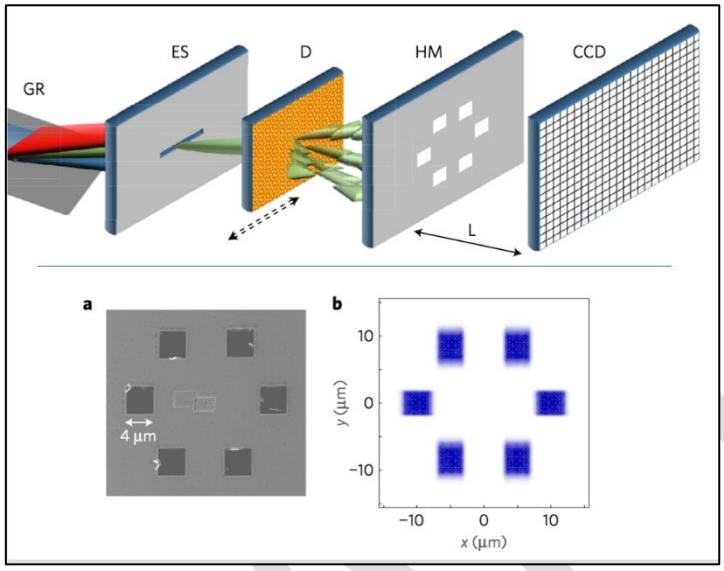

Figure 3.2: The first demonstration of incoherent diffraction using a microscale patterned mask at the FLASH XFEL.[21] (Top) Experimental setup with grating (GR), exit slit (ES), diffusor (D), hole mask (HM), and a CCD detector. a) Hole mask, b) reconstructed image.

3.2.3 Structural dynamics and beyond

Ultrafast x-ray scattering at XFELs is beginning to make it possible to observe structural dynamics at the fundamental femtosecond (10^{-15} s) timescale of nuclear motion. Since information on the structural evolution of a molecular system is not readily available from ultrafast spectroscopy, this brings unique insights into the atomic motions that underpin transformations in matter. With sufficient spatial and temporal resolution, it is possible to observe the fundamental steps in bond-breaking, bond-making, and atomic re-arrangements, for instance following photoexcitation. Recent experiments at LCLS demonstrated structure determination in excited molecules undergoing coherent vibrations[53] and the dynamics associated with rapid electrocyclic ring-opening reactions[54]. As the resolution increases, it will become possible to track the time-evolution of the quantum wavepacket for excited systems and directly observe intrinsically quantum phenomena such as dispersion, coherence, and interference[55,56].

Such measurements will inherently transgress simplistic notions of structural dynamics, as analysis of the ultrafast x-ray scattering data can reveal normal modes and associated frequencies, thus combining sub-Ångström resolution of atomic displacements with resolution of *e.g.* harmonic motions[57,58]. Importantly, the scattered x-ray photons carry an imprint of the actual electron density of the material system. This means, at least in principle, that specific electronic states should be identifiable, and one may conceive of experiments that simultaneously track not just the structural dynamics of a molecule but also the changes in electronic states that are a primary driver of the observed dynamics. Such experiments would begin to approach a complete characterisation of photochemical and photophysical processes. Even for static molecules, more accurate measurements

made possible by the large X-ray photon flux may reveal intrinsic correlation effects in electronic structure, leading to further methodological and theoretical advances in electronic structure theory.

3.2.4 Physics of scattering with coherent x-rays

The coherence in the incident x-ray radiation, combined with the ultrashort time-duration of the pulses, may lead to new observable phenomena that appear as interferences between different inelastic transitions. This new phenomenon in x-ray scattering, sometimes referred to as coherent mixed scattering[59], has been theoretically predicted to carry the signatures of ultrafast electron dynamics[60],transient nuclear coherences,[59] and transitions between different electronic states due to nonadiabatic coupling[61] or at conical intersections[62].

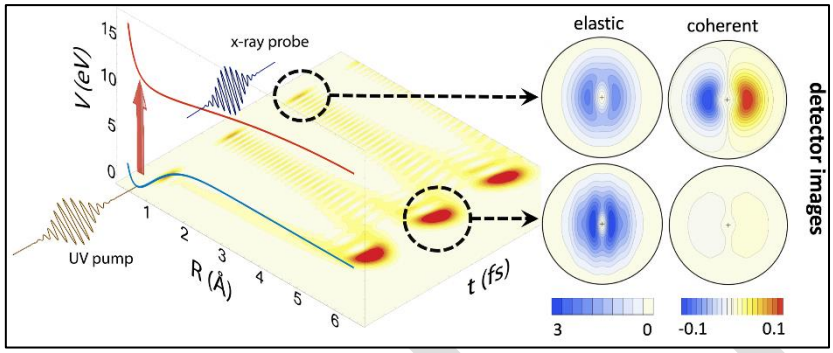

Figure 3.3: Coherent mixed scattering appears as a consequence of coherent electron dynamics and may help characterise complex dynamic processes in matter.[59-63] On the left-hand side, an optically pumped wavepacket is shown, with the x-ray scattering detector images showing elastic and coherent mixed scattering shown on the right

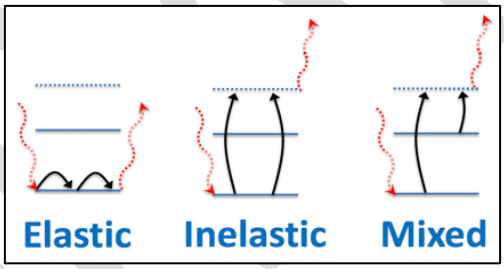

Figure 3.4. Schematic illustration of the main components in x-ray scattering. Populated states are shown as solid straight lines, scattering transitions as curved arrows (one for each scattering matrix element), and incident and scattered photons as curly arrows.

The coherent mixed scattering is predicted to appear alongside elastic and inelastic scattering and stems from an interference of scattering amplitudes from different electronic states populated in an excited molecule,[59,63] as shown in Fig. 3.2.2 and 3.2.3. The effect requires coherence between populated electronic states, meaning that their nuclear wavefunctions must overlap. Such coherences emerge transiently during photochemical reactions when electronic states are coupled and transitions between them occur. Coherent mixed scattering should thus provide distinct fingerprints of internal conversion and intersystem crossing during photochemical and photophysical processes. It could furthermore be used to measure the role of coherence in energy transport[64] and charge migration[65].

3.3 Attosecond science and non-linear X-ray spectroscopy

Electron dynamics, typically occurring on attosecond to femtosecond timescales, play a crucial role in a vast array of physical, biological and technological processes. High temporal resolution X-ray probes are essential to understanding and harnessing these processes, and will impact on knowledge and control of, for example, excitons in light harvesting systems, primary steps in photocatalysis, advanced photodetectors, and photodynamic therapy.

3.3.1 Introduction to new attosecond X-ray FEL capability

There has been a rapid advance in short pulse operation modes at X-ray FELs since LCLS first started operation in 2009[66]. Low-bunch charge modes were soon found to produce self-amplified spontaneous emission (SASE) pulses as short as 3 fs[67]; emittance spoiler based methods followed[68], and the two-colour fresh-slice mode[69] was developed and is now routinely used[70]. Two pulse/two colour X-ray modes are subject to orders of magnitude less inherent jitter (sub-femtosecond) than laser-X-ray experiments and so, at present, offer the highest temporal resolution pump-probe capabilities. When millijoule-level femtosecond duration SASE pulses are focussed, high intensities (> 10^{18} Wcm^{-2}) are routinely attainable. Such high intensities are required to drive even relatively low order non-linear X-ray processes, since the relevant interaction strengths scale strongly with wavelength, leading to much diminished non-linear cross-sections in the X-ray range. Nevertheless, two-photon ionisation[71], stimulated Raman[72] and stimulated emission[73] have been observed, as well as XFEL-pumped atomic X-ray lasers[74]. The challenge now is to go beyond multi-spiked stochastic SASE pulses, to permit more controllable non-linear interactions.

The introduction of seeding[75] and echo enabled seeding at FERMI[76] has shown that almost transform-limited (fully temporally coherent) femtosecond pulses can be delivered in the XUV and soft-X-ray range. These seeded pulses have enabled the first transient grating XUV FEL experiments[77] and prospects to scale these to higher photon energies look promising. Enhanced SASE (eSASE) has been discussed for some time as it offers[78] a way to restrict the SASE lasing to a single SASE spike with a field that much more closely approaches the *ideal* transform limit. This technique was recently demonstrated[79] with the generation of one and two colour eSASE pulses of sub-femtosecond duration and large coherent bandwidth. Using a circularly polarised laser field streaking method, these pulses were fully characterized in the 500 – 1000 eV range and found to give 200 – 500 attosecond pulse durations [Figure 3.3.1], with a relatively narrow distribution over multiple shots. Moreover, these short pulses were accompanied by a large coherent bandwidth in the range 5 – 10 eV, and the pulse energy was some nine orders of magnitude higher than that obtained by high harmonic generation (HHG), the only other source of attosecond pulses. This breakthrough development is opening the path to important new opportunities in attosecond domain pump-probe measurements, and non-linear X-ray spectroscopy.

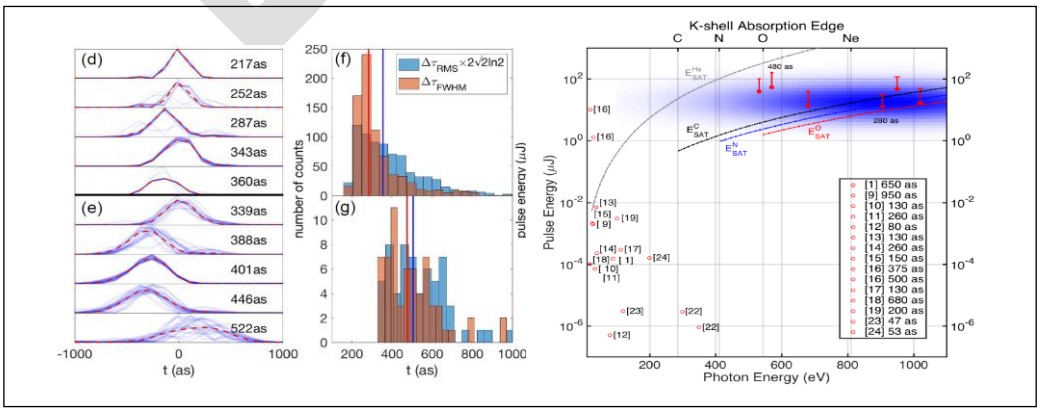

Figure 3.5: Recent results from LCLS showing (top) the measured 200 – 500 attosecond pulses in the SXR region, and (bottom) the comparison to HHG attosecond sources (from Duris et al (2020)[20])

3.3.2 Attosecond science

The timescale of electronic dynamics in matter is naturally very fast; for example, the orbit time of an electron in the lowest Bohr level of the hydrogen atom is just 150 attoseconds. When superpositions of electronic valence states are formed, fast electronic dynamics are manifested as an observable effect, e.g. through the ultrafast time dependent localisation of charge density. Given that the typical energy spacings of valence states can span several electron-volts or more, the resulting beating timescale is typically a few-femtoseconds to sub-femtoseconds. The primary events of photoexcitation and radiolysis will intrinsically occur on such timescales when considered at the single system quantum level. The wider impact of this on science and technology is through the importance of photo-excitation/photo-ionisation in renewable energy (e.g. light harvesting technology), photocatalysis (e.g. photo-driven water splitting and biofuel generation) and biomedicine (e.g. photodynamic therapy, photoactivated fragmentation of biomolecules in mass spectrometry and radiation damage and therapy).

The new X-ray attosecond pulse capability from eSASE provides the prospect of applying X-ray spectroscopic probes that allow, for the first time, the study of electron dynamics with full spatial resolution through atomically localized probing as well as the required temporal resolution. For example, in the X-ray ionisation of matter by a short pulse, the high kinetic energy of the outgoing electron leads to a "sudden ionisation" event that can project the resulting charged system into superposition of valence states, resulting in large amplitude charge density oscillation across the system with attosecond timescales. This "charge migration" situation has been widely studied theoretically, but can only now be realised in the context of true sudden ionization. Ultrafast charge migration following sudden ionization or excitation is believed to be a universal response of extended molecules, and is also likely to occur in some form in many condensed phase systems[80]. It is now understood that there is intrinsic coupling to the nuclear wavefunction through both zero-point geometry spread and subsequent rapid motion[81], which will take place on a short (< 10 fs) timescale, so it is expected that coupling to nuclear modes will rapidly become important[82]. Understanding ultrafast electron-nuclear coupling poses an enormous challenge, requiring fully quantum dynamics calculations that go beyond the Born-Oppenheimer approximation, and experimental benchmarking is now vital.

Electron wavepackets excited by attosecond pulses lead to a new regime in photochemistry where the electronic state dynamics drive the reaction and the nuclear dynamics follow, in contrast to the usual case where nuclear dynamics drive the reaction and the electronic motion follows. Such charge directed reactivity has been suggested to explain laser ionisation dynamics in molecules,[83] and may offer routes to control reactions in the future.

Ultrafast hole evolution and motion is of critical importance to many aspects of photochemistry and photophysics, where there is hitherto little experimental data at these short timescales. At present, attosecond science relies heavily on the process of HHG as a means to generate attosecond pulses in the soft-X-ray photon energy range[84,85], but, despite progress in the generation efficiency and shortness of the pulse duration,[86] the power levels are currently found to be very low (picojoules in the soft X-ray range). This has prohibited applications to direct pump-probe measurements and instead techniques have been developed that use an intense IR field either as the pump[87] or the probe [88 89]. The strong IR field will, however, induce profound modifications to any extended multi-electron system[90] and so inhibit the ability to make measurements on the native charge migration process without unwanted strong field distortion.

3.3.3 Attosecond spectroscopy and impulsive X-ray Raman interactions: Electronic excitation in matter localised in space and time

X-ray attosecond pulse pairs open up new routes for the pump-probe study of charge migration and other attosecond timescale electronic processes. A resonant core state to valence hole probing scheme enabled by attosecond X-ray pulses is far superior to current methods, in that the interaction

ensures a non-perturbative measurement of the intrinsic electron dynamics, whilst it also permits an atomically localised probing of the electronic state through the atomic specificity of core state spectroscopy[91]. In addition, attosecond streaking with circularly polarized fields is now being used to time-resolve the electron photoemission process and subsequent Auger cascades,[92] and future extensions of such streaking base methods are anticipated to the XUV and hard X-ray ranges as new attosecond capabilities are developed.

With the new generation of eSASE capability, likely to be extended across a wide photon energy range in a future light source, we will have the means to measure time-dependent information on the electron-hole evolution, and localization in a wide range of situations in both gas and condensed phase systems. We also anticipate better synchronization and better time-stamping (e.g. via circular streaking offering sub-femtosecond measurement resolution) between laser fields and X-rays in future facilities. Such advances will allow attosecond resolved measurements on excited state neutrals that will extend these X-ray probing methods to chemical excited state dynamics in gas and liquid phases and excitons in condensed phase materials, and open prospects for control of photo-processes through manipulation of the new resource of electronic state superpositions.

New concepts in nonlinear X-ray spectroscopy have been proposed and explored theoretically, including 1-d[93] and 2-d coherent X-ray Raman scattering[94]. One method already being realised is *impulsive* X-ray Raman scattering (IXRS), which relies upon the large coherent bandwidth within a single attosecond X-ray pulse to provide both the pump and the Stokes transition frequencies required to excite a valence *electronic* excited state in the neutral. This is analogous to stimulated impulsive Raman in the optical domain (visible to UV), which primarily couples to *vibrational* states of matter. IXRS offers unprecedented opportunities for creating localized coherent electronic wave packets in *un-ionised* states that can be employed to probe electronic couplings between atomic sites in a molecule or a condensed phase material.

Early experiments on IXRS in the NO molecule tuned near the O 1s-π* resonance have shown promising results. Tuning the X-ray photon energy resonances between inner shell and valence states in the molecule boosts the two-photon (Raman) excitation of excited state neutral atoms by a large factor. Through strong resonance enhancement, the Raman process can select only atoms of a single species through a virtual transition to this core-excited intermediate state. The process can, therefore, lead to localized excitation at a specific site (site *a* in the *flagship experiment* box) within a neutral molecule, and it is possible to control which sites are excited by tuning the X-ray photon energy. A second delayed pulse, tuned to a different resonance, can then be used to induce a Raman transition at a nearby atomic site (site *b*). The electronic excitation transfer from site *a* to site *b* can then be determined in changes to the stimulated X-ray emission spectrum induced in the second Raman transition. As a result, this process provides the perfect tool to probe the transfer of electronic excitation within a molecule or a condensed phase system with atomic spatial and sub-fs temporal resolution, and is ultimately a *photon in – photon-out* method that lends itself to gas, solid and liquid phase systems.

Building on our experience so far, we can envision the development of new experimental techniques to probe electronic dynamics in femtosecond to attosecond timescales. In the future, with multi-pulse/multi-colour attosecond operation, it may become feasible to create a localized electronic excitation at one atomic site and then probe, with attosecond resolution, the motion of that excitation to *multiple* other atomic sites within the molecule or material, by observing stimulated emission at different X-ray frequencies (see Box 3.3). Further developments to more elaborate X-ray four-wave mixing scenarios are at the level of theoretical investigation and promise to yield a new type of multi-dimensional spectroscopy that can, in principle, examine the full range of nuclear, electronic and electronic-nuclear couplings in a material. Extension of the transient grating method to the X-ray range to investigate ultrafast transport in materials is one prospect, but this will require fully coherent broad-bandwidth pulses (such as those available with eSASE) with a high measure of phase coherence across a wide range of frequencies. ESASE already provides two-colour pulses, each with ~ 10 eV of coherent bandwidth, and it is likely that the full array of X-ray tools needed for these advanced spectroscopies will be developed over the next decade.

SPACE TIME LOCALIZED MEASUREMENTS OF ELECTRONIC COUPLING

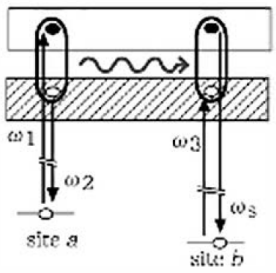

A double impulsive Raman sequence can excite a valence state wave-packet localized at one atomic site and probe at a second atomic site after a controlled delay[30]. This creates a unique opportunity for spatial/temporal resolved probing and quantum control. Such a flagship experiment is a stepping-stone to attosecond multi-dimensional spectroscopy, with creation and probing of localised electronic wave-packets in matter of all kinds.

Box 3.3 New concepts to create and track coherent electronic wavepackets through materials

3.4 Capturing conformational dynamics and rare thermodynamic states

Chemical reactions catalysed by biomolecules and transformations of matter such as crystallisation or phase transitions progress via complex trajectories across rare thermodynamic states. Many of the transitions and fluctuations critical to these processes happen at timescales too fast to be captured by any existing methods. X-ray FEL imaging methods, coupled to advanced data sorting algorithms, offer a unique way to capture these changes essential to understanding how, for instance, biomolecules function in their native state

3.4.1 Introduction

For many decades the key to our scientific understanding and control of matter in its various forms - molecules, polymers, solid materials (metals, semi-conductors, dielectrics) and biomolecules - has stemmed in large part from our ability to determine their atomic scale structure. In structural biology, the tight connection between structure and function is an underpinning paradigm that supports nearly all of biology and is responsible for the vast majority of new treatments linked to human health. Our scientific understanding of structure was delivered by the capability to use X-ray, neutron and electron diffraction, and imaging methods to determine the atomic scale arrangement of complex material. As successful as this picture has been, it nevertheless misses a key part of the story.

The challenge is that many processes in condensed phases, such as enzyme catalysis, crystallisation [95] [96], phase transitions[97] [98] [99],or dynamic heterogeneity[100] occur via rare states accessed via thermodynamic fluctuations. Yet, we only detect an ensemble averaged behaviour, strongly dominated by the stable endpoints of the process, rather than capturing the underlying transformational dynamics at a single molecule level. For example, in the context of biomolecules, scientists fit an atomic model to X-ray diffraction data from crystal comprised of 10^6 copies of the macromolecule, each of which may include tens of thousands of atoms in complex 3D arrangement. Functional information often comes from measuring the reaction kinetics and or spectroscopic signals of an ensemble average reaction in solution. Overall reaction rates are typically rather slow (microseconds or longer) for biomolecules, although the dynamics of the critical sub-steps that manifest the functional processes nearly always happen on a much faster timescale (picosecond to nanosecond). Up until very recently, we have not had the appropriate tools to capture atomic structures of dynamic systems engaged in performing their function. Thus, the ability to routinely measure the structure and function of macromolecules engaged in physiological processes under physiological temperature and pressure, would be transformative.

If we can directly image key conformational steps, *i.e*. the rare thermodynamic states crucial to function, then the ensuing mechanistic insights will answer profound questions in condensed phase, including physics, biology and chemistry:

- How do enzyme-catalysed reactions occur in a living cell?
- How do molecular machines efficiently cross energy barriers to drive biological processes?
- What are the fluctuation dynamics of solvation networks in liquids?
- What are the initial steps in crystallisation and how do the initial crystal seeds grow?
- What are the mechanistic aspects that control phase transitions?
- How do spontaneous fluctuations and nanoscale heterogeneity relate in functional materials?

New X-ray diffraction and coherent diffraction imaging capabilities at XFELs enable single-shot structure determination/imaging, that exploit pulses short enough to capture individual

conformations. For each single molecular or biomolecular assembly probed with femtosecond pulses, we will capture an instantaneous conformation that is not smeared by a long exposure time. This capability, combined with advanced data analysis techniques, offers a route to resolve the questions posed above and many others.[101,102] Using these methods, and with sufficient data, it is possible to map out the conformational trajectory through the free-energy landscape associated with a particular reaction path.[103] In common with cryoEM, this potential capability for single-particle imaging sets X-ray scattering data apart from ensemble-averaged methods such as X-ray crystallography and NMR spectroscopy that cannot capture the single-molecule conformations.

Whilst the most common technique to measure dynamics are by the pump-probe methodology, this is *not* viable for capturing the plethora of reactions occurring at room temperature but driven by far from equilibrium transient conformational changes (*e.g*. barrier crossings). For instance, the molecular conformation(s) required by enzyme catalysis are very likely to be significantly different than the equilibrium structure of the macromolecule in its ground state. An alternative to pump-probe strategies is to take multiple short pulsed data points and then splice these together to create stop-motion views of the functional cycle. This often exploits either X-ray diffraction from a periodic array as in serial micro-crystallography methods, or coherent diffraction imaging from non-regular specimens as in single-particle imaging techniques, at high spatial localization to avoid spatial averaging. Importantly, the density of the data sampling must be high enough that the rarely occupied high-energy states of the system are present within the data set. Moreover, the exposure time must be short enough to capture the various stages of these conformational changes without time averaging, scrambling or blurring. If these criteria are met, then the data techniques can in principle retrieve the structural dynamics of these critical events at high atomic and temporal resolution.

3.4.2 Data driven approaches to structural dynamics

Pioneering work by the group of Ourmazd[104] took pump-probe experimental data[105] that visualised the molecular rotational wavepacket in N_2 using Coulomb explosion. Despite that the original data had 300 fs timing uncertainty, Ourmazd *et al*. were able to reconstruct the dynamics with a few femtosecond precision, including a transient aligned states of the molecule. The key feature of this data-analysis method is that it does not require precise control of timing, as would be the case in a conventional pump-probe experiment. Instead it uses random, and essentially noisy data from the large dataset, and applies advanced algorithms for sorting the data in order to reconstruct the rare events.

For some cases such as cryoEM, the relatively low temporal resolution available from freeze-quench methods (~ a millisecond) are adequate to capture the dynamics of slow processes. But the ability to go to much faster timescales, corresponding to the actual inherent time-scales of many intermediate states, and the opportunity to avoid artefacts from low temperature conditions, presses us to explore the possibilities with ultrafast X-ray sources. Furthermore, cryoEM data sets are typically rather small due to the time associated with the freeze-quench preparation and data collection, which limits the ability to "see" critical rate-limiting high-energy conformational states. CryoEM is, and will likely remain, the dominant method for single molecule conformational state determination with near atomic resolution. In contrast, lower resolution X-ray single-shot imaging may have a considerable role in uncovering the large conformational changes associated with high-energy, rate-limiting processes.

Another example applied to single-molecule coherent diffractive imaging of the PR772 virus with low spatial resolution (in the 10 nanometer range) allowed Ourmazd *et al*. to visualize a rare event, the growth of a tubular structure from a portal vertex potentially associated with release of the virus genome.[106] This indicates the potential for application to X-ray snapshot imaging. Success of the technique was also demonstrated with cryoEM data where the conformational and energy landscape of the 80S ribosome extracted from yeast was mapped.[107]

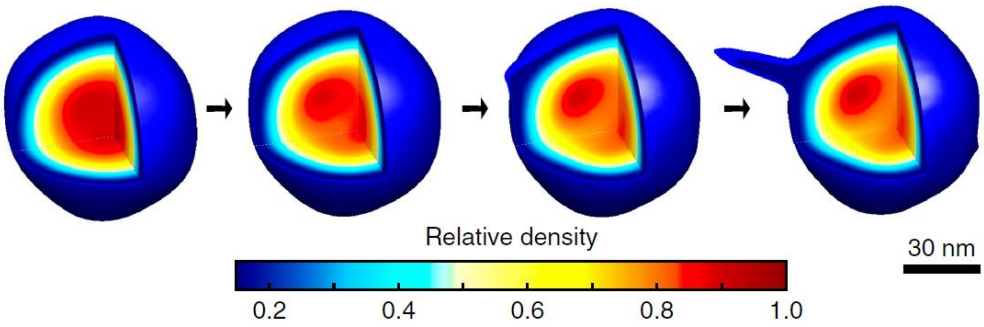

Figure 3.6: 3D structures revealed by conformational analysis of 37,550 single-particle X-ray snapshots of the PR772 virus grouped by conformational parameter. The rare tubular structure is captured in the rightmost conformer.

3.4.3 Developing methods for tracking conformational dynamics through the energy landscape

The further development of these methods will require some significant technical advances for which a UK XFEL facility can be optimised. Firstly, improved resolution of X-ray single-particle imaging is an important goal. The Single Particle Imaging Initiative at LCLS and other efforts globally have improved the methodology and resolution[108] but it is believed there is still considerable scope for further improvement. This includes improved control of imaging conditions (X-ray intensity, spectrum, beam profile), an improved particle hit rate, and higher precision positioning in the focus, less variation in the thickness of the hydrating water jacket around each sample and further improvements on scattered background and on analysis algorithms. Evidence is emerging that the highest intensities are not required for imaging and that if a nanometre resolution is sought, then soft or tender X-ray wavelengths rather than hard X-rays may be optimal.

The central advantage of the XFEL based technique is the possibility to record very large datasets. The probability of a specific conformer within the free energy landscape is determined by the Boltzmann factor, hence the highest energy states furthest from equilibrium will also be the rarest. To be sure of sampling with sufficient numbers *all* of the relevant conformers for a reaction with a high-energy transition state (as in processes driven by ATP hydrolysis) will require billions of individual snapshots. This is well within reach of an XFEL, even one at modest repetition rate of 10 kHz, which will require only hours under optimised conditions, but this will remain very challenging for cryoEM. Moreover, the very short pulses (few femtoseconds) of the XFEL will eliminate any possibility of temporal smearing, which remains a real issue given the freeze-quench time of cryoEM.

It therefore appears that a high repetition rate seeded source operating at ~1 keV and with high flux harmonics (to 3 keV) may be a very appropriate source for furthering the method to sub-nanometre resolution. The seeding would ensure stable shot to shot conditions and a reproducible beam and spectrum. This would need to be coupled to the most innovative state of the art sample delivery system.

Another area where focussed effort will be needed is in algorithm develop to support the efficient conformational determination and sorting from the large data sets. For ultimate resolutions a high rep-rate hard X-ray source with some form of seeding could prove optimal. These capabilities are likely to have impact also in capturing the complex structural dynamics in condensed phase systems and quantum materials where fluctuations on the mesoscopic scale can play a critical role.

3.5 Non-linear X-ray Physics and Physics beyond the Standard Model with XFELs

With the development of high intensity X-ray lasers one can envision new non-linear X-ray interaction physics and groundbreaking precision tests of observables that are manifest only at very high-energies. This allows probes of quantum gravity and tests for deviations from the Standard Model of particle physics while being far below the Planck scale of 10^{19}GeV that is beyond the direct reach of any particle accelerator.

3.5.1 XFEL-driven nonlinear dynamics in matter and vacuum

The combination of high photon frequency and high intensity means that X-ray free electron lasers are ideally suited for studying matter in extreme conditions. However, a future XFEL system that aimed for *relativistic intensity*, at XUV to soft X-ray wavelengths, could be used to study nonlinear behaviour not only in matter, but in the vacuum itself [109] [110]. According to quantum field theory, it is possible to interact with transient electron-positron pairs, whose lifetime is restricted by the uncertainty principle. There are longstanding theoretical predictions that the vacuum, through this coupling, behaves as a *nonlinear*, birefringent medium. Yet none of these interactions have been observed with real photons. As the probabilities for the relevant processes generically increase with photon frequency and field intensity, a high-intensity XFEL would be a unique platform that could be used to pump, or probe, vacuum birefrigence or even Schwinger pair creation[111]: the electromagnetically driven `breakdown' of the vacuum into electron-positron pairs. Here we summarise three scientific opportunities, illustrated in Box 3.5, that would be available with XFEL pulses that are focused to high intensity.

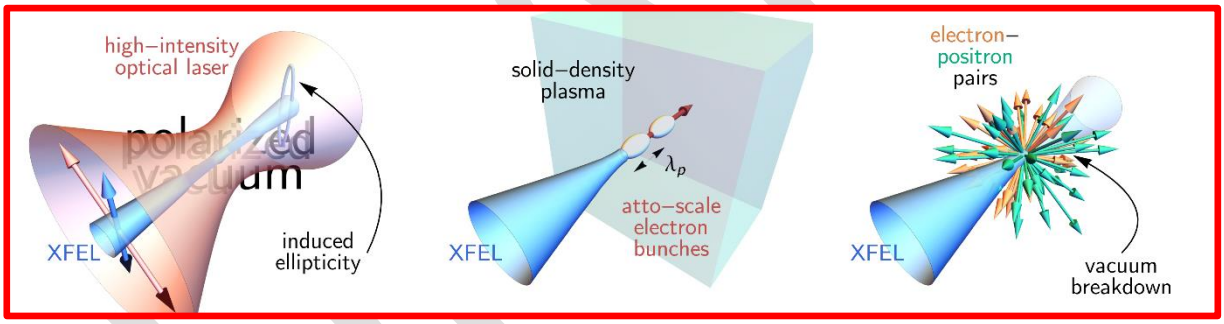

Box 3.5: *(left) An XFEL probes the vacuum polarized by a high-power optical laser.*

(centre) An XFEL drives a nonlinear plasma wake in a high-density plasma, accelerating atto-scale electron bunches at gradients of TeV/cm.

(right) An XFEL, focused to ultrahigh intensity, sparks electron-positron pair creation from the vacuum

3.5.1.1 Vacuum birefringence

In classical electromagnetism, light does not interact with light, a fact that is expressed mathematically by the linearity of Maxwell's equations in vacuum. QED, however, predicts that it is possible for two photons to scatter off one another, the cross section being $\sigma_{\gamma\gamma} = 10^{-31} (\hbar\omega^*/mc^2)^6 \, cm^{-2}$ for centre-of-mass photon energies $\hbar\omega^*$ much smaller than the electron rest energy mc^2. The cross section is so small, and the necessary photon fluxes therefore so high, that light-by-light scattering has not yet been observed with real photons. It could be, using the combination of an XFEL and a high-intensity optical laser, because of the strong scaling of $\sigma_{\gamma\gamma}$ with photon frequency. The cross section is 11 orders of magnitude larger for XFEL-laser scattering than for laser-laser scattering, and 33 orders larger for XFEL-XFEL scattering (as attempted at SACLA[112]). The advantage of using a high-intensity optical laser is that signal is enhanced by coherence. The large separation in energy scales (keV vs. eV) means that the X-

ray photons primarily scatter forward, with altered helicity, rather than momentum: in other words, an initially linearly polarized XFEL beam would acquire a small ellipticity, as if it had passed through a birefrigent medium[113]. The difference here is that the medium is not a material, but the vacuum, which is polarized by the strong electromagnetic field of the optical laser. This leads to a non-isotropic permittivity tensor with two non-trivial refractive indices.

The induced ellipticity, $\delta = \omega L \Delta n/2$, is proportional to the *difference* in the refractive indices $\Delta n = 2 \alpha I_{laser} / 15 I_{crit}$. It is maximised by increasing the X-ray frequency ω and the laser intensity I_{laser} ($I_{crit} = 2 \times 10^{29}$ Wcm^{-2}). The primary experimental challenge is that the ellipticity change is of order $\delta = 10^{-10}$, which requires high initial polarization purity[114]. Nevertheless, lab-based measurements of vacuum birefringence are much in demand, as the same phenomenon should occur around highly magnetized compact objects, such as magnetars[115], and claims of observation are disputed[116] [117]. Furthermore, as the difference in refractive index Δn is zero in Born-Infeld theory[118], an experiment could rule out this alternative theory of nonlinear electrodynamics. At higher centre-of-mass photon energies, close to the pair-creation threshold, it becomes possible to probe *anomalous dispersion*, i.e. the energy dependence of the vacuum refractive indices.

3.5.1.2 Plasma acceleration at solid density

In the case of a vacuum birefringence measurement, the XFEL beam plays the role of probe, rather than pump. An example of the latter would be using an XFEL to drive a wakefield in a solid-density plasma [2] [119], thereby scaling a laser-plasma accelerator[120] from optical to XUV or soft-X-ray wavelengths. This leverages the considerably higher frequency of an XFEL; as the plasma frequency of a medium increases with the electron density n_e, increasing the driver frequency renders higher density targets transparent. The plasma wavelength, λ_p [μm] = $n_e^{-0.5}$[10^{21}cm^{-3}] , which controls the size of the accelerating structure and therefore the size of the electron bunches, is significantly reduced. For optical lasers, the use of high-pressure gas jet 10^{18} - 10^{19} cm^{-3} yields a cavity size of 10 μm and therefore electron bunches that are tens of femtoseconds in duration. Driving a solid of density 10^{23} – 10^{25} cm^{-3} with X rays, focused to an intensity ~ $10^{18} \lambda^{-2}$ [μ m] W cm^{-2}, could yield electron bunches with durations as short as 10^{-17} – 10^{-15} s. These could be used to generate secondary beams of γ rays, for example, of comparable duration.

3.5.1.3 Schwinger pair creation and vacuum breakdown

Pair creation from vacuum becomes likely when the applied electromagnetic field can deliver work equal to $2mc^2$, i.e. twice the rest energy of an electron-positron pair, over a Compton length $\lambda_c = \hbar/(mc)$ ~ 386 fm. The process is often called *Schwinger pair creation* [3] and it is a landmark prediction of nonlinear QED. Exponential suppression of the rate is overcome by fields that satisfy $E^2 - c^2B^2 > E^2_{cr}$, which requires either tight focusing or the overlap of two or more beams of extreme intensity. However, the characteristic field strength, E_{cr} ~ 1.3 x10^{18} Vm^{-1}, is so large that it is currently out of reach in a laboratory environment. In fields of critical strength, the electrons and positrons so created can be accelerated so strongly that they radiate hard gamma rays, which stimulate further pair creation, radiation emission, and thus an electromagnetic cascade. It is speculated that triggering such a cascade is what limits the highest intensity that could ever be achieved with a tightly focused, optical laser[121] [122]. However, the higher photon frequency of an XFEL, as compared to an optical laser, means that it is possible to reduce the volume of the focal region, suppressing cascade growth that could limit the largest field achieved. It is predicted that a terawatt XFEL, focused close to the diffraction limit, could provide the first observation of Schwinger pair creation[123] . Here, capability for diffraction-limited focusing is essential: if the focal spot radius is 20 nm, rather than 0.1 nm, the power requirements increase from 2 TW to 50 PW.

3.5.2 Physics beyond the Standard Model with X-ray Free Electron Lasers

Intense, ultra-short pulsed X-ray beams are expected to deliver unprecedented intensities at very short wavelength, possibly achieving values in excess of 10^{20} W/cm^2. An electron placed at the focus of such beams should experience enormous acceleration[124], comparable to what it would feel if placed near

the event horizon of a $6x10^{18}$ kg ($=3x10^{-12}$ M_{sun}) black hole. Indeed for such low mass black holes the surface gravity is strong enough that pairs of entangled photons can be produced from the vacuum, with one of the pair escaping to infinity. The black hole can then radiate, and the spectrum of such radiation is a blackbody at the so-called Hawking temperature[125]. This relation is at the foundations of quantum gravity phenomenology, since, by virtue of the equivalence principle, it is impossible to distinguish between an accelerated frame in flat spacetime or gravitational effects. In flat space-time, the observation of thermal photons by an accelerated detector is called the Unruh effect[126].

All proposals aimed at the observation of the Hawking/Unruh effect have so far been unable to reach the required conditions[127] [128] or separate this effect from the background. Hawking radiation, information loss-paradox, as well as searches for dark-matter are now within the grasp of new high intensity optical facilities [129] [130] [131]. While optical laser experiments are in principle able to achieve the required acceleration, they have the constraint that separating the Unruh emission from any other classical or quantum (e.g., radiation reaction) effect is very challenging [132] [133]. High-intensity, high-energy X-ray laser facilities thus offer a new approach that could provide a successful route towards the experimental demonstration of the Hawking/Unruh effect. For an electron accelerated by a 10^{19} W/cm^2 laser, the Unruh temperature corresponds to the optical frequency band. Thus, it becomes much simpler to separate the Unruh emission from the X-ray background.

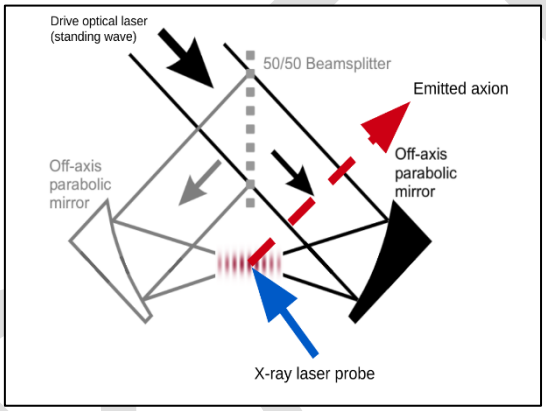

Figure 3.7: Probing production of dark matter in with an intense X-ray field interacting with and intense optical laser standing wave

At these high X-ray intensities very light particles can also be created via similar mechanisms[23]. These axion-like particles (ALPs) are a possible dark-matter candidate[134] [135]. An XFEL facility could then be included in the worldwide effort of searches for dark matter, as synchrotron have, in the past, been used in light-shining-through-walls (LSW) experiments, both at ESRF[136] and SPring-8[137]. The advantage of an XFEL in LSW searches is the 10^{17}-10^{18} increase in the number of photons/s, implying a factor 20-30 improvement in the predicted exclusion bounds. While LSW searches have the advantage of being model-free, the parameter space they can access remains much smaller than those achieved by searches that already assumes ALPs are a constituent of dark matter (such as ADMX[138]) or that axions are produced in the Sun (such as CAST[139]). The combination of x-ray and optical laser sources at an XFEL facility may be able to circumvent this limitation of laboratory-based searches. As shown in the Figure 3.5.1, the collision of two laser beams can resonantly produce axions[140], with their presence inferred by a signal photon detected after magnetic reconversion[141], but with a much larger cross-section thanks to resonant excitation – achieving exclusion bounds comparable to CAST, but without any assumption on the axion generation in stars. The additional advantage of an XFEL based search is the energy tunability, thus providing a natural means to scan across a broad energy range - which is needed given that the ALPs mass is relatively unconstrained by theory[142].

While cosmological and astrophysical evidence for dark matter is very compelling, however as yet all attempts to identify the elusive particle itself have failed. On the other hand, recent satellite observations with XMM-Newton and Chandra in the *Perseus* cluster have shown an unidentified emission line near 3.5 keV[143,144]. It has been suggested that this line may be the result of resonant

excitation of dark matter particles. XFEL experiments could then provide an ideal experimental tool (because of the narrow bandwidth and high photon number) to resonantly excite dark matter particles and then measure their subsequent decay into x-ray photons. Initial calculations shows that it might be possible to detect of order 1–10 photons a week in this way, thereby potentially opening up a new search strategy for dark matter

3.6 High brightness relativistic electron beam science

High brightness electron beams, in addition to powering the XFEL, can also be used for electron beam-driven plasma wakefield acceleration (PWFA), a unique inverse Compton scattering gamma source and new precision tests of the Standard Model. The incorporation of plasma photocathodes in PWFA can boost electron energy and brightness, which can have a transformative impact on photon pulses produced by the UK XFEL in the future. The gamma source would be a major research asset for nuclear science and the nuclear industry in the UK.

3.6.1 Physics of plasma photocathodes and production of ultrabright electron beams

By transferring energy from a *driver* electron pulse, that sets up the plasma wave, to a following *witness* electron pulse located in the accelerating phase of the plasma wave, the electron energy of the witness beam can be multiplied on sub-metre-scale distance because of the ~100 GV m^{-1} scale plasma accelerator gradients [1]. However, the controlled generation of electron beams with sufficient quality in particular with regard to emittance and energy spread has been a well-known challenge for the plasma accelerator community – and thus far was a showstopper for achieving lasing of electron beams from plasma-based accelerators in undulators.

A novel approach of beam generation in plasma-based accelerators, invented [2] and computationally [3] and experimentally [4] pioneered by a UK-led collaboration, opens a transformative path towards controlled production of electron beams of substantially improved quality compared to state-of-the-art. In the plasma photocathode (a.k.a. "Trojan Horse") method, a synchronized, focused laser pulse is used to release electrons directly within the electron beam-driven plasma wave via tunnelling ionization of a higher ionization level of the background gas. These electrons are liberated within the tight laser focus region, where its intensity exceeds the tunnelling ionization threshold, and have vanishing transverse momenta. Rapid acceleration in ~100 GV m^{-1} accelerating and focusing fields of the plasma then produces electron bunches that are intrinsically compressed to few femtosecond (fs) duration or shorter, with ultralow nmrad-scale emittance and corresponding ultrahigh brightness.

This combination of plasma photogun, compressor and accelerator in a single, compact plasma accelerator stage allows generation of ultrashort (fs to sub-fs-scale), high-current (multi-kA) electron beams with extremely compact transverse phase space and therefore ultralow emittance $\varepsilon_{nx,ny}$ down to the nm rad-scale – three orders of magnitude smaller than state-of-the-art levels. In addition to its capability of superior emittance, the plasma photocathode process is largely decoupled from details of the electron driver beam per-shot pattern. The process can therefore be very robust to shot-to-shot driver beam jitters [4] and nearly completely insensitive to energy spread variations. This decoupling gives rise to potential for very high stability, and an extremely wide parameter range of reproducible ultrabright electron beam populations, including multi-colour beam trains with variable separation in colour and temporal distance.

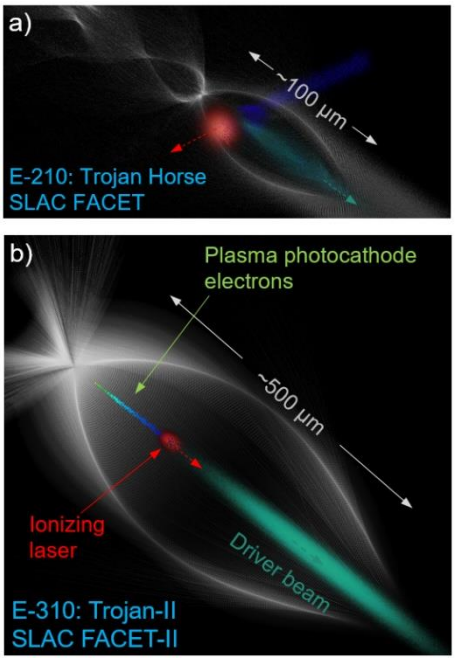

The first demonstration of a plasma photocathode was recently achieved at SLAC's FACET facility in the "E-210: Trojan Horse" experiment [4] in 90° geometry between electron drive beam and plasma photocathode laser. In this configuration, the emittance of produced beams was already of the order of state-of-the-art linacs – and additionally this setup also allowed the first realization of optical density downramp injection (a.k.a. "Plasma Torch"), that is also a

promising candidate for production of high quality electron beams. The top panel in the figure to the right shows a 3D particle-in-cell (VSim) representation of this experiment. The SLAC FACET linac electron beam (green) propagates to the bottom right and sets up the plasma wave by expelling hydrogen electrons (white). The plasma photocathode laser pulse (red) comes from the right and crosses the plasma wave to tunnel ionize electrons from neutral helium gas within the plasma wave. These helium electrons are then captured and constitute the witness beam.

Further improvement of electron beam quality is expected from advanced versions of plasma photocathodes e.g. in collinear geometry, as shown in the bottom panel of the figure. This is part of the "E-310: Trojan Horse-II" R&D at SLAC FACET-II that aims to generate electron beams with 10-nm-scale emittance, sub-fs duration and kA-scale currents.

The large energy spread, an intrinsic by-product of the huge accelerating gradient in plasma accelerators, is a well-known threshold barrier for beam quality preservation during extraction and transport from the plasma stage, and the process of free-electron lasing in the undulator itself. A further innovation, exploiting the tunability of the plasma photocathode, promises reduction of energy spread from the typical few-%-level by ~two orders of magnitude, down to relative energy spreads at the $\Delta W_{rms}/W < 0.01\%$ level already at $W \approx 3$ GeV witness beam energies [3]. This is well below the FEL energy threshold given by the Pierce parameter even for very hard x-ray radiation. Since the emittance of plasma photocathodes can yield nm rad-scale emittance levels in both planes ε_{nx} and ε_{ny}, the corresponding 5D-beam brightness $B_{5D} = 2I_p / (\varepsilon_{nx}\varepsilon_{ny})$ as well as the 6D-brightness $B_{6D} = B_{5D} / (0.1\% \Delta W_{rms}/W)$ reach is many orders of magnitude larger than those of state-of-the-art electron beams from conventional accelerators.

It should be emphasized that the experimental realization and exploitation of the plasma photocathode technology is still in its infancy [4]. Nevertheless, the plasma photocathode so far experimentally has behaved exactly as expected based on theory and simulation, and the confidence level is therefore very high that ultrahigh beam qualities can be realized and harnessed. The UK XFEL is in a symbiotic relation with PWFA: the UK XFEL can be exploited for plasma photocathode PWFA R&D and to realize increasingly bright electron beams, and in turn these electron beams can be harnessed for accessing fundamentally new photon science regimes.

3.6.2 Impact of ultrabright electron beams on photon science

The UK STFC has assumed leadership in the exploration of such ultrabright electron beams for photon science in the "PWFA-FEL" project "Exploratory Study of PWFA-FEL at CLARA" 2019-2023, a UK-US collaboration that brings together plasma photocathode wakefield accelerator and XFEL experts [5]. Jointly with FACET-II, Stanford and LCLS personnel, investigation of the addition of PWFA-FEL capabilities into the existing hard x-ray FEL facilities LCLS [6] and/or LCLS-II has been initiated. These ambitions, however, have to deal with existing facility layouts that were designed before invention and existence of plasma photocathodes, and before their potential for superior emittance and brightness, and the resulting impact for photon science capabilities, had been understood.

The emerging UK XFEL project allows tailored integration of PWFA-XFEL capabilities *ab ovo* instead of retrospectively investigating options that may be compatible with existing facility layouts. Provision of dedicated beamlines for plasma accelerator research and applications would enable wide-ranging enhanced exploitation for photon science, but would not increase the spatial and financial footprint of the facility significantly. Intriguingly, in addition or alternatively to dedicated plasma accelerator beamline(s) directly powered by the linac, one could also accommodate the use of linac-generated electron beams *after* their passage through the undulators. When propagating through an undulator, the electron beam transfers only a fraction of its energy to the photon field, and the concomitant electron beam quality loss does not compromise the capability of these electron beams to drive a PWFA significantly. A particularly cost-effective and potentially 'high-gain' approach could therefore be integration of plasma wakefield brightness and energy afterburners into the linac-based UK XFEL

after the undulator section, instead of only diagnosing and disposing the electron beam into a beam dump.

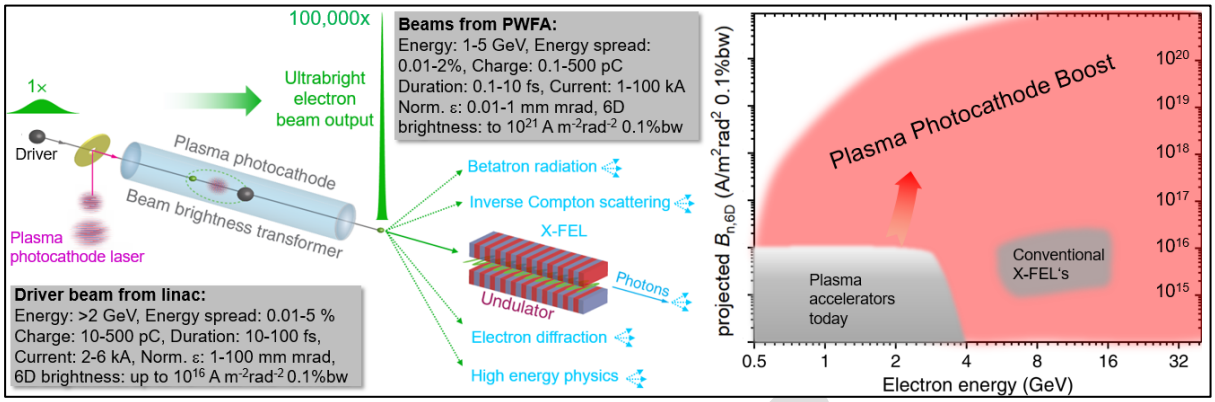

Figure 3.8: Layout for a plasma photocathode based PWFA (left) and the potential beam brightness boost (right)

Figure 3.1 above (left) summarizes the scheme and potential parameters for a plasma-based accelerator stage driven by a linac-based UK XFEL precision machine, and the boosted output electron beam. The plasma photocathode will increase the electron beam parameter range of the UK XFEL substantially, and will provide a strategic advantage compared with other existing or planned XFEL facilities. The overarching impact from plasma photocathodes for photon science arises from their capability to produce ultrashort, high-current electron beams with superior emittances – the emittance improvement being at the root of this impact. The figure above (right) highlights the witness beam 6D brightness boost that may be realized from plasma photocathode PWFA stages. The plasma photocathode laser required needs to reach tunnel ionisation intensities for He (~ 10^{16} Wcm^{-2}) which is compatible with commercially available kHz rep-rate laser systems generating ~ 1 mJ pulses.

Such ultrabright output electron beams potentially enable completely new photon science modalities to be explored. A core requirement for coherent emission of x-ray photons is reflected by the energy spread threshold $\Delta W_{rms}/W < \eta$, where $\Delta W_{rms}/W$ is the relative energy spread, which reduces as $1/\gamma$ during the acceleration process, and $\eta \propto 1/\gamma$ is the FEL Pierce parameter, and by the emittance threshold $\lambda_{min} \approx 4\pi\varepsilon_n/\gamma$ required to achieve saturation at x-ray wavelengths λ_{min}. First, the consequence of ultrahigh brightness electron beams is significant reduction in gain length L_{1D} in the undulator section because of the 1D gain length scaling $L_{1D} \propto B_{6D}^{-1/3}$. Second, such high gain leads to rapid growth of the photon field, and thus minimizes slippage between the emerging radiation and the electron beam. This enables a potential route towards operation of the FEL in a single-spike regime for fully coherent ultrashort photon pulses. Such photon pulses would enable novel scientific capabilities for femto-chemistry, material science, and imaging of electronic distributions, their motion and ultrafast charge transfer e.g. in biomolecules on their natural timescale. Beyond this, the dramatically reduced emittance opens a path towards hard x-ray wavelengths λ_{min} already at few GeV electron energies, or conversely there can be a push towards even harder photon energies [7]. Lower electron energies are particularly interesting in this connection, because the rate of mean energy loss to incoherent radiation scales as $\propto \gamma^2$, and an even more severe fundamental limitation towards harder photon energies arises from the quantum fluctuation of synchrotron radiation, which scales with γ^4. These scalings [8] entail dramatic growth of energy spread for high energy beams and impose insurmountable challenges for realization of gamma-FELs with conventional electron beams with high energies and moderate emittance values. In contrast, low energy, ultralow emittance and high brightness beams from plasma photocathodes allow exploration of exciting possibilities towards gamma-ray FELs as well as for quantum FELs [7] e.g. for precision studies of nuclear processes, and may allow realization of photon-photon colliders e.g. for Breit–Wheeler electron-positron pair production.

Further tailored 'designer' electron beams can broaden the impact of plasma photocathode-generated electron beams on photon science at the UK XFEL, e.g. via synchronized and versatile multi-colour and

pump-probe setups. Finally, as indicated in the conceptual figure above (also see appendix 3.2), ultralow emittance and ultrahigh brightness beams also allow for exploration of a range of wider opportunities, such as betatron and inverse Compton scattering sources and ion channel lasers for photon science. While experimental realization of PWFA plasma photocathode-based production of ultrahigh brightness beams is only beginning, the arising opportunities are potentially transformative. The integration of plasma wakefield accelerator of beamlines for research and applications into the UK XFEL will allow full harnessing of this potential, and will provide unique capabilities and a broad path to future-proof competitiveness and upgrade options.

3.6.3 Inverse Compton Scattering Gamma source

The injector and first ~1 GeV of the superconducting electron accelerator for the MHz repetition rate soft X-ray FEL beamlines of UK-XFEL can be readily adapted to include Energy Recovery (SC-ERL). The resulting capability to produce high average electron currents (10 – 100 mA) would enable a high-flux, narrowband gamma source based on inverse Compton scattering (ICS).

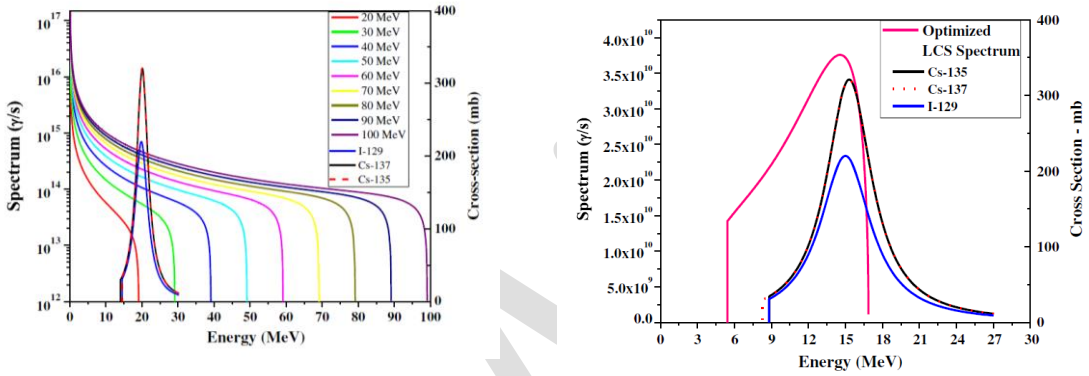

Figure 3.9: Bremsstrahlung (left) and collimated ICS (right) gamma spectra compared to photonuclear dipole resonances of Cs-135, Cs-135 and I-129 (right only). From Rehman et. al. "Comparison of laser Compton scattering and conventional bremsstrahlung X-rays for photonuclear transmutation" Int J Energy Res. 2018;42:236-244

The production of 1-100 MeV gammas via ICS of relativistic electrons on an external laser results in gamma properties fundamentally improved with respect to standard bremsstrahlung generation. Bremsstrahlung is broadband emission peaked at low energy with a cut-off at the electron energy. ICS has a correlation between the angle of emission and energy, therefore in combination with angular collimation, narrowband (or "monoenergetic") gamma beams can be produced [9,10]. In addition, ICS preserves the polarisation of the incident laser. Presently the worlds brightest narrowband gamma source is the High Intensity Gamma Source (HIGS) at Duke University [9]. In the construction phase is the EU funded Extreme Light Infrastructure – Nuclear Physics (ELI-NP) Gamma Beam System (GBS) in Magurele, Romania [10].

To quantify the potential of an ICS source driven by an SC-ERL enabled UK-XFEL front end, initial calculations of the source properties have been produced and are shown in Table 3.1 and Figure 3.10 (Peter Williams & Bruno Muratori (ASTeC, STFC Daresbury Lab), Joe Crone & Hywel Owen (U. Manchester)).

Table 3.1: Conservative input parameters used for ICS source calculation for electron beam and laser system. We cover the nominal gamma energy from 1 to 100 Mev using electron beam extracted at three locations. For the laser-electron interaction point we assume a Fabry-Perot bow-tie like resonator cavity as demonstrated at KEK by Agaki et. al.

Beam Parameters	Value		
Beam Energy (MeV)	340	680	1020
RF Frequency (MHz)	802		
Repetition Rate (MHz)	100		
Bunch Charge (pC)	100		
Average Beam Current (mA)	10		
Normalised Transverse Emittance (mm-mrad)	0.5		
Recoil Parameter	0.006	0.012	0.018
Nd:YAG Laser System Parameters	**Value**		
Wavelength (nm)	1064		
Repetition Rate (MHz)	100		
Pulse Energy (μJ)	100		
Average Stored Cavity Power (kW)	10		
Spot Size at IP (circular spot) (μm)	25		
Stored Pulse Width (ps)	5.7		
Field Strength of the Normalised Laser Vector Potential a_0	6.05×10^{-4}		

Parameter	340 MeV			680 MeV			1020 MeV		
γ-ray Peak energy (MeV)	2.05			8.17			18.27		
Flux per Shot (ph)	4076			4750			5027		
Bandwidth	raw	0.5%	0.1%	raw	0.5%	0.1%	raw	0.5%	0.1%
Flux	4.08×10^{11}	6.24×10^{9}	4.05×10^{9}	4.75×10^{11}	6.24×10^{9}	4.08×10^{8}	5.03×10^{11}	6.24×10^{9}	4.11×10^{8}
Average Brilliance (ph/s mm^2-mrad^2)	-	2.79×10^{14}	1.81×10^{13}	-	1.12×10^{15}	7.32×10^{13}	-	2.52×10^{15}	1.66×10^{14}
Peak Brilliance (ph/s mm^2-mrad^2)	-	3.77×10^{16}	2.45×10^{15}	-	1.51×10^{17}	9.88×10^{15}	-	3.40×10^{17}	2.24×10^{16}
Spectral Density (ph/s eV)	-	2.41×10^{5}	7.81×10^{4}	-	6.01×10^{4}	1.96×10^{4}	-	2.67×10^{4}	8.79×10^{3}

Figure 3.10: Resulting ICS source brilliances and spectral energy densities for the three example extracted electron beam energies as detailed in Table 3.1

This corresponds to at least two orders of magnitude greater spectral energy density than HIGS, and likely similarly exceed the performance of ELI-NP-GBS. It should be noted that this calculation uses conservative, previously demonstrated parameters as input, and therefore should be viewed as a lower bound. Narrowing the energy bandwidth below 0.5% whilst retaining significant flux, as shown in Table 3.1, will enable the resolution of individual nuclear excitations according to the nuclear shell model. This is because the source bandwidth would be less than predicted typical spacings between adjacent energy levels. Simulated improvement in the knowledge of an example photonuclear cross section is shown in Fig. 3.6.3. This would lead to the establishment / consolidation of new field of science, Nuclear Photonics, named by analogy to the field of atomic photonics opened up by lasers from the 1960s onwards. This is because the ICS source would be a step change in high-flux, tune-able, narrowband gamma production.

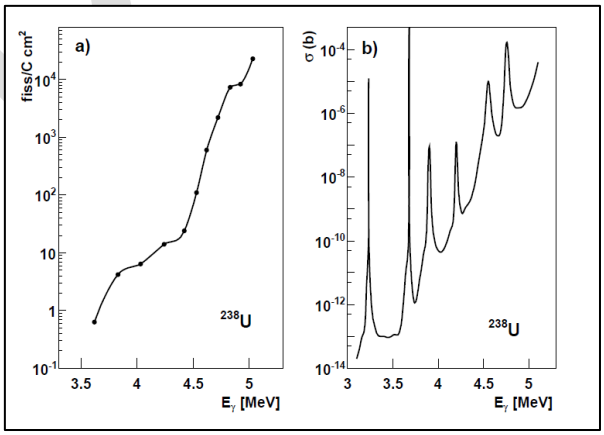

Figure 3.11: Left - Observed, bremsstrahlung induced photofission Giant Dipole Resonance (GDR) of Uranium-238. Right - predicted "hidden" resonances within GDR revealed by an ICS narrowband gamma source. From "Perspectives for photofission studies with highly brilliant, monochromatic gamma beams". P. G. Thirolf et. al. EPJ Web of Conferences 38, 08001 (2012)

In particular, the use of fully linearly-polarised gamma beams in photon induced reaction results in distinct angular distributions for the two transition multipolarities (electric E or magnetic M) and the associated excitation modes can then easily be disentangled. Hence, ICS gamma beams are a sensitive probe of the nuclear electric (E1) [11] and magnetic (M1) [12] dipole response. Since the photon is not charged, for an interaction it physically needs to hit the object nucleus, resulting in a low scattering cross section. At existing facilities in order to compensate for this, large amounts of target material (order of grams) is required, which limits the application to stable or quasi-stable nuclei with a half-life in the order of 107 years. The 100-fold increase in flux enabled by an SC-ERL driven source will alleviate this restriction.

The E1 response is dominated by the well-known Giant Dipole Resonance (GDR) [13,14]; however, in the last two decades on the low-energy tail of the GDR, an additional E1 contribution has been established. This so-called Pygmy Dipole Resonance (PDR) [15,16] is located near the particle thresholds and it has been shown to have an enormous influence on neutron capture rates as encountered in the astrophysical rapid and slow neutron capture processes [17], which synthesise all chemical elements heavier than iron. The PDR is often visualised as an oscillation of a neutron skin versus a core with nearly equal proton and neutron numbers, though this interpretation is controversial. Nevertheless, this geometric interpretation suggests a connection to the asymmetry term of the nuclear equation of state, required to describe properties of the heaviest known objects: neutron stars. Recently, the PDR has even been linked to the reactor antineutrino anomaly [18], which causes a previously unexplained heat generation in operational nuclear reactors.

For the M1 response, the Gamow-Teller (spin-isospin) resonances are of particular importance, dominating inelastic neutrino-nucleus interactions. These provide an additional heating to supernova type-II events, which otherwise would not explode [19]. Furthermore, they are mandatory in order to reliable estimate the cross sections for neutrino detectors (e.g., see ref. [20]).

Given the gamma fluxes at presently available (HIGS) or facilities in construction (ELI-NP-GBS), various interesting physics cases are not feasible, but would become so with an SC-ERL driven ICS source. One example is the investigation of the E1 response of the octupole-correlated nucleus Ra-226 (T_(1/2)≈1600 years), which very likely has a strong quadrupole-octupole coupling enhanced CP-violating Schiff moment in the ground state [21]. Recently, admixtures of the low-lying E1 strength have been proposed as a second enhancement mechanism [22]. Another example is the measurement of parity violating physics exploiting J^π=1^± parity doublets (close lying 1- and 1+ levels) as, for example, found in Ne-20 [23].

In the context of particle physics, the ICS gamma source would enable unprecedented measurements of Delbrück scattering (QED vacuum) and light-by-light scattering. A SC-ERL driven ICS source would not only be of great interest in academic physics and astrophysics, but have direct societal and economic benefits in the nuclear security, civil nuclear power and medical radio-nuclide sectors. For further details see Section 8.4.5

3.6.4 High Luminosity Internal Gas Target Interaction Point

A ~1 GeV, high current (10 – 100 mA), high brightness (< 1 mm mrad), low energy spread (<10-5) electron beam such as that capable of being produced by the UK-XFEL SC front end with energy recovery is recognised as high potential for fundamental physics requiring highly intense electron beams.

High luminosity (> 10^{36} cm-2s-1) e-A scattering can be used as precision tests of Standard Model and Beyond the Standard Model physics. For example, measurements of the weak mixing angle and direct searches for dark matter particles. The DarkLight experiment at Jefferson Lab [24] and MAGIX at MESA, U. Mainz [25] are examples of present and future experiments of this type. The paradigm is to bring the electron beam into collision with a supersonic gas jet surrounded by a 4-pi tracking detector, then energy recover the electron beam after disruption to enable large currents (and the correspondingly high luminosities). This setup has potential to greatly exceed limits established by beam dump and

storage ring alternatives, such as those at CEBAF. Of utmost importance in these types of experiments is the precision with which one knows the electron energy and therefore the ERL transport should be optimised to minimise the energy spread. It should be possible to maintain the gun projected energy spread to the IP (300 – 1000 MeV) leading to energy spreads potentially at the 10^{-5} level.

References

[1] A. Valentini et al., "Optomechanical Control of Quantum Yield in Trans–Cis Ultrafast Photoisomerization of a Retinal Chromophore Model", Ange. Chem. Int. Ed., 56, 3842 (2017), DOI: 10.1002/anie.201611265

[2] L.A. Baker et al., "A Perspective on the Ultrafast Photochemistry of Solution-Phase Sunscreen Molecules", Phys. Chem. Lett., 7, 22, 4655 (2016), DOI: 10.1021/acs.jpclett.6b02104

[3] E. Romero et al., "Quantum coherence in photosynthesis for e-cient solar-energy conversion", Nat. Phys., 10, 676 (2014), DOI: 10.1038/NPHYS3017

[4] V.I. Prokhorenko et al., "New Insights into the Photophysics of DNA Nucleobases", J. Phys. Chem. Lett. 7, 22, 4445 (2016), DOI: 10.1021/acs.jpclett.6b02085

[5] P. Vasa and D. Mathur "Ultrafast Quantum Mechanical Processes in Animals", in "Ultrafast Biophotonics" Springer, Cham, pp 145-157 (2016), DOI: 10.1007/978-3-319-39614-9_8

[6] A.A. Lutman et al., "Polarization control in an X-ray free-electron laser", Nat. Phot., 10, 468 (2016), DOI: 10.1038/nphoton.2016.79

[7] L. Young et al., "Roadmap of ultrafast x-ray atomic and molecular physics", J. Phys. B, 51, 032003 (2018), DOI: 10.1088/1361-6455/aa9735

[8] P.M. Kraus et al., "The ultrafast X-ray spectroscopic revolution in chemical dynamics", Nat. Rev. Chem., 2, 82 (2018), DOI: 10.1038/s41570-018-0008-8

[9] A. Kumar and M. D. Sevilla, "Proton-Coupled Electron Transfer in DNA on Formation of Radiation-Produced Ion Radicals", Chem. Rev., 110, 7002 (2010): DOI: 10.1021/cr100023g

[10] M. Duarante et al., "Faster and safer? FLASH ultra-high dose rate in radiotherapy" Brit. J. Rad., 91: 20170628 (2018), DOI: 10.1259/bjr.20170628

[11] L. Nahon et al., "Valence shell one-photon photoelectron circular dichroism in chiral systems", J. El. Spect. Rel. Phen., 204, 322 (2015), DOI: 10.1016/j.elspec.2015.04.008

[12] C. Lux et al., "Circular Dichroism in the Photoelectron Angular Distributions of Camphor and Fenchone from Multiphoton Ionization with Femtosecond Laser Pulses", Ange. Chem. Int. Ed., 51, 1 (2012), DOI: 10.1002/anie.201109035

[13] A. Comby et al., "Real-time determination of enantiomeric and isomeric content using photoelectron elliptical dichroism", Nat. Comm., 9, 5212 (2018), DOI: 0.1038/s41467-018-07609-9

[14] M. Tia et al., "Observation of Enhanced Chiral Asymmetries in the Inner-Shell Photoionization of Uniaxially Oriented Methyloxirane Enantiomers", J. Phys. Chem. Lett., 8, 2780 (2017), DOI: 10.1021/acs.jpclett.7b01000

[15] S. Beaulieu et al., "Universality of photoelectron circular dichroism in the photoionization of chiral molecules", N. J. Phys., 18, 121001 (2016), DOI: 10.1088/1367-2630/18/10/102002

[16] A.M. Beckley et al., "Full Poincaré beams II: partial polarization", Opt. Exp., 20, 9357 (2012), DOI: 10.1364/OE.20.009357

[17] S. Rozen et al., "Controlling Subcycle Optical Chirality in the Photoionization of Chiral Molecules", Phys. Rev. X, 9, 031004 (2019), DOI: 10.1103/PhysRevX.9.031004

[18] J. Morgan et al., "Orbital Angular Momentum From SASE", 39th Free Electron Laser Conf., TUP071, 219 (2019), DOI: 10.18429/JACoW-FEL2019-TUP072

[19] D. Ayuso et al., "Synthetic chiral light for efficient control of chiral light–matter interaction", Nat. Phot., 13, 866 (2019), DOI: 10.1038/s41566-019-0531-2

[20] J. Rouxel et al., "Photoinduced molecular chirality probed by ultrafast resonant X-ray spectroscopy", Struct. Dyn., 4, 044006 (2017), DOI: 10.1063/1.4974260

[21] N. Berrah, "Molecular dynamics induced by short and intense x-ray pulses from the LCLS", Phys. Scr., T169, 014001 (2016), DOI: 10.1088/0031-8949/2016/T169/014001

[22] A. Rudenko et al., "Femtosecond response of polyatomic molecules to ultra-intense hard X-rays", Nature, 546, 103 (2017), DOI: 10.1038/nature22373

[23] L. Young et al., "Femtosecond electronic response of atoms to ultra-intense X-rays", Nature, 466, 56 (2010), DOI: 0.1038/nature09177

[24] Berrah et al, "Femtosecond resolved observation of fragmentation of buckminsterfullerene following X-ray multiphoton ionisation", Nat.Phys., 15, 1279 (2019), DOI:10.1038/s41567-019-0665-7

[25] C.S. Slater et al., "Coulomb-explosion imaging using a pixel-imaging mass-spectrometry camera", Phys. Rev. A, 91, 053424 (2015), DOI: 10.1103/PhysRevA.91.053424

[26] M. Pitzer et al., "How to determine the handedness of single molecules using Coulomb explosion imaging", J. Phys. B, 50, 153001 (2017), DOI: 10.1088/1361-6455/aa77a9

[27] E. Kukk et al., "Coulomb implosion of tetrabromothiophene observed under multiphoton ionization by free-electron-laser soft-x-ray pulses", Phys. Rev. A, 99, 023411 (2019), DOI: 10.1103/PhysRevA.99.023411

[28] M. Fisher-Levine et al., "Time-resolved ion imaging at free-electron lasers using TimepixCam", J. Synchrotron Rad., 25, 336 (2018), DOI: 10.1107/S1600577517018306

[29] D. You et al., "Multi-particle momentum correlations extracted using covariance methods on multiple-ionization of diiodomethane molecules by soft-X-ray free-electron laser pulses", PCCP, 22, 2648 (2020), DOI: 10.1039/c9cp03638e

[30] T. Driver et al., "Partial covariance two-dimensional mass spectrometry for determination of biomolecular primary structure", arXiv:1904.05946

[31] Nobel Prize in Physiology or Medicine 1962 https://www.nobelprize.org/prizes/medicine/1962/summary/

[32] Nobel Prize in Chemistry 1962 https://www.nobelprize.org/prizes/chemistry/1962/summary/

[33] Nobel Prize in Physics 1915 https://www.nobelprize.org/prizes/physics/1915/summary/

[34] The Protein Data Bank (Wikipedia, 29 August 2019, https://tinyurl.com/y6f8lo4n) and the Cambridge Structural Database (Wikipedia, 29 August 2019,

https://tinyurl.com/y62accha), with the number of structures in the latter surpassing 1 million in 2018

[35] R. Neutze et al. Nature 406 752 (2000) *Potential for biomolecular imaging with femtosecond X-ray pulses*

[36] Z. Kam Macromolecules 10(5) 927-934 (1977) *Determination of macromolecular structure in solution by spatial correlation of scattering fluctuations*

[37] Z. Kam, M. H. Koch, J. Bordas, Proc. Nat. Acad. Sci. 78 3559 (1981) *Fluctuation x-ray scattering from biological particles in frozen solutions by using synchrotron radiation*

[38] P. Wochner et al. Proc. Nat. Acad. Sci. 106 11511 (2009) *X-ray cross correlation analysis uncovers hidden local symmetries in disordered matter*

[39] B. Ardenne, M. Mechelke, and H. Grubmüller, Nat. Comm., 9 2375 (2018) *Structure determination from single molecule X-ray scattering with three photons per image*

[40] T. B. Pittman et al. Phys. Rev. A 52 3429 (1995) *Optical imaging by means of two-photon quantum entanglement*

[41] R. S. Bennink, S. J. Bentley, R. W. Boyd, Phys. Rev. Lett. 89 113601 (2002) *Two-photon coincidence imaging with a classical source*

[42] A. Gatti et al. Phys. Rev. Lett. 93 93602 (2004) *Ghost imaging with thermal light: comparing entanglement and classical correlation*

[43] Y. Y Kim et al. Phys. Rev. A 101 013820 (2020) *Ghost Imaging at an XUV Free-Electron Laser*

[44] . T. J. Lane and D. Ratner arXiv:1907.12178v2 (24 Aug 2019) *What are the advantages of ghost imaging? Multiplexing for x-ray and electron imaging*

[45] R. S. Aspden et al. Optica 2 1049 (2015) *Photon-sparse microscopy: visible light imaging using infrared illumination*

[46] A. M. Kingston et al., Optica, 5 1516 (2018) *Ghost tomography*

[47] D. Ratner et al. Phys. Rev. X 9 011045 (2019) *Pump-probe Ghost Imaging with SASE FELs*

[48] S. Asban, K. E. Dorfman, S. Mukamel, Proc. Nat. Acad. Sci. 116 11673 (2019) *Quantum phase-sensitive diffraction and imaging using entangled photons*

[49] A. Classen et al. Phys. Rev. Lett. 117 253601 (2016) *Superresolving imaging of arbitrary one-dimensional arrays of thermal light sources using multiphoton interference*

[50] A. Classen et al. Phys. Rev. Lett. 119 053401 (2017) *Incoherent diffractive imaging via intensity correlations of hard x rays*

[51] R. Schneider et al. Nat. Phys. 14 126 (2018) *Quantum imaging with incoherently scattered light from a free-electron laser*

[52] C. Thiel et al. Phys. Rev. Lett. 99 133603 (2007) *Quantum imaging with incoherent photons*

[53] B. Stankus et al. Nat. Chem. 11 716 (2019) *Ultrafast X-ray scattering reveals vibrational coherence following Rydberg excitation*

[54] M. Minitti et al. Phys. Rev. Lett. 114 255501 (2015) *Imaging molecular motion: femtosecond X-ray scattering of an electrocyclic chemical reaction*

[55] J. M. Glownia et al. Phys. Rev. Lett. (2016) *Self-referenced coherent diffraction X-ray movie of Ångström- and femtosecond-scale atomic motion*

[56] A. Kirrander and P. Weber Applied Science 7 534 (2017) *Fundamental Limits on Spatial Resolution in Ultrafast X-ray Diffraction*

[57] M. R. Ware et al. Phil. Trans. R. Soc. A 377 20170477 (2019) *On the limits of observing motion in time-resolved X-ray scattering*

[58] M. R. Ware et al. Phys. Rev. A 100 033413 (2019) *Characterizing dissociative motion in time-resolved x-ray scattering from gas-phase diatomic molecules*

[59] M. Simmermacher et al. Phys. Rev. Lett. 122 073003 (2019) *Electronic coherence in ultrafast X-ray scattering from molecular wave packets*

[60] G. Dixit, O. Vendrell, R. Santra, Proc. Nat. Acad. Sci. 109 11636 (2012) *Imaging electronic quantum motion with light*

[61] M. Kowaleski, K. Bennet, S. Mukamel, Struct. Dyn. 4 054101 (2017) *Monitoring nonadiabatic avoided crossing dynamics in molecules by ultrafast X-ray diffraction*

[62] K. Bennet, M. Kowalewski, J. R. Rouxel, S. Mukamel, Proc. Nat. Acad. Sci. 115 6538 (2018) *Monitoring molecular nonadiabatic dynamics with femtosecond X-ray diffraction*

[63] M. Simmermacher et al. J. Chem. Phys. 151 174302 (2019) *Theory of ultrafast x-ray scattering by molecules in the gas phase*

[64] G. D. Scholes et al. Nature 543 7647 647 (2017) *Using coherence to enhance function in chemical and biophysical systems*

[65] P. M. Kraus et al. Science 350 790 (2015) *Measurement and laser control of attosecond charge migration in ionized iodoacetylene*

[66] Emma et al, "First lasing and operation of an angstrom free electron laser", Nature Photonics, 4, 64 (2010) DOI: 10.1038/NPHOTON.2010.176

[67] Y. Ding et al, "Measurements and Simulations of Ultralow Emittance and Ultrashort Electron Beams in the Linac Coherent Light Source", Phys.Rev.Lett, 102 254801 (2009) DOI: 10.1103/PhysRevLett.102.254801

[68] Y. Ding et al, "Femtosecond X-Ray Pulse Characterization in Free-Electron Lasers Using a Cross-Correlation Technique" Phys.Rev.Lett, 109 254802 (2012), DOI: 10.1103/PhysRevLett.109.254802

[69] A. Lutman et al, "Fresh-slice multicolour X-ray free electron lasers", Nature Photonics, 10, 745 (2016) DOI: 10.1038/NPHOTON.2016.201

[70] N. Berrah et al, "Femtosecond observation of the fragmentation of C_{60} following X-ray multiphoton ionization", Nature Physics, 15, 1279 (2019) DOI: 10.1038/s41567-019-0665-7

[71] G. Doumy et al, "Nonlinear atomic response to intense ultrashort X-rays", Phys.Rev.Lett, 106, 083002 (2011) DOI: 10.1103/PhysRevLett.106.083002

[72] C. Weninger et al, "Stimulated electronic Raman scattering", Phys.Rev.Lett. 111, 233902 (2013), DOI: 10.1103/PhysRevLett.111.233902

[73] T. Kroll et al, "Stimulated X-ray emission spectroscopy in transition metal complexes", Phys.Rev.Lett, 120, 133203 (218) DOI: 10.1103/PhysRevLett.120.133203

[74] N. Rohringer et al, "Atomic inner shell X-ray laser at 1.46 nm pumped by an X-ray FEL", Nature, 488, 7413 (2012) DOI: 10.1038/nature10721

[75] E. Allaria et al, "Highly coherent and stable pulses from the FERMI seeded free-electron laser in the extreme ultraviolet", Nature Photonics, 6, 699 (2012) DOI: 10.1038/NPHOTON.2012.233

[76] P.R. Ribic et al, "Coherent soft X-ray pulses from echo-enabled harmonic generation free electron laser", Nature Photonics, 13, 555 (2019) DOI: 10.1038/s41566-019-0427-1

[77] F. Bencivenga et al, "Four-wave mixing experiments with extreme ultraviolet transient gratings", Nature, 520, 205 (2015) DOI: 10.1038/nature14341
[78] A.A. Zholents, W.M. Fawley, "Proposal for intense Attosecond Radiation from an X-ray Free Electron Laser", Phys.Rev.Lett, 92 224801 (2004), DOI: 10.1103/PhysRevLett.92.224801
[79] J. Duris et al, "Tunable isolated attosecond X-ray pulses with gigawatt peak power from a free-electron laser", Nature Photonics, 14, 30 (2020) DOI: 10.1038/s41566-019-0549-5
[80] F. Remacle and R. D. Levine, "An electronic time scale in chemistry", PNAS 103 6793 (2006), DOI: 10.1073/pnas.0601855103; J. Breidbach and L. S. Cederbaum, "Migration of holes…", J. Chem. Phys. 118 3983 (2003), DOI: 10.1063/1.1540618
[81] M. Vacher et al, "Electron dynamics upon ionization of polyatomic molecules…", Phys.Rev.Lett.118, 083001 (2017), DOI: 10.1103/PhysRevLett.118.083001
[82] M. Vacher et al, "Coupled electron-nuclear dynamics: Charge migration and charge transfer initiated near a conical intersection", J Chem Phys, 139 044110 (2013), DOI: 10.1063/1.4815914; M. Vacher et al., "Electron dynamics following photoionization…", PRA 92, 040502(R) (2015), DOI: 10.1103/PhysRevA.92.040502
[83] L.S. Cederbaum and J. Zobeley, "Ultrafast charge migration by electron correlation", Chem. Phys. Lett. 307 205 (1999), DOI: 10.1016/S0009-2614(99)00508-4; R. Weinkauf et al., "Nonstationary Electronic States and Site-selective Reactivity", J. Phys. Chem. 101 7702 (1997), DOI: 10.1021/jp9715742
[84] M. Drescher et al., "X-ray Pulses Approaching the Attosecond Frontier", Science 291 1923 (2001), DOI: 10.1126/science.1058561
[85] F. Frank et al., "Technology for Attosecond Science", Rev. Sci. Inst. 83 071101 (2012), DOI: 10.1063/1.4731658
[86] F. Ferrari et al., "High-energy isolated attosecond pulses and applications to molecular physics", Nature Photonics 4 875 (2011), DOI: 10.1364/HILAS.2011.HThB2; T. Popmintchev et al., "The attosecond nonlinear optics of bright coherent X-ray generation", Nature Photonics 4 822 (2010), DOI: 10.1038/nphoton.2010.256
[87] E. Goulielmakis et al., "Real-time observation of valence electron motion", Nature 466 739 (2010), DOI: 10.1038/nature09212
[88] F. Calegari et al, "Ultrafast electron dynamics in phenylalanine intiated by attosecond pulses", Science, 2014, Vol. 346, 336, DOI: 10.1126/science.1254061
[89] A.L. Cavalieri et al., "Attosecond spectroscopy in condensed matter", Nature 4491029 (2007), DOI: 10.1038/nature06229
[90] M. Lezius et al., "Polyatomic molecules in strong laser fields: Nonadiabatic multielectron dynamics", J. Chem. Phys. 117 1575 (2002), DOI: 10.1063/1.1487823
[91] B. Cooper et al, "Analysis of a measurement scheme for ultrafast hole dynamics…", Faraday Discussion 171, 93 (2014), DOI: 10.1039/C4FD00051J
[92] N. Hartmann, et al., "Attosecond time-energy structure of X-ray free electron laser pulses", Nature Photon. 12 (2018), DOI: 10.1038/s41566-018-0107-6
[93] S. Tanaka and S. Mukamel, "Coherent X-Ray Raman Spectroscopy: A Nonlinear Local Probe for Electronic Excitations", PRL 89, 043001 (2002), DOI: 10.1103/PhysRevLett.89.043001; S. Tanaka and S. Mukamel, "Probing exciton dynamics using Raman resonances in femtosecond x-ray four-wave mixing", PRA 67, 033818 (2003), DOI: 10.1103/PhysRevA.67.033818
[94] I.V. Schweigert and S. Mukamel, "Coherent Ultrafast Core-Hole Correlation Spectroscopy: X-Ray Analogues of Multidimensional NMR", PRL 99, 163001 (2007), DOI: 10.1103/PhysRevLett.99.163001; J.D. Biggs et al, "Two-dimensional stimulated resonance Raman spectroscopy of molecules with broadband x-ray pulses", J Chem Phys 136, 174117 (2012), DOI: 10.1063/1.4706899
[95] H. Kulla et al. Cryst. Growth Des. 17 1190 (2017) *Knowing When to Stop – Trapping Metastable Polymorphs in Mechanochemical Reactions*
[96] A. Alexander and P. Camp. J. Chem. Phys. 150 040901 (2019) *Non-photochemical laser-induced nucleation*
[97] G. J. Snyder and E. S. Toberer, Nat. Mater. 7 105 (2008) *Complex thermoelectric materials*
[98] . C. Xiao et al. J. Am. Chem. Soc. 134 4287 (2012) *Superionic Phase Transition in Silver Chalcogenide Nanocrystals Realizing Optimized Thermoelectric Performance*
[99] S. Raoux, Mater. Res. 39 25 (2009) *Phase Change Materials*
[100] R. Pecore, Ed., *Dynamic Light Scattering* (Plenum Press, New York, 1985)
[101] A.Ourmazd in "X-ray free electron lasers: Applications in materials, chemistry, and biology", Energy and Environment Series. ed U.Bergmann et al, 418 (RSC (2017))
[102] A.Hosseinizadeh et al, "Single-particle structural determination by X-ray FELS…", Struc.Dynamics. 2, 041601 (2015) DOI:/10.1063/1.4919740
[103] A.Ourmazd "Cryo-EM, XFELs and the structure conundrum in structural biology", Comment, Nature Methods, 16, 941 (2019) DOI:/10.1038/s41592-019-0587-4
[104] R.Fung et al, "Dynamics from random data with extreme timing uncertainty", Nature 532, 471 (2016) DOI: 10.1038/nature17627
[105] J.Glownia et al,"Time resolved pump-probe experiments at LCLS", Opt.Express 18, 17620 (2010) DOI:10.1364/OE.18.017620
[106] A.Hosseinizadeh et al,"Conformational landscape of a virus by single particle X-ray scattering", Nat.Met. 14, 877 (2017) DOI:10.1038/NMETH.4395
[107] A.Dashti et al, "Trajectories of the ribosome as a Brownian nanomachine", PNAS, 111, 17492 (2014) DOI: 10.1073/pnas.1419276111
[108] A.Munke et al, "Coherent diffraction imaging of single Dwarf Rice particles using hard X-rays at the LCLS", Sci.Data 3, 160064 (2016) DOI:10.1038/sdata.2016.4
[109] M. Marklund and P. Shukla, "Nonlinear collective effects in photon-photon and photon-plasma interactions", Rev. Mod. Phys. 78, 591 (2006)
[110] T. Tajima, "Laser acceleration in novel media", Eur. J. Phys. Spec. Top. 223, 1037--1044 (2014)
[111] J. Schwinger, "On Gauge Invariance and Vacuum Polarization", Phys. Rev. 82, 666--679 (1951)
[112] T. Inada et al, "Search for Photon-Photon Elastic Scattering in the X-ray Region", Phys. Lett. B 732, 356--359 (2014)
[113] T. Heinzl, B. Liesfeld, K. Amthor, H.Schwoerer, R. Sauerbrey and A. Wipf, "On the observation of vacuum birefringence", Opt. Commun. 267, 318--321 (2006)
[114] H.-P. Schlenvoigt, T. Heinzl, U. Schramm, T. E. Cowan, and R. Sauerbrey, "Detecting vacuum birefringence with

x-ray free electron lasers and high-power optical lasers: a feasibility study", Phys. Scr. 91, 023010 (2016)
[115] R. C. Duncan and C. Thompson, "Formation of very strongly magnetized neutron stars - Implications for gamma-ray bursts", Astrophys. J. 392, L9 (1992)
[116] R. P. Mignani et al, "Evidence for vacuum birefringence from the first optical-polarimetry measurement of the isolated neutron star" RX J1856.5-3754, Mon. Not. R. Astron. Soc. 465, 492--500 (2017)
[117] L. M. Capparelli et al, "A note on polarized light from magnetars", Eur. Phys. J. C 77, 754 (2017)
[118] M. Born and L. Infeld, "Foundations of the new field theory", Proc. R. Soc. Lond. A 144, 425--451 (1934)
[119] B. Svedung Wettervik, A. Gonoskov, and M. Marklund, "Prospects and limitations of wakefield acceleration in solids", Phys. Plasmas 25, 013107 (2018)
[120] E. Esarey, C. B. Schroeder, and W. P. Leemans, Physics of laser-driven plasma-based electron accelerators, Rev. Mod. Phys. 81, 1229 (2009)
[121] A. M. Fedotov, N. B. Narozhny, G. Mourou, and G. Korn, "Limitations on the Attainable Intensity of High Power Lasers", Phys. Rev. Lett. 105, 080402 (2010)
[122] S. S. Bulanov, T. Zh. Esirkepov, A. G. R. Thomas, J. K. Koga, and S. V. Bulanov, "Schwinger Limit Attainability with Extreme Power Lasers", Phys. Rev. Lett. 105, 220407 (2010)
[123] A. Ringwald, "Pair production from vacuum at the focus of an X-ray free electron laser", Phys. Lett. B 510, 107--116 (2001)
[124] Mourou, G. A., Tajima, T. & Bulanov, S. V. *Optics in the relativistic regime*. Rev. Mod. Phys. 78, 309 (2006).
[125] Hawking, S. W. *Black hole explosions?* Nature 248, 30 (1974).
[126] Unruh, W. G. *Notes on black-hole evaporation*. Phys. Rev. D 14, 870 (1976).
[127] Weinfurtner, S., Tedford, E. W., Penrice, M. C., Unruh, W. G. & Lawrence, G. *Measurement of Stimulated Hawking Emission in an Analogue System*. Phys Rev Lett 106, 021302 (2011).
[128] Nova, J. R. M. de, Golubkov, K., Kolobov, V. I. & Steinhauer, J. *Observation of thermal Hawking radiation and its temperature in an analogue black hole*. Nature 569, 688 (2019).
[129] Chen, P. & Tajima, T. *Testing Unruh Radiation with Ultraintense Lasers*. Phys Rev Lett 83, 256 (1999).
[130] Chen, P. & Mourou, G. *Accelerating Plasma Mirrors to Investigate the Black Hole Information Loss Paradox*. Phys Rev Lett 118, 045001 (2017).
[131] Wadud, M. A., King, B., Bingham, R. & Gregori, G. *Axion particle production in a laser-induced dynamical spacetime*. Phys Lett B 777, 388 (2018).
[132] Brodin, G., Marklund, M., Bingham, R., Collier, J. & Evans, R. *Laboratory soft X-ray emission due to the Hawking–Unruh effect?* Class. Quantum Grav. 25, 145005 (2008).
[133] Peña, I. & Sudarsky, D. *On the possibility of measuring the Unruh Effect*. Found Phys 44, 689 (2014).
[134] Weinberg, S. *A New Light Boson?* Phys Rev Lett 40, 223 (1978).
[135] Wilczek, F. *Problem of Strong P and T Invariance in the Presence of Instantons*. Phys Rev Lett 40, 279 (1978).
[136] Battesti, R. et al. *Photon Regeneration Experiment for Axion Search Using X-Rays*. Phys Rev Lett 105, 250405 (2010).
[137] Inada, T. et al. *Results of a search for paraphotons with intense X-ray beams at SPring-8*. Phys Lett B 722, 301–304 (2013).
[138] Du, N. et al. *Search for Invisible Axion Dark Matter with the Axion Dark Matter Experiment*. Phys Rev Lett 120, (2018).
[139] Anastassopoulos, V. et al. *New CAST limit on the axion-photon interaction*, Nature Physics 13, 584 (2017).
[140] Beyer, K. A., Marocco, G., Bingham, R. & Gregori, G. *Axion detection through resonant photon-photon collisions*, arXiv:2001.03392 (2020)
[141] Sikivie, P. *Experimental Tests of the Invisible Axion*. Phys Rev Lett 51, 1415 (1983).
[142] Rosenberg, L. J. *Dark-matter QCD-axion searches*. Proc Nat Acad Sci 112, 12278 (2015).
[143] Bulbul, E. et al., *Detection of an unidentified emission line in the stacked X-ray spectrum of galaxy clusters*. Astrophys. J. 789, 13 (2014).
[144] Boyarsky, A. et al., *Unidentified line in X-ray spectra of the andromeda galaxy and perseus galaxy cluster*. Phys. Rev. Lett. 113, 251301 (2014).

4. Science opportunities for Matter in Extreme Conditions

Matter at extreme pressures and temperatures is a rich source of novel phenomena in condensed matter physics and materials science, and dominates the interiors of planets and exoplanets. Femtosecond X-ray pulses can probe extreme phases of matter in unprecedented detail, providing new knowledge and understanding as to its behaviour, and how it might be controlled and tailored in the future.

4.1 Shocked materials and matter at extremes

Matter at extreme density, where ion cores overlap significantly and the electronic structure is unique to the high-density regime, where periodicity is often lost and the zero-point energies become significant, holds the promise of breakthroughs in our understanding of both solid and liquid phases

4.1.1 Introduction to Matter at Extremes

The study of materials at high energy densities, or equivalently very high pressures, is a rich source of novel phenomena in condensed matter physics and materials science, is a route to new phases and materials, and provides stringent tests of fundamental condensed matter theory, computation and simulation[1]. It is essential for understanding the interior of the Earth and exoplanets, for developing models of material response in aerospace engineering and defence applications, and is increasingly making an impact in chemistry and materials science[2].

Matter can be compressed and heated dynamically to extreme pressures and temperatures on nanosecond (or even sub-nanosecond) timescales via illumination by high energy optical lasers, a method that has been at the forefront of recent international efforts to achieve Inertial Confinement Fusion (ICF). Laser compression offers the only means by which matter can be created at multi-megabar pressures and temperatures of 104 K in a laboratory environment[3], the conditions that otherwise occur only deep within gas or ice-giant planets such as Jupiter or Neptune, and within the plethora of exoplanets discovered by the likes of the Kepler space mission.

Understanding the internal structure of such planets relies on our knowledge of the densities and compressibilities of the solid and liquid phases that make up their interior, and on the crystalline structure adopted by the solid phases. For decades, these structures were assumed to be “simple”, with the atoms packed closely together. The high density phases were also assumed to become free electron-like metals at high enough pressures as a result of the kinetic energy of the electrons (which scales as V–2/3) increasingly dominating over their potential energy (which scales as V–1/3 for Coulomb interactions). However, there was little experimental evidence to support these very broad assumptions.

4.1.2 The Importance of X-ray Studies

The arrival of 3rd generation synchrotron sources in the 1990s, and advances in electronic structure calculations, completely overturned these assumptions. The new picture that emerged was one of complexity, where the structure of high-density matter was found to be as complex, if not more so, than that observed at ambient conditions. It was also found that materials might transform into semiconductors or insulators at high densities rather than metals, and new forms of bonding, involving core electrons were seen to enrichen the structural landscape.

Key to these breakthroughs was the advent of advanced X-ray diffraction and spectroscopic techniques. However, even the most advanced synchrotrons remain insufficiently bright to probe the very short-lived extreme states created as a result of laser irradiation and/or compression. The ultra-high brightness X-ray pulses from XFELs, on the other hand, can be focussed to sub-micron dimensions, are extremely well collimated, spatially coherent, and the 100 fsec pulse length is well-matched to probing the shortest-lived extreme states. Indeed, the pulse length is so short that even “smearing” of the data resulting from hydrodynamic motion can be removed.

XFELs thus enable us to study the structure and dynamics of extreme states of dense matter for the first time. Using the LCLS, UK researchers have made the first measurement of material strength at the same spatial (<1 μm) and temporal (<50 ps) scales as multimillion-atom molecular dynamics simulations[4]; shown that melting and solid-solid phase transitions in shocked compressed metals take place on ns timescales[5,6], that complex, even incommensurate, forms are created on such timescales[7,8], probed the equation of state and resolved the ionic interactions at atomic length scales in dense metals[9,10] and carbon[11,12]; and created and probed the absorption of solid-density plasmas (see **Section 4.2**).

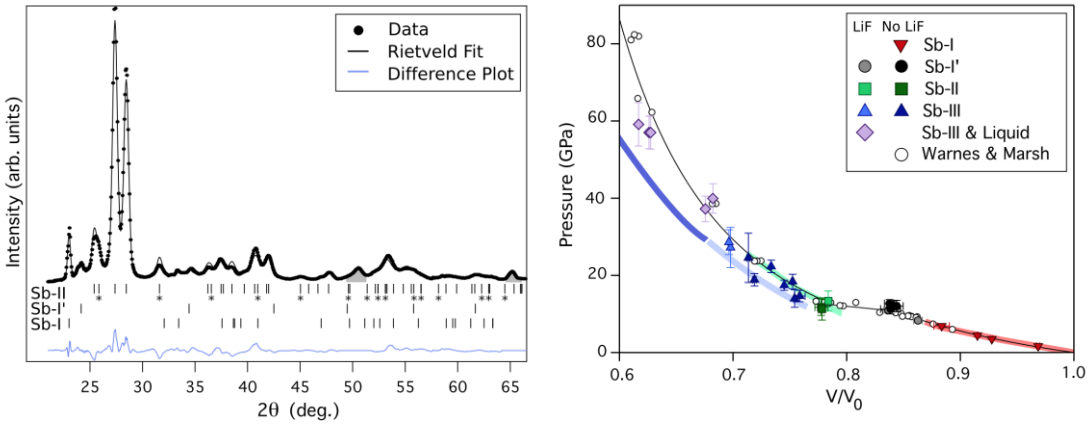

Figure 4.1: Examples of Synchrotron quality diffraction data from an ordered incommensurate host-guest structure (left) and complex phase evolution with pressure (right) in shock compressed antimony. Taken from Coleman et al[7].

Although much of the work above has focussed on elemental materials, work on more complex systems is becoming commonplace. This includes deformation of brittle materials such as ceramics[13], compression of hydrocarbons[14,15] including the observation of precipitation of diamond like carbon under loading[16], and planetary relevant compounds such as SiO_2[17,18] and water[19].

An example of the remarkable complexity present even in 'simple' elemental systems can be seen in **Figure 4.1**. This work on shock compressed antimony followed structural evolution from ambient conditions up to melt along the shock Hugoniot. This study demonstrates two of the key themes permeating the field. Firstly, it was able to access complex phase transitions into an incommensurate host-guest phase on nanosecond timescales. Such structures, observed at moderate pressures in static experiments, are expected to be common at TPa pressures, and as such, their observation in nanosecond timescale experiments is a critical validation of the potential of dynamic compression to access complex stable structures at astrophysically relevant conditions.

The same work also shows the formation of the previously unobserved phase (Sb-I'), which appears to be unique to dynamic loading conditions. This demonstrates the potential for the large shear stresses and restricted deformation timescales inherent to dynamic loading to lead to unique material behaviour hitherto unseen in static studies. An understanding of these phenomena is important not just to interpretation of data of planetary relevance, but more fundamentally to understanding the dynamic compression and failure processes underlying key aeronautical and defence applications. Thus, it is key to explore and understand, at the microstructural level, the full sample journey through both compression and release.

The study of such systems has been made possible by the development of a suite of X-ray diagnostic capabilities. X-ray diffraction remains the workhorse of high energy density structural determination. More recently, this has been combined with imaging techniques to allow for detailed probing of systems with complex multi-wave loading, and thus spatially inhomogeneous structure[20,21]. Initial experiments have been conducted to demonstrate X-ray absorption spectroscopy as a tool for probing chemical environment within high density matter[22]. Most recently, inelastic scattering techniques have been demonstrated which hold the potential to provide temperature measurements in the 0.1 - 1 eV range likely to be accessed in these experiments, completing our understanding of material equation of state[23].

4.1.3 Opportunities for future study

Despite the rapid advances made in the study of dynamically compressed matter since the advent of XFELs, there is still considerable scope for growth and innovation in the field.

In particular, there is still a significant range of pressure unexplored in XFEL science. Current capabilities at LCLS only allow studies up to 3 Mbar[9], with the majority of work being at no more than 1 - 2 Mbar. This compares to the 3.5Mbar of Earth's core, or the 40 - 50 Mbar estimated core pressure of Jupiter. Studies will be extended at European-XFEL from 2021, where the UK's £8M DiPOLE diode-pumped, 100 J, 10 Hz optical laser, will be installed. DiPOLE is vastly superior to its LCLS equivalent, having 3-times the energy, 2000-times the repetition rate, and, crucially, the ability to fine tune the time-profile of the laser pulses it provides in almost real time, thereby allowing routine access to an extremely wide range of P-T states at unparalleled rates. However, even here, pressures will likely be limited to below 10Mbar for most experiments. It should however be noted that both of these facilities have planned upgrade paths to low rep-rate kJ scale optical lasers within the early-mid 2020's.

The potential of exploiting a wider range of pressure is significant. For example, in the same way that diamond is a familiar metastable high-pressure allotrope of carbon, a number of other high-pressure structures are predicted to be metastable at ambient conditions. One example is the proposed BC8 phase of carbon, which is notable for having a hardness comparable to, and potentially exceeding that of diamond[24]. Any such metastability from a phase with a transition pressure above, or composition differing from, Earth's mantle would potentially represent an entirely new material. The extreme structural and electronic properties of these phases means that such materials may exhibit extreme strength or density, have novel bandgaps suitable for exploitation in electronic or photovoltaic applications, or potentially exhibit superconductivity[25].

In order to probe such materials, a full understanding of crystal and electronic structure in situ will be required. XRD as a structural probe, utilising 10 – 25 keV X-rays is almost routine at XFELs, but accompanying spectroscopic techniques suitable for probing electronic properties often require quite disparate X-ray conditions. For example, techniques such as XANES[22] or XAS HEROS[26] require tuning to the vicinity of an absorption edge (typically <10 keV), which is usually avoided for scattering measurements. An XFEL capable of providing true 2 colour modes of operation, allowing simultaneous structural and electronic probing, would open up new avenues for comprehensive understanding of high-pressure states, and potentially recoverable materials.

Super-Earths and Beyond – Probing the cores of planetary giants

Box 4.1: Ab-initio predictions of the solid phase and liquid (hatched) fields of stability in Fe – a key core constituent for planets[27]. Earth core conditions lie on the edge of current static technique capabilities, with 5 Earth-mass and Jupiter core lying in a regime accessible only to dynamic techniques with a multi kJ class optical laser driver. The two red lines denote the isentrope (lower) and the Hugoniot (upper).

Via a combination of X-ray diffraction and spectroscopic techniques an advanced UK FEL could fully map this region, determining the equation of state, phase and chemical properties key to understanding planetary structure and evolution

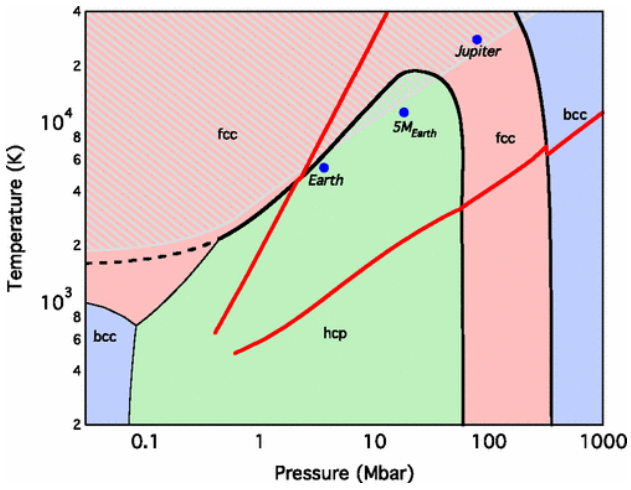

As discussed above, one key shortcoming of current experimental efforts is the inability to sample temperature due optically opaque nature of the material, and relatively low (typically sub eV) temperatures. One potential avenue to provide information on this final crucial component of equation of state is inelastic scattering, which employs high resolution (<10meV) X-ray scattering measurements to directly observe phonon (ion-acoustic) modes whose occupation is directly related to thermodynamic temperature[23]. However, the low efficiency of such scattering processes requires significant integration of shots, and thus limits exploration of configuration space. This limitation could be alleviated by a self-seeded linac with the inherent capability to reach ~10meV bandwidth in the hard X-ray regime. Once again, with suitable machine capability, such a technique is potentially compatible with diffraction/spectroscopy approaches, further broadening the information one can capture on these novel high pressure states.

4.1.4 Conclusions

The study of matter in extremes offers a window into understanding of a wide range of phenomena from the astrophysical to fundamental material deformation. As a field experiencing rapid growth, there remains significant opportunity for discovery. Although both LCLS and the European XFEL have dedicated instruments for such studies, they are limited by the scale and ambition of the driver for compression, as well as the available X-ray parameters, and thus viability of X-ray techniques.

The UK has world leading capability in many of the underpinning technological requirements for this science. STFC efforts in high repetition laser technology and microtarget assembly have already been foundational for the European XFEL's HED instrument and early experiments on LCLS.

A UK XFEL offers a unique opportunity to collocate a world class, large scale laser compression platform alongside an advanced XFEL source. A high repetition rate, high energy (10kJ class), temporally tuneable laser system would allow access to a plethora of hitherto unexplored structures in a range of materials. This would go meaningfully beyond the scale envisaged for existing FELs allowing a UK system to access and explore a unique range of P-T states.

Coupled to this, a high photon energy, high pulse energy, narrow bandwidth, two colour photon source would allow for the full suite of X-ray diagnostic techniques to be brought to bear to allow for full structural, electronic and equation of state knowledge of the material to be acquired. All of this will lead to unprecedented understanding of the high pressure and dynamic deformation regimes, but also open up routes to systematic searches for new metastable materials with potentially transformative scientific and industrial applications.

4.2 Quantum plasmas: warm and hot dense matter

The vast majority of the visible universe is in the plasma state, and extreme states of matter are routinely found in all astrophysical bodies from (exo)planets to stars. A comprehensive understanding of the structure and dynamics of such high energy density plasmas is thus of fundamental physical interest in its own right, but also forms the basis for progress in planetary physics, astrophysics, applications using laser-plasma interactions to generate compact radiation sources, and in providing the foundation to laboratory-based fusion energy. High temporal resolution X-ray probes, synchronized with high-energy drivers, will allow us to create these extreme conditions in a controlled laboratory setting and explore them on the fundamental temporal and spatial scales.

4.2.1 Introduction

Significant advances in X-ray science over the past decade have transformed our capability to study how matter behaves in extreme conditions of pressure, temperature and density. Of particular interest is the dense plasma regime where quantum effects and correlations are important and dominate plasma dynamics. Matter in these conditions is prevalent across the universe in stellar[28] and (exo)planetary interiors[29], is commonly encountered in most laser-plasma interactions[30], and is of considerable interest within the context of inertial confinement fusion energy research[31]. In contrast to high-temperature classical plasmas that are well described by kinetic theory, the properties of quantum plasmas are governed by the complex interplay between Coulomb interactions, quantum correlations, and kinetics, all comparable in size. This leads to a rich spectrum of plasma properties, albeit one that has proven highly challenging to both model computationally and to investigate experimentally.

Since energies from quantum interactions are in competition with thermal energies, the domain where quantum effects dominate has historically been confined to low-temperature (i.e., cryogenic) systems at relatively high densities. However, quantum effects and correlations remain important in systems up to temperatures on the order of their Fermi energy. Since Fermi energies can exceed 10s of eV in high density systems (see **Figure 4.2**), quantum effects can remain important even at high temperatures. Matter in this regime cannot be described by classical plasma theory and is known as warm-dense matter. Its equation of state has strong implications for planetary physics as planetary cores are found in this regime, and its transport properties underly much of planetary formation and evolution. This research area is of growing interest in light of the observation of over a thousand planet candidates outside our solar system, and that many of them do not have analogues within our own solar system[32]. While these observation-based discoveries are among the most exciting in a generation, they provide limited insight into the nature of these objects, i.e., their interior structure, evolutionary pathways, potential habitability, and physical and chemical processes that shape their geology and atmosphere. It is here that laboratory-based experiments can provide valuable insight into the behaviour of relevant high energy density (HED) systems, and guide future exploration. Similarly, our understanding of the structure, composition and evolution of stars also depends on a range of processes in the HED regime. Standard solar models[33] using the revised element abundances were found to disagree with helioseismic observations that determine the internal solar structure using acoustic oscillations. Recent experimental work on the Z-pinch machine at Sandia from Bailey and collaborators[28,34] showed that the opacity of Fe in the boundary region between the convective and radiative zones in the Sun could be partially responsible for this discrepancy. From this work it emerges that the opacity of open L-shell mid-Z ions (Cr, Fe) are relatively poorly understood and cannot be explained by current state-of-the-art modelling efforts, while closed-shell ions (Ni) do not lead to similar difficulties. This emphasises the importance of benchmarking astrophysical data in the HED regime to guide developments, and highlights the role of well-characterized HED experiments in supporting this effort. Other work from the Linac Coherent Light Source FEL has shown more generally that our overall understanding of the electronic structure of partially-ionized plasmas in the hot-dense conditions relevant to stellar envelopes remains incomplete[35], and significant discrepancies remain between experiments and theoretical predictions of even fundamental quantities such as degree of continuum lowering[36-38].

4.2.2 HED Science on XFELs to Date

The first plasma experiments at FEL facilities[39] have successfully demonstrated the capability of X-rays to isochorically heat matter to temperatures between a few eV up to in excess of 100 eV (>1 million K), providing access to the temperature-density conditions present in a range of stellar, white dwarf, and planetary interior conditions[35,40,41] . More recent work using nano-focused X-ray pulses suggests further isochoric heating of Fe to temperatures exceeding 1 keV at solid density, with electron densities well above 10^{24} cm^{-3}. The range of temperature-density conditions currently reachable via isochoric heating is schematically shown in Fig. 1, alongside the temperature-density tracks for our sun and a typical white dwarf star. Such hot systems lend themselves well to be probed via X-ray emission spectroscopy, which has been successfully deployed to study the collisional dynamics of hot-dense plasmas[42,43], their opacity[44,45], and shed light on the physics of ionization potential depression[36-38], all with unprecedented accuracy and control of experimental conditions. Investigations of warm-dense plasmas relevant to planetary astrophysics has also yielded important new insight into the structure and equation of state of planetary interiors[16,46,47], their transport properties[48,49], opacity[50] , and degree of ionization and continuum lowering[51-53]. To date, source limitations have constrained much of the high-temperature work to time-integrated experiments. Extending this research into the time domain, and to much higher densities, while accurately controlling the HED conditions of the generated plasmas (and independently measuring the temperature, ionization and density), remain among the most promising future research avenues in this area.

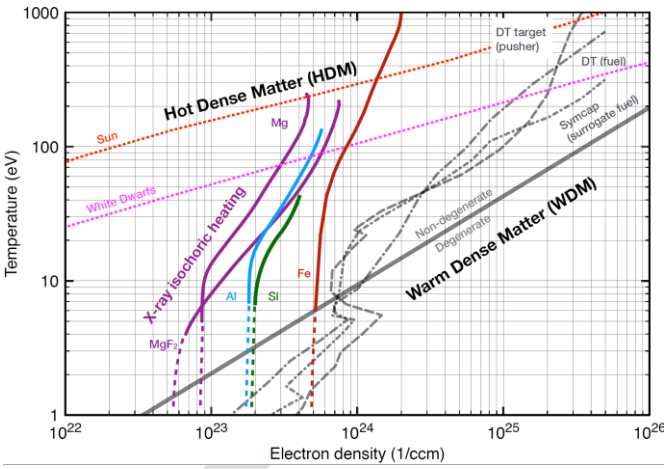

Figure 4.2: Temperatures and densities accessible in the laboratory using X-ray FEL isochoric heating: we can study a broad spectrum of extreme conditions, from planetary cores to stellar interiors. High energy compression drivers will allow us to investigate the

Time Resolved Iron Opacity Measurements in Stellar Envelopes

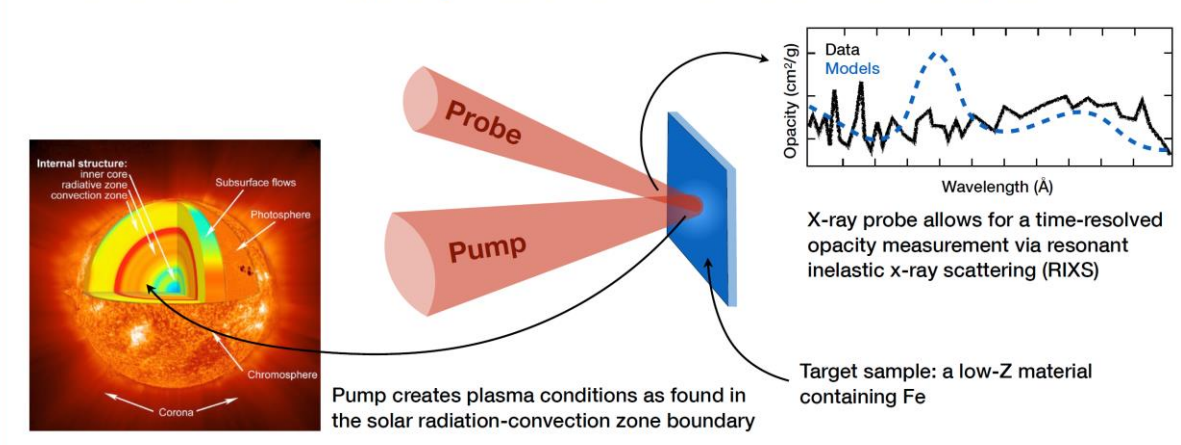

Box 4.2: Schematic of an experimental platform to study the opacity of mid-Z elements such as Fe in stellar interior conditions. The plasma is generated isochorically by a soft X-ray pump and heated to the required conditions. After a time delay the system is probed at harder X-ray wavelengths and the L-shell opacity is determined via resonant inelastic X-ray scattering.

4.2.3 Future Opportunities

X-ray free-electron lasers, coupled with energetic high-energy optical laser drivers, provide a unique opportunity to investigate extreme state of matter. X-ray isochoric heating has already been shown to heat solid density systems to temperatures exceeding 1 keV on femtosecond timescales, while compression experiments on large scale laser facilities have shown how we can tune the inter-atomic spacing in matter to the point where it becomes comparable to the de Broglie wavelength, providing access to a new quantum frontier in high energy density science, potentially pushing quantum behaviour to the macro-scale. While these extreme capabilities are separately available at select flagship facilities around the world today, no facility can currently both create such extreme conditions, and subsequently probe them using the range of cutting-edge X-ray techniques provided by X-ray FELs. In addition to this, high repetition-rate lasers and FELs will prove revolutionary to HED physics in that they will enable, for the first time, statistical analyses of many identical HED events, rather than the current norm based on isolated-event experiments. Access to insight into how rare events (e.g., nucleation of phases and dislocations, ejecta, and detonation) lead to transformations will also enable new science.

Future developments in FEL technology may provide viable approaches to significantly increasing the energy output of an FEL from the mJ level currently available to close to 1 J. A Joule-class X-ray FEL would have several transformative advantages to HED physics investigations, and would enable research opportunities unrivalled elsewhere. Firstly, it would allow us to access the ultra-high energy density regime via isochoric heating, generating dense plasmas at temperatures considerably in excess of those found in the centre of stars. It would further enable single-shot measurements of photon hungry diagnostics such as inelastic or diffuse scattering, and would make it possible to apply novel non-linear spectroscopy techniques to HED investigations for the first time. A substantial increase in photons would also enhance the usefulness of beam-splitting techniques, and would, at least in principle, enable the generation of energetic X-ray comb pulse structures which would provide new opportunities for multi-frame ultra-fast time-resolved studies.

The main future scientific objectives will be linked to the ability to perform well-characterized, time-resolved studies to drive progress in HED science. Of particular interest will be experiments aimed at observing the real-time dynamics of dense plasmas, and of phase transitions of dynamically compressed materials. This includes studies into the transport of heat, charge and particles across interfaces, and the experimental characterization of conductivity, diffusivity, viscosity, instabilities, and plasma opacity. Transport properties such as viscosity and thermal diffusivity in the warm dense matter regime in particular are essential inputs for models of planetary evolution and nuclear fusion processes, and progress on this front will have an impact extending significantly beyond the realm of pure HED physics. Within this context, measurements of the opacity at the hot-dense conditions of relevance to the solar interior, performed in a well-characterized time-resolved experiment that demonstrates thermal equilibrium, may be possible for the first time, addressing key outstanding issues in solar modelling (see highlight box).

The direct investigation of the electronic structure and excitation spectrum of highly compressed, dense plasmas is also of critical interest, not only because of its role in determining the overall partition functions and thermodynamics of extreme HED systems, but also because it will shed light on the mechanisms of core-electron interactions and on how they give rise to the observed emergence of structural complexity at high pressures. At the highest pressures it may be possible that such mechanisms lead to the discovery of new states of matter, where quantum effects emerge and dominate material structure and dynamics even at very high temperatures. While access to such extreme regimes may already be possible in some aspects on the largest facilities such as the National Ignition Facility, key diagnostic techniques are still lacking and we currently cannot probe fundamental excitation mechanisms and ultra-fast electron dynamics in the most extreme conditions. These techniques, largely based on high-resolution inelastic X-ray scattering, necessitate a tuneable, narrow-bandwidth, bright X-ray source, which is where an X-ray FEL would prove transformative.

4.3 Laser wakefield acceleration

By utilising compact laser-driven, plasma-based accelerators we can generate complementary X-ray and gamma ray sources for probing warm dense states, as well as accessing the extreme science of fundamental particle interactions, allowing us to test the fundamental theories of quantum electrodynamics

As described in more detail in **Appendix 3.2**, in a laser wakefield accelerator (LWFA) an intense laser pulse drives a plasma wakefield, within which are generated electric fields of order 100 GV m^{-1}, which can be used to accelerate charged particles. To date LWFAs have generated electron beams with an energy up to 8 GeV from an accelerator stage only 20 cm long. The electron beams produced by LWFAs have been used to generate incoherent radiation from 100 eV to 1 MeV via magnetic undulators, betatron oscillations in the plasma wakefield, and by Compton scattering.

Since they are relatively inexpensive, and compact, LWFAs could be operated alongside the XFEL, greatly expanding the science which could be done whilst also providing an opportunity to drive advances in LWFAs themselves.

As shown schematically in **Figure 4.3**, it would be possible for LWFAs to utilize the auxiliary laser systems required by XFEL users. One or more LWFAs could be driven by using the lasers used for HED science to pump a short-pulse (50 fs) laser driver for an LWFA.

LWFA-driven photon sources could provide femtosecond-duration pulses of incoherent radiation in the keV to MeV range via betatron emission[54] or Compton scattering[55-57] part of the LWFA drive laser with LWFA-generated electrons. Note that using a plasma mirror to retro-reflect the LWFA drive laser provides a convenient, self-aligning geometry and can generate narrow-band X-rays of sufficient brightness for single-shot radiography[57]. These X-ray sources would be tightly synchronized to each other, and to other lasers used in the target areas (for example to compress matter). Hence LWFA-driven photon sources could provide additional, synchronized ultrafast probes for X-ray imaging, scattering, and absorption measurements.

The X rays produced by LWFAs are unique in that they are both broadband and have a femtosecond duration. This makes them an ideal tool for X ray absorption spectroscopy of rapidly evolving systems. In particular this could provide an ideal probe of the extreme states of matter far from equilibrium that can be generated at the focus of an XFEL beam. Work in this area has started at LCLS[58], and is a focus of UK[59] and international LWFA groups[60].

The combination of laser wakefield accelerators with an XFEL also offers some unique opportunities in fundamental science. One specific example is the study of photon-photon interactions. In 1934, Breit and Wheeler predicted that when two photons collide, they can produce an electron and a positron[61], a process called "inelastic photon-photon scattering". This process is crucial in a range of astrophysical phenomena yet has never been observed in the laboratory. For example, extremely-high-energy gamma rays should not propagate across the universe due to their interaction with the cosmic microwave background[62], and observations of TeV gamma rays are showing some tension with predictions based on the Breit-Wheeler process[63].

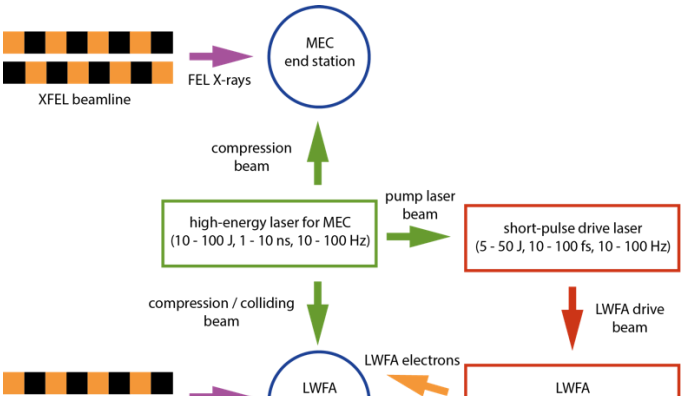

Figure 4.3: Schematic diagram illustrating how auxiliary lasers could drive a LWFA

Elastic photon-photon scattering, when two photons collide and change angle and energy, is one of the fundamental predictions of quantum electrodynamics but it has never been observed with real photons. So far it has only been observed with very high-energy "virtual" photons[64]. In astrophysical scenarios, scattering of photons plays an important role in determining primordial abundances, and in the gamma-ray spectra we can observe from events early in the universe[65]. Attempts to measure low energy photon-photon scattering have not been successful (e.g. using keV photons from an XFEL[66] or eV photons using lasers) due to the very small cross section at these low energies. Crucially, for both elastic and inelastic photon-photon scattering, the regime of relevance to astrophysics requires the invariant mass of the collision between two photons to be close to the rest mass of an electron-positron pair. With an XFEL pulse consisting few keV photons, this therefore requires collision with photon energies around a few hundred MeV. LWFA are ideal source of such photons, either through bremsstrahlung conversion or Compton back scattering[67,68]. Colliding ~100 MeV photons with 1-10 keV XFEL photons will enable fundamental studies of photon-photon physics in the laboratory for the first time.

4.4 Coupling an XFEL to a Laser-driven Spherical Compression Facility

The coupling of a laser-driven spherical-compression facility to a sufficiently hard XFEL would enable the diagnosis of extreme states of matter in unprecedented detail, leading to advances both in the pursuit of fusion energy and our understanding of the universe. This would be a transformative marriage of technologies which would be globally unique, enabling the UK to attain a leadership position in the associated science and technologies.

4.4.1 Introduction

Laser-driven spherical-compression enables the creation of temperature and density states otherwise inaccessible within the laboratory. These conditions are similar to those in the cores of stars, supernovae, and giant planets. Historically, research in this area has been focussed on two main areas: laser inertial confinement fusion[69] (one of two 'mainline' routes to fusion energy) and nuclear weapons research. In recent years, research on such facilities has become increasingly diverse, and now includes areas such as Laboratory Astrophysics, Nuclear Astrophysics, Planetary Physics, Plasma Physics, Matter at Extreme Conditions, Warm Dense Matter, Opacity, Equations of State, Laser-Plasma Interactions and Quantum Electro-Dynamics (QED).

International spherical compression facilities include the USA's National Ignition Facility (~2MJ of laser energy[1]), France's Laser MegaJoule (similar to NIF), Russia's ISKRA-6 (2.8MJ, under construction), China's SGIII (180kJ) and SGII (320kJ upgrade in progress), and the USA's Omega (30kJ). However, due to the small spatial scales of the compressed plasma and the brief duration of peak compression, the limited precision of experimental diagnosis obstructs a detailed understanding of the physics of these extreme states of matter. Coupling a laser-driven spherical compression facility to the UK XFEL would enable a transformation in our understanding; state-of-the-art experiments are typically limited to spatial resolutions of ~3um and temporal resolutions of $1x10^{-11}$s (but usually significantly worse), in contrast an XFEL can achieve spatial resolutions of ~30nm and temporal resolutions of $1x10^{-14}$ s, an increase of 100 and 1000-fold respectively.

4.4.2 Applications

The key advantage of spherical compression is the capability to probe a *far* greater density and temperature parameter space than that which can be created through any other method, as illustrated in Figure 4.4.

A laser-driven spherical compression facility sited alongside an XFEL would have a diverse range of applications in the fields of Laboratory Astrophysics, Nuclear Astrophysics, Planetary Physics, Plasma Physics, Matter at Extreme Conditions, Warm Dense Matter, Opacity, Equations of State, Laser-Plasma Interactions and Quantum Electro-Dynamics (QED). Rather than re-visiting these topics which are detailed elsewhere in the 'Matter at Extreme Conditions', we instead highlight that spherical compression would greatly increase the scope of these research areas by enlarging the accessible density and temperature parameter space.

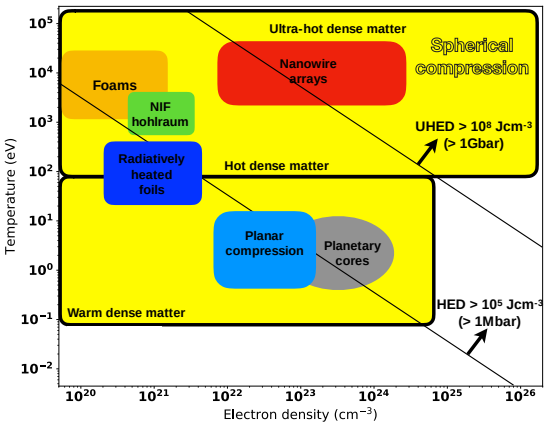

Figure 4.4: The region of density and temperature parameter space which can be explored via spherical compression (both yellow regions).

[1] Laser energy is indicative of the relative size and hence capital cost of these facilities

Below we outline some areas where the coupling of a spherical compression facility to an XFEL would be truly transformative, creating a world-leading capability. This would enable these systems to be studied in unprecedented detail, with concomitant improvements in our understanding of the underlying science.

Laser Fusion: Laser inertial fusion is, along with magnetic confinement fusion, one of two highly advanced, credible approaches to fusion energy. Currently the National Ignition Facility (NIF) has entered the alpha heating regime and has made substantial progress towards meeting the Generalised Lawson Criterion for ignition. Further progress is expected to require either an improved understanding of the implosion performance and fuel assembly conditions, or an increase in the implosion scale; progress is ongoing on both fronts. The unprecedented spatio-temporal resolution of an XFEL would enable ultra-high-resolution X-ray Compton scattering or phase contrast imaging of the implosion with effectively no temporal blurring. Coupled to a more modest (e.g. 100kJ) spherical compression facility, this would transform our understanding of the implosion process, accelerating progress towards fusion energy gain. Importantly, by exploring more energetically efficient implosion techniques such as Laser Direct Drive[70,71], the insights gained on such a facility could pave the way to ignition on significantly smaller scale lasers than NIF, which in turn would enhance the economics of laser fusion power production through the reduction in capital cost.

Fusion Materials: A key challenge for fusion is the engineering of materials able to withstand the fast ion and neutron irradiation created by fusion reactions. The coupling of a spherical compression facility to an XFEL may enable the real-time evaluation of damage mechanisms caused by atomic displacements within the lattice.

The Intensity Frontier: Spherical compression requires quite significant laser energy, meaning a system would likely be at least in the high 10s of kJ in order to be globally competitive. Chirped Pulse Amplification (CPA, the subject of a recent Nobel Prize) enables this laser energy to be compressed in time. If the available laser energy were harnessed in this way, the achievable laser intensity would far exceed that of any existing or planned facility. Such a laser, when coupled to an XFEL, would enable the exploration of a raft of exotic fundamental physics (see section 3.5).

Matter at Extreme Conditions: understanding mechanisms of deformation, melt, recrystallisation and polymorphic phase transitions. Current studies are limited to planar geometries in which shear plays a significant role in deformation dynamics, significantly complicating the interpretation of such experiments. A spherical implosion facility combined with an XFEL would enable hydrostatic (shear-free) compression to extreme states of matter to be studied in unprecedented detail.

Advanced manufacturing: the development of precision targetry for such a facility would greatly enhance existing cutting-edge UK manufacturing capabilities, such as those at Scitech Precision Ltd. Furthermore, the required laser developments would consolidate the Central Laser Facility's position as world-leaders in the design and manufacture of high-energy, high repetition rate lasers. With these technologies in place, the UK would be excellently placed to capitalise on potential economic benefits if power production via Laser Fusion were to become a commercial reality.

Defence: The combination of spherical compression with an XFEL would enable opacity and equation of state studies to be performed with unprecedented fidelity. Potentially such a machine could enter the burning plasma regime, unlocking a wealth of physics, the detailed understanding of which is critical in the nuclear test-ban era.

References

1 Hemley, R. J. & Ashcroft, N. W. The Revealing Role of Pressure in the Condensed Matter Sciences. *Phys. Today* **51**, 26-32, doi:10.1063/1.882374 (1998).

2 McMillan, P. F. New materials from high-pressure experiments. *Nat. Mater.* **1**, 19-25, doi:10.1038/nmat716 (2002).

3 Smith, R. F. *et al.* Ramp compression of diamond to five terapascals. *Nature* **511**, 330-333, doi:10.1038/nature13526 (2014).

4 Milathianaki, D. *et al.* Femtosecond visualization of lattice dynamics in shock-compressed matter. *Science* **342**, 220-223, doi:10.1126/science.1239566 (2013).

5 Gorman, M. G. *et al.* Direct Observation of Melting in Shock-Compressed Bismuth With Femtosecond X-ray Diffraction. *Phys. Rev. Lett.* **115**, 095701, doi:10.1103/PhysRevLett.115.095701 (2015).

6 McBride, E. E. *et al.* Phase transition lowering in dynamically compressed silicon. *Nat. Phys.* **15**, 89-94, doi:10.1038/s41567-018-0290-x (2019).

7 Coleman, A. L. *et al.* Identification of Phase Transitions and Metastability in Dynamically Compressed Antimony Using Ultrafast X-Ray Diffraction. *Phys. Rev. Lett.* **122**, 255704, doi:10.1103/PhysRevLett.122.255704 (2019).

8 Briggs, R. *et al.* Ultrafast X-Ray Diffraction Studies of the Phase Transitions and Equation of State of Scandium Shock Compressed to 82 GPa. *Phys. Rev. Lett.* **118**, 025501, doi:10.1103/PhysRevLett.118.025501 (2017).

9 Wehrenberg, C. E. *et al.* In situ X-ray diffraction measurement of shock-wave-driven twinning and lattice dynamics. *Nature* **550**, 496-499, doi:10.1038/nature24061 (2017).

10 Sliwa, M. *et al.* Femtosecond X-Ray Diffraction Studies of the Reversal of the Microstructural Effects of Plastic Deformation during Shock Release of Tantalum. *Phys. Rev. Lett.* **120**, 265502, doi:10.1103/PhysRevLett.120.265502 (2018).

11 Kraus, D. *et al.* The complex ion structure of warm dense carbon measured by spectrally resolved X-ray scatteringa). *Physics of Plasmas* **22**, doi:10.1063/1.4920943 (2015).

12 Kraus, D. *et al.* Nanosecond formation of diamond and lonsdaleite by shock compression of graphite. *Nat Commun* **7**, 10970, doi:10.1038/ncomms10970 (2016).

13 Tracy, S. J. *et al.* In situ observation of a phase transition in silicon carbide under shock compression using pulsed X-ray diffraction. *Physical Review B* **99**, doi:10.1103/PhysRevB.99.214106 (2019).

14 Hartley, N. J. *et al.* Evidence for Crystalline Structure in Dynamically-Compressed Polyethylene up to 200 GPa. *Sci Rep* **9**, 4196, doi:10.1038/s41598-019-40782-5 (2019).

15 Hartley, N. J. *et al.* Liquid Structure of Shock-Compressed Hydrocarbons at Megabar Pressures. *Phys Rev Lett* **121**, 245501, doi:10.1103/PhysRevLett.121.245501 (2018).

16 Kraus, D. *et al.* Formation of diamonds in laser-compressed hydrocarbons at planetary interior conditions. *Nature Astronomy* **1**, 606-611, doi:10.1038/s41550-017-0219-9 (2017).

17 Gleason, A. E. *et al.* Ultrafast visualization of crystallization and grain growth in shock-compressed SiO2. *Nat. Commun.* **6**, 8191, doi:10.1038/ncomms9191 (2015).

18 Gleason, A. E. *et al.* Time-resolved diffraction of shock-released SiO2 and diaplectic glass formation. *Nat Commun* **8**, 1481, doi:10.1038/s41467-017-01791-y (2017).

19 Gleason, A. E. *et al.* Compression Freezing Kinetics of Water to Ice VII. *Phys. Rev. Lett.* **119**, 025701, doi:10.1103/PhysRevLett.119.025701 (2017).

20 Schropp, A. *et al.* Imaging Shock Waves in Diamond with Both High Temporal and Spatial Resolution at an XFEL. *Sci. Rep.* **5**, 11089, doi:10.1038/srep11089 (2015).

21 Brown, S. B. *et al.* Direct imaging of ultrafast lattice dynamics. *Sci Adv* **5**, eaau8044, doi:10.1126/sciadv.aau8044 (2019).

22 Harmand, M. *et al.* X-ray absorption spectroscopy of iron at multimegabar pressures in laser shock experiments. *Physical Review B* **92**, doi:10.1103/PhysRevB.92.024108 (2015).

23 McBride, E. E. *et al.* Setup for meV-resolution inelastic X-ray scattering measurements and X-ray diffraction at the Matter in Extreme Conditions endstation at the Linac Coherent Light Source. *Rev. Sci. Instrum.* **89**, 10F104, doi:10.1063/1.5039329 (2018).

24 Sun, J., Klug, D. D. & Martonák, R. Structural transformations in carbon under extreme pressure: beyond diamond. *J. Chem. Phys.* **130**, 194512, doi:10.1063/1.3139060 (2009).

25 Drozdov, A. P., Eremets, M. I., Troyan, I. A., Ksenofontov, V. & Shylin, S. I. Conventional superconductivity at 203 kelvin at high pressures in the sulfur hydride system. *Nature* **525**, 73-76, doi:10.1038/nature14964 (2015).

26 Błachucki, W. *et al.* High energy resolution off-resonant spectroscopy for X-ray absorption spectra free of self-absorption effects. *Phys. Rev. Lett.* **112**, 173003, doi:10.1103/PhysRevLett.112.173003 (2014).

27 Stixrude, L. Structure of Iron to 1 Gbar and 40 000 K. *Phys. Rev. Lett.* **108**, 1-5, doi:10.1103/PhysRevLett.108.055505 (2012).

28 Bailey, J. E. *et al.* A higher-than-predicted measurement of iron opacity at solar interior temperatures. *Nature* **517**, 56-59, doi:10.1038/nature14048 (2015).

29 Smith, R. F. *et al.* Equation of state of iron under core conditions of large rocky exoplanets. *Nature Astronomy* **2**, 452-458, doi:10.1038/s41550-018-0437-9 (2018).

30 Shukla, P. K. & Eliasson, B. Nonlinear aspects of quantum plasma physics. *Physics-Uspekhi* **53**, 51-76, doi:10.3367/UFNe.0180.201001b.0055 (2010).

31 Gaffney, J. A. *et al.* A Review of Equation-of-State Models for Inertial Confinement Fusion Materials. *High Energy Density Physics* **28**, 7-24, doi:10.1016/j.hedp.2018.08.001 (2018).

32 Lissauer, J. J. *et al.* A closely packed system of low-mass, low-density planets transiting Kepler-11. *Nature* **470**, 53-58, doi:10.1038/nature09760 (2011).

33 Bahcall, J. N., Huebner, W. F., Lubow, S. H., Parker, P. D. & Ulrich, R. K. Standard solar models and the uncertainties in predicted capture rates of solar neutrinos. *Reviews of Modern Physics* **54**, 767-799, doi:10.1103/RevModPhys.54.767 (1982).

34 Nagayama, T. *et al.* Systematic Study of L-Shell Opacity at Stellar Interior Temperatures. *Phys Rev Lett* **122**, 235001, doi:10.1103/PhysRevLett.122.235001 (2019).

35 Vinko, S. M. *et al.* Creation and diagnosis of a solid-density plasma with an X-ray free-electron laser. *Nature* **482**, 59-62, doi:10.1038/nature10746 (2012).

36 Ciricosta, O. *et al.* Direct Measurements of the Ionization Potential Depression in a Dense Plasma. *Phys. Rev. Lett.* **109**, 065002, doi:10.1103/PhysRevLett.109.065002 (2012).

37 Vinko, S. M., Ciricosta, O. & Wark, J. S. Density functional theory calculations of continuum lowering in strongly coupled plasmas. *Nat Commun* **5**, 3533, doi:10.1038/ncomms4533 (2014).

38 Ciricosta, O. *et al.* Measurements of continuum lowering in solid-density plasmas created from elements and compounds. *Nat Commun* **7**, 11713, doi:10.1038/ncomms11713 (2016).

39 Emma, P. *et al.* First lasing and operation of an ångstrom-wavelength free-electron laser. *Nature Photonics* **4**, 641-647, doi:10.1038/nphoton.2010.176 (2010).

40 Lévy, A. *et al.* The creation of large-volume, gradient-free warm dense matter with an X-ray free-electron laser. *Physics of Plasmas* **22**, doi:10.1063/1.4916103 (2015).

41 Ciricosta, O. *et al.* Detailed model for hot-dense aluminum plasmas generated by an X-ray free electron laser. *Physics of Plasmas* **23**, doi:10.1063/1.4942540 (2016).

42 Vinko, S. M. *et al.* Investigation of femtosecond collisional ionization rates in a solid-density aluminium plasma. *Nat Commun* **6**, 6397, doi:10.1038/ncomms7397 (2015).

43 van den Berg, Q. Y. *et al.* Clocking Femtosecond Collisional Dynamics via Resonant X-Ray Spectroscopy. *Phys Rev Lett* **120**, 055002, doi:10.1103/PhysRevLett.120.055002 (2018).

44 Preston, T. R. *et al.* Measurements of the K-Shell Opacity of a Solid-Density Magnesium Plasma Heated by an X-Ray Free-Electron Laser. *Phys Rev Lett* **119**, 085001, doi:10.1103/PhysRevLett.119.085001 (2017).

45 Hollebon, P. *et al.* Ab initio simulations and measurements of the free-free opacity in aluminum. *Phys Rev E* **100**, 043207, doi:10.1103/PhysRevE.100.043207 (2019).

46 Fletcher, L. B. *et al.* Ultrabright X-ray laser scattering for dynamic warm dense matter physics. *Nature Photonics* **9**, 274-279, doi:10.1038/nphoton.2015.41 (2015).

47 Kraus, D. *et al.* X-ray scattering measurements on imploding CH spheres at the National Ignition Facility. *Phys Rev E* **94**, 011202, doi:10.1103/PhysRevE.94.011202 (2016).

48 Faustlin, R. R. *et al.* Observation of ultrafast nonequilibrium collective dynamics in warm dense hydrogen. *Phys Rev Lett* **104**, 125002, doi:10.1103/PhysRevLett.104.125002 (2010).

49 Sperling, P. *et al.* Free-electron X-ray laser measurements of collisional-damped plasmons in isochorically heated warm dense matter. *Phys Rev Lett* **115**, 115001, doi:10.1103/PhysRevLett.115.115001 (2015).

50 Williams, G. O. *et al.* Tracking the ultrafast XUV optical properties of X-ray free-electron-laser heated matter with high-order harmonics. *Physical Review A* **97**, doi:10.1103/PhysRevA.97.023414 (2018).

51 Fletcher, L. B. *et al.* X-ray Thomson scattering measurements of temperature and density from multi-shocked CH capsules. *Physics of Plasmas* **20**, doi:10.1063/1.4807032 (2013).

52 Fletcher, L. B. *et al.* Observations of continuum depression in warm dense matter with X-ray Thomson scattering. *Phys Rev Lett* **112**, 145004, doi:10.1103/PhysRevLett.112.145004 (2014).

53 Kraus, D. *et al.* Characterizing the ionization potential depression in dense carbon plasmas with high-precision spectrally resolved X-ray scattering. *Plasma Physics and Controlled Fusion* **61**, doi:10.1088/1361-6587/aadd6c (2019).

54 Kneip, S. *et al.* Bright spatially coherent synchrotron X-rays from a table-top source. *Nature Physics* **6**, 980-983, doi:10.1038/nphys1789 (2010).

55 Powers, N. D. *et al.* Quasi-monoenergetic and tunable X-rays from a laser-driven Compton light source. *Nature Photonics* **8**, 28-31, doi:10.1038/nphoton.2013.314 (2013).

56 Khrennikov, K. *et al.* Tunable all-optical quasimonochromatic thomson X-ray source in the nonlinear regime. *Phys Rev Lett* **114**, 195003, doi:10.1103/PhysRevLett.114.195003 (2015).

57 Döpp, A. *et al.* An all-optical Compton source for single-exposure X-ray imaging. *Plasma Physics and Controlled Fusion* **58**, doi:10.1088/0741-3335/58/3/034005 (2016).

58 Albert, F. Applications of Light Sources Driven by Laser-Wakefield Acceleration, presented at the 9th Int. Particle Accelerator Conf. (IPAC'18), Vancouver, BC, Canada. (2018).

59 Kettle, B. *et al.* Single-Shot Multi-keV X-Ray Absorption Spectroscopy Using an Ultrashort Laser-Wakefield Accelerator Source. *Phys Rev Lett* **123**, 254801, doi:10.1103/PhysRevLett.123.254801 (2019).

60 Mahieu, B. *et al.* Probing warm dense matter using femtosecond X-ray absorption spectroscopy with a laser-produced betatron source. *Nat Commun* **9**, 3276, doi:10.1038/s41467-018-05791-4 (2018).

61 Breit, G. & Wheeler, J. A. Collision of Two Light Quanta. *Physical Review* **46**, 1087-1091, doi:10.1103/PhysRev.46.1087 (1934).

62 Gould, R. J. & Schréder, G. P. Pair Production in Photon-Photon Collisions. *Physical Review* **155**,

1404-1407, doi:10.1103/PhysRev.155.1404 (1967).

63 Meyer, M., Horns, D. & Raue, M. First lower limits on the photon-axion-like particle coupling from very high energy gamma-ray observations. *Physical Review D* **87**, doi:10.1103/PhysRevD.87.035027 (2013).

64 ATLAS Collaboration. Evidence for light-by-light scattering in heavy-ion collisions with the ATLAS detector at the LHC. *Nature Physics* **13**, 852-858, doi:10.1038/nphys4208 (2017).

65 Svensson, R. & Zdziarski, A. Photon-photon scattering of gamma rays at cosmological distances. *The Astrophysical Journal* **349**, doi:10.1086/168325 (1990).

66 Yamaji, T. *et al.* An experiment of X-ray photon–photon elastic scattering with a Laue-case beam collider. *Physics Letters B* **763**, 454-457, doi:10.1016/j.physletb.2016.11.003 (2016).

67 Sarri, G. *et al.* Generation of neutral and high-density electron-positron pair plasmas in the laboratory. *Nat Commun* **6**, 6747, doi:10.1038/ncomms7747 (2015).

68 Ta Phuoc, K. *et al.* All-optical Compton gamma-ray source. *Nature Photonics* **6**, 308-311, doi:10.1038/nphoton.2012.82 (2012).

69 Nuckolls, J., Wood, L., Thiessen, A. & Zimmerman, G. Laser Compression of Matter to Super-High Densities: Thermonuclear (CTR) Applications. *Nature* **239**, 139-142, doi:10.1038/239139a0 (1972).

70 Craxton, R. S. *et al.* Direct-drive inertial confinement fusion: A review. *Physics of Plasmas* **22**, doi:10.1063/1.4934714 (2015).

71 Gopalaswamy, V. *et al.* Tripled yield in direct-drive laser fusion through statistical modelling. *Nature* **565**, 581-586, doi:10.1038/s41586-019-0877-0 (2019).

5. Science Opportunities in Quantum and Nanomaterials

The properties of condensed phase materials have long been a key driver in technology; electronics, optoelectronics, data storage, superconductivity and light sources. The rich interplay of phenomena between the nanoscopic and mesoscopic scale leads to the emergent properties of the material. To understand this, we require incisive probes of electronic state, geometric structure and spin state. This is never more so than in the case of *quantum* or *strongly coupled* materials where there is a complex interplay and coupling between these states of the system. Such quantum materials, along with nanostructured materials, provide new technology opportunities with properties that can be tailored to specific functions. XFELs provide ideal probes to uncover these rich phenomena via X-ray scattering, X-ray photoelectron spectroscopy and resonant inelastic scattering.

5.1 Magnetic materials and control of ultrafast magnetisation

Ultrafast photo-excitation of quantum materials that exhibit intricate coupling between charge, spin and orbital degrees of freedom hold great promise for understanding and controlling the properties of non-equilibrium and hidden states. Here we discuss the state-of- the-art and introduce time-resolved resonant inelastic X-ray scattering (trRIXS) as a means of measuring charge, spin and orbital excitations. These excitations encode the correlations and interactions that determine the detailed properties of the generated states and may advance the technology of for instance fast, energy efficient, data storage.

5.1.1 Introduction to magnetic dynamics measured with FELs

Magnetism has fascinated mankind since its discovery over two thousand years ago. Although magnetic fields can be conceptualized using classical physics, the existence of magnetic materials can only be understood in terms of the fundamentally quantum mechanical nature of the world around us. Our ability to manipulate magnetism via ultra-fast laser excitation has therefore attracted considerable excitement within the scientific community. In terms of applications, ultrafast magnetism provides routes to fast switching of electronic devices, which often store information in different magnetic states [1]. From a more fundamental point of view ultrafast magnetism addresses questions: what are the fundamental principles governing the interactions of photons with matter[2]? And can we use ultrafast excitations to generate magnetic states that are in-accessible in equilibrium[3]? Magnetic or spin degrees of freedom are also intimately tied to many of the most interesting emergent electronic properties of materials, such as high temperature superconductivity quantum spin liquids, colossal magnetoresistance etc. [4,5]. Understanding quantum magnetism is therefore important to nascent efforts to realize and manipulate such states transiently.

Our current understanding of ultrafast magnetism tends to be based on simple magnetic order parameter ideas, of which the so-called three-temperature model is the most popular [6]. This involves defining effective temperatures for the lattice, electrons and spins and constructing a phenomenological picture based on rates of energy-exchange between these degrees of freedom. This can, for example, capture the common phenomenology of a magnetic order being suppressed by high-fluence high-energy optical pulses before its recovers slowly. This theoretical approach is rather natural in terms of the common tools for characterizing transient magnetism, which are benchtop optical experiments that measure the net ferromagnetic order parameter using the Faraday or magneto-optical Kerr effects. Since most experiments measure simple order parameter dynamics there is limited information and motivation to develop more sophisticated theories.

Working within this paradigm is, however, very limited, as it is most appropriate for states that are similar to those that are accessible via equilibrium thermal heating. This paradigm excludes many of the most interesting ideas such as magnetic switching [7], generating transient superconductivity [8], realizing topological lattice or electronic structures [9,10] or rotating spin with terahertz or mid-infrared excitation [11-13].

5.1.2 State of the art in probing magnetic dynamics

Despite the increasing sophistication of table-top probes of magnetism, the information extracted tends to be held-back by the low energy of the beams. The wavelength of optical light is far longer than the atomic spacing and the lengthscales usually relevant to magnetism, meaning that a lot of the details of transient magnetic states are inaccessible to such experiments. This is perhaps the primary reason why optical experiments tend to probe the net ferromagnetic order parameters. Using X-rays provides a direct way to access lengthscale-dependent properties and a more complete description. The most obvious way to do so is by studying spatially modulated states such as antiferromagnetism,

orbital order or charge density waves [14-18]. These states have staggered order parameter as a function of position in the crystal lattice, which average to zero in spatially integrating probes.

Standard x-ray scattering with arbitrary x-ray energies interacts primarily via the Thompson cross section and probes the atomic structure of the material. Resonant x-ray scattering, as illustrated in **Figure 5.1** (left) involves tuning the x-ray energy to excite a core hole resonance. This provides a means to couple x-rays to magnetic and orbital degrees of freedom and probe electronic order. The use of resonant diffraction was impressively illustrated in studies of perovskite manganite Pr0.5Ca0.5MnO3, in which the authors probe electronic and structural degrees of freedom after photo-excitation and were able to describe the electronic behaviour of the material in terms of a set of atomic displacements illustrated in **Figure 5.1** (right) [14].

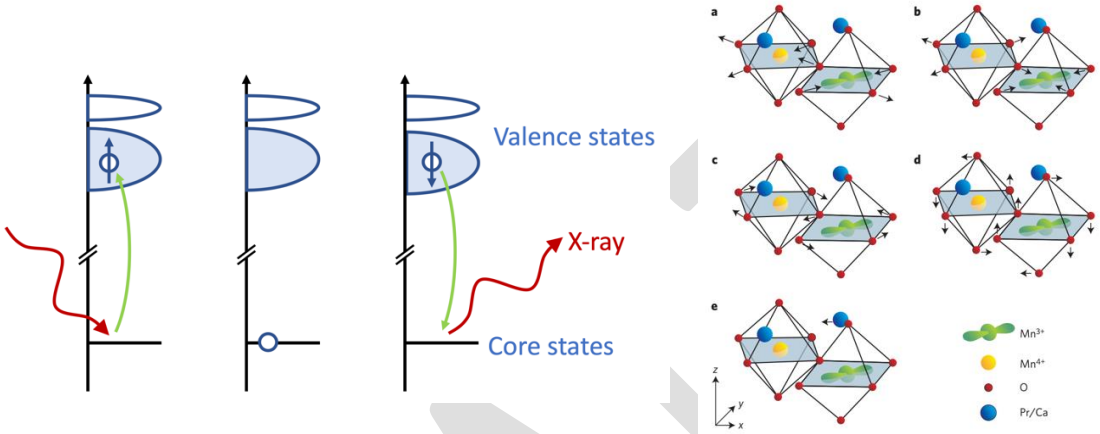

Figure 5.1: Ultrafast resonant diffraction. Left: A schematic of the resonant scattering process. The initial, intermediate, and final states are shown from left to right. Photons are represented as wavy red lines and electronic transitions are shown as green arrows. In this process spin excitations are created and their dispersion can be measured by determining the energy and momentum change of the photon [19]. Right diagram of optical phonon modes related to the different elements of electronic order in Pr0.5Ca0.5MnO3. Taken from [14].

Another important class of experiments probe the statistical distribution of magnetism with x-rays [7,20-22]. If one measures a ferromagnet with a characteristic domain size using x-ray resonant magnetic scattering, the diffraction pattern will be azimuthally symmetric with a peak that reflects the inverse domain size as seen in Figure 5.2(left) [7]. Previous experiments have applied this approach at XFELs in order to probe magnetism and have shown unique capabilities for separately probing different magnetic species at different lengthscales [7,20-22].

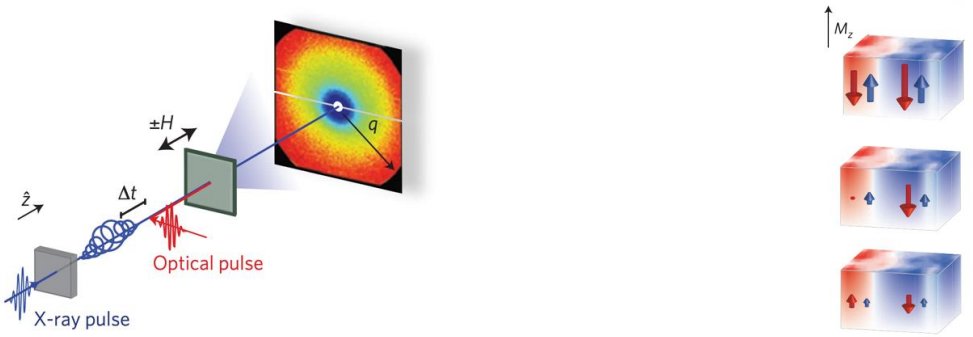

Figure 5.2: Magnetic domain dynamics. Left the experimental setup for magnetic diffraction from domains. Right an illustration of the evolution of iron and gadolinium moments out of equilibrium. Taken from [7].

5.1.3 Future opportunities in magnetic dynamics

We identify three main categories of new experiments. The first involves more sophisticated and high time-resolution pump schemes such as THz or mid-infra excitation. This lower energy photo-excitation can couple more directly to magnetism or drive phonon modes in order to realize novel electronic states. Dedicated instrumentation for the pump and probe is highly desirable here as the x-ray element of the experiment needs to be implemented in a more stable and straightforward way in order to allow more challenging photo-excitation schemes.

A very appealing, but underexplored, area is performing XFEL experiments in the perturbative regime in which the ground state is only slightly disturbed and small changes are seen in the magnetic state. In this limit, the sample response can reflect the equilibrium dynamical susceptibility and coupling between different degrees of freedom. This scheme has been compellingly employed to provide parameter-free determination of electron-phonon coupling via the measurement of crystal structure and electronic band-structure after photo-excitation [23]. To the authors idea has not yet been applied to XFEL experiments of magnetism. Experiments involving small changes are especially well-suited to high-repetition-rate XFEL sources as high average flux is needed to measure small changes in a weak magnetic order parameter signal.

Our final area is the prospect of performing spectroscopy of collective excitations in transient states. Collective excitations encode key details about the interactions and short-range correlations in transient states. Time-resolved RIXS, as illustrated in Figure 5.1.3, has recently emerged as a practical means to probe such correlations and has measured magnons in photo-excited iridates [16,24]. Such a spectroscopy is could answer some of the most profound questions such as how can we modify different components of the magnetic exchange on ultra-fast timescales? Or can we soften different components of the magnetic excitation spectra in order to transiently stabilize different magnetic ground states? An XFEL with a dedicated spectrometer for such experiments would have unique opportunities to help understand transient magnetism.

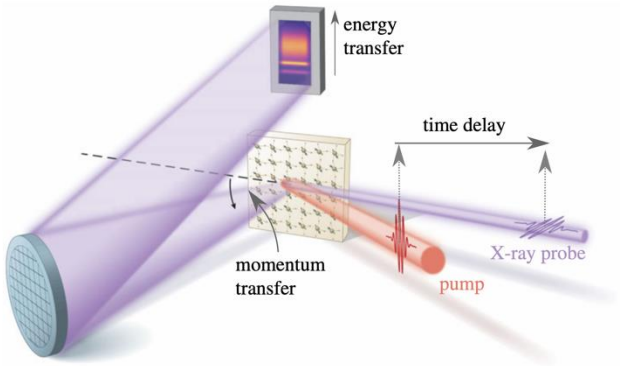

Figure 5.3: Time-resolved RIXS as recently realized in [16,24,25]. The momentum transfer is determined by the angle between the incident and scattered X-rays from the sample, along with the wavelength of the X-ray. The energy of the scattered photons is resolved by dispersing the x-rays with a grating or crystal analyzer onto a two-dimensional detector. In tr-RIXS, a second pump laser pulse is used which arrives at a controllable time ahead of the incident X-rays.

References

[1.] C. D. Stanciu, F. Hansteen, A. V. Kimel, A. Kirilyuk, A. Tsukamoto, A. Itoh, and T. Rasing, Physical Review Letters 99, 047601 (2007).

[2.] J.-Y. Bigot, M. Vomir, and E. Beaurepaire, Nature Physics 5, 515 (2009).

[3.] Department of Energy Grand Challenges, https://science.osti.gov/bes/efrc/Research/Grand-Challenges.

[4.] D. N. Basov, R. D. Averitt, and D. Hsieh, Nature Materials 16, 1077 (2017).

[5.] J. Zhang and R. D. Averitt, Annual Review of Materials Research 44, 19 (2014).

[6.] E. Beaurepaire, J. C. Merle, A. Daunois, and J. Y. Bigot, Physical Review Letters 76, 4250 (1996).

[7.] C. E. Graves et al., Nature Materials 12, 293 (2013).

[8.] D. Fausti et al., Science 331, 189 (2011).

[9.] Y. H. Wang, H. Steinberg, P. Jarillo-Herrero, and N. Gedik, Science 342, 453 (2013).

[10.] E. J. Sie et al., Nature 565, 61 (2019).

[11.] S. Baierl, M. Hohenleutner, T. Kampfrath, A. K. Zvezdin, A. V. Kimel, R. Huber, and R. V. Mikhaylovskiy, Nature Photonics 10, 715 (2016).

[12.] D. Afanasiev, J. R. Hortensius, B. A. Ivanov, A. Sasani, E. Bousquet, Y. M. Blanter, R. V. Mikhaylovskiy, A. V. Kimel, and A. D. Caviglia, arXiv e-prints, arXiv:1912.01938 (2019).

[13.] I. Radu et al., Nature 472, 205 (2011).

[14.] P. Beaud et al., Nature Materials 13, 923 (2014).

[15.] A. Kogar et al., Nature Physics 16, 159 (2020).

[16.] M. P. M. Dean et al., Nature Materials 15, 601 (2016).

[17.] N. Thielemann-Kühn, D. Schick, N. Pontius, C. Trabant, R. Mitzner, K. Holldack, H. Zabel, A. Föhlisch, and C. Schüßler-Langeheine, Physical Review Letters 119, 197202 (2017).

[18.] L. Rettig et al., Physical Review Letters 116, 257202 (2016).

[19.] M. P. M. Dean, Journal of Magnetism and Magnetic Materials 376, 3 (2015).

[20.] E. Iacocca et al., Nature Communications 10, 1756 (2019).

[21.] B. Pfau et al., Nature Communications 3, 1100 (2012).

[22.] B. Vodungbo et al., Nature Communications 3, 999 (2012).

[23.] S. Gerber et al., Science 357, 71 (2017).

[24.] Y. Cao, D. G. Mazzone, D. Meyers, J. P. Hill, X. Liu, S. Wall, and M. P. M. Dean, Philosophical Transactions of the Royal Society A: Mathematical, Physical and Engineering Sciences 377, 20170480 (2019).

[25.] D. G. Mazzone, D. Meyers, and others, 2020).

5.2 Structural dynamics and light induced phases in quantum materials

The transiently modification of structure in quantum materials by femtosecond pulses of laser light can induce new properties that do not appear in equilibrium. Coupling with an ultra-fast x-ray probe can provide unprecedented insight into how electrons, phonons and spins interact to determine the properties of materials, such as magnetism, insulator-metal transitions and superconductivity. Here we discuss how light can be used to effectively and efficiently manipulate these interactions in order to control material properties.

5.2.1 Introduction to the structural dynamics measured with FELs

The atomic structure of quantum materials has a profound effect of the material's electronics and magnetic properties. Understanding this connection between the underlying atomic structure and the resulting functionality of the material is one of the key challenges in the physics of quantum materials. In many quantum materials small, picometer, atomic displacements can result in materials with vastly different properties. These displacements are capable of changing a magnetic insulator into a metal or even a superconductor. The sensitivity to distortions represent significant challenges to understand quantum materials, as they intrinsically require highly accurate and precise measurements and theories [1] in order to accurately capture and characterize the subtle structural changes. However, this sensitivity also presents new opportunities for control. As only small atomic displacements are required to induce new electronic and magnetic properties, intense light pulses can distort the crystal structure of the lattice. This has led to a new field with the aim of controlling the properties of quantum materials "on demand" [2].

Several experiments have shown that light can transiently modify the structure of materials to induce new properties that do not appear in equilibrium in the host material. Light tuned to a structural resonance in order to shake specific bonds has been shown to induce insulator-metal[3], magnetic[4] and superconducting[5] transitions. However, these first experiments have essentially been performed "blind" from a structural point of view. These effects were observed before the first X-ray FELs could look at the atomic structure on the appropriate timescale and lattice motion that resulted from the optical excitation could only be inferred through indirect methods. FELs are now enabling a step change in our understanding of lattice dynamics as they can probe the structural changes directly, capturing snapshots of the atomic configuration as it changes in real time. This new information will enable completely new insights into both how small atomic displacements alter the functionality of quantum materials and how light can manipulate these changes, which ultimately could lead to new paradigms in both our theoretical understanding of quantum materials and in future devices which can exploit the dynamic control of the material's phase.

5.2.2 Structural dynamics in quantum materials

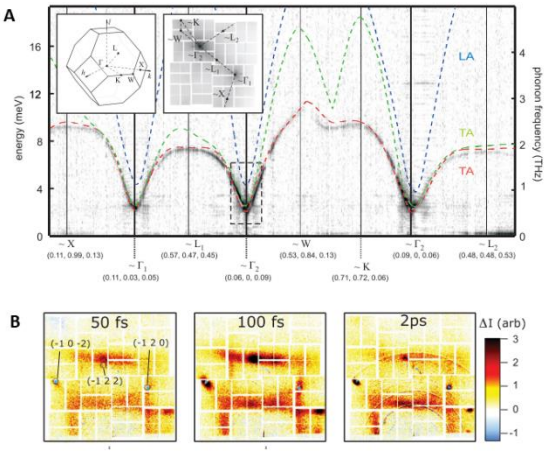

*Figure 5.4: Time-resolved diffuse X-ray scattering. **A** Fourier Transform inelastic X-ray scattering is now able to measure phonon dynamics in Ge throughout the entire Brillouin Zone with sub meV energy resolution (Take from ref[6]). **B** Time-resolved diffuse scattering changes during a structural phase transition in VO_2, showing that lattice disorder dominates at early timescales (taken from ref[7]).*

While femtosecond X-ray sources have enabled the study aspects of light induced phase transitions in quantum materials for some time[8], the advent of ultrafast and ultra-bright FEL laser pulses has transformed our understanding of ultrafast structural transitions. Correcting for the intrinsic timing jitter between X-rays and the exciting laser has been key for much of the progress. Real-time jitter correction can time-stamp each measurement with a precision of 6 fs[9], which is sufficient to observe most structural motion. Initial measurements on light-induced phase transitions focused on exploiting the time-resolution of XFELs to study vibrational coherences induced by optical excitation through Bragg scattering[10]. More recent advances have been driven by combining Bragg scattering with new methods to control the lattice, specifically mid-IR[11] and THz[12] excitation. By combining state of the art X-ray sources with start of the art laser based methods to excite the system, new insights into how below-gap light can coherently modify the structures of materials is emerging and enabling a new states of materials to form.

In addition to the advances that come from combining advanced pumping techniques with femtosecond X-rays, new techniques, are beginning to emerge that can take advantage of the high photon flux. Phonons cause deviations from a perfect lattice by modulate the atomic structure on the length scale set by their wavelength. This transfers some scattered intensity from the 'ideal' Bragg peak into diffuse scattering between the peaks. As the phonon displacements are small, the intensity redistribution is weak, and had been largely inaccessible to time-resolved studies. Ultra-bright XFELs, however, are intense enough to resolve this scattering with ease. Fourier Transform inelastic X-ray scattering[13] is a new technique that exploits this scattering to measure coherent phonon dynamics over the entire Brillouin zone for the first time (See Figure 5.2.1**A**). This time-domain approach is excellent for measuring low energy oscillations and sub-meV resolution phonon dynamics have already been reported [6], making this technique competitive with inelastic X-ray scattering in terms of energy resolution.

Furthermore, this technique can be used to examine how phonon populations change dynamically when the system is rapidly driven through a phase transition. This was performed for the first time on the prototypical quantum material VO_2 [7] (Fig 5.2.1**B**), where it was observed that phonons are excited rapidly but incoherently throughout the entire Brillouin zone. This disorder-like process, only visible due to the high brightness and high momentum resolution of the FEL, overturned the pervious description, obtained from electron diffraction, that the transition was a coherent-like process resulting from well-defined regular atomic motions [14].

5.2.3 Future opportunities in structural dynamics

The study of structural dynamics and phase transitions with XFELs is rapidly developing. There are several directions in future progress can be made, specifically combining state of the art optical pump sources with the new probing techniques short and intense X-ray pulses provide.

X-FELS have many properties that make them the leading source for measuring dynamics of quantum materials. X-rays have significantly higher q-resolution and the pulse durations can be an order of magnitude shorter than electron sources, which is a key competitor. These are key factors for observing small and fast displacements. However, most significantly X-rays are insensitive to the mechanism used to excite the sample. X-rays are not directly perturbed by the pump pulse and only respond to the resulting changes in the material, whereas electrons are charged and can thus feel the electric field of the pump pulse during transit to the sample. This becomes particularly significant when the pump wavelength is increased, which increases the ponderomotive force applied on the electron beam.

However, there are several technical drawbacks that X-rays face. The wavelength of current hard X-ray sources is low and to fully map out and measure the lattice structure in a single experimental geometry and samples have to be rotated. While this is not a problem for static measurements, it introduces many challenges for dynamic measurements. Freely rotating samples while cooling and providing optical access has limited most experiments to temperatures above 100 K. Furthermore, in order to match pump and probe penetration depths experiments must be performed in a near grazing geometry. This results in large spots sizes which limits the field strengths that can be reached. Furthermore, due to the large optical anisotropy of many quantum materials rotating samples for X-ray diffraction can result in very different pumping geometries, which makes comparing results challenging.

One way to overcome this limitation a move to hard X-rays >20 keV. If high quality free standing samples can be obtained, a transmission Laue diffraction geometry would enable the measurement of multiple diffraction peaks in a single experimental geometry. This would also significantly simply the experimental setup and cooling requirements, enabling much lower base temperatures to be reached that those achieved to date. Further benefits would arise from a 'normal incident' geometry, specifically high peak electric fields could be generated which would could drive the sample into new regimes, while nanofocusing of the X-ray source could enable direct probing of macroscopic inhomogeneity.

References

[1] Varignon, J., Bibes, M. & Zunger, A. Origin of band gaps in 3d perovskite oxides. *Nat. Commun.* **10**, 1658 (2019).4).

[2] Basov, D. N., Averitt, R. D. & Hsieh, D. Towards properties on demand in quantum materials. *Nat. Mater.* **16**, 1077-1088 (2017).

[3] Rini, M. *et al.* Control of the electronic phase of a manganite by mode-selective vibrational excitation. *Nature* **449**, 72-4 (2007).

[4] Först, M. *et al.* Driving magnetic order in a manganite by ultrafast lattice excitation. *Phys. Rev. B* **84**, 241104 (2011).

[5] Fausti, D. *et al.* Light-Induced Superconductivity in a Stripe-Ordered Cuprate. *Science (80-.).* **331**, 189-191 (2011).

[6] Zhu, D. *et al.* Phonon spectroscopy with sub-meV resolution by femtosecond x-ray diffuse scattering. *Phys. Rev. B* **92**, 054303 (2015).

[7] Wall, S. *et al.* Ultrafast disordering of vanadium dimers in photoexcited VO_2. *Science (80-.).* Pending publication. (2018).

[8] Cavalleri, A. *et al.* Femtosecond Structural Dynamics in VO2 during an Ultrafast Solid-Solid Phase Transition. *Phys. Rev. Lett.* **87**, 237401 (2001).

[9] Harmand, M. *et al.* Achieving few-femtosecond time-sorting at hard X-ray free-electron lasers. *Nat. Photonics* **7**, 215-218 (2013).

[10] Beaud, P. *et al.* A time-dependent order parameter for ultrafast photoinduced phase transitions. *Nat. Mater.* **13**, 923-927 (2014).

[11] Mankowsky, R. *et al.* Nonlinear lattice dynamics as a basis for enhanced superconductivity in YBa2Cu3O6.5. *Nature* **516**, 71-73 (2014).

[12] Kozina, M. *et al.* Terahertz-driven phonon upconversion in SrTiO 3. *Nat. Phys.* **15**, 387-392 (2019).

[13] Trigo, M. *et al.* Fourier-transform inelastic scattering from time- and momentum-dependent phonon - phonon correlations. *Nat. Phys.* **9**, 790-794 (2013).

[14] Baum, P., Yang, D.-S. & Zewail, A. H. 4D Visualization of Transitional Structures in Phase Transformations by Electron Diffraction. *Science (80-.).* **318**, 788-792 (2007).

5.3 Imaging Dynamics in Nanomaterials

The ability to directly image in three-dimensions time varying phenomena in nanoscale materials at the surface and in the bulk can greatly increase our understanding of how novel phases develop and how they influence the material properties. Coherent diffractive imaging (CDI) without lenses is a form of microscopy that can permit high resolution imaging where the use of conventional optics is not feasible. When combined with ultra-fast x-rays, time-resolved Bragg CDI provides a novel and robust means to image ordered material systems with sub-angstrom sensitivity. Such insight will greatly aid our understanding of nanomaterials and will serve as a platform to develop next generation materials and devices.

5.3.1 Introduction to science topic

Nanomaterials are materials in which the defining characteristics of the material are size dependent. Technologies developed from nanomaterials are the subject of multidisciplinary research stemming from more traditional disciplines that routinely study the physical, chemical, biological, engineering and electronic aspects of materials. Nanomaterials have found use in a wide range of disciplines owing to their unique and often tunable physical, chemical and biological properties that often differ widely from the bulk material. [1]

When materials are reduced to the nanoscale, their behaviour often differs widely from the bulk material due to quantum confinement effects and the increased surface to volume ratio that may result in behaviour that is dominated by surface properties. [2] It is for this reason that our ability to directly image materials in three-dimensions at the surface and in the bulk can greatly increase our understanding of how novel phases develop and influence the material properties. Progress in the study of nanomaterials will require tools to characterise the nanoscale structure in three-dimensions with atomic precision.

The dynamics of nanomaterials are governed by their quantum properties. Strong coupling between lattice, charge, spin and orbital degrees of freedom often give rise to emergent behaviour and multi-functional properties. [3-6] Such materials are of great interest because the different properties may work together in uniquely different ways and lead to exciting new applications, if we could understand this better. For example, the coupling between magnetic spin and ferroelectric charge ordering can be utilised to develop magnetoelectronic devices where spin transport can be controlled electrically. This is advantageous for technological applications including novel sensors and ultra-low power memory devices. As a result there is a vibrant effort to understand the underlying mechanisms at work. [7-9]

Nanomaterials where degrees of freedom are strongly correlated can exhibit novel short-lived non-equilibrium phases that occur on the femtosecond time-scale. They include light-induced superconductivity, terahertz induced ferroelectricity and ultra-fast solid-phase structural transformations. [10-14] Efforts to shed light on these hidden phases are further compounded by limited theoretical framework that is able to adequately describe the spontaneous emergence of new phases of materials due to external excitation. In addition, Few studies are dedicated to time resolved measurements due to the limitations on adequate tools. For example, electron microscopes are able to resolve atomic scale features of sufficiently thin materials but have poor time resolution. [15] In addition, femtosecond laser systems (excluding hard X-ray sources, treated here) have poor spatial resolution and cannot resolve atomic structural changes. The key to deciphering these phenomena lies in measuring time-dependent changes in the materials structure in three dimensions. The ability to directly image these processes in three-dimensions at the surface and in the bulk will greatly increase our understanding of how the phase is initiated, proliferates and gives rise to emergent properties.

With the advent of 4th generation x-ray free electron laser (XFEL) facilities, it has become possible to study ultra-fast structural dynamics in nanoscale materials for the first time. [16,17] This is enabled by the femtosecond coherent x-ray pulses produced by the XFEL. Three-dimensional imaging at the

surface and bulk of structural properties in nanoscale materials is made possible through lens-less imaging techniques such as coherent x-ray imaging (CDI). [18] The following section provides an overview of the current state of the art in imaging of dynamics in nanomaterials at XFEL facilities. Imaging of biological nanomaterials is omitted and is instead treated in sections 3.4 and 7.5.

5.3.2 Background including earlier research at XFELs and by other methods

Traditional non-destructive methods for the study of nanomaterials such as scanning electron microscopy (SEM), transmission electron microscopy (TEM), atomic force microscopy (AFM) and numerous spectroscopic techniques can provide detailed information on the surface structure but do not directly probe the structure within its volume as a whole. Coherent diffraction imaging (CDI) is a powerful lens-less imaging technique for probing nanometre sized crystalline materials with sub-angstrom sensitivity. It is an attractive alternative to electron microscopy because of the better penetration of the electromagnetic waves in materials of interest, which are often less damaging to the sample than electrons. [18,19] There are a number of important variations on the conventional CDI method. They include forward scattering CDI which is ideally performed on non-periodic structures and Bragg Coherent X-ray diffraction Imaging (BCXDI). [20-25] Forward scattering CDI has found many uses including serial crystallography and imaging extended objects (see sections 3.4 and 7.5)

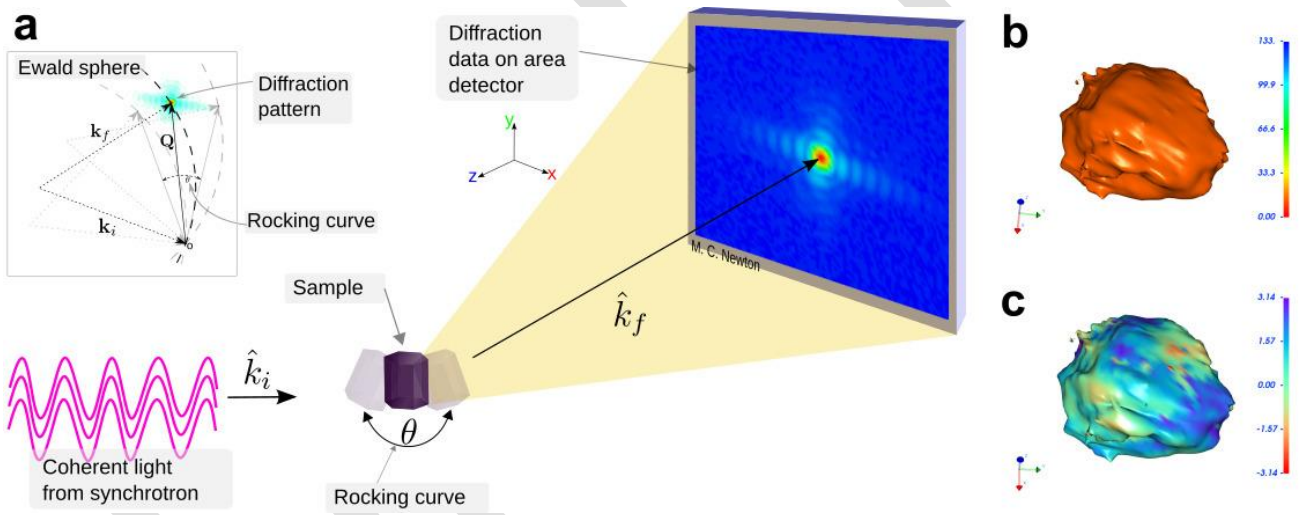

Figure 5.5: Illustration of the BCXDI imaging experiment. ***a****, Schematic of the BCXDI imaging experiment showing coherent X-ray illumination of a single nanocrystal in the Bragg geometry. The inset illustrates Evald sphere construction of the experimental geometry in reciprocal space.* ***b****, Reconstruction of the electron density amplitude of a single nanocrystal approximately 300 nm in length.* ***c****, Phase information shown at the surface of the nanocrystal in* ***b****.*

BCXDI is the reflection scattering variant of CDI. [18] BCXDI holds great promise for understanding transient phases in correlated nanomaterials (Figure 5.5). It is also largely non-destructive and provides structural information at the surface and throughout the bulk of a material. BCXDI was first applied to the study of gold nanocrystals [20, 22] Later it was shown that BCXDI also offers a means to determine in three-dimensions any structural changes due to strain, most likely to occur for nanocrystals that experience a structural distortion due to defects or external perturbation. [26]

When coupled with an ultra-fast coherent x-ray excitation source, BCXDI can be performed in a stroboscopic mode to provide time-resolved images in three-dimensions with nanometre resolution and angstrom sensitivity. The spatial coherence of an XFEL beam ensures that BCXDI is feasible. The earliest example of time-resolved three dimensional imaging of nanomaterials was performed on gold nanocrystals at the Linac Coherent Light Source (LCLS). [27] By utilising femtosecond laser pulses to excite the nanomaterial and femtosecond x-rays to probe in a 'pump-probe' experiment, it was

possible to obtain three-dimensional images of the generation and subsequent evolution of coherent acoustic phonons on the picosecond time scale within a single gold nanocrystal thus providing insights into the physics of the phenomenon. Further studies have focussed on a broader range of materials systems such ultra-fast processes in complex transition metal-oxides. [28-31]

5.3.3 What are the important future opportunities with XFELs

Ultra-short pulses of coherent x-rays beams hold the unique potential to record time-varying three-dimensional images of electronic, magnetic and crystalline structural properties in quantum nanomaterials. The potential to image the inner workings of transient phenomena in and out of equilibrium including (multiferroic) phase-domain structures, dislocations, topological nanocrystals, strong-phase structures and structural phase transitions in three-dimensions will provide a potential route to solving long standing problems that are driven by strong correlations. There remains a wide range of prototype quantum material systems that are not fully understood and yet lend themselves to XFEL experiments. They include multiferroic perovskite materials [32,33] (e.g. $BiFeO_3$, $YMnO_3$, La_xCa_{x-1} MnO_3 (LCMO), $La_xSr_{x-1}FeO_3$ (LSFO), $La_xSr_{x-1}MnO_3$ (LSMO) and $PbVO_3$) for electronically mediated spin transport devices, structural phase change materials (e.g. $BaTiO_3$, VO_2) for femto-second ultra-fast optoelectronic switches, [34,35] and ion diffusion in battery materials such as $LiCoO_2$.

The remaining challenges for imaging quantum material systems are two fold. The first is the difficulty measuring nanoscale materials using single extremely intense and short x-ray pulses before the onset of radiation damage (diffraction before destruction). For nanomaterials other than simple metals, this can pose a challenge when employed in a pump-probe measurement. The second is related to the ultimate resolution of attainable by x-ray imaging methods which is ~5 nm at present. Further development of XFEL facilities with increased x-ray brilliance will enable CDI methods to achieve atomic resolution and realise a long standing dream of an atomic-resolution x-ray microscope. [18,36]

5.3.4 Summary/Conclusion

The UK has significant strength in theoretical research into quantum materials and nanotechnology. There is also a strong global community in x-ray diffraction imaging techniques. For the UK's x-ray facilities to maintain world class status, it is essential that important scientific questions are addressed and emerging techniques such as ultrafast CDI are continuously developed and utilised. An XFEL that can reveal ultra-fast processes that occur on the femtosecond time scale and beyond will prove an invaluable asset for the development of next generation quantum technologies and will solicit the UK as world leading in ultra-fast imaging of quantum materials.

References

[1] Nanoscience and nanotechnologies: opportunities and uncertainties, The Royal Society and Royal Academy of Engineering (2004).

[2] Volokitin, Y., Sinzig, J., de Jongh, L. et al. Quantum-size effects in the thermodynamic properties of metallic nanoparticles. Nature 384, 621-623 (1996).

[3] Morosan, E., Natelson, D., Nevidomskyy, A.H. and Si, Q., Strongly Correlated Materials. Adv. Mater. 24, 4896-4923 (2012).

[4] Elbio Dagotto, Complexity in Strongly Correlated Electronic Systems, Science 08, 257-262 (2005)

[5] Multiferroics march on, Nature Materials 18, 187-187 (2019)

[6] Spaldin, N. A. & Ramesh, R., Ad- vances in magnetoelectric multiferroics, Nature Materials 18, 203-212 (2019).

[7] Vogel, E. Technology and metrology of new electronic materials and devices. Nature Nanotech 2, 25-32 (2007).

[8] Yang, J., Strukov, D. & Stewart, D. Memristive devices for computing. Nature Nanotech 8, 13-24 (2013).

[9] Tan, D.H.S., Banerjee, A., Chen, Z. et al. From nanoscale interface characterization to sustainable energy storage using all-solid-state batteries. Nature Nanotech 15, 170-180 (2020).

[10] D. Fausti, R. I. Tobey, N. Dean, S. Kaiser, A. Dienst, M. C. Hoffmann, S. Pyon, T. Takayama, H. Takagi, A. Cavalleri, Light-Induced Superconductivity in a Stripe-Ordered Cuprate, Science 14, 189-191 (2011)

[11] S. Kaiser, C. R. Hunt, D. Nicoletti, W. Hu, I. Gierz, H. Y. Liu, M. Le Tacon, T. Loew, D. Haug, B. Keimer, and A. Cavalleri, Optically induced coherent transport far above Tc in underdoped $YBa_2Cu_3O_{6+\delta}$, Phys. Rev. B 89, 184516 (2014).

[12] Hu, W., Kaiser, S., Nicoletti, D. et al. Optically enhanced coherent transport in YBa2Cu3O6.5 by ultrafast redistribution of interlayer coupling. Nature Mater 13, 705-711 (2014).

[13] By Xian Li, Tian Qiu, Jiahao Zhang, Edoardo Baldini, Jian Lu, Andrew M. Rappe, Keith A. Nelson, Terahertz field-induced ferroelectricity in quantum paraelectric $SrTiO_3$, Science14, 1079-1082 (2019).
[14] Newton, Marcus C., Sao, Mayu, Fujisawa, Yuta, Onitsuka, Rena, Kawaguchi, Tomoya, Tokuda, Kazuya, Sato, Takahiro, Togashi, Tadashi, Yabashi, Makina, Ishikawa, Tetsuya, Ichitsubo, Tetsu, Matsubara, Eiichiro, Tanaka, Yoshihito and Nishino, Yoshinori, Time-Resolved Coherent Diffraction of Ultrafast Structural Dynamics in a Single Nanowire, Nano Letters 14, 2413-2418 (2014).
[15] Hyun Soon Park, Oh-Hoon Kwon, J. Spencer Baskin, Brett Barwick, and Ahmed H. Zewail, Direct Observation of Martensitic Phase-Transformation Dynamics in Iron by 4D Single-Pulse Electron Microscopy, Nano Letters 9 (11), 3954-3962 (2009).
[16] Emma, P., Akre, R., Arthur, J. et al. First lasing and operation of an ångstrom-wavelength free-electron laser. Nature Photon 4, 641-647 (2010).
[17] Margaritondo G. and Ribic P.R., A simplified description of X-ray free-electron lasers, Journal of Synchrotron Radiation 18(2), 101-108 (2011).
[18] Jianwei Miao, Tetsuya Ishikawa, Ian K. Robinson, Margaret M. Murnane, Beyond crystallography: Diffractive imaging using coherent x-ray light sources, Science, 530-535 (2015).
[19] Robinson, I., Harder, R. Coherent X-ray diffraction imaging of strain at the nanoscale. Nature Mater 8, 291-298 (2009).
[20] I. K. Robinson, I. A. Vartanyants, G. J. Williams, M. A. Pfeifer, J. A. Pitney, Reconstruction of the shapes of gold nanocrystals using coherent x-ray diffraction. Phys. Rev. Lett. 87, 195505 (2001).
[21] J. Miao, T. Ishikawa, B. Johnson, E. H. Anderson, B. Lai, K. O. Hodgson, High resolution 3D x-ray diffraction microscopy. Phys. Rev. Lett. 89, 088303 (2002).
[22] M. A. Pfeifer, G. J. Williams, I. A. Vartanyants, R. Harder, I. K. Robinson, Three-dimensional mapping of a deformation field inside a nanocrystal. Nature 442, 63-66 (2006).
[23] H. N. Chapman, A. Barty, M. J. Bogan, S. Boutet, M. Frank, S. P. Hau-Riege, S. Marchesini, B. W. Woods, S. Bajt, W. H. Benner, R. A. London, E. Plönjes, M. Kuhlmann, R. Treusch, S. Düsterer, T. Tschentscher, J. R. Schneider, E. Spiller, T. Möller, C. Bostedt, M. Hoener, D. A. Shapiro, K. O. Hodgson, D. van der Spoel, F. Burmeister, M. Bergh, C. Caleman, G. Huldt, M. M. Seibert, F. R. N. C. Maia, R. W. Lee, A. Szöke, N. Timneanu, J. Hajdu, Femtosecond diffractive imaging with a soft-X-ray free-electron laser. Nat. Phys. 2, 839-843 (2006).
[24] G. J. Williams, H. M. Quiney, B. B. Dhal, C. Q. Tran, K. A. Nugent, A. G. Peele, D. Paterson, M. D. de Jonge, Fresnel coherent diffractive imaging. Phys. Rev. Lett. 97, 025506 (2006).
[25] J. M. Rodenburg, A. C. Hurst, A. G. Cullis, B. R. Dobson, F. Pfeiffer, O. Bunk, C. David, K. Jefimovs, I. Johnson, Hard-x-ray lensless imaging of extended objects. Phys. Rev. Lett. 98, 034801 (2007).
[26] M. C. Newton, S. J. Leake, R. Harder, I. K. Robinson, Three-dimensional imaging of strain in a single ZnO nanorod. Nat. Mater. 9, 120-124 (2010).
[27] J. N. Clark, L. Beitra, G. Xiong, A. Higginbotham, D. M. Fritz, H. T. Lemke, D. Zhu, M. Chollet, G. J. Williams, M. Messerschmidt, B. Abbey, R. J. Harder, A. M. Korsunsky, J. S. Wark, I. K. Robinson, Ultrafast three-dimensional imaging of lattice dynamics in individual gold nanocrystals. Science 341, 56-59 (2013).
[28] D. Rudolf, C. La-O-Vorakiat, M. Battiato, R. Adam, J. M. Shaw, E. Turgut, P. Maldonado, S. Mathias, P. Grychtol, H. T. Nembach, T. J. Silva, M. Aeschlimann, H. C. Kapteyn, M. M. Murnane, C. M. Schneider, P. M. Oppeneer, Ultrafast magnetization enhancement in metallic multilayers driven by superdiffusive spin current. Nat. Commun. 3, 1037 (2012).
[29] A. Barty, S. Boutet, M. J. Bogan, S. Hau-Riege, S. Marchesini, K. Sokolowski-Tinten, N. Stojanovic, R. Tobey, H. Ehrke, A. Cavalleri, S. Düsterer, M. Frank, S. Bajt, B. W. Woods, M. M. Seibert, J. Hajdu, R. Treusch, H. N. Chapman, Ultrafast single-shot diffraction imaging of nanoscale dynamics. Nat. Photonics 2, 415-419 (2008).
[30] J.-D. Nicolas, T. Reusch, M. Osterhoff, M. Sprung, F. J. R. Schülein, H. J. Krenner, A. Wixforth, T. Salditt, Time-resolved coherent X-ray diffraction imaging of surface acoustic waves. J. Appl. Cryst. 47, 1596-1605 (2014).
[31] Marcus C. Newton, Mayu Sao, Yuta Fujisawa, Rena Onitsuka, Tomoya Kawaguchi, Kazuya Tokuda, Takahiro Sato, Tadashi Togashi, Makina Yabashi, Tetsuya Ishikawa, Tetsu Ichitsubo, Eiichiro Matsubara, Yoshihito Tanaka, and Yoshinori Nishino, Time-Resolved Coherent Diffraction of Ultrafast Structural Dynamics in a Single Nanowire, Nano Letters 14 (5), 2413-2418 (2014).
[32] Choi, T., Lee, S., Choi, Y. J., Kiryukhin, V. & Cheong, S.-W., Switch- able Ferroelectric Diode and Photovoltaic Effect in BiFeO3, Science 324, 63-66 (2009).
[33] Bibes, M. & Barthelemy, A., Multiferroics: Towards a magnetoelectric memory, Nature Materials 7, 425-426 (2008).
[34] Cavalleri, A. et al., Femtosecond Structural Dynamics in VO2 during an Ultrafast Solid-Solid Phase Transition, Phys. Rev. Lett. 87, 237401 (2001).
[35] Nakano, M. et al., Collective bulk carrier delocalization driven by electrostatic surface charge accumulation, Nature 487, 459-462 (2012).
[36] Vartanyants, I. A., Robinson, I. K., McNulty, I., David, C., Wochner, P. & Tschentscher, Th., J. Synchrotron Rad. 14, 453-470 (2007).

5.4 Electronic Dynamics in Quantum Materials

Ultra-fast photoelectron spectroscopy (PES) is an enabling technique to prove insight into spin, orbital and charge degrees of freedom of chemical bonding characteristics in quantum materials. PES techniques combined with ultra-fast x-rays will provide much needed answers to questions related to dynamic behaviour on the femto-second timescale.

5.4.1 Introduction to science topic

Correlating the structure and electronic structure of materials lies at the core of our understanding of functional materials. When moving from bulk to quantum materials we encounter a significant increase in complexity due to the special confinement of electronic states, e.g. at surfaces and interfaces. In many technologically relevant device systems, the overall electronic behaviour is dominated solely by interfaces rather than the surrounding extended structures. Even minute changes in the structure of a material can lead to significant differences in its electronic structure and the resulting electronic behaviour, determining whether a material is a metal, semimetal, semiconductor or insulator. The detailed nature of the electronic structure, including band structure, intrinsic and extrinsic charge carriers, and defect and trap states, is of great importance to further develop future device generations.

To date, physical characterisation techniques are predominantly confined to the study of the electronic structure in static, often bulk samples. Dynamic behaviour is often inferred by combining electrical measurements and physical characterisation at specific points, which are “frozen in time”. FELs provide an unmatched opportunity to study electronic structure dynamics in energy, space and time providing a high level of understanding of quantum materials, which is essential to future application developments.

5.4.2 Background including earlier research at XFELs and by other methods

One of the key techniques to study the electronic structure of matter is photoelectron spectroscopy (PES). Excitation sources from the UV to soft and hard X-rays are used to probe the occupied valence states and in specific cases occupied conduction states of materials including gases, liquids and solids. The technique is intrinsically referenced to the Fermi energy of the sample and can provide not only information on the chemical nature of bands in solids, but also their overall alignment. The correlation of changes of the electronic structure of a material with both core level and valence spectra is immensely powerful to study local chemical environments as well as the electron density and distribution of a system.

Standard PES is performed routinely in laboratories worldwide, but synchrotron sources are necessary for advanced studies. In particular, probing of low occupation states, often vital to electronic behaviour, necessitates the high flux provided by synchrotrons to enable the detection of such low intensity features. In addition, the energy tunability of synchrotrons enables measurements under resonant conditions and the associated discrimination between states of different orbital character enables the identification of specific contributions to the overall complex band structure. XFELs are expanding the dimensions PES can explore from energy, space and spin to time enabling multi-dimensional analysis of electronic structure dynamics.

The most important limitation for PES at FELs is the existence of vacuum space charge effects. The extremely brilliant FEL pulses generate a dense cloud of photoelectrons at the sample surface and the Coulomb repulsion of the electrons leads to a strong distortion of the initial photoelectron energy distribution. This leads to shifting and overall broadening of spectra and therefore a loss in effective energy resolution. Both computational and experimental solutions to this challenge are being proposed and are at the core of current developments.[1-4]

One completely new area that XFELs have opened up is X-ray two-photon photoelectron spectroscopy (XTPPS). This technique exploits the femtosecond timescales provided at XFELs and follows the formation of single or two site double core hole (ssDCH, tsDCH) states caused by the sequential absorption of two X-ray photons at a time scale matching the lifetime of Auger decay (below 10 fs). The DCH states have been shown to probe the local chemical environment more sensitively compared to single core hole (SCH) states as they are directly coupled to any changes in valence electron structure of the two core hole atomic sites.[5-7] Figure 5.6shows a schematic of the different accessible core hole states. Access to this new regime in PES enables a detailed investigation of both core and valence structure of matter.

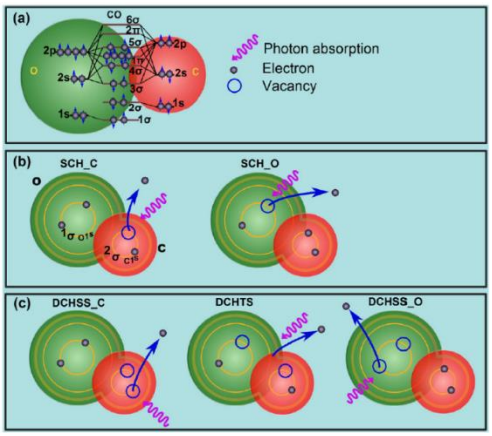

Figure 5.6: Cartoon design of (a) the electronic structure of the CO molecule, (b) the SCH ionization at the C K-edge and the O K-edge, and (c) the ssDCH ionization at the C K-edge, the ssDCH ionization of the O K-edge and the tsDCH ionization. Taken from Ref. [7]

Time-resolved PES including XPS (trPES, trXPS) enables access to electronic state dynamics in quantum materials. To date, experiments have been performed using laboratory laser sources and synchrotrons [8,9] as well as XFELs. [1,10] Pioneering work by Hellmann and co-workers focused on understanding metal-insulator transitions essential for so many electronic devices.[8,10] Their work focused on the Mott insulator 1T-TaS_2 and they successfully employed femtosecond time-resolved core-level photoelectron spectroscopy as well as time-resolved angle-resolved PES (trARPES) to explore atomic-site specific charge-order dynamics of the charge-density wave and the relative contributions of electron-electron and electron-phonon interactions to electronic order in momentum space. Figure 5.7 shows time-resolved ARPES spectra of a range of layered compounds.[8]

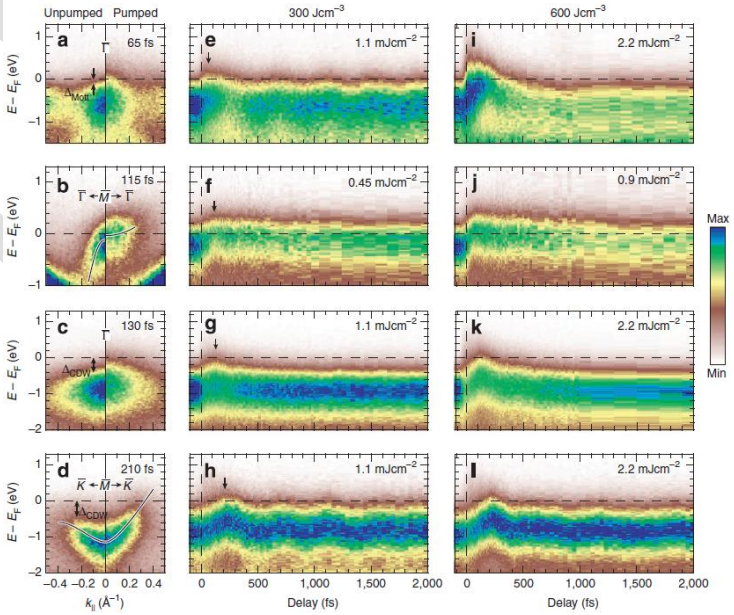

Figure 5.7: Time-resolved momentum-space view of the electronic structure in layered charge-density-wave compounds, including 1T-TaS_2, 1T-$TiSe_2$, and 1T-TaS_2. Taken from Ref.[8]

Beyond soft X-ray PES, recent years have shown considerable development of time-resolved hard X-ray PES (trHAXPES) setups and experiments. [11,12] The main advantage of HAXPES over XPS is the significant increase in probing depth enabling the exploration of bulk systems and buried layers and interfaces often crucial to material behaviour in a device context. Oloff and co-workers could show that it is possible to resolve intrinsic charge-carrier recombination dynamics in electron-doped $SrTiO_3$ establishing trHAXPES as a well-placed technique to study intrinsic charge-carrier dynamics on ultrafast time scales.[12]

Recent work by Kutnyakhov and co-workers presents the culmination of current developments for muldimensional PES.[3] They developed a novel setup at FLASH which combines full-field momentum imaging and time-of-flight energy recording. Combined with the photon energies available at FLASH and other FELs this will enable time-resolved experiments from core level to valence band spectroscopy and photoelectron diffraction exploiting the tunability of the photon energy to access varying probing depths.

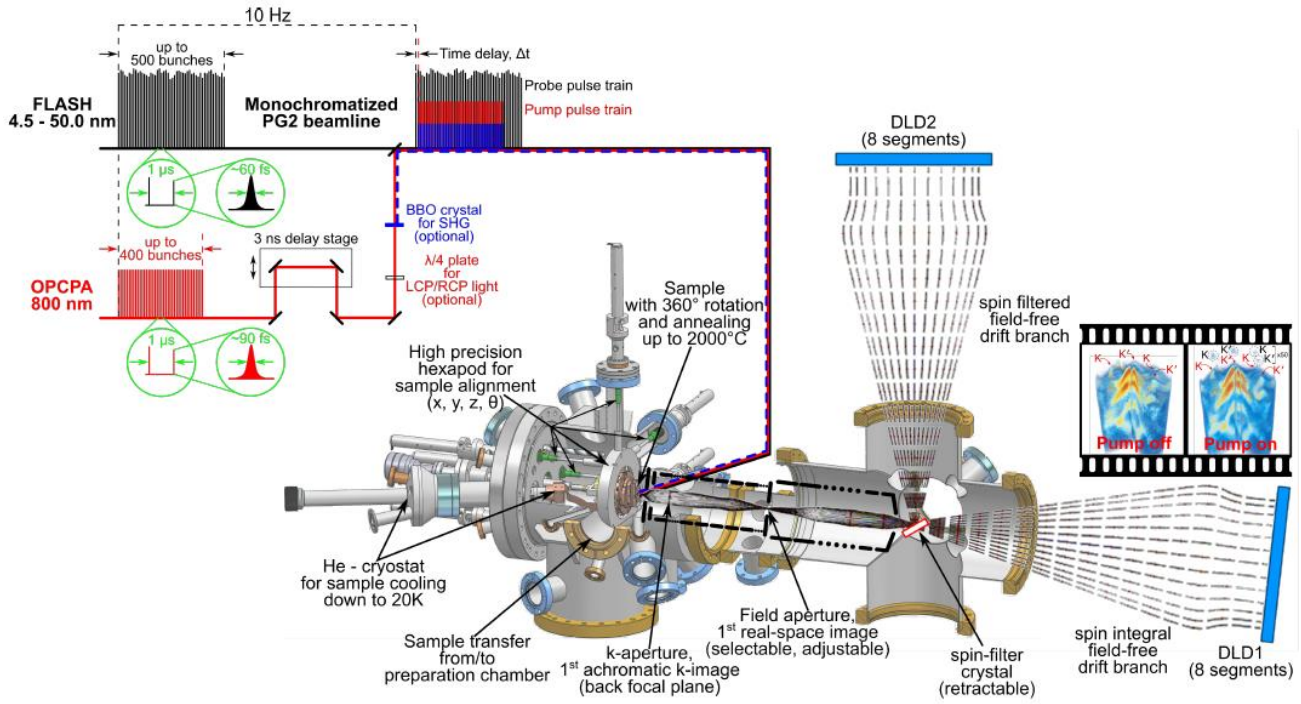

Figure 5.8: Simplified overview of the FLASH pulse structure, the PG2 beamline with synchronized pump laser (top left) and the experimental setup (middle) used to perform time-resolved momentum microscopy and acquire volumetric band-mapping movies (right inset) by means of a multidimensional recording scheme. Taken from Ref. [3]

5.4.3 What are the important future opportunities with XFELs

XFELs already routinely provide access to femtosecond timescales and first measurement with attosecond resolution have been reported. This provides access to electronically relevant time scales allowing to probe electron dynamics in real time. XFELs will enable to go beyond static measurements of electronic structure towards a full dynamic picture of the electronic behaviour of charge carriers.

Several challenges remain when wanting to probe electronic structure both statically and dynamically in quantum materials. One of the biggest practical limitations to date is the difficulty of obtaining useable signals from often small spectral features using short, extremely intense X-ray pulses without acquiring data influenced by radiation damage. Sample delivery and data acquisition systems for nanomaterials as well as structured multilayer materials including buried interfaces will need substantial further development to enable probing of low intensity contributions to e.g. density of states.

As mentioned above, space charge is a fundamental problem for PES and high repetition rate sources combined with high efficiency electron detectors are necessary to combat it negative effects. Detector developments, e.g. the introduction of single-shot data acquisition system which can be combined with existing high-resolution hemispherical electron energy analysers are an integral part of future advances.[13] In parallel, ongoing development of powerful momentum microscope systems for both the soft and hard X-ray regimes is pushing towards three-dimensional data acquisition, collecting electron energies and their distribution in k-space on relevant time scales.[14-19]

Multiple ionisation events and their use as chemical and electronic probes in PES are an exciting emerging area of study which promises new insights into both core and valence electronic nature of materials. Ongoing research is focusing on the extension of current work on small molecular species to more complex materials in the view to establish this technique for quantum materials.

5.4.4 Summary/Conclusion

The UK has a strong, long standing record in photoelectron spectroscopy and its application to study the electronic structure of matter. This is complemented by an outstanding theory community supporting experimental efforts. The continuous development of experimental techniques at X-ray facilities is crucial to the understanding and development of future electronic materials and their applications.

The possibility to investigate ultrafast electron dynamics across a wide range of both chemical and physical systems using time-resolved PES is a game changer in the area of quantum technologies. The simultaneous detection of the electronic, spin, and overall structure of a material on relevant timescales in the femto- and attosecond regime will open up a completely new way to directly probe the interactions between electronic, spin and lattice dynamics in quantum materials enabling the emergence of new technological applications.

References

[1] Hellmann, S., Sohrt, C., Beye, M., Rohwer, T. & Sorgenfrei, F. Time-resolved x-ray photoelectron spectroscopy at FLASH. *New J. Phys.* **14**, 013062 (2012).

[2] Pietzsch, A. *et al.* Towards time resolved core level photoelectron spectroscopy with femtosecond x-ray free-electron lasers. *New J. Phys.* **10**, 033004 (2008).

[3] Kutnyakhov, D. *et al.* Time- and momentum-resolved photoemission studies using time-of-flight momentum microscopy at a free-electron laser. *Rev. Sci. Instrum.* **91**, 013109 (2020).

[4] Schönhense, B. *et al.* Multidimensional photoemission spectroscopy - the space-charge limit. *New J. Phys.* **20**, 033004 (2018).

[5] Salén, P. *et al.* Experimental Verification of the Chemical Sensitivity of Two-Site Double Core-Hole States Formed by an X-Ray Free-Electron Laser. *Phys. Rev. Lett.* **108**, 153003 (2012).

[6] Fukuzawa, H. *et al.* Deep Inner-Shell Multiphoton Ionization by Intense X-Ray Free-Electron Laser Pulses. *Phys. Rev. Lett.* **110**, 173005 (2013).

[7] Berrah, N. & Fang, L. Chemical analysis: Double core-hole spectroscopy with free-electron lasers. *J. Electron Spectrosc. Relat. Phenom.* **204**, 284-289 (2015).

[8] Hellmann, S. *et al.* Time-domain classification of charge-density-wave insulators. *Nat. Commun.* **3**, 1069 (2012).

[9] Pressacco, F. *et al.* Laser induced phase transition in epitaxial FeRh layers studied by pump-probe valence band photoemission. *Struct. Dyn.* **5**, 034501 (2018).

[10] Hellmann, S. *et al.* Ultrafast Melting of a Charge-Density Wave in the Mott Insulator 1 T − TaS 2. *Phys. Rev. Lett.* **105**, 187401 (2010).

[11] Oloff, L.-P. *et al.* Time-resolved HAXPES at SACLA: probe and pump pulse-induced space-charge effects. *New J. Phys.* **16**, 123045 (2014).

[12] Oloff, L.-P. *et al.* Time-resolved HAXPES using a microfocused XFEL beam: From vacuum space-charge effects to intrinsic charge-carrier recombination dynamics. *Sci. Rep.* **6**, 35087 (2016).

[13] Oura, M. *et al.* Development of a single-shot CCD-based data acquisition system for time-resolved X-ray photoelectron spectroscopy at an X-ray free-electron laser facility. *J. Synchrotron Radiat.* **21**, 183-192 (2014).

[14] Tusche, C., Krasyuk, A. & Kirschner, J. Spin resolved bandstructure imaging with a high resolution momentum microscope. *Ultramicroscopy* **159**, 520-529 (2015).

[15] Tusche, C. *et al.* Multi-MHz time-of-flight electronic bandstructure imaging of graphene on Ir(111). *Appl. Phys. Lett.* **108**, 261602 (2016).

[16] Medjanik, K. *et al.* Direct 3D mapping of the Fermi surface and Fermi velocity. *Nat. Mater.* **16**, 615-621 (2017).

[17] Medjanik, K. *et al.* Progress in HAXPES performance combining full-field *k* -imaging with time-of-flight recording. *J. Synchrotron Radiat.* **26**, 1996-2012 (2019).

[18] Fedchenko, O. *et al.* High-resolution hard-x-ray photoelectron diffraction in a momentum microscope—the model case of graphite. *New J. Phys.* **21**, 113031 (2019).

[19] Babenkov, S. *et al.* High-accuracy bulk electronic bandmapping with eliminated diffraction effects using hard X-ray photoelectron momentum microscopy. *Commun. Phys.* **2**, 107 (2019).

5.5 Time Resolved Pair Distribution Functions

Persistent disorder in quantum materials can appear in various forms including chemical, electronic, magnetic and geometric. Correlations present within the disorder often give rise to novel phases in the physical and chemical properties of quantum materials. Pair Distribution Function (PDF) measurements are able to probe disorder and when combined with ultra-fast x-rays, provide a potent method to identify the symmetry breaking transitions.

5.5.1 Introduction to science topic

There is strong community interested in total scattering and Pair Distribution Function (PDF) techniques in the UK using both X-rays and neutrons and exploiting the Diamond and ISIS facilities. The PDF is the Fourier transform of the total scattering intensity, which maps the probabilities of distances between all pairs of atoms [1]. This function can be modelled precisely. We expect there will be significant interest in developing the instrumentation and methodology needed to measure time-resolved X-ray PDFs at the future UK-XFEL. Many of the problems of interest to this community will carry over into the time domain with the provision of a pump-probe methodology.

One immediate application would be to address the important Orbital Degeneracy Lifting (ODL) ideas, widespread in Quantum Materials, particularly those containing transition metal elements with partially filled d-orbitals [2]. The ability to access the femto- and picosecond time domain will enable a completely new dimension of understanding of ODL physics by investigating the speed of its response to an ultrafast laser stimulus. ODL is a local state lacking long-range order, established to lift orbital degeneracies imposed by the high temperature crystal structure. Being electronic in nature and breaking crystal symmetry, it is expected both to fluctuate rapidly and to respond to a driving laser excitation. ODL leads to a subtle kind of local order that is invisible to most other X-ray analytical techniques, but can be clearly seen through the real-space PDF approach. ODL is hard to measure with X-ray Bragg diffraction because it is a local effect within a crystal that does not change its overall symmetry; it therefore produces broad diffuse scattering in reciprocal space. ODL could be responsible for local the local symmetry-breaking electronic nematicity found in a range of quantum materials, especially complex oxides and chalcogenides [3,4].

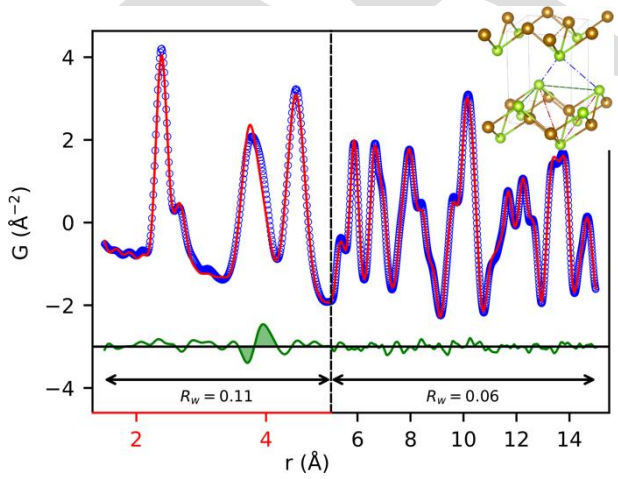

Figure 5.9: X-ray Pair Distribution Function measured from tetragonal FeSe at 300K, well above its orthorhombic phase transition at 90K. Local fluctuations are apparent in the second-neighbour peak at 3.9Å, indicating local symmetry breaking. [5] It is believed this is driven by local fluctuations in the d-orbitals, whose time-dependence could be tracked in a future tr-PDF experiment at the UK XFEL.

5.5.2 Background including earlier research at XFELs and by other methods

PDF is a potent method to identify the symmetry breaking which, in extreme cases, leads to crystals with one lattice symmetry at large distances and a completely different symmetry over the short range distance scale. A simple example of ODL explains the symmetry breaking found in FeSe [5]. PDF structural analysis of FeSe has revealed the presence of a local orthorhombic distortion (which lifts the degeneracy of d_{xz} and d_{yz} t_{2g} orbitals and which we have identified as an ODL state) with a correlation length of about 4 nm at temperatures where the average symmetry is tetragonal. FeSe is tetragonal above 90 K, with C_4 rotational symmetry about the c axis. The low-temperature orthorhombic structure

has C_2 symmetry. Fig. 5.5.1 shows that the C_4 structure fits the high-temperature PDF data at distances beyond 6Å, but not below, where the C_2 structure is needed. This large local orthorhombic distortion in FeSe persists over wide ranges of temperatures, including into the nematic state at low temperatures, where the magnitude of the local distortion is much larger than the average crystallographic distortion, suggesting an imperfect long-range ordering of the local state below Ts=90K. Our results point to a model where ODL fluctuations, which persist up to at least 300 K, order at low temperature into the macroscopically orthorhombic phase.

The goal of a UK-XFEL based time-resolved PDF measurement of FeSe would be to investigate the sequence of events following optical pumping into the valence band, followed by occupation of the Fe d-orbitals relevant to ODL and the subsequent local distortion of the lattice. Ultrafast Electron Diffraction (UED) studies of FeSe have already shown the sort of information that might be learned [6].

Another class of materials which will be accessible by trPDF are the "relaxor ferroelectrics". This behaviour is typically found in perovskite complex oxide crystals, most famously in lead magnesium niobate, $PbMg_{1/3}Nb_{2/3}O_3$ (PMN), which shows unusual local structure and electrical properties. Conventional ferroelectrics exhibit a sharp first-order phase transition from a high temperature paraelectric state to a spontaneously polarized state at the Curie temperature T_C. The phase transformation at T_C is unambiguously associated with a structural phase transition, which provides vital guidance to the design and scientific development of this class of materials. In comparison, relaxor ferroelectrics have a broader transition and never fully order below T_C, but simply slow down to form a glass-like low-temperature state with the same average crystal symmetry as at high temperature. The low-temperature state is called an ergodic relaxor (ER) state [7], often explained by nanometer scale regions, called "polar nano regions" (PNRs), which possess randomly oriented dipole moments.

The existence of these PNRs has a dramatic effect on the electrical behavior and shows a characteristic frequency dependence of the dielectric constant. Unlike the conventional ferroelectrics, which exhibit a Curie-Weiss divergence of ε at T_C, PMN and other relaxors exhibit a rounded peak, which shifts to higher temperatures with frequency. The peak in ε depends very strongly on the measurement frequency, which indicates that there are relaxational dynamics with timescales that freeze out at different temperatures. The origin of this time scale, its dependence on other experimental parameters has been phenomenologically explained by a thermally activated reconfiguration of the polarization [8], but this explanation is not microscopically understood despite extensive neutron [9] and X-ray [10] diffuse scattering studies and X-ray PDF investigation [11, 10].

5.5.3 What are the important future opportunities with XFELs

To develop the tr-PDF method at the UK-XFEL will present some challenges. First and foremost, high energy X-rays are need ideally up to 50keV. A large area detector sensitive to these high energy X-rays, such as the Rayonix (MAR) MX340-XFEL will then have to be augmented with a CdTe sensor. The lowest conceivable energy would be about 25keV. This is needed to obtain a wide enough Q-range, with $Q_{max} = 25Å^{-1}$ needed to fully resolve the peaks in the PDF in real space, as seen in Figure 5.9. New detector geometries, conceivably a wrap-around back-scattering layout, could be introduced to get to high Q_{max} with lower energy X-rays. PDF structure refinements and simulations can then be obtained with the existing PDFgui program suite [12] or RMCProfile codes [13].

A general challenge in all pump-probe experiments is to obtain a good laser/X-ray overlap to ensure that every part of the sample responds to the laser pump. For PDF experiments, we could use spin-coating to make thin layer samples of finely ground material on Si_3N_4 membrane windows, aiming for say 10um crystals in a close packed single layer. This design would allow every crystal to see the laser at normal incidence. The photo-stimulated electrons generated by the pump laser would traverse the grain quickly in the metallic state to provide overlap everywhere, not just within the electromagnetic skin depth. The X-ray beam will be spread over 100's of microns, even up to $1mm^2$. This helps the powder averaging and spreads the dose so we can stay below the sample damage threshold. But it is important to avoid "shadowing" of grains that would not see the laser.

References

[1] D. A. Keen and A. L. Goodwin "The crystallography of correlated disorder" Nature **521** 303 (2015)

[2] E. S. Bozin, W.G. Yin, R. J. Koch, M. Abeykoon, Y. S. Hor, H. Zheng, H. C. Lei, C. Petrovic, J. F. Mitchell and S. J. L. Billinge, Local orbital degeneracy lifting as a precursor to an orbital-selective Peierls transition, Nature Comms **10** 3638 (2019)

[3] J. Wu, A. T. Bollinger, X. He and I. Bozovic, Spontaneous breaking of rotational symmetry in copper oxide superconductors, Nature **547** 432 (2017)

[4] S. A. Kivelson, Fradkin, E. and Emery, V. J. Electronic liquid-crystal phases of a doped Mott insulator. Nature **393** 550-553 (1998)

[5] R. J. Koch, T. Konstantinova, M. Abeykoon, A. Wang, C. Petrovic, Y. Zhu, E. S. Bozin, S. J. L. Billinge, Room temperature local nematicity in FeSe superconductor, Phys. Rev. B **100** 020501 (2019)

[6] T. Konstantinova, L. Wu, M. Abeykoon, R. J. Koch, A. F. Wang, R. K. Li, X. Shen, J. Li, J. Tao, I. A. Zaliznyak, C. Petrovic, S. J. L. Billinge, X. J. Wang, E. S. Bozin and Y. Zhu, Photoinduced dynamics of nematic order parameter in FeSe, Phys. Rev. B **99** 180102 (2019)

[7] A. A. Bokov, Z.-G. Ye "Recent Progress in Relaxor Ferroelectrics with Perovskite Structure" J. Materials Sci. **41** 31 (2006)

[8] F. M. Jiang and S. Kojima, "Microheterogeneity and relaxation in $0.65Pb(Mg_{1/3}Nb_{2/3})O_3$-$0.35PbTiO_3$ relaxor single crystals," Appl. Phys. Lett. **77** 1271 (2000)

[9] G. Y. Xu, G. Shirane, J. R. D. Copley, P. M. Gehring "Neutron elastic diffuse scattering study of $Pb(Mg_{1/3}Nb_{2/3})O_3$", Phys. Rev. B **69** 064112 (2004)

[10] A. Bosak, D. Chernyshov, S. Vakhrushev, M. Krisch, Diffuse scattering in relaxor ferroelectrics: true three-dimensional mapping, experimental artefacts and modelling. Acta Cryst. **A68** 117-123 (2012)

[11] S. Vakhrushev, A. Nabereznov, S. K. Sinha, Y. P. Feng, T. Egami, "Synchrotron X-ray scattering study of lead magnoniobate relaxor ferroelectric crystals", J. Phys. Chem. Solids **57** 1517 (1996)

[12] Farrow, C. L. et al. PDFfit2 and PDFgui: computer programs for studying nanostructure in crystals. J. Phys. Condens. Matter. **19** 335219 (2007)

[13] Tucker, M. G. et al. RMCProfile: reverse Monte Carlo for polycrystalline materials. J. Phys.: Condensed Matter **19** 335218 (2007)

6. Science opportunities in the Chemical Sciences and Energy

Virtually any chemical reaction, regardless of the means of its initiation, is enabled and accompanied by simultaneously occurring structural changes, ranging from a complete dissociation of a chemical bond, to subtle fluctuations in local geometries, changes in electronic structure, and often changes of spin-states. XFELs give unique and incisive access to these dynamics, which is vital to scientific understanding and myriad applications of chemistry to real-world applications.

The revolutionary impact of the proposed XFEL on Chemical Sciences – as an integral part of all science and technology areas in the age of multi-disciplinary approaches – will be enabled by a combination of key unique capabilities. Those include high repetition rate of 100 KHz or higher to enable the required sensitivity and signal-to-noise ratio, high brightness of $>10^{12}$ photon/pulse, the broad coverage of X-ray energies – from soft to hard (200 eV to 25 keV) which enable to investigate pretty much all of the periodic table, and the flexibility of combining multiple methods of initiation and monitoring, combining X-rays, electron beams, and optical methods.

To bring about the new level of understanding of areas as diverse as chemistry in space and the origin of life on Earth to photocatalysis or information storage, these processes need to be followed with atomic precision as the system evolves along the multidimensional, multi-parameter landscape. A potential game-changer, ***a combination of X-ray pulses with optical VUV, UV, Vis, IR, THz excitation and detection pulses mixed-and-matched-by-demand,*** is now within reach.

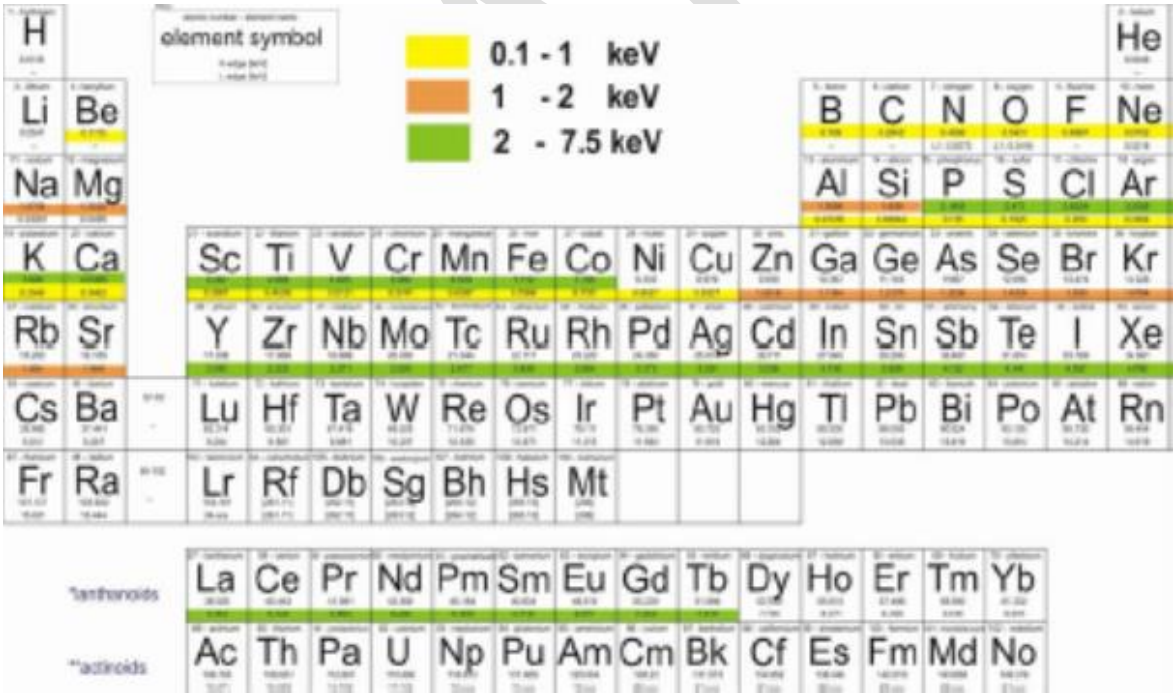

Figure 6.1: The Periodic Table of X-rays (courtesy of C Bressler)

Selected areas discussed below include real-time molecular movies of reactions, transformations, and catalysts with atomic precision, on the timescales from femtosecond upwards; the next level of understanding of the interplay of fundamental nuclear, electronic, and spin dynamics underpinning much of the new 2D-materials, photofunctional materials, materials for energy storage and capture, and catalysis; atmospheric, environmental, and analytical chemistry; chemistry in space; new diagnostics and therapies in medicine – to name but a few.

6.1 Fundamentals of Reaction Dynamics: Coupling between nuclear, electronic and spin degrees of freedom

Chemical dynamics encompasses the entanglement of phenomena across decades of timescales, from femtoseconds (a vibrational period of a chemical bond) to seconds (photosynthesis), involving structural, electronic, and spin sta3tes evolving together. The UK-XFEL source bring about a combination of sufficiently short pulses of photons with energies tuneable from THz to X-ray, sufficiently high repletion rate of >100 KHz, and greatly enhanced brightness of 10^{12} ph/pulse to finally enable a comprehensive interrogation of chemical reactions, non-equilibrium processes, and transformations, "watching chemistry happen".

6.1.1 Introduction

The last decades brought about an explosive development of interrogation of optical phenomena in molecules and materials on the ever shorter time-scales, approaching the very act of breaking or formation of a chemical bond and reaching out into the attosecond domain.[1] Key questions the must be answered include: *Can we possibly ever record a meaningful molecular movie, where the convolved structural, electronic, vibrational, and spin dynamics are resolved simultaneously?*[2] *Can we now establish the role of coherent processes – electronic, vibronic – in charge and energy transport on the nanoscale? Can we do element-specific imaging concurrently with electron density, spin density, and structural changes with fs resolution?*[3–5] Yet optics-based methods cannot measure sub-Angstrom displacement and femtosecond motion in molecules and alternative methods are urgently needed.

A powerful combination of diverse femtosecond X-ray methods with optical methods could potentially answer the underlying questions, including (i) How long does it take the atoms to move?; (ii) Where is the motion localised/delocalised within the molecule or material?; (iii) What is the amplitude and the phase of this motion? (iv) What is the reaction coordinate(s); (v) the role of coherence(s) in ultrafast transformations; (vi) can we alter the outcome of a chemical reaction at will.

The UK XFEL and associated infrastructure of ultrafast optical methods will bring about a combination of short pulses of photons with energies tuneable from THz to X-ray, high repetition rate of >100 KHz, and high brightness to finally enable a comprehensive interrogation of chemical reactions, non-equilibrium processes, and transformations, in a real-time molecular movie. Combining multiple means of initiation and interrogation, we can reach new milestones such as structure of excited/transition states with <0.01 Å resolution; follow coherent vibrations in polyatomic molecules; or direct observation of conical intersections, which are the key part of the mechanism of ultrafast light-driven reactions yet remain elusive experimentally. *The methods of X-ray absorption that p*robes structure and unoccupied electronic density of states, *X-ray emission to p*robe occupied density of states, r*esonant X-ray emission to enable h*igh resolution experiments,[6] *X-ray Raman*[7] *to p*robe edges of light elements using harder X-rays, and multiple emerging methods must be combined. It is also crucial that both light- and heavy-elements can be followed in the same experiment, as illustrated in the *Periodic Table of X-rays* (Figure 6.1), to simultaneously interrogate various metal centers and organic ligands, or multiple metal and/or light elements in molecules and materials – one of the key essential features is a simultaneous delivery of hard- and soft X-rays. This combined approach will finally visualise "molecular movies" that provide vital new insights into mechanisms of reactions and processes in physics, chemistry, and biology, from molecular level upwards.

Since much of chemistry occurs in complex systems, we require the ability to make such measurements on systems of varying complexity, for example, ranging from isolated gas phase molecules, nanoscale solvated clusters, species adsorbed at metal and liquid interfaces, through to large molecular systems in solution. The ability to make ultrafast measurements in such dilute and diverse samples requires both high photon numbers and high repetition rates.

It is also important to acknowledge that only a small fractions of (bio)chemical reaction can be triggered with (visible) light, and therefore other means of triggering ultrafast reactions need to be coupled with X-ray interrogation techniques– such as T-jump, vibrational (THz, IR) excitation, electron injection or even another X-ray pulse. Of critical importance is that the trigger and the probe pulses are synchronized to ~5 fs.

The pioneering contributions of ultrafast X-ray spectroscopies to approaching the "movie" goal emerged in the last decade in many a demonstrative example – such as ligand dissociation in small metal complexes,[8,9], vibrational wave-packet dynamics in Fe-carbene photosensitizer determined with femtosecond X-ray emission and scattering[10], the first demonstration of picosecond X-ray absorption spectroscopy to probe ligand binding to heme proteins in physiological media, [11] ultrafast spin-change in spin-crossover materials or single-molecule molecular magnets for new methods of information storage. *Selected areas where such studies can bring transformative change are exemplified below.*

6.1.2 Ultrafast spin dynamics in molecules and biomolecules

The importance of deciphering the interplay of electronic and structural dynamics is well-illustrated in spin-crossover molecules[12] containing e.g. $Fe^{2+/3+}$ or Co^{2+} which are able to change the spin-state in response to external perturbation, such as light,[13] temperature, or pressure. The change in spin-states is usually ultrafast, sub-100 fs, and accompanied by a dramatic change in magnetic (ortho/para), structural (one most famous example is oxygen binding in heme; the bond lengths changes can be several tenth of A), or optical properties. The potential for targeted control of properties by external means opens up diverse applications of SCO in materials and devices, such as magnetic switching[14], all-optical magnetic recognition in iron garnet,[15] or photocatalytic CO_2 reduction (section 6.4).

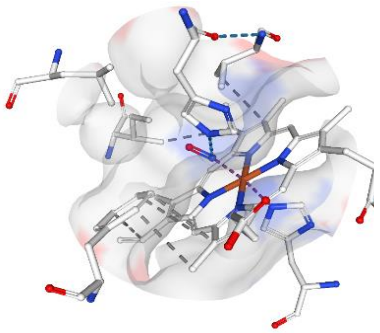

Figure 6.2. *Nitrosyl Horse Heart Myoglobin. --- show bonds which reversibly form& break. PDB 2FRJ.*

An example of the correlated spin and structural dynamics is the dissociation/recombination of NO from/to Fe-center in Myoglobin.[11] Here, huge advances have been made in following structures of the short-lived intermediates by XAS and WAXS; obtaining spin information by XES (K_β, 3p-1s and K_α, 2p-1s) monitoring high spin/low-spin transition. The next step, we want to follow formation and breaking of H-bonds (dashed lines, Figure 6.2), and changes of electron density not only on and around the Fe center, but of the ligand/protein itself. This major task calls for higher sensitivity, high repetition rate, and crucially, multiple detection, bringing in correlative XAS and XES methods, and RIXS to follow the changes in the ligand itself. [16]

In materials, the coupling between electronic and structural degrees of freedom is at the origin of the emergence of functions that can be triggered by direct or indirect excitation of various degrees of freedom, such as spin, electron, phonon, and lattice. These ultrafast phenomena affect various properties such as conductivity, magnetism and ferroelectricity. Understanding the complex out-of-equilibrium dynamics induced by light in these diverse systems requires both detailed calculations and molecular model compounds. Polynuclear metal complexes can serve as mimics of materials such as transition metal oxides, two-dimensional dichalcogenides, charge and orbital ordered manganites (anti-to-ferromagnetic phase transitions,[17] cyano-bridged photomagnets,[18] or mixed transition-metal/lanthanides.[19]

The fundamental understanding of the structure-function relationship requires the interplay between the oxidation states, electron density distribution along the molecule or material, spin-states, geometric changes to be resolved for (ideally) all atoms involved on the ultrafast time-scales. The UK XFEL's high repetition rate and brightness will enable new non-linear X-ray and optical/X-ray experiments, , which together with the tuneability, the ability to track changes in several metal centers and organic components by simultaneous detection in several spectral regions, will give principally

new insights into charge-transfer/electronic (such as change in oxidation state), structural and spin dynamics – and, ultimately, into chemical reactivity.

6.1.3 Ground-state chemistry and solvent-solute interactions

A major challenge across chemical science is to understand molecular reorganization in complex environments in terms of both intra-molecular and environment dynamics. The reorganization of the environment of a molecule influences processes by solvation perturbations and outer-sphere molecular co-ordination and often dictates transition states, chemical outcomes, and product state distributions. However, these problems are technologically challenging. Current laser technology provides time-resolved IR capability, but with limited spectral coverage; currently the region below ~ 800 cm^{-1} is inaccessible. Extension of the spectral coverage to provide a full temporally resolved 4000 – 1 cm^{-1} spectrum would allow for example the study of large collective motions of proteins such as alpha helical stretches, also the hindered rotations or vibrational structure of solvent molecules which influence solvent reorganization dynamics in liquids, the direct probing of metal-carbon and metal-metal atom motions in surface science problems, and identification of key biologically active radical species during radical migration during DNA strand breaks.

The vast majority of chemical transformations are thermally activated, but how one can trigger it in order to resolve structural dynamics? The ability to trigger a reaction in the electronic ground state, by e.g. ultrafast T-Jump, a THz or IR pulse, and follow the accompanying structural, electronic, vibronic and spin changes, on the ultrafast timescale would be of obvious fundamental and practical importance in understanding chemical reactivity. Ultrafast structural dynamics on the ground state potential energy surface can be investigated following photoexcitation and relaxation to the ground state, as shown by ultrafast X-ray scattering on a dinuclear Pt complex in solution,[20] a deep-UV triggered ground-state ring-opening dynamics of 1,3-cyclohexadiene in gas phase,[21] or a reaction of sulfine in its hot ground state leading to *nine* different products within < 1 ps.[22]

Figure 6.3. *Different motions contributing to the solvation of species formed in 220 nm photolysis of BrCN in perfluorohexane.*[25]

Photoinduced isomerization reactions, including ring-opening reactions, are one notable example of reactions with ultrafast structural changes. Recently, time-resolved photoelectron spectroscopy with a seeded XUV FEL traced the ultrafast ring opening of a thiophene molecule in gas phase after 265 nm excitation, and show that the initial ring opening and non-adiabatic coupling to the electronic ground state was driven by ballistic Sulfur-Carbon bond extension within 350 fs.[2324] These XFEL experiments provide unprecedented insights into both electronic and nuclear dynamics of this fundamental class of reactions – and illustrate how similar approach can be used to follow almost any reaction.

The structure of solute species and the solvent around them is fundamental to the understanding of the multitude of chemical reactions that take place in solution, with multitude of optical spectroscopies providing insight into inter-mode coupling and energy transfer. Resolving contributions from rotational, vibrational, and translational modes into overall solvent-solute interactions (Figure 6.3) can also help understanding interactions at the interfaces and on surfaces.[25] This important field of fundamental research underpins vast areas of chemistry, biochemistry, and medicine. X-ray absorption (EXAFS, XANES) is a particularly powerful technique here due to its element specificity, its wide-ranging applicability to the characterisation of the local environment of selected atoms in solids, liquids and even gases, and high sensitivity which makes it applicable to local structural studies from ultra-dilute to pure substances.

Vibrational energy redistribution in molecules and materials following an external perturbation, or within a product of a chemical reaction, is an important fundamental question. 2DIR-spectroscopy is now broadly used to answer this question, by following changes in vibrational frequencies, but requires specific IR-reporting groups. Time-resolved X-ray spectroscopy on the sub-10 ps time-scale to detect directly changes associated with C, N, and O-movements, in combination with 2DIR data, will allow the "molecular movie" of ground state catalysts, proton transfer reactions, or to follow photoisomerization pathways in proteins.[26]

6.1.4 Organic reactions, protein dynamics, DNA damage, and photoprotection

From fundamental organic photochemistry in gas phase and solution-phase, to free radicals in biology and medicine, to DNA damage and photoprotection, enzyme catalysis or drug-target interactions, one of the major challenges in investigations of ultrafast structural, electronic & spin dynamics is the prevalence of light elements, C, N, O, H.[27] It is extremely important to have access to all organic molecules via C, N, and O-edges. Time-resolved photoelectron spectroscopy with XUV (21 – 30 eV) will be instrumental in investigating all of the above. We must deliver the "molecular movie" in this area of research without relying on heavy elements, and extremely challenging task which can be solved with the UK-XFEL, providing access to nπ* and ππ* excited states which are present in virtually every organic molecule.

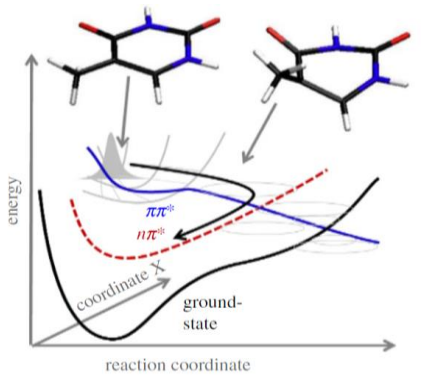

Figure 6.4. *Photochemistry of DNA. TR-AES and TR-NEXAFS reveals possible relaxation paths a ππ* state of thymine populated by UV-pulse, to the dark nπ* state and to the ground state through conical intersections.[27, 31]*

An example of ultrafast molecular transformation involving light molecules is the dynamics of –SS-bridges in proteins which respond to photoexcitation and oxidative stress. How does –SS-bond cleave? What is the sequence of steps in radical/ion formation, and recombination? Is structural change following the primary photo-chemical event or vice versa? fs-TRXAS studies showed that a model molecule dimethyl-disulfide H_3C-S-S-CH_3 undergoes direct dissociation to two H_3C-S-radicals within 120 fs upon UV-excitation.[28] This pioneering work prepared the grounds for investigating the same reaction in photocaged proteins, and under physiological conditions, where the high photon flux and high, 10 – 100 KHz repetition rate, will be essential to ensure the necessary sensitivity.

The high sensitivity and near-attosecond time resolution would enable direct mapping of structural changes as the system evolves through conical intersections which are postulated but rarely[29] observed experimentally in the majority of reactions occurring on the ultrafast time-scale away from Born-Oppenheimer approximation. Conical intersections (CIs) dominate the pathways and outcomes of virtually all photophysical and photochemical molecular processes. Despite extensive experimental effort, CIs have not been directly observed yet and the experimental evidence is being inferred from fast reaction rates and some vibrational signatures. Recent work shows that short X-ray (rather than optical) pulses can directly detect the passage through a CI with the adequate temporal and spectral sensitivity.[30]

Recent pioneering work on organic excited states[31] demonstrated how a combination of time-resolved Auger electronic spectroscopy with TR-NEXAFS resolve structural and electronic changes induced by UV-excitation in the nucleobase thymine (Fig 6.4), establishing the elongation of –C-O bond and non-adiabatic ππ* to the "dark" nπ* transition. Such direct observation of non-adiabatic dynamics in small molecules is unprecedented, whilst detecting dark states is intrinsically hard in optical spectroscopy. The ultrafast soft X-ray capability at UK-XFEL will enable the next step of this research – moving from individual nucleobases to DNA, understanding DNA damage. One step further will be real-time imaging of DNA damage/repair in living cells, and watching the action of light-activated therapy such as PDT in real time.

6.1.5 Fundamental Dynamics of Energy and Charge, Coherent and Optical Control of Reaction Dynamics

The development of new chemical processes relies upon the advancement of our mechanistic understanding of chemical change in complex systems. Since chemical change occurs on the timescales of nuclear motion, femtosecond time resolution is a key requirement. Ultrafast chemical reactions are often mediated by the complex non-adiabatic couplings between electronic and nuclear motions that occur when the Born-Oppenheimer approximation breaks down. Combining non-linear methods, multipulse optical and X-ray spectroscopies, on the femtosecond time-scale will enable one to track the evolving structural, electronic, and spin landscape following the trigger. [32]

Transition metal complexes, differently to organic entities, often exhibit ultrafast intersystem crossing (ISC) in the excited state, leading to long-lived excited state which determines their applications in photocatalysis (Re(I) for CO_2 reduction), PLEDs, or in photodynamic therapies (Pt, Ir, Ru). Ultrafast structural, electronic, spin, and vibrational dynamics occur simultaneously, and to follow them requires multipulse experiments where each parameter can be probed independently following a common trigger. The mechanism of ultrafast ISC is likely to involve spin-vibronic effects, as spin-orbit and vibrational coupling now occur on a similar, ultrafast time-scale.[33]

Time-resolved X-ray studies, using a variety of available methods, have been conducted on e.g. Cu-complexes which exhibit huge structural change in the excited state (Figure 6.5),[34,35] on dinuclear Pt(II) photocatlyst,[36,37] and on a multitude of Fe complexes (see "Spin dynamics" section), all of which demonstrated complex dynamics. It is hoped that ultrafast multipulse Xray studies with optical triggering, combined with THz, 2DIR, and 2DUV spectroscopies, will allow one to identify reaction coordinates responsible for the ISC in transition metal complexes, as well as in materials.

The ability to control chemical reactivity is one of the holy grails of chemistry. Diverse methods have been designed to achieve this goal (some of which are covered in the Attosecond Sciences section), such as coherent control[32,38] or bond-specific perturbation in molecules undergoing photoinduced electron transfer[39] and in organic PV materials.[40] Various degrees of control of chemical reactivity have been achieved, yet the control mechanisms remain elusive, especially in condensed phase. Ultrafast multipulse and nonlinear structural methods should enable us to resolve vibrational and vibronic coupling in charge and energy transfer reactions, identify reaction coordinates, follow energy transfer from one vibronic mode to another, and visualise where exactly the energy and charge are distributed along the molecules, in space and time, and which reaction pathways are driven by what vibrations. It may also long-term bring about rational control and design not only of molecules – single-molecule magnets, molecular conductors for example – but also of materials, and may bring us one step further to fulfilling the dream of "reactivity at will".

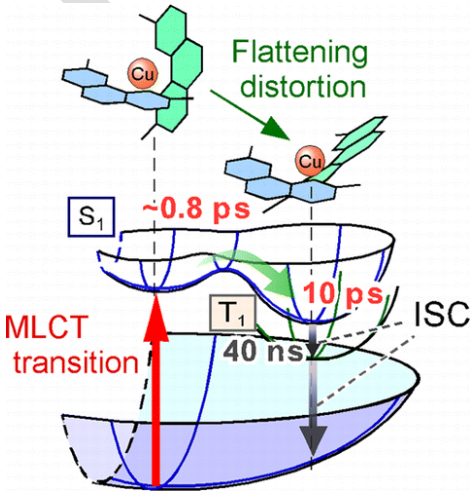

Figure 6.5. *Light-triggered distortion in a Cu-complex. Nuclear, electronic, and spin dynamics are convolved on the ultrafast timescale.*[34]

XFEL for Chemical Sciences can open up new horizons in Chemical Sciences and at the interface with materials, physics, biology, and medicine, by bringing about unprecedented degree of scrutiny of reactions happening in gas phase, liquids and solids; yielding with atomic precision and femtosecond resolution, real time molecular movies; and paving the way for new photoactive materials, catalysts, and drugs.

References

1. T. Elsaesser. "*Introduction: Ultrafast Processes in Chemistry*". *Chem. Rev.* 117, 10621, (2017) DOI: 10.1021/acs.chemrev.7b00226.

2. R. J. D. Miller. "*Femtosecond Crystallography with Ultrabright Electrons and X-rays: Capturing Chemistry in Action*". *Science (80-.).* 343, 1108, (2014) DOI: 10.1126/science.1248488.

3. G. D. Scholes *et al.* "*Perspective: Detecting and measuring exciton delocalization in photosynthetic light harvesting.*". *J. Chem. Phys.* 140, 110901, (2014) DOI: 10.1063/1.4869329.

4. F. Fassioli *et al.* "*Designs for molecular circuits that use electronic coherence*". *Faraday Discuss.* 163, 341, (2013) DOI: 10.1039/c3fd00009e.

5. C. Consani *et al.* "*Quantum control spectroscopy of competing reaction pathways in a molecular switch.*". *J. Phys. Chem. A* 118, 11364, (2014) DOI: 10.1021/jp509382m.

6. M. Maiuri *et al.* "*Ultrafast Spectroscopy: State of the Art and Open Challenges*". *J. Am. Chem. Soc.* 142, 3, (2020) DOI: 10.1021/jacs.9b10533.

7. V. Kimberg *et al.* "*Stochastic stimulated electronic x-ray Raman spectroscopy*". *Struct. Dyn.* 3, (2016) DOI: 10.1063/1.4940916.

8. P. Wernet *et al.* "*Orbital-specific mapping of the ligand exchange dynamics of Fe(CO)5 in solution*". *Nature* 520, 78, (2015) DOI: 10.1038/nature14296.

9. P. Wernet. "*Chemical interactions and dynamics with femtosecond X-ray spectroscopy and the role of X-ray free-electron lasers*". *Philos. Trans. R. Soc. A Math. Phys. Eng. Sci.* 377, (2019) DOI: 10.1098/rsta.2017.0464.

10. K. Kunnus *et al.* "*Vibrational wavepacket dynamics in Fe carbene photosensitizer determined with femtosecond X-ray emission and scattering*". *Nat. Commun.* 11, 634, (2020) DOI: 10.1038/s41467-020-14468-w.

11. R. Monni *et al.* "*Tryptophan-to-heme electron transfer in ferrous myoglobins*". *Proc. Natl. Acad. Sci.* 201423186, (2015) DOI: 10.1073/pnas.1423186112.

12. N. Huse *et al.* "*Femtosecond Soft X-ray Spectroscopy of Solvated Transition-Metal Dynamics*". 880, (2011).

13. H. T. Lemke *et al.* "*Coherent structural trapping through wave packet dispersion during photoinduced spin state switching*". *Nat. Commun.* 8, 15342, (2017) DOI: 10.1038/ncomms15342.

14. W. F. Koehl *et al.* "*All-optical control of ferromagnetic thin films and nanostructures*". 345, (2014).

15. A. Stupakiewicz *et al.* "*Selection rules for all-optical magnetic recording in iron garnet*". *Nat. Commun.* 10, 612, (2019) DOI: 10.1038/s41467-019-08458-w.

16. W. Zhang *et al.* "*Tracking excited-state charge and spin dynamics in iron coordination complexes.*". *Nature* 509, 345, (2014) DOI: 10.1038/nature13252.

17. T. Li *et al.* "*Femtosecond switching of magnetism via strongly correlated spin–charge quantum excitations*". *Nature* 496, 69, (2013) DOI: 10.1038/nature11934.

18. S. Ohkoshi *et al.* "*Light-induced spin-crossover magnet*". *Nat. Chem.* 3, 564, (2011) DOI: 10.1038/nchem.1067.

19. A. R. Khorsand *et al.* "*Element-Specific Probing of Ultrafast Spin Dynamics in Multisublattice Magnets with Visible Light*". *Phys. Rev. Lett.* 110, 107205, (2013) DOI: 10.1103/physrevlett.110.107205.

20. K. Haldrup *et al.* "*Ultrafast X-Ray Scattering Measurements of Coherent Structural Dynamics on the Ground-State Potential Energy Surface of a Diplatinum Molecule*". *Phys. Rev. Lett.* 122, 63001, (2019) DOI: 10.1103/physrevlett.122.063001.

21. J. M. Ruddock *et al.* "*A deep UV trigger for ground-state ring-opening dynamics of 1,3-cyclohexadiene*". *Sci. Adv.* 5, eaax6625, (2019) DOI: 10.1126/sciadv.aax6625.

22. B. Mignolet *et al.* "*Rich Athermal Ground-State Chemistry Triggered by Dynamics through a Conical Intersection*". *Angew. Chemie Int. Ed.* 55, 14993, (2016) DOI: 10.1002/anie.201607633.

23. J. a. Borek *et al.* "*Azide-water intermolecular coupling measured by 2-color 2D IR spectroscopy*". *EPJ Web Conf.* 41, 6005, (2013) DOI: 10.1051/epjconf/20134106005.

24. S. Pathak *et al.* "*Tracking the Ultraviolet Photochemistry of Thiophenone During and Beyond the Initial Ultrafast Ring Opening*". (2019).

25. M. P. Grubb *et al.* "*Translational, rotational and vibrational relaxation dynamics of a solute molecule in a non-interacting solvent*". *Nat. Chem.* 8, 1042, (2016) DOI: 10.1038/nchem.2570.

26. M. G. Romei *et al.* "*Electrostatic control of photoisomerization pathways in proteins*". *Science (80-.).* 367, 76, (2020) DOI: 10.1126/science.aax1898.

27. T. J. A. Wolf *et al.* "*Probing ultrafast ππ*/nπ* internal conversion in organic chromophores via K-edge resonant absorption*". *Nat. Commun.* 8, 29, (2017) DOI: 10.1038/s41467-017-00069-7.

28. K. Schnorr *et al.* "*Tracing the 267 nm-Induced Radical Formation in Dimethyl Disulfide Using Time-Resolved X-ray Absorption Spectroscopy*". *J. Phys. Chem. Lett.* 10, 1382, (2019) DOI: 10.1021/acs.jpclett.9b00159.

29. A. J. Musser *et al.* "*Evidence for conical intersection dynamics mediating ultrafast singlet exciton fission*". *Nat. Phys.* 11, (2015) DOI: 10.1038/nphys3241.

30. M. Kowalewski *et al.* "*Catching Conical Intersections in the Act: Monitoring Transient Electronic Coherences by Attosecond Stimulated X-Ray Raman Signals*". *Phys. Rev. Lett.* 115, (2015) DOI: 10.1103/physrevlett.115.193003.

31. T. J. A. Wolf *et al.* "*Photochemical pathways in nucleobases measured with an X-ray FEL*". *Philos. Trans. R. Soc. A Math. Phys. Eng. Sci.* 377, (2019) DOI: 10.1098/rsta.2017.0473.

32. M. Först *et al.* "*Mode-Selective Control of the Crystal Lattice.*". *Acc. Chem. Res.* (2015) DOI: 10.1021/ar500391x.

33. T. J. Penfold *et al.* "*Spin-Vibronic Mechanism for Intersystem Crossing*". *Chem. Rev.* 118, 6975, (2018) DOI: 10.1021/acs.chemrev.7b00617.

34. M. Iwamura *et al.* "*Ultrafast Excited-State Dynamics of Copper(I) Complexes*". *Acc. Chem. Res.* 48, 782, (2015) DOI: 10.1021/ar500353h.

35. T. Katayama *et al.* "*Tracking multiple components of a nuclear wavepacket in photoexcited Cu(I)-phenanthroline complex using ultrafast X-ray spectroscopy*". *Nat. Commun.* 10, 1, (2019) DOI: 10.1038/s41467-019-11499-w.

36. R. M. van der Veen *et al.* "*Vibrational relaxation and intersystem crossing of binuclear metal complexes in solution.*". *J. Am. Chem. Soc.* 133, 305, (2011) DOI: 10.1021/ja106769w.

37. M. Chergui *et al.* "*Photoinduced Structural Dynamics of Molecular Systems Mapped by Time-Resolved X-ray Methods*". *Chem. Rev.* 117, 11025, (2017) DOI: 10.1021/acs.chemrev.6b00831.

38. D. Meshulach *et al.* "*Coherent quantum control of two-photon transitions by a femtosecond laser pulse*". *Nature* 396, 239, (1998).

39. M. Delor *et al.* "*Toward control of electron transfer in donor-acceptor molecules by bond-specific infrared excitation.*". *Science* 346, 1492, (2014) DOI: 10.1126/science.1259995.

40. A. A. Bakulin *et al.* "*The Role of Driving Energy and Delocalized States for Charge Separation in Organic Semiconductors.*". *Science.* 335, 1340, (2012) DOI: 10.1126/science.1217745.

6.2 Exploring Complex Energy Landscapes through Chemical Activation

Physical, chemical and biological processes are all governed by interactions across complex potential energy surfaces. Understanding these surfaces is fundamentally important for everything from chemical reactivity and protein folding through to crystal structure prediction and developing new materials and pharmaceuticals. To understand these surfaces in ever great detail across multiple length and time scales, we need new experimental tools that can demonstrate control over the electronic, spin and ionic degrees of freedom of a material to engineer transient states of matter far from equilibrium, regulate transitions across barriers and explore new phases and materials with exotic and novel properties.

6.2.1 Introduction

All chemical processes are governed by dynamics that occur across complex energy landscapes. These landscapes need to be understood across multiple length and timescales, in particular, it is often the ultrafast events in nature that are accompanied by equally fast structural and electronic changes that are crucial to any chemical understanding. To understand the mechanism behind, e.g. chemical reactions, ultrafast magnetization, phonon triggered changes in structure, photon induced processes within materials and at interfaces, and we need to be able to measure these ultrafast changes in real time (~10 fs – 10 ps). The ultrafast X-ray methods that would be enabled by UK XFEL are perfect tools for this as they capture all the timescales of motion associated with changes in any complex matter system while providing a probe that is sensitive to both the structural and electronic change in a system. However, key to these developments at UK XFEL will be the ability to initiate chemical change using a diverse range of synchronized ultrafast pump sources including optical pump fields from the THz to the XUV, and pulsed radiolysis with electron beams. Of critical importance is that the pump (event trigger) and probe pulses are sufficiently well synchronized to permit temporal resolution approaching the sub-5 fs limit. This in-turn would enable complex pulse sequences to be used to build on the more established multidimensional optical techniques[1-4] with the inclusion of a (or multiple) X ray probe(s) over a range of energies (see section 6.1) which will provide time-resolved structural information that is often only inferred by other measurement techniques. It is essential that any new light source will provide an array of pump-probe and multidimensional capabilities that will collectively resolve the ultrafast structure and dynamics in a wide range of chemical processes.

A number of possible pumping options have been specifically highlighted throughout this case including THz, IR, UV and X-ray. In this section we highlighted two important options (THz and ultrafast electrons) that provide opportunities for exciting chemical science by providing unique capabilities at UK XFEL.

6.2.2 Intense THz excitation combined with ultrafast X-ray measurement techniques

Absorption at THz frequencies can be complex, and governed by many different physical mechanisms that are fundamentally important to understand. In simple crystalline materials the absorption is dominated by strongly coupled phonons[5-7] while in complex crystalline systems these are mixed with low-frequency internal motions.[8, 9] In amorphous materials,[10, 11] a large number of overlapping bands often give rise to a featureless spectral vibrational density of-states that is very difficult to interpret — even for apparently simple systems such as water.[12] However, THz absorption shows exceptional sensitivity to long-range order and dynamics, whether it be in polymorph formation,[13] structural formation in solutions,[14] and ionic liquids,[15] and sensitivity to enzyme functional dynamics.[16, 17]

THz frequency normal modes are particularly interesting because they have been linked to reaction pathways and dynamics in majority of reactions with specific examples including the initiation of

energetic materials,[9] enzymatic reactions, in particular proton tunnelling,[16] solid-state phase transitions in metal-organic frameworks (MOFs),[20-22] materials that exhibit solid-state phase transitions[7] and catalytic surface chemistry.[19]

Recently, the development of a range of methods to generate intense THz pulses has led to a very dynamic research field to manipulate matter.[23, 24] Recent examples relevant to the chemical sciences include the orientation of OCS molecules in the gas phase[25] and THz induced crystallisation of carbamazepine and indomethacin from an amorphous phase to different polymorphic phases in comparison to temperature induced crystallisation.[26] This has obvious implications in the study of the relative stability of pharmaceutical compounds but has the potential to provide a new insight into the important processes of nucleation and crystallisation which in turn may provide new perspectives to aid first-principles structure prediction — one of the grand challenges of the chemical sciences.[27]

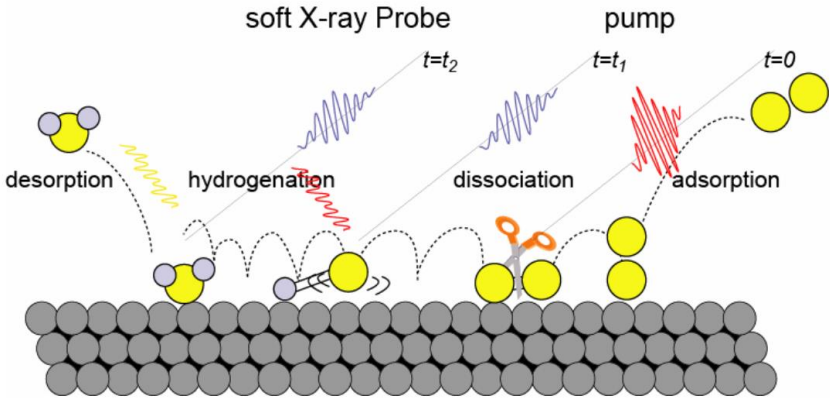

Figure 6.6. *An initial intense THz pump manipulating a molecule adsorbed to a catalytic surface. This initiates a reaction that is then probed by a series of time-delayed X-ray pulses which provide spectroscopic and structural information in real time. Intense THz electric fields can strongly interact with molecules adsorbed on a surface or the electron bath of the catalytic surface. This has been shown to selectively induce CO oxidation on a Ru (0001) surface. The addition of measurement techniques such as time-resolved XAS and XES would provide a greater understanding of the reaction dynamics and intermediate species formed which will in turn pave the way for the development of the next generation of more efficient and selective catalysts. Importantly the low energy of THz radiation, coupled with the high peak electric (< 100MV/cm) and magnetic fields (< 33 T) that can be generated may provide a universal way to manipulate matter without the excess energy associated with optical excitation.*[18, 19]

Measurements have also demonstrated that high-field THz pulses can promote specific reaction pathways on a catalytic surface, for instance selectively inducing CO oxidation on a Ru (0001) surface (Figure 6.6).[18, 19] There are also a number of studies that show the manipulation of lattice and spin dynamics including the discovery of novel phases through the direct manipulation of phonons and magnons using high-field THz pulses (Figure 6.7).[2, 5, 6, 28]

Recent measurements have also used ultrafast X-ray pulses to probe this THz electric-field driven manipulation of dynamics (i.e. see Figure 6.7). In $BaTiO_3$, the modulations of the ferroelectric polarization[29] were detected while in $SrTiO_3$ coupling of phonon modes[6] and the identification of a metastable ferroelectric phase has been observed.[5] These studies, however, are limited by the range of accessible Bragg reflections, and by the signal to noise at current XFELs. Extensions to higher energy (> 25 keV), using PDF approaches, or to higher repetition rate (for both XFEL and THz sources), would provide the first direct visualizations of these local atomic-scale motions — a crucial step in making these experimental tools practically useful for exploring increasingly complex materials.

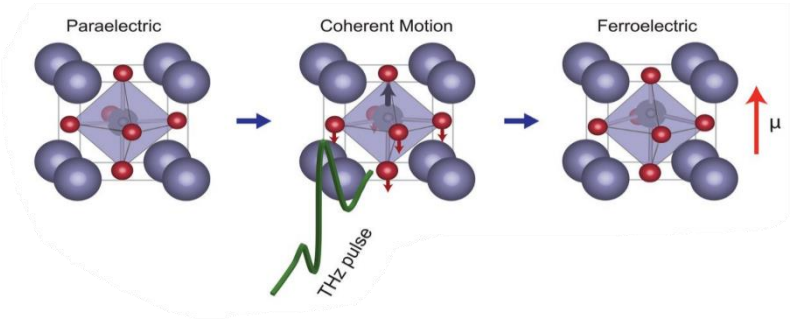

Figure 6.7. *A single-cycle THz electric field which moves all the ions it encounters toward their positions in a new ferroelectric crystalline phase. In STO, the initial high-symmetry configuration around each Ti^{4+} ion has no dipole moment and the crystal is paraelectric. The incident field drives the "soft" lattice vibrational mode, moving the ions along the directions indicated into a lower-symmetry geometry with a dipole moment.[5] This ion movement can be probed directly with X-rays.*

What's particularly exciting is that in all these studies and more, THz pumping has enabled the exploration of the complex energy landscapes that underpin reactivity and dynamics. These systems do not require the chromophores needed for most optical excitation, suggesting the THz excitation could become a universal pumping source for majority of materials. It has the ability to manipulate matter on an ultrafast timescale and provides the capability to achieve insight into the fundamental dynamics of processes, which in turn can be used to underpin the future rational design of materials with tailored physical and chemical properties.

Future applications of intense THz excitation could also be found in the life sciences – examples include the potential disruption of H-bonding in a solvent network surrounding a protein whose structure has already been probed by low-intensity THz radiation,[14, 30, 31] or through the pumping of enzymatic promoting modes[16] which have been suggested for some time as being directly linked to the reaction coordinate in complex enzymatic reactions, particularly where electric field controlled catalytic mechanism[32] are thought to be involved and these high peak THz-fields could be used to resonantly (and non-resonantly) influence the reaction pathway in these complex bio-materials. For all the examples discussed here and more what is required is a high-field (> 100 MV/cm), narrowband and tuneable THz pump source that could be used to selectively excite specific modes in a material, combined with a plethora of broadly tuneable XFEL and laser-based sources for providing ultrafast spectroscopic and structural information as the material changes. This would require a tuneable accelerator-based THz source (< 10 μm) combined with laser-based systems for higher wavelengths.

6.2.3 Electron induced radiolysis combined with ultrafast X-ray measurement techniques

An ultrafast pulsed electron beam is a complementary and powerful method for the generation of chemical intermediates, excited states and free radicals. Its major difference from laser initiation is that the primary excitation step involves interaction of electrons with the media and doesn't rely on the absorption by a chromophore of the laser light of a particular wavelength, thus opening up the possibility of understanding electron transfer and radiochemical processes that cannot be optically initiated.

As such, pulse radiolysis as a trigger to accompany soft X-ray probes of structural change will be an exciting and important avenue of research with a diverse range of applications throughout chemistry including within geochemistry,[33, 34] nanoscience,[35] ionic liquids,[36, 37] radiation induced corrosion[38] and other radiation induced processes with particular applications in understanding how living tissue, and in particular DNA, responds to radiation.[39-42] In particular, it can be used to determine the fundamental radiochemical processes occurring in any media exposed to ionizing radiation through the determination of kinetics in radiation tracks and how they influence the overall radiation chemical processes. A pulsed electron beam is often the method of choice to generate and determine the

properties of radical ions, reactive oxygen species and initiate charge migration and proton transfer processes. The ability to generate charged species will also allow studies of charge mobility in electronic devices and artificial light-harvesting systems.

The coupling of ultrashort (< 100 fs) electron pulses (~ 5 – 15 MeV) as a trigger for chemical change with the X-ray probe techniques to monitor structural change in real time would represent a unique capability internationally. In particular, compared to existing pulse radiolysis facilities worldwide,[43-45] this would give the UK a leading edge in terms of both structural sensitivity and time resolution. The combination of XUV pulses[46] (especially in the 10 – 30 eV range) and pulsed radiolysis at the same facility will also allow direct comparison of optically induced dynamics with those of radiolysis, another potential key international defining feature for the new XFEL.

Particular areas of interest include the radiolysis of water[47, 48] and other solvents[36, 49] along with larger molecular systems[50] where the elementary processes associated with ionization of the material including initial ionization, the formation of solvent holes and geminate recombination processes are fundamental for understanding radiation-matter interactions in chemistry and biology. While water has been heavily studied using a range of pump sources to measure the dynamics of the hydrated electron only very recent work[47] using an optical pump – ultrafast X-ray probe scheme has provided the first spectral evidence of its partner arising from ionization of liquid water, H_2O^+.

Increased time resolution and signal-to-noise ratios would enable more accurate H_2O^+ lifetime measurements (tentatively assigned to be 46 ± 10 fs) and at the same time permit the observation of ultrafast dynamics involving hole alignment, coherences, and nonadiabatic dynamics induced by radiolysis.[47] A comparison of lifetimes measured using electron and optical excitation would be particularly useful. Understanding these processes is fundamentally important in delineating the consequences of radiotherapy with recent studies showing that ~67 % of DNA radiation damage that occurs during treatment is initiated indirectly via water ionisation — with the reasons for this being very poorly understood.[51] The development of an electron beam instrument with a beam energy of 5 – 15 MeV would also allow increased penetration through thicker samples and while maintaining a tighter focus inside a sample, providing a facility where more biologically relevant samples including cells and tissues could potentially be investigated via radiolysis.

The combination of a facility where a direct comparison of radiation damage induced by optical, X-ray and electron pulses could be directly compared would be unprecedented. Synergistically, a suitable ultrafast electron pump source would also be ideal for ultrafast electron diffraction (UED) and in the development of plasma wakefield acceleration.

While the recent science enabled by the development of new THz/e-beam sources is ground breaking, the development of a high brightness (> 10^{12} Photons per pulse), high repetition rate (upto 1 MHz) XFEL, combined with accelerator based THz and electron beam pump sources (along with numerous synchronized of laser based sources) will be a world-first, enabling a plethora of new science by exploration of potential energy landscapes for increasingly complex materials using novel experimental tools that combine these pump sources with multiple in-situ spectroscopic probes simultaneously.

References

1. N.T. Hunt, "*2D-IR spectroscopy: ultrafast insights into biomolecule structure and function",* Chem. Soc. Rev., 38, 1837, (2009), DOI: 10.1039/B819181F.
2. J. Lu, et al., "*Two-dimensional spectroscopy at terahertz frequencies",* in *Multidimensional Time-Resolved Spectroscopy*, T. Buckup, et al., Editors. Springer, Cham. 275, (2019).
3. M. Delor, et al., "*On the mechanism of vibrational control of light-induced charge transfer in donor–bridge–acceptor assemblies",* Nat. Chem., 7, 689, (2015), DOI: 10.1038/nchem.2327.
4. M. Delor, et al., "*Toward control of electron transfer in donor-acceptor molecules by bond-specific infrared excitation",* Science, 346, 1492, (2014), DOI: 10.1126/science.1259995.
5. X. Li, et al., "*Terahertz field–induced ferroelectricity in quantum paraelectric $SrTiO_3$",* Science, 364, 1079, (2019), DOI: 10.1126/science.aaw4913.
6. M. Kozina, et al., "*Terahertz-driven phonon upconversion in $SrTiO_3$",* Nat. Phys., 15, 387, (2019), DOI: 10.1038/s41567-018-0408-1.
7. R.J.D. Miller, "*Mapping atomic motions with ultrabright*

electrons: The chemists' gedanken experiment enters the lab frame", Annu. Rev. Phys. Chem., 65, 583, (2014), DOI: 10.1146/annurev-physchem-040412-110117.

8. A.D. Burnett, et al., "*Effect of molecular size and particle shape on the terahertz absorption of a homologous series of tetraalkylammonium salts",* Anal. Chem., 85, 7926, (2013), DOI: 10.1021/ac401657r.

9. S. Ye, et al., "*Energy transfer rates and impact sensitivities of crystalline explosives",* Combust. Flame, 132, 240, (2003), DOI: 10.1016/S0010-2180(02)00461-3.

10. J. Sibik, et al., "*Terahertz response of organic amorphous systems: experimental concerns and perspectives",* Philos. Mag., 96, 842, (2016), DOI: 10.1080/14786435.2015.1111528.

11. K.A. Niessen, et al., "*Terahertz optical measurements of correlated motions with possible allosteric function",* Biophys. Rev., 7, 201, (2015), DOI: 10.1007/s12551-015-0168-4.

12. A. Beneduci, "*Which is the effective time scale of the fast Debye relaxation process in water?",* J. Mol. Liq., 138, 55, (2008), DOI: 10.1016/j.molliq.2007.07.003.

13. E.P. Parrott, et al., "*Terahertz time-domain and low-frequency Raman spectroscopy of organic materials",* Appl. Spectrosc., 69, 1, (2015), DOI: 10.1366/14-07707.

14. V. Conti Nibali, et al., "*New insights into the role of water in biological function: Studying solvated biomolecules using terahertz absorption spectroscopy in conjunction with molecular dynamics simulations",* J. Am. Chem. Soc., 136, 12800, (2014), DOI: 10.1021/ja504441h.

15. C. Roth, et al., "*The importance of hydrogen bonds for the structure of ionic liquids: Single-crystal X-ray diffraction and transmission and attenuated total reflection spectroscopy in the terahertz region",* Angew. Chem. Int. Ed., 49, 10221, (2010), DOI: 10.1002/anie.201004955.

16. S. Hay, et al., "*Good vibrations in enzyme-catalysed reactions",* Nat. Chem., 4, 161, (2012), DOI: 10.1038/nchem.1223.

17. K.A. Niessen, et al., "*Protein and RNA dynamical fingerprinting",* Nature Communications, 10, 1026, (2019), DOI: 10.1038/s41467-019-08926-3.

18. J.L. Larue, et al., "*THz-pulse-induced selective catalytic CO oxidation on Ru",* Phys. Rev. Lett., 115, 036103, (2015), DOI: 10.1103/PhysRevLett.115.036103.

19. A. Nilsson, et al., "*Catalysis in real time using X-ray lasers",* Chem. Phys. Lett., 675, 145, (2017), DOI: 10.1016/j.cplett.2017.02.018.

20. M.R. Ryder, et al., "*Identifying the role of terahertz vibrations in metal-organic frameworks: from gate-opening phenomenon to shear-driven structural destabilization",* Phys. Rev. Lett., 113, 215502, (2014), DOI: 10.1103/PhysRevLett.113.215502.

21. N.Y. Tan, et al., "*Investigation of the terahertz vibrational modes of ZIF-8 and ZIF-90 with terahertz time-domain spectroscopy",* Chem. Commun., 51, 16037, (2015), DOI: 10.1039/c5cc06455d.

22. T. Itakura, et al., "*The role of lattice vibration in the terahertz region for proton conduction in 2D metal–organic frameworks",* Chemical Science, (2020), DOI: 10.1039/c9sc05757a.

23. P. Salén, et al., "*Matter manipulation with extreme terahertz light: Progress in the enabling THz technology",* Phys. Rep., (2019), DOI: 10.1016/j.physrep.2019.09.002.

24. T. Kampfrath, et al., "*Resonant and nonresonant control over matter and light by intense terahertz transients",* Nat. Phot., 7, 680, (2013), DOI: 10.1038/nphoton.2013.184.

25. S. Fleischer, et al., "*Molecular orientation and alignment by intense single-cycle THz pulses",* Phys. Rev. Lett., 107, 163603, (2011), DOI: 10.1103/PhysRevLett.107.163603.

26. M.T. Ruggiero, et al., "*The significance of the amorphous potential energy landscape for dictating glassy dynamics and driving solid-state crystallisation",* PCCP, 19, 30039, (2017), DOI: 10.1039/c7cp06664c.

27. S.L. Price, "*Control and prediction of the organic solid state: a challenge to theory and experiment",* Proc. R. Soc. London, Ser. A, 474, 20180351, (2018), DOI: 10.1098/rspa.2018.0351.

28. J. Lu, et al., "*Coherent two-dimensional terahertz magnetic resonance spectroscopy of collective spin waves",* Phys. Rev. Lett., 118, 207204, (2017), DOI: 10.1103/PhysRevLett.118.207204.

29. F. Chen, et al., "*Ultrafast terahertz-field-driven ionic response in ferroelectric $BaTiO_3$",* Phys. Rev. B: Condens. Matter, 94, 180104, (2016), DOI: 10.1103/PhysRevB.94.180104.

30. M.-C. Bellissent-Funel, et al., "*Water determines the structure and dynamics of proteins",* Chem. Rev., 116, 7673, (2016), DOI: 10.1021/acs.chemrev.5b00664.

31. M. Heyden, et al., "*Dissecting the THz spectrum of liquid water from first principles via correlations in time and space",* Proc. Natl. Acad. Sci. U.S.A., 107, 12068, (2010), DOI: 10.1073/pnas.0914885107.

32. S.D. Fried, et al., "*Electric fields and enzyme catalysis",* Annu. Rev. Biochem, 86, 387, (2017),

33. N. Laanait, et al., "*X-ray–driven reaction front dynamics at calcite-water interfaces",* Science, 349, 1330, (2015), DOI: 10.1126/science.aab3272.

34. M.A. Pasek, "*Rethinking early Earth phosphorus geochemistry",* Proc. Natl. Acad. Sci. U.S.A., 105, 853, (2008), DOI: 10.1073/pnas.0708205105.

35. H. Gu, et al., "*Nanoscale hybrid multidimensional perovskites with alternating cations for high performance photovoltaic",* Nano Energy, 65, 104050, (2019), DOI: 10.1016/j.nanoen.2019.104050.

36. L. Das, et al., "*Pulse radiolysis and computational studies on a pyrrolidinium dicyanamide ionic liquid: Detection of the dimer radical anion",* J. Phys. Chem. A, 122, 3148, (2018), DOI: 10.1021/acs.jpca.8b00978.

37. D.R. Macfarlane, et al., "*Energy applications of ionic liquids",* Energy Environ. Sci., 7, 232, (2014), DOI: 10.1039/C3EE42099J.

38. C.M. Lousada, et al., "*Gamma radiation induces hydrogen absorption by copper in water",* Sci. Rep., 6, 24234, (2016), DOI: 10.1038/srep24234.

39. F.E. Garrett-Bakelman, et al., "*The NASA Twins Study: A multidimensional analysis of a year-long human spaceflight",* Science, 364, eaau8650, (2019),

40. E. Alizadeh, et al., "*Precursors of solvated electrons in radiobiological physics and chemistry",* Chem. Rev., 112, 5578, (2012), DOI: 10.1021/cr300063r.

41. J. Ma, et al., "*Ultrafast electron attachment and hole transfer following ionizing radiation of aqueous uridine monophosphate",* J. Phys. Chem, 9, 5105, (2018), DOI: 10.1021/acs.jpclett.8b02170.

42. F. Boussicault, et al., "*The fate of C5′ radicals of purine nucleosides under oxidative conditions",* J. Am. Chem. Soc., 130, 8377, (2008), DOI: 10.1021/ja800763j.

43. J.F. Wishart, et al., "*The LEAF picosecond pulse radiolysis facility at Brookhaven National Laboratory",* Rev. Sci. Instrum., 75, 4359, (2004), DOI: 10.1063/1.1807004.

44. J.L. Marignier, et al., "*Time-resolved spectroscopy at the picosecond laser-triggered electron accelerator ELYSE",* Radiat. Phys. Chem., 75, 1024, (2006), DOI:

10.1016/j.radphyschem.2005.10.020.
45. J. Yang, et al., "*Pulse radiolysis based on a femtosecond electron beam and a femtosecond laser light with double-pulse injection technique",* Radiat. Phys. Chem., 75, 1034, (2006), DOI: 10.1016/j.radphyschem.2005.09.016.
46. V. Svoboda, et al., "*Real-time observation of water radiolysis and hydrated electron formation induced by extreme-ultraviolet pulses",* Science Advances, 6, eaaz0385, (2020), DOI: 10.1126/sciadv.aaz0385.
47. Z.-H. Loh, et al., "*Observation of the fastest chemical processes in the radiolysis of water",* Science, 367, 179, (2020), DOI: 10.1126/science.aaz4740.
48. B.C. Garrett, et al., "*Role of water in electron-initiated processes and radical chemistry: Issues and scientific advances",* Chem. Rev., 105, 355, (2005), DOI: 10.1021/cr030453x.
49. A.R. Cook, et al., "*Rapid "step capture" of holes in chloroform during pulse radiolysis",* J. Phys. Chem. A, 117, 7712, (2013), DOI: 10.1021/jp405349u.
50. A.R. Cook, et al., "*Sudden, "step" electron capture by conjugated polymers",* J. Phys. Chem. A, 115, 11615, (2011), DOI: 10.1021/jp205790k.
51. D.R. Spitz, et al., "*An integrated physico-chemical approach for explaining the differential impact of FLASH versus conventional dose rate irradiation on cancer and normal tissue responses",* Radiotherapy and Oncology, 139, 23, (2019), DOI: 10.1016/j.radonc.2019.03.028.

6.3 Energy Materials and Devices: Solar Cells and Batteries

Our energy systems are rapidly evolving, driven by the challenges of associated with decarbonisation, an ageing infrastructure and shifts in societal expectations. Achieving a radical shift in how we supply, manage and consume energy calls for new materials and a detailed understanding of how they function. Yet in many energy technologies there remains fundamental processes related to function which we simply do not understand, and such lack of understanding severely impedes the progress in the field. Ultrafast X-ray probing will unprecedented insight into the function of materials on the atomic scale of time (femtosecond) and length (Angströms) leading to a greatly more detailed understanding of structure-property relationships in materials for energy applications.

6.3.1 Introduction

Energy demands are increasing throughout the world and provision is currently being met by a mix of sources including fossil fuels, nuclear power, hydroelectricity and renewables, such as wind and solar energy. However, despite this, many challenges remain and need to be overcome to realise the global energy revolution required to limit the detrimental effects on the planet. Solutions must be found that allow an increase in energy consumption whilst reducing the environmental impact, in order to meet the UK obligations under the Paris Agreement on Climate Change[1] and the ambition of a net zero emissions energy policy by 2050[2]. This will only be possible by improving all aspects of energy conversion, storage, transmission and low-power device efficiency.

For energy conversion, technologies focus upon the transition from polluting fossil fuels to low-carbon sources such as wind, tidal and solar power. However, these technologies are inherently intermittent and consequently must be concurrently developed alongside new directions for highly efficient grid and off-grid storage solutions such as batteries or chemical storage. Crucially, this will not be overcome without new classes of zero-carbon materials that are produced sustainably and allow higher efficiency energy conversion with better operational stability than current materials.

The challenge is that materials underpinning many energy conversion/storage processes are complex and poorly understood, especially on the atomic scale. Indeed, they often exhibit functional structural disorder and contain dynamical properties that are needed for their operation, but which are also responsible for energy losses and device instabilities and degradation during decade-long operation under harsh, non-equilibrium conditions. This lack of understanding means that the design of new materials is often focused upon large-scale synthetic programs as epitomised by the extensive literature reporting new potential candidates. Ultimately, few candidate materials make the transition to application in practically useful devices. This *status-quo* leads to incremental progress, stagnation of research fields and makes designing materials costly and time-consuming.

The development and utilization of ultrafast X-ray methods will play an important role in providing crucial understanding into material properties down to the atomic scale of time (femtosecond) and length (Angströms). This understanding can subsequently be used to control the physics and chemistry of emerging materials for energy conversion/storage.

By exploiting a broad range of excitation (pump) pulses in the UV, visible, IR or THz region, it will be possible to address a broad range of challenges in energy materials using optical, vibrational and thermal excitations. Probe techniques such as Resonant X-ray Emission Spectroscopy (RXES) will provide powerful insight into the properties of the materials required to address the above challenges. Presently the repetition rate of X-FELs severely limits their ability to acquire RXES spectra, while 3rd generation light sources cannot achieve the temporal resolution for understanding. These techniques will also be combined with complementary techniques such as X-ray Photoelectron Spectroscopy (XPS), X-ray Scattering, X-ray Magnetic Circular Dichroism and X-ray Raman to facilitate the study of dynamical processes Interfaces. Indeed, these X-ray techniques can disentangle the coupled motion of the spins, electrons and nuclear dynamics, making them uniquely powerful for studying energy.

Combined with the remarkable capabilities of UK-FEL (ultrafast time resolution and high repetition rate) delivers potentially transformative new approaches to address fundamental and use-inspired questions in energy materials.

6.3.2 Photovoltaics

Everyday approximately 200 Wm^{-2} of radiant energy in the form of natural light arrives on earth from the sun. The ability to convert this solar radiation into energy is core to attempts to reduce our reliance on unsustainable fuel sources. Crystalline and amorphous silicon photovoltaics (PV) are used owing to their stability and high-power conversion efficiency, but they have distinct drawbacks including, for example, indirect band gap and processing costs. The global photovoltaic (PV) market is forecast to grow significantly in the coming years with emerging technologies predicted to account for 25% of this with potential examples including dye-sensitised nanoparticles, organic bulk heterojunctions, thin film semiconductors such as lead-halide perovskites. These technologies are appealing as they are based around low cost solution processing or vacuum deposition that are highly scalable.

However, they are currently limited by a number of factors, including efficiency and stability. They rely on sunlight to generate charge carriers (electrons and holes) and consequently, to improve performance it is crucial to understand the room temperature creation, separation, transport, and trapping of the photogenerated holes and electrons over a wide distribution of time and length scales. These dynamics begin on the ultrafast timescale and therefore require ultrashort pulses to track all of the competing processes. The ultrashort timescales and the complex interplay of structural and electronic effects means that many of these processes and various relaxation pathways remain poorly understood.

Time-resolved X-ray spectroscopy has recently increasingly been used to investigate the fate of charge carriers in photoexcited these photovoltaic materials[3], and because the valence and conduction of semiconductors are often dominated by the orbitals of specific atomic constituents. The element-specificity of X-ray spectroscopy can be exploited to achieve electronic band selectivity. In essence, it is reducing the complexity of band structures to the simplicity of atomic sites to provide important insights into the charge carrier dynamics and the effect of morphology, defects and band level alignment.

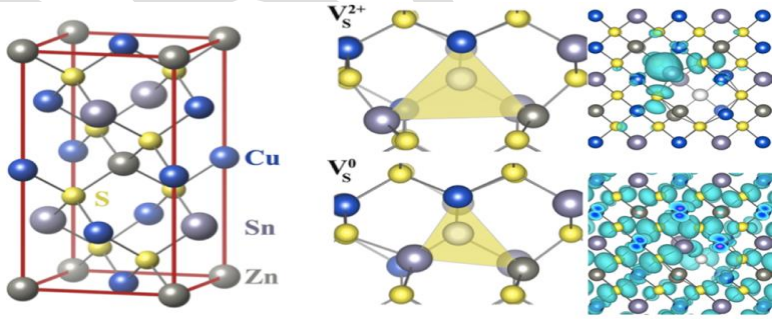

Figure 6.8. *Left: The atomic structure of the Kesterite like Cu_2ZnSnS_4 (CZTS) system. Right: Key defects proposed to be responsible for nonradiative electron-hole recombination and charge density associated with them. Figure reproduced from Ref. 6.3.4.*

In this area, there has been a significant research effort in the development of ternary and quaternary semiconductors such as CIGS ($CuIn_xGa_{1-x}Se_2$) or kesterite structures (Figure 6.8) such as CZTS (Cu_2ZnSnS_4), halide perovskite structured semiconductors such as methylammonium lead iodide ($CH_3NH_3PbI_3$)[5]. Specifically, for the case of the earth abundant solar absorber, CZTS, band gap excitation would excite an electron from the Cu-3d/S-3p state (valence band) to the Sn-5s/S-3p state (conduction band)[6]. Time-resolved X-ray absorption and emission spectroscopy can be used to monitor the photocarrier generation, localization and recombination occurring on the femto- and picosecond timescale from the perspective of multiple atomic sites. Through chemical modifications the effect of the interstitial atoms, vacancies and grain boundary on the excited carrier dynamics can be

investigated[7], while dopants can be introduced to improve photon absorption and shift the energy levels to refine the performance of promising materials. The capability of fs X-ray spectroscopy and the insights obtained from these measurements will enable us to reveal a detailed structural understanding of ultrafast charge carrier dynamics and propose avenues for improving the performance of these materials.

6.3.3 Electrochemical Energy Storage

Many forms of renewable energies, like solar and wind, are intermittent. Consequently, to meet the current worldwide energy demand and control the load exerted on the national grid, a wide variety of energy storage solutions are required to be integrated. The development of the Li-ion battery[8] has revolutionized technology, however the ever-increasing need for energy storage beyond portable electronics places an increasingly heavy demand on battery capacity and developing other approaches to electrochemical storage, e.g. redox flow batteries[9].This calls for further improvements of energy density and a continuous reduction of cost. The need for affordable large-scale grid storage is urgent and can only be achieved through a detailed understanding of the competing processes occurring in operational batteries.

The operation of all electrochemical storage solutions relies on the movement and/or changes in chemical state of ions, which is accompanied by solvation and desolvation processes of these ions. The rate of electron transfer involved in the redox process strongly determines the electrochemical activity and therefore achieving a detailed understanding is essential. The energy and temporal resolution provided by UK-FEL combined with the high repetition rate will enable X-ray spectroscopy, X-ray Raman, X-ray scattering and photoelectron spectroscopy measurements capable of deeper understanding the fundamental processes leading to involved in battery performance and degradation. The high time resolution which can be achieved by UK-FEL will be exploited to probe fundamental charge transfer and solvation dynamics around the ions which occur on the femto- to picosecond timescale[10], with a particular focus in the region of the interface.

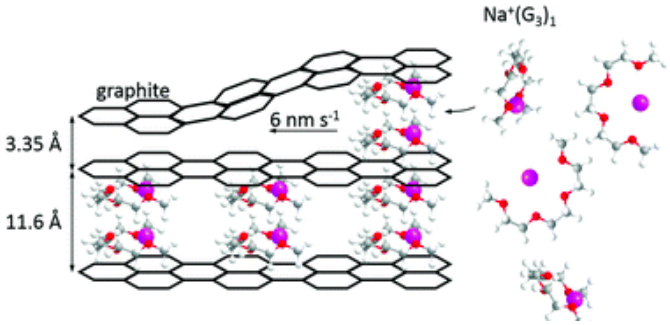

Figure 6.9. *A Schematic of the solvent assisted Na intercalation mechanism. The size of the Na:solvent complex leads to a ~7 Å increase in the interlayer spacing in Graphite[14].*

Pulse radiolysis pump combined with X-ray probe experiments can be used to make it possible to study, on the picosecond timescale, the reaction of the electrons with the ions and the electrolytes[11] and reveal structural dynamics leading to degradation mechanisms. IR-pump / X-ray probe studies will provide structural insights into the solvation dynamics so important to the systems[12]. The increased brightness will concurrently allow the collection of high-quality data of weak signal in are in situ studies of systems under operational conditions, such as materials/liquid interfaces in batteries.

An example of where UK-FEL could contribute a step-change includes providing new insights into the contrasting mechanism for intercalation observed in Li-ion batteries (LIB) and Na-ion batteries (NIBs). Research in the latter has experienced rapid growth in recent years, owing to the elemental abundance of Na in the earth's crust, which is about three orders of magnitude larger than Li [13]. However, NIBs still exhibit inferior energy, power density and reversibility compared to Li-ion batteries (LIB). Overcoming these performance limitations requires a fundamental understanding of electrode materials and the effect of the larger ionic radius of the Na-ion on its intercalation behavior is required. Despite the large size it has been shown that Na-ion intercalation only occurs with the solvation shell, and consequently usually an ether-based electrolyte such as di-glymine is used. Importantly, upon

Na:solvent intercalation, the graphite interlayer spacing expands from 3.35 to 10.9 Å[14], as illustrated schematically in Figure 6.9. Given this large expansion it is astonishing that these systems can be cycled several thousand times without a significant loss in capacity.

A combination of X-ray Raman and resonant X-ray emission can be used to investigate the dynamic properties of electrodes during fast charge/discharge process from the perspective of both the electrode material, the ions and the solvent. Although the time scale for these processes is often not ultrafast, the high brightness of UK-FEL will facilitate the collection of high-quality data of photon-in/photon-out spectroscopies in operando, which have previously been shown to provide significant insight into the dynamical mechanism in batteries. Other examples include atomic scale insight into the crucial electron transfer mechanism between redox couples in redox flow batteries[9].

6.3.4 New Generation Data Storage

Magnetism in novel nanoscale materials is a key ingredient in modern information technology. Manipulating magnetic materials is the cornerstone of hard drive technology, where binary digital information is recorded by aligning the direction of the magnetic poles in the hard drive. New technologies are urgently needed because it is estimated that by 2025, up to 20% of the world's energy will be consumed by information technologies, where data centres consume ca one third of this energy. Data storage servers are already emitting as much carbon dioxide as the whole aviation industry. With the ever-increasing use of big data for driverless cars, robots, video surveillance and artificial intelligence etc, there is an urgent need to develop a new generation data storage devices.

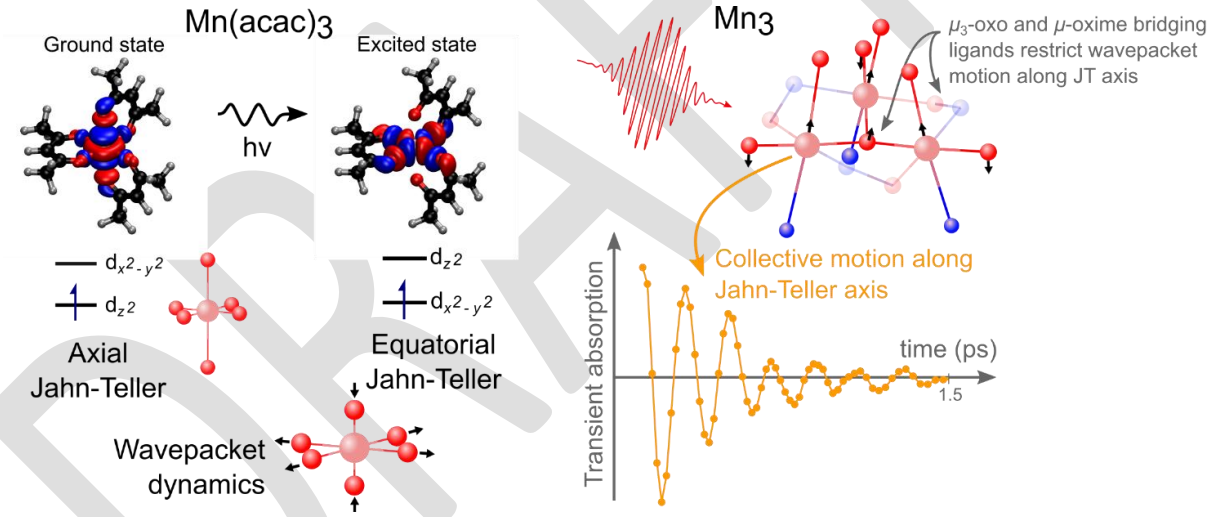

Figure 6.10. *Photophysics of Mn^{3+} complexes. The antibonding nature of the e_g orbitals lead to a rapid switch of the JT distortion in the excited state of $Mn(acac)_3$ (left). In Mn_3, the strong bonds in the triangle prevent equatorial expansion and the Mn ion (right)[16].*

Recent developments in ultrafast magnetism have resulted in photo-magnetic recording in materials which has the distinct advantage of faster sequential switching rates due to the non-thermal mechanism[15]. These experiments make use of specific optical transitions, exciting the electrons from one atomic orbital to another which in turn changes the magneto-crystalline anisotropy[15]. However, the microscopic mechanisms responsible are difficult to understand because they involve a high density of electronically excited states, vibrational motion, and different spin states which are all highly coupled (see 6.1). At present, this lack of a detailed understanding hinders the development of new materials to achieve fast, energy-efficient and also miniaturising the magnetic grains towards the nanoscale.

The capability of fs X-ray spectroscopy will facilitate unprecedented new insights into the mechanism of emerging photo-magnetic materials, such as the trinuclear SMM $[Mn^{III}_3O(Et\text{-}sao)_3(\beta\text{-}pic)_3(ClO_4)]$[16], as performed for light-induced excited spin-state trapping (LIESST) systems[17]. In this case vibrational

wavepacket, closely linked to the Jahn-Teller distortion (Figure 6.10) upon excitation were found to be closely linked the magnitude and orientation of the magnetic anisotropy. These results highlight the strong coupling between electronic and nuclear degrees of freedom, and the strong electron correlation between electrons on Mn sites in the polynuclear molecule important for the photo-magnetic properties. The ability to probe the electronic (XAS, XES), structural (XAS) and spin (XES) dynamics of these complex materials and related analogues on the timescale upon which they operate, i.e. femtoseconds, will enable fine control of the magnetic properties and coherence times of these materials and provide crucial new insights urgently required to develop to new storage materials.

References

[1] *Adoption of the Paris Agreement* FCCC/CP/2015/L.9/Rev.1 (UNFCCC, 2015).

[2]Committee on Climate Change Report to Parliament – Meeting Carbon Budgets: Closing the Policy Gap(2017) https://www.theccc.org.uk/publication/2017-report-to-parliament-meeting-carbon-budgets-closing-the-policy-gap/

[3] *a*) TJ Penfold *et al.* Nature Comm. 9 (2018) 478, b) Y. Uemura *et al. Angew*. Chem., Int. Ed. 55 (2016) 1364-1367.

[4] S. Kim *et al.* ACS Energy Lett. 3 (2018) 496−500.

[5] H.J. Snaith Nature Mater. 17 (2018) 372-376.

[6] J. Paier *et al.* Phys. Rev. B, 79 (2009) 115126.

[7] J.S. Park, *et al.* Nature Rev. Mater. 3 (2018) 194–210.

[8] F. Wu *et al. Chem. Soc. Rev.* https://doi.org/10.1039/C7CS00863E (2020).

[9] P. Leung, *et al.* J. Power Sources 360 (2017) 243-283.

[10] V.T. Pham *et al.* J. Am. Chem. Soc. 133 (2011) 12740-12748.

[11] D. Ortiz, *et al. ChemSusChem* 8 (2015) 3605-3616.

[12] K-K. Lee *et al. Nature Comm.* 8 (2017): 14658.

[13] V. Palomares, *et al. Energy Environ. Sci.* 5 (2012) 5884-5901.

[14] Z-L Xu, *et al.* Nature Comm. 10 (2019) 2598.

[15] A. Stupakiewicz et al. *Nature* 542 (2017) 71–74.

[16] F. Liedy et al. Nature Chem. (2020). https://doi.org/10.1038/s41557-020-0431-6

[17] a) G. Auböck et al. Nature Chem. 7 (2015): 629-633, b) W. Zhang et al Nature 509 (2014) 345-348.

6.4 Understanding Catalysis

Although catalysts are often the key to invaluable chemical and biochemical processes, their complex and elusive nature has by and large defied our current abilities to characterise and understand their microscopic action. This situation has partly arisen from the very fast timescales involved in their role as agents of chemical action, which are faster than conventional characterisation capabilities. The recent developments in femtosecond XFEL technology and instrumentation have finally opened the door on this fascinating research area, and we now have an unprecedented opportunity to capture the behaviour of catalysts in their active state. These developments are expected to now deliver on the long-standing dream of catalyst by design, as opposed to trial and error.

6.4.1 Introduction to catalysis

Catalysis is fundamental for the sustainability of our modern way of life. Most of the products that we use regularly, such as medicines, fuels, fertilizers, perfumes and those products designed for the purification of air and water make use of a catalyst at some point during their manufacture. Catalysts can also be found in nature, where they facilitate critical reactions. It is estimated that 90% of all chemical processes involve the use of a catalyst[1]. From an economic point of view, catalysis generates £50 billion a year for the UK economy through the nation's chemical industry. In 2016, this industry accounted for £12.1 billion of the UK economy's Gross Value Added (GVA)[2] and approximately 100,000 direct jobs[3].

The discovery of new and improved catalysts is becoming ever more important in order to produce sustainable materials as efficiently as possible. Typical methods that are used in catalyst development are often based on a trial and error approach, where a catalyst is exposed to several types of substrates and analysed, and the process is repeated with adjusted design and operational parameters[4]. Although this approach is often successful, it is heavily resource intensive both in terms of researcher time and materials, which are often rare and precious metals, whilst still effectively being very narrow in scope. The rational development of catalysts is the alternative approach, but it needs deep understanding of a catalyst's specific functionality and reaction mechanisms. Effective progress by this route can only be achieved by knowing the detailed geometrical structure of the catalyst's atomic and molecular environments, as well as their active electronic structure, and how all these factors change during chemical processes.

Most catalytic studies focus on either the structural characterization of the product outcome or on the low energy intermediates formed long after the activation period. However, most catalytic mechanisms require an activation point from where a low energy state material, or pre-catalyst, needs to be 'pumped' to form the true catalyst which exists in a highly reactive state. This true catalyst can then undergo chemistry that either could not otherwise be performed or with a high selectivity towards the generation of one product type. The characterisation of either the activation route or the properties of the activated species is a challenging prospect, as by its very nature the complex is highly unstable and often short-lived, but in spite of this difficulty this issue is critical to address as it clearly pre-determines the future catalyst's operational ability. To produce a major shift forwards in the field of catalysis, the focus must therefore shift from the analysis of product distribution and kinetic outlooks, to a direct method of experimental characterisation of the active species paired with advanced computational theory.

X-ray Free Electron Lasers (XFEL) are nowadays capable of providing intense and short X-ray pulses, presenting an exciting opportunity to enable the determination of the nature of transient catalytic intermediates and the dynamics with which they are formed, so we can understand, predict and control the resulting chemical processes. X-ray Absorption Near Edge Structure (XANES) spectroscopy, X-ray Emission Spectroscopy (XES), X-ray Scattering (XS) and Resonant Inelastic X-ray Scattering (RIXS) are some of the techniques that have successfully been used in XFELs for the study of catalytic reactions.

6.4.2 Catalysis and XFEL

Photocatalysts are set to become some of the most important materials in terms of sustainability, looking to harness the sun's energy in order to perform high energy transformations, such as water splitting or fuel production[5,6]. Laser pump/X-ray probe studies are proving to be a truly unique characterisation tool for these materials, identifying the highly active species and key excited state chemistry. Many pump-probe studies in catalysis have been performed using the temporal probe capabilities of third generation synchrotron sources, enabling investigations on time scales of hundreds of picocoseconds[7–10]. Although time resolutions below the picosecond have been achieved at synchrotron sources using original timing schemes, such as laser-electron slicing, this has been attained at a significantly reduced flux[11,12]. The emergence of XFEL sources has enabled studies in femtosecond timescales with high flux, that have subsequently allowed the electron and nuclear movements to be followed in real time far from thermal equilibrium, both in the soft and hard X-ray regimes. Here we will review the most significant catalysis studies performed at XFEL facilities in recent years.

Most of the catalytic system studies on femtosecond time scales in the hard x-ray regime have been focussed on understanding the photochemistry of transition metal complexes, as they play essential roles as photosensitizers for hydrogen evolution[13] or for solar energy conversion[14]. Transition metal complexes are widely used for photochemical application due to their ability to absorb light, and subsequently create energetic excited states with holes and electrons that are well separated between the metal centre and the ligands. XANES spectroscopy is ideally suited to investigate the electronic and geometric structure of transition metal centres, taking advantage of the element specificity of the technique to provide access to the d-d electronic transitions in the excited state that cannot be directly detected by optical spectroscopy. The first femtosecond time-resolved XANES (TR-XANES) experiment in the hard X-ray regime was carried out in 2010 at the Linac Coherent Light Source (LCLS)[15] achieving a time-resolution of 500 fs, limited by the instability of the XFEL pulses in arrival time. Since then, the situation has been improved upon, using several technological advances[16–19], enabling numerous femtosecond XANES investigations.

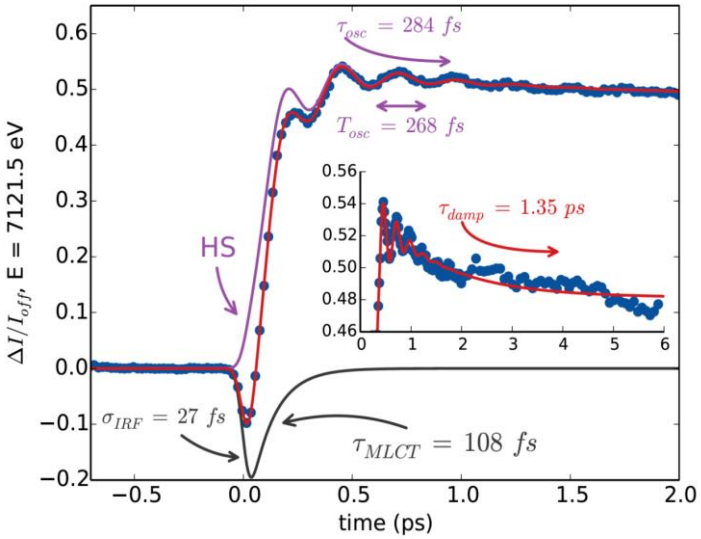

Figure 6.11. *Fit to the femtosecond transient XANES of $[Fe(bpy)_3]^{2+}$ measured at 7121.5 eV, showing the contribution of the MLCT and of the oscillating high spin state (ref. 20).*

One recent example by Lemke et al.[20] used TR-XANES to investigate nuclear wave packet oscillations of the solvate iron (II) bipyridine complex for the first time, extracting valuable information of the Fe-N breathing vibrational mode (Figure 6.11). The system was previously studied using the time resolution available at synchrotron sources[21,22], and although the structural dynamics of the spin crossover was revealed, the molecular breathing was not observed due to the insufficient signal to noise ratio. In a similar experiment, Katayama et al.[23] managed to track multiple components of the coherent nuclear wavepacket dynamics in a copper (I) phenanthroline complex, showing that the amplitude of the identified vibration modes can be modified by changing the incident X-ray energy. The increased stability of the XFELs has facilitated the performance of X-ray Absorption Spectroscopy experiments in an extended energy range. Following the publication of the first steady-state Extended X-ray Absorption Fine Structure (EXAFS) spectrum acquired at the LCLS[24], Britz et al.[25] collected a full

range time resolved EXAFS spectrum up to 500 eV above the absorption edge on a Fe(II) polypyridine complex in solution.

While XANES is used to provide information about the empty electronic states of transition metal centres, XES is used to provide information about the occupied density of states projected on the absorbing atom. Although time resolved XES (TR-XES) has been performed in synchrotron sources to determine the spin state of transition elements with picosecond time resolution[26], the technique has benefitted greatly from the high pulse intensity and high time resolution of XFEL sources. Many investigations have been performed on the study of the K_α and K_β emission lines of 3d transition metals in molecules, taking advantage of the sensitivity of these emission lines to the oxidation state and the number of unpaired electrons of the transition[27].

The valence electronic structure of transition metal complexes in solution has also been studied with X-ray spectroscopy in the soft X-ray range with femtosecond time resolution at XFEL sources[28,29]. Time-resolved RIXS (TR-RIXS) at the Fe L_3 edge has been performed to study the ligand exchange dynamics of $Fe(CO)_5$, concluding that the photoinduced removal of CO generates a 16-electron $Fe(CO)_4$ species in an excited singlet state, that either converts to the triplet ground state or combines with a solvent molecule to regenerate a penta-coordinated low spin singlet state Fe species (Figure 6.12). It can also recombine with a CO molecule to regenerate the initial state.

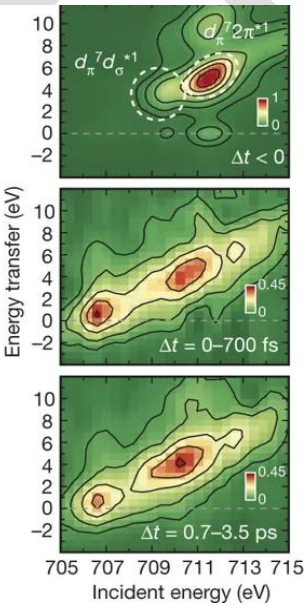

Figure 6.12. *Time-resolved RIXS at the Fe L_3 edge sheds light on the ligand exchange dynamics of $Fe(CO)_5$. Measured Fe L3-RIXS intensities versus energy transfer and incident photon energy. Top: ground-state $Fe(CO)_5$. Middle and bottom: difference intensities for delay intervals of 0–700 fs and 0.7–3.5 ps, respectively (ref. 28)*

Femtosecond soft X-ray pulses have also been used to probe the real-time dynamic evolution of the adsorbate electronic structure of different transient species during chemical reactions using TR-XANES and TR-XES. These studies are important to increase our microscopic understanding of surface reactions, a longstanding goal in heterogeneous catalysis, where chemical reactions occur at the solid surface. In these studies, the optical laser is used to start the reaction, while the XFEL pulse is used to follow the changes in the electronic structure of the adsorbate[30]. Several studies have been focussed on the study of the desorption of a CO molecule from a Ru (0001) surface[31,32] at both the O and the C K-edge[33]. Ultrafast X-ray spectroscopy has also been used to identify the short-lived intermediates that are formed during reaction of CO with O_2 on a ruthenium surface[34]. In this study, the optical laser pulse excites motions of CO and O_2 on the surface, allowing the reactants to collide, while new electronic states are shown in the oxygen TR-XANES spectrum.

The ability to perform time resolved XS (TR-XS) in solution is also widely used in XFEL sources for the study of catalytically relevant systems, as it provides information on the structural changes in the system under study, including the changes in the solvent cage and the dynamics of the bulk solvent after excitation. TR-XS has been used to extract information of the excited state dynamics in iridium based dimeric complexes in acetonitrile solution[35], and has also been used to study the ultrafast structural dynamics of bond formation in $[Au(CN)_2^-]_3$ in solution[36,37].

As the experimental requirements for TR-XES and in-solution TR-XS are very similar, requiring the use of a fixed incident energy, several investigations have been performed combining both techniques at XFEL sources, illustrating the complementary nature of the techniques: while XES provides information on the changes of the electronic structure, XS provides information on the structural changes. This has been used for the study of photocatalytic dyads[38], and the study of the solvent-solute interactions that occur simultaneously to the spin transition on aqueous Fe(II) bipyridine [39].

6.4.3 Opportunities in catalysis

As seen in the previous section, XFEL sources are now beginning to make a significant impact upon the way that we understand chemical processes. The examples demonstrate that the short duration and high flux of the XFEL pulses can be used effectively to observe atomic motions and electronic transitions in real time, moving from the scenario where experiments were limited to study only thermally relaxed transient states. The ultimate goal in catalysis is to be able to record movies of chemical processes, where molecular electronic and nuclear structural dynamics are acquired, and XFEL sources are well along the path to delivering this capability. The resulting insights will ultimately bring control of reactions at the electronic and atomic level, when they are initiated by light or other stimuli.

Although spectroscopy and scattering techniques are currently being used with success at XFEL sources to help understand catalytic systems, especially in the field of photocatalysis, most of these studies have so far only been performed on model molecular systems far from real conditions of concentration. It is expected that in future, profiting from technological developments, it will become possible for more challenging systems to be studied at XFEL sources under more realistic conditions of concentration and within complicated sample environments. Developments of this type are clearly of considerable interest in catalysis, where often low amounts of the active species are used, and reactions are often performed under harsh conditions of high temperature with toxic and/or flammable gas atmospheres.

It is however important to note that, the more complicated the system to study, the more difficult it will be to obtain a complete picture of the chemical process with a single structural technique, and the application of multiple techniques simultaneously is going to be necessary if the comprehensive insight required for knowledge guided process optimisation is to be obtained. Chemical studies at synchrotrons reflect this, as multidisciplinary methods under realistic conditions are nowadays routinely used to deliver the full hierarchical characterisation of materials. The study of chemical processes at XFEL sources is not an exception, and many XFEL end-stations now offer the instrumentation needed to perform both spectroscopy and scattering. XES and in-solution XS are frequently used simultaneously, providing complementary information: XES providing information on the electronic configuration dynamics through probing the unoccupied density of states, and in-solution XS providing information on the nuclear motion and changes in the solvent structure. Both methods need a fixed wavelength to be performed and there is no need for scanning the incident beam, and they both profit from the pulse nature of the XFEL source, collecting the entire spectrum in a single acquisition. XANES is often available together with XES and XS, providing complementary information about the occupied density of states of the absorbing element, but as the technique requires the incident energy to be scanned, it cannot be collected using the XFEL single pulse. In future, one could envisage being able to get information about the occupied density of states using the pulse nature of the XFEL sources. This can be achieved using High Energy Resolution Off-Resonant Spectroscopy (HEROS). This method, when performed using an X-ray spectrometer operating in a dispersive geometry, allows measurements of a scattered X-ray spectrum in a single acquisition using monochromatic incident beam. The feasibility of the method was first demonstrated at the Swiss Light Source (SLS), but due to the extremely weak scattering cross section of the off-resonant signal, it has not been exploited at synchrotron sources[40]. More recently, HEROS has been used at the LCLS to record the static spectra of copper and copper oxide with femtosecond time resolution, taking advantage of the brightness of the XFEL pulses[41]. The next step will be to use this method to study the electronic dynamics of ultrafast chemical processes and combine it with the simultaneous collection of XS data to get structural information, as it is nowadays possible to do when combining XES and XS.

An additional method that will be able to provide complementary spectroscopy information in the hard x-ray regime is X-ray Raman Scattering (XRS). The technique uses hard X-rays for performing XANES spectroscopy of light elements, such as O, C, N, etc... The use of hard X-rays makes this method

a bulk sensitive probe that can be used with a broad range of sample environments, removing the experimental difficulties of working in the soft x-ray regime. Providing access to the study of the electronic structure of low Z materials in the bulk is of significant interest in the study of catalytic reactions, particularly in the field of heterogeneous catalysis, where most systems are composed of an active support that is used for the conversion of small molecules consisting of C, O, N and H. The Raman cross section is orders of magnitude smaller than that of the photoelectric absorption, so this method will benefit greatly from the high flux available in XFEL sources, as experiments will be feasible at more realistic concentration conditions than what is currently achievable at synchrotron sources. The combination of XRS with other techniques, such as XES and XS, will provide a more complete picture of the catalytic process.

Sometimes in catalysis, the 'one-pot' approach, in which more than one catalyst is used in a single reactor to perform sequential transformations, is used instead of the more traditional stepwise-mediated synthetic approaches. In other cases, the catalytic species contains more than one active site, each catalysing a different step in a chemical process, as is the case of mixed metal photocatalysts. The determination of the electronic and structural dynamics of all the active species involved in the catalytic process is necessary in both scenarios in order to elucidate the reaction mechanism, and to understand how the changes of one active site correlate to the others during the reaction. The use of element sensitive techniques, such as X-ray spectroscopies, is an ideal way to acquire this understanding, allowing the disentanglement of the role of the different sites by tuning the energy to the selected element. These sorts of studies have traditionally been performed in a sequential manner, both at synchrotron and XFEL sources, focussing on one active site after another. Very recently, a novel experiment has been performed at the European XFEL in a Fe-Co dyad, where the iron centre acts as the photosensitizer while the cobalt centre catalyses the reaction once the intra-molecular charge transfer has occurred[42]. The experiment used two dispersive emission spectrometers simultaneously, one aligned to collect the emission spectrum of the iron centre, and the other, the Co centre. By measuring the two sites simultaneously, the authors of that study managed to correlate the electronic dynamics of both active sites within the photocatalyst. Although this pioneering experiment represents an important step forwards towards the understanding of the electronic dynamics of mixed metal catalysts, the system was chosen carefully so that the absorption edges of the two active sites are close enough in energy to allow the simultaneous collection of the emission spectra. However, it is not easy to extend this methodology to other systems where the absorption edges of the elements of interest are at very different energies, but this restriction could be overcome by using two X-ray beams impinging in the sample simultaneously, in similar fashion to what has been done at Diamond Light Source, where a soft and a hard X-ray beam are used for electron spectroscopy[43]. Such a development would make the collection of simultaneous XES for more than one element much more generally applicable, including the possibility to study elements with absorption edges in the hard and soft X-ray energy regimes (Figure 6.13). In these cases, not only mixed catalysts can be studied, but also metal transition catalysts with low Z ligands, i.e., the hard X-ray beam will be used to study the electronic dynamics of the transition metal active site, while the soft x-ray beam will be used to study the electronic changes in the ligand donor. This methodology will provide unprecedented insight into electronic movements from two or more atomic sites simultaneously.

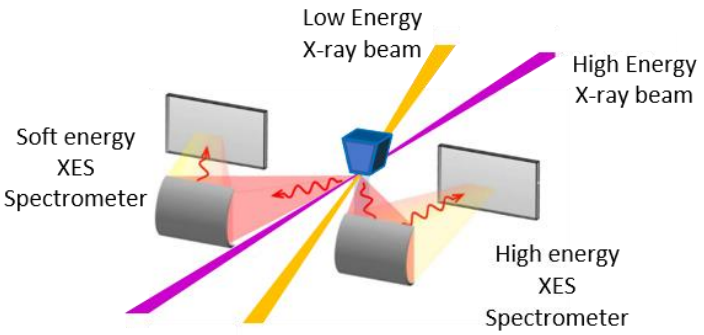

Figure 6.13. *Schematic of a XES experiment performed in the soft and the hard X-ray regime simultaneously (adapted from ref. 19).*

References

1. G. Ertl *et al. Handbook of Heterogeneous Catalysis*. (Wiley-VCH, Weinheim, 2008). DOI: 10.1524/zpch.1999.208.part_1_2.274.
2. *GDP(O) Low Level Aggregates National Accounts, ONS, 2017*.
3. *'Employee Jobs by Industry', ONS, September 2017*.
4. Q. Zhao *et al.* "*N-Heterocyclic Carbene Complexes in C-H Activation Reactions*". *Chemical Reviews* vol. 120 1981, (2020) DOI: 10.1021/acs.chemrev.9b00634.
5. J. K. McCusker. "*Photocatalysis: Fuel from photons*". *Science* vol. 293 1599, (2001) DOI: 10.1126/science.1064112.
6. M. Grätzel. "*Solar energy conversion by dye-sensitized photovoltaic cells*". *Inorg. Chem.* 44, 6841, (2005) DOI: 10.1021/ic0508371.
7. L. X. Chen *et al.* "*Photochemical processes revealed by X-ray transient absorption spectroscopy*". *J. Phys. Chem. Lett.* 4, 4000, (2013) DOI: 10.1021/jz401750g.
8. S. A. Bartlett *et al.* "*Monitoring the Formation and Reactivity of Organometallic Alkane and Fluoroalkane Complexes with Silanes and Xe Using Time-Resolved X-ray Absorption Fine Structure Spectroscopy*". *J. Am. Chem. Soc.* 141, 11471, (2019) DOI: 10.1021/jacs.8b13848.
9. L. X. Chen *et al.* "*Tracking electrons and atoms in a photoexcited metalloporphyrin by X-ray transient absorption spectroscopy*". *J. Am. Chem. Soc.* 129, 9616, (2007) DOI: 10.1021/ja072979v.
10. L. X. Chen *et al.* "*X-ray snapshots for metalloporphyrin axial ligation*". *Chem. Sci.* 1, 642, (2010) DOI: 10.1039/c0sc00323a.
11. R. W. Schoenlein *et al.* "*Generation of femtosecond pulses of synchrotron radiation*". *Science* 287, 2237, (2000) DOI: 10.1126/science.287.5461.2237.
12. P. Beaud *et al.* "*Spatiotemporal stability of a femtosecond hard-X-ray undulator source studied by control of coherent optical phonons*". *Phys. Rev. Lett.* 99, 1, (2007) DOI: 10.1103/physrevlett.99.174801.
13. J. I. Goldsmith *et al.* "*Discovery and high-throughput screening of heteroleptic iridium complexes for photoinduced hydrogen production*". *J. Am. Chem. Soc.* 127, 7502, (2005) DOI: 10.1021/ja0427101.
14. H. B. Gray *et al.* "*Solar chemistry of metal complexes*". *Science* 214, 1201, (1981) DOI: 10.1126/science.214.4526.1201.
15. H. T. Lemke *et al.* "*Femtosecond x-ray absorption spectroscopy at a hard x-ray free electron laser: Application to spin crossover dynamics*". *J. Phys. Chem. A* 117, 735, (2013) DOI: 10.1021/jp312559h.
16. T. Katayama *et al.* "*Femtosecond x-ray absorption spectroscopy with hard x-ray free electron laser*". *Appl. Phys. Lett.* 103, (2013) DOI: 10.1063/1.4821108.
17. T. Katayama *et al.* "*A beam branching method for timing and spectral characterization of hard X-ray free-electron lasers*". *Struct. Dyn.* 3, 034301, (2016) DOI: 10.1063/1.4939655.
18. K. Nakajima *et al.* "*Software for the data analysis of the arrival-timing monitor at SACLA*". *J. Synchrotron Radiat.* 25, 592, (2018) DOI: 10.1107/s1600577517016654.
19. Y. Kayser *et al.* "*Core-level nonlinear spectroscopy triggered by stochastic X-ray pulses*". *Nat. Commun.* 10, 1, (2019) DOI: 10.1038/s41467-019-12717-1.
20. H. T. Lemke *et al.* "*Coherent structural trapping through wave packet dispersion during photoinduced spin state switching*". *Nat. Commun.* 8, (2017) DOI: 10.1038/ncomms15342.
21. W. Gawelda *et al.* "*Structural determination of a short-lived excited iron(II) complex by picosecond X-ray absorption spectroscopy*". *Phys. Rev. Lett.* 98, 6, (2007) DOI: 10.1103/physrevlett.98.057401.
22. C. Bressler *et al.* "*Femtosecond XANES study of the light-induced spin crossover dynamics in an iron(II) complex*". *Science* 323, 489, (2009) DOI: 10.1126/science.1165733.
23. T. Katayama *et al.* "*Tracking multiple components of a nuclear wavepacket in photoexcited Cu(I)-phenanthroline complex using ultrafast X-ray spectroscopy*". *Nat. Commun.* 10, 1, (2019) DOI: 10.1038/s41467-019-11499-w.
24. R. Chatterjee *et al.* "*XANES and EXAFS of dilute solutions of transition metals at XFELs*". *J. Synchrotron Radiat.* 26, 1716, (2019) DOI: 10.1107/s1600577519007550.
25. A. Britz *et al.* "*Resolving structures of transition metal complex reaction intermediates with femtosecond EXAFS*". *Phys. Chem. Chem. Phys.* 22, 2660, (2020) DOI: 10.1039/c9cp03483h.
26. G. Vankó *et al.* "*Picosecond time-resolved X-ray emission spectroscopy: Ultrafast spin-state determination in an iron complex*". *Angew. Chemie - Int. Ed.* 49, 5910, (2010) DOI: 10.1002/anie.201000844.
27. W. Zhang *et al.* "*Tracking excited-state charge and spin dynamics in iron coordination complexes*". *Nature* 509, 345, (2014) DOI: 10.1038/nature13252.
28. P. Wernet *et al.* "*Orbital-specific mapping of the ligand exchange dynamics of Fe(CO)5 in solution*". *Nature* 520, 78, (2015) DOI: 10.1038/nature14296.
29. K. Kunnus *et al.* "*Identification of the dominant photochemical pathways and mechanistic insights to the ultrafast ligand exchange of Fe(CO)5 to Fe(CO)4EtOH*". *Struct. Dyn.* 3, (2016) DOI: 10.1063/1.4941602.
30. T. Katayama *et al.* "*Ultrafast soft X-ray emission spectroscopy of surface adsorbates using an X-ray free electron laser*". *J. Electron Spectros. Relat. Phenomena* 187, 9, (2013) DOI: 10.1016/j.elspec.2013.03.006.
31. M. Dell'Angela *et al.* "*Real-Time Observation of Surface Bond Breaking with an X-ray Laser*". *Science* 339, 1302, (2013) DOI: 10.1126/science.1231711.
32. M. Beye *et al.* "*Selective ultrafast probing of transient hot chemisorbed and precursor states of CO on Ru(0001)*". *Phys. Rev. Lett.* 110, 1, (2013) DOI: 10.1103/physrevlett.110.186101.
33. H.-Y. Wang *et al.* "*Time-resolved observation of transient precursor state of CO on Ru(0001) using carbon K-edge spectroscopy*". *Phys. Chem. Chem. Phys.* 22, 2677, (2020) DOI: 10.1039/c9cp03677f.
34. H. Öström *et al.* "*Probing the transition state region in catalytic CO oxidation on Ru*". *Science* 347, 978, (2015) DOI: 10.1126/science.1261747.
35. T. B. Van Driel *et al.* "*Atomistic characterization of the active-site solvation dynamics of a model photocatalyst*". *Nat. Commun.* 7, (2016) DOI: 10.1038/ncomms13678.
36. K. H. Kim *et al.* "*Direct observation of bond formation in solution with femtosecond X-ray scattering*". *Nature* 518, 385, (2015) DOI: 10.1038/nature14163.
37. K. H. Kim *et al.* "*Femtosecond X-ray solution scattering reveals that bond formation mechanism of a gold trimer complex is independent of excitation wavelength*". *Struct. Dyn.* 3, (2016) DOI: 10.1063/1.4948516.
38. S. E. Canton *et al.* "*Visualizing the non-equilibrium dynamics of photoinduced intramolecular electron transfer*

with femtosecond X-ray pulses". *Nat. Commun.* 6, 1, (2015) DOI: 10.1038/ncomms7359.
39. K. Haldrup *et al.* "*Observing Solvation Dynamics with Simultaneous Femtosecond X-ray Emission Spectroscopy and X-ray Scattering*". *J. Phys. Chem. B* 120, 1158, (2016) DOI: 10.1021/acs.jpcb.5b12471.
40. J. Szlachetko *et al.* "*High energy resolution off-resonant spectroscopy at sub-second time resolution: (Pt(acac) 2) decomposition*". *Chem. Commun.* 48, 10898, (2012) DOI: 10.1039/c2cc35086f.
41. J. Szlachetko *et al.* "*The electronic structure of matter probed with a single femtosecond hard x-ray pulse*". *Struct. Dyn.* 1, (2014) DOI: 10.1063/1.4868260.
42. M. Bauer. "*Private Communication*".
43. T. L. Lee *et al.* "*A Two-Color Beamline for Electron Spectroscopies at Diamond Light Source*". *Synchrotron Radiat. News* 31, 16, (2018) DOI: 10.1080/08940886.2018.1483653.

6.5 Chemistry and the Environment: Aerosols, Atmospheric, Space Chemistry, Combustion, Corrosion

The chemistry of complex mixtures inherent in environmental and industrial situations, provides some of the most challenging examples of chemistry to study. The multiscale nature of the problems, combined with random mixing and, complex kinetics of multiple competing chemical processes, means that accurate measurements are vital for producing the quantitative models that can be used for material capability studies and process optimisation. Current approaches leave us some way from this point. The capability of a high repetition rate XFEL to provide temporally, spatially and chemically specific maps of reaction mixtures during the process will provide mechanistic detail far beyond current capabilities. The information rich data will provide new perspectives on the chemical and physical properties and processes that control efficiency and material degradation, providing new routes to process optimisation, control and environmental reform.

6.5.1 Chemistry and the Environment

Chemistry in the environment covers a broad range of atmospherically and industrially important processes. The key features that links these aspects together is the complex interplay between the chemical changes occurring and the inhomogeneous mixing, driven by complex gas or fluid dynamics.[1] The combined effects lead to localised chemical changes with almost chaotic spatial and temporal characteristics in some circumstances. This combination of the multiscale (in both length and time) nature of the system characteristics with the inherent spatial inhomogeneities means accurate measurements remain a significant challenge to conventional light sources. The ability of XFELS to measure spectra in a single laser pulse, combined with chemical specificity and particle detection make XFELs a potentially game changing source for the study of the chemistry of these complex mixtures and materials.

In all cases, the ability to initiate chemistry with a variety of pump sources (IR, UV, VUV, e-Beam) provides routes to studying different reaction types of relevance to various environmental areas. Combined with measurement of ion, electron energy or photon absorption and emission provides a multiplexed approach to complex chemical problems that would be impossible to solve with a single technique alone.

6.5.2 Combustion

As well as driving the development of next generation energy production and storage materials (Section 6.3), the UK XFEL can continue to drive efficiency savings in the energy sector through increased understanding of combustion dynamics. Combustible fuels form an integral and, currently irreplaceable, part of our energy landscape. They provide a high energy density material that is easily stored and transported, making them a key commodity for the foreseeable future. While the UK has committed to banning the sale of new Petrol and Diesel vehicles from 2035, the use of combustible fuels in other areas is set to continue, such that the challenges associated with driving ever increasing efficiencies should continue to be met. As an example of the impact of efficiency savings, around 80% of energy used within the UK still derives from combustion sources. Despite the ever-increasing energy demands of a growing population and the UKs continued reliance on combustible fuels, UK emissions continue to fall and in 2018 were 44% below 1990 levels[2], in large part driven by increased efficiency. The UK moves towards the target of net zero emissions by 2050, meeting which will require the combined effect of both new technologies and an increase in energy efficiency, both of which are areas where the capabilities of a UK XFEL source can address open questions.

Intelligent routes to increasing the efficiency of combustion sources requires temporally and spatially resolved, species specific measurements of the complex chemistry occurring. This data is a prerequisite for the development of predictive models that can direct next generation system development. For combustion this means detailed and accurate measurements of the dynamic chemical distribution

within the flames are required. Optical and fluorescence measurements have limited applicability due to the highly scattering environments and variability in pressure creating spatially dependent quenching rates, limiting data reliability and availability.[3] Synchrotron based methods can provide time averaged speciation maps through soft X-ray absorption and fluorescence measurements[4,5] but currently miss the temporal changes in species and how this links to gas dynamics and time dependent local changes in density, pressure and temperature. The unique capabilities of an XFEL in providing high X-ray fluxes at potentially high repetition rates would allow single shot spectral measurements across large spatial areas, providing temporally and spatially resolved species specific maps during the combustion process. Spatially tracking the production, distribution, growth and loss of polycyclic aromatic hydrocarbons (PAHs) for example, will provide details of the early stages of particulate formation and how the local physical characteristics as well as the chemical environment either enhances or perturbs their formation, Figure 6.14. This has further links to the chemistry of hot and cold plasmas in planetary atmospheres and to the chemistry of space (Section 6.5.4) where, PAHs form around 20% of all galactic carbon but question remain over whether their formation is a top down process, deriving from the breakup of soot from carbon stars, or bottom up from small unsaturated chemical species.

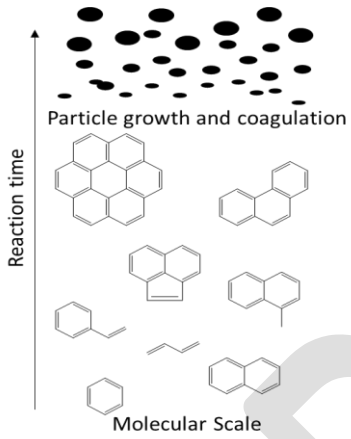

Figure 6.14. *Schematic reaction scheme of the formation of soot particulates in combustion. XFEL probes can potentially map all stages from the molecular growth and formation of PAHs through XANES and XES spectroscopy, through to particle size distribution via scattering and surface chemistry and structure through X-ray surface second harmonic generation. The techniques will cover timescales and length scales, from femtoseconds and Angstroms at the molecular level, through to 100s of nm and microsecond for the particulate formation.*

This ability becomes increasingly important as we move to higher efficiency engine types, such as those based on Homogeneous Charge Compression Ignition (HCCI). HCCI engines provide much higher fuel efficiency than other internal combustion engines, achieving both CO_2 and NO_x reduction.[6] In HCCI engines, the ignition of the fuel is driven by compression leading to autoignition. The much higher pressure and much lower temperature make the resulting chemistry quite different[7] to a standard engine, and makes measurements challenging. Utilising the high brightness X-rays from an XFEL will allow for dynamic imaging of the combustion process. By moving beyond state-averaged quantities, such as mixing fractions, to tracking of real time and spatially resolved chemical changes, fully correlative analysis of the turbulent reaction mixtures can be performed. Laser-derived perturbations, e.g. laser filaments, can then drive changes in processes like particle formation,[8] allowing for measurements covering timescales from femto- to micro-seconds. Species-specific probing can be further enhanced through the use of stimulated X-ray Raman probes to monitor changing bonding character in specific reactive intermediates and stable molecules through the flame.[9] The highly detailed and information-rich data will provide detail far beyond the current state of the art, allowing for new insights into the complex interplay of chemistry, fluid dynamics, nucleation and particulate formation that define the fundamental chemical and physical processes that affect energy conversion efficiency.

6.5.3 Corrosion and Biofilms

Material suitability and lifetime is often defined by the corrosion processes that degrade material quality over time. Our molecular level understanding of the chemical processes and mechanisms that drive material degradation is limited which means our ability to design and manage materials over extended periods is far from optimal. Typical corrosion prevention methods rely on sacrificial layers or

the control of diffusion through the use of structured surfaces and coatings. Mechanistic information could lead to a breakthrough technology that impedes the chemistry that drives corrosion helping to reduce the trillion-pound cost of corrosion to global economies and preserve precious material resources.[10]

To develop these controls requires a molecular level understanding of the degradation pathways and how the surface level interaction are affected by the coatings and structures currently used. Such studies require detailed structural information of the surface topography and chemical state. Measurement of localised oxidation state changes and identification of deposits and corrosion products requires high sensitivity and rapid spectral data collection. Similar to the combustion studies, the ability to map spatial regions in a single shot removes state averaging and allows for correlative analysis of the changes across all aspects. In electrochemically driven processes this could include information on the etching and structuring of the surface combined with oxidation state changes and chemical product formation, providing the multivariable analysis required in order to understand the interplay between physical, chemical and structural effects.

Another pressing concern of material suitability and corrosion surrounds the development of biofilms. Biofilms form due to the collective growth of microorganism over surfaces. While this presents material opportunities, their growth over implants and in fuel and chemical storage containers causes bacterial infections, corrosion of surfaces and degradation of stored material.[11] Large scale investment into the prevention, detection and management of biofilms is driven by the needs of wide-ranging industries affected by these issues. There are fundamental questions surrounding the composition and dynamics of biofilm growth and how adaptions to the molecular framework could be used to direct growth and control activity for potentially beneficial applications. For this to become reality standardised models need to be developed which must be based on detailed experimental data.

For both corrosion and biofilm studies probes that are sensitive to surface properties and reactions are required. Newly emerging techniques that are only possible at high intensity XFEL facilities are moving non-linear optical probes developed in the visible and infrared into the X-ray regime. In recent experiments at the FERMI XFEL soft X-ray second harmonic generation experiments were performed on graphite surfaces and showed surface level sensitivity with element specificity.[12] These non-linear X-ray techniques will play a key role in understanding these surface driven process and will have strong links to the catalysis experiments (section 6.4). The increased penetration depth and atom specificity of the X-ray second harmonic generation experiments will detail active site information and molecule specific kinetics even at buried layers and interfaces.[12] Moreover, by simultaneously following biofilm growth the activity of bacteriophages at controlling and removing biofilms can be integrated at the molecular level, impacting on the boundary between chemistry, life sciences and industry.

6.5.4 Atmospheric and Space Sciences

Atmospheric science shares many of the experimental challenges associated with studies of low temperature combustion. The generation of radical and reactive species through exothermic reactions leads to local heating and pressure changes that redistribute the reactive species setting off chains of chemical reactions that depend on the local chemical composition. With the ever-increasing range and complexity of chemicals in the atmosphere creating challenges in the measurement and characterisation,[13] it is from this starting point that wide and varied chemistries can occur leading to reactions with trace pollutants, aerosol or particulate formation, or termination through recombination. The relevance of these effect will of course bridge across all planetary atmospheres. Impacting on our understanding of the development and chemistry of other planetary atmospheres where, detailed measurements of systems both within our solar system (e.g. Titan, Jupiter, etc) and outside (exoplanets) are increasing in number and relevance.

Almost all these processes proceed through complex multi-welled potential energy surfaces. The formation of bound intermediates leads to indirect reactions, multiple branching points and complex kinetics.[7] Identifying key intermediates of the many possibilities requires highly sensitive probes that

can identify small changes in bonding and structure. The complexity is highlighted in Figure 6.15, where the currently identified reactions of isoprene are outlined.[18] Isoprene is a naturally occurring VOC that forms a trace chemical species found in green spaces. From this single molecule the molecular branching space is huge such that tracing these species and their reactivity with atmospheric oxidants plays a major role in understanding our environment. Other important examples include the reactions of alkenes with ozone and the formation of Criegee intermediates.[21-23] The ozonolysis of alkenes contain a similarly complex series of reactions and side reactions meaning their kinetics and mechanisms of reaction are poorly understood. The ability of a high repetition rate XFEL to monitor the dynamics associated with complex formation and reaction in both time and spatially resolved modes through sheet or line imaging of X-ray absorption or emission will provide detailed mechanistic information and kinetic profiles that can be fed into improved atmospheric models, while mechanistic details can be obtained for VUV/XUV XFEL probes combined with photoelectron and photo-ion coincidence detection methods.

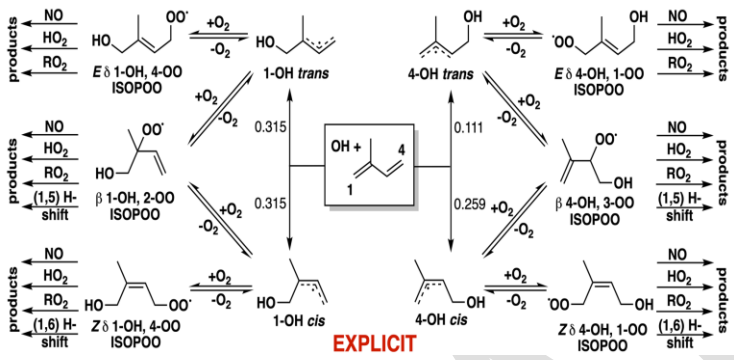

Figure 6.15. *Reaction scheme for isoprene highlighting the complex branching space and kinetics required in understanding atmospheric composition and chemistry.*[19]

Additionally, atmospheric aerosol and particulate concentrations have a major impact on human health and climate change.[14, 15] Reduction in particulates forms a major component of the UKs clean air strategy due to the particularly strong impacts of breathing in small particulates in polluted atmospheres, while the effects of atmospheric aerosols and particulates on climate change models have large uncertainties limiting reliability.[16] Part of the problems associated with controls and climate models result from fundamental questions about the production and characteristics of formation. In atmospheric science (as in combustion) the process by which aerosols and particulates forms is unclear. The uncertainty lies not only in the nucleation and growth processes (see also Section 8.2), but also in the chemical composition, arrangement and surface activity of the resulting aerosols and particulates as they grow. This can affect removal processes, reactivity and atmospheric lifetime all of which feed into climate models.

X-ray probes from an XFEL can provide information on particle growth, size and morphology through Hard X-ray scattering and on composition and functionality through linear and non-linear soft and hard X-ray spectroscopies such as XANES, XES and XCARS (Section 3.5), with surface sensitivity possible through recently demonstrated techniques such as X-ray second harmonic generation which only become viable with the high flux and high intensity available at XFEL facilities.

Another key region of the environment is the interfacial layer where the oceans and the atmosphere form a coupled system, exchanging heat, momentum, and water, and a large variety of chemical species at the air–sea interface. These exchanges exert a considerable and complex influence on the climate system, as well as have more local effects on regional air quality and marine biological productivity. The emission and deposition of trace chemical species at the air–sea interface has important environmental implications, hence the chemical and physical processes involved need to be far better understood. Key to this is an understanding of the structure, composition and chemistry of the sea-surface microlayer (SSM) that defines the uppermost tens to hundreds microns of the ocean, its equilibrium and interaction with the atmosphere.

The chemical and biological complexity of the SSM (enriched concentrations of amphiphiles, colloids, aggregates, halogenated VOCs, and phytoplankton) mean the important interactions bridge across

biology, chemistry, physics, and oceanography and have the potential to impact the environment, at almost all scales. Experiments with high flux XFEL sources on laboratory analogues of the SSM provide opportunities to monitor the coupled reactions involved in environmentally important process (such as the production and subsequent reaction of molecular iodine) as a function of controlled parameters (e.g. temperature, humidity, pH, sea-salt concentrations, ozone levels, nature of microalgae). Important experiments would cover the full range potentially available at the UK XFEL, with VUV/XUV XFEL radiation used in liquid microjet experiments to monitor reactants, reaction intermediates and products with time and spatial resolution, using photoelectron spectroscopy, and photoelectron-photoion coincidence spectroscopy (PEPICO), through to methods that take advantage of the highly penetrating nature of hard X-rays to probe processes deeper in the solution with atom and oxidation state specificity.

The surface sensitivity and potentially broad energy range available from the XFEL and supporting sources also allows for measurements of relevance to space chemistry. Many of the reactions of relevance to the interstellar medium occur on ice grain boundaries and can lead to much more complex chemicals than may otherwise be expected.[17] With the data from space-based observing platforms tuned to the mid- and far-IR regions (James Webb Space Telescopei) and tasked with the observation of star forming regions through observations of icy dust (IceAge Project[20]), and identifying small molecular coolants (small hydrides, water etc.) as well as more chemically complex systems. Large numbers of chemical systems are being identified. The UK XFEL provides opportunities to study the mechanism of formation through the use of synchronized THz to XUV ultrafast light sources with ultrafast X-ray probes. The use of high energy pump sources creates the short-lived radicals involved while THz or X-ray probes provide chemical identification and track changes in bonding and structure. Combining this with non-linear X-ray probes that provide site specific detail of the chemical changes promises to provide the most detailed insight into how the molecules of life (e.g. peptides)[18] are formed and through the use of X-ray probes of chirality (Section 3.1.3) we can investigate the fundamental origins of their formation in such inhospitable environments.

References

[1] J. B. Bell, *et al*., "Simulation of nitrogen emissions in a premixed hydrogen flame stabilized on a low swirl burner," Proceedings of the Combustion Institute 34, 1173 (2013).

[2] UK Greenhouse Gas Emissions National Statistics. Available from https://www.gov.uk/government/collections/final-uk-greenhouse-gas-emissions-national-statistics

[3] M. J. Evans and P. R. Medwell. "Understanding and Interpreting Laser Diagnostics in Flames: A Review of Experimental Measurement Techniques" Front. Mech. Eng., 5 1 (2019) | https://doi.org/10.3389/fmech.2019.00065

[4] J. H. Frank, *et al*., "In situ soft X-ray absorption spectroscopy of flames". Appl. Phys. B 117, 493 (2014). DOI: 10.1007/s00340-014-5860-8.

[5] J. Dunnmon, *et al., "*Characterization of scalar mixing in dense gaseous jets using X-ray computed tomography". Exp Fluids, 56, 193 (2015) DOI: 10.1007/s00348-015-2057-9

[6] M R Kamesh, *et al*., "Approaches and solutions to HCCI - a review energy systems: fuel and combustion, injection and atomization" IOP Conf. Series: Materials Science and Engineering 402, 012204, (2018) DOI:10.1088/1757-899X/402/1/012204

[7] D. L. Osborn. "Reaction Mechanisms on Multiwell Potential Energy Surfaces in Combustion (and Atmospheric) Chemistry". Annu. Rev. Phys. Chem. 68, 233 (2017) DOI: 10.1146/annurev-physchem-040215-112151

[8] H. Zang, *et al*. "Ultrafast swelling and shrinking of soot in alkanol–air flames induced by femtosecond laser filamentation", Combust. Flame, 212, 345 (2020), DOI: 10.1016/j.combustflame.2019.11.009.

[9] S. Tanaka, and S. Mukamel, "Coherent X-ray Raman spectroscopy: A nonlinear local probe for electronic excitation," Physical Review Letters 89, 043001 (2002).

[10] G. Kock. in "Trends in Oil and Gas Corrosion Research and Technologies" ed. A. M. El-Sherik, Woodhead Publishing, 1st edn, 2017, ch. 1, pp 3-30, DOI: 10.1016/B978-0-08-101105-8.00001-2

[11] H. Koo, *et al*. "Targeting microbial biofilms: current and prospective therapeutic strategies" Nat. Rev. Microbiol. 15, 740, (2017) DOI: 10.1038/nrmicro.2017.99

[12] R. K. Lam *et al., Soft X-Ray Second Harmonic Generation as an Interfacial Probe,* Phys. Rev. Lett., 120, 023901, (2018). DOI: 10.1103/PhysRevLett.120.023901

[13] B. I. Escher *et al. Tracking Complex Mixtures of Chemicals in our Changing Environment*, Science, 367, 388, (2020) DOI: 10.1126/science.aay6636

[14] U. Pöschl. Atmospheric Aerosols: Composition, Transformation, Climate and Health Effects. Angewandte Chemie International Edition, 44, 7520, (2005). DOI: 10.1002/anie.200501122

[15] D. Yang, *et al*. "Changes in anthropogenic $PM_{2.5}$ and the resulting global climate effects under the RCP4.5 and RCP8.5 scenarios by 2050. Earth's Future, 8, e2019EF001285, (2020). DOI: 10.1029/2019EF001285

[16] T. C. Bond, *et al*. "Bounding the role of black carbon in the climate system: A scientific assessment", J. Geophys. Res. Atmos., 118, 5380, (2013) DOI:10.1002/jgrd.50171.

[17] A. Belloche, *et al*., "Detection of a branched alkyl molecule in the interstellar medium: iso-propyl cyanide" Science 345, 1584, (2014) DOI: 10.1126/science.1256678

[18] R. I. Kaiser, *et al.*, "On the formation of dipeptides in interstellar model ices" Astrophys. J. 765, 111 (2013) DOI:10.1088/0004-637X/765/2/111

[19]K. H. Bates and D. J. Jacob. "A new model mechanism for atmospheric oxidation of isoprene: global effects on oxidants, nitrogen oxides, organic products, and secondary organic aerosol", Atmos. Chem. Phys., 19, 9613, (2019) DOI:10.5194/acp-19-9613-2019

[20]http://www.stsci.edu/jwst/observing-programs/approved-ers-programs/program-1309

[21]C.A.Taatjes, *et al.* "Direct Measurements of Conformer-Dependent Reactivity of the Criegee Intermediate $(CH_3)CHOO$ " Science 340, 177-180 (2013)

[22]C.A.Taatjes, *et al.* "Intermediates just want to react" Nature Chem. 6, 461 (2014)

[23] C.A.Taatjes, *et al*. "Research frontiers in the chemistry of Criegee intermediates and tropospheric ozonolysis" Phys. Chem. Chem. Phys 16, 1704 (2014) DOI: 10.1039/C3CP52842A.

7. Science Opportunities in the Life Sciences

The strongest XFEL use case in life science is serial femtosecond crystallography (SFX) and time-resolved SFX. These methods exploit slurries of nano- to micro-crystalline samples at near-physiological temperature and pressure to generate atomic resolution models and probe authentic function from the same sample. Reaction cycles for time-resolved SFX are initiated by light or mixing strategies and many are generalizable across all of biology. Thus, dynamic structural biology and molecular movies of macromolecular function will become routine. In many cases, especially metal-dependent systems, complementary spectroscopic information can also be collected from the same samples and X-ray pulses to provide even more detailed mechanistic insights. Structure-functional results will translate into better drugs and treatments impacting human health, and better catalysis for clean energy and agriculture. A frontier XFEL challenge is to extend single particle imaging methods of biomolecules in solution so that nearly all dynamic processes in biology can be studied with high temporal and spatial resolution.

Crystallographers frequently observe microcrystal showers measuring only a few microns on a side that arise from initial sparse matrix screens used early in most projects. These conditions are then "optimized" to yield large single crystals typically measuring ~ 25 - 100(s) µm or more on at least two sides. Next, they establish cryogenic conditions that are suitable for low temperature diffraction data collection with a synchrotron or lab-based X-ray source. During data collection, the X-ray dose is often distributed throughout as much of the entire crystal volume as possible, by combinations of rotation and translation motions.[1-8] As a result, one crystal often yields one atomic model that likely includes radiation-induced alterations to local (*e.g.* transition metal centres) and general sites (*e.g.* decarboxylation of some amino acids and/or disruptions of disulphide bonds, etc).

Thus, microcrystals are ubiquitous but often overlooked because they can be more difficult to use and/or perceived to be inappropriate for structural analysis. However, the characteristics of XFELs change the sample requirements for macromolecular crystallography (MX). Indeed, showers of microcrystals are ideal for XFELs that deliver hard X-rays with high flux density in a very well-focused fs-long pulse. Membrane proteins are an important and under-resented class in the Protein Data Bank (PDB) because they are often difficult to crystalize for traditional MX methods. But many membrane proteins do produce microcrystals that are well-suited for serial femtosecond crystallography (SFX) methods.[9-14] Microcrystals are also ideal for time-resolved studies of reactions initiated by either visible light photons or reagent mixing. The impacts of SFX have translated to analogous serial MX strategies at synchrotron micro-focus beamlines at Diamond, anticipated for Diamond II, and all similar facilities around the world. Uniquely at XFELs, the SFX data is obtained before any radiation-induced effects manifest within the sample, even at the most sensitive local sites such as metal centres.[15-18] Although each XFEL pulse destroys each sample, the fs pulse duration is so short that the still diffraction pattern yields a snap-shot with extremely sharp temporal and atomic resolution of the ordered atoms within the crystal, before the Coulombic explosion consumes it. Thousands of still images from thousands of microcrystals, each in a random orientation, are needed to fill out the Ewald sphere for each complete dataset. Several sample delivery methods have been developed to rapidly replenish fresh sample for each pulse. Most of these operate at room-temperature and readily support time-resolved studies. Thus, one of the great promises of XFEL-based methods is that time-resolved SFX naturally blends functional and structural analyses in the same experiment. This is often described as, *Dynamic Structural Biology*.

More than 99% of all organisms that have ever lived on the earth are now extinct; and yet the current diversity of life is still staggering.[19] With life spans that range from hours to dozens of millennia, organisms tolerate temperatures from about -15 °C to 125 °C, pressures from the vacuum of space to up to 1,100 atmospheres, pH values between 0 to 12.5, visible light conditions ranging from full sun to 5 x 10^6 fold attenuation, UV and/or ionizing radiation up to ≥1,000 J m^{-2} or 50 Gy/hr (12,000 Gy in an acute dose).[20] Despite these taxonomic characteristics, modern biology today is often defined and

underpinned by genomic analyses (Figure 7.1). Indeed, the impact of the human genome project is enormous as suggested by the statement from Battelle (Columbus, Ohio) and the United for Medical Research[1] collation,[21, 22]

> *The reference human genome is to biology what the periodic table is to chemistry: a fundamental platform for understanding and advancing science for generations.*

Genomes derive from "individuals," whereas in contrast, metagenomic analyses help reveal complex relationships amongst organisms and their environments.[23-26] As of January 2020, the Kyoto Encyclopedia of Genes and Genomes (KEGG) database lists complete genomes from 536 Eukaryotes, 5543 Bacteria, 315 Archaea, and 341 viruses, as well as metagenomes from 477 environmental and 712 organismal samples.[27-30] Table 7.1 indicates millions of expressed genes that exhibit massive diversity and cover all macromolecular and enzyme classes. About half of the gene products have also been mapped or linked to metabolic or signalling pathways or many other important biological functions. Interactions between organisms range from benign to symbiotic to pathogenic; however, deciphering the fundamental principles that dictate the scale, scope, and consequence(s) of these interactions remains a grand challenge in biology. Answering this challenge will have profound

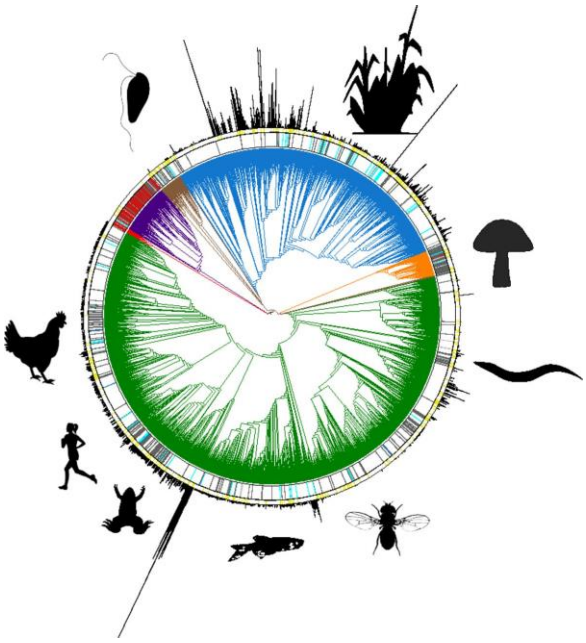

Figure 7.1: Current status of the sequencing of life. Open Tree of Life (opentreeoflife.org) synthesis of phylogeny for all of life with resolution to the genus level, and showing phylogenetic information for Archaea (red), Bacteria (purple), Fungi (orange), Plantae (blue), Protista (brown), and Animalia (green). The current state of genomic information available from NCBI's GenBank is shown in the inner circle, with complete genomes colored in red, chromosome level in blue, scaffolds in dark gray, and contigs in light gray. The second circle shows the transcriptomes from the NCBI Transcriptome Shotgun Assembly Sequence Database (www.ncbi.nlm.nih.gov/genbank/tsa/). Genome size as C value is displayed in bars around the outer circle. Data for animals is from the Animal Genome Size Database (www.genomesize.com/), data for plants is from the Royal Botanic Gardens, Kew (cvalues.science.kew.org/), and data for fungi is from the Fungal Genome Size Database (www.zbi.ee/fungal-genomesize/). From Lewin et al (2018) *Proc Natl Acad Sci USA 115*, 4325-4333

Table 7.1: KEGG GENES Annotation Statistics (as of 23 Feb 2020) [a]

Category	Protein-based genes		RNA-based genes		Pathway linked genes	Enzyme genes with EC numbers
	All genes	KO assigned genes [b]	All genes	KO assigned genes [b]		
KEGG organisms	29,649,273	14,264,286	612,196	342,637	8,289,646	6,029,364
Viruses	367,069	10,057	5,497	24	N/A	5,202
Addendum	4,524	4,433	N/A	N/A	N/A	3,625

[a] Source: www.genome.jp/kegg/docs/genes_statistics.html
[b] Annotated with the KEGG Orthology (KO) system; the basis for cross-species annotation in KEGG. The set of genes in the genome that can be mapped to KEGG reference pathways and BRITE reference hierarchies to generate organism-specific pathways and hierarchies.

[1] The coalition groups consist of the American Association for Cancer Research, American Cancer Society Cancer Action Network, American Diabetes Association, American Heart Association, Association of American Universities, Association of Public and Land Grant Universities, BD, Biotechnology Industry Organization, Boston University, Corning, FasterCures, Harvard University, Johns Hopkins University, Life Technologies, Massachusetts Institute of Technology, Melanoma Research Alliance, Northwestern University, Pancreatic Cancer Action Network, Partners Healthcare, PhRMA, Research!America, Stanford University, The Endocrine Society, Thermo Fisher Scientific, University of Pennsylvania, University of Southern California, Vanderbilt University, and Washington University in St. Louis.

implications to human health, renewable energy sources and climate change, species extinction versus survival, and food production for a human population expected to reach 11.2 billion by the end of the century.[31]

The answers will not come exclusively from genomic analyses, but rather are greatly influenced by structural biology and many complementary methods (Figure 7.2). X-ray crystallography (MX)[15-18, 32-34] and cryo-Electron Microscopy (cryo-EM)[35-41] are essential and well established tools for structural biologists worldwide (see also Appendix 2.2). The impact is amplified by ten Nobel Prizes awarded in the past decade with a component linked to structural biology. Synchrotron X-ray sources or cryo-EM were vital to the R&D efforts in each of the Nobel laureates' laboratories. Synchrotron facilities also serve the entire structural biology community, who now leverage these capabilities on a daily basis.[32, 33] As a result, more than 160,000 atomic models are currently curated by the Protein Data Bank (PDB), with an estimated economic value of more than $16B.[42-44] Furthermore, structural biology was critical to 93% of all drugs approved by the US FDA between 2010 and 2016.[45-48]

The PDB has released 143,187 atomic models linked to X-ray crystallography, 12,913 to cryo-EM, and 4437 to NMR spectroscopy (compiled on 27 Feb 2020).[49] Despite these impressive results, and the important biological insights derived from them, the known genes summarized in Table 7.1 are tallied in the tens of millions. For instance, there are more than 6 million enzyme genes listed in the KEGG databases. Thus, one might conclude that we are incredibly ignorant with respect to an atomic level understanding of biology on a global scale, and that there is a tremendous amount of new information still to be discovered. To these ends, structural biology results via MX and cryo-EM methods are critical. They are also complemented by many important methods including, neutron diffraction and small angle scattering[50-53], macromolecular structure prediction[54-57], small and wide angle X-ray scattering of biomolecules in solution[58-62], super resolution fluorescence microscopy[63], optogenetics[64, 65], DNA and RNA sequencing and multimodal data analysis technologies applied to single cells[66, 67], cryo-electron tomography[68-70], X-ray microscopy, tomography and ptychography[71-76], electron diffraction from micron to submicron-size crystals[77-82], and a variety of methods to establish interaction networks between biomolecules[83]. Thus, biologists are analysing integrated structural, functional and dynamic data. This applies to macromolecules in pure states, through to increasing complexity of heterogenous samples, and ultimately to physiological conditions such as within whole cells or tissues.

The vast majority of the MX datasets are collected from one to a few macro-sized crystal(s), rotated about one or more axis during data collection and held at 100 K in a cryostream.[84] Similarly, nearly all of the cryo-EM atomic models are collected from cryo-cooled samples. But life is dynamic and function is not compatible with the cryogenic conditions. Selected timescales in biology are illustrated in Figure 7.2 and range from fs for electronic transitions and bond vibrations, to ps for light-induced charge separation, photoisomerisation and amino acid side chain rotation, to µs for domain motion and ion transport and fast enzyme reactions, to ms for most enzyme reaction rates and fast protein folding, to seconds for protein synthesis and DNA or RNA replication/synthesis.

XFELs offer new opportunities in structural biology, especially for samples at near-physiological conditions and for time-resolved studies.[15-18, 85, 86] The unparalleled XFEL intensity reduces the crystal size requirements such that even submicron size crystals yield high quality diffraction data collected from samples at room temperature.[87] The fs pulse duration also provides extraordinary temporal resolution and data without radiation-induced alterations to highly reactive intermediates. These characteristics prompted the following statement from Tetsuya Ishikawa, (Director, RIEKEN SPring-8 Center, Sayo, Hyoga, Japan) at SLAC National Accelerator Laboratory, Menlo Park CA USA on 02 May 2014:

> *The basis of science is observation. The most fundamental way of observation is by light. X-rays are a form of light that can probe atoms and molecules. X-ray lasers can probe atoms and molecules on their fundamental time scales, femtoseconds. X-ray lasers are therefore one of the fundamentally most powerful tools for science.*

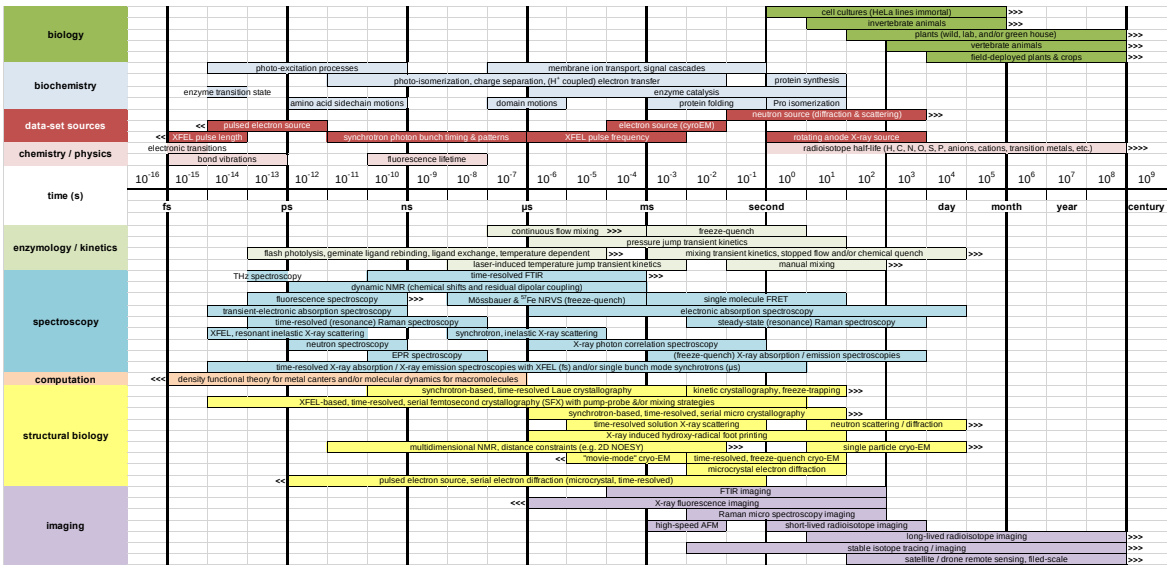

Figure 7.2 A comparison of X-ray sources and types of phenomena they are used to study. Biochemical processes span orders of magnitude in time (top). The X-ray dose and time required to elicit a spectroscopic change and an X-ray diffraction pattern to high resolution at a modern synchrotron or XFELs range from µs to fs at synchrotrons and XFELs, respectively. For comparison, examples of complementary methods are shown along the bottom. Biologists will often use many of these methods in their research.

Sixty years ago, at the dawn of structural biology, Nobel laureate Max Perutz attempted to measure the structural impact of O_2 binding to hemoglobin crystals. His large crystals did not survive exposure to O_2 because it triggered significant and functionally relevant conformational changes in each protein within the crystal lattice.[88, 89] When Perutz conducted his experiments, he used a weak, lab-based X-ray source that required large crystals to collect as much of the diffraction data as possible from a small number of samples at room temperature. One hypothesis is that the crystal lattice, which is held together by weak interactions, builds up strain across large crystal upon O_2 binding to hemoglobin and breaks into smaller and smaller fragments -- essentially dissolving. Importantly, the lattice also did not prevent the dynamic and functional consequences of O_2 binding to hemoglobin; although there was nothing useful left considering the instrumentation at the time.

Today we are experiencing a step-change in macromolecular crystallography. This derives from serial MX and time-resolved functional studies that are directly linked to XFELs and the use of micron-size samples.[15-18] One important hypothesis is that micron-sized crystals minimize or eliminate barriers to relieving strain that builds up when conformational changes propagate across molecules and unit cells. A dramatic case in point is an aptamer of messenger RNA, a riboswitch that binds adenosine and undergoes a large conformational change that ultimately regulates gene expression.[90-92] Using a slurry of micron-size RNA crystals and mix-and-inject methods, Stagno et al reported time-resolved SFX results that demonstrate ligand binding-induced conformational changes so significant that the crystals changed symmetry, but they did not shatter.[93, 94] This remarkable result has also recently been observed via atomic force microscopy wherein the probe-tip is scanned across the outer layers of microcrystals. These experiments demand the intensity and tight focus of the XFEL beam; without either, these experiments would not be feasible.

Biologists will continue to use all of the tools available to them over the next several decades, including those exploiting X-rays and electrons for structural analysis. Structural biology is also experiencing a step-change linked to cryo-EM methods.[36-38, 41] This was noted by the 2017 Nobel Prize in Chemistry awarded to Dubochet, Frank, and Henderson for "developing cryo-electron microscopy (cryo-EM) for the high-resolution structure determination of biomolecules in solution."[39, 95] Because methods and microscopes are improving rapidly[40, 96, 97], and national centers supporting the high-end instruments are more common, more high resolution structures of smaller macromolecules are being released on

a daily basis. Facilities like eBIC at Diamond provide scientists with state-of-the-art experimental equipment and expertise, for both single particle analysis and cryo-tomography.[98] It is part of the UK infrastructure that overall fields more than 20 high end microscopes. Similarly, three US NIH funded national electron microscopy centers are operational in New York, Oregon and California.

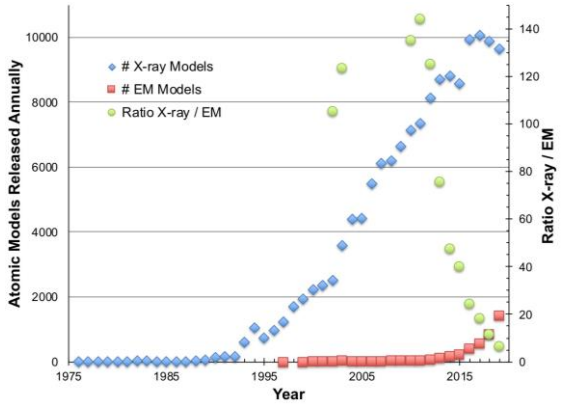

Figure 7.3. Growth of the PDB archive from X-ray and cryo-EM methods (compiled 27 Feb 2020). The tally algorithm does not account for thousands of models related to fragment screening results (at Diamond and elsewhere), consequently the numbers for MX are still increasing.

However, there is still room to improve cryo-EM technologies especially with respect to the quantum efficiency of detectors, recovering all of the high-resolution signal in the presence of various types of noise, selection of the appropriate electron energy, sample preparations methods and data analysis algorithms. Improvements in all of these areas will bring the method closer to its theoretical limits. Together, MX and cryo-EM have the potential over the coming decade(s) to provide the necessary tools to establish the structural basis of nearly every functional aspect from any type of cell.

With such large global effort and many important biological targets (see Table 7.1), progress across all of biology has been profound and will continue with increasing pace.[99] This is reflected in the recent PDB statistics (Figure 7.3) indicating that the ratio of X-ray to cryo-EM in 2019 was 6.8; compared to a few years earlier when the ratio was greater than 100. It is very likely that parity will be reached soon. Although cryo-EM does not require a crystal lattice, the data is collected under cryo-conditions that are far from physiological and do not allow for dynamic conformational changes. However, freeze-quench methods are being developed to enable time-resolved cryo-EM with about ms time resolution.[100-102]

Sample preparation and delivery are unmet challenges in both serial MX and cryo-EM methods. This offers significant opportunities for technology transfer between the fields. They each must manipulate on-demand nano- to picoliter volumes of either macromolecules in solutions or as a slurry of microcrystals.[101-108] Freeze-quench methods in cryo-EM will likely be limited to about 100s µs to ms time range because of constraints linked to sample grid preparation; however, this is an active area of R&D. High-quality SFX and time-resolved SFX data collected at XFEL facilities already approach fs time resolution for light-triggered reactions. For mixing strategies, it is likely that enzyme reactions will be studied from 100s µs through seconds. With more XFEL facilities, some running with MHz repetition rates, scientists will be able to significantly improve the correlations between the electronic and atomic structures, even potentially on a crystal by crystal basis.

7.1 Serial femtosecond crystallography enabled by XFELs - a new era in structural biology

Serial nano-crystallography presents a revolutionary opportunity to solve structures from the large number of proteins that can only form tiny crystals. The high brightness of the XFEL enables a diffract-before-destroy methodology allows structures to be rapidly solved from accumulated data.

Serial femtosecond crystallography (SFX) is a new technique developed to exploit the fs pulses from XFELs and to use thousands of micron-size crystals or smaller.[15-18] It is the dominant method in life sciences at all five XFELs since it was first reported in 2011 by Chapman and colleagues at the LCLS.[109, 110] The impact of SFX is summarized in Table 7.2, wherein atomic models released by the PDB is a measure of impact. These atomic models are almost always accompanied by a primary citation. It is noteworthy that 58% of the primary citations since 2011 were in high profile publications such as *Science*, *Nature* or *Cell*, etc. One might argue that the impact is modest, but the entire volume of these results derives from only a handful of facilities (some still in commissioning phases) and each facility only fields experiments for structural biology for a fraction of each operational period. In contrast, more than 100 synchrotron MX beamlines and hundreds of high-end cryo-EM instruments all collect data nearly continuously and simultaneously around the world.

Table 7.2: Macromolecular atomic models linked XFEL released by the PDB [a]

LCLS (USA, 2011 to date; CXI, XPP, MFX beamlines) • 185 models released • 76 primary citations • 54 high profile citations [b]
SACLA (Japan, 2014 to date; BL2, BL3 beamlines) • 104 models released • 39 primary citations • 13 high profile citations [b]
European XFEL (Germany, 2018 to date; SPB/SFX instrument) • 12 models released • 4 primary citations • 4 high profile citations [b]
PAL-XFEL (South Korea, 2019 to date; NCI - SFX beamline) • 7 models released • 3 primary citations • 0 high profile citations [b]
SwissFEL (Switzerland, 2019 to date; Aramis, Bernina beamlines) • 1 model released • 0 primary citations • 0 high profile citations [b]

[a] Compiled on 04 Feb 2020

[b] Primary citation appeared in either *Science*, *Nature*, *Cell*, *Proc Nat Acad Sci USA*, *Nature Methods*, *Nature Communications*, *Nature Chemistry*, or *Structure*

SFX studies are very often conducted at room temperature, from which one still diffraction pattern is recorded from each microcrystal in a random orientation. XFEL beams are typically well-focused to deliver submicron or 1 - 3 µm size at the sample, and are about nine orders of magnitude brighter than synchrotrons like Diamond Light Source. Because so much energy is deposited into the sample, it explodes.[111] Consequently, SFX methods require a unique sample for each diffraction pattern. To this end, sample delivery methods for serial MX is a very active R&D effort in the field. The aim is to rapidly and efficiently deliver sample, without wasting precious material, at a rate that matches the XFEL pulse frequency and/or the detector characteristics.

A variety of methods have been developed to deliver a slurry of microcrystals into the XFEL interaction region, which range from liquid or viscous jets[13, 109, 112-117], to on-demand micro-droplets that may be coupled to a conveyor belt transport system[106-108, 118-123], to fixed targets that raster a sample array through the X-ray beam interaction region[108, 124-133], to goniometer-based methods at the XFEL.[134-137] Many of these methods are readily adaptable to time-resolve studies in which the reaction is triggered by either light or mixing. Light-activated systems are relatively rare in biology, but are easier to initiate and many have the potential to probe rates from fs and slower. In contrast, enzymes are ubiquitous throughout biology, but the reactions are slower, in part because substrate binding events are required. One of the most active areas of research include developing new methods to initiate enzyme reaction cycles by adding/mixing substrates into the microcrystal slurry at some variable time before reaching the X-ray beam. An important additional strategy is to use caged substrates or caged proteins to initiate enzyme reactions via a light flash that decages the substrate or the protein.[138-140] Although SFX was first demonstrated in 2011 at the LCLS[109, 110], serial MX methods are now also available at

nearly all major synchrotron facility around the world.[33, 141-146] Moreover, beamlines dedicated to serial MX are often identified as a flagship capability at facilities undergoing upgrades to diffraction-limited lattice configurations.[147] Thus, room-temperature, serial MX methods that couple dynamics and functional studies with structural analysis will soon become routine around the world. This trend will continue to expand and impact all of life sciences.

About 30% of the human genome codes for membrane proteins.[10, 148-150] Because they are located and function at the interface between cells or organelles, they are critical mediators / sensors of environmental conditions, nutrient transport, and cell communication and signalling. Not surprisingly then, membrane proteins are targets for more than 50% of all drugs available worldwide.[151, 152] The PDB currently curates 10,024 membrane protein atomic models, of which 8097 were determined by X-ray diffraction and 847 by cryo-EM. Furthermore, SFX methods at three XFELs facilities have been used for 88 of the recently released atomic models. Because membrane proteins are hard to crystalize and often only yield microcrystals, they are ideally suited to structural analysis at high intensity well focused sources such as XFELs.[10, 11, 150, 153]

Light source characteristics that includes a CW high repetition rate and increased stability parameters will allow the further development of the accuracy of stationary serial MX. Specifically, there are two areas where the analysis of stationary diffraction can exploit such capabilities. Firstly, post-refinement is being developed to improve the quality of the retrieved amplitudes.[154-162] With the necessary increased frame rate of area detectors, orders of magnitude improvement in data collection rates relative to current 'warm Linac' hard X-ray FELs will be achieved. For example, the European XFEL fields AGPIDs[163-165] and JUNGFRAU[166, 167] detectors wherein the former can collect 3520 data frames per second overall, out of the 27,000 pulses per second delivered in 4.5 MHz trains lasting no more than 600 μs; compared to warm Linac machines that deliver pulses at up to 120 Hz. In addition, increased stability will allow a more accurate X-ray geometry determination to improve post-refinement methods for further enhancements of the structure factor amplitude determination. A discussion of the crystallographic signal-to-noise and the new molecular physics that may be probed in such a regime has been presented.[168] These include the detection and analysis of vibrational coherence dynamics in addition to resolving reactive mode displacements on ultrafast time scale. A second opportunity for analysis of stationary diffraction is the explicit retrieval of ultrafast population information through application of optical crystallography theory.[168, 169] This is an important example that provides one of several strong cases for high-repetition rate and increased sensitivity of time resolved SFX.

Specifically, for all classes of uniaxial and biaxial symmetries (trigonal, tetragonal, hexagonal, triclinic, monoclinic and orthorhrombic crystal classes) the resulting birefringence connects the orientation dependence of electric field decomposition to the explicit analysis of power density dependent population transfer. Inversion of an indexing matrix for a stationary diffraction image from time-resolved SFX data will allow a calculation of orthogonal field directions in the X-ray crystallographic coordinate frame from solving Maxwell's polarised wave equations in anisotropic media (Figure 7.3). While this requires explicit knowledge of the intrinsic birefringence value and wavelength dependence depending on the point group symmetry, opportunities for population analysis specifically exploit the high repetition rate regime. With knowledge of linear and non-linear optical cross sections, the time-resolved SFX data can be separated in data bins according to the calculated photoselection of linear and non-linear population under intense femtosecond optical excitation. With currently available signal-to-noise and crystallographic statistics, time resolved studies effectively average the full Debye-Scherrer range of individual reflections, while high repetition rate studies will separate the population difference that exist within (Figure 7.4). This provide additional compelling motivation for the development of high repetition rate, increased stability and high accuracy crystallography. It is evident that such applications will be possible and successful with the availability of many more stationary diffraction observations. A second compelling motivation for increased sensitivity is the control and observation of small amplitude coherent motion, discussed in section 7.4.

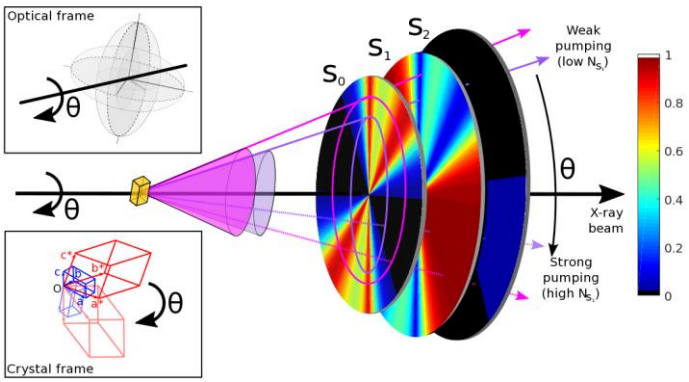

Figure 7.4. Illustration of the analysis of orientation dependence of photoinduced populations with reference to both the optical orientation and the X-ray crystallographic orientation. Tracing a Debye-Scherrer ring in revolution, the polarisation directions are modified according to the solutions to Maxwell's polarized wave equations. Therefore, population transfer may be analysed radially in the detector plane, as illustrated with a physical calculation example for a uniaxial case. From Hutchison et al (2019)

7.2 Structural dynamics in photosensitive biomolecules

A remaining frontier challenge of structural biology is to determine time-resolved structures at atomic resolution directly from systems engaged in function at physiological temperatures and pressures. XFEL methods are making important advances towards this goal.

General time resolved structural biology is separated from ultrafast applications by fundamental time scales of decoherence, which is typically completed within few picoseconds. Coherent dynamics are separately discussed in section 7.3, while pure population dynamics at slower time scales are the focus of biochemistry applications discussed here. The concept is illustrated in Figure 7.5 and couples reaction dynamics with sample preparation and/or data collection. Dynamic structural biology is as much a philosophy as a set of tools to collect as much data as possible, from every sample and every X-ray pulse, at physiological temperature and pressure, with an aim to create time-resolved molecular movies of macromolecules engaged in function. Diffusion-triggered methods for time-resolved crystallography experiments were proposed in 2000 by the LCLS Scientific Advisory Committee, in 'First Scientific Experiments for LCLS' (http://www.slac.stanford.edu/pubs/slacreports/reports03/slac-r-611.pdf).[170]

> *Time-resolved structural studies on diffusive processes in crystalline enzymes are difficult due to problems with mixing enzyme and reactant in the crystal. With submicron-sized samples, the vast majority of solution techniques and methodologies will suddenly become available for time-resolved structural investigations at the LCLS.*

One of the great promises of serial MX methods at XFELs and synchrotrons is to combine structural and functional studies by exploiting slurries of microcrystals at room temperature for time-resolved data analysis from the same sample. Heretofore the *status quo* in structural biology is to use many separate samples, from which different types of data are collected under different conditions. Some of the experimental conditions may be very far from physiological. For example, traditional MX or cryo-EM methods usually provide insightful atomic models of a particular ground state molecule from a sample held at 100 K. In contrast, most functional studies are conducted in solution, at room-temperature, and often include binding, conformational changes, and/or other types of dynamics.

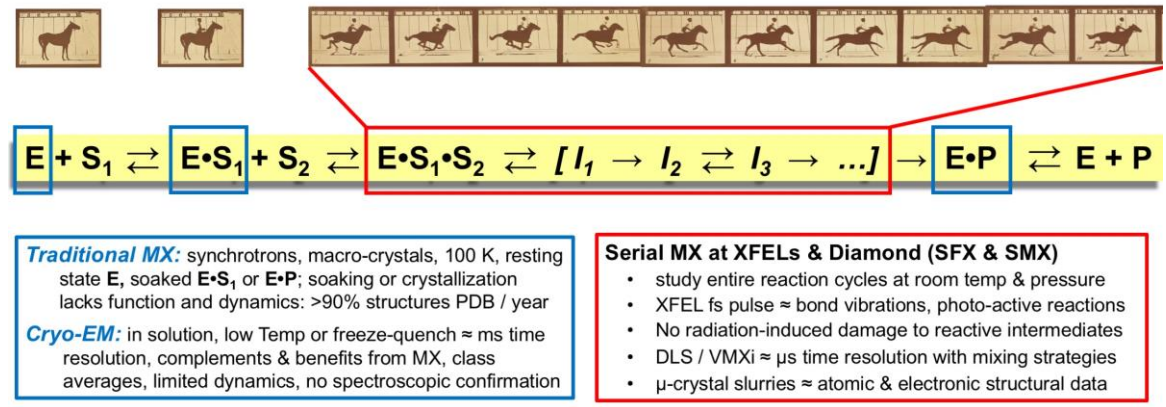

Figure 7.5. Concepts of time-resolved structural biology. Snap-shots of data inspired by Muybridge's "horse in motion" photographs (Palo Alto CA, June 1878, 500 µs shutter speed). Stable, ground-state complexes are studied by traditional MX and cryo-EM methods, most often at 100 K. Time-resolved cryo-EM methods use freeze-quench techniques, typically with ms time resolution. Serial MX methods with microcrystals and monochromatic X-rays at synchrotrons or XFELs collect still diffraction images at room temperature with µs - fs exposures, respectively, at different Δt intervals after optical laser flash(es) or ligand mixing.

It is not unexpected then that ultrafast time-resolved spectroscopic experiments performed on photo-active proteins in solution have provided many important insights into the very early events after absorbing a photon. Because XFELs are still new, analogous time-resolved SFX experiments are still

emerging. Often comparisons between time-resolved SFX and spectroscopic results with similar pump-probe delay times do not yield one-to-one correlations. One possible explanation is that the crystal versus solution conditions are sufficiently different that ultrafast spectroscopic experiments have not been performed at the same pH, viscosity, ionic strength, among many other potential variables. Furthermore, the desire of structural biologists to observe and maximize illumination-dependent differences in electron density maps has often pushed experimental conditions into the multi-photon regime. Recently has it become clear that visible light power studies are critically important to nearly all light-activated time-resolved SFX experiments. Unfortunately, in part because beamtime is so rare, scientists may underprioritize these "control" experiments, and as a result these types of data are often sacrificed under time-pressure situations.

Examples of XFEL experiments involving light-activated systems include photosystem I[110, 171 172-175], photosystem II[176-178 106, 107, 118, 136, 139, 179-187], photoactive yellow protein[188-190], human rhodopsin[191, 192], bacteriorhodopsins[115, 193-199], jumping spider rhodopsin[200, 201], light activated ion channels[202], fluorescent proteins[203-206], several phytochromes[106, 207], DNA photolyase, and photo-dissociation studies of myoglobin-CO[208] or cytochrome c oxidase-CO[209, 210]. Of these systems, photosystems I and II have evolved mechanisms to diffuse the excess energy absorbed in multiphoton events through the network of internal chromophores. Therefore, they are less susceptible to the impact of single versus multiphoton time-resolved SFX studies. The photo-dissociation of CO from metalloproteins can be considered outside their normal function and less constrained by illumination conditions. The remaining systems evolved to react to visible photons, and single photon methods are likely to be most physiological. Moreover, many of these systems experience photo-driven conformational changes that are often linked to photoisomerization of the chromophore. Such events are often very fast and require timing tools to help coordinate the pump-probe experiment.[211-214]

Photosystem II (PS-II) is a high-value, benchmark system for time-resolved SFX studies with results coming principally from three international teams of researchers in the USA, Asia, and Europe.[118, 172, 176-181, 184, 185] The enzyme is responsible for the "great oxidation event" approximately 2.4 billion years ago that transformed the earth from an anaerobic reducing atmosphere to the O_2 rich and oxidizing atmosphere today. PS-II is a large integral membrane protein expressed in all plant and most photosynthetic microorganisms. The protein uses four photons to catalyse the four electron oxidation of two water molecules that form one O_2 molecule plus four H^+ that help establish a proton gradient used for ATP generation by ATP synthase. The PS-II reaction is driven by visible light photons that initiate very rapid charge separation events (fs - ps), and much slower electron-transfer events (hundreds of ms) to reduce the quinone pool.

Thus, PS-II is an ideal system for time-resolved SFX studies; but the entire reaction cycle spans more than 12 orders of magnitude in time, which creates experimental challenges. A large collaborative group developed an on-demand, acoustic droplet ejection onto tape system (Figure 7.6).[106, 108, 118, 120, 181, 186, 187, 215] It transports discrete nL droplets across a laser illumination platform before they reach the X-ray interaction region. This allows for multiple illumination / equilibration perturbations to advance the reaction cycle for time-resolved SFX experiments. An added benefit of the design is that the region between the droplet ejection and the X-ray interaction region can also be fitted with either an O_2 reaction chamber or a second pL droplet ejector system, both of which enable a wide range of mixing based time-resolved reactions.

O_2 bond formation within PS-II is catalysed by the oxygen evolving complex (OEC) that include a Mn_4O_5Ca cluster (Figure 7.7).[216, 217] When a photon is absorbed by the P680 chromophore, it results in charge separation and electron transfer to the quinone site. The oxidized P680 is then reduced by the OEC, which advances one oxidation state with each photon absorption event. In the Kok cycle, the first photon promotes the S_1 to S_2 transition, the second photon S_2 to S_3, and the third photon from S_3 to S_4. The S_4 state catalyses the conversion of two water molecules into O_2 resulting in the S_0 state of the OEC. Absorption of a fourth photon produces the stable S_1 starting state.

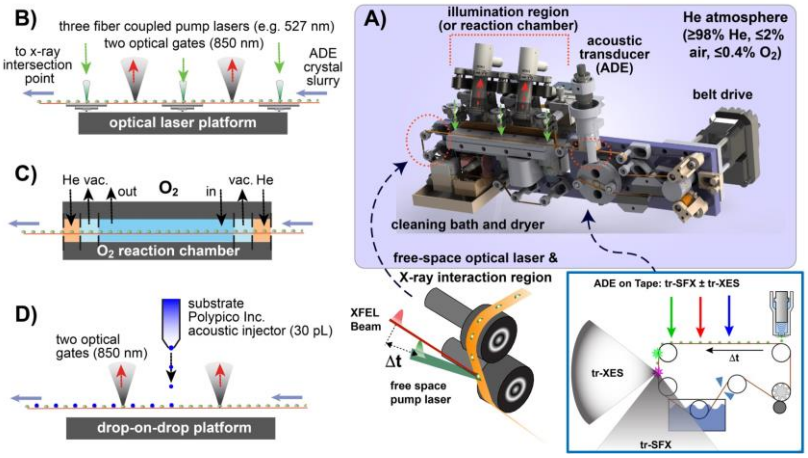

Figure 7.6. Acoustic tape drive system for pump-probe time-resolved SFX and XES measurements of PS-II (A & B) and options for O_2 dependent reactions (C) or drop-on-drop ligand additions (D). See also Fuller et al (2017) *Nature Methods* 14, 443-449.

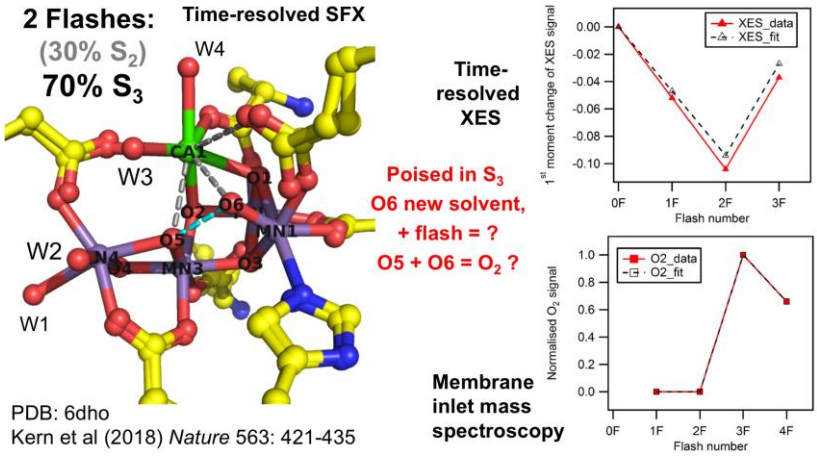

Figure 7.7. Correlated time-resolved SFX and XEX results from PS-II. (left) the 2.09 Å resolution atomic model for S3. (right, top) The first moment change of the Mn $K\beta_{1,3}$ XES spectra from PS-II crystals obtained *in situ* simultaneously with SFX. (right, bottom) Flash-induced O_2 yield in crystal slurry as a function of flash number.

The Mn atoms within the cluster act as a redox "buffer" and each oxidation state has a unique $K\beta_{1,3}$ X-ray emission spectrum (XES). Consequently, time-resolved XES collected simultaneously with time-resolved SFX provides complementary data on the electronic and atomic structures of the catalytic centre.[118, 181, 184-187, 218] Groups working principally at the LCLS and LBNL developed methods to simultaneously collect time-resolved SFX data in the forward direction and time-resolved X-ray emission spectroscopy (XES) at 90°, from each sample and each X-ray pulse.[106, 107, 118, 181, 183, 185-187, 218-220] Some of the results for PS-II are shown in Figure 7.7 for the OEC poised in the S_3 state where µs time-resolved structures demonstrate motion of the Mn atoms and entry of a new solvent atom (label O6 in the image).[118] The atomic model is correlated with oxidation of the Mn atoms within the OEC and the O_2 generation assays from crystal slurries. Details for the time-resolved reaction that forms the O_2 molecule remain ill-defined; however, the deepest mechanistic insights will likely depend upon correlated studies and benefit from XFEL sources.

Light-driven strategies to initiate catalysis in systems that are not naturally light sensitive include: a) caged compounds, b) caged proteins, c) ligand exchange, or d) temperature jump methods.[138, 140, 221-235] Each of these must satisfy the requirements of high selectivity, high quantum yield and temporal resolution. To these ends, *o*-nitrobenzyl moieties are among the most common photocaging groups for substrates and amino acids, but their decaging photochemistry may not be as fast nor as clean as *p*-hydroxyphenacyl or coumarylmethyl derivatives. Caged substrates are either co-crystallized with the target macromollecule, or soaked into slurries of microcrystals. Incorporation of non-natural amino acids that convert a given protein into a caged protein is more difficult (*e.g.* Figure 7.8). Consequently, caged protein approaches typically include a computational evaluation stage, followed by protein translation using *amber* TAG codon-suppression methods, or post-translational modification strategies. The photo-active moiety is most often linked to thio, amino, carboxy, or hydroxy groups of proteins or substrate ligands, and are then cleaved by irradiation with UV to visible

light. Photo-cleavage of the caging group varies in rate (ps - µs) and quantum yield (<0.2 - 1), which then generates: *i)* authentic substrate in the active site vicinity, ii) a rapid pH shift, *iii)* a temperature jump, *iv)* removes an active site barrier and enables substrate binding, or *v)* eliminates a dynamic or conformational restraint required for catalysis. Ligand exchange methods include photolabile metal-CO or NO complexes that mimic a metal-O_2 intermediates in a reaction cycle. Photodissociation of the blocking diatomic molecules then allows for O_2 binding and the ensuing reaction. All of these methods are experiencing a resurgence of R&D activity and provide important opportunities for time-resolved structural biology at XFELs. Some of these techniques will require careful coordination of the timing between the visible light pump laser and the XFEL probe pulse.

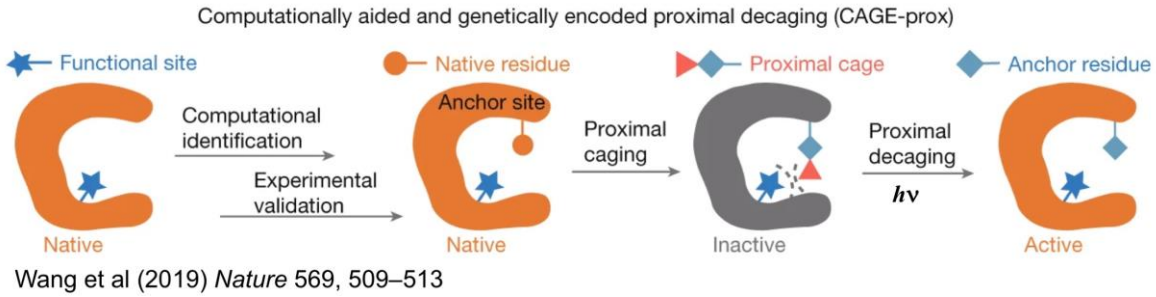

Figure 7.8. Schematic concept of the CAGE-prox strategy. A proximal cage can be genetically incorporated at an anchor site in close proximity to the protein functional site for temporal blockage of its activity. Proximal decaging can lead to rapid rescue of protein functions, as long as the decaged anchor residue has negligible influence on protein activity.

7.3 Dynamic Structural Biology: molecular movies of enzyme catalysis

Time-resolved SFX studies exploiting mixing methods have significant potential for revealing the dynamics of enzyme catalysis.

Macromolecular crystals are typically about 50% protein and 50% solvent, which is similar to the overall concentration inside cells. The average reaction time for enzyme catalysis in solution is about 60 ms. Dynamics play important but often ill-defined roles in enzyme catalysis.[236-245] A driving hypothesis for time-resolved serial MX is that because small molecule substrates diffuse as fast as 1 $\mu m^2 \bullet \mu s^{-1}$, enzyme microcrystals will equilibrate with substrates faster than catalytic turnover.[171, 246-252] This implies that time-resolve structural biology methods are generalizable when exploiting micron-size crystals or smaller. With 6,029,364 enzyme genes listed in the KEGG databases (Table 7.1.1), there is an enormous reaction landscape to be explored. However, due to the very limited availability of XFEL beamtime, relatively few time-resolved SFX experiments exploiting mixing strategies have been conducted at fully commissioned XFEL facilities.[93, 106, 249, 253]

To date, most time-resolved SFX studies that exploit mixing methods used liquid gas dynamic virtual nozzle (GDVN) style jets or microfluidic devices that have been developed by several groups. [93, 94, 113, 114, 171, 249, 253-256] For the majority of cases, GDVNs typically achieve sample injection speeds of 10 - 30 m s^{-1} and are suitable for 10 - 120 Hz repetition rate XFEL sources. Many of these mixing-injectors are slow and need on the order of seconds to fully mix substrate with crystals. Other types of devices mix on the ms time scale, but require high-dilution ratios to infuse substrate into the crystal slurry stream. These types consume large amounts of substrate or ligand and dilute the crystal concentration, which also reduces the overall SFX data collection rates. All of the GDVN nozzle methods are prone to clogging or freezing when used in vacuum chambers and benefit from cleaning between samples.

For MHz sources, sample injection speeds need to be on the order of 50 - 100 m s^{-1} so that fresh material is presented to each XFEL pulse.[111, 173, 257-260] Mixing injectors that produce such high jet velocities must have very small orifices and therefor can only accommodate microcrystals. This matches the desire to use less than ~3 µm crystals and is consistent with rapid equilibration of ligands throughout the crystal. These constraints also impact GDVN nozzle fabrication. For instance, a recent example developed for MHz data collection at the European XFEL used a high-end 3D printer (Nanoscribe GmbH) and two photon stereolithography methods to achieve free-form geometries with submicron precision.[113] Devices like those illustrated in Figure 7.9 produce 50 - 225 µm jet lengths, diameters as low as 536 ± 35 nm with a liquid flow rates of 2.4 ± 0.12 µl min^{-1} and a gas flow rates of 22.5 ± 0.2 mg min^{-1}. At the SPB/SFX instrument at the European XFEL, a similar design with a gas and liquid orifice size of 60 and 50 µm diameter, respectively, were used to inject microcrystals of up to 6 to 8 µm in size at velocities of up to 100 m s^{-1}.[259, 260] The delay timepoint(s) achievable for high velocity mix-inject jets is principally a function of the flow rate and the distance the sample-ligand mixture travels to the nozzle exit; the time of flight to the beam will only be ~ 1 - 3 µs and thus very short compared to most enzyme reaction times (average turnover time of ~ 60 ms).

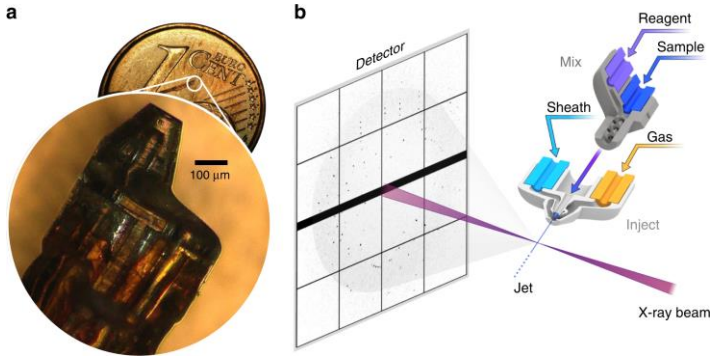

Figure 7.9. A microfluidic device for time-resolved SFX. **a)** Through micro-3D-printing Knoška *et al* fabricate microfluidic devices of a few 100 µm in size. Magnified view of a nozzle placed on a 1 cent coin for scale reference. **b)** This technique can realize integrated nozzle assemblies to jet protein crystal suspension into the X-ray interaction region for diffractive imaging. From Knoska, et al, (2020) *Nat Commun 11*, 657 doi: 10.1038/s41467-020-14434-6

The acoustic tape drive system describe above (see Figure 7.6) can also be used for mixing-based time-resolved SFX ± XES; for example, metalloenzyme reactions with O_2.[106] It is difficult to study oxygen-Fe intermediates by traditional, synchrotron-based MX methods because their reactivity also makes them very sensitive to photoreduction by the X-ray beam. In those studies, because an Fe(IV)=O intermediate is produced in the reaction cycle, it is also important to include X-ray emission spectroscopy to help differentiate it from Fe(II)-OH_2, and Fe(III)-OH species. The electron density maps for these three moieties are nearly identical except at extraordinarily high resolution and are susceptible to X-ray radiation-induced artifacts, but the spectroscopic signatures are very different. This strategy provides critical correlations between atomic and electronic structures (especially first row transition metal centres) from the same sample and X-ray pulse. These types of complementary datasets will continue to yield deeper mechanistic insights on more metalloenzyme systems. For instance, this also represents an opportunity to include time-resolved XES measurements into the time-resolved SFX data processing pipelines so that only diffraction patterns that also exhibit the appropriate spectroscopic signature are merged together into a timepoint dataset. Such a strategy will provide more confidence in the electron density map interpretation and the resulting atomic models deposited to the PDB that are released to the whole structural biology community.

In parallel and complementary to XFEL efforts, time-resolved MX methods are under development at synchrotron facilities too, especially those that provide pink-beam and microfocus capabilites.[143, 144, 146, 261] At XFEL or synchrotron facilities, the reactions in crystals must be synchronized throughout all unit cells in order to observe high resolution diffraction from reaction cycle intermediates. For mixing strategies this will depend upon viscosity and the size of the substrate molecules traversing channels within the crystal lattice and macromolecules themselves.[262-264] Therefore, best practices dictate that when possible scientists should measure reactivity in the solid state and from more than one space group with different lattice packing. The homogeneity of the microcrystal slurry is also an important optimization parameter for mixing-based time-resolved SFX experiments.[265, 266]

Electron diffraction (ED) also generates high resolution atomic models from slurries of microcrystals; however, the crystal thickness is restricted to several hundred nanometers because electrons interact with matter more strongly than X-rays.[78, 79, 81, 82] Submicron size samples reduce problems associated with inelastic scatter, multiple scattering events, or simply diminishing returns of information. A pulsed electron source coupled with sub-micron size crystals that are injected into the interaction regions are a perfect match for time-resolved dynamic structural biology; provided that various challenges are overcome.[267-269] Many of these issues are synergistic with time-resolved SFX at XFELs and include sample delivery with mixing strategies and data processing pipelines with near-real time feedback.

7.4 Controlling and measuring nuclear and electronic coherence within biological systems

Some photo-induced biochemical processes are so fast that nuclear and electronic quantum coherence are believed to have a role. XFELs are offering a new incisive window into this behaviour.

The current and future abilities for ultrafast protein X-ray crystallography hold great potential for the development of methods and new approaches to interrogate protein dynamics. The field of ultrafast spectroscopy has traditionally used indirect methods for observation of structural dynamics, such as spectral shift analysis. Direct ultrafast crystal structure determination and electron density dynamics will allow many advances in structural dynamics that are not directly possible with spectroscopy. The development of time-resolved SFX at XFEL facilities has enabled the detection of nuclear coherent motions with application of ultrafast pump-probe techniques. For such applications, access to the ultrafast time scale is necessary and needs the ability to combine a femtosecond optical laser excitation pump with an X-ray probe from an XFEL pulse at Ångstrom wavelength, femtosecond duration and delay time(s), and high X-ray photon flux.

A number of successful time-resolved protein X-ray crystallography experiments have been reported which included delays in the sub-picosecond time scale that includes vibrational coherence dynamics.[189, 195, 208] For time-resolved macromolecular crystallography, the combination of large unit cell dimensions, light atoms having small cross section, often small isomorphous differences, dictate the X-ray source requirements.[109, 110, 172, 176, 260, 270, 271] The photoinduced differences for protein crystals are analysed in real space from the electron density differences obtained by inverse Fourier transform rather than on the level of $\Delta I/I$ of individual Bragg diffraction spots.[272] This requires strict isomorphism which is maintained on ultrafast time scale in protein crystals.

Because the atomic cross section, which dominates the valence electron density contribution, determines the measurements of protein structural dynamics by X-ray crystallography, it is rapidly dominated by displacements and order-disorder transitions through the analysis of isomorphous differences. It is well established from the ultrafast vibrational spectroscopy field that the typical dephasing time scale measured for protein samples is on the order of ~1-2 ps depending on the system of interest.[273-277] The ultrafast time-resolved SFX of proteins thus must include contributions from coherent vibrational dynamics.[168, 272] This is a relatively new experimental ability that has been demonstrated in recent years but has opened up a new field of application. Electronic coherence properties may not be readily available from X-ray crystallography, but a new type of application can be proposed to apply phase-locked two-pulse femtosecond excitation for time-resolved SFX experiments that would in principle provide a frequency correlation measurement from the coherence time alteration.[168]

The emerging area of ultrafast time-resolved SFX can exploit and build on decades of ultrafast vibrational spectroscopy research and coherence theory.[168, 272] A close analogy can be made between the technique of impulsive Raman spectroscopy which is an ultrafast time-domain technique, and the ultrafast time-resolved SFX observation.[273, 275] The comparison additionally identifies clear and obvious opportunities for future development of time-resolved SFX particularly with emphasis of growing the experimental bandwidth and improving the signal-to-noise ratio. Impulsive Raman spectroscopy can achieve observation of vibrational wavepacket motion at frequencies exceeding 3000 cm^{-1} employing few-femtosecond laser pulses.[278] The detection in transmission resolves the four-wave mixing signals which modulate the population dynamics signals with typically very small amplitudes, from the transition probability modification of coherent motion in the ground and excited state. In the pump-probe time-resolved SFX experiment the creation of ground and excited state wavepackets are population and displacement driven, respectively, and result from the field-dipole interaction with rank of two which is sufficient to create interstate coherence.[168, 279] Their properties have been

evaluated on the basis of theoretical considerations.[168] In the case of protein crystallography which lacks the atomic and subatomic information, charge density analysis is typically not available and detection of electron density differences are primarily caused by atomic displacements. This places limits on the frequency range of nuclear coherence that can be expected to contribute to the measurements, judged from the calculation of displacements and reduced masses for harmonic frequency calculations of proteins.[272] In addition, the Huang-Rhys factors as well as anharmonicities must be evaluated in order to analyse their real-space displacements. Therefore, currently the explicit measurement of fingerprint modes in the ~800-1800 cm^{-1} frequency range, which have few pm characteristic displacements are currently not accessible. Similarly, high frequency hydrogen stretching modes (3000-3500 cm^{-1}) are not accessible for reasons of small displacement, experimental bandwidth and additionally from the small cross section of hydrogen.

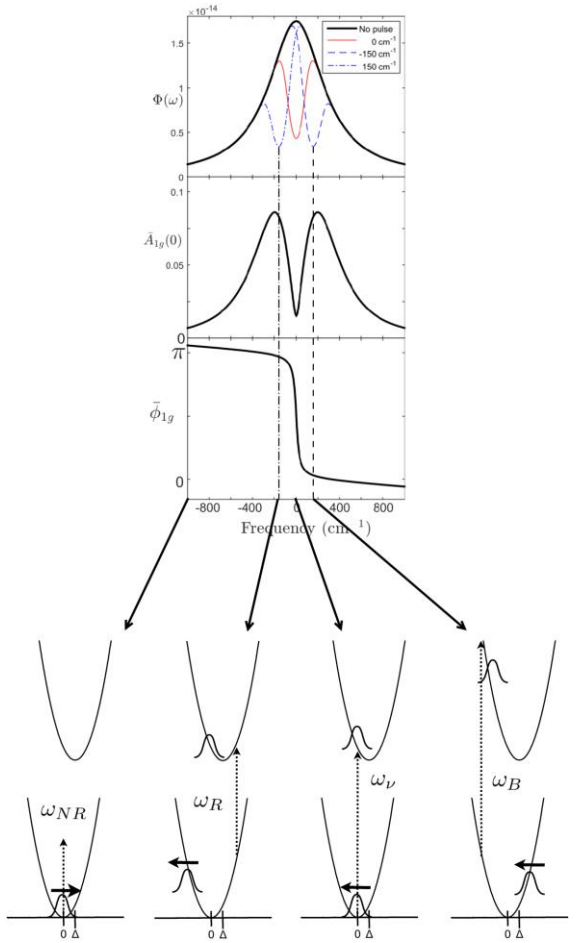

Figure 7.10. Illustration of the lineshape theory treatment of ground and excited state vibrational coherence calculation using additional wavepacket representations. Laser excitation of a homogeneously broadened line Φ(ω) with carrier frequency below (ω_R), on (ω_v), or above (ω_B) resonance creates a total impulsive ground state coherence A_{1g} with phase φ_{1g}. The resulting ground coherence is shown for the high temperature case (300K). From van Thor, J. J. (2019) *Struct Dyn* 6, 050901 doi: 10.1063/1.5110685

The Raman spectroscopy literature includes ample evidence that the study of fingerprint modes is particularly desirable for the functional analysis of protein dynamics. In contrast, current time-resolved SFX capabilities include measurements that can only be strongly dominated by low frequency modes (below few-hundred wavenumbers) which have large displacement as the result of significant associated reduced mass.[275, 278] An additional reason that the frequency range is limited to low frequency modes is a physical limit to the crystallographic signal-to-noise that arises from the current sub-KHz repetition rate and source and detector capabilities. In this regime it is shown that very intense femtosecond optical excitation is a requirement, or otherwise no light induced differences will be resolved. Practically, this requires the stretching of optical pulses in the range of 100-200 fs. A detailed discussion of non-linear optical transformation in this regime has been presented previously.[2168, 272, 280, 281]

The case for development of increased experimental bandwidth and signal-to-noise is therefore particularly compelling. Since the experimental bandwidth for pump-probe application of SFX is currently dominated by the optical pulse rather than the XFEL pulse duration, increased sensitivity of the pump-induced difference measurements will allow improvement of the time resolution. This would be achieved through increased repetition rate of a hard X-ray XFEL light source as well as the area detector frame-rate to achieve orders of magnitude improvement in data rate. In addition, the improvement of source stability will significantly contribute. The latter includes pulse intensity, carrier frequency, spectral distribution and bandwidth stabilisation on a shot-to-shot basis. Such future capabilities will increase the ability to resolve ground and excited state coherent vibrational motion at frequencies higher than the current ~ 300 cm^{-1} limit by time-resolved SFX from crystallographic coordinates directly (Figure 7.10). The novel capabilities will significantly develop results from decades of ultrafast Raman spectroscopy methods and theory.

7.5 Capturing biological function in single molecules

The potential for near atomic resolution of macromolecular dynamics under their working conditions remains a driver for XFEL based coherent diffraction imaging of single particles.

Among the important science drivers for the development of the LCLS was the potential to observe structures of macromolecules from close to physiological conditions, without requiring crystals.[170] The concepts of single particle imaging (SPI) were supported by timely theoretical considerations by Hadju and Neutze *et al*.[246, 282, 283] However, as discussed in the sections above, SFX methods succeed "easily" because they depend upon collecting Bragg reflections from nano- to micron-size crystals; in essence a strongly diffracting sample with data originating from a strong, well-focused X-ray beam. In a way, Gati *et al* approached the SPI goal by using extremely small crystals, the naturally occurring granulovirus OBs, which consists of about 9,000 unit cells.[87] Based upon their analysis, they conclude, "It should be possible, under ideal experimental conditions, to obtain data from protein crystals with only 100 unit cells in volume [and] that single-molecule imaging of individual biomolecules could almost be within reach."

Single particle imaging, in contrast to SFX, demands that one measure a weak signal from a strong beam that is further complicated or obscured by any and all other scattering structures in the beam. The challenges have been extreme and originating from many perspectives, ranging from sample delivery all the way through data processing. To address the challenges, an international collaboration formed to coordinate activities amongst groups, the SPI initiative.[284, 285] For SPI experiments the typical LCLS pulse energy is about 2 - 5 mJ, which at the AMO instrument equals 7.80 x 10^{12} to 1.95 x 10^{13} photons/pulse at 1.6 keV and at the CXI instrument equals about 1.78 to 4.46 x 10^{12} photons/pulse at 7.0 keV. To date, at the LCLS they have achieved about 6 Å resolution with hard X-rays at the CXI instrument and abut 10 Å resolution with soft X-rays at the AMO instrument. Thus, the potential to study macromolecular dynamics in near-physiological conditions, and to capture (ultrafast) biological, chemical and physical processes remains a grand challenge for XFEL facilities.

As alluded to in previous sections, cryo-EM has overtaken single particle X-ray imaging as the dominant method for macromolecular structure determination from non-crystalline, frozen hydrated samples. Nevertheless, Chapman states[15]

> *"The promise of more photons per atom recorded in a diffraction pattern than electrons per atom contributing to an electron micrograph may enable diffraction measurements of single molecules, although challenges remain."*

Some of the challenges include:

a. developing methods to introduce homogenous macromolecules into the interaction region with high and sustainable overlap between sample stream and X-ray pulses
b. delivering high enough X-ray intensity in a very tightly focused beam (need > 10^{14} photons μm^{-2} of 4 - 10 keV photons focused into tens of nm^{-2} size)
c. eliminating background scattering, or limiting it to no more than about 100 photon counts per diffraction pattern
d. delivering a stream of reproducible and uncontaminated particles (perhaps at variable delay time(s) after initiating a reaction via mixing or pump-probe strategies)
e. acquiring tens of thousands to millions of patterns per dataset
f. interpreting the noisy diffraction data

XFEL facility repetition rate and detector frame rate both impact the quality and quantity of SPI data that can be collected in a given time (Table 7.3). To date, the main limitation has been achieving adequate and sustainable sample hit rates. However, to realize higher resolution single particle imaging, the field needs faster detectors with lower noise such that it is easier to differentiate single

scattered photons from the sample compared to those from the various sources of background noise. Thus, a faster X-ray source does not necessarily translate into a faster detector. Indeed, a 100 kHz detector is a distant R&D objective, and yet MHz sources are available now.

Table 7.3. Main detector characteristics used at several XFEL facilities

	AMO / LCLS	CXI / LCLS	TXI / LCLS-II	SPB/SFX / Eu.XFEL	BL2 / SACLA	SwissFEL
Detector	pnCCD	CSPAD [b]	ePix10k	AGIPD [d]	MPCCD	JUNGFRAU [f]
Pixel Size (μm^{-2})	75 x 75	110 x 110	100 x 100	200 x 200	50 x 50	75 x 75
Single Photon Sensitivity	yes	yes	yes	yes	yes [e]	yes
Quantum Efficiency	> 80% @ 0.3~12 keV	~97% @ 8 keV	~85% @ 5 keV	> 80% @ 0.3~25 keV	~ 85% @ 5.5 keV	Up to 85% @ 12 keV
Dynamic Range	10^3 @ 2 keV	3.5 x 10^2 @ 8 keV	~ 10^4 @ 8 keV	> 10^4 @ 12.5 keV	1.2 x 10^3 @ 6 keV	>10^4 @ 12 keV
Noise (e^-)	20 / 2 [a]	300	120	265	300	100
Pulse Rate (kHz)	0.12	0.12	0.48 / 2~4 / 10~20 [c]	4500	0.06	0.1~2.4

Taken from Sun, Z. B., Fan, J. D., Li, H. Y., and Jiang, H. D. (2018) Current Status of Single Particle Imaging with X-ray Lasers, *Appl Sci-Basel 8* doi: ARTN 132; 10.3390/app8010132.
[a] For pnCCD, the readout noise is 20 e^- for low gain, 2 e^- for high gain.
[b] The dynamic range and ASIC noise for CSPAD under high gain mode are 350 photons @ 8 keV and 300 e^- r.m.s. For low gain mode, they're 2700 photons @ 8 keV and 1000 e^- r.m.s.
[c] The current version is about 480 Hz. For digital domain multiplexing, the frame rate will be 2~4 kHz. For fast ADCs, the frame rate will be 10~20 kHz.
[d] See D. Greiffenberg, *J. Instrum.* 2012, 7, C0110 and A. Allahgholi, et al *J. Instrum.* 2015, 10, C01023 for information.
[e] Keeping the single photon detection capability for X-ray photon energy higher than 6 keV.
[f] See J. H. Jungmann-Smith, et al *J. Synchrotron Radiat.* 2016, 23, 385–394 for detailed information.

Insert a short section on small angle solution scattering *aka* (Pande, K., Donatelli, J. J., Malmerberg, E., Foucar, L., Bostedt, C., Schlichting, I., and Zwart, P. H. (2018) Ab initio structure determination from experimental fluctuation X-ray scattering data, *Proc Natl Acad Sci U S A 115*, 11772-11777 doi: 10.1073/pnas.1812064115) …

Insert a short section outlining time-resolved SFX to correlate experiments with computational modelling and molecular dynamics …

7.6 Conclusion and Summary

Biology is a large and high-impact area at all synchrotron and XFEL facilities. About 50% of the total user community at Diamond focuses on life sciences; although they frequently rely upon highly automated data collection strategies and use a smaller overall fraction of Diamond beamlines. The number of important biological targets is staggering as illustrated by the KEGG databases statistics listed in Table 7.1.1. Moreover, new and novel threats to human health are always emerging. For example, proteins from the COVID-19 virus were recently used for cryo-EM structures and MX-based ligand screening at the XChem facility at Diamond Light Source.[286-295] Those are prime examples of high-throughput data collection and analysis that is enabled by mature and optimized facilities.

Structure-based drug discovery and fragment-based screening are major strategies used by all pharmaceutical companies to bring new drugs to market. And yet, most new drugs fail because they lack efficacy. These strategies often rely upon ground-state crystal structures determined at 100 K. An emerging alternative that de-risks new therapeutic avenues, is to study the whole dynamic reaction cycle, which will reveal and mediate changes that are focused upon particular function. Indeed, XChem is very likely to expand capabilities to room-temperature complexes or reaction cycles inspired by serial MX approaches.

Scientists working at the forefront of biology will use many of tools available to them in an increasingly integrative approach (Figure 7.2). For structural biology, some frontier challenges for synchrotrons, XFELs and cryo-EM / electron diffraction (ED) are summarized in Table 7.4 In the sections above, several areas of common synergistic overlap are identified. Consequently, R&D effort in one area, is very likely to rapidly transfer to other areas.

Table 7.4. Frontier challenges in structural biology and some approaches for progress

Goal	Synchrotrons	XFELs	cryo-EM & ED
to determine time-resolved structures directly from systems engaged in catalysis at physiological temperature and pressure	• RT serial µ-crystal methods • focused µ-beams • µs – ms datasets to dose limits • kinetics within µ-crystals correlated w/ spectroscopy	• on-demand sample delivery methods • mixing injectors • kinetics within n – µ-crystals correlated w/ spectroscopy • SFX processing pipelines	• automated, time-resolved sample grid preparation • high resolution from smaller targets • RT serial & time-resolved ED
to determine structures from single molecules in native-like conditions (in solution or membranes, in pure complexes)	• continuous diffractive imaging from n – µ-crystals with coherent sources	• single particle imaging & sample delivery methods • continuous diffractive imaging	• imaging processing & better detectors • low-energy electron holography
to understand structure/function/dynamics in native context	• X-ray microscopy with correlated imaging of metals and/or labels	• *in-situ* SFX of n – µ-crystals • imaging processing	• liquid / whole cells • high resolution microscopy

Exciting future challenges lie in the ability to observe dynamic enzymes and macromolecular complexes at high spatial and temporal resolution, both in purified/reconstituted forms and *in situ/in vivo*, and the ability to correlate these dynamics with physiological changes from the cell to the tissue and organism. There are clear opportunities to exploit the synergies between all of the current structural biology techniques including but not limited to: *i)* synchrotron- and XFEL-based MX including serial methods, *ii)* cryo-EM single particle techniques, *iii)* cryo electron tomography, *iv)* serial and time-

resolved electron diffraction from sub-micron macromolecular crystals, *v)* NMR and *vi)* other spectroscopic methods. To meet these challenges, there is strong consensus in the UK, and the wider life science community, that anything that can be done to improve XFEL access and training would be very useful. To these ends, there is a need to widen the applications of XFELs in life sciences especially by:

- Making SFX and time-resolved SFX methods more accessible to smaller groups through automation in sample delivery and data processing
- Coordinating training of expertise, building capacity, and engagement with the XFEL Hub at Diamond by the UK community to make best use of all five XFEL facilities
- Establishing a XFEL Doctoral Training Centre for studying biological dynamics should be a Priority Theme for EPSRC/BBSRC, as well as providing short term training courses
- Increasing industry involvement – dynamics of enzymes and protein-ligand interactions will have major implications in drug discovery

The options available to the life science community (Table 7.5) are broad and range from currently active (*e.g.* the XFEL Hub at Diamond) to long term development (*e.g.* this UK XFLE project) with additional opportunities in between (*e.g.* partnerships with existing XFEL facilities). For instance, the XFEL Hub at Diamond is a first in the world and was formed with grant support from the Wellcome, MRC and BBSRC awarded to Jim Naismith *et al* in 2014. The three full-time Hub scientists reside at a synchrotron, develop technologies for XFELs, and look to take advantage of synergies between XFELs and synchrotrons to better enable users to solve biomedical questions, especially by accessing the time domain with high resolution structural biology. The Hub helps users compete for beamtime on the global XFEL market. Because XFEL beamtime is massively oversubscribed, we take it as a measure of success that the Hub has participated in more than 45 XFEL experiments at all five operating XFELs worldwide since October 2015. The Hub has also provided travel assistance to more than 100 UK-based scientists for their participation in XFEL experiments. The overwhelming majority of these were given to students and Post-docs to participate directly in XFEL experiments. Staff at the XFEL Hub at Diamond also pursue science driven projects in close collaboration with users and other synchrotron and XFEL scientists. To these ends, the Hub has active R&D projects with Diamond beamline staff at I04, I24, VMXi and VMXm, as well as with eBIC.

Table 7.5. Some options for life sciences in XFEL research and development

Time frame	Main objectives and/or goals	Relative cost
Short term (0 - 2 years)	• Full support &/or expansion of the XFEL Hub at Diamond and XFEL Hub for physical sciences • CDT / DTP PhD studentships in life and physical sciences dedicated to XFEL research • Sample delivery collaboration between Diamond and SwissFEL for time-resolved SFX ± XES	0.005 - 0.02
Medium term (3 - 5 years)	• Partnership with SwissFEL &/or European XFEL to construct hard X-ray beamline(s) within existing accelerator tunnel for dynamic structural biology & imaging • Partnership between Diamond and SACLA to develop EH5 end station exploiting photons from SPring-8 and SACLA for X-ray pump - X-ray probe, time-resolved structural biology • Institute for XFEL Science	0.1 - 0.25
Long term (> 10 years)	• Build UK XFEL with hard X-ray capability for dynamic structural biology and imaging • Intersect UK XFEL beamline with one or more Diamond II beamlines for coordinated, time-resolved experiments	1.0

Although the XFEL Hub at Diamond is much smaller in scale, there are parallels between it and BioXFEL (https://www.bioxfel.org/), a Science and Technology Center funded by the US National Science Foundation. BioXFEL is a multi-institutional and international center established with a $25M grant in

2013, which was awarded a 5-year renewal in 2018 with a $22.5M grant. The BioXFEL does not have a specific user support role. Rather they are mandated to address education, outreach, research and development with aims to develop biological applications for XFELs. As a result, BioXFEL has extensive collaborations throughout the global SFX community.

The XFEL Hub at Diamond has established a "Dynamic Structural Biology at Diamond and XFLEs" beamtime allocation group at Diamond. It introduces and brings serial MX capabilities to users, advances dynamic structural biology, and helps reduce the barrier to access to XFELs for SFX and time-resolved studies of reactive intermediates generated *in situ*. This provides valuable training to new users, enables scientist to collect important preliminary data for XFEL beamtime applications, and also generates results that stand on their own. Judging from the increasing access of UK to XFEL sources the XFEL Hub has already had a useful catalytic role, despite its modest scale. There is strong consensus in the UK that the XFEL Hub at Diamond should be fully supported by the STFC/UKRI and expanded to increase its impact across a larger cross-section of structural biology R&D.

Mid-term options to life sciences include partnerships with existing facilities to build out their infrastructure. For instance, two unoccupied tunnels are already drilled at the European XFEL. One of these could be developed to support dynamic structural biology with an intra-train pulse rate of 4 MHz over up to 600 µs that repeats at 10 Hz. Eventually the European XFEL may strive to achieve CW-like operations. SwissFEL also has room for another hard X-ray beamline that will deliver X-ray pulses at 100 Hz and at lower flux density. There are program development options at SPring-8 and SACLA where the UK can have an impact. For instance, experimental hutch 5 (EH5) is situated between both facilities and has possibilities to take photons from both into one interaction region. The geometry is such that the X-ray photons reach the sample from opposite directions, but could be used to develop novel X-ray pump and X-ray probe experiments in time resolved structural biolgy. These experiments are relevant to very common electron-driven reactions in biology. Finally, an Institute for XFEL Science would bring research groups into a coordinated space similar to Center for Free-Electron Laser Science - CFEL on the DESY campus in Hamburg Germany (https://www.cfel.de/). These options all have significant merits and will be considered further in section 9.x.

Long-term options include building the UK XFEL. For life sciences, the desired machine will deliver 5 - 25 keV X-ray pules at about 100 kHz or faster, of 0.1 - 25 fs duration, in a well-focused beam (~0.02 - 2 μm^2) with at least 10^{12} photons per pulse. There are strong incentives to site the UK XFEL adjacent to Diamond II. For example, the science community is eager to develop options to exploit X-ray photons from both sources that arrive at the sample in a nearly collinear manner. Further details of a potential machine are detailed in Appendix 1 following the demands of the analysis in section 9.

References

[1] Henderson, R. (1995) The potential and limitations of neutrons, electrons and X-rays for atomic resolution microscopy of unstained biological molecules, *Q Rev Biophys 28*, 171-193 doi: 10.1017/s003358350000305x

[2] Henderson, R. (1990) Cryoprotection of Protein Crystals against Radiation-Damage in Electron and X-Ray-Diffraction, *P Roy Soc B-Biol Sci 241*, 6-8 doi: DOI 10.1098/rspb.1990.0057

[3] de la Mora, E., Coquelle, N., Bury, C. S., Rosenthal, M., Holton, J. M., Carmichael, I., et al, Weik, M. (2020) Radiation damage and dose limits in serial synchrotron crystallography at cryo- and room temperatures, *Proc Natl Acad Sci U S A 117*, 4142-4151 doi: 10.1073/pnas.1821522117

[4] Bury, C. S., Brooks-Bartlett, J. C., Walsh, S. P., and Garman, E. F. (2018) Estimate your dose: RADDOSE-3D, *Protein Sci 27*, 217-228 doi: 10.1002/pro.3302

[5] Garman, E. F., and Weik, M. (2017) Radiation Damage in Macromolecular Crystallography, *Methods Mol Biol 1607*, 467-489 doi: 10.1007/978-1-4939-7000-1_20

[6] Zeldin, O. B., Brockhauser, S., Bremridge, J., Holton, J. M., and Garman, E. F. (2013) Predicting the X-ray lifetime of protein crystals, *Proc Natl Acad Sci U S A 110*, 20551-20556 doi: 10.1073/pnas.1315879110

[7] Holton, J. M., and Frankel, K. A. (2010) The minimum crystal size needed for a complete diffraction data set, *Acta Crystallogr D Biol Crystallogr 66*, 393-408 doi: 10.1107/S0907444910007262

[8] Holton, J. M. (2009) A beginner's guide to radiation damage, *J Synchrotron Radiat 16*, 133-142 doi: 10.1107/S0909049509004361

[9] Li, D., and Caffrey, M. (2020) Structure and Functional Characterization of Membrane Integral Proteins in the Lipid Cubic Phase, *J Mol Biol* doi: 10.1016/j.jmb.2020.02.024

[10] Zhang, Q., and Cherezov, V. (2019) Chemical tools for membrane protein structural biology, *Curr Opin Struct Biol 58*, 278-285 doi: 10.1016/j.sbi.2019.06.002

[11] Mishin, A., Gusach, A., Luginina, A., Marin, E., Borshchevskiy, V., and Cherezov, V. (2019) An outlook on using serial femtosecond crystallography in drug discovery, *Expert Opin Drug Dis 14*, 933-945 doi: 10.1080/17460441.2019.1626822

[12] Neutze, R., Branden, G., and Schertler, G. F. (2015) Membrane protein structural biology using X-ray free electron lasers, *Curr Opin Struct Biol 33*, 115-125 doi: 10.1016/j.sbi.2015.08.006

[13] Weierstall, U., James, D., Wang, C., White, T. A., Wang, D., Liu, W., et al, Cherezov, V. (2014) Lipidic cubic phase injector facilitates membrane protein serial femtosecond crystallography, *Nat Commun 5*, 3309 doi: 10.1038/ncomms4309

[14] Caffrey, M. (2015) A comprehensive review of the lipid cubic phase or in meso method for crystallizing membrane and soluble proteins and complexes, *Acta Crystallogr F Struct Biol Commun 71*, 3-18 doi: 10.1107/S2053230X14026843

[15] Chapman, H. N. (2019) X-Ray Free-Electron Lasers for the Structure and Dynamics of Macromolecules, *Annu Rev Biochem 88*, 35-58 doi: 10.1146/annurev-biochem-013118-110744

[16] Schlichting, I. (2015) Serial femtosecond crystallography: the first five years, *IUCrJ 2*, 246-255 doi: 10.1107/S205225251402702X

[17] Fromme, P. (2015) XFELs open a new era in structural chemical biology, *Nat Chem Biol 11*, 895-899 doi: 10.1038/nchembio.1968

[18] Spence, J. C. H. (2017) XFELs for structure and dynamics in biology, *IUCrJ 4*, 322-339 doi: 10.1107/S2052252517005760

[19] Barnosky, A. D., Matzke, N., Tomiya, S., Wogan, G. O., Swartz, B., Quental, T. B., et al, Ferrer, E. A. (2011) Has the Earth's sixth mass extinction already arrived?, *Nature 471*, 51-57 doi: 10.1038/nature09678

[20] McKay, C. P. (2014) Requirements and limits for life in the context of exoplanets, *Proc Natl Acad Sci U S A 111*, 12628-12633 doi: 10.1073/pnas.1304212111

[21] Battelle. (2013) The Impact of Genomics on the U.S. Economy, Battelle Memorial Institute, http://unitedformedicalresearch.org/wp-content/uploads/2013/06/The-Impact-of-Genomics-on-the-US-Economy.pdf, access date 26 Feb 2020

[22] Wadman, M. (2013) Economic return from Human Genome Project grows, *Nature* doi: 10.1038/nature.2013.13187

[23] Human Microbiome Project, C. (2012) A framework for human microbiome research, *Nature 486*, 215-221 doi: 10.1038/nature11209

[24] Gilbert, J. A., and Lynch, S. V. (2019) Community ecology as a framework for human microbiome research, *Nat Med 25*, 884-889 doi: 10.1038/s41591-019-0464-9

[25] Lewin, H. A., Robinson, G. E., Kress, W. J., Baker, W. J., Coddington, J., Crandall, K. A., et al, Zhang, G. (2018) Earth BioGenome Project: Sequencing life for the future of life, *Proc Natl Acad Sci U S A 115*, 4325-4333 doi: 10.1073/pnas.1720115115

[26] Gilbert, J. A., Jansson, J. K., and Knight, R. (2014) The Earth Microbiome project: successes and aspirations, *BMC Biol 12*, 69 doi: 10.1186/s12915-014-0069-1

[27] Du, J., Yuan, Z., Ma, Z., Song, J., Xie, X., and Chen, Y. (2014) KEGG-PATH: Kyoto encyclopedia of genes and genomes-based pathway analysis using a path analysis model, *Mol Biosyst 10*, 2441-2447 doi: 10.1039/c4mb00287c

[28] Altermann, E., and Klaenhammer, T. R. (2005) PathwayVoyager: pathway mapping using the Kyoto Encyclopedia of Genes and Genomes (KEGG) database, *BMC Genomics 6*, 60 doi: 10.1186/1471-2164-6-60

[29] Kanehisa, M., and Goto, S. (2000) KEGG: kyoto encyclopedia of genes and genomes, *Nucleic Acids Res 28*, 27-30 doi: 10.1093/nar/28.1.27

[30] Kanehisa, M., Sato, Y., Furumichi, M., Morishima, K., and Tanabe, M. (2019) New approach for understanding genome variations in KEGG, *Nucleic Acids Res 47*, D590-D595 doi: 10.1093/nar/gky962

[31] Roser, M. (2020) Future Population Growth, https://ourworldindata.org/future-population-growth, access date 26 Feb 2020

[32] Owen, R. L., Juanhuix, J., and Fuchs, M. (2016) Current advances in synchrotron radiation

instrumentation for MX experiments, *Arch Biochem Biophys 602*, 21-31 doi: 10.1016/j.abb.2016.03.021

[33] Grimes, J. M., Hall, D. R., Ashton, A. W., Evans, G., Owen, R. L., Wagner, A., et al, Stuart, D. I. (2018) Where is crystallography going?, *Acta Crystallogr D Struct Biol 74*, 152-166 doi: 10.1107/S2059798317016709

[34] Gruner, S. M., and Lattman, E. E. (2015) Biostructural Science Inspired by Next-Generation X-Ray Sources, *Annu Rev Biophys 44*, 33-51 doi: 10.1146/annurev-biophys-060414-033813

[35] (2016) Method of the Year 2015, *Nature Methods 13*, 1-1 doi: 10.1038/nmeth.3730

[36] Fernandez-Leiro, R., and Scheres, S. H. (2016) Unravelling biological macromolecules with cryo-electron microscopy, *Nature 537*, 339-346 doi: 10.1038/nature19948

[37] Elmlund, D., and Elmlund, H. (2015) Cryogenic electron microscopy and single-particle analysis, *Annu Rev Biochem 84*, 499-517 doi: 10.1146/annurev-biochem-060614-034226

[38] Cheng, Y., Grigorieff, N., Penczek, P. A., and Walz, T. (2015) A primer to single-particle cryo-electron microscopy, *Cell 161*, 438-449 doi: 10.1016/j.cell.2015.03.050

[39] Shen, P. S. (2018) The 2017 Nobel Prize in Chemistry: cryo-EM comes of age, *Anal Bioanal Chem 410*, 2053-2057 doi: 10.1007/s00216-018-0899-8

[40] Subramaniam, S. (2019) The cryo-EM revolution: fueling the next phase, *IUCrJ 6*, 1-2 doi: 10.1107/S2052252519000277

[41] Glaeser, R. M. (2019) How Good Can Single-Particle Cryo-EM Become? What Remains Before It Approaches Its Physical Limits?, *Annu Rev Biophys 48*, 45-61 doi: 10.1146/annurev-biophys-070317-032828

[42] Berman, H. M., Kleywegt, G. J., Nakamura, H., and Markley, J. L. (2012) The Protein Data Bank at 40: reflecting on the past to prepare for the future, *Structure 20*, 391-396 doi: 10.1016/j.str.2012.01.010

[43] Sullivan, K. P., Brennan-Tonetta, P., and Marxen, L. J. (2017) Economic Impacts of the Research Collaboratory for Structural Bioinformatics (RCSB) Protein Data Bank, New Brunswick, NJ, Office of Research Analytics, Rutgers New Jersey Agricultural Experiment Station, https://cdn.rcsb.org/rcsb-pdb/general_information/about_pdb/Economic%20Impacts%20of%20the%20PDB.pdf, access date 06 October 2018

[44] Markosian, C., Di Costanzo, L., Sekharan, M., Shao, C., Burley, S. K., and Zardecki, C. (2018) Analysis of impact metrics for the Protein Data Bank, *Sci Data 5*, 180212 doi: 10.1038/sdata.2018.212

[45] Goodsell, D. S., Zardecki, C., Di Costanzo, L., Duarte, J. M., Hudson, B. P., Persikova, I., et al, Burley, S. K. (2020) RCSB Protein Data Bank: Enabling biomedical research and drug discovery, *Protein Sci 29*, 52-65 doi: 10.1002/pro.3730

[46] Zardecki, C., Westbrook, J., and Burley, S. K. (2019) PDB Structure Data Impacted Discovery and Development of Recently FDA-Approved Drugs, *The FASEB Journal 33*, 779.753-779.753 doi: 10.1096/fasebj.2019.33.1_supplement.779.53

[47] Westbrook, J. D., and Burley, S. K. (2019) How Structural Biologists and the Protein Data Bank Contributed to Recent FDA New Drug Approvals, *Structure 27*, 211-217 doi: 10.1016/j.str.2018.11.007

[48] Westbrook, J. D., Soskind, R., Hudson, B. P., and Burley, S. K. (2020) Impact of the Protein Data Bank on antineoplastic approvals, *Drug Discov Today* doi: 10.1016/j.drudis.2020.02.002

[49] Berman, H. M., Adams, P. D., Bonvin, A. A., Burley, S. K., Carragher, B., Chiu, W., et al, Sali, A. (2019) Federating Structural Models and Data: Outcomes from A Workshop on Archiving Integrative Structures, *Structure 27*, 1745-1759 doi: 10.1016/j.str.2019.11.002

[50] Helliwell, J. R. (2020) Fundamentals of neutron crystallography in structural biology, *Methods Enzymol 634*, 1-19 doi: 10.1016/bs.mie.2020.01.006

[51] Schroder, G. C., O'Dell, W. B., Myles, D. A. A., Kovalevsky, A., and Meilleur, F. (2018) IMAGINE: neutrons reveal enzyme chemistry, *Acta Crystallogr D Struct Biol 74*, 778-786 doi: 10.1107/S2059798318001626

[52] Mahieu, E., and Gabel, F. (2018) Biological small-angle neutron scattering: recent results and development, *Acta Crystallogr D Struct Biol 74*, 715-726 doi: 10.1107/S2059798318005016

[53] Kwon, H., Langan, P. S., Coates, L., Raven, E. L., and Moody, P. C. E. (2018) The rise of neutron cryo-crystallography, *Acta Crystallogr D Struct Biol 74*, 792-799 doi: 10.1107/S205979831800640X

[54] Yang, J., Anishchenko, I., Park, H., Peng, Z., Ovchinnikov, S., and Baker, D. (2020) Improved protein structure prediction using predicted interresidue orientations, *Proc Natl Acad Sci U S A 117*, 1496-1503 doi: 10.1073/pnas.1914677117

[55] Ovchinnikov, S., Park, H., Kim, D. E., DiMaio, F., and Baker, D. (2018) Protein structure prediction using Rosetta in CASP12, *Proteins 86 Suppl 1*, 113-121 doi: 10.1002/prot.25390

[56] Deng, H., Jia, Y., and Zhang, Y. (2018) Protein structure prediction, *Int J Mod Phys B 32* doi: 10.1142/S021797921840009X

[57] Baker, D., and Sali, A. (2001) Protein structure prediction and structural genomics, *Science 294*, 93-96 doi: 10.1126/science.1065659

[58] Levantino, M., Yorke, B. A., Monteiro, D. C., Cammarata, M., and Pearson, A. R. (2015) Using synchrotrons and XFELs for time-resolved X-ray crystallography and solution scattering experiments on biomolecules, *Curr Opin Struct Biol 35*, 41-48 doi: 10.1016/j.sbi.2015.07.017

[59] Meisburger, S. P., Thomas, W. C., Watkins, M. B., and Ando, N. (2017) X-ray Scattering Studies of Protein Structural Dynamics, *Chem Rev 117*, 7615-7672 doi: 10.1021/acs.chemrev.6b00790

[60] Cammarata, M., Levantino, M., Schotte, F., Anfinrud, P. A., Ewald, F., Choi, J., et al, Ihee, H. (2008) Tracking the structural dynamics of proteins in solution using time-resolved wide-angle X-ray scattering, *Nature Methods 5*, 881 doi: 10.1038/nmeth.1255 https://www.nature.com/articles/nmeth.1255#supplementary-information

[61] Pande, K., Donatelli, J. J., Malmerberg, E., Foucar, L., Poon, B. K., Sutter, M., et al, Zwart, P. H. (2018) Free-electron laser data for multiple-particle fluctuation scattering analysis, *Sci Data 5*, 180201 doi: 10.1038/sdata.2018.201

[62] Pande, K., Donatelli, J. J., Malmerberg, E., Foucar, L., Bostedt, C., Schlichting, I., and Zwart, P. H. (2018) Ab initio structure determination from experimental fluctuation X-ray scattering data, *Proc Natl Acad Sci U S A 115*, 11772-11777 doi: 10.1073/pnas.1812064115

[63] (2009) Method of the Year 2008, *Nature Methods 6*, 1-1 doi: 10.1038/nmeth.f.244

[64] (2011) Method of the Year 2010, *Nature Methods 8*, 1-1 doi: 10.1038/nmeth.f.321

[65] Deisseroth, K. (2011) Optogenetics, *Nature Methods 8*, 26-29 doi: 10.1038/Nmeth.F.324

[66] (2014) Method of the Year 2013, *Nature Methods 11*, 1-1 doi: 10.1038/nmeth.2801

[67] (2020) Method of the Year 2019: Single-cell multimodal omics, *Nat Methods 17*, 1 doi: 10.1038/s41592-019-0703-5

[68] Strack, R. (2020) Structures in situ, *Nature Methods 17*, 21-21 doi: 10.1038/s41592-019-0704-4

[69] Schaffer, M., Pfeffer, S., Mahamid, J., Kleindiek, S., Laugks, T., Albert, S., et al, Plitzko, J. M. (2019) A cryo-FIB lift-out technique enables molecular-resolution cryo-ET within native Caenorhabditis elegans tissue, *Nat Methods 16*, 757-762 doi: 10.1038/s41592-019-0497-5

[70] Schur, F. K. (2019) Toward high-resolution in situ structural biology with cryo-electron tomography and subtomogram averaging, *Curr Opin Struct Biol 58*, 1-9 doi: 10.1016/j.sbi.2019.03.018

[71] Du, M., and Jacobsen, C. (2018) Relative merits and limiting factors for x-ray and electron microscopy of thick, hydrated organic materials, *Ultramicroscopy 184*, 293-309 doi: 10.1016/j.ultramic.2017.10.003

[72] Rawson, S. D., Maksimcuka, J., Withers, P. J., and Cartmell, S. H. (2020) X-ray computed tomography in life sciences, *BMC Biol 18*, 21 doi: 10.1186/s12915-020-0753-2

[73] Sala, S., Kuppili, V. S. C., Chalkidis, S., Batey, D. J., Shi, X., Rau, C., and Thibault, P. (2018) Multiscale X-ray imaging using ptychography, *J Synchrotron Radiat 25*, 1214-1221 doi: 10.1107/S1600577518007221

[74] Do, M., Isaacson, S. A., McDermott, G., Le Gros, M. A., and Larabell, C. A. (2015) Imaging and characterizing cells using tomography, *Arch Biochem Biophys 581*, 111-121 doi: 10.1016/j.abb.2015.01.011

[75] Guo, J., and Larabell, C. A. (2019) Soft X-ray tomography: virtual sculptures from cell cultures, *Curr Opin Struct Biol 58*, 324-332 doi: 10.1016/j.sbi.2019.06.012

[76] Ekman, A. A., Chen, J. H., Guo, J., McDermott, G., Le Gros, M. A., and Larabell, C. A. (2017) Mesoscale imaging with cryo-light and X-rays: Larger than molecular machines, smaller than a cell, *Biol Cell 109*, 24-38 doi: 10.1111/boc.201600044

[77] Nannenga, B. L., and Gonen, T. (2016) MicroED opens a new era for biological structure determination, *Curr Opin Struct Biol 40*, 128-135 doi: 10.1016/j.sbi.2016.09.007

[78] Bücker, R., Hogan-Lamarre, P., Mehrabi, P., Schulz, E. C., Bultema, L. A., Gevorkov, Y., et al, Dwayne Miller, R. J. (2020) Serial protein crystallography in an electron microscope, *Nature Communications 11*, 996 doi: 10.1038/s41467-020-14793-0

[79] Xu, H., Lebrette, H., Clabbers, M. T. B., Zhao, J., Griese, J. J., Zou, X., and Hogbom, M. (2019) Solving a new R2lox protein structure by microcrystal electron diffraction, *Sci Adv 5*, eaax4621 doi: 10.1126/sciadv.aax4621

[80] Khakurel, K. P., Angelov, B., and Andreasson, J. (2019) Macromolecular Nanocrystal Structural Analysis with Electron and X-Rays: A Comparative Review, *Molecules 24* doi: 10.3390/molecules24193490

[81] Wolff, A. M., Young, I. D., Sierra, R. G., Brewster, A. S., Martynowycz, M. W., Nango, E., et al, Thompson, M. C. (2020) Comparing serial X-ray crystallography and microcrystal electron diffraction (MicroED) as methods for routine structure determination from small macromolecular crystals, *IUCrJ 7*, 306-323 doi: doi:10.1107/S205225252000072X

[82] Martynowycz, M. W., Zhao, W., Hattne, J., Jensen, G. J., and Gonen, T. (2019) Qualitative Analyses of Polishing and Precoating FIB Milled Crystals for MicroED, *Structure 27*, 1594-1600 e1592 doi: 10.1016/j.str.2019.07.004

[83] Hawe, J. S., Theis, F. J., and Heinig, M. (2019) Inferring Interaction Networks From Multi-Omics Data, *Front Genet 10*, 535 doi: 10.3389/fgene.2019.00535

[84] Berman, H. M., Burley, S. K., Kleywegt, G. J., Markley, J. L., Nakamura, H., and Velankar, S. (2016) The archiving and dissemination of biological structure data, *Curr Opin Struct Biol 40*, 17-22 doi: 10.1016/j.sbi.2016.06.018

[85] Bergmann, U., Yachandra, V., and Yano, J. (2017) *X-Ray Free Electron Lasers: Applications in Materials, Chemistry and Biology*, The Royal Society of Chemistry, London, UK.

[86] Boutet, S., Fromme, P., and Hunter, M. S. (2018) *X-ray Free Electron Lasers; A Revolution in Structural Biology*, 1 ed., Springer International Publishing, Springer Nature Switzerland AG.

[87] Gati, C., Oberthuer, D., Yefanov, O., Bunker, R. D., Stellato, F., Chiu, E., et al, Chapman, H. N. (2017) Atomic structure of granulin determined from native nanocrystalline granulovirus using an X-ray free-electron laser, *Proc Natl Acad Sci U S A 114*, 2247-2252 doi: 10.1073/pnas.1609243114

[88] Perutz, M. F., Rossmann, M. G., Cullis, A. F., Muirhead, H., Will, G., and North, A. C. (1960) Structure of haemoglobin: a three-dimensional Fourier synthesis at 5.5-Å resolution, obtained by X-ray analysis, *Nature 185*, 416-422 doi: 10.1038/185416a0

[89] Perutz, M. F., Bolton, W., Diamond, R., Muirhead, H., and Watson, H. C. (1964) Structure of Haemoglobin. An X-Ray Examination of Reduced Horse Haemoglobin, *Nature 203*, 687-690 doi: 10.1038/203687a0

[90] Breaker, R. R. (2018) Riboswitches and Translation Control, *Cold Spring Harb Perspect Biol 10* doi: 10.1101/cshperspect.a032797

[91] Breaker, R. R. (2012) Riboswitches and the RNA world, *Cold Spring Harb Perspect Biol 4* doi: 10.1101/cshperspect.a003566

[92] Bhandari, Y. R., Fan, L., Fang, X., Zaki, G. F., Stahlberg, E. A., Jiang, W., et al, Wang, Y. X. (2017) Topological Structure Determination of RNA Using Small-Angle X-Ray Scattering, *J Mol Biol 429*, 3635-3649 doi: 10.1016/j.jmb.2017.09.006

[93] Stagno, J. R., Liu, Y., Bhandari, Y. R., Conrad, C. E., Panja, S., Swain, M., et al, Wang, Y. X. (2017) Structures of riboswitch RNA reaction states by mix-and-inject XFEL serial crystallography, *Nature 541*, 242-246 doi: 10.1038/nature20599

[94] Stagno, J. R., Bhandari, Y. R., Conrad, C. E., Liu, Y., and Wang, Y. X. (2017) Real-time crystallographic studies of the adenine riboswitch using an X-ray free-electron laser, *FEBS J 284*, 3374-3380 doi: 10.1111/febs.14110

[95] Nobelprize.org. (2017) The 2017 Nobel Prize in Chemistry - Press Release, Nobel Media AB 2014, https://www.nobelprize.org/nobel_prizes/chemistry/laureates/2017/, access date

[96] Muench, S. P., Antonyuk, S. V., and Hasnain, S. S. (2019) The expanding toolkit for structural biology: synchrotrons, X-ray lasers and cryoEM, *IUCrJ 6*, 167-177 doi: 10.1107/S2052252519002422

[97] Ourmazd, A. (2019) Cryo-EM, XFELs and the structure conundrum in structural biology, *Nature Methods* doi: 10.1038/s41592-019-0587-4

[98] Clare, D. K., Siebert, C. A., Hecksel, C., Hagen, C., Mordhorst, V., Grange, M., et al, Zhang, P. (2017) Electron Bio-Imaging Centre (eBIC): the UK national research facility for biological electron microscopy, *Acta Crystallogr D Struct Biol 73*, 488-495 doi: 10.1107/S2059798317007756

[99] Callaway, E. (2020) Revolutionary cryo-EM is taking over structural biology, *Nature 578*, 201 doi: 10.1038/d41586-020-00341-9

[100] Kaledhonkar, S., Fu, Z., White, H., and Frank, J. (2018) Time-Resolved Cryo-electron Microscopy Using a Microfluidic Chip, *Methods Mol Biol 1764*, 59-71 doi: 10.1007/978-1-4939-7759-8_4

[101] Frank, J. (2017) Time-resolved cryo-electron microscopy: Recent progress, *J Struct Biol 200*, 303-306 doi: 10.1016/j.jsb.2017.06.005

[102] Kontziampasis, D., Klebl, D. P., Iadanza, M. G., Scarff, C. A., Kopf, F., Sobott, F., et al, White, H. D. (2019) A cryo-EM grid preparation device for time-resolved structural studies, *IUCrJ 6* doi: doi:10.1107/S2052252519011345

[103] Jain, T., Sheehan, P., Crum, J., Carragher, B., and Potter, C. S. (2012) Spotiton: a prototype for an integrated inkjet dispense and vitrification system for cryo-TEM, *J Struct Biol 179*, 68-75 doi: 10.1016/j.jsb.2012.04.020

[104] Dandey, V. P., Wei, H., Zhang, Z., Tan, Y. Z., Acharya, P., Eng, E. T., et al, Carragher, B. (2018) Spotiton: New features and applications, *J Struct Biol 202*, 161-169 doi: 10.1016/j.jsb.2018.01.002

[105] Kaledhonkar, S., Fu, Z., Caban, K., Li, W., Chen, B., Sun, M., et al, Frank, J. (2019) Late steps in bacterial translation initiation visualized using time-resolved cryo-EM, *Nature 570*, 400-404 doi: 10.1038/s41586-019-1249-5

[106] Fuller, F. D., Gul, S., Chatterjee, R., Burgie, E. S., Young, I. D., Lebrette, H., et al, Yano, J. (2017) Drop-on-demand sample delivery for studying biocatalysts in action at X-ray free-electron lasers, *Nat Methods 14*, 443-449 doi: 10.1038/nmeth.4195

[107] Roessler, C. G., Agarwal, R., Allaire, M., Alonso-Mori, R., Andi, B., Bachega, J. F. R., et al, Zouni, A. (2016) Acoustic Injectors for Drop-On-Demand Serial Femtosecond Crystallography, *Structure 24*, 631-640 doi: 10.1016/j.str.2016.02.007

[108] Davy, B., Axford, D., Beale, J. H., Butryn, A., Docker, P., Ebrahim, A., et al, Aller, P. (2019) Reducing sample consumption for serial crystallography using acoustic drop ejection, *Journal of Synchrotron Radiation 26*, 1820-1825 doi: doi:10.1107/S1600577519009329

[109] Boutet, S., Lomb, L., Williams, G. J., Barends, T. R., Aquila, A., Doak, R. B., et al, Schlichting, I. (2012) High-resolution protein structure determination by serial femtosecond crystallography, *Science 337*, 362-364 doi: 10.1126/science.1217737

[110] Chapman, H. N., Fromme, P., Barty, A., White, T. A., Kirian, R. A., Aquila, A., et al, Spence, J. C. (2011) Femtosecond X-ray protein nanocrystallography, *Nature 470*, 73-77 doi: 10.1038/nature09750

[111] Stan, C. A., Milathianaki, D., Laksmono, H., Sierra, R. G., McQueen, T. A., Messerschmidt, M., et al, Boutet, S. (2016) Liquid explosions induced by X-ray laser pulses, *Nat Phys 12*, 966-971 doi: 10.1038/Nphys3779

[112] Kim, D., Echelmeier, A., Cruz Villarreal, J., Gandhi, S., Quintana, S., Egatz-Gomez, A., and Ros, A. (2019) Electric Triggering for Enhanced Control of Droplet Generation, *Anal Chem 91*, 9792-9799 doi: 10.1021/acs.analchem.9b01449

[113] Knoska, J., Adriano, L., Awel, S., Beyerlein, K. R., Yefanov, O., Oberthuer, D., et al, Heymann, M. (2020) Ultracompact 3D microfluidics for time-resolved structural biology, *Nat Commun 11*, 657 doi: 10.1038/s41467-020-14434-6

[114] Oberthuer, D., Knoska, J., Wiedorn, M. O., Beyerlein, K. R., Bushnell, D. A., Kovaleva, E. G., et al, Bajt, S. (2017) Double-flow focused liquid injector for efficient serial femtosecond crystallography, *Sci Rep 7*, 44628 doi: 10.1038/srep44628

[115] Nogly, P., Panneels, V., Nelson, G., Gati, C., Kimura, T., Milne, C., et al, Standfuss, J. (2016) Lipidic cubic phase injector is a viable crystal delivery system for time-resolved serial crystallography, *Nat Commun 7*, 12314 doi: 10.1038/ncomms12314

[116] DePonte, D. P., Weierstall, U., Schmidt, K., Warner, J., Starodub, D., Spence, J. C. H., and Doak, R. B. (2008) Gas dynamic virtual nozzle for generation of microscopic droplet streams, *Journal of Physics D: Applied Physics 41*, 195505 doi:

[117] Kovacsova, G., Grunbein, M. L., Kloos, M., Barends, T. R. M., Schlesinger, R., Heberle, J., et al, Schlichting, I. (2017) Viscous hydrophilic injection matrices for serial crystallography, *IUCrJ 4*, 400-410 doi: 10.1107/S2052252517005140

[118] Kern, J., Chatterjee, R., Young, I. D., Fuller, F. D., Lassalle, L., Ibrahim, M., et al, Yachandra, V. K. (2018) Structures of the intermediates of Kok's photosynthetic water oxidation clock, *Nature 563*, 421-425 doi: 10.1038/s41586-018-0681-2

[119] Orville, A. M. (2017) CHAPTER 18 Acoustic Methods for On-demand Sample Injection into XFEL Beams, In *X-Ray Free Electron Lasers: Applications in Materials, Chemistry and Biology*, pp 348-364, The Royal Society of Chemistry.

[120] Soares, A. S., Engel, M. A., Stearns, R., Datwani, S., Olechno, J., Ellson, R., et al, Orville, A. M. (2011) Acoustically mounted microcrystals yield high-resolution X-ray structures, *Biochemistry 50*, 4399-4401 doi: 10.1021/bi200549x

[121] Wu, P., Noland, C., Ultsch, M., Edwards, B., Harris, D., Mayer, R., and Harris, S. F. (2016) Developments in the Implementation of Acoustic Droplet Ejection for Protein Crystallography, *J Lab Autom 21*, 97-106 doi: 10.1177/2211068215598938

[122] Mafune, F., Miyajima, K., Tono, K., Takeda, Y., Kohno, J. Y., Miyauchi, N., et al, Yabashi, M. (2016) Microcrystal delivery by pulsed liquid droplet for serial femtosecond crystallography, *Acta Crystallogr D Struct Biol 72*, 520-523 doi: 10.1107/S2059798316001480

[123] Hadimioglu, B., Stearns, R., and Ellson, R. (2016) Moving Liquids with Sound: The Physics of Acoustic Droplet Ejection for Robust Laboratory Automation in Life Sciences, *J Lab Autom 21*, 4-18 doi: 10.1177/2211068215615096

[124] Hunter, M. S., Segelke, B., Messerschmidt, M., Williams, G. J., Zatsepin, N. A., Barty, A., et al, Frank, M. (2014) Fixed-target protein serial microcrystallography with an x-ray free electron laser, *Sci Rep 4*, 6026 doi: 10.1038/srep06026

[125] Doak, R. B., Kovacs, G. N., Gorel, A., Foucar, L., Barends, T. R. M., Grunbein, M. L., et al, Schlichting, I. (2018) Crystallography on a chip - without the chip: sheet-on-sheet sandwich, *Acta Crystallogr D 74*, 1000-1007 doi: 10.1107/S2059798318011634

[126] Oghbaey, S., Sarracini, A., Ginn, H. M., Pare-Labrosse, O., Kuo, A., Marx, A., et al, Miller, R. J. (2016) Fixed target combined with spectral mapping: approaching 100% hit rates for serial crystallography, *Acta Crystallogr D Struct Biol 72*, 944-955 doi: 10.1107/S2059798316010834

[127] Sherrell, D. A., Foster, A. J., Hudson, L., Nutter, B., O'Hea, J., Nelson, S., et al, Owen, R. L. (2015) A modular and compact portable mini-endstation for high-precision, high-speed fixed target serial crystallography at FEL and synchrotron sources, *J Synchrotron Radiat 22*, 1372-1378 doi: 10.1107/S1600577515016938

[128] Mueller, C., Marx, A., Epp, S. W., Zhong, Y., Kuo, A., Balo, A. R., et al, Dwayne Miller, R. J. (2015) Fixed target matrix for femtosecond time-resolved and in situ serial micro-crystallography, *Struct Dyn 2*, 054302 doi: 10.1063/1.4928706

[129] Aller, P., Sanchez-Weatherby, J., Foadi, J., Winter, G., Lobley, C. M., Axford, D., et al, Walsh, M. A. (2015) Application of in situ diffraction in high-throughput structure determination platforms, *Methods Mol Biol 1261*, 233-253 doi: 10.1007/978-1-4939-2230-7_13

[130] Lieske, J., Cerv, M., Kreida, S., Komadina, D., Fischer, J., Barthelmess, M., et al, Meents, A. (2019) On-chip crystallization for serial crystallography experiments and on-chip ligand-binding studies, *IUCrJ 6*, 714-728 doi: 10.1107/S2052252519007395

[131] Roedig, P., Ginn, H. M., Pakendorf, T., Sutton, G., Harlos, K., Walter, T. S., et al, Meents, A. (2017) High-speed fixed-target serial virus crystallography, *Nat Methods 14*, 805-810 doi: 10.1038/nmeth.4335

[132] Roedig, P., Duman, R., Sanchez-Weatherby, J., Vartiainen, I., Burkhardt, A., Warmer, M., et al, Meents, A. (2016) Room-temperature macromolecular crystallography using a micro-patterned silicon chip with minimal background scattering, *J Appl Crystallogr 49*, 968-975 doi: 10.1107/S1600576716006348

[133] Roedig, P., Vartiainen, I., Duman, R., Panneerselvam, S., Stube, N., Lorbeer, O., et al, Meents, A. (2015) A micro-patterned silicon chip as sample holder for macromolecular crystallography experiments with minimal background scattering, *Sci Rep 5*, 10451 doi: 10.1038/srep10451

[134] Shelby, M. L., Gilbile, D., Grant, T. D., Seuring, C., Segelke, B. W., He, W., et al, Frank, M. (2020) A fixed-target platform for serial femtosecond crystallography in a hydrated environment, *IUCrJ 7*, 30-41 doi: 10.1107/S2052252519014003

[135] Chreifi, G., Baxter, E. L., Doukov, T., Cohen, A. E., McPhillips, S. E., Song, J., et al, Poulos, T. L. (2016) Crystal structure of the pristine peroxidase ferryl center and its relevance to proton-coupled electron transfer, *Proc Natl Acad Sci U S A 113*, 1226-1231 doi: 10.1073/pnas.1521664113

[136] Baxter, E. L., Aguila, L., Alonso-Mori, R., Barnes, C. O., Bonagura, C. A., Brehmer, W., et al, Cohen, A. E. (2016) High-density grids for efficient data collection from multiple crystals, *Acta Crystallogr D Struct Biol 72*, 2-11 doi: 10.1107/S2059798315020847

[137] Cohen, A. E., Soltis, S. M., Gonzalez, A., Aguila, L., Alonso-Mori, R., Barnes, C. O., et al, Hodgson, K. O. (2014) Goniometer-based femtosecond crystallography with X-ray free electron lasers, *Proc Natl Acad Sci U S A 111*, 17122-17127 doi: 10.1073/pnas.1418733111

[138] Tosha, T., Nomura, T., Nishida, T., Saeki, N., Okubayashi, K., Yamagiwa, R., et al, Kubo, M. (2017) Capturing an initial intermediate during the P450nor enzymatic reaction using time-resolved XFEL crystallography and caged-substrate, *Nat Commun 8*, 1585 doi: 10.1038/s41467-017-01702-1

[139] Suga, M., Shimada, A., Akita, F., Shen, J. R., Tosha, T., and Sugimoto, H. (2020) Time-resolved studies of metalloproteins using X-ray free electron laser radiation at SACLA, *Biochim Biophys Acta Gen Subj 1864*, 129466 doi: 10.1016/j.bbagen.2019.129466

[140] Deiters, A., Groff, D., Ryu, Y., Xie, J., and Schultz, P. G. (2006) A genetically encoded photocaged tyrosine, *Angew Chem Int Ed Engl 45*, 2728-2731 doi: 10.1002/anie.200600264

[141] Zhao, F. Z., Zhang, B., Yan, E. K., Sun, B., Wang, Z. J., He, J. H., and Yin, D. C. (2019) A guide to sample delivery systems for serial crystallography, *FEBS J 286*, 4402-4417 doi: 10.1111/febs.15099

[142] Martiel, I., Muller-Werkmeister, H. M., and Cohen, A. E. (2019) Strategies for sample delivery for femtosecond crystallography, *Acta Crystallogr D Struct Biol 75*, 160-177 doi: 10.1107/S2059798318017953

[143] Meents, A., Wiedorn, M. O., Srajer, V., Henning, R., Sarrou, I., Bergtholdt, J., et al, Chapman, H. N. (2017) Pink-beam serial crystallography, *Nat Commun 8*, 1281 doi: 10.1038/s41467-017-01417-3

[144] Mehrabi, P., Schulz, E. C., Agthe, M., Horrell, S., Bourenkov, G., von Stetten, D., et al, Miller, R. J. D. (2019) Liquid application method for time-resolved analyses by serial synchrotron crystallography, *Nature Methods* doi: 10.1038/s41592-019-0553-1

[145] Martin-Garcia, J. M., Conrad, C. E., Nelson, G., Stander, N., Zatsepin, N. A., Zook, J., et al, Liu, W. (2017) Serial millisecond crystallography of membrane and soluble protein microcrystals using

synchrotron radiation, *IUCrJ 4*, 439-454 doi: 10.1107/S205225251700570X

[146] Martin-Garcia, J. M., Zhu, L., Mendez, D., Lee, M. Y., Chun, E., Li, C., et al, Liu, W. (2019) High-viscosity injector-based pink-beam serial crystallography of microcrystals at a synchrotron radiation source, *IUCrJ 6*, 412-425 doi: 10.1107/S205225251900263X

[147] Chenevier, D., and Joly, A. (2018) ESRF: Inside the Extremely Brilliant Source Upgrade, *Synchrotron Radiation News 31*, 32-35 doi: 10.1080/08940886.2018.1409562

[148] Fagerberg, L., Jonasson, K., von Heijne, G., Uhlen, M., and Berglund, L. (2010) Prediction of the human membrane proteome, *Proteomics 10*, 1141-1149 doi: 10.1002/pmic.200900258

[149] Almen, M. S., Nordstrom, K. J., Fredriksson, R., and Schioth, H. B. (2009) Mapping the human membrane proteome: a majority of the human membrane proteins can be classified according to function and evolutionary origin, *BMC Biol 7*, 50 doi: 10.1186/1741-7007-7-50

[150] Ishchenko, A., Abola, E. E., and Cherezov, V. (2017) Crystallization of Membrane Proteins: An Overview, *Methods Mol Biol 1607*, 117-141 doi: 10.1007/978-1-4939-7000-1_5

[151] Yildirim, M. A., Goh, K. I., Cusick, M. E., Barabasi, A. L., and Vidal, M. (2007) Drug-target network, *Nat Biotechnol 25*, 1119-1126 doi: 10.1038/nbt1338

[152] Wu, Z., Li, W., Liu, G., and Tang, Y. (2018) Network-Based Methods for Prediction of Drug-Target Interactions, *Front Pharmacol 9*, 1134 doi: 10.3389/fphar.2018.01134

[153] Stauch, B., and Cherezov, V. (2018) Serial Femtosecond Crystallography of G Protein-Coupled Receptors, *Annu Rev Biophys 47*, 377-397 doi: 10.1146/annurev-biophys-070317-033239

[154] White, T. A., Mariani, V., Brehm, W., Yefanov, O., Barty, A., Beyerlein, K. R., et al, Chapman, H. N. (2016) Recent developments in CrystFEL, *J Appl Crystallogr 49*, 680-689 doi: 10.1107/S1600576716004751

[155] White, T. A. (2014) Post-refinement method for snapshot serial crystallography, *Philos Trans R Soc Lond B Biol Sci 369*, 20130330 doi: 10.1098/rstb.2013.0330

[156] Winter, G., Waterman, D. G., Parkhurst, J. M., Brewster, A. S., Gildea, R. J., Gerstel, M., et al, Evans, G. (2018) DIALS: implementation and evaluation of a new integration package, *Acta Crystallogr D Struct Biol 74*, 85-97 doi: 10.1107/S2059798317017235

[157] Brewster, A. S., Waterman, D. G., Parkhurst, J. M., Gildea, R. J., Young, I. D., O'Riordan, L. J., et al, Sauter, N. K. (2018) Improving signal strength in serial crystallography with DIALS geometry refinement, *Acta Crystallogr D Struct Biol 74*, 877-894 doi: 10.1107/S2059798318009191

[158] Waterman, D. G., Winter, G., Gildea, R. J., Parkhurst, J. M., Brewster, A. S., Sauter, N. K., and Evans, G. (2016) Diffraction-geometry refinement in the DIALS framework, *Acta Crystallogr D Struct Biol 72*, 558-575 doi: 10.1107/S2059798316002187

[159] Sauter, N. K. (2015) XFEL diffraction: developing processing methods to optimize data quality, *J Synchrotron Radiat 22*, 239-248 doi: 10.1107/S1600577514028203

[160] Yefanov, O., Gati, C., Bourenkov, G., Kirian, R. A., White, T. A., Spence, J. C., et al, Barty, A. (2014) Mapping the continuous reciprocal space intensity distribution of X-ray serial crystallography, *Philos Trans R Soc Lond B Biol Sci 369*, 20130333 doi: 10.1098/rstb.2013.0333

[161] Ginn, H. M., Brewster, A. S., Hattne, J., Evans, G., Wagner, A., Grimes, J. M., et al, Stuart, D. I. (2015) A revised partiality model and post-refinement algorithm for X-ray free-electron laser data, *Acta Crystallogr D Biol Crystallogr 71*, 1400-1410 doi: 10.1107/S1399004715006902

[162] Gevorkov, Y., Yefanov, O., Barty, A., White, T. A., Mariani, V., Brehm, W., et al, Chapman, H. N. (2019) XGANDALF - extended gradient descent algorithm for lattice finding, *Acta Crystallogr A Found Adv 75*, 694-704 doi: 10.1107/S2053273319010593

[163] Allahgholi, A., Becker, J., Delfs, A., Dinapoli, R., Goettlicher, P., Greiffenberg, D., et al, Graafsma, H. (2019) The Adaptive Gain Integrating Pixel Detector at the European XFEL, *Journal of Synchrotron Radiation 26*, 74-82 doi: doi:10.1107/S1600577518016077

[164] Allahgholi, A., Becker, J., Bianco, L., Delfs, A., Dinapoli, R., Goettlicher, P., et al, Zimmer, M. (2015) AGIPD, a high dynamic range fast detector for the European XFEL, *J Instrum 10* doi: Artn C01023; 10.1088/1748-0221/10/01/C01023

[165] Greiffenberg, D., and Collaboration, A. (2012) The AGIPD detector for the European XFEL, *J Instrum 7* doi: Artn C01103; 10.1088/1748-0221/7/01/C01103

[166] Leonarski, F., Mozzanica, A., Brückner, M., Lopez-Cuenca, C., Redford, S., Sala, L., et al, Wang, M. (2020) JUNGFRAU detector for brighter x-ray sources: Solutions for IT and data science challenges in macromolecular crystallography, *Structural Dynamics 7*, 014305 doi: 10.1063/1.5143480

[167] Leonarski, F., Redford, S., Mozzanica, A., Lopez-Cuenca, C., Panepucci, E., Nass, K., et al, Wang, M. (2018) Fast and accurate data collection for macromolecular crystallography using the JUNGFRAU detector, *Nature Methods 15*, 799-804 doi: 10.1038/s41592-018-0143-7

[168] van Thor, J. J. (2019) Advances and opportunities in ultrafast X-ray crystallography and ultrafast structural optical crystallography of nuclear and electronic protein dynamics, *Struct Dyn 6*, 050901 doi: 10.1063/1.5110685

[169] Hutchison, C. D. M., and van Thor, J. J. (2019) Optical control, selection and analysis of population dynamics in ultrafast protein X-ray crystallography, *Philos Trans A Math Phys Eng Sci 377*, 20170474 doi: 10.1098/rsta.2017.0474

[170] Shenoy , G. K., Stöhr, J., Freeman, R. R., Bucksbaum, P. H., Kulander, K., Young, L., et al, Yu, L.-H. (2003) LCLS The First Experiments, Stanford Linear Accelerator Center, Stanford University, https://www.slac.stanford.edu/pubs/slacreports/reports03/slac-r-611.pdf, access date February 2020

[171] Aquila, A., Hunter, M. S., Doak, R. B., Kirian, R. A., Fromme, P., White, T. A., et al, Chapman, H. N. (2012) Time-resolved protein nanocrystallography using an X-ray free-electron laser, *Optics Express 20*, 2706-2716 doi: 10.1364/Oe.20.002706

[172] Johansson, L. C., Arnlund, D., Katona, G., White, T. A., Barty, A., DePonte, D. P., et al, Neutze, R. (2013) Structure of a photosynthetic reaction centre determined by serial femtosecond crystallography, *Nat Commun 4*, 2911 doi: 10.1038/ncomms3911

[173] Wiedorn, M. O., Awel, S., Morgan, A. J., Ayyer, K., Gevorkov, Y., Fleckenstein, H., et al, Chapman, H. N. (2018) Rapid sample delivery for megahertz serial crystallography at X-ray FELs, *IUCrJ 5*, 574-584 doi: 10.1107/S2052252518008369

[174] Echelmeier, A., Kim, D., Cruz Villarreal, J., Coe, J., Quintana, S., Brehm, G., et al, Ros, A. (2019) 3D printed droplet generation devices for serial femtosecond crystallography enabled by surface coating, *J Appl Crystallogr 52*, 997-1008 doi: 10.1107/S1600576719010343

[175] Gisriel, C., Coe, J., Letrun, R., Yefanov, O. M., Luna-Chavez, C., Stander, N. E., et al, Zatsepin, N. A. (2019) Membrane protein megahertz crystallography at the European XFEL, *Nat Commun 10*, 5021 doi: 10.1038/s41467-019-12955-3

[176] Kupitz, C., Basu, S., Grotjohann, I., Fromme, R., Zatsepin, N. A., Rendek, K. N., et al, Fromme, P. (2014) Serial time-resolved crystallography of photosystem II using a femtosecond X-ray laser, *Nature 513*, 261-265 doi: 10.1038/nature13453

[177] Ayyer, K., Yefanov, O. M., Oberthur, D., Roy-Chowdhury, S., Galli, L., Mariani, V., et al, Chapman, H. N. (2016) Macromolecular diffractive imaging using imperfect crystals, *Nature 530*, 202-206 doi: 10.1038/nature16949

[178] Suga, M., Akita, F., Sugahara, M., Kubo, M., Nakajima, Y., Nakane, T., et al, Shen, J. R. (2017) Light-induced structural changes and the site of O=O bond formation in PSII caught by XFEL, *Nature 543*, 131-135 doi: 10.1038/nature21400

[179] Suga, M., Akita, F., Yamashita, K., Nakajima, Y., Ueno, G., Li, H., et al, Shen, J. R. (2019) An oxyl/oxo mechanism for oxygen-oxygen coupling in PSII revealed by an x-ray free-electron laser, *Science 366*, 334-338 doi: 10.1126/science.aax6998

[180] Suga, M., Akita, F., Hirata, K., Ueno, G., Murakami, H., Nakajima, Y., et al, Shen, J. R. (2015) Native structure of photosystem II at 1.95 A resolution viewed by femtosecond X-ray pulses, *Nature 517*, 99-103 doi: 10.1038/nature13991

[181] Young, I. D., Ibrahim, M., Chatterjee, R., Gul, S., Fuller, F. D., Koroidov, S., et al, Yano, J. (2016) Structure of photosystem II and substrate binding at room temperature, *Nature 540*, 453-457 doi: 10.1038/nature20161

[182] Sierra, R. G., Gati, C., Laksmono, H., Dao, E. H., Gul, S., Fuller, F., et al, DeMirci, H. (2016) Concentric-flow electrokinetic injector enables serial crystallography of ribosome and photosystem II, *Nat Methods 13*, 59-62 doi: 10.1038/nmeth.3667

[183] Kern, J., Yachandra, V. K., and Yano, J. (2015) Metalloprotein structures at ambient conditions and in real-time: biological crystallography and spectroscopy using X-ray free electron lasers, *Curr Opin Struct Biol 34*, 87-98 doi: 10.1016/j.sbi.2015.07.014

[184] Kern, J., Tran, R., Alonso-Mori, R., Koroidov, S., Echols, N., Hattne, J., et al, Yachandra, V. K. (2014) Taking snapshots of photosynthetic water oxidation using femtosecond X-ray diffraction and spectroscopy, *Nat Commun 5*, 4371 doi: 10.1038/ncomms5371

[185] Kern, J., Alonso-Mori, R., Tran, R., Hattne, J., Gildea, R. J., Echols, N., et al, Yano, J. (2013) Simultaneous femtosecond X-ray spectroscopy and diffraction of photosystem II at room temperature, *Science 340*, 491-495 doi: 10.1126/science.1234273

[186] Alonso-Mori, R., Kern, J., Gildea, R. J., Sokaras, D., Weng, T. C., Lassalle-Kaiser, B., et al, Bergmann, U. (2012) Energy-dispersive X-ray emission spectroscopy using an X-ray free-electron laser in a shot-by-shot mode, *Proc Natl Acad Sci U S A 109*, 19103-19107 doi: 10.1073/pnas.1211384109

[187] Fransson, T., Chatterjee, R., Fuller, F. D., Gul, S., Weninger, C., Sokaras, D., et al, Yano, J. (2018) X-ray Emission Spectroscopy as an in Situ Diagnostic Tool for X-ray Crystallography of Metalloproteins Using an X-ray Free-Electron Laser, *Biochemistry 57*, 4629-4637 doi: 10.1021/acs.biochem.8b00325

[188] Tenboer, J., Basu, S., Zatsepin, N., Pande, K., Milathianaki, D., Frank, M., et al, Schmidt, M. (2014) Time-resolved serial crystallography captures high-resolution intermediates of photoactive yellow protein, *Science 346*, 1242-1246 doi: 10.1126/science.1259357

[189] Pande, K., Hutchison, C. D., Groenhof, G., Aquila, A., Robinson, J. S., Tenboer, J., et al, Schmidt, M. (2016) Femtosecond structural dynamics drives the trans/cis isomerization in photoactive yellow protein, *Science 352*, 725-729 doi: 10.1126/science.aad5081

[190] Pandey, S., Bean, R., Sato, T., Poudyal, I., Bielecki, J., Cruz Villarreal, J., et al, Schmidt, M. (2019) Time-resolved serial femtosecond crystallography at the European XFEL, *Nature Methods* doi: 10.1038/s41592-019-0628-z

[191] Kang, Y., Zhou, X. E., Gao, X., He, Y., Liu, W., Ishchenko, A., et al, Xu, H. E. (2015) Crystal structure of rhodopsin bound to arrestin by femtosecond X-ray laser, *Nature 523*, 561-567 doi: 10.1038/nature14656

[192] Zhou, X. E., Gao, X., Barty, A., Kang, Y., He, Y., Liu, W., et al, Xu, H. E. (2016) X-ray laser diffraction for structure determination of the rhodopsin-arrestin complex, *Sci Data 3*, 160021 doi: 10.1038/sdata.2016.21

[193] Nakane, T., Hanashima, S., Suzuki, M., Saiki, H., Hayashi, T., Kakinouchi, K., et al, Mizohata, E. (2016) Membrane protein structure determination by SAD, SIR, or SIRAS phasing in serial femtosecond crystallography using an iododetergent, *Proc Natl Acad Sci U S A 113*, 13039-13044 doi: 10.1073/pnas.1602531113

[194] Nango, E., Royant, A., Kubo, M., Nakane, T., Wickstrand, C., Kimura, T., et al, Iwata, S. (2016) A three-dimensional movie of structural changes in bacteriorhodopsin, *Science 354*, 1552-1557 doi: 10.1126/science.aah3497

[195] Nogly, P., Weinert, T., James, D., Carbajo, S., Ozerov, D., Furrer, A., et al, Standfuss, J. (2018) Retinal isomerization in bacteriorhodopsin captured by a femtosecond x-ray laser, *Science 361* doi: 10.1126/science.aat0094

[196] Wickstrand, C., Nogly, P., Nango, E., Iwata, S., Standfuss, J., and Neutze, R. (2019) Bacteriorhodopsin: Structural Insights Revealed

Using X-Ray Lasers and Synchrotron Radiation, *Annual Review of Biochemistry, Vol 88 88*, 59-83 doi: 10.1146/annurev-biochem-013118-111327

[197] Weinert, T., Skopintsev, P., James, D., Dworkowski, F., Panepucci, E., Kekilli, D., et al, Standfuss, J. (2019) Proton uptake mechanism in bacteriorhodopsin captured by serial synchrotron crystallography, *Science 365*, 61-65 doi: 10.1126/science.aaw8634

[198] Panneels, V., Wu, W., Tsai, C. J., Nogly, P., Rheinberger, J., Jaeger, K., et al, Schertler, G. (2015) Time-resolved structural studies with serial crystallography: A new light on retinal proteins, *Struct Dyn 2*, 041718 doi: 10.1063/1.4922774

[199] Nass Kovacs, G., Colletier, J. P., Grunbein, M. L., Yang, Y., Stensitzki, T., Batyuk, A., et al, Schlichting, I. (2019) Three-dimensional view of ultrafast dynamics in photoexcited bacteriorhodopsin, *Nat Commun 10*, 3177 doi: 10.1038/s41467-019-10758-0

[200] Varma, N., Mutt, E., Muhle, J., Panneels, V., Terakita, A., Deupi, X., et al, Lesca, E. (2019) Crystal structure of jumping spider rhodopsin-1 as a light sensitive GPCR, *Proc Natl Acad Sci U S A 116*, 14547-14556 doi: 10.1073/pnas.1902192116

[201] Nagata, T., Koyanagi, M., Tsukamoto, H., Mutt, E., Schertler, G. F. X., Deupi, X., and Terakita, A. (2019) The counterion-retinylidene Schiff base interaction of an invertebrate rhodopsin rearranges upon light activation, *Commun Biol 2*, 180 doi: 10.1038/s42003-019-0409-3

[202] Yun, J. H., Li, X., Park, J. H., Wang, Y., Ohki, M., Jin, Z., et al, Lee, W. (2019) Non-cryogenic structure of a chloride pump provides crucial clues to temperature-dependent channel transport efficiency, *J Biol Chem 294*, 794-804 doi: 10.1074/jbc.RA118.004038

[203] Hutchison, C. D. M., Cordon-Preciado, V., Morgan, R. M. L., Nakane, T., Ferreira, J., Dorlhiac, G., et al, van Thor, J. J. (2017) X-ray Free Electron Laser Determination of Crystal Structures of Dark and Light States of a Reversibly Photoswitching Fluorescent Protein at Room Temperature, *International Journal of Molecular Sciences 18* doi: ARTN 1918; 10.3390/ijms18091918

[204] Woodhouse, J., Nass Kovacs, G., Coquelle, N., Uriarte, L. M., Adam, V., Barends, T. R. M., et al, Weik, M. (2020) Photoswitching mechanism of a fluorescent protein revealed by time-resolved crystallography and transient absorption spectroscopy, *Nat Commun 11*, 741 doi: 10.1038/s41467-020-14537-0

[205] Colletier, J. P., Sliwa, M., Gallat, F. X., Sugahara, M., Guillon, V., Schiro, G., et al, Weik, M. (2016) Serial Femtosecond Crystallography and Ultrafast Absorption Spectroscopy of the Photoswitchable Fluorescent Protein IrisFP, *J Phys Chem Lett 7*, 882-887 doi: 10.1021/acs.jpclett.5b02789

[206] Coquelle, N., Sliwa, M., Woodhouse, J., Schiro, G., Adam, V., Aquila, A., et al, Weik, M. (2018) Chromophore twisting in the excited state of a photoswitchable fluorescent protein captured by time-resolved serial femtosecond crystallography, *Nat Chem 10*, 31-37 doi: 10.1038/nchem.2853

[207] Edlund, P., Takala, H., Claesson, E., Henry, L., Dods, R., Lehtivuori, H., et al, Westenhoff, S. (2016) The room temperature crystal structure of a bacterial phytochrome determined by serial femtosecond crystallography, *Sci Rep 6*, 35279 doi: 10.1038/srep35279

[208] Barends, T. R., Foucar, L., Ardevol, A., Nass, K., Aquila, A., Botha, S., et al, Schlichting, I. (2015) Direct observation of ultrafast collective motions in CO myoglobin upon ligand dissociation, *Science 350*, 445-450 doi: 10.1126/science.aac5492

[209] Ishigami, I., Zatsepin, N. A., Hikita, M., Conrad, C. E., Nelson, G., Coe, J. D., et al, Rousseau, D. L. (2017) Crystal structure of CO-bound cytochrome c oxidase determined by serial femtosecond X-ray crystallography at room temperature, *Proc Natl Acad Sci U S A 114*, 8011-8016 doi: 10.1073/pnas.1705628114

[210] Shimada, A., Kubo, M., Baba, S., Yamashita, K., Hirata, K., Ueno, G., et al, Tsukihara, T. (2017) A nanosecond time-resolved XFEL analysis of structural changes associated with CO release from cytochrome c oxidase, *Sci Adv 3*, e1603042 doi: 10.1126/sciadv.1603042

[211] Nakajima, K., Joti, Y., Katayama, T., Owada, S., Togashi, T., Abe, T., et al, Yabashi, M. (2018) Software for the data analysis of the arrival-timing monitor at SACLA, *J Synchrotron Radiat 25*, 592-603 doi: 10.1107/S1600577517016654

[212] Katayama, T., Owada, S., Togashi, T., Ogawa, K., Karvinen, P., Vartiainen, I., et al, Yabashi, M. (2016) A beam branching method for timing and spectral characterization of hard X-ray free-electron lasers, *Struct Dyn 3*, 034301 doi: 10.1063/1.4939655

[213] Sanchez-Gonzalez, A., Johnson, A. S., Fitzpatrick, A., Hutchison, C. D. M., Fare, C., Cordon-Preciado, V., et al, van Thor, J. J. (2017) Coincidence timing of femtosecond optical pulses in an X-ray free electron laser, *J Appl Phys 122* doi: Artn 203105

10.1063/1.5012749

[214] Yabuuchi, T., Kon, A., Inubushi, Y., Togahi, T., Sueda, K., Itoga, T., et al, Yabashi, M. (2019) An experimental platform using high-power, high-intensity optical lasers with the hard X-ray free-electron laser at SACLA, *J Synchrotron Radiat 26*, 585-594 doi: 10.1107/S1600577519000882

[215] Roessler, C. G., Kuczewski, A., Stearns, R., Ellson, R., Olechno, J., Orville, A. M., et al, Heroux, A. (2013) Acoustic methods for high-throughput protein crystal mounting at next-generation macromolecular crystallographic beamlines, *J Synchrotron Radiat 20*, 805-808 doi: 10.1107/S0909049513020372

[216] Yano, J., and Yachandra, V. (2014) Mn4Ca cluster in photosynthesis: where and how water is oxidized to dioxygen, *Chem Rev 114*, 4175-4205 doi: 10.1021/cr4004874

[217] Hillier, W., and Wydrzynski, T. (2008) O-18-Water exchange in photosystem II: Substrate binding and intermediates of the water splitting cycle, *Coordin Chem Rev 252*, 306-317 doi: 10.1016/j.ccr.2007.09.004

[218] Alonso-Mori, R., Sokaras, D., Zhu, D., Kroll, T., Chollet, M., Feng, Y., et al, Bergmann, U. (2015) Photon-in photon-out hard X-ray spectroscopy at the Linac Coherent Light Source, *J Synchrotron Radiat 22*, 612-620 doi: 10.1107/S1600577515004488

[219] Alonso-Mori, R., Asa, K., Bergmann, U., Brewster, A. S., Chatterjee, R., Cooper, J. K., et al, Yano, J. (2016) Towards characterization of photo-excited electron transfer and catalysis in natural and artificial systems using XFELs, *Faraday Discuss 194*, 621-638 doi: 10.1039/c6fd00084c

[220] Jensen, S. C., Sullivan, B., Hartzler, D. A., Aguilar, J. M., Awel, S., Bajt, S., et al, Pushkar, Y. (2019) X-ray Emission Spectroscopy at X-ray Free Electron Lasers: Limits to Observation of the Classical Spectroscopic Response for Electronic Structure Analysis, *J Phys Chem Lett 10*, 441-446 doi: 10.1021/acs.jpclett.8b03595

[221] Wang, J., Liu, Y., Liu, Y., Zheng, S., Wang, X., Zhao, J., et al, Chen, P. R. (2019) Time-resolved protein activation by proximal decaging in living systems, *Nature 569*, 509-513 doi: 10.1038/s41586-019-1188-1

[222] Givens, R. S., Rubina, M., and Wirz, J. (2012) Applications of p-hydroxyphenacyl (pHP) and coumarin-4-ylmethyl photoremovable protecting groups, *Photochem Photobiol Sci 11*, 472-488 doi: 10.1039/c2pp05399c

[223] Johnson, L. N. (1992) Time-resolved protein crystallography, *Protein Sci 1*, 1237-1243 doi: 10.1002/pro.5560011002

[224] Austin, R. H., Beeson, K. W., Eisenstein, L., Frauenfelder, H., and Gunsalus, I. C. (1975) Dynamics of ligand binding to myoglobin, *Biochemistry 14*, 5355-5373 doi: 10.1021/bi00695a021

[225] Mondal, P., and Meuwly, M. (2018) Solvent Composition Drives the Rebinding Kinetics of Nitric Oxide to Microperoxidase, *Sci Rep 8*, 5281 doi: 10.1038/s41598-018-22944-z

[226] Murakawa, Y., Nagai, M., and Mizutani, Y. (2012) Differences between protein dynamics of hemoglobin upon dissociation of oxygen and carbon monoxide, *J Am Chem Soc 134*, 1434-1437 doi: 10.1021/ja209659w

[227] Beece, D., Eisenstein, L., Frauenfelder, H., Good, D., Marden, M. C., Reinisch, L., et al, Yue, K. T. (1979) Dioxygen replacement reaction in myoglobin, *Biochemistry 18*, 3421-3423 doi: 10.1021/bi00582a032

[228] Flanagan, J. C., and Baiz, C. R. (2019) Ultrafast pH-jump two-dimensional infrared spectroscopy, *Opt Lett 44*, 4937-4940 doi: 10.1364/OL.44.004937

[229] Abbruzzetti, S., Sottini, S., Viappiani, C., and Corrie, J. E. (2005) Kinetics of proton release after flash photolysis of 1-(2-nitrophenyl)ethyl sulfate (caged sulfate) in aqueous solution, *J Am Chem Soc 127*, 9865-9874 doi: 10.1021/ja051702x

[230] Thompson, M. C., Barad, B. A., Wolff, A. M., Sun Cho, H., Schotte, F., Schwarz, D. M. C., et al, Fraser, J. S. (2019) Temperature-jump solution X-ray scattering reveals distinct motions in a dynamic enzyme, *Nat Chem 11*, 1058-1066 doi: 10.1038/s41557-019-0329-3

[231] Keedy, D. A., Kenner, L. R., Warkentin, M., Woldeyes, R. A., Hopkins, J. B., Thompson, M. C., et al, Fraser, J. S. (2015) Mapping the conformational landscape of a dynamic enzyme by multitemperature and XFEL crystallography, *Elife 4* doi: 10.7554/eLife.07574

[232] Reddish, M. J., Callender, R., and Dyer, R. B. (2017) Resolution of Submillisecond Kinetics of Multiple Reaction Pathways for Lactate Dehydrogenase, *Biophys J 112*, 1852-1862 doi: 10.1016/j.bpj.2017.03.031

[233] Winter, M. B., Herzik, M. A., Jr., Kuriyan, J., and Marletta, M. A. (2011) Tunnels modulate ligand flux in a heme nitric oxide/oxygen binding (H-NOX) domain, *Proc Natl Acad Sci U S A 108*, E881-889 doi: 10.1073/pnas.1114038108

[234] Alberding, N., Frauenfelder, H., and Hanggi, P. (1978) Stochastic theory of ligand migration in biomolecules, *Proc Natl Acad Sci U S A 75*, 26-29 doi: 10.1073/pnas.75.1.26

[235] Alberding, N., Austin, R. H., Chan, S. S., Eisenstein, L., Frauenfelder, H., Good, D., et al, Yue, K. T. (1978) Fast reactions in carbon monoxide binding to heme proteins, *Biophys J 24*, 319-334 doi: 10.1016/S0006-3495(78)85380-6

[236] Walsh, C. (2001) Enabling the chemistry of life, *Nature 409*, 226-231 doi: 10.1038/35051697

[237] Benkovic, S. J., and Hammes-Schiffer, S. (2003) A perspective on enzyme catalysis, *Science 301*, 1196-1202 doi: 10.1126/science.1085515

[238] Hammes, G. G. (2002) Multiple conformational changes in enzyme catalysis, *Biochemistry 41*, 8221-8228 doi: 10.1021/bi0260839

[239] Warshel, A., and Bora, R. P. (2016) Perspective: Defining and quantifying the role of dynamics in enzyme catalysis, *J Chem Phys 144*, 180901 doi: 10.1063/1.4947037

[240] Agarwal, P. K. (2019) A Biophysical Perspective on Enzyme Catalysis, *Biochemistry 58*, 438-449 doi: 10.1021/acs.biochem.8b01004

[241] Henzler-Wildman, K. A., Thai, V., Lei, M., Ott, M., Wolf-Watz, M., Fenn, T., et al, Kern, D. (2007) Intrinsic motions along an enzymatic reaction trajectory, *Nature 450*, 838-844 doi: 10.1038/nature06410

[242] Henzler-Wildman, K. A., Lei, M., Thai, V., Kerns, S. J., Karplus, M., and Kern, D. (2007) A hierarchy of timescales in protein dynamics is linked to enzyme catalysis, *Nature 450*, 913-916 doi: 10.1038/nature06407

[243] Kohen, A. (2015) Role of dynamics in enzyme catalysis: substantial versus semantic controversies, *Acc Chem Res 48*, 466-473 doi: 10.1021/ar500322s

[244] Frauenfelder, H., Chen, G., Berendzen, J., Fenimore, P. W., Jansson, H., McMahon, B. H., et al, Young, R. D. (2009) A unified model of protein dynamics, *Proc Natl Acad Sci U S A 106*, 5129-5134 doi: 10.1073/pnas.0900336106

[245] Frauenfelder, H., Sligar, S. G., and Wolynes, P. G. (1991) The energy landscapes and motions of proteins, *Science 254*, 1598-1603 doi: 10.1126/science.1749933

[246] Hajdu, J., Neutze, R., Sjogren, T., Edman, K., Szoke, A., Wilmouth, R. C., and Wilmot, C. M. (2000) Analyzing protein functions in four dimensions, *Nat Struct Biol 7*, 1006-1012 doi: 10.1038/80911

[247] Schmidt, M. (2019) Time-Resolved Macromolecular Crystallography at Pulsed X-ray Sources, *International Journal of Molecular Sciences 20* doi: ARTN 1401 10.3390/ijms20061401

[248] Schmidt, M. (2017) Time-Resolved Macromolecular Crystallography at Modern X-Ray Sources, *Methods*

Mol Biol 1607, 273-294 doi: 10.1007/978-1-4939-7000-1_11

[249] Kupitz, C., Olmos, J. L., Jr., Holl, M., Tremblay, L., Pande, K., Pandey, S., et al, Schmidt, M. (2017) Structural enzymology using X-ray free electron lasers, *Struct Dyn 4*, 044003 doi: 10.1063/1.4972069

[250] Schmidt, M., and Saldin, D. K. (2014) Enzyme transient state kinetics in crystal and solution from the perspective of a time-resolved crystallographer, *Struct Dyn 1*, 024701 doi: 10.1063/1.4869472

[251] Schmidt, M. (2013) Mix and Inject: Reaction Initiation by Diffusion for Time-Resolved Macromolecular Crystallography, *Advances in Condensed Matter Physics 2013*, 10 doi: 10.1155/2013/167276

[252] van den Bedem, H., and Fraser, J. S. (2015) Integrative, dynamic structural biology at atomic resolution--it's about time, *Nat Methods 12*, 307-318 doi: 10.1038/nmeth.3324

[253] Olmos, J. L., Jr., Pandey, S., Martin-Garcia, J. M., Calvey, G., Katz, A., Knoska, J., et al, Schmidt, M. (2018) Enzyme intermediates captured "on the fly" by mix-and-inject serial crystallography, *BMC Biol 16*, 59 doi: 10.1186/s12915-018-0524-5

[254] Calvey, G. D., Katz, A. M., and Pollack, L. (2019) Microfluidic Mixing Injector Holder Enables Routine Structural Enzymology Measurements with Mix-and-Inject Serial Crystallography Using X-ray Free Electron Lasers, *Anal Chem 91*, 7139-7144 doi: 10.1021/acs.analchem.9b00311

[255] Calvey, G. D., Katz, A. M., Schaffer, C. B., and Pollack, L. (2016) Mixing injector enables time-resolved crystallography with high hit rate at X-ray free electron lasers, *Struct Dyn 3*, 054301 doi: 10.1063/1.4961971

[256] Monteiro, D. C. F., Vakili, M., Harich, J., Sztucki, M., Meier, S. M., Horrell, S., et al, Trebbin, M. (2019) A microfluidic flow-focusing device for low sample consumption serial synchrotron crystallography experiments in liquid flow, *J Synchrotron Radiat 26*, 406-412 doi: 10.1107/S1600577519000304

[257] Grunbein, M. L., and Nass Kovacs, G. (2019) Sample delivery for serial crystallography at free-electron lasers and synchrotrons, *Acta Crystallogr D Struct Biol 75*, 178-191 doi: 10.1107/S205979831801567X

[258] Grunbein, M. L., Shoeman, R. L., and Doak, R. B. (2018) Velocimetry of fast microscopic liquid jets by nanosecond dual-pulse laser illumination for megahertz X-ray free-electron lasers, *Opt Express 26*, 7190-7203 doi: 10.1364/OE.26.007190

[259] Grünbein, M. L., Bielecki, J., Gorel, A., Stricker, M., Bean, R., Cammarata, M., et al, Schlichting, I. (2018) Megahertz data collection from protein microcrystals at an X-ray free-electron laser, *Nature Communications 9*, 3487 doi: 10.1038/s41467-018-05953-4

[260] Wiedorn, M. O., and Oberthür, D., and Bean, R., and Schubert, R., and Werner, N., and Abbey, B., et al, Barty, A. (2018) Megahertz serial crystallography, *Nature Communications 9*, 4025 doi: 10.1038/s41467-018-06156-7

[261] Sanchez-Weatherby, J., Sandy, J., Mikolajek, H., Lobley, C. M. C., Mazzorana, M., Kelly, J., et al, Sorensen, T. L. M. (2019) VMXi: a fully automated, fully remote, high-flux in situ macromolecular crystallography beamline, *J Synchrotron Radiat 26*, 291-301 doi: 10.1107/S1600577518015114

[262] Pravda, L., Berka, K., Svobodova Varekova, R., Sehnal, D., Banas, P., Laskowski, R. A., et al, Otyepka, M. (2014) Anatomy of enzyme channels, *BMC Bioinformatics 15*, 379 doi: 10.1186/s12859-014-0379-x

[263] Juers, D. H., and Ruffin, J. (2014) MAP_CHANNELS: a computation tool to aid in the visualization and characterization of solvent channels in macromolecular crystals, *J Appl Crystallogr 47*, 2105-2108 doi: 10.1107/S160057671402281X

[264] Coleman, R. G., and Sharp, K. A. (2009) Finding and characterizing tunnels in macromolecules with application to ion channels and pores, *Biophys J 96*, 632-645 doi: 10.1529/biophysj.108.135970

[265] Heymann, M., Opthalage, A., Wierman, J. L., Akella, S., Szebenyi, D. M., Gruner, S. M., and Fraden, S. (2014) Room-temperature serial crystallography using a kinetically optimized microfluidic device for protein crystallization and on-chip X-ray diffraction, *IUCrJ 1*, 349-360 doi: 10.1107/S2052252514016960

[266] Abdallah, B. G., Zatsepin, N. A., Roy-Chowdhury, S., Coe, J., Conrad, C. E., Dorner, K., et al, Ros, A. (2015) Microfluidic sorting of protein nanocrystals by size for X-ray free-electron laser diffraction, *Struct Dyn 2*, 041719 doi: 10.1063/1.4928688

[267] Zhu, P. F., Zhu, Y., Hidaka, Y., Wu, L., Cao, J., Berger, H., et al, Wang, X. J. (2015) Femtosecond time-resolved MeV electron diffraction, *New J Phys 17* doi: Artn 063004

10.1088/1367-2630/17/6/063004

[268] Vecchione, T., Denes, P., Jobe, R. K., Johnson, I. J., Joseph, J. M., Li, R. K., et al, Zhang, D. (2017) A direct electron detector for time-resolved MeV electron microscopy, *Rev Sci Instrum 88*, 033702 doi: 10.1063/1.4977923

[269] Nunes, J. P. F., Ledbetter, K., Lin, M., Kozina, M., DePonte, D. P., Biasin, E., et al, Wang, X. J. (2020) Liquid-phase mega-electron-volt ultrafast electron diffraction, *Struct Dyn 7*, 024301 doi: 10.1063/1.5144518

[270] Barty, A., Caleman, C., Aquila, A., Timneanu, N., Lomb, L., White, T. A., et al, Chapman, H. N. (2012) Self-terminating diffraction gates femtosecond X-ray nanocrystallography measurements, *Nat Photonics 6*, 35-40 doi: 10.1038/nphoton.2011.297

[271] Kirian, R. A., White, T. A., Holton, J. M., Chapman, H. N., Fromme, P., Barty, A., et al, Spence, J. C. (2011) Structure-factor analysis of femtosecond microdiffraction patterns from protein nanocrystals, *Acta Crystallogr A 67*, 131-140 doi: 10.1107/S0108767310050981

[272] Hutchison, C. D. M., and van Thor, J. J. (2017) Populations and coherence in femtosecond time resolved X-ray crystallography of the photoactive yellow protein, *Int Rev Phys Chem 36*, 117-143 doi: 10.1080/0144235x.2017.1276726

[273] Kumar, A. T. N., Rosca, F., Widom, A., and Champion, P. M. (2001) Investigations of ultrafast nuclear response induced by resonant and nonresonant laser pulses, *J Chem Phys 114*, 6795-6815 doi: Doi 10.1063/1.1356011

[274] Kumar, A. T. N., Rosca, F., Widom, A., and Champion, P. M. (2001) Investigations of amplitude

and phase excitation profiles in femtosecond coherence spectroscopy, *J Chem Phys 114*, 701-724 doi: Doi 10.1063/1.1329640

[275] Rosca, F., Kumar, A. T. N., Ye, X., Sjodin, T., Demidov, A. A., and Champion, P. M. (2000) Investigations of coherent vibrational oscillations in myoglobin, *J Phys Chem A 104*, 4280-4290 doi: DOI 10.1021/jp993617f

[276] Bardeen, C. J., Wang, Q., and Shank, C. V. (1998) Femtosecond chirped pulse excitation of vibrational wave packets in LD690 and bacteriorhodopsin, *J Phys Chem A 102*, 2759-2766 doi: DOI 10.1021/jp980346k

[277] McClelland, A., Demidov, A., Benabbas, A., Sun, Y., Venugopal, K., Sage, T., et al, Champion, P. (2010) Direct Observations of Low Frequency Vibrational Coherences in wt-GFP, *AIP Conference Proceedings 1267*, 674-675 doi: 10.1063/1.3482744

[278] Kuramochi, H., Takeuchi, S., and Tahara, T. (2016) Femtosecond time-resolved impulsive stimulated Raman spectroscopy using sub-7-fs pulses: Apparatus and applications, *Review of Scientific Instruments 87* doi: Artn 043107 10.1063/1.4945259

[279] van Thor, J. J. (2019) Coherent two-dimensional electronic and infrared crystallography, *J Chem Phys 150* doi: Artn 124113 10.1063/1.5079319

[280] Hutchison, C. D. M., Kaucikas, M., Tenboer, J., Kupitz, C., Moffat, K., Schmidt, M., and van Thor, J. J. (2016) Photocycle populations with femtosecond excitation of crystalline photoactive yellow protein, *Chem Phys Lett 654*, 63-71 doi: 10.1016/j.cplett.2016.04.087

[281] Lincoln, C. N., Fitzpatrick, A. E., and van Thor, J. J. (2012) Photoisomerisation quantum yield and non-linear cross-sections with femtosecond excitation of the photoactive yellow protein, *Phys Chem Chem Phys 14*, 15752-15764 doi: 10.1039/c2cp41718a

[282] Neutze, R., Wouts, R., van der Spoel, D., Weckert, E., and Hajdu, J. (2000) Potential for biomolecular imaging with femtosecond X-ray pulses, *Nature 406*, 752-757 doi: 10.1038/35021099

[283] Neutze, R., and Hajdu, J. (1997) Femtosecond time resolution in x-ray diffraction experiments, *Proc Natl Acad Sci U S A 94*, 5651-5655 doi:

[284] Aquila, A., Barty, A., Bostedt, C., Boutet, S., Carini, G., dePonte, D., et al, Williams, G. J. (2015) The linac coherent light source single particle imaging road map, *Struct Dyn 2*, 041701 doi: 10.1063/1.4918726

[285] Sun, Z. B., Fan, J. D., Li, H. Y., and Jiang, H. D. (2018) Current Status of Single Particle Imaging with X-ray Lasers, *Appl Sci-Basel 8* doi: ARTN 132; 10.3390/app8010132

[286] Yan, R., Zhang, Y., Li, Y., Xia, L., Guo, Y., and Zhou, Q. (2020) Structural basis for the recognition of the SARS-CoV-2 by full-length human ACE2, *Science* doi: 10.1126/science.abb2762

[287] Wrapp, D., Wang, N., Corbett, K. S., Goldsmith, J. A., Hsieh, C. L., Abiona, O., et al, McLellan, J. S. (2020) Cryo-EM structure of the 2019-nCoV spike in the prefusion conformation, *Science 367*, 1260-1263 doi: 10.1126/science.abb2507

[288] Walls, A. C., Park, Y. J., Tortorici, M. A., Wall, A., McGuire, A. T., and Veesler, D. (2020) Structure, Function, and Antigenicity of the SARS-CoV-2 Spike Glycoprotein, *Cell* doi: 10.1016/j.cell.2020.02.058

[289] Velavan, T. P., and Meyer, C. G. (2020) The COVID-19 epidemic, *Trop Med Int Health 25*, 278-280 doi: 10.1111/tmi.13383

[290] Shen, Z., Xiao, Y., Kang, L., Ma, W., Shi, L., Zhang, L., et al, Li, M. (2020) Genomic diversity of SARS-CoV-2 in Coronavirus Disease 2019 patients, *Clin Infect Dis* doi: 10.1093/cid/ciaa203

[291] Thomas, S. E., Collins, P., James, R. H., Mendes, V., Charoensutthivarakul, S., Radoux, C., et al, Blundell, T. L. (2019) Structure-guided fragment-based drug discovery at the synchrotron: screening binding sites and correlations with hotspot mapping, *Philos Trans A Math Phys Eng Sci 377*, 20180422 doi: 10.1098/rsta.2018.0422

[292] Zhang, D., Markoulides, M. S., Stepanovs, D., Rydzik, A. M., El-Hussein, A., Bon, C., et al, Schofield, C. J. (2018) Structure activity relationship studies on rhodanines and derived enethiol inhibitors of metallo-beta-lactamases, *Bioorg Med Chem 26*, 2928-2936 doi: 10.1016/j.bmc.2018.02.043

[293] Collins, P. M., Douangamath, A., Talon, R., Dias, A., Brandao-Neto, J., Krojer, T., and von Delft, F. (2018) Achieving a Good Crystal System for Crystallographic X-Ray Fragment Screening, *Methods Enzymol 610*, 251-264 doi: 10.1016/bs.mie.2018.09.027

[294] Bowkett, D., Talon, R., Tallant, C., Schofield, C., von Delft, F., Knapp, S., et al, Brennan, P. E. (2018) Identifying Small-Molecule Binding Sites for Epigenetic Proteins at Domain-Domain Interfaces, *ChemMedChem 13*, 1051-1057 doi: 10.1002/cmdc.201800030

[295] Collins, P. M., Ng, J. T., Talon, R., Nekrosiute, K., Krojer, T., Douangamath, A., et al, von Delft, F. (2017) Gentle, fast and effective crystal soaking by acoustic dispensing, *Acta Crystallogr D Struct Biol 73*, 246-255 doi: 10.1107/S205979831700331X

8. Opportunities for UK Industry, Society and Defence

The case presented so far has been focused on scientific opportunities, but throughout there is also a strong case for connections to technology and broader utility of the methods and knowledge. As discussed in the **Introduction**, the capability to measure matter at the quantum scales of both *time* and *space* inevitably immediately connects to advanced technologies. We now explicitly address some of the opportunities we foresee for UK Industry, Society and Defence. This survey is not complete, as we anticipate myriad industrial and societal impacts, but the ones we highlight are hopefully illustrative of the broad potential.

We start by discussing the impact of a UK XFEL in the context of the Grand Challenges identified in the UK government's Industrial Strategy, and connect also to the emerging UKRI themes. We then examine a sample of areas we see as having highest potential impact: shocked materials, crystallization and nucleation in soft materials, dynamic processes in advanced manufacturing, nuclear materials and nuclear security using gamma ray probes and life sciences on pharma and bio-tech. In this last area we highlight the importance of having the full range of science tools in our armoury for rapid deployment in a crisis such as the current Covid-19 situation. Finally, we present a broad-brush economic impact analysis that should be seen as the start point for a fuller Business Case analysis if the project moves to the next stage.

8.1 Addressing national strategic priorities

A UK XFEL will impact science across almost all disciplines and be an underpinning resource for future technologies in vital sectors such as healthcare, defence and green energy. It is thus in a prime position to address UK government strategic priorities. It will boost skills training in essential areas and cultivate STEM subjects across the nation.

8.1.1 Mapping to scientific and technological strategic priorities

It is clear that the scientific, technological and economic impact of a UK-XFEL will be broad and far reaching and directly resonant with the ambitions of the government's Industrial Strategy. The evidence for this comes from the analysis already conducted for this science case (see Sections 3-7 and especially sections 8.1-8.5), and from the experience of the five major FEL facilities already operating where national strategic priorities were implicitly part of their justification. Within UKRI it will enable developments across the science portfolio and is well matched to the key UKRI priorities, for example:

- *Advancing Technology* – through quantum scale structural dynamics
- *Healthcare* – through structural biology and conformational mapping
- *Frontiers of Knowledge* – through access to brightest ultrafast X-ray pulses
- *Net Zero Growth* – through unravelling photo-chemical/catalytic cycles
- *Economic Strengths* – through skills and research outcomes

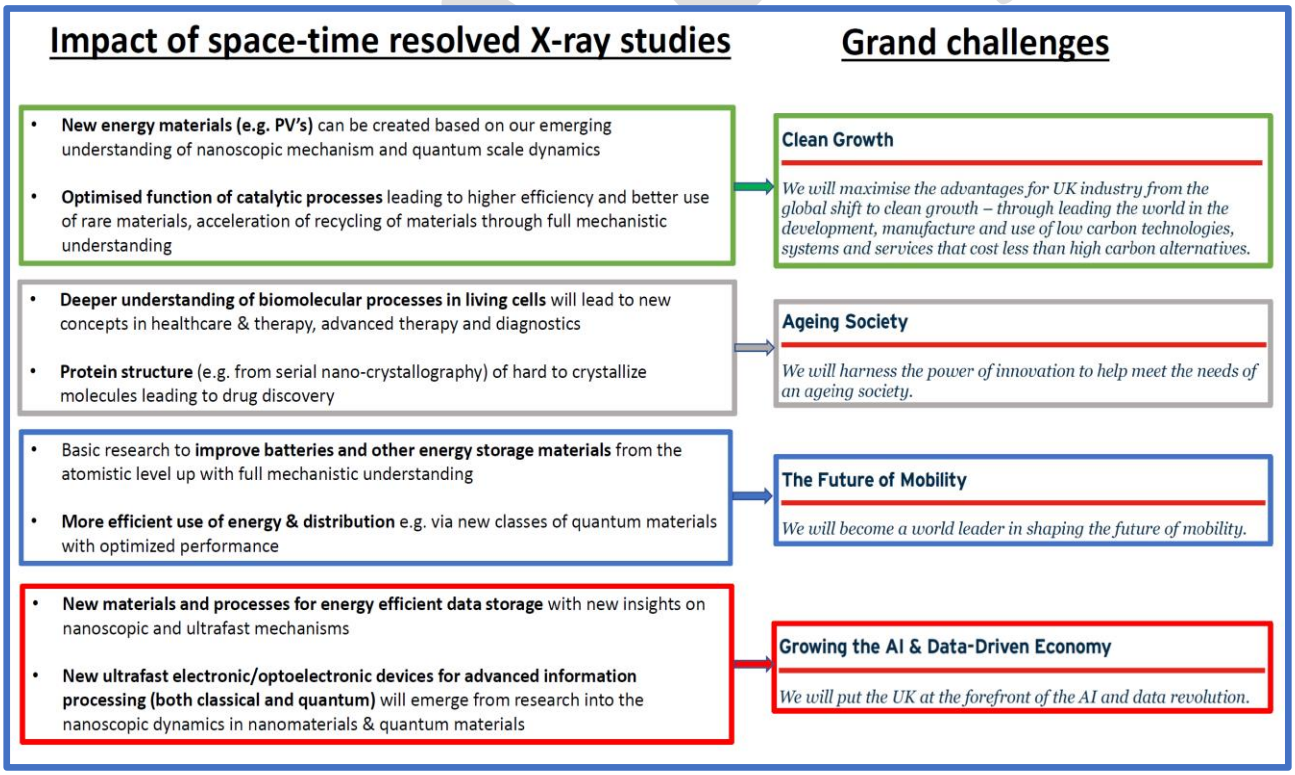

Box 8.1 Mapping to Grand Challenges identified in Industrial Strategy

A summary of the connection between science and technology enabled by the combined high space-time resolution enabled by X-rays and the Grand Challenges identified in the Government Industrial Strategy is shown in **Box 8.1** to illustrate some of these mappings.

In the **energy sector**, a UK-XFEL will provide new insight into complex light harvesting materials and solar biofuels, stimulating new, low cost energy generation and storage technologies (see Sections 6.3), which are essential for ensuring our future growth is as clean and carbon neutral as possible**.**

Aligned to this, a UK-XFEL will aid the development of **green technologies**, new catalysts for example (Section 6.4), to ensure clean industrial processes and sustainable industrial chemistry**.** It will enable the development of new and **advanced materials** with direct applicability to industry, mobility, digital manufacturing (Section 5), nuclear energy (Sections 3.6 and 8) and the defence community (Section 4). It will contribute critical new understanding at the nanoscopic level to **energy efficient fast data storage** that is crucial for the expansion of the data driven economy (Sections 5.2 and 6.3). In the **life sciences**, it will permit the mapping of conformational pathways for biomolecules (Section 3.4) and aid the understanding of the chemistry of complex molecular processes (Sections 6 and 7) that govern life and disease – beyond what is possible using current approaches. Advanced imaging capabilities will, when applied to structural biology (Section 7), aid the discovery of advanced drugs and new antibiotics essential to address the challenges of an ageing society.

8.1.2 Building a skilled workforce

This investment will naturally support advanced **STEM skills** development in the UK workforce, both locally where the machine is built and nationally within its user community. Many thousands of **scientists, engineers, computer scientists, technicians and apprentices** will pass through the UK-XFEL over its life-cycle. This will seed the skills base with essential capabilities – addressing everything from the challenges of the civil engineering for such a precision machine through to the handling the vast quantities of data such a machine will generate. Extracting maximum value from these data sets will stimulate advances in artificial intelligence as already demonstrated at LCLS.

The facility activities will support skills development in UK workforce particularly in key areas of high value to the economy**:**

- Advanced electronics
- Control systems
- Optics (from THz to Hard X-ray)
- Hardware for handling unprecedented data volumes
- AI and machine-learning to operate the facility and manage the huge data flow
- Advanced modelling of materials at the quantum scale
- Precision engineering and advanced manufacturing
- Detector technologies
- Cryo-technology
- Carbon neutral operation of large infrastructure

It is anticipated that UK XFEL will operate its own apprenticeship schemes and that although a large fraction will be initially retained as employees following training many will, in the fullness of time, move out into the wider workforce taking with them their skills. STFC's existing large facilities employ 131 apprentices across 15 diverse disciplines from Mechanical Engineering to Project Management and IT Infrastructure. As well as providing specialist technical training on a world-leading facility, apprenticeship and graduate schemes should provide core transferable training in areas such as communication skills, team-working and leadership. Likewise, undergraduate degree, masters and PhD level trained staff will also be required in large number to staff the facility. Some of their training can be associated with activities at the facility, with existing facilities such as ISIS, Diamond and the CLF providing around 20,000 training days per year for university PhD students. The typically rapid churn associated with such staff will also efficiently seed the wider workforce benefiting the industrial, defence, finance, medical and university sectors.

There are large opportunities for technical and research internships, some leading to permanent jobs, and this has been used at LCLS to deliberately increase diversity in the workforce by recruiting from local high schools with a strong emphasis on women and ethnic minorities.

As a user facility, thousands of scientists will use the machine each year and the benefit of the investment will, as a result, be nationally distributed. There will be opportunities to directly influence diversity within it and the broader scientific community, especially via choice of location and stimulus of the user base. And of course, such a machine will act as a beacon for UK science internationally, attracting the best and the brightest to the UK, championing the UK's place in the world.

8.1.3 Intellectual property and enterprise

The user research of the facility is likely to play a large role in innovation and discovery leading to the creation of intellectual property as has been the experience of the large scale facilities at STFC's national laboratories. IP can be either generated by (and reside with) the home university and investigator, or by the laboratory through research and development programmes into end-station capabilities, procedures and sample preparation. Hence there is also large scope for IP generation with the ownership residing primarily with the facility. This IP can be further exploited via Proof of Concept Funding, technology transfer into spin out companies and licensing technology and skills transfer to industry. By the end of 2017-2018 FY STFC's national labs had generated over 200 patents and supported the creation of 19 spin-out companies. These companies have raised over £78m in third-party investment and created over 232 jobs.

Experience has shown (Daresbury, Diamond, DESY, SLAC) that a cluster of new businesses grow up around large facilities driven by entrepreneurs moving out from the facility to develop their own ideas and others coming from further afield to position themselves as suppliers of equipment, consumables and services or simply to benefit from the locally created high-tech ecology. It is no accident that Sand Hill Road, Menlo Park is the centre of Silicon Valley's massive venture capital industry – it is the street on which the main gate to SLAC is located! The combined UK Research and Innovation campuses of Daresbury and Harwell were established in order to co-locate academia, industry and commercial organisations with cutting-edge large scale facilities. Together these are home to over 300 companies employing over 6,500 people. Provision of space on or close to the site to establish a science park and potential small business incubator support services could be a very beneficial additional investment.

8.1.4 Outreach and promoting public understanding of science

As a state-of-the art facility conducting cutting edge scientific and technological research across many disciplines UK XFEL will be a focus for activities centred around outreach and public understanding. Every effort should be made to involve the public (young people especially) with the science programmes of the facility, in order to both encourage young people into STEM subjects and to convey the benefits of scientific research to the UK's wider economy and society generally.

It can have a large programme of outreach to schools both regionally and nationally and host visitor facilities to ensure visits are informative, stimulating and fun. Equivalent large facilities based at Harwell typically host around 3000 school visitors per year, with many more students reached by facility staff visiting schools in the local area and nationwide. It can thus be a very concrete and high-profile recruiter and promoter of STEM subjects in school age children, with feedback frequently showing that outreach events with primary and secondary school students boosts future interest in pursuing STEM subjects by 28-44% depending on school age. The possibility of internships (see above) should also be used to ensure the growth of a diverse training programme starting with school age young people. Older members of the public should not be overlooked and an appropriate visitor centre to cater for their interests must also be a priority. Facility open days could also be used to promote the broad range of cutting-edge science technological development that a UK XFEL would undertake and emphasise the wider impact of such work on wider society. The Harwell Open Week in 2015 that included large facilities such as Diamond, ISIS and the CLF welcomed 16,000 visitors who got an opportunity to go behind-the-scenes and meet the many scientists, engineers and technologists who work there.

So that UK XFEL can play a full role in promoting the sciences and technology it is important that it be as visually striking as possible, both from the ground and from the air. In that way it can be an iconic

symbol for the sciences that propagates through the media, newspapers, social media and in the public consciousness.

8.1.5 Selected areas of industrial and societal Impact

Throughout this case we have endeavoured to highlight important areas of application in the science and technology opportunities discussed. In the remainder of this section we look at selected areas of special relevance to industry and society where an XFEL will have significant impact. These are: Properties of shocked materials for engineering and defence, Nucleation, solidification and crystallization in soft-matter, Dynamic processes in additive manufacturing, combustion, laser machining and photolithography, Nuclear security and materials in nuclear industry, Industrial inspirations from deeper insights into biology: pharma to clean energy. We conclude with an overview of anticipated economic benefits associated with construction and operation of a UK XFEL.

8.2 Properties of shocked materials for engineering and defence

The properties of materials under shock loading conditions are both of fundamental scientific interest and important across a wide range of engineering domains, from aerospace through to defence [1]. XFEL technology is driving rapid progress in the underpinning science in this area and represents an accelerated pathway for the manufacturing and qualification of the next generation of engineering materials and processes.

8.2.1 New understanding of materials response at multiple scales

With the advent of high-brilliance, femtosecond duration hard x-ray FEL sources, an understanding of the rich array of the underlying microscopic processes which govern the macroscopic response of heterogenous engineering-relevant materials to rapid loading and unloading is now within reach. The routes by which materials deform and respond to external stresses are complex, as they depend not only on the underlying structure (that is to say the particular crystal phase), but also on the evolution of the population of defects within the system that mediate plastic flow. Given that defect density itself is strain and strain-rate dependent, a comprehensive understanding of material strength, and response to impact, all the way from the microscale of the lattice dynamics to the macroscale of system response on engineering length-scales remains largely elusive. X-Ray Free electron lasers are starting to have significant impact in bridging this important gap in our knowledge, with large angle diffraction techniques (that measure structure, lattice spacings and orientations) and small angle scattering (which can measure void evolution) combining to provide hitherto inaccessible insights into the pertinent physics on the atomic scale. Furthermore, the femtosecond nature of the x-ray beam ensures that all measurements are free from motional blurring, with the diffraction signals being recorded on a timescale even shorter than that of the oscillation period of atomic vibrations.

Importantly, these measurements can also now be augmented with computer simulations on precisely the same length scales (several microns) and timescales (spanning hundreds of picosecond to nanoseconds). Multi-million (or billion) atom molecular dynamics simulations can now be performed, from which simulated diffraction patterns (linking the micro and macro properties) can be extracted and compared with experiment. The fidelity of these simulations itself relies on a good knowledge of the interatomic potentials between atoms, but here a feedback loop engendered by a comparison of experimental results and theoretical prediction will play an increasingly important role in verifying the development of the potentials themselves.

An understanding of material flow under rapid impact is important in both fundamental and applied sciences. At the fundamental level, impact phenomena have played an important part in the evolution and modification of our own and other planets, and the resultant flow of material can be seen at the extremes of the macroscale in geological features such as the Chicxulub crater on our own planet, or are readily apparent from a casual glance upwards at our moon. In the applied sciences arena, the applications in the defence industry are obvious, whilst the response of matter to high velocity impact is also important in design of protection for satellites, the space station, future space habitats and their electronics from impact with high velocity grains of dust of even few micron dimension [2]. What is perhaps less known is that laser-ablative impact treatment of materials via so-called ‘laser-peening’ can induce residual compressive stresses in the surface of materials, which can retard crack initiation and growth, thus increasing the fatigue strength of important engineering components [3, 4]. However, very little in situ experimental data exists on the underpinning evolution of the defect landscape and microstructure during this process, and enhanced physical understanding could well lead to improved material-properties outcomes.

Progress to date in using x-ray FELS to reveal lattice-level information has already been spectacular. As noted above, both structure and strain rate play important roles in the dynamic response of materials. At extremely high strain rates, it had long been predicted that the initial response of a

material would be purely elastic until its ultimate yield strength limit (100s times greater than realised in practice) was reached, as even pre-existing defects and dislocations would not have time to relieve plastic flow under high-velocity impact for the first few tens of picoseconds [5]. Such 'super-elastic' response, reaching the ultimate compressive strength of a pure crystal but within an initially defective sample has been demonstrated and observed via such femtosecond diffraction in copper samples [6]. It is also now known that some of the most complex phase transitions that a single element can undergo can be induced and observed within samples compressed for just a few nanoseconds, with the transitions in both Scandium [7] and Antimony [8] exhibiting the change from regular crystalline matter to a complex incommensurate 'host-guest' phase under rapid compression.

The opportunity to study the relative importance of plasticity mechanisms within a given sample has also been demonstrated. The femtosecond pulses of x-rays not only afford information on structure and lattice spacing, but also on the orientation of the lattice planes during deformation, allowing us to distinguish between the amount of impact damage internalised as twinning, as opposed to direct dislocation motion – such proof of principle experiments have been conducted in Tantalum samples [9]. Importantly, the defective nature of the sample was monitored during the release of the shock pressure from the sample, and the microstructural changes induced by the shock (that is to say the density of both twins and lattice rotation due to other defects) was shown to be largely annihilated upon rarefaction [10]: the state of the sample (in terms of its microstructure) during impact is very different from that which one would observe in a sample that was recovered and analysed after the event itself. This observation highlights the imperative on performing such in situ experiments that x-ray lasers make possible.

In other experiments, small-angle x-ray scattering has been used to diagnose the details of cavitation underlying spall failure and excellent agreement was obtained with molecular dynamics simulations [11]. These experiments typically employ a sample thickness on the order of a few microns and x-ray photon energy on the order of 10 keV, although an FEL with higher photon energies would allow study of thicker samples approaching engineering length scales, as well as provide for greater exploration of reciprocal space, which would be especially useful in eludidating complex structures formed under shock and ramp compression.

At the mesoscale, the relationship between material response and microstructural parameters such as grain size distribution and orientation (texture) must be understood. With this understanding, the opportunity for new engineering materials with designed-in properties arises [12]. Molecular dynamics calculations of the role of individual and idealised collections of grains under impact has started to be studied, [13] affording opportunities for transferring the lessons learnt from the modelling to the design of specific FEL-based experiments to learn about grain-grain interactions, and the dependence of material response on grain size as well as texture.

It should be noted that the methods described above are not limited to metals and metal alloys but are applicable to a wide range of engineering materials which include polymers, ceramics and their composites. These systems too have outstanding fundamental questions surrounding their responses to impact loading. Explosives for example, are heterogeneous systems containing grains, pores and cracks [14], and consequently exhibit complex physical phenomena over multiple length scales [15] (see Figure 8.1) which underpin performance and safety. Recently, XFEL experiments employing explosive samples have studied phase changes under shock compression and the role of micron-scale inhomogeneities in detonation initiation [16].

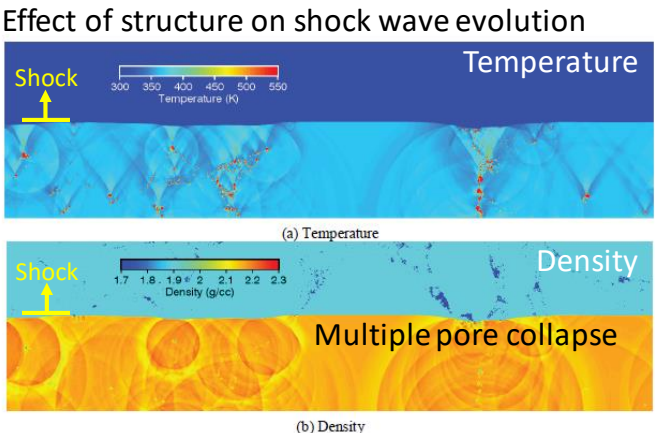

Figure 8.1: from Ref. 8 showing shock propagation in an explosive

At the macroscale, the sample size is representative of components used in applications and engineering processes can be studied and optimised. These include (as noted above) laser peening [3,4], foreign object damage to turbine blades [17], laser powder additive manufacturing (AM) [18, Section 8.3] and explosive initiators [19]. At the typical operating scale of several millimetres, x-ray energies up to ~100keV are required for single-shot imaging and x-ray diffraction studies [20]. Although these processes occur on relatively slow timescales (<100ns), the fast time resolution offered by an XFEL can help to elucidate dynamics occurring very early in time.

8.2.2 Future Opportunities

In order to access the high-pressure shock conditions of interest in samples with thickness of a few microns, an optical driver is necessary, and this would also be a requirement for a UK XFEL facility. The newly developed UK DiPOLE laser system [21], for example, can access multi-MBar pressures at a 10Hz repetition rate (Section 4.1). Such a laser would also find application in laser peening and particle impact studies (in the latter case by using the laser to propel a particle off a surface towards a target), but a higher energy (multi-kJ) system would allow us to access even higher pressures taking us into the regime of relevance for planetary science. Opportunities exist for overlap with interests in a laser-driven compression facility (see section 4.4).

For studies at longer length-scales and loading durations, a bespoke precision impact system, analogous to a single- or multiple-stage gas gun, will be required. Such a system will enable sustained loading over several 10s of nanoseconds in samples ranging from 10s – 100s micrometers, thereby bridging the gap between crystal physics and the mesoscale, permitting study of cumulative deformation and damage processes such as adiabatic shear, spallation, jetting, and fragmentation, and potentially the study of samples of shape and geometry that are analogous to those in real engineering applications. We note that the coupling of such a mechanical driver to a short-pulse x-ray source has already been proven at the Advanced Photon Source synchrotron,[22] albeit with x-ray pulses of much longer duration (100-psec) than can be produced at a FEL. As we move up in length scale and Z, the photon energies required will increase, and further studies of the flux of the higher harmonics of any FEL design will need to be taken into consideration. Finally, we note that as well as shock drivers specifically tailored for the FEL, this branch of science will also require state-of-the-art secondary shock diagnostics to understand the states generated, including, velocimetry, pyrometry, and imaging.For other applications, specialised equipment is required - such as a process replicator for AM studies [18].

References

[1] M. A. Meyers, "Dynamic Behavior of Materials" (Wiley & Sons, New York, 1994), DOI:10.1002/9780470172278

[2] A. C. Fletcher et al., "Particle-in-cell simulations of an RF emission mechanism associated with hypervelocity impact plasmas", Physics of Plasmas 24, 053102 (2017); DOI:10.1063/1.4980833

[3] R. Sundar et al., "Laser Shock Peening and its Applications: A Review", Lasers in Manufacturing and Materials Processing **6**, 424–463 (2019); DOI: 10.1007/s40516-019-00098-8

[4] S. J. Laine et al., "Microstructural characterisation of metallic shot peened and laser shock peened Ti-6Al-4V", Acta Materialia **123**, 350 (2017); DOI: 10.1016/j.actamat.2016.10.044

[5] E. Bringa et al., "Shock deformation of face-centred-cubic metals on subnanosecond timescales", Nat. Materials, **5**, 805, (2006) DOI: 10.1038/nmat1735

[6] D. Milathianaki et al., "Femtosecond visualization of lattice dynamics in shock-compressed matter", Science **342** 220-223 (2013) DOI: 10.1126/science.1239566

[7] R. Briggs et al., "Ultrafast X-Ray Diffraction Studies of the Phase Transitions and Equation of State of Scandium Shock Compressed to 82 GPa", Phys. Rev. Lett. **118**, 025501 (2017) DOI: 10.1103/PhysRevLett.118.025501

[8] A.L. Coleman et al., "Identification of Phase Transitions and Metastability in Dynamically Compressed Antimony Using Ultrafast X-Ray Diffraction", Phys. Rev. let. **122**, 255704 (2019) DOI: 10.1103/PhysRevLett.122.255704

[9] C. E. Wehrenberg *et al*., "In situ X-Ray diffraction measurement of shock-wave-driven twinning and lattice dynamics", Nature **550,** 496–499 (2017) DOI: 10.1038/nature24061

[10] M. Sliwa et al., "Femtosecond X-Ray Diffraction Studies of the Reversal of the Microstructural Effects of Plastic Deformation during Shock Release of Tantalum," Phys. Rev. Lett., 120 265502 (2018) DOI: 10.1103/PhysRevLett.120.265502

[11] James Coakley, (Private Communication, 2020)

[12] https://www.lanl.gov/science-innovation/science-facilities/dmmsc/index.php

[13] P.D. Heighway et al., "Molecular dynamics simulations of grain interactions in shock-compressed highly textured columnar nanocrystals", Phys. Rev. Materials, 3,083602 (2019) DOI: 10.1103/PhysRevMaterials.3.083602

[14] B. Lambourn and C. Handley, "A two-temperature model for shocked porous explosive", AIP Conf. Proc. **1793**, 120025 (2017) DOI: 10.1063/1.4971707

[15] C. Handley et al., "Understanding the shock and detonation response of high explosives at the continuum and meso scales", Appl. Phys. Rev. **5**, 011303 (2018) DOI: 10.1063/1.5005997

[16] R. L. Sandberg et al., "Studying Shocked Material Dynamics with Ultrafast X-Rays", Microsc. Microanal. **21** (Suppl 3), 1851 (2015) DOI: 10.1017/S143192761501003X

[17] P. G. Frankel et al., "Residual stress fields after FOD impact on flat and aerofoil-shaped leading edges", Mechanics of Materials **55**, 130 (2012). DOI: 10.1016/j.mechmat.2012.08.007

[18] C. L. A. Leung et al., "In situ X-ray imaging of defect and molten pool dynamics in laser additive manufacturing", Nature Communications **9** 1355 (2018) DOI: 10.1038/s41467-018-03734-7

[19] N. J. Sanchez et al., "Dynamic exploding foil initiator imaging at the advanced photon source", AIP Conference Proceedings **1979**, 160023 (2018) DOI: 10.1063/1.5045022

[20] B. R. Maddox et al., "Single-pulse x-ray diffraction using polycapillary optics for in situ dynamic diffraction", Rev. Sci. Inst. **87**, 083901 (2016) DOI: 10.1063/1.4960812

[21] P. Mason et al., "Development of a 100J, 10Hz laser for compression experiments at the High Energy Density instrument at the European XFEL", High Power Laser Science and Engineering, **6**, E65 (2018) DOI: 10.1017/hpl.2018.56

[22] S.N. Luo et al., "Gas gun shock experiments with single-pulse x-ray phase contrast imaging and diffraction at the Advanced Photon Source", Review of Scientific Instruments **83**, 073903 (2012); DOI: 10.1063/1.4733704

8.3 Nucleation, Solidification and Crystallization in Soft-Matter

Consumer products, chemical and pharmaceutical manufacturing are part of the chemistry-using industries and make a gross value-added (GVA) annual contribution of more than £65bn to the UK Economy.[1] Especially the properties of organic crystalline solids present enormous industrial R&D challenges, because key transformations are poorly understood at the molecular level. These include, for example, nucleation, crystal growth, dissolution and agglomeration. For decades, the science of these phenomena has been slow due to the experimental challenges of localised spatiotemporally rare events. The time and imaging capabilities afforded by XFEL scattering and spectroscopies now open up a realistic perspective to progress in this area.

The entire UK manufacturing sector relies on chemistry to generate £600 billion of annual aggregate sales to the economy. The chemicals sector itself has an annual turnover of £60 billion, and generates an annual £5 billion trade surplus. The chemistry-using industries' growth strategy[2] aims to increase its gross value-added (GVA) contribution from £195bn to £300bn by 2030, building on £200bn of market opportunities.[3] Just the subset of consumer products, chemical and pharmaceutical manufacturing represents an annual GVA over £65bn.[1]

Practical bottlenecks in chemical product design and manufacture arise from the challenging properties of crystalline solids. Especially for organic materials, crystal structure, size, morphology, mechanical properties, solubility and surface properties of particles combine to set up complex manufacturing demands. Predictive design of products would need a deep understanding of key transformations (e.g., nucleation, crystal growth, dissolution, agglomeration) and of the impact of typical process conditions (temperature, pressure, composition, mixing). The associated complex multiscale transformations are characterised by localised rare events at the molecular level that are insufficiently understood to permit the establishment of predictive structure/performance relationships.

For decades, scientific progress has been slow due to the experimental challenges of localised spatiotemporally rare events. For example, a particularly challenging gap is the uncertain molecular nature of self-assembled nuclei of new phases, their dynamics and rates of formation.[5–7] Nucleation events create structure from the molecular and nanoscale all the way up to the colloidal domain that are characterised by complex interfacial energetics involving electrostatics, covalent and non-covalent interactions. It has recently been recognised through time-resolved synchrotron X-ray phase contrast imaging that a seemingly simple process such as nucleation in antisolvent crystallisation can follow self-assembly paths that are fundamentally different from the hypothetical nucleation processes used in conventional modelling (Figure 8.2).[4]

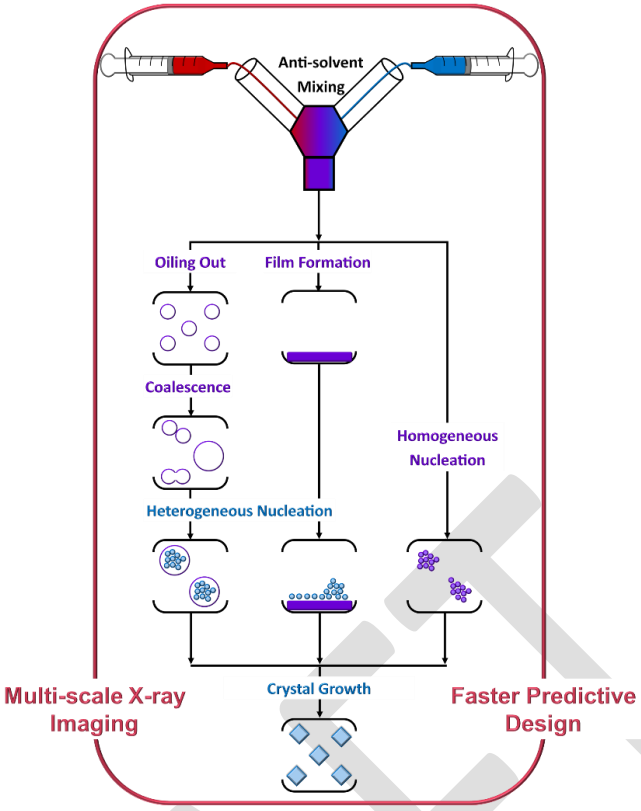

Figure 8.2. Alternative nucleation and crystal growth pathways in anti-solvent crystallisation process.[4]

Indeed, crystallisation from solution is one example that is central to the processing of materials and manufacturing of chemical products. In the process of particle formation from homogeneous solution a nucleus (or nuclei) must be formed by self-association of solute molecules, and subsequently phase-separation from the bulk solution must take place.[6–8] Classical Nucleation Theory (CNT) is usually applied as a conceptual framework for modelling these processes.[5,9] CNT assumes that nucleation occurs from supersaturated solutions, leading to nuclei of a critical size whose internal structure matches that of the bulk material.[10,11] Dynamic equilibria create unstable small clusters ('sub-critical nuclei') and other transient aggregates. Supercritical nuclei may even re-dissolve again.[9,11] The challenges for experimental work detecting such nucleation events are tremendous, because one seeks to detect rare nanoscale events that are stochastic in time and (at least for homogeneous nucleation) in space. More importantly, it is now believed that nucleation pathways exist that are not captured by CNT (Figure 8.3). It has been demonstrated that localisation of homogeneous events by, e.g, use of liquid liquid interfaces[12] and small volume electron microscopy imaging[13] is a viable way forward, but they also interfere with the nucleation dynamics through interface formation or radiolysis.

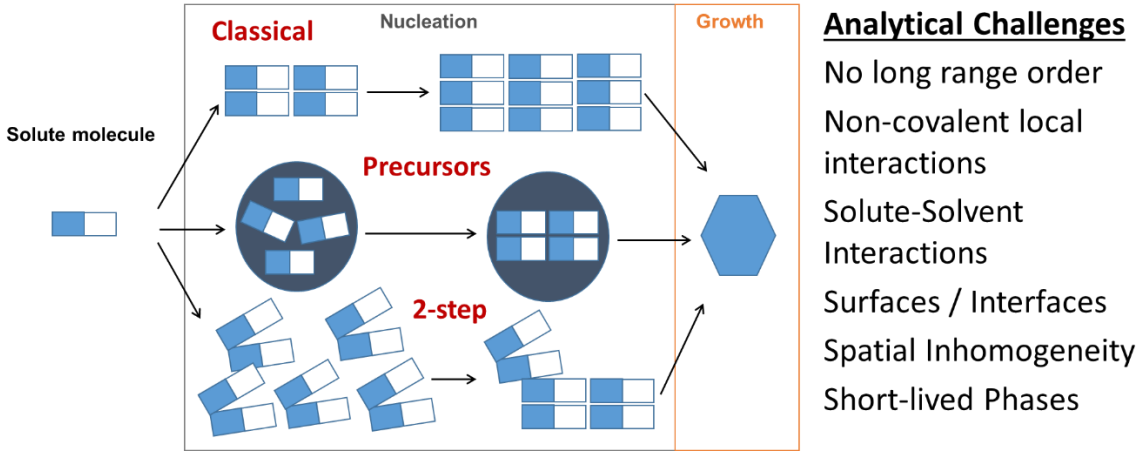

Figure 8.3 Alternatives to classical nucleation theory pathways in crystallisation, and the associated experimental science challenges to nucleation science.[14,15]

XFEL scattering and spectroscopy methodologies will for the first time provide the required combination of time and spatial resolution to overcome these challenges through high experiment repetition rate, multi-technique multiscale probing and molecular level imaging taking snapshots of small sample volumes under nucleation conditions. Advanced synchrotron and neutron characterisation with core level spectroscopies, PDF (see also section 5.5), scattering and diffraction methods (*vide supra*) has indicated that, in combination with modelling, these techniques can provide the required deep structural understanding. For taking this field of hybrid fundamental and applied research in small molecule crystallography forward we can take cues from the already fledgling field of time-resolved serial femtosecond crystallography (SFX) of proteins. Indeed, SFX studies of enzyme reactions are one of the major use cases for XFELs in life science (see section 7).[16-20] Just as in applied particle research, R&D efforts are significantly impacted by crystal size and size-distribution within the slurry (homogeneity).[20-23] The principal reason is because the fraction of macromolecules on the surface of a crystal increases with smaller crystals. Consider for example, a cubic crystal with 150 Å unit cell dimensions (Figure 8.4), which is a typical size for enzymes. A slurry comprised of 1 µm crystals will have just under 10% of the unit cells on the exterior layer of each crystal. But the exterior surface layer of 0.3 µm crystals includes 30% of the unit cells. Substrates must diffuse throughout the mother liquor and the microcrystals to initiate enzyme reactions. Macromolecular crystals are about 50% solvent/mother liquor and 50% protein[24-27] Enzymes on the surface of the crystal will bind substrates faster than those buried inside. Typical substrate molecules diffuse at roughly 1 $\mu m^2\ \mu s^{-1}$ and the rate depends upon viscosity as well as the size, shape and electrostatics of the intermolecular solve channels within the crystal lattice.[28-33] Diffusion through micron-size crystals is significantly faster than the average 60 ms reaction time for enzyme catalysis. A variety of mix and inject sample delivery methods are available and there is significant R&D activity in this area.[31-37] Therefore, time-resolved SFX is generalizable; however, cleaner results will be derived from more homogenous microcrystal slurries.

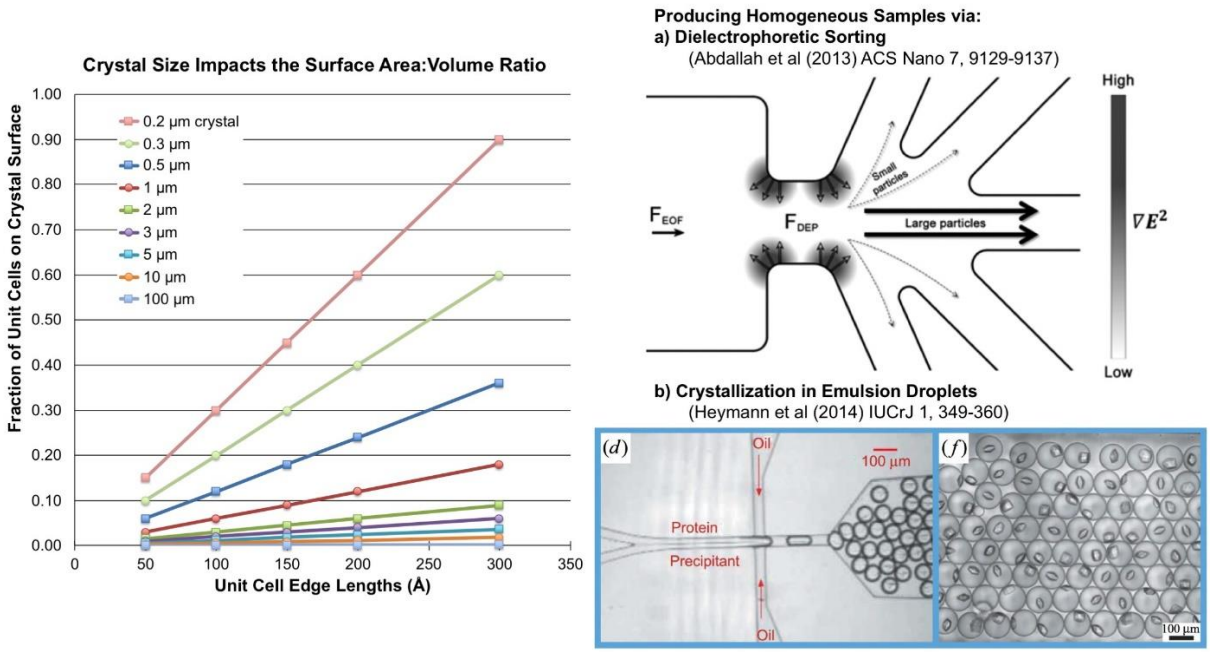

Figure 8.4 (Left) The fraction of unit cells on the surface of a crystal increases with smaller crystal size. (Right) Some methods to produce uniform slurries of microcrystal that are suitable for time-resolved SFX studies. Adapted from Abdallah, et al (2013) ACS Nano 7, 9129-9137 and Heymann et al (2014) IUCrJ 1, 349-360

The influences of the homogeneity of the slurry, crystal size, morphology, lattice packing, and solvent content upon the reaction rates have not been quantified. These should be measured for each system of interest and include more than one space group and/or crystal morphology whenever possible. For example, the ratio of surface area to volume changes as a function of crystal size and becomes pronounced in samples of submicron crystals composed of macromolecules in large unit cells. This may impact the overall k_{cat} measured from a slurry, especially if the molecules on the outside catalyse reactions with a different rate than those buried within the interior. If so, this suggests that lattice constraints may impact the reaction of interest, which may be alleviated in an alternative space group with different crystal packing. To date, microcrystal slurries are often grown in batch mode with relatively few constraints that do not always produce homogenous results. Therefore, heterogeneous microcrystal slurries can be filtered through pores of know size and/or sorted with microfluidic methods and dielectrophoresis (DEP) focusing.[38-40] In contrast, producing homogenous slurries of microcrystals often benefits from the use of microfluidic methods to grow individual crystals of predefined dimensions based upon nucleation in nL volume drops encapsulated in oil.[41] Using thE SFX approach we can therefore realistically hope to also unravel sequences of events in the nucleation and crystal growth processes in small molecule systems. Moreover, we can build on a rich existing knowledge transfer network in the field of small molecule particle science, including an engrained culture of industrial collaborations, perhaps exemplified best by the EPSRC CMAC Hub, which brings 7 UK Universities together with dozens of companies, including the Tier 1 partners AstraZeneca, Bayer, Eli Lilly, GlaxoSmithKline, Novartis, Pfizer, Roche and Takeda. These existing dissemination and collaboration relationships can be built on seamlessly for creating economic impact.

References

1 Office for National Statistics, *Annual Business Survey*, 2012.

2 Chemistry Growth Strategy Group, *Chemistry at Work - Strategy for Delivering Chemistry-Fuelled Growth of the UK Economy*, 2013.

3 Society of the Chemical Industry, *The Chemistry Council Sector Deal - Sustainable Innovation for a Better World*, 2019.

4 G. Das, S. Marathe, A. Pallipurath, R. Miller, K. Wanelik, J. Leng, T. Kathyola, L. H. Al-Madhagi, S. Y. Chang, C. Rau, J. McGinty, J. Sefcik and S. L. M. Schroeder, X-ray phase-contrast imaging of nucleation and crystal growth in anti-solvent crystallization of small molecule organics.

5 M. J. W. Povey, Crystal nucleation in food colloids, *Food Hydrocoll.*, 2014, **42**, 118–129.
6 R. J. Davey, S. L. M. Schroeder and J. H. Ter Horst, Nucleation of organic crystals - A molecular perspective, *Angew. Chemie - Int. Ed.*, 2013, **52**, 2167–2179.
7 G. C. Sosso, J. Chen, S. J. Cox, M. Fitzner, P. Pedevilla, A. Zen and A. Michaelides, *Chem. Rev.*, 2016, 116, 7078–7116.
8 D. Gebauer, M. Kellermeier, J. D. Gale, L. Bergström and H. Cölfen, Pre-nucleation clusters as solute precursors in crystallisation, *Chem. Soc. Rev.*, 2014, **43**, 2348–2371.
9 D. Kashchiev and G. M. van Rosmalen, Review: Nucleation in solutions revisited, *Cryst. Res. Technol.*, 2003, **38**, 555–574.
10 D. Kashchiev, *Nucleation: Basic Theory with Applications*, Butterworth-Heinemann, Oxford, 2000.
11 D. Erdemir, A. Y. Lee and A. S. Myerson, Nucleation of Crystals from Solution: Classical and Two-Step Models, *Acc. Chem. Res.*, 2009, **42**, 621–629.
12 S. Y. Chang, Y. Gründer, S. G. Booth, L. B. Molleta, A. Uehara, J. F. W. Mosselmans, G. Cibin, V. T. Pham, L. Nataf, R. A. W. Dryfe and S. L. M. Schroeder, Detection and characterisation of sub-critical nuclei during reactive Pd metal nucleation by X-ray absorption spectroscopy, *CrystEngComm*, 2016, **18**, 674–682.
13 M. H. Nielsen, S. Aloni and J. J. De Yoreo, In situ TEM imaging of CaCO3 nucleation reveals coexistence of direct and indirect pathways, *Science (80-.).*, 2014, **345**, 1158–1162.
14 R. J. Davey, S. L. M. Schroeder and J. H. ter Horst, Keimbildung organischer Kristalle aus molekularer Sichtweise, *Angew. Chemie*, 2013, **125**, 2220–2234.
15 D. Gebauer and H. Cölfen, Prenucleation clusters and non-classical nucleation, *Nano Today*, 2011, **6**, 564–584.
16 Chapman, H. N. (2019) X-Ray Free-Electron Lasers for the Structure and Dynamics of Macromolecules, *Annu Rev Biochem 88*, 35-58 doi: 10.1146/annurev-biochem-013118-110744
17 Fromme, P. (2015) XFELs open a new era in structural chemical biology, *Nat Chem Biol 11*, 895-899 doi: 10.1038/nchembio.1968
18 Schlichting, I. (2015) Serial femtosecond crystallography: the first five years, *IUCrJ 2*, 246-255 doi: 10.1107/S205225251402702X
19 Spence, J. C. H. (2017) XFELs for structure and dynamics in biology, *IUCrJ 4*, 322-339 doi: 10.1107/S2052252517005760
20 Schmidt, M. (2019) Time-Resolved Macromolecular Crystallography at Pulsed X-ray Sources, *International Journal of Molecular Sciences 20* doi: ARTN 1401 10.3390/ijms20061401
21 Schmidt, M. (2017) Time-Resolved Macromolecular Crystallography at Modern X-Ray Sources, *Methods Mol Biol 1607*, 273-294 doi: 10.1007/978-1-4939-7000-1_11
22 Schmidt, M., and Saldin, D. K. (2014) Enzyme transient state kinetics in crystal and solution from the perspective of a time-resolved crystallographer, *Struct Dyn 1*, 024701 doi: 10.1063/1.4869472
23 Schmidt, M. (2013) Mix and Inject: Reaction Initiation by Diffusion for Time-Resolved Macromolecular Crystallography, *Advances in Condensed Matter Physics 2013*, 10 doi: 10.1155/2013/167276
24 Weichenberger, C. X., and Rupp, B. (2014) Ten years of probabilistic estimates of biocrystal solvent content: new insights via nonparametric kernel density estimate, *Acta Crystallogr D Biol Crystallogr 70*, 1579-1588 doi: 10.1107/S1399004714005550
25 Chruszcz, M., Potrzebowski, W., Zimmerman, M. D., Grabowski, M., Zheng, H., Lasota, P., and Minor, W. (2008) Analysis of solvent content and oligomeric states in protein crystals--does symmetry matter?, *Protein Sci 17*, 623-632 doi: 10.1110/ps.073360508
26 Kantardjieff, K. A., and Rupp, B. (2003) Matthews coefficient probabilities: Improved estimates for unit cell contents of proteins, DNA, and protein-nucleic acid complex crystals, *Protein Sci 12*, 1865-1871 doi: 10.1110/ps.0350503
27 Matthews, B. W. (1968) Solvent content of protein crystals, *J Mol Biol 33*, 491-497 doi: 10.1016/0022-2836(68)90205-2
28 Pravda, L., Berka, K., Svobodova Varekova, R., Sehnal, D., Banas, P., Laskowski, R. A., et al, Otyepka, M. (2014) Anatomy of enzyme channels, *BMC Bioinformatics 15*, 379 doi: 10.1186/s12859-014-0379-x
29 Juers, D. H., and Ruffin, J. (2014) MAP_CHANNELS: a computation tool to aid in the visualization and characterization of solvent channels in macromolecular crystals, *J Appl Crystallogr 47*, 2105-2108 doi: 10.1107/S160057671402281X
30 Coleman, R. G., and Sharp, K. A. (2009) Finding and characterizing tunnels in macromolecules with application to ion channels and pores, *Biophys J 96*, 632-645 doi: 10.1529/biophysj.108.135970
31 Olmos, J. L., Jr., Pandey, S., Martin-Garcia, J. M., Calvey, G., Katz, A., Knoska, J., et al, Schmidt, M. (2018) Enzyme intermediates captured "on the fly" by mix-and-inject serial crystallography, *BMC Biol 16*, 59 doi: 10.1186/s12915-018-0524-5
32 Oberthuer, D., Knoska, J., Wiedorn, M. O., Beyerlein, K. R., Bushnell, D. A., Kovaleva, E. G., et al, Bajt, S. (2017) Double-flow focused liquid injector for efficient serial femtosecond crystallography, *Sci Rep 7*, 44628 doi: 10.1038/srep44628
33 Kupitz, C., Olmos, J. L., Jr., Holl, M., Tremblay, L., Pande, K., Pandey, S., et al, Schmidt, M. (2017) Structural enzymology using X-ray free electron lasers, *Struct Dyn 4*, 044003 doi: 10.1063/1.4972069
34 Knoska, J., Adriano, L., Awel, S., Beyerlein, K. R., Yefanov, O., Oberthuer, D., et al, Heymann, M. (2020) Ultracompact 3D microfluidics for time-resolved structural biology, *Nat Commun 11*, 657 doi: 10.1038/s41467-020-14434-6
35 Bohne, S., Heymann, M., Chapman, H. N., Trieu, H. K., and Bajt, S. (2019) 3D printed nozzles on a silicon fluidic chip, *Rev Sci Instrum 90*, 035108 doi: 10.1063/1.5080428
36 Wiedorn, M. O., Awel, S., Morgan, A. J., Ayyer, K., Gevorkov, Y., Fleckenstein, H., et al, Chapman, H. N. (2018) Rapid sample delivery for megahertz serial crystallography at X-ray FELs, *IUCrJ 5*, 574-584 doi: 10.1107/S2052252518008369
37 Stagno, J. R., Liu, Y., Bhandari, Y. R., Conrad, C. E., Panja, S., Swain, M., et al, Wang, Y. X. (2017) Structures of riboswitch RNA reaction states by mix-and-inject XFEL serial crystallography, *Nature 541*, 242-246 doi: 10.1038/nature20599
38 Abdallah, B. G., Zatsepin, N. A., Roy-Chowdhury, S., Coe, J., Conrad, C. E., Dorner, K., et al, Ros, A. (2015) Microfluidic sorting of protein nanocrystals by size for X-ray free-electron laser diffraction, *Struct Dyn 2*, 041719 doi: 10.1063/1.4928688

39 Luo, J., Muratore, K. A., Arriaga, E. A., and Ros, A. (2016) Deterministic Absolute Negative Mobility for Micro- and Submicrometer Particles Induced in a Microfluidic Device, *Anal Chem 88*, 5920-5927 doi: 10.1021/acs.analchem.6b00837
40 Abdallah, B. G., Roy-Chowdhury, S., Coe, J., Fromme, P., and Ros, A. (2015) High throughput protein nanocrystal fractionation in a microfluidic sorter, *Anal Chem 87*, 4159-4167 doi: 10.1021/acs.analchem.5b00589
41 Heymann, M., Opthalage, A., Wierman, J. L., Akella, S., Szebenyi, D. M., Gruner, S. M., and Fraden, S. (2014) Room-temperature serial crystallography using a kinetically optimized microfluidic device for protein crystallization and on-chip X-ray diffraction, *IUCrJ 1*, 349-360 doi: 10.1107/S2052252514016960

8.4 Dynamic processes in additive manufacturing, combustion, laser machining and photolithography

Various advanced technologies vital to the manufacturing base including friction welding, additive manufacturing and laser machining require an understanding of microstructural phenomena frequently occurring at fast timescales. XFELs offer probing capabilities that surpass the current state-of-the-art and allow these processes to be followed from milliseconds to sub-picosecond timescales. Soft X-ray/extreme UV pulses of high brightness from a high repetition rate XFEL may lead to new prospects in matching Moore's law with nanometre scale resolution photolithography.

8.4.1 Rapid Events in Materials Science and Advanced Manufacturing

During various novel manufacturing processes (e.g. friction welding, laser micro-machining, additive manufacturing, forging, etc…), metallic materials experience rapid microstructural events due to the high temperatures and stresses during these process, especially when accompanied by both high strain rate deformation (~10^3/s) and high heating rates (10^6-10^9 K/s). These microstructural phenomena need to be understood and controlled in order to achieve the required quality and performance. This has raised the need for experimental tools that enable real-time observation of the microstructural development and phase transformations (PTs) during these manufacturing processes. Synchrotron X-ray diffraction (XRD) and in-situ high temperature microscopy (Attallah et al.) have been successfully used in several studies to in-situ investigate the phase evolution during melting and solidification, as well as the solid-to-solid phase transformations. However, more studies are needed within a synchrotron XFEL context, and higher temporal resolution demanded to capture all of the timescales of these processes.

Friction Welding: high strain rate thermo-mechanical deformation and rapid heating

During friction welding or forging operations, the material experiences rapid thermomechanical deformation (typically in a shear deformation mode). Friction welding is a high integrity welding process that is employed in welding aero-engine components; notably the bladed disk (BLISK) structures. Previous work used high speed imaging to visualise the complex thermomechanical deformation (Figure 8.5). Future investigations can develop new material models to describe the rapid thermal and thermomechanical conditions associated with friction welding, taking into consideration microstructural development in addition to the flow stress/strain behaviour at these rapid rates. This will address the limitation in the current models, which rely on thermomechanical and thermodynamic/phase transformation data that do not consider the rapid and transient nature of the thermal and thermomechanical fields during friction welding. Such a limitation hinders the development of models to predict the microstructure-property development in friction welds. Some of the proposed work can include in-situ X-ray diffraction measurements during high strain rate testing (Hopkison bar) at high temperature, to deliver both flow-stress/strain behaviour as well as microstructural (phase transformation) information to understand the microstructural phenomena (e.g. dynamic recrystallisation, precipitation, etc…) and micromechanical development (e.g. crystallographic texture). Furthermore, the influence of rapid heating on the phase transformations kinetics and other microstructural phenomena (e.g. liquation) can be explored to model the microstructural development within the heat-affected zone (HAZ).

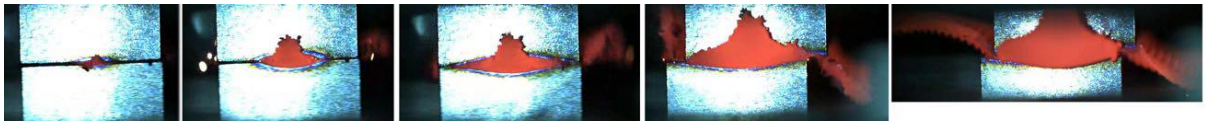

Figure 8.5. High speed imaging still shots during linear friction welding, showing the extrusion of the hot material during the process (typical weld cycle is <5 s) [1]

Additive Manufacturing: Laser-Material Interaction

Recently, there has been a growing interest in the development and utilisation of *in-situ* synchrotron techniques [2] and high-speed imaging [3] to study the physical phenomena of additive manufacturing (Figure 8.6), especially the laser-material interaction to understand the defect formation mechanisms. Further studies are needed to improve our understanding of the rapid phenomena during additive manufacturing, specifically by exploring the following areas:

- Residual stress development: it is important to understand the influence of the repeated thermal cycling during additive manufacturing on the development of residual stresses due to their detrimental impact on the mechanical properties, part tolerances, and process.
- Phase transformations: additive manufacturing is estimated to have a cooling rate of 106 K/s, and a very high heating rate. Understanding the impact of the rapid phenomena on the solid-to-solid and liquid-to-solid phase transformation will achieve the holy grail of additive manufacturing, which is enabling localised microstructural control and customisation of the local properties to improve the product performance.

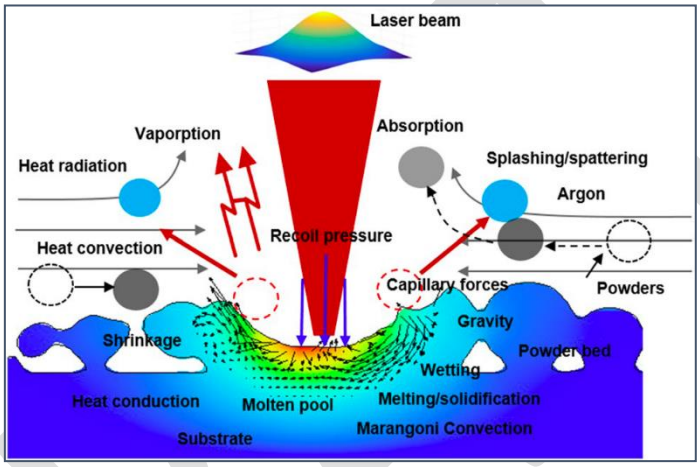

Figure 8.6: An overview of the physical phenomena associated with laser-material interaction during metallic materials additive manufacturing [4]

To implement this research 2D detectors will be required to record crystallographic information, EDX detectors to record residual stress development from white beams, tomographic detectors. Acquisition rates should be faster than >1 kHz.

Figure 8.7: Example experimental additive manufacturing platform that can fitted within the experimental facilities, the 'shoe box' laser additive manufacturing system which was used by Bidare et al. in monitoring the process using high speed imaging.

8.4.2 Laser Machining

Laser machining is a widely used technology in UK industrial production and there are domestic companies providing automated tooling for this process. In the engineering literature there is ongoing discussion on the choice between short-pulse (fs), long-pulse (ns) or continuous-wave (CW) lasers. Often different solutions are used for different applications, but there are fundamental questions why these choices produces such different results.

The high-power laser research world is similarly divided between the “petawatt (PW)” communities exploring very fast electron processes in molecules or materials, and the “kilojoule” communities interested in compression, ramping, pressure generation and heating processes in materials. These represent the same differences between the fs and ns laser worlds.

Comparisons of the results of fs and ns laser hole drilling, carried out side-by-side on samples of thin sheets of aluminium [5] and steel [6] are shown in Fig 8.8. The authors both note striking improvements in the sharpness of the laser cut obtained with the fs pulses, and also the presence of a “heat affected zone” in the case of the ns cutting. This is only qualitatively understood at the present time.

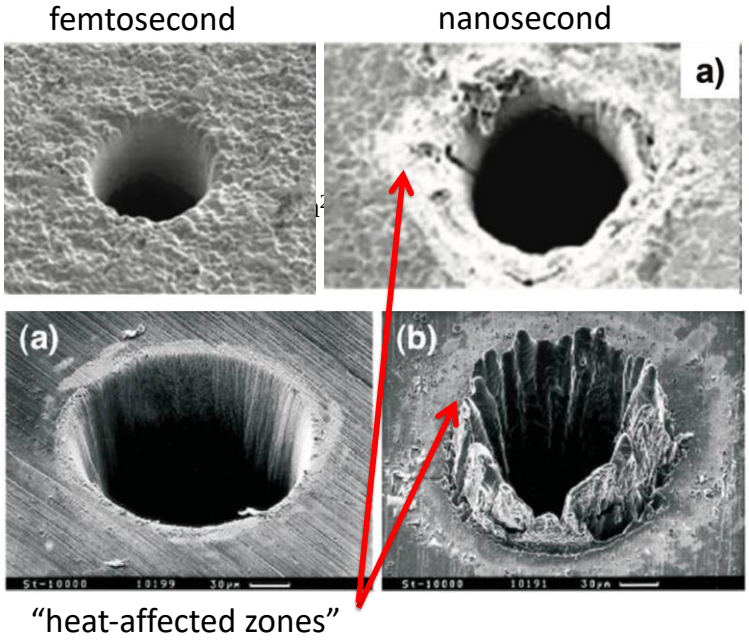

Figure 8.8: Comparisons of the results of fs and ns laser machining, in thin sheets of aluminium [5] and steel [6]

An example of a recent result [7], representing possible future direction of study that could be undertaken at the UK XFEL is illustrated in Figure 8.9. A 300nm thin film of gold was melted with a single laser pulse tuned to just provide enough heat to melt the film over a 100um focussed area. A single X-ray pulse from the PAL XFEL facility in South Korea was brought in to measure the X-ray Diffraction pattern of a 50um region in the centre of the focus, as a function of time delay. From the shape of the diffraction showing a split peak, it was clear that the melting of the polycrystalline film takes place inhomogeneously. The model in the figure assumes that all the energy is deposited at the grain boundaries, where the heated electrons couple to the crystal lattice. This heat conducts on a ps time scale into the surrounding grains, which are micron-sized. The result is a pair of melt fronts, separating in time, which bracket a block of gold undergoing melting by absorption of the latent heat of melting. This block gives the distinct second peak seen in the transient diffraction pattern seen.

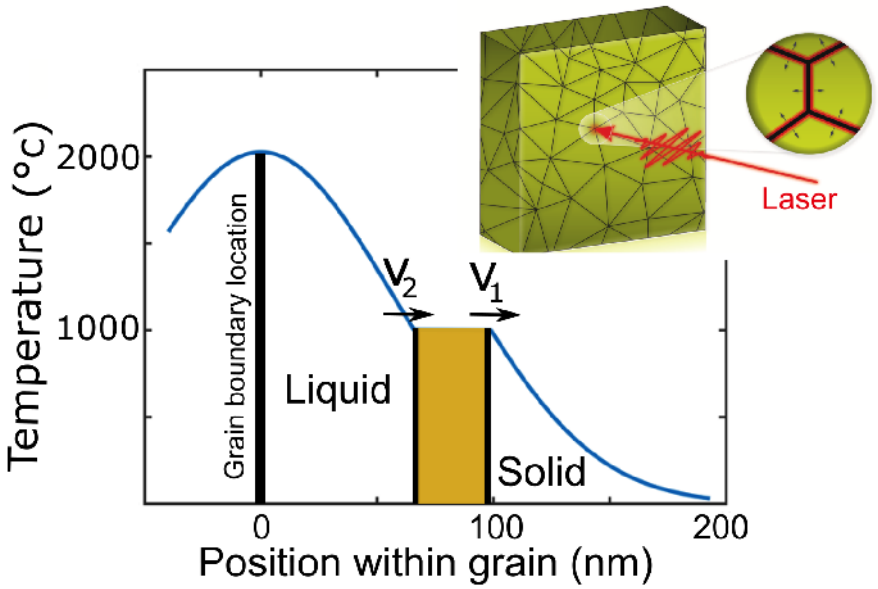

Figure 8.9: Model of the behaviour seen in Laser pump, XFEL X-ray probe measurements of the spatial of melting of a 300nm gold thin film near a grain boundary [7]

8.4.3 Extreme Ultraviolet Lithography

Standard lithography of semiconductor chips with ArF laser-produced 193 nm radiation is gradually being augmented / replaced by the finer patterning enabled by 13.5nm illumination, referred to in the industry as EUV. This is the main contemporary technique allowing the industry to keep up with Moore's Law. Currently, EUV is produced through the excitation of a tin or xenon plasma with an excimer laser, commercial scanners can now produce EUV at the few 100 W level. An alternative method would be the deployment at chip fabrication plants of an EUV FEL capable of operating at multi-kW average power. Such a possibility has been investigated in detail by a leading company in lithography apparatus, but as yet the low level of technical maturity of FELs has prohibited commercial commitment. Driving the UK-XFEL soft X-ray FEL with a ~1 GeV Energy Recovery Linac (ERL) would enable multi-kW production of EUV. This would benefit the global semiconductor industry by allowing study of FEL capabilities at an industrial output level, and developing and proving kW-capable EUV optical elements / beamlines for photon transport to chip scanners.

References

[1] F Schröder, RM Ward, AR Walpole, RP Turner, MM Attallah, JC Gebelin, RC Reed. Materials Science and Technology, 2015, vol. 31, pp. 372-84.
[2] Leung *et al.*, Additive Manu., 2018.
Leung *et al.*, Nature Comm., 2018.
[3] P Bidare, I Bitharas, RM Ward, MM Attallah, AJ Moore: Fluid and particle dynamics in laser powder bed fusion. Acta Materialia 142, 107-120, 2018.
[4] Chen *et al.,* Appl. Phys. A, 2019
[5] Pico- and Femtosecond Laser Micromachining for Surface Texturing, Tatsuhiko Aizawa and Tadahiko Inohara, InTech Open Book (2018)
[6] Femtosecond laser three-dimensional micro- and nanofabrication, K. Sugioka and Y. Cheng, Appl. Phys. Rev. 1 041303 (2014)
[7] Melt-front Dynamics in Polycrystalline Gold Thin Films Tadesse A. Assefa, Yue Cao, Soham Banerjee, Sungwon Kim, Dongjin Kim, Sunam Kim, Jae Hyuk Lee, Sang-Youn Park, Intae Eom, Jaeku Park, Daewoog Nam, Sangsoo Kim, Sae Hwan Chun, Hyojung Hyun, Kyung Sook Kim, Pavol Juhas, Emil S. Bozin, Ming Lu, Changyong Song, Hyunjung Kim, Simon J. L. Billinge and Ian K. Robinson, Science Advances 6 eaax2445 (2020)

8.5 Gamma Source Application in Nuclear Security and Materials in Nuclear Industry

Because of the globally unique quality and quantity of gamma production from the ICS source [Section 3.3], a number of techniques of great value to nuclear security and industry sectors will become possible. Impact would be in the fields of nuclear waste management, nuclear forensics such as active SNM and contraband detection, and medical isotope production. Further applications may include treaty verification and stockpile stewardship.

Presently, the most intense dedicated ICS source at MeV energies is the High Intensity Gamma Source (HIGS) at Duke University, USA. Important measurements have been made, such as photonuclear resonances in U-235, where 13 new resonances were identified. This data was important in the development of nuclear resonance fluorescence as an assay methodology. HIGS is, however, limited in flux and bandwidth as it is a storage ring based source. The key technology improvement proposed for the UK-XFEL ICS source that allows for orders of magnitude increase in flux (and narrowing of bandwidth) is the replacement of the electron storage ring with an Energy Recovery Linac (ERL). Higher flux means shorter integration times in the applications described below; narrower bandwidth means better energy resolution and the ability to tune into narrow nuclear resonances with less background signal and less absorbed dose into the subject.

8.5.1 Non-Destructive Assay via Radiography, Nuclear Resonance Fluorescence and Photofission

Radiographic imaging (< 10 MeV) of assemblies (e.g. shipping container contents) can be conducted with broadband (bremsstrahlung) systems, but a near-monoenergetic ICS source would significantly simplify the deconvolution of detector and filter responses during the post-processing of radiographic data whilst reducing dose to the subject. Tuneability of the source (including below 1 MeV) may permit some degree of discrimination between materials.

1 – 5 MeV photons with ~few percent bandwidth are expected to enable development of verification techniques for non-proliferation security through nuclear resonance fluorescence (NRF) computed tomography. AWE desire to be partners as this would be a source of high quality underpinning data for future, smaller systems deployable in the field (e.g. at ports of entry into the UK). Specifically, nuclear cross-sections and the resonance characteristics of materials could be acquired across the photon energy range of operational interest. The narrow bandwidth and tune-ability of the source are also key in that specific resonances can be targeted with the aim of demonstrating materials identification from the resulting fluorescence signature. Furthermore, the narrowband nature of the ICS source ensures that the input dose to the target can be significantly reduced compared to existing broadband sources. NNL desire to be partners in the context of the non-destructive assay of components through the whole nuclear fuel cycle, for example spent fuels and unknown legacy wastes. The gamma rays from the ICS system would allow fast, high-resolution, isotopically sensitive, probing of waste packages, allowing nuclear assay even through shielded flask walls.

From a national security perspective, the ICS source could be used to demonstrate the feasibility of using induced photofission signatures (5 MeV < E < 10 MeV) for low-dose identification of specific isotopes. As for NRF, underpinning materials data (in this case, nuclear photofission cross-sections) acquired using the ICS source would be central for developing this new detection methodology

8.5.2 Nuclear Waste Management via Photonuclear Transmutation

Combining NRF with irradiation at higher photon energy (5 – 40 MeV) and narrower bandwidth (0.1 – 0.01 %) are expected to enable development of techniques to possibly selectively transmute specific isotopes. This would allow investigation of improved nuclear waste management techniques via induced photofission of actinides and long-lived fission products. Crucially, a high value source or

product oxide could be purified without the need for wet chemical partitioning. Thus allowing purification of a mixture of isotopes, or alternatively selective destruction of a contaminant that has grown into a material. For example, ingrowth of Am-241 in a can of PuO2 greatly increases operator dose when this is recycled as MOX fuel. This could be mitigated if the Am-241 could be eliminated in situ.

Future reprocessing plant are looking at new reprocessing strategies to segregate actinides in differing combinations to improve long term waste handling options. It may be practical to selectively destroy a specific high hazard actinide or alternatively a fission product waste such as I-129 or Tc-99. To be economically viable, the waste volume would need to be small and specific long term waste storage and waste stabilisation costs be high. Major economic benefit may therefore arise in, for example, reconfiguring the long-term management of the UKs current and future stockpiles of problematic legacy wastes on the Sellafield site

8.5.3 Medical Radionuclide Production

The high spectral flux available may make the production of novel medical radioisotopes economically viable, including by harvesting them from legacy material currently considered as waste. The pencil nature of the gamma beam implies potential for very high specific activity in the material produced. Applications would include new medical diagnostic techniques such as gamma-PET (photonuclear generation of Ti-44, Pt-195m, Sn-117m, Sc-44).

8.5.4 Detector Calibration

For example, calibrated gas Cherenkov detectors (GCD) are routinely used to monitor burn characteristics in Inertial Confinement Fusion (ICF) schemes (M. S. Rubery et al., Rev. Sci. Instr. 84, 073504 (2013)). The monochromatic but tuneable characteristics of the ICS source are ideal for determining detector response as a function of gamma photon energy.

References

[1] Production of medical radioisotopes with high specific activity in photonuclear reactions with gamma beams of high intensity and large brilliance, D. Habs &U. Koster, Applied Physics B (2011) 108: 501 519

[2] The state of the art of the non-destructive assay of spent nuclear fuel assemblies – a critical review of the spent fuel NDA project of the US Department of Energy's next generation safeguards initiative, Bolind & Seya, Review for Japan Atomic Energy Agency 2015-027, DOI:10.11484/jaea-review-2015-027

[3] Impact of monoenergetic photon sources on nonproliferation applications, C. Geddes et. al., Idaho National Laboratory Report INL/EXT-17-41137 (March 2017) prepared for US Department of Energy

[4] Comparison of laser Compton scattering and conventional bremsstrahlung for photonuclear transmutation, Rehman, Lee & Kim, Int J. Energy Res. 2018;42:236-244

[5] Photo-transmutation of long-lived nuclear waste Cs-135 by intense Compton gamma-ray source, Zhu et. al. Annals of Nuclear Energy 89 (2016) 109-114

[6] Iodine transmutation through laser Compton scattering gamma rays, Li et. al., Journal of Nuclear Science & Technology, 46:8, 831-835 (2009)

[7] Discrete deexcitations in U-235 below 3 MeV from nuclear resonance fluorescence, Kwan et. al., Phys. Rev. C 83 041601 (2011)

[8] Perspectives for photofission studies with highly brilliant, monochromatic gamma-ray beams, Thirolf et. al., EPJ Web of Conferences 38 08001 (2012)

[9] Nondestructive assay of plutonium and minor actinide in spent fuel using nuclear resonance fluorescence with laser Compton scattering gamma-rays, Nuclear Instruments & Methods in Physics Research A 621 (2010) 695-700

[10] Demonstration of a transmission nuclear resonance fluorescence measurement for a realistic radioactive waste canister scenario, Angell et. al., Nuclear Instruments & Methods in Physics Research B 347 (2015) 11-19

[11] Exploratory study of fission product yield determination from photofission of Pu-239 at 11 MeV with monoenergetic photons, Bhike et. al., Phys. Rev. C 95 024608 (2017)

[12] Monoenergetic photon-induced fission cross-section ratio measurements for U-235, U-238 and Pu-239 from 9.0 to 17.0 MeV, Krishichayan et. al., Phys. Rev. C 98 014608 (2018)

[13] Development of general nuclear resonance fluorescence model, Ogawa et. al., Journal of nuclear science & technology 53:11, 1766-1773 (2016)

8.6 Industrial inspirations from deeper insights into biology: pharma to clean energy

Industrial XFEL users in life science want faster, better structures from smaller samples. They demand reliability and automation, especially for proprietary R&D efforts. Industry is already using Diamond and eBIC extensively, and starting to explore options at XFELs. They are watching for developments in cryo-EM, serial crystallography, and time-resolved studies that couple structure and function from the same sample. New opportunities for drug discovery impacting human health are profound and progress has recently been demonstrated with serial femtosecond crystallography (SFX) results on several membrane proteins involved cell signalling. Time resolved SFX results targeting photosystem II, hydrogenases, and nitrogenases promise molecular level insights that will inspire the next generation of solar and full cells, and green catalysts to convert N_2 into fertilizer.

An outstanding grand challenge in life sciences is to understand the molecular basis of symbiosis *versus* pathogenicity. Why are some interactions beneficial, and how can these be protected or enhanced while simultaneously degrading those that cause disease? The need to distinguish between "friend or foe" impacts the entire biosphere and is one of the critical factors that drive evolution on earth; often a life or death process. This ongoing struggle is a fundamental underlying basis of the $1.2 trillion pharmaceutical industry focused upon human health, and similar global efforts targeting agriculture. Despite the extinction of more than 99% of all organisms that have ever lived on earth (see Section 7), the current diversity of life is immense and always evolving.[1]

As we write this, the Covid-19 pandemic is roiling around the word with 529,591 confirmed cases and 23,970 deaths reported at 11:53 UTC on 26 March 2020 (Figure 8.10).[2-5] This is the third coronavirus outbreak to emerge in the 21st century that causes severe respiratory syndrome and death on a large scale (SARS in 2002, MERS in 2012, and Covid-19 in December 2019). Covid-19 is likely to have evolved recently from a SARS precursor. Consequently, humans have no immunity to this novel, positive-strand RNA virus and treatments, ranging from symptom mitigation to vaccines, will take time to develop. In the meantime, social distancing is the dominant health strategy.

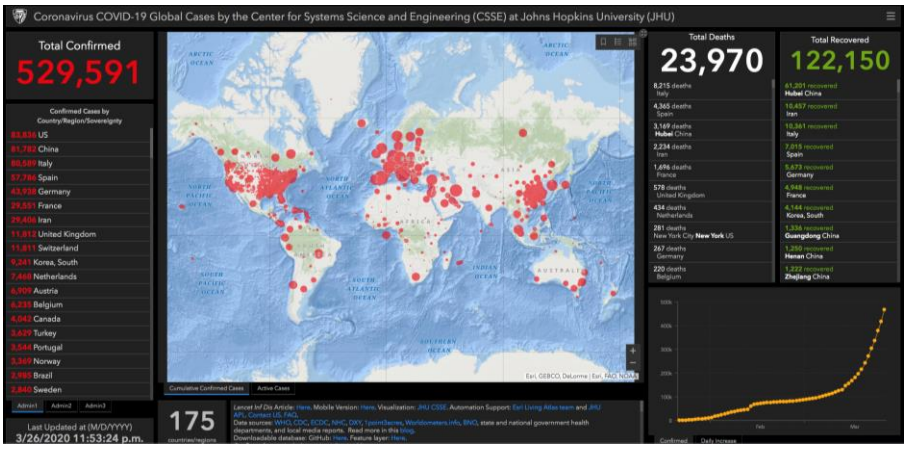

Figure 8.10. A snapshot on 26 March 2020 of the Covid-19 outbreak that started in Dec 2019 as tracked by the Johns Hopkins University Coronavirus COVID-19 Global Cases server.

Dong, E., Du, H., and Gardner, L. (2020) *Lancet Infect Dis* doi: 10.1016/S1473-3099(20)30120-1

Structural biologists in academic and industrial labs around the world are vigorously working on the problem, including analyses of key proteins from the Covid-19 virus genome using cryo-EM, X-ray crystallography and homology modelling approaches (Figure 8.11).[6-12] Among the first results are cryo-EM single particle analysis of the whole virus and the complex that likely mediates entry into human cells. These results suggest that the Covid-19 virus hijacks the normal physiological roles of angiotensin-converting enzyme 2 (ACE2) and transporters for the uptake of large neutral amino acids like B^0AT1 and/or its homologues. In parallel, chemical fragment library screening with X-ray

crystallography at Diamond target inhibition of the Covid-19 protease that is critical to the virus life cycle. The XChem crystallographic results link directly to industrial partners including Exscientia (Oxford, UK) to assay hits and follow-up lead compounds, and Enamine (Rīga, Latvia) for selected compounds to be used for bioassays. The rapid progress across all R&D fronts is impressive.

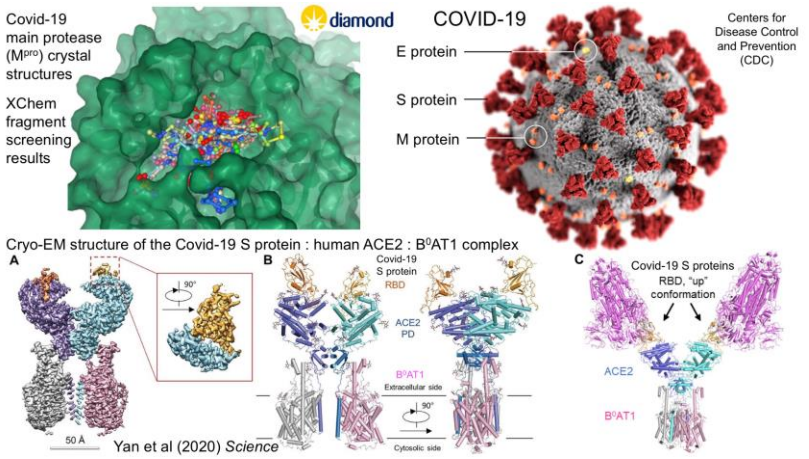

Figure 8.11. Morphology of the Covid-19 virus (top right) and structure-based drug discovery. (top left) Fragment screening by crystallography of the M^{pro} protease at Diamond identified > 50 ligand hits in and around the active site. (bottom) 2.9 Å resolution cryo-EM map (A) and overall structure (B) of the RBD-ACE2-B^0AT1 ternary complex. (C) The ternary complex superimposed with the S protein of Covid-19 (PDB code: 6VSB); adapted from Yan, et al (2020) *Science* doi: 10.1126/science.abb2762

However, this is also a tragic example of a missed opportunity. The original SARS outbreak in 2002 actually did yield high resolution crystal structures of the main protease, which is very homologous to the Cocid-19 main protease.[6, 13, 14] As Dr Stephen Burley (director of the Research Collaboratory for Structural Bioinformatics Protein Data Bank, Institute for Quantitative Biomedicine, Rutgers, The State University of New Jersey) said on 04 March 2020, "Had an effective blocker of the SARS main protease been discovered and developed [to fruition] in 2003, it would have stopped the current infection dead in its tracks."[15] Since they are so closely related by evolution, an inhibitor developed for the SARS coronavirus main proteas will also very likely be effective against Covid-19.

Although very successful, these approaches largely ignore dynamic components because they derive from samples held at cryogenic temperature. In contrast, many of the XFEL-based approaches described in Section 7 are performed at physiological temperature and thereby enable scientists to simultaneously probe dynamics and structure. This capability is germane to Covid-19 R&D efforts. The receptor binding domain (RBD) of the Covid-19 spike protein has at least two configurations, up and down. The molecular basis and dynamics for the transition between these two states is unknown; however, only the up state binds to ACE2. The interactions between the Covid-19 S protein and ACE2 indicate that the new virus binds with 4 times higher affinity than its SARS precursor (1.2 nM compared to 5.0 nM) and that most of this difference is apparent in the slower off-rate kinetics for Covid-19 (1.6×10^{-4} s^{-1} versus 7.1×10^{-4} s^{-1}).[9] The fragment screening results do not address any of the dynamic steps within the protease reaction kinetics or catalytic mechanism.

Structure-based drug discovery and/or design is a hallmark strategy used across the pharmaceutical industry. Its success is illustrated by the fact that more than 90% of new molecular entities (NEM) to receive US FDA approval since 2010 leveraged structural biology.[16-18] Almost all of the atomic models for the new drug targets were released into the public domain, and many about 10 years before a drug compound came to market. Thus, the linkages between the public and private sectors are historic and extensive.[19] At Diamond, up to 10% of the available experiment time is set aside for proprietary access used by many industrial partners. More than 160,000 atomic models are curated by the PDB with estimated economic value of more than $16B. Screening macromolecular targets against the vast chemical space using fragment libraries is highly automated, especially at the XChem facility at Diamond Light Source.[20-26] To date, this has almost always exploited cryogenic conditions. XFELs offer new opportunities to couple functional dynamics with ligand discovery of new drugs and therapies at physiological temperature.

XFEL-based structural biology methods efficiently use slurries of micron-size crystals to generate high resolution atomic models. An example of the impact is illustrated with G protein-coupled receptors (GPCRs, Figure 8.12).[27-32] These integral membrane proteins tend to exhibit a seven transmembrane protein fold that is often difficult to crystallize and study by traditional methods. Nevertheless, many have produced microcrystals with lipidic cubic phase conditions, that have generated important results from XFELs using SFX approaches.[33-44] There are more than 800 human GPCRs that respond to thousands of chemicals or photons, and elicit responses that touch nearly every physiological aspect of cells. Ligand binding or photoisomerization elicit dynamic conformational changes that propagate across the membrane and initiate intracellular signalling cascades. More than 40% of all prescribed drugs target GCPRs with impact to the central nervous, cardiovascular, immune, metabolic, and reproductive systems, as well as to many human cancers. The importance of GPCRs was the recognized by the 2012 Nobel Prize in Chemistry to Lefkowitz and Kobilka "for studies of G-protein-coupled receptors." Membrane proteins, and especially GPCRs, will be a strong use case for Industrial users for XFELs in the coming decades.

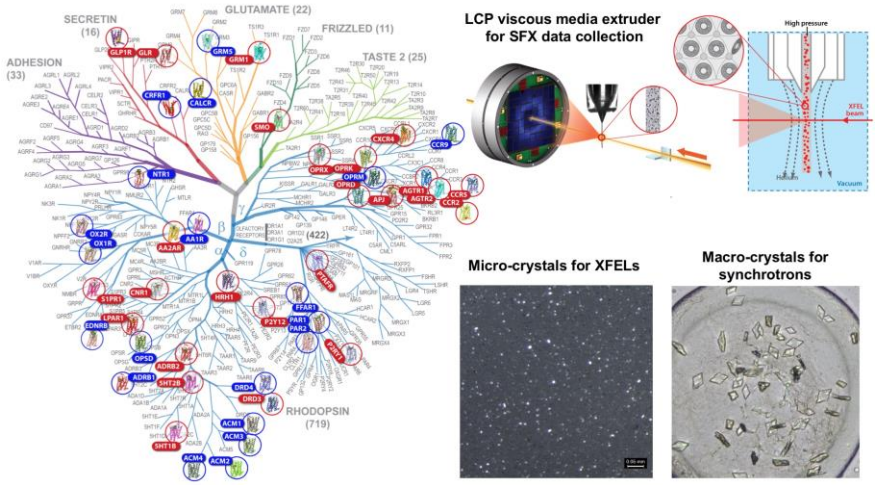

Figure 8.12. (Left) High-resolution crystal structures of GPCRs in 2019 superimposed upon the phylogenomic family tree. (Top right) SFX data collection strategy using an LCP injector at XFELs and microcrystal. (Bottom right) Comparison of micro- and macro-crystals. Adapted from Stauch & Cherezov, *Annu Rev Biophys* (2018) 47: 377–397 and Katritch, et al (2012) *Trends Pharmacol Sci* 33, 17-27

Metalloenzymes catalyse the most difficult reactions in biology.[45-49] They evolved to produce high energy intermediates when and where they are needed to transform a wide range of compounds. For instance, section 7.2 highlights photosystem II and how XFELs provide experimental approaches to watch visible light photons elicit charge separation, that sequentially oxidizes the Mn atoms within the oxygen evolving complex, that ultimately converts two H_2O molecules into O_2.[50-60] These mechanistic insights serve as inspiration for advanced generation photovoltaic cells for industrial applications. Fuel cells will also take inspiration from hydrogenases, metalloenzyme that use complex iron-sulfur and nickel clusters to catalyse the reversible reaction of two H^+ plus two electrons to produce H_2.[61-71] Methane monooxygenase uses dinuclear iron centre to catalyse the conversion of methane into methanol by creating a bis-Fe(IV)=O reactive intermediate.[72-84] Indeed, Fe(IV)=O intermediates are critically important across all aerobic life and are extraordinarily difficult to study by traditional synchrotron methods because they are easily perturbed by photoelectrons generated during the X-ray exposure.[46, 49, 85, 86] Metalloproteins will be a strong use case at XFELs and will inspire small molecule catalysis for many industrial applications.

For most of earth's history, natural sources have provided enough bio-available nitrogen to support all life in the biosphere. The most important reason is nitrogenase, a class of complex metalloenzymes that evolved in microbes to fix N_2 at atmospheric pressure and ambient temperature converting it to NH_3.[87, 88] The enzyme needs eight electrons and uses the energy released by ATP hydrolysis to drive protein conformational changes (Figure 8.13). Microbial species that carry genes for nitrogenase are widely distributed across terrestrial and oceanic environments. Some symbiotic bacteria inhabit the root nodules of legumes and express nitrogenases, which supply all of the reduced nitrogen needed

by the plant. In exchange, the plants supply reduced carbon from photosynthesis to the microbes, which is used for carbon and energy needed to fix N_2. The photosynthetic cyanobacteria *Crocosphaera watsonii* in the ocean expresses photosystem II during the day to generate electrons and fix CO_2. Then during the night, it express nitrogenase to fix N_2.[89-91] An outstanding frontier challenge is to understand the molecular basis of nitrogenase catalysis, especially how protein and metal cluster dynamics impact reactivity. Indeed, structural and spectroscopic results demonstrate that the ground-state crystal structures of nitrogenase determined at cryogenic temperatures are inactive.[92-104] This supports the hypothesis that dynamic motion of the active site cluster is essential to catalysis..

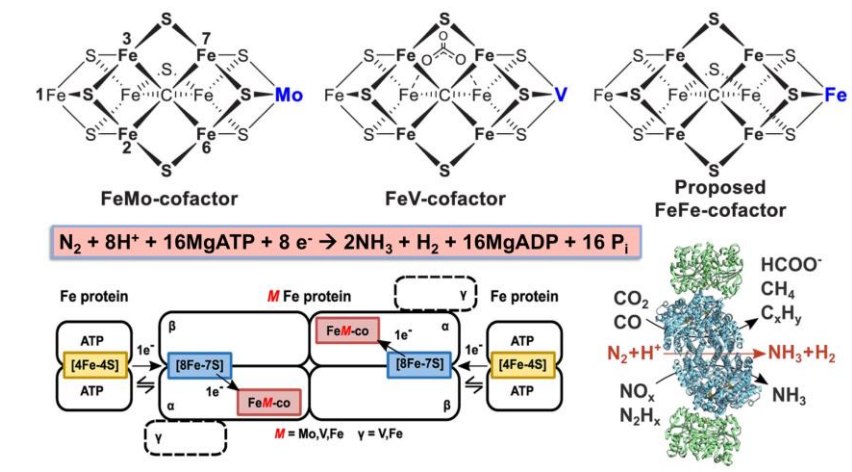

Figure 8.13. (Bottom, left) Schematic of nitrogenase structures showing the electron delivery Fe protein component and the catalytic MFe protein component (M = Mo, V, Fe). (Bottom, right) Overall structure of Fe protein - MoFe protein complex and reactions catalysed. (Centre) The nitrogenase reaction is catalysed by the metal Fe*M*-co centres (top) that incorporate similar but distinct clusters from various microbes.

Adapted from Seefeldt, et al (2020) *Chem Rev* doi: 10.1021/acs.chemrev.9b00556

The Haber-Bosch process is the industrial equivalent of nitrogenase and N_2 fixation.[87, 88] It was invented just over 100 years ago and now produces as much NH_3 globally as all natural sources. It has not changed significantly over the past century. Unfortunately, the Haber-Bosch process requires high pressure and temperature, as well as annually consumes about 5% of the global natural gas. Thus, it is not sustainable. Moreover, feeding the current world population of ~7.7 billion critically depends upon industrial fertilizers; but natural N_2 fixation processes alone can support only about 50% of the current population.[88, 105, 106] Consequently, there is an urgent need to develop alternatives to the Haber-Bosh process. Clearly a better understanding of the structure, dynamics and function of nitrogenase is an inspirational guidepost and XFELs will play a major role in the R&D effort in the years to come. The industrial scale application of green chemistry strategies to produce new N_2 fixing catalysts inspired by structural biology is essential to human survival.

References

[1] Barnosky, A. D., Matzke, N., Tomiya, S., Wogan, G. O., Swartz, B., Quental, T. B., et al, Ferrer, E. A. (2011) Has the Earth's sixth mass extinction already arrived?, *Nature 471*, 51-57 doi: 10.1038/nature09678

[2] Dong, E., Du, H., and Gardner, L. (2020) An interactive web-based dashboard to track COVID-19 in real time, *Lancet Infect Dis* doi: 10.1016/S1473-3099(20)30120-1

[3] Wu, F., Zhao, S., Yu, B., Chen, Y. M., Wang, W., Song, Z. G., et al, Zhang, Y. Z. (2020) A new coronavirus associated with human respiratory disease in China, *Nature 579*, 265-269 doi: 10.1038/s41586-020-2008-3

[4] Shen, Z., Xiao, Y., Kang, L., Ma, W., Shi, L., Zhang, L., et al, Li, M. (2020) Genomic diversity of SARS-CoV-2 in Coronavirus Disease 2019 patients, *Clin Infect Dis* doi: 10.1093/cid/ciaa203

[5] Chen, Y., Liu, Q., and Guo, D. (2020) Emerging coronaviruses: Genome structure, replication, and pathogenesis, *J Med Virol 92*, 418-423 doi: 10.1002/jmv.25681

[6] Zhang, L., Lin, D., Sun, X., Curth, U., Drosten, C., Sauerhering, L., et al, Hilgenfeld, R. (2020) Crystal structure of SARS-CoV-2 main protease provides a basis for design of improved alpha-ketoamide inhibitors, *Science* doi: 10.1126/science.abb3405

[7] Yan, R., Zhang, Y., Li, Y., Xia, L., Guo, Y., and Zhou, Q. (2020) Structural basis for the recognition of the SARS-CoV-2 by full-length human ACE2, *Science* doi: 10.1126/science.abb2762

[8] Wrapp, D., Wang, N., Corbett, K. S., Goldsmith, J. A., Hsieh, C. L., Abiona, O., et al, McLellan, J. S. (2020) Cryo-EM structure of the 2019-nCoV spike in the prefusion

conformation, *Science 367*, 1260-1263 doi: 10.1126/science.abb2507
[9] Walls, A. C., Park, Y. J., Tortorici, M. A., Wall, A., McGuire, A. T., and Veesler, D. (2020) Structure, Function, and Antigenicity of the SARS-CoV-2 Spike Glycoprotein, *Cell* doi: 10.1016/j.cell.2020.02.058
[10] Dong, S., Sun, J., Mao, Z., Wang, L., Lu, Y. L., and Li, J. (2020) A guideline for homology modeling of the proteins from newly discovered betacoronavirus, 2019 novel coronavirus (2019-nCoV), *J Med Virol* doi: 10.1002/jmv.25768
[11] Lan, J., Ge, J., Yu, J., Shan, S., Zhou, H., Fan, S., et al, Wang, X. (2020) Crystal structure of the 2019-nCoV spike receptor-binding domain bound with the ACE2 receptor, *bioRxiv*, 2020.2002.2019.956235 doi: 10.1101/2020.02.19.956235
[12] Jin, Z., Du, X., Xu, Y., Deng, Y., Liu, M., Zhao, Y., et al, Yang, H. (2020) Structure of M^{pro} from COVID-19 virus and discovery of its inhibitors, *bioRxiv*, 2020.2002.2026.964882 doi: 10.1101/2020.02.26.964882
[13] Yang, H., Yang, M., Ding, Y., Liu, Y., Lou, Z., Zhou, Z., et al, Rao, Z. (2003) The crystal structures of severe acute respiratory syndrome virus main protease and its complex with an inhibitor, *Proc Natl Acad Sci U S A 100*, 13190-13195 doi: 10.1073/pnas.1835675100
[14] Lu, I. L., Mahindroo, N., Liang, P. H., Peng, Y. H., Kuo, C. J., Tsai, K. C., et al, Wu, S. Y. (2006) Structure-based drug design and structural biology study of novel nonpeptide inhibitors of severe acute respiratory syndrome coronavirus main protease, *J Med Chem 49*, 5154-5161 doi: 10.1021/jm060207o
[15] Hill, M. (2020) How a Rutgers Team Is Working to Crack the Coronavirus Code, New Jersy Public Media, https://www.njtvonline.org/news/video/how-a-rutgers-team-is-working-to-crack-the-coronavirus-code/?utm_source=newsletter&utm_medium=email&utm_campaign=rutgerstoday&utm_content=research, access date (29 March 2020)
[16] Westbrook, J. D., Soskind, R., Hudson, B. P., and Burley, S. K. (2020) Impact of the Protein Data Bank on antineoplastic approvals, *Drug Discov Today* doi: 10.1016/j.drudis.2020.02.002
[17] Goodsell, D. S., Zardecki, C., Di Costanzo, L., Duarte, J. M., Hudson, B. P., Persikova, I., et al, Burley, S. K. (2020) RCSB Protein Data Bank: Enabling biomedical research and drug discovery, *Protein Sci 29*, 52-65 doi: 10.1002/pro.3730
[18] Westbrook, J. D., and Burley, S. K. (2019) How Structural Biologists and the Protein Data Bank Contributed to Recent FDA New Drug Approvals, *Structure 27*, 211-217 doi: 10.1016/j.str.2018.11.007
[19] Blundell, T. L. (2017) Protein crystallography and drug discovery: recollections of knowledge exchange between academia and industry, *IUCrJ 4*, 308-321 doi: 10.1107/S2052252517009241
[20] Thomas, S. E., Collins, P., James, R. H., Mendes, V., Charoensutthivarakul, S., Radoux, C., et al, Blundell, T. L. (2019) Structure-guided fragment-based drug discovery at the synchrotron: screening binding sites and correlations with hotspot mapping, *Philos Trans A Math Phys Eng Sci 377*, 20180422 doi: 10.1098/rsta.2018.0422
[21] Thomas, S. E., Mendes, V., Kim, S. Y., Malhotra, S., Ochoa-Montano, B., Blaszczyk, M., and Blundell, T. L. (2017) Structural Biology and the Design of New Therapeutics: From HIV and Cancer to Mycobacterial Infections: A Paper Dedicated to John Kendrew, *J Mol Biol 429*, 2677-2693 doi: 10.1016/j.jmb.2017.06.014
[22] Bowkett, D., Talon, R., Tallant, C., Schofield, C., von Delft, F., Knapp, S., et al, Brennan, P. E. (2018) Identifying Small-Molecule Binding Sites for Epigenetic Proteins at Domain-Domain Interfaces, *ChemMedChem 13*, 1051-1057 doi: 10.1002/cmdc.201800030
[23] Pearce, N. M., Krojer, T., Bradley, A. R., Collins, P., Nowak, R. P., Talon, R., et al, von Delft, F. (2017) A multi-crystal method for extracting obscured crystallographic states from conventionally uninterpretable electron density, *Nat Commun 8*, 15123 doi: 10.1038/ncomms15123
[24] Collins, P. M., Douangamath, A., Talon, R., Dias, A., Brandao-Neto, J., Krojer, T., and von Delft, F. (2018) Achieving a Good Crystal System for Crystallographic X-Ray Fragment Screening, *Methods Enzymol 610*, 251-264 doi: 10.1016/bs.mie.2018.09.027
[25] Pearce, N. M., Bradley, A. R., Krojer, T., Marsden, B. D., Deane, C. M., and von Delft, F. (2017) Partial-occupancy binders identified by the Pan-Dataset Density Analysis method offer new chemical opportunities and reveal cryptic binding sites, *Struct Dyn 4*, 032104 doi: 10.1063/1.4974176
[26] Bradley, A. R., Echalier, A., Fairhead, M., Strain-Damerell, C., Brennan, P., Bullock, A. N., et al, von Delft, F. (2017) The SGC beyond structural genomics: redefining the role of 3D structures by coupling genomic stratification with fragment-based discovery, *Essays Biochem 61*, 495-503 doi: 10.1042/EBC20170051
[27] Shimada, I., Ueda, T., Kofuku, Y., Eddy, M. T., and Wuthrich, K. (2019) GPCR drug discovery: integrating solution NMR data with crystal and cryo-EM structures, *Nat Rev Drug Discov 18*, 59-82 doi: 10.1038/nrd.2018.180
[28] Munk, C., Mutt, E., Isberg, V., Nikolajsen, L. F., Bibbe, J. M., Flock, T., et al, Gloriam, D. E. (2019) An online resource for GPCR structure determination and analysis, *Nat Methods 16*, 151-162 doi: 10.1038/s41592-018-0302-x
[29] Weis, W. I., and Kobilka, B. K. (2018) The Molecular Basis of G Protein-Coupled Receptor Activation, *Annu Rev Biochem 87*, 897-919 doi: 10.1146/annurev-biochem-060614-033910
[30] Hilger, D., Masureel, M., and Kobilka, B. K. (2018) Structure and dynamics of GPCR signaling complexes, *Nat Struct Mol Biol 25*, 4-12 doi: 10.1038/s41594-017-0011-7
[31] Latorraca, N. R., Venkatakrishnan, A. J., and Dror, R. O. (2017) GPCR Dynamics: Structures in Motion, *Chem Rev 117*, 139-155 doi: 10.1021/acs.chemrev.6b00177
[32] Katritch, V., Cherezov, V., and Stevens, R. C. (2012) Diversity and modularity of G protein-coupled receptor structures, *Trends Pharmacol Sci 33*, 17-27 doi: 10.1016/j.tips.2011.09.003
[33] Li, D., and Caffrey, M. (2020) Structure and Functional Characterization of Membrane Integral Proteins in the Lipid Cubic Phase, *J Mol Biol* doi: 10.1016/j.jmb.2020.02.024
[34] Stein, R. M., Kang, H. J., McCorvy, J. D., Glatfelter, G. C., Jones, A. J., Che, T., et al, Dubocovich, M. L. (2020) Virtual discovery of melatonin receptor ligands to modulate circadian rhythms, *Nature* doi: 10.1038/s41586-020-2027-0

[35] Stauch, B., Johansson, L. C., McCorvy, J. D., Patel, N., Han, G. W., Huang, X. P., et al, Cherezov, V. (2019) Structural basis of ligand recognition at the human MT1 melatonin receptor, *Nature 569*, 284-288 doi: 10.1038/s41586-019-1141-3
[36] Johansson, L. C., Stauch, B., McCorvy, J. D., Han, G. W., Patel, N., Huang, X. P., et al, Cherezov, V. (2019) XFEL structures of the human MT2 melatonin receptor reveal the basis of subtype selectivity, *Nature 569*, 289-292 doi: 10.1038/s41586-019-1144-0
[37] Gusach, A., Luginina, A., Marin, E., Brouillette, R. L., Besserer-Offroy, E., Longpre, J. M., et al, Cherezov, V. (2019) Structural basis of ligand selectivity and disease mutations in cysteinyl leukotriene receptors, *Nat Commun 10*, 5573 doi: 10.1038/s41467-019-13348-2
[38] Stauch, B., and Cherezov, V. (2018) Serial Femtosecond Crystallography of G Protein-Coupled Receptors, *Annu Rev Biophys 47*, 377-397 doi: 10.1146/annurev-biophys-070317-033239
[39] Che, T., Majumdar, S., Zaidi, S. A., Ondachi, P., McCorvy, J. D., Wang, S., et al, Roth, B. L. (2018) Structure of the Nanobody-Stabilized Active State of the Kappa Opioid Receptor, *Cell 172*, 55-67 e15 doi: 10.1016/j.cell.2017.12.011
[40] Zhang, H., Unal, H., Gati, C., Han, G. W., Liu, W., Zatsepin, N. A., et al, Cherezov, V. (2015) Structure of the Angiotensin receptor revealed by serial femtosecond crystallography, *Cell 161*, 833-844 doi: 10.1016/j.cell.2015.04.011
[41] Kang, Y., Zhou, X. E., Gao, X., He, Y., Liu, W., Ishchenko, A., et al, Xu, H. E. (2015) Crystal structure of rhodopsin bound to arrestin by femtosecond X-ray laser, *Nature 523*, 561-567 doi: 10.1038/nature14656
[42] Weierstall, U., James, D., Wang, C., White, T. A., Wang, D., Liu, W., et al, Cherezov, V. (2014) Lipidic cubic phase injector facilitates membrane protein serial femtosecond crystallography, *Nat Commun 5*, 3309 doi: 10.1038/ncomms4309
[43] Liu, W., Wacker, D., Gati, C., Han, G. W., James, D., Wang, D., et al, Cherezov, V. (2013) Serial femtosecond crystallography of G protein-coupled receptors, *Science 342*, 1521-1524 doi: 10.1126/science.1244142
[44] Ishchenko, A., Stauch, B., Han, G. W., Batyuk, A., Shiriaeva, A., Li, C., et al, Cherezov, V. (2019) Toward G protein-coupled receptor structure-based drug design using X-ray lasers, *IUCrJ 6*, 1106-1119 doi: doi:10.1107/S2052252519013137
[45] Meier, K. K., Jones, S. M., Kaper, T., Hansson, H., Koetsier, M. J., Karkehabadi, S., et al, Kelemen, B. (2018) Oxygen Activation by Cu LPMOs in Recalcitrant Carbohydrate Polysaccharide Conversion to Monomer Sugars, *Chem Rev 118*, 2593-2635 doi: 10.1021/acs.chemrev.7b00421
[46] Jasniewski, A. J., and Que, L., Jr. (2018) Dioxygen Activation by Nonheme Diiron Enzymes: Diverse Dioxygen Adducts, High-Valent Intermediates, and Related Model Complexes, *Chem Rev 118*, 2554-2592 doi: 10.1021/acs.chemrev.7b00457
[47] Huang, X., and Groves, J. T. (2018) Oxygen Activation and Radical Transformations in Heme Proteins and Metalloporphyrins, *Chem Rev 118*, 2491-2553 doi: 10.1021/acs.chemrev.7b00373
[48] Holm, R. H., Kennepohl, P., and Solomon, E. I. (1996) Structural and Functional Aspects of Metal Sites in Biology, *Chem Rev 96*, 2239-2314 doi: 10.1021/cr9500390
[49] Solomon, E. I., Goudarzi, S., and Sutherlin, K. D. (2016) O2 Activation by Non-Heme Iron Enzymes, *Biochemistry 55*, 6363-6374 doi: 10.1021/acs.biochem.6b00635
[50] Muh, F., and Zouni, A. (2020) Structural basis of light-harvesting in the photosystem II core complex, *Protein Sci* doi: 10.1002/pro.3841
[51] Cox, N., Pantazis, D. A., and Lubitz, W. (2020) Current Understanding of the Mechanism of Water Oxidation in Photosystem II and Its Relation to XFEL Data, *Annu Rev Biochem* doi: 10.1146/annurev-biochem-011520-104801
[52] Kern, J., Chatterjee, R., Young, I. D., Fuller, F. D., Lassalle, L., Ibrahim, M., et al, Yachandra, V. K. (2018) Structures of the intermediates of Kok's photosynthetic water oxidation clock, *Nature 563*, 421-425 doi: 10.1038/s41586-018-0681-2
[53] Young, I. D., Ibrahim, M., Chatterjee, R., Gul, S., Fuller, F. D., Koroidov, S., et al, Yano, J. (2016) Structure of photosystem II and substrate binding at room temperature, *Nature 540*, 453-457 doi: 10.1038/nature20161
[54] Kern, J., Tran, R., Alonso-Mori, R., Koroidov, S., Echols, N., Hattne, J., et al, Yachandra, V. K. (2014) Taking snapshots of photosynthetic water oxidation using femtosecond X-ray diffraction and spectroscopy, *Nat Commun 5*, 4371 doi: 10.1038/ncomms5371
[55] Kern, J., Alonso-Mori, R., Tran, R., Hattne, J., Gildea, R. J., Echols, N., et al, Yano, J. (2013) Simultaneous femtosecond X-ray spectroscopy and diffraction of photosystem II at room temperature, *Science 340*, 491-495 doi: 10.1126/science.1234273
[56] Suga, M., Akita, F., Yamashita, K., Nakajima, Y., Ueno, G., Li, H., et al, Shen, J. R. (2019) An oxyl/oxo mechanism for oxygen-oxygen coupling in PSII revealed by an x-ray free-electron laser, *Science 366*, 334-338 doi: 10.1126/science.aax6998
[57] Suga, M., Akita, F., Sugahara, M., Kubo, M., Nakajima, Y., Nakane, T., et al, Shen, J. R. (2017) Light-induced structural changes and the site of O=O bond formation in PSII caught by XFEL, *Nature 543*, 131-135 doi: 10.1038/nature21400
[58] Suga, M., Qin, X., Kuang, T., and Shen, J. R. (2016) Structure and energy transfer pathways of the plant photosystem I-LHCI supercomplex, *Curr Opin Struct Biol 39*, 46-53 doi: 10.1016/j.sbi.2016.04.004
[59] Ayyer, K., Yefanov, O. M., Oberthur, D., Roy-Chowdhury, S., Galli, L., Mariani, V., et al, Chapman, H. N. (2016) Macromolecular diffractive imaging using imperfect crystals, *Nature 530*, 202-206 doi: 10.1038/nature16949
[60] Kupitz, C., Basu, S., Grotjohann, I., Fromme, R., Zatsepin, N. A., Rendek, K. N., et al, Fromme, P. (2014) Serial time-resolved crystallography of photosystem II using a femtosecond X-ray laser, *Nature 513*, 261-265 doi: 10.1038/nature13453
[61] Lu, Y., and Koo, J. (2019) O2 sensitivity and H2 production activity of hydrogenases-A review, *Biotechnol Bioeng 116*, 3124-3135 doi: 10.1002/bit.27136
[62] Ilina, Y., Lorent, C., Katz, S., Jeoung, J. H., Shima, S., Horch, M., et al, Dobbek, H. (2019) X-ray Crystallography and Vibrational Spectroscopy Reveal the Key Determinants of Biocatalytic Dihydrogen Cycling by [NiFe] Hydrogenases, *Angew Chem Int Ed Engl 58*, 18710-18714 doi: 10.1002/anie.201908258

[63] Volbeda, A., Mouesca, J. M., Darnault, C., Roessler, M. M., Parkin, A., Armstrong, F. A., and Fontecilla-Camps, J. C. (2018) X-ray structural, functional and computational studies of the O2-sensitive E. coli hydrogenase-1 C19G variant reveal an unusual [4Fe-4S] cluster, *Chem Commun (Camb) 54*, 7175-7178 doi: 10.1039/c8cc02896f
[64] Schuchmann, K., Chowdhury, N. P., and Muller, V. (2018) Complex Multimeric [FeFe] Hydrogenases: Biochemistry, Physiology and New Opportunities for the Hydrogen Economy, *Front Microbiol 9*, 2911 doi: 10.3389/fmicb.2018.02911
[65] Beaton, S. E., Evans, R. M., Finney, A. J., Lamont, C. M., Armstrong, F. A., Sargent, F., and Carr, S. B. (2018) The structure of hydrogenase-2 from Escherichia coli: implications for H2-driven proton pumping, *Biochem J 475*, 1353-1370 doi: 10.1042/BCJ20180053
[66] Shomura, Y., Taketa, M., Nakashima, H., Tai, H., Nakagawa, H., Ikeda, Y., et al, Higuchi, Y. (2017) Structural basis of the redox switches in the NAD(+)-reducing soluble [NiFe]-hydrogenase, *Science 357*, 928-932 doi: 10.1126/science.aan4497
[67] Kalms, J., Schmidt, A., Frielingsdorf, S., van der Linden, P., von Stetten, D., Lenz, O., et al, Scheerer, P. (2016) Krypton Derivatization of an O2 -Tolerant Membrane-Bound [NiFe] Hydrogenase Reveals a Hydrophobic Tunnel Network for Gas Transport, *Angew Chem Int Ed Engl 55*, 5586-5590 doi: 10.1002/anie.201508976
[68] Evans, R. M., Brooke, E. J., Wehlin, S. A., Nomerotskaia, E., Sargent, F., Carr, S. B., et al, Armstrong, F. A. (2016) Mechanism of hydrogen activation by [NiFe] hydrogenases, *Nat Chem Biol 12*, 46-50 doi: 10.1038/nchembio.1976
[69] Ogata, H., Nishikawa, K., and Lubitz, W. (2015) Hydrogens detected by subatomic resolution protein crystallography in a [NiFe] hydrogenase, *Nature 520*, 571-574 doi: 10.1038/nature14110
[70] Fritsch, J., Lenz, O., and Friedrich, B. (2013) Structure, function and biosynthesis of O(2)-tolerant hydrogenases, *Nat Rev Microbiol 11*, 106-114 doi: 10.1038/nrmicro2940
[71] Volbeda, A., Amara, P., Darnault, C., Mouesca, J. M., Parkin, A., Roessler, M. M., et al, Fontecilla-Camps, J. C. (2012) X-ray crystallographic and computational studies of the O2-tolerant [NiFe]-hydrogenase 1 from Escherichia coli, *Proc Natl Acad Sci U S A 109*, 5305-5310 doi: 10.1073/pnas.1119806109
[72] Banerjee, R., Jones, J. C., and Lipscomb, J. D. (2019) Soluble Methane Monooxygenase, *Annu Rev Biochem 88*, 409-431 doi: 10.1146/annurev-biochem-013118-111529
[73] Elango, N., Radhakrishnan, R., Froland, W. A., Wallar, B. J., Earhart, C. A., Lipscomb, J. D., and Ohlendorf, D. H. (1997) Crystal structure of the hydroxylase component of methane monooxygenase from Methylosinus trichosporium OB3b, *Protein Sci 6*, 556-568 doi: 10.1002/pro.5560060305
[74] Banerjee, R., Proshlyakov, Y., Lipscomb, J. D., and Proshlyakov, D. A. (2015) Structure of the key species in the enzymatic oxidation of methane to methanol, *Nature 518*, 431-434 doi: 10.1038/nature14160
[75] Shu, L., Nesheim, J. C., Kauffmann, K., Munck, E., Lipscomb, J. D., and Que, L., Jr. (1997) An Fe2IVO2 diamond core structure for the key intermediate Q of methane monooxygenase, *Science 275*, 515-518 doi: 10.1126/science.275.5299.515
[76] Nesheim, J. C., and Lipscomb, J. D. (1996) Large kinetic isotope effects in methane oxidation catalyzed by methane monooxygenase: evidence for C-H bond cleavage in a reaction cycle intermediate, *Biochemistry 35*, 10240-10247 doi: 10.1021/bi960596w
[77] Lee, S. K., Nesheim, J. C., and Lipscomb, J. D. (1993) Transient intermediates of the methane monooxygenase catalytic cycle, *J Biol Chem 268*, 21569-21577 doi:
[78] Lee, S. J., McCormick, M. S., Lippard, S. J., and Cho, U. S. (2013) Control of substrate access to the active site in methane monooxygenase, *Nature 494*, 380-384 doi: 10.1038/nature11880
[79] Sazinsky, M. H., and Lippard, S. J. (2005) Product bound structures of the soluble methane monooxygenase hydroxylase from Methylococcus capsulatus (Bath): protein motion in the alpha-subunit, *J Am Chem Soc 127*, 5814-5825 doi: 10.1021/ja044099b
[80] Whittington, D. A., Rosenzweig, A. C., Frederick, C. A., and Lippard, S. J. (2001) Xenon and halogenated alkanes track putative substrate binding cavities in the soluble methane monooxygenase hydroxylase, *Biochemistry 40*, 3476-3482 doi: 10.1021/bi0022487
[81] Whittington, D. A., and Lippard, S. J. (2001) Crystal structures of the soluble methane monooxygenase hydroxylase from Methylococcus capsulatus (Bath) demonstrating geometrical variability at the dinuclear iron active site, *J Am Chem Soc 123*, 827-838 doi: 10.1021/ja003240n
[82] Rosenzweig, A. C., Brandstetter, H., Whittington, D. A., Nordlund, P., Lippard, S. J., and Frederick, C. A. (1997) Crystal structures of the methane monooxygenase hydroxylase from Methylococcus capsulatus (Bath): implications for substrate gating and component interactions, *Proteins 29*, 141-152 doi:
[83] Rosenzweig, A. C., Frederick, C. A., Lippard, S. J., and Nordlund, P. (1993) Crystal structure of a bacterial non-haem iron hydroxylase that catalyses the biological oxidation of methane, *Nature 366*, 537-543 doi: 10.1038/366537a0
[84] Cutsail, G. E., 3rd, Banerjee, R., Zhou, A., Que, L., Jr., Lipscomb, J. D., and DeBeer, S. (2018) High-Resolution Extended X-ray Absorption Fine Structure Analysis Provides Evidence for a Longer Fe...Fe Distance in the Q Intermediate of Methane Monooxygenase, *J Am Chem Soc 140*, 16807-16820 doi: 10.1021/jacs.8b10313
[85] Kal, S., Xu, S., and Que, L., Jr. (2019) Bio-inspired Nonheme Iron Oxidation Catalysis: Involvement of Oxoiron(V) Oxidants in Cleaving Strong C-H Bonds, *Angew Chem Int Ed Engl* doi: 10.1002/anie.201906551
[86] Pau, M. Y., Lipscomb, J. D., and Solomon, E. I. (2007) Substrate activation for O2 reactions by oxidized metal centers in biology, *Proc Natl Acad Sci U S A 104*, 18355-18362 doi: 10.1073/pnas.0704191104
[87] Seefeldt, L. C., Yang, Z. Y., Lukoyanov, D. A., Harris, D. F., Dean, D. R., Raugei, S., and Hoffman, B. M. (2020) Reduction of Substrates by Nitrogenases, *Chem Rev* doi: 10.1021/acs.chemrev.9b00556
[88] Chen, J. G., Crooks, R. M., Seefeldt, L. C., Bren, K. L., Bullock, R. M., Darensbourg, M. Y., et al, Schrock, R. R. (2018) Beyond fossil fuel-driven nitrogen transformations, *Science 360* doi: 10.1126/science.aar6611

[89] Saito, M. A., Bertrand, E. M., Dutkiewicz, S., Bulygin, V. V., Moran, D. M., Monteiro, F. M., et al, Waterbury, J. B. (2011) Iron conservation by reduction of metalloenzyme inventories in the marine diazotroph Crocosphaera watsonii, *Proc Natl Acad Sci U S A 108*, 2184-2189 doi: 10.1073/pnas.1006943108
[90] Saito, M. A., McIlvin, M. R., Moran, D. M., Goepfert, T. J., DiTullio, G. R., Post, A. F., and Lamborg, C. H. (2014) Multiple nutrient stresses at intersecting Pacific Ocean biomes detected by protein biomarkers, *Science 345*, 1173-1177 doi: 10.1126/science.1256450
[91] Tagliabue, A., Bowie, A. R., Boyd, P. W., Buck, K. N., Johnson, K. S., and Saito, M. A. (2017) The integral role of iron in ocean biogeochemistry, *Nature 543*, 51-59 doi: 10.1038/nature21058
[92] Keable, S. M., Vertemara, J., Zadvornyy, O. A., Eilers, B. J., Danyal, K., Rasmussen, A. J., et al, Peters, J. W. (2018) Structural characterization of the nitrogenase molybdenum-iron protein with the substrate acetylene trapped near the active site, *J Inorg Biochem 180*, 129-134 doi: 10.1016/j.jinorgbio.2017.12.008
[93] Sippel, D., and Einsle, O. (2017) The structure of vanadium nitrogenase reveals an unusual bridging ligand, *Nat Chem Biol 13*, 956-960 doi: 10.1038/nchembio.2428
[94] Morrison, C. N., Spatzal, T., and Rees, D. C. (2017) Reversible Protonated Resting State of the Nitrogenase Active Site, *J Am Chem Soc 139*, 10856-10862 doi: 10.1021/jacs.7b05695
[95] McGale, J., Cutsail, G. E., 3rd, Joseph, C., Rose, M. J., and DeBeer, S. (2019) Spectroscopic X-ray and Mossbauer Characterization of M6 and M5 Iron(Molybdenum)-Carbonyl Carbide Clusters: High Carbide-Iron Covalency Enhances Local Iron Site Electron Density Despite Cluster Oxidation, *Inorg Chem 58*, 12918-12932 doi: 10.1021/acs.inorgchem.9b01870
[96] Keable, S. M., Zadvornyy, O. A., Johnson, L. E., Ginovska, B., Rasmussen, A. J., Danyal, K., et al, Peters, J. W. (2018) Structural characterization of the P(1+) intermediate state of the P-cluster of nitrogenase, *J Biol Chem 293*, 9629-9635 doi: 10.1074/jbc.RA118.002435
[97] Tezcan, F. A., Kaiser, J. T., Howard, J. B., and Rees, D. C. (2015) Structural evidence for asymmetrical nucleotide interactions in nitrogenase, *J Am Chem Soc 137*, 146-149 doi: 10.1021/ja511945e
[98] Henthorn, J. T., Arias, R. J., Koroidov, S., Kroll, T., Sokaras, D., Bergmann, U., et al, DeBeer, S. (2019) Localized Electronic Structure of Nitrogenase FeMoco Revealed by Selenium K-Edge High Resolution X-ray Absorption Spectroscopy, *J Am Chem Soc 141*, 13676-13688 doi: 10.1021/jacs.9b06988
[99] Sippel, D., Rohde, M., Netzer, J., Trncik, C., Gies, J., Grunau, K., et al, Einsle, O. (2018) A bound reaction intermediate sheds light on the mechanism of nitrogenase, *Science 359*, 1484-1489 doi: 10.1126/science.aar2765
[100] Spatzal, T., Perez, K. A., Einsle, O., Howard, J. B., and Rees, D. C. (2014) Ligand binding to the FeMo-cofactor: structures of CO-bound and reactivated nitrogenase, *Science 345*, 1620-1623 doi: 10.1126/science.1256679
[101] Spatzal, T., Aksoyoglu, M., Zhang, L., Andrade, S. L., Schleicher, E., Weber, S., et al, Einsle, O. (2011) Evidence for interstitial carbon in nitrogenase FeMo cofactor, *Science 334*, 940 doi: 10.1126/science.1214025
[102] Schmid, B., Ribbe, M. W., Einsle, O., Yoshida, M., Thomas, L. M., Dean, D. R., et al, Burgess, B. K. (2002) Structure of a cofactor-deficient nitrogenase MoFe protein, *Science 296*, 352-356 doi: 10.1126/science.1070010
[103] Einsle, O., Tezcan, F. A., Andrade, S. L., Schmid, B., Yoshida, M., Howard, J. B., and Rees, D. C. (2002) Nitrogenase MoFe-protein at 1.16 A resolution: a central ligand in the FeMo-cofactor, *Science 297*, 1696-1700 doi: 10.1126/science.1073877
[104] Schindelin, H., Kisker, C., Schlessman, J. L., Howard, J. B., and Rees, D. C. (1997) Structure of ADP x AlF4(-)-stabilized nitrogenase complex and its implications for signal transduction, *Nature 387*, 370-376 doi: 10.1038/387370a0
[105] Smil, V. (1999) Detonator of the population explosion, *Nature 400*, 415-415 doi: 10.1038/22672
[106] Erisman, J. W., Sutton, M. A., Galloway, J., Klimont, Z., and Winiwarter, W. (2008) How a century of ammonia synthesis changed the world, *Nat Geosci 1*, 636-639 doi: 10.1038/ngeo325

8.7 Overall economic context

A UK-XFEL would be a cutting-edge large scale scientific facility that would operate a world-leading programme of frontier research. Researchers from the UK and worldwide would tackle fundamental scientific challenges across the Life and Physical Sciences, creating substantial benefits to skills and innovation in science and technology. This fundamental research will lead to multiple innovative applications, supporting technological innovation and commercialisation over many decades.

A UK-XFEL would be a strategic asset to the UK for the manufacturing, defence, medical and technology sectors. As well as the fundamental benefit to the UK economy from construction, procurement and operation, a world leading XFEL facility with unique x-ray capabilities would enhance the UK's position as a centre for advanced science and innovation. UK Industry that can collaborate with cutting-edge facilities are able to increase the rate of technological progress, improve process and hence deliver enhanced economic benefits and job growth over the long term. Without investment in a UK XFEL industry would not easily be able to access such a unique X-ray source due to the access challenges and higher costs of collaborating with existing facilities internationally. These sources are likely to become increasingly an essential national technology resource in the coming decades. A UK XFEL would safeguard future research and innovation capability for industrial and defence sectors for years to come, giving them access to a world-class facility and relevant scientific and technological experts.

Locating an XFEL in the UK will create greater benefit for local firms and workers and lead to greater capitalisation from the training of skilled scientists and engineers that would be required to design, build and operate such a facility. In addition, a UK XFEL would act as a catalyst for regional development, creating new industrial clusters and attracting investment and highly skilled workers.

Large scale research facilities in the UK typically provide thousands of days of user access to PhD students. During this time they are receiving training and gaining valuable 'on-the-job' skills and knowledge that can be applied in the UK academic and wider economy over their future working life. Overseas students would naturally be attracted to such a flagship facility, and many of these would settle (or return) to the UK to pursue their future careers. Staff and users of the UK-XFEL would be expected to learn specialist skills that are highly valuable to industry. Aside from pursuing careers in industry following time at the facility, industry would be able to access these skills via collaborative research or knowledge exchange programmes.

8.7.1 Areas of Economic Impact

Many potential economic benefits would be realised from the building of a UK XFEL. These include:

- Economic benefit to external suppliers through direct employment and purchasing – construction, upgrades and maintenance of a UK XFEL. A significant fraction of the expenditure for a UK XFEL would go to companies and suppliers based in the UK, many of which would be local.
- Creation of new businesses / spin-outs to capitalise on the outputs of user research or facility developments and subsequent benefits to the supply chain of these companies. Based on the experience of other large-scale research facilities in the UK it is expected that a number of 'spin-out' companies will be formed during the lifetime of a UK XFEL. Societal benefits from fundamental research can often take years to realise. Government-funded large facilities, however, have proven experience in accelerating this process by exploiting innovative research through IP protection, proof-of-concept funding and support for spin-out companies.
- Employment of Facility Staff – A UK XFEL would require hundreds of staff, many highly skilled, to operate the facility.

- PhD and Post-doctoral wage premiums for students who receive training on the facility – as a result of receiving skills-related training on site during their visits, many thousands of PhD and post-doctoral visitors will benefit from an earnings premium over their subsequent career.
- Apprenticeships and training of non-scientific staff in engineering, analytical technology, chemical- and bio-technology, IT and big data (including machine learning), optics and advanced electronics.
- Economic benefit to firms from commercial and industrial access to the XFEL, e.g. through improvements to existing materials and processes.
- Agglomeration benefits from the formation of science and technology clusters co-located with the facility. The co-location of firms working in similar sectors has been shown to positively impact rates of innovation and productivity.
- Economic benefit of visitors to the facility – It is anticipated that there would many thousand individual scientific visits (as a user or for collaborative work) to a UK XFEL facility per year, as well as members of industry, commercial or other public bodies. These visitors would have a positive impact on the local economy in terms of spend of accommodation, subsistence and travel.

8.7.2 Return on Investment

One of the primary methods to determine the value for money (VfM) of building a large-scale facility such as UK XFEL is to look at the estimated impact of R&D that results from the facility on the overall economy (see section above). While an estimate of the possible benefits that can be directly attributed to the creation of a new facility can be performed (a 'bottom-up' approach) it is important to recognise the broader benefits to the UK economy that would result from investment in an UK XFEL. For example, fundamental research performed in the short term is likely to drive technological innovation in the longer term that uses knowledge developed indirectly from user experiments and facility developments. * Directly estimating the benefit of attracting highly skilled scientists and organisations to cutting-edge XFEL facility can also be hard to quantify.

An alternative 'top-down' approach can use published literature on rates of return on investment in science and technology. This approach covers the direct rate of return on the investment to the funder (the UK Government) as well as wider benefits to the UK economy. Published literature (a summary of which is contained in "Rates of return to investment in science and innovation" – Frontier Economics 2014) estimates a mean rate of return of 30% on the investment to the funding source, with a mean social rate (which covers broader societal benefits through spill-over effects) of two to three times that. A recent comprehensive analysis was undertaken for STFC's Extreme Photonics Applications Centre (EPAC), a facility which will use high power lasers to produce unique secondary radiation sources for fundamental science and industrial applications. While EPAC is different in terms of the driving technology and capability, there are striking similarities in terms of the opportunities that both facilities would offer across many science and technology sectors. The total benefit of the related R&D of the EPAC facility was found to have a mean R&D multiplier value of 1.85. This factor would be applied to anticipated expenditure on a UK XFEL in order to estimate the broader economic benefits of such investment.

The uniqueness of a UK XFEL would likely generate greater returns than this figure owing to the many areas of applied research across technology, engineering and healthcare that rely on high levels of contribution from core academic research.

9. UK Facility Requirements and Options Analysis

The science opportunities discussed in the preceding sections will require an ambitious machine with new capabilities beyond those currently available anywhere. Here we examine what capabilities are needed, both in terms of the X-ray characteristics and the other supporting features available at end-stations, to allow the full realisation of the science. The X-ray requirements include the need for a high repetition rate machine across a significant photon energy range, as well as high brightness, narrow bandwidth and ultrashort pulses. Even with a superb X-ray capability, the facility will not deliver the most exciting science without properly equipped end-stations that bring the full range of laser, THz and electron beams to the interaction point. These science needs are used to define a facility specification that informs the set of concept outline designs presented in **Appendix 1**. These new machine options, along with other options to proceed that do not involve building a facility in the UK, are examined in an options analysis that weighs the pros and cons of a number of ways to go forward.

9.1 Facility X-ray requirements: photon energy, bandwidth, pulse duration, repetition rate and pulse energy

A diverse and ambitious range of scientific opportunities has been described in Sections 3 to 8. This section summarises the key X-ray requirements from all of these science areas. An analysis has also been carried out to identify key requirements of common interest across the science areas, which would lead to unique facility capability. A landscape of the various requirements has been identified that would inform facility design choices in future.

9.1.1 Key requirements by science area

Each of the science areas described in **Sections 3 to 8** contains a wide variety of experimental interests and methods. A summary of such a rich and complex landscape cannot capture every intricate detail. Rather, some of the key requirements central to the mission of each science area have been identified: these are presented in **Figure 9.1**, and are described in turn below.

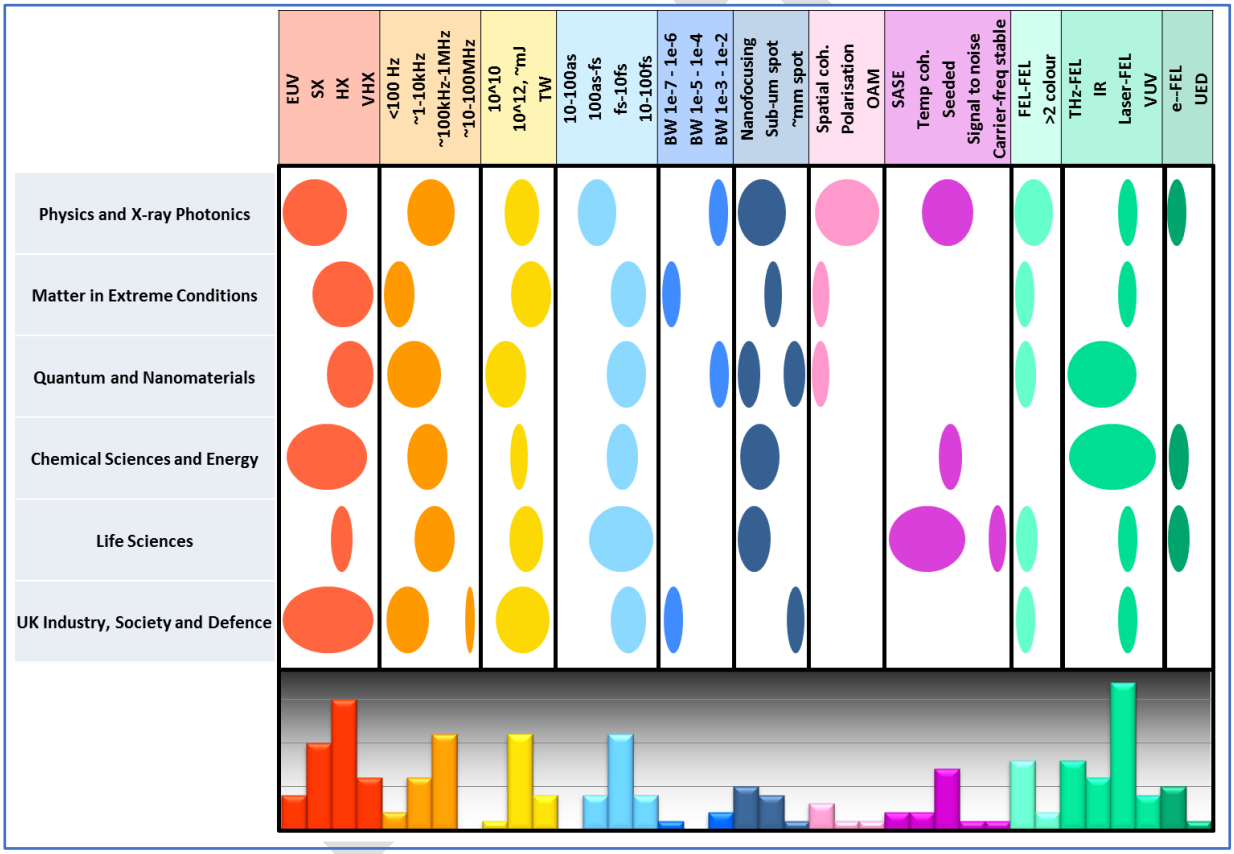

Figure 9.1: Summary of the key requirements of the different science areas

Key: *The different colours correspond to properties of the X-ray light (photon energy, repetition rate, etc.), including additional sources to be used in combination (THz, IR, etc.). Each coloured category features an internal scale or range of options (sub-category).*

*The science requirements of **Sections 3 to 8** were analysed for key features. The coloured ellipses represent the requirements in each category, for each science area. The bar chart indicates the number of sub-sections in the text (or direct input) that highlight that sub-category – allowing requirements of the highest common interest (e.g. hard X-rays, combination with optical lasers) to be identified. Associations between certain properties can also be identified.*

9.1.1.1 Physics and X-ray Photonics

The key requirements are for attosecond pulses (~100 as) across a broad range of photon energies, from 200 eV to hard X-ray, with sub-femtosecond synchronisation to optical lasers (combination with electrons and other FEL pulses is also of interest). Control of pulse properties, such as polarisation and orbital angular momentum, and through seeding are also highlighted. High repetition rates (> 10 kHz) are preferred.

9.1.1.2 Matter in Extreme Conditions

The key requirements are for X-ray pulses with high pulse energy (mJ to orders of magnitude higher) and high photon energy (up to 30-50 keV), in combination with very high-energy optical lasers. Repetition rate is generally less demanding. Narrow bandwidth (10 meV), two-colour FEL capability and sub-micron spot sizes are called for.

9.1.1.3 Quantum and Nanomaterials

The key requirements are for soft to very hard X-rays (up to ~50 keV would open up new opportunities), in combination with pump sources across a broad range of wavelengths (THz to visible), as well as two-colour FEL capability. Sub-femtosecond synchronisation is important in all cases. Repetition rate can be as low as 10 Hz in some experiments, due to sample recovery times, but high average flux is needed in others.

9.1.1.4 Chemical Sciences and Energy

The key feature of the requirements for this science area is to combine XFEL pulses with a multitude of different sources: accelerator based THz, electron beam pump sources, along with numerous synchronized laser-based sources. The X-rays should be soft to very hard (> 25 keV for some experiments) and high repetition rate (1 kHz to 1 MHz). For some experiments, a bandwidth below 1×10^{-4} is needed. Two-colour FEL operation is also important, with the possibility of combining two XFEL pulses in various combinations of soft (from 200 eV to 3000 eV) and hard X-rays (from 5 to 25 keV).

9.1.1.5 Life Sciences

This science area calls for hard X-rays (5 - 25 keV) at high repetition rates (1 kHz to potentially as high as 1 MHz, depending on detector capabilities). A key requirement is for precise control of the X-ray pulse properties - stability of carrier frequency, pulse energy, instantaneous bandwidth and spectrum. Two-colour FEL operation with the ability for large variation in temporal (fs – µs) and energy separation is important, as well as combination with electrons.

9.1.2 Requirements of common interest and unique facility capability

Through analysis of the requirements of each of the science areas, it is possible to identify features of common interest associated with unique capability. These are indicated in **Figure 9.1** and are summarised below.

9.1.2.1 Photon energy

The requirements for photon energy are focused on hard and soft X-rays, but also with significant interest above the current state of the art (~25 keV), up to approximately 50 keV. There is also interest in lower photon energies, down to ~200 eV.

9.1.2.2 Repetition rate

The majority of the science areas call for high repetition rates: from 1 kHz up to 100 kHz, and to 1 MHz in some cases. Some areas (EUV lithography, gammas for nuclear application) would benefit from still higher rates (~100 MHz). A few areas are limited to 10 - 100 Hz, due to sample recovery time, etc.

9.1.2.3 Pulse duration/bandwidth

There is significant interest in extremes of pulse duration (ultra-short pulses to ~100 attoseconds) and bandwidth (ultra-narrow $\sim 10^{-7}$ relative bandwidth).

9.1.2.4 Two-colour modes

There is interest in two-colour modes, including soft and hard X-ray options.

9.1.2.5 Other spatio-temporal properties

There is a major requirement to improve control of pulse properties, including shot-to-shot reproducibility through the use of seeding. There is significant interest in sub-micron spot sizes, as well as recognition of the importance of controlling polarisation and orbital angular momentum.

9.1.2.6 Combination between sources

The most frequently highlighted requirement of all is to combine X-rays with optical lasers, while combination with THz-IR and electrons are also frequently requested. These requirements are discussed in **Section 9.2**. Two-colour or multi-colour FEL capabilities are also frequently highlighted, with unique capabilities including extending the range of energy/temporal separation.

9.1.3 Associated requirements

The requirements of common interest identified in **Section 9.1.2** above are clearly not all required simultaneously in any one experiment. By recognising associations between the different requirements, an indication of the optimal way of meeting them can be determined. This could inform facility design choices in future (see **Appendix 1**). Some of the key associated parameter combinations are as follows:

- **Photon energy and repetition rate:** the science areas indicate a general trend for high repetition rates at lower photon energies, and somewhat lower repetition rates at high photon energies, as shown in **Figure 9.2**.
- **Pulse energy and photon energy:** in general, it is required to have higher energy per pulse for experiments at high photon energy (matter in extremes, industrial applications etc.).

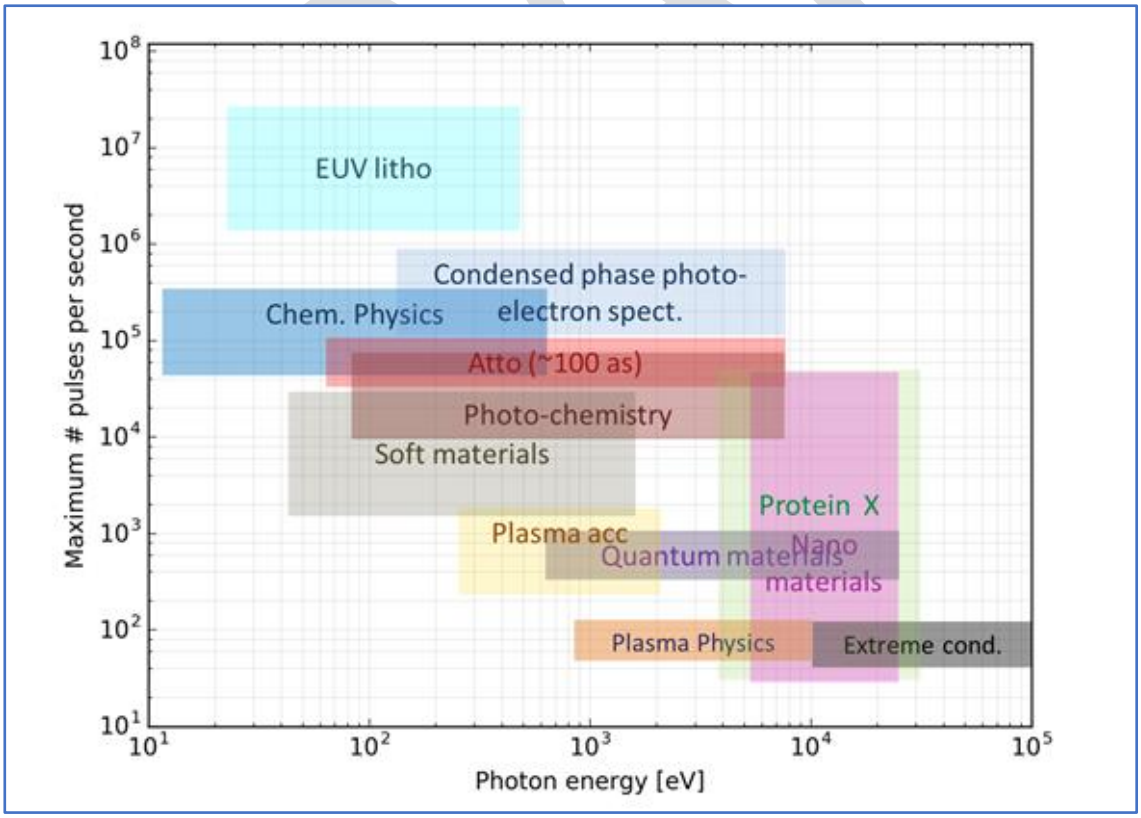

Figure 9.2: Requirements of different areas of the science case in terms of photon energy and repetition rate

Specific categories of the science case are used to clearly demonstrate the trade-off between the parameters

9.2 Facility General Requirements

Although the unique X-ray properties are at the core of the new science made possible by XFELs, a successful XFEL facility with maximal scientific reach must have provision for many other features.

A great deal of the added value of the UK XFEL plans can come from these auxiliary features that will enable a broad swathe of new science not possible elsewhere. These general requirements are discussed here. They are informed by the Science Cases (**Sections 3 – 8**) and by the many years of collective experience of XFEL users and operators of existing facilities.

Since the time-resolved capabilities of XFELs arise largely from pump-probe experiments it is inevitable that ultrafast lasers are a key requirement. By looking to the latest optical technologies we can ensure the availability of ultrafast pulses spanning the wavelength range from 10 µm to less than 100 nm (photon energies 0.12 – 12 eV). The synchronisation and time tool strategies explained in 9.1 can then be used to deliver pump-probe timing determination approaching 1 fs (and eventually shorter than this). For still longer wavelengths of importance to, for example, chemistry and condensed phase systems accelerator based THz options (based on bends or short undulators) can be developed (see below). For some of the most adventurous physical science in this case (**Sections 3.5** and **3.6**, and **Section 4**) high power lasers capable of reaching focused intensities > 10^{19} Wcm^{-2} are required to operate at a repetition rate matching to the HXR beamlines. For shock compression and high energy density systems a rep-rated high energy laser (of a kJ class) would permit world leading science. Other capabilities offered at the interaction points with the X-rays that will greatly extend the science range are electron beams and high magnetic fields. Beyond this sample delivery and sample preparation of the most advanced kind are required to enable a truly world-beating range of experiments. The most advanced detectors, for X-rays and emitted charged particles, of exceptional sensitivity, dynamic range and able to accept the full repetition rate of the X-rays pulses are also essential. All the detectors and diagnostics systems will generate vast quantities of data and the hardware, software and administrative strategies to handle these must be designed into the facility at the outset.

9.2.1 Femtosecond optical pump sources 10 µm to less than 100 nm

The dynamics of matter can be studied by selectively probing excitations e.g. electronic, vibrational and rotational. These naturally lie in a range of photon energies (wavelengths) ranging from the deep UV through the optical to the far IR part of the electromagnetic spectrum, as reflected by the commensurate timescales illustrated in **Figure 9.1**. Electronic excitations of the valence states of neutrals and ions lie in energy ranges typically from 20 eV to 0.4 eV (50 nm to 2 µm). Vibrational excitations/ phonons lie in the range from 0.4 eV – 0.02 eV (2 – 20 µm), whilst rotations are at still lower energies/ longer wavelengths. Raman excitation, as opposed to direct single photon excitation, offers ways to access these excitations using shorter wavelength sources, but sometimes direct excitation is required. This sets a wide variety of target photon energies/wavelengths that must be accessed from a femtosecond laser. This is generally done using a range of non-linear optical techniques: optical parametric amplification (OPA), difference frequency generation (DFG), harmonic generation (second-, third-, fourth, fifth-), and high harmonic generation. OPAs are especially attractive, as they offer continuous tunability over significantly wide wavelength ranges and can access a wide range of other wavelengths through coupling to the other non-linear techniques.

Most early experiments at XFELs used Ti:S CPA architecture femtosecond lasers, but, as the repetition rates of XFELs have increased, this technology is sometimes limiting, although it will doubtless still continue as a workhorse for decades to come. New technologies include: disc laser pumped OPCPA lasers offering 100 -200 kHz repetition rate and intrinsically short pulses; and fibre lasers using coherent combination of multiple fibre outputs that can approach the 1 MHz repetition rate, be pulse compressed to short duration, and be used in conjunction with OPAs and other non-linear methods to cover the required spectral ranges. It is likely a UK XFEL will embrace all of these technologies, plus

others under development, to access the full range of required wavelengths at the required repetition rate.

Although in most current XFEL facilities pump laser pulse durations of 30 fs have been deemed adequate, as the X-ray pulses become shorter the laser pump pulses must be matched with comparably short pulses. Some XFEL end-stations are starting to use hollow core fibre pulse compression, and new fibre and structured fibre technologies are likely to see widespread use across diverse wavelength ranges. Recent work has shown the utility of structured (Kagome) fibres for deep UV pulses of ~ 3 fs duration[1], and exceptional performance of stretched hollow core fibres in non-linear pulse generation across a broad spectral range[2].

The need to go to longer wavelengths will require a combination of laser-based THz generation methods to reach to 10 THz, and potentially machine-based THz methods to cover the 10 – 30 THz range (see below). These pulses are necessarily far longer in duration than the optical domain pulses (picoseconds rather than femtoseconds), but their key role in exciting the modes of importance to thermally-excited samples (**Section 6**), and of driving condensed phase systems beyond normal equilibrium (**Section 5**), mandate that they be available.

For wavelengths shorter than 220 nm a number of options exist. There are some promising structured and hollow fibre based approaches that offer relatively high power to around 120 nm[3,4]. To reach into the VUV - XUV range (10 – 50 eV), the conventional choice is high order harmonic generation that has been shown to be driven by high repetition rate lasers[5]. In the energy range to 25 eV, relatively high conversion efficiencies (10^{-5} - 10^{-6}) have been demonstrated, so pulses of 1 - 10 nJ are possible, even for high repetition rates, which are of sufficient energy to pump the small sample volumes probed in typical XFEL experiments.

9.2.2 High energy and high power lasers

The requirement for LWFA and other MEC-related high energy density pumping (**Section 4**) necessitates the availability of a high power multi-Petawatt class laser with <30 fs pulse duration, that can be focused to intensities from 10^{18} Wcm^{-2} to those exceeding 10^{22} Wcm^{-2}. Multiple focusing geometries (and hence focused laser intensities), coupled with high repetition-rate targetry, would permit access to a broad range of extreme conditions and laser-driven secondary sources. To provide a really unique capability, we should aspire to a 100 Hz repetition rate laser system. These higher repetition rates will greatly benefit the observation of rare events, including the study of non-linear QED systems driven by ultra-intense electromagnetic fields, where statistical analysis of multiple events will be required. Many applications of secondary sources generated by high intensity lasers will also require higher repetition rates. A new high repetition-rate, high intensity laser would provide an attractive platform to optimise existing applications and draw users from a broad range of research fields when coupled with a powerful X-ray probe. Conversely a high power laser could also be used to probe XFEL-driven non-linear dynamics; hence a high-repetition rate source should be a priority, to exploit the capability of an ultra-intense hard X-ray source.

The rapid advancement of diode-pumped laser technology has made possible the construction of lasers such as D100-X (developed by the Central Laser Facility in the UK and recently installed at the European XFEL). D100-X uses innovative diode-pumped, cryogenically gas cooled amplification medium to produce high energy (>100 J) laser pulses at high repetition rates (10 Hz). The same diode pumped laser system will also power the 10 Hz petawatt laser source for the new Extreme Photonics Applications Centre (EPAC), for which construction is currently underway. This innovative technology could be scaled to produce higher energies and/or repetition rates, depending on the evolution of the science drivers.

To ensure unique new science is possible in the shock compression area and studies of warm dense matter (WDM), a kJ class nanosecond laser is required in order to reach the highest energy densities and pressures. A 10 Hz repetition rate is an aspiration – going to higher as the technology evolves. Multiple high-energy beams could be combined in order to provide novel geometries for compressed

matter experiments, as well as to provide a more scalable path to the highest laser energies (and hence experimental pressures). The laser temporal profile should also be tuneable (as per D-100X), in order to provide access to a range of energy states.

9.2.3 THz, high magnetic fields and relativistic e-beams at interaction points

It is possible to obtain intense pulses of THz light, synchronised to the FEL pulse, from electron beams using a number of different mechanisms. The FEL electron beam is used at the TeraFERMI beamline[6] after it has passed through the FEL and just before it is dumped. In this example, the electrons pass through a thin metal foil and emit coherent transition radiation. An alternative is to pass the spent beam through a long period undulator to generate the THz, as is the case at FLASH[7], although this becomes much less attractive at higher electron beam energies as the undulator period becomes unfeasibly large. Another option to consider would be the generation of a low energy, short bunch, electron beam (of order 10 MeV) close to the FEL beamline for efficient undulator light production. This electron beam would be well synchronised to the FEL pulse using established techniques, and could also be used as a source for electron diffraction at the end-stations.

The interaction of materials with magnetic fields is a rich source of information on their magnetic and spin quantum properties. Work at LCLS investigating X-ray scattering from materials using their 30 T pulsed magnetic field apparatus has revealed new insights into quantum materials[8]. It would seem an excellent aspiration to equip at least one hard X-ray end-station with a pulsed high B field facility to progress research in this direction. The possibility for a high field DC magnet might also be considered, given that the pulse repetition rate in both hard- and soft-X-ray would deliver unprecedented measurement sensitivity that could transform our understanding. The options for doing this would need to be further reviewed under the activities associated with preparing a Conceptual Design Report.

The demands for pulsed radiolysis (**Section 6**) and the prospects for UED (**Appendix 2.1**), potentially combined with correlated X-ray spectroscopy and X-ray scattering on the same sample, demand that a synchronized relativistic (1 - 5 MeV) electron gun be located at least at one of the end-stations. This will open up new science not available at any existing XFEL facility, as well as enabling an independent programme of research driven by UED alone. The technology of these guns is now mature enough that we can be confident that this is achievable[9]. The CDR process will need to analyse the strategies for synchronization with the X-rays, the extent to which a common suite of scattering detectors can be used, and radiological protection issues. Other laser accelerated electron and ion beam capability will be developed to extend possibilities to higher energy electrons to the GeV range (see **Section 4.3**), accelerated protons and various ions. This will lead to a world-leading capability.

9.2.4 Sample delivery, sample environments and fabrication

The particular characteristics of X-ray scattering experiments at XFELs, i.e. the powerful concept of “diffract-before-destroy” that has driven progress in serial nanocrystallography and coherent diffraction imaging, have demanded the development of new concepts in sample delivery. Great progress was made by the development of an array of liquid injector and gas dynamic virtual nozzle (GVDN) injectors[10]. The challenge now is to increase the throughput and develop sample on demand technology that will ensure every X-ray pulse results in useful data (rather than the high fraction of “misses” that is the current norm). Technology is moving quickly, with sample array technologies as well as sample on demand injectors being developed. The aspiration should be to ensure the most efficient data collection and highest throughput. A further aspiration is that users need not even accompany their samples to the XFEL, which will greatly expand the number of scientists and Pharma companies who use XFELs as a routine part of their research efforts.

For X-ray spectroscopy, a similarly wide array of liquid jet technologies is available that can optimise the measurement using XAS, XES and RIXS[11 12]. An important motivation for high repetition rate is that very dilute samples, for example consistent with the concentrations in naturally occurring biochemistry, can be studied and optimised sample environments, that minimize noise in the detection channel, must be further developed.

Solid state samples of importance in materials science face a limitation due to sample damage (both pump beam and X-ray induced). This effect has hitherto limited data acquisition to relatively low repetition rates. Sample growth facilities to provide a ready supply of high-quality samples, and moving sample holders that allow a fresh region to be probed even at a high repetition rate, must be developed to fully exploit the capabilities of the XFEL. Solid samples for high energy density (HED) science, and diamond anvil cells transparent to X-ray probing, will also need to be developed. HED science has traditionally been performed at low-repetition rate, high energy laser facilities (with repetition rates below a minute) and, as the sample must be replaced for each shot, this has become the low through-put working mode. It is reasonable to move towards faster sample refreshment that could see a step change in data quality, enabled by far higher repetition rate X-ray pulses (for directly creating warm dense matter (WDM)) and the rep-rated high energy laser. To achieve the higher-rep rate objective, developments in target fabrication and presentation to the beams will be required.

9.2.5 Advanced X-ray detectors

X-ray imaging detectors of high sensitivity and dynamic range, and operable at high repetition rate, are essential for all X-ray scattering measurement, and also for momentum-spectrum resolved RIXS and spectroscopy measurements. This has been an area of dedicated progress across a number of organisations over a long period of time (including RAL UK, PSI Switzerland, DESY Germany and SLAC USA) and excellent detectors for the current range of repetition rates are available. For anticipated higher repletion rates (> 50 kHz) new detectors are under development, but approaching the near future 1 MHz rates are still seen as a major challenge.

The development of hybrid technology detectors, with charge integrating front-end electronics instead of photon counting, has been critical for XFEL sources, where many photons arrive at the detector in a very short period of time due to the pulsed nature of the source. These detectors need to have single photon sensitivity (i.e. the detector equivalent noise charge must be smaller than the charge released in the sensor by a single photon event) and they also need to be able to detect a large number of photons at one time (up to 10^6 photons/pulse) without going into saturation. Hybrid integrating detectors are in use at existing XFEL sources, such as LPD, AGIPD, and DSSC developed for the European XFEL, ePix detector developed for LCLS at Stanford, and the JUNGFRAU detector developed for the SwissFEL. The JUNGFRAU detector can run at a frame rate up to 2.4 kHz, and the development team is planning further improvements of the chip that aim to bring the maximum frame rate to around 4 kHz. At SACLA, CITIUS, an integrating detector with a frame rate of 17.4 kHz, is under development.

Further initiatives are currently underway to meet the challenges that are posed by the next generation of XFELs, such as LCLS-II or the upgrade of the European XFEL. These new sources will require detectors running at a frame rate of 100 kHz and above, expected to be in routine operation within the next 10 years. For instance, at LCLS the plans are based around the ePIX detector family with ePIXHR (5 kHz) now being rolled out for LCLS II, and future models ePIXHR2.5D (25 kHz) and ePIXUHR (100 kHz-1 MHz) in the development pipeline. Nevertheless, at SLAC it has been recognised that no single detector solution will satisfy all future applications. There remains an urgent need for innovation and continuing R & D in this arena, but on the timescale of 10 years off-the-shelf solutions will be ready for UK XFEL, likely up to the 100 kHz rate.

9.2.6 Electron and charge particle detection

Many measurement modes utilise emitted electrons and ions that carry the signatures of dynamical changes, e.g. in X-ray photoelectron spectroscopy (XPS), angle resolved electron spectroscopy (ARPES), and coincidence-based momentum imaging. Favoured techniques, such as velocity map imaging (VMI) and electron/ion time-of-flight (TOF) measurements, can still be used at higher rep-rates, but there will be limits placed at high repletion rates (on readout speeds in the case of VMI and flight times in the case of TOFs). Technical developments to provide efficient high throughput analogues to TOF and VMI will be required to optimise instruments at a number of end-stations. ARPES using standard hemispherical analysers is in principle compatible with high repetition rates, but, unless integration

over many shots is required, upgraded fast readout detectors will need to be used to access single shot data. Momentum imaging techniques, such as COLTRIMs, are intrinsically designed for high data rate acquisition, and the REMI instrument at the European XFEL and the soon to be commissioned DREAM instrument at LCLS are already able to handle the higher repetition rates.

Most end-stations should be configured with a dedicated set of high calibre instrumentation, to ensure high quality data and high scientific productivity. Nevertheless, some provision for "roll-up" user supplied end-stations should be retained, to ensure operational flexibility and future-proofing through the development of new experimental concepts.

9.2.7 Data infrastructure and management for operating at high rep-rate

Along with the massive scientific advantages associated with the high data rate from a high repetition rate XFEL comes a heavy cost in terms of data transfer, storage and management. At the existing high repetition rate facilities, it has been realised that the cost of proceeding without significant data compression and intelligent data retention policies is too high to be viable (estimated at around $0.25 billion in the case of LCLS II and would grow further). Analysis of LCLS II suggests that each working end-station operating at 1 MHz will generate in the range of 100 Gb/s – 1 TB/s. In their planning, the account for a factor of 10 reduction through data compression to 10 GB/s – 100 Gb/s. Part of this compression will be in the form of on-chip data reduction using FGPA's integrated to the front-end detectors. Compression via feature extraction, vetos, and multi-event reduction must all form part of the strategy. At the same time, it is vital to provide the possibility of fast feedback to the users in real-time during the experiment to ensure efficient use of beamtime. Very large off-line data storage and analysis capability will be essential, requiring multiple 100 PB storage capacity. To manage this will require the implementation of an intelligent set of policies on data retention. It is important to start planning hardware, software and administrative policies from the outset, to avoid serious problems later.

The advantages of greater coherence and stability of X-rays by going beyond SASE modes (seeding, eSASE, superradiance schemes) is that the required experimental signal may be measured in a greatly reduced number of shots compared to conventional SASE operation. Experience with two-pulse SASE X-ray modes, where spectral/temporal/intensity fluctuations effecting both pulses in the pair requires aggressive data sorting, has shown that a down selection by several orders of magnitude is often required, which would be greatly improved were seeded and stable operation to be available. Moreover, the pulse-to-pulse X-ray diagnostics are very expensive in terms of data volume, especially if they involve detector arrays (e.g. spectral or temporal measurements like XTCAV) - it has been shown that machine learning approaches to X-ray diagnostics can be hugely beneficial in this regard[13].

A fully integrated controls environment must be developed for the entire facility, including all end-stations and experimental installations. The experience required to do this is available from Diamond. LCLS, European XFEL etc.

9.2.8 Auxiliary support facilities

To allow the efficient delivery of the science mission of UK XFEL will require an extensive array of state-of-the-art support facilities, as well as excellently equipped end-stations.

Capability for sample preparation and fabrication will be central to supporting the best science. Nanofabrication capability on-site, including nanoscribe, fast-ion beam (FIB), sample growth and nano-lithography, will be required. Laboratories for safe preparation of high-quality chemical and biological samples will likewise be required. If the industry demand arises, there may need to be facilities for handling nuclear materials. Additionally, first class machine shop, optical testing and coating, and electronics workshop facilities will be necessary to support both the in-house facility development and the R & D programmes, as well as the user science programme. This includes local testing and measurement labs equipped with sample characterisation capability, such as LEED, TEM, and SEM, as well as standard optical and 2-photon microscopy.

Further measurement modalities, other than X-ray based, can be very valuable in establishing integrative approaches to the science and so stretching the scientific capability; an example of this is co-location of UED capabilities (**Appendix 2.1**). Laser laboratories for optical only time-resolved measurements, CryoEM capability for single molecule imaging, and NMR capability might also be integrated into the scientific offer of the UK XFEL, either at the same site or distributed across the STFC facility network.

9.2.9 User support infrastructure

Users are at the core of the scientific success of any facility. A UK XFEL must offer appropriate user support just as any other large-scale user facility, such as the CLF, Diamond or ISIS. In many respects the user support infrastructure in terms of accommodation, transport, catering, safety initiation and training, technical training and data policies will be much the same as at these existing facilities, although attention will be given to ensuring the user experience is as efficient and productive as possible, and that innovations and best practice are applied.

At this relatively early stage in their development, however, the use of XFELs is perceived to be much more challenging than for established methods and this has presented a significant barrier to the adoption of their use for routine science. A UK XFEL must do all that is possible to support new users and lower substantially this access barrier, both that perceived and the actual one caused by the complexity of end-stations and the rapid development that the technology is still undergoing. Measures to accomplish this are being pioneered at the facilities that are already operating in terms of offering end-station scientist support and transparent to operate end-station controls, and we will adopt all best practice. Some things that must be done are to make some classes of measurement, e.g. diffract-before-destroy CDI, serial nano-crystallography, time-resolved X-ray spectroscopy and RIXS, far more routine and fully supported, so that in many instances users need only send a sample and collaborate with the staff scientists on the data analysis. Where this is not practical, standard end-station configurations should be developed that minimise facility staff and user time in swapping between experiments, thus making high quality data taking more certain and efficient. Finally, an extensive training support programme will need to be offered by the facility to provide new users with the necessary skills: this ought to be mirrored by university-based academic training actions.

9.3 Options Analysis

To guide the decision making as to the way forward, with the objective to deliver all or most of the scientific opportunities identified in this Science Case, we have looked at a range of options. These span from building a world-leading machine to simply building on the status quo. A discussion of the pros and cons of each option is offered.

Given the science and technology opportunities highlighted in this Science Case, we must now address how best to realise these opportunities in the fullest form. We have developed the following analysis of different options, or at least analysed groups of options that lie in a similar range, to guide in this process. The most ambitious options (A and B) carry the highest cost, but also provide the greatest benefits for the UK science base and the economy. In contrast, the latter options (C - F) are relatively cheaper, but will return progressively less gain to the UK science base and the economy.

A. Build a unique UK XFEL optimised for new capability

This group of options would deliver a unique UK XFEL, fully optimised with some of the most advanced X-ray capabilities in the world with, for instance, high repetition rate across a significant photon energy range. In this category are *Concept outline 1* and *Concept outline 2*, overviewed in **Appendix 1**. Seeding would be available up to at least 1 keV, and attosecond pulse pairs across the entire photon energy range from soft to hard X-rays. It would offer a farm of end-stations equipped with the most advanced lasers, THz radiation sources, electron beams and other auxiliary equipment, and have the highest specification high energy and high-power laser integrated into the facility. A high repetition-rate end station for X-ray photolithography could be part of the facility. It would also provide science access to the electron beam for plasma wakefield and other accelerator technology research, as well as a high brightness gamma ray source. The fully superconducting *Concept outline 1* would be the most expensive, but it would deliver high repetition rate across the entire photon energy range at full power and so, in this respect, be directly as capable as LCLS II HE. The hybrid superconducting/normal conducting accelerator in *Concept outline 2* would be more restricted in having high repetition rate X-rays at full power only to 2 - 3 keV, but with lower power harmonics (3^{rd} and 5^{th}) into the hard X-ray range, but it could still have the full range of other unique features as *Concept outline 1*. Pushing the repetition rate of the normally conducting linac for the hard X-rays could deliver repetition rates as high as 5 kHz at full power, although R & D is required to deliver this.

The main advantages of these options are that they would provide the UK with a world-leading XFEL capability, giving maximum scientific reach and the largest potential scientific impact (see **Sections 8.6** and **8.7**). Such an international flagship facility would attract some of the world's best scientists across the physical, chemical, material and life sciences to our shores as users and staff scientists, and into the UK university sector. There would be maximum benefit to the UK skills pipeline, and the high-profile activity would attract young people in STEM subjects and foster growing public appreciation of science. Such a facility would likely attract an exciting array of partners from around the world, perhaps contributing financially to running costs and governance, including EU, USA, Japan, Korea and China along with nations not yet invested in this technology, such as India, Australia, Canada, Latin American nations, Israel, Middle Eastern Nations, and emerging economies in the Pacific rim. Nevertheless, the UK would be in control of all major decisions and strategic directions. Sovereign capabilities would be safeguarded for the long-term. The facility would signal global scientific and technical leadership.

On the other hand, the cost of such an option would be the highest and the timescale to delivery would be the longest, necessitating other measures to be taken in the interim. As new features and new combinations of features would be combined into the facility, there are moderate technical risks to manage, although no completely new technology needs to be developed for this option.

B. Build a UK XFEL providing capacity well beyond 10 years

This option would be focused on providing national capacity in XFEL science and technology for the long-term. It could include still some novel features and combinations of capabilities that would make it a world competitive facility, but not the full array envisioned under Option A. It would be in the character of a class of option referred to in the 2016 panel exercise as "Swiss FEL +". *Concept outline 3* presented in **Appendix 1** is in this category. We would still anticipate it addressing the majority of our needs for time-resolved X-ray science from soft to hard X-rays, and could have seeding and/or attosecond modes over a moderate photon energy range. It would not, however, provide high-repetition rate (> 500 Hz) over any of the photon energy range. Scope for a full array of lasers and other light sources would still be open, and future upgrades could provide a very exciting array of end-station capabilities.

As the technology for this option is already fully developed, and the scale of the infrastructure significantly smaller than Option A, both cost and delivery time are reduced. We estimate a cost of around 60% of *Concept outline 2*, and delivery time may be appreciably shorter (two-thirds). It would still safeguard a wide range of scientific, technological and sovereign capability. The impact on the UK skills pipeline would still be strong, and it would still be a national flagship for attracting students into STEM subjects. The UK would be in full control of all decisions and strategy, including the nature of future upgrades. There would be some scope for international partnerships, to assist in running costs for instance.

This option would not deliver a comparable level of kudos to the UK as Option A and would indicate that, whilst the UK is a competitive environment for X-ray science, it is not a global leader in science and technology. Options to attract scientists from overseas would also be possible, but more likely restricted into specific areas where the facility proves itself especially effective. Some of the UK's XFEL science would likely as not still need to be carried out at more capable overseas facilities. Project risks would be less than in Option A, but it would still require rigorous project management.

C. Invest more in dedicated UK facilities at existing XFELs

As partners in European XFEL, and users of the other main XFELs globally, we would be in a strong position to influence and invest in upgrades. Exactly which of these are most attractive, and/or available to our investment, would require further analysis. There would be scope for doing this at LCLS, SACLA or PAL FEL (Korea) if an upgrade opportunity matching our aspirations were to become apparent. At European XFEL there are already two unfilled tunnels that could house two undulators dedicated for particular performance ranges, for which input in their development is actively being sought at the current time and in which the UK could become a strong partner. It is thus this option that is analysed specifically here.

This approach could provide end-stations tailored to the needs of a significant fraction of the UK user community with, presumably, some arrangement for preferred access (although unlikely to be exclusive access). As the superconducting electron linear accelerator already exists, the extra costs are much lower than Options A or B (estimate 10 - 20% of Option A cost). Delivery time could be on the order of five years, but we would need to move rapidly to stake our intentions and to bring along like-minded partners. This could certainly be flagged as a national or shared (e.g. German/UK) end-station, politics permitting, which would bring moderate kudos and may attract some star players in the relevant areas to locate at UK universities.

The impact on the UK science and technology base would be modest. As the construction would be overseas, there would be no direct benefits to the UK economy. The limited space available in the European XFEL end hall will lead to significant restrictions on what can be done. Additionally, the pulsed nature of the European XFEL RF, leading to a complex temporal structure in the electron bunches, has a restraining impact on the science that can be planned. A small impact on UK skills may ensue from additional UK staff scientists and technicians seconded to European XFEL, but the volume would likely be relatively small compared to Options A or B. Some training opportunities might be

created, but again nothing like on the scale of Options A or B. Moreover, we would not have long-term control over the arrangements, and, although doubtless we would have a say, we could not solely determine the future strategy. UK sovereign capability would not be secured and, in the long-term, access to this capability might still be subject to, as yet, unforeseen geopolitical uncertainties (as well as those already all too apparent). There is thus some risk to the UK science and technology base in pursuing this option.

D. Increase investment to support users in exploiting existing opportunities (e.g. long term grant funding schemes, CDTs, "UK XFEL Institute")

This option is concerned with building the UK XFEL scientific community so that it has a competitive size, comparable to those in Germany or the USA where the existence of a national facility has greatly accelerated growth. The UK user community is very dynamic and has led many important developments in the early years of XFEL science, but it is still relatively small although growing steadily. To better position UK science to exploit the numerous scientific benefits offered by XFELs, a coordinated programme of community development and training ought to be undertaken urgently. Such a measure is equally important if we decide to build our own facility, as we will need a community ready to take full advantage of all the science opportunities. Large scale community building, aimed at bringing new groups into XFEL activity that would at the same time allow existing groups to be more effective, should be part of this. These could support the growth of the community by funding research fellows and technicians, networking activity, travel and the required equipment at the home base for preparing XFEL experiments across a wide range of disciplines. Building of specific instruments to be permanently stationed at end-stations might also form an important part of this activity (akin to the contribution of the DiPOLE laser in the HIBEF project). In parallel PhD training support is urgently needed. This could be delivered through a set of inter-related CDT doctoral training programmes. Several of these, for instance, centred on serial nanocrystallography, chemical dynamics, HEDs, materials, time-resolved imaging and X-ray physics, could support the science mission whilst providing a high-quality multidisciplinary training environment. Establishing a Scientific Institute (or several Institutes) to promote ultrafast X-ray science could be an additional highly effective measure, such as the very effective PULSE Institute at Stanford and CFEL at DESY.

The advantage of these measures is that they would accelerate the growth of the science base in the relevant areas, whilst also making a modest contribution to the broader skills pipeline. The cost of such activities would be modest compared to Options A - C, and could be spread across the research councils. We would estimate costs in the range £10 – 30M over five years, depending on the scale of activities undertaken. It could catalyse actions by the universities to recruit academic staff in the area. It would help to make the UK better able to benefit from the world XFEL infrastructures by being more competitive at winning beamtimes and delivering high quality science.

This option, however, offers limited additional economic benefit to the UK and will have only a modest impact on skills outside of the PhD training actions. For instance, it does nothing to support the UK accelerator science capability. Neither does it add significant new scientific capability or capacity to any of the XFELs that would be used. We would still be reliant on access to the facilities hosted by other nations and so fully subject to the rules and strategies of external agencies. UK sovereign capability would not be secured and, in the long-term, access to the scientific capability would still be subject to uncertainties. There is thus some risk to the wider UK science and technology base in pursuing this option.

E. Dedicated R & D effort towards a future XFEL ("test facility")

An action that could have significant value is an XFEL test facility for dedicated R & D. This could support in the longer term an ambitious future XFEL. Already such an action is partly underway in the form of CLARA. That project might be built upon to satisfy these long term R & D needs. This would also play an important role in supporting critical R & D if we go ahead to build an XFEL (Options A or B) on a faster time-line. A detailed analysis of the essential R & D steps that are required to achieve the aims

of the preferred XFEL option is required. These essential steps could include proving of novel FEL schemes and pre-production accelerator system demonstrations, such as a very high repetition rate photoinjector, an optimised superconducting RF cryomodule, and high gradient-low repetition rate/low gradient-high repetition rate normal conducting linac systems. Following this analysis a test facility would be proposed which would be optimised for achieving these R & D milestones. This might be an upgraded CLARA or a completely new test facility.

This option would be a stepping-stone to a future facility and would carry only a moderate cost over the next five years (£15 – 30M), of similar scale to Option D. It would at least maintain and modestly grow UK skills in accelerator science, and maintain the UK in a position to be competitive in the required technology. It would be possible to test some very advanced concepts not yet mature enough to be incorporated on the critical path for design of Options A or B (e.g. plasma wakefield acceleration mediated by dielectric or metallic structures).

This option, if carried out alone, would not contribute to the health of the wider science base in the UK in the short or intermediate terms. It would require a recurrent budget and a long-term commitment (~ 10 years) to the activity for it to be effective. It would also not, if carried out in isolation, deliver any of the economic, national or skills benefit of a larger scale facility. It would thus carry with it a moderate risk to UK science and innovation, and embed lost opportunities for at least the intermediate term. The motivation for doing this, if it is not to be seen as part of a long-term strategy to build a UK XFEL, would need to be carefully considered.

F. Extend activities of existing Life and Physical Sciences Hubs

The Life Science hub at Diamond has proven a great success in promoting UK FEL activity in the structural biology subject area. The Physical Science hub hosted by the CLF has just begun and is an opportunity to similarly promote the growth of UK XFEL users in other areas of science. These activities must at least be maintained and, for a modest investment, could be expanded and made more effective. Other community actions are currently being discussed (e.g. Oxford/Imperial plus others) are looking at better co-ordinated post-graduate training for XFEL science in the chemical/life sciences area, as a step towards a university hosted CDT. Although these activities are only a modest growth from the status quo, they are welcome and of value far exceeding their cost.

To grow these activities, perhaps by guaranteeing long-term funding and a couple of additional staff positions, would be the cheapest option towards delivering on the science opportunities. It would at least support a modest growth in the UK community and would help a number of additional groups to integrate XFEL-based measurements/experiments into their research programmes. If properly promoted, it could encourage universities to consider creation of new academic positions in this area.

Even with some net growth in the UK XFEL user community under this option, we are likely to fall back steeply against international competitors in relative terms as their community growth accelerates. As this would be widely perceived as doing nothing much new, there is a risk of a brain-drain from currently active university researchers who will see better prospects in overseas universities and institutes perceived to be more favourable to their science . As a “user” only nation, we would have little or no influence on future policies and strategy at the overseas XFELs. There would be a serious risk of lost access due to geopolitical circumstances and changes in access policy (e.g. it has been mooted that at least one major XFEL may bring in charging for access at market rates). No substantive general economic or skills boost would ensue from this option, although some of the individual research projects may create impact. Overall this would carry the highest risks to UK science, innovation and industrial competitiveness.

9.3.1 Summary of options analysis

In summary, the options that involve least cost and sit closest to the status quo carry the highest risks to the UK science base and economy. Nevertheless, a combination of Options D, E and F should be considered in some form, as they are required steps towards building a machine – which will

necessarily benefit from expanding the UK scientific user community and the technical capabilities of UK accelerator science. Option C could also sit efficiently in conjunction with Options A and B, as a way of effectively filling a gap not readily satisfied by the planned machine (e.g. very high repetition rate serial nanocrystallography).

"Do nothing" or a "do little" strategies are now the riskiest options and could potentially damage national competitiveness, technology and sovereign capability, and international scientific standing. The more ambitious the machine the lower the future risks to UK science and technology.

[1] C.Brahms et al, "Direct characterization of tune-able few-femtosecond dispersive wave pulses in the deep UV", Opt.Letts. 44, 2990 (2019)

[2] J.C.Travers et al, "High energy pulse self-compression and ultraviolet generation through soliton dynamics in hollow capillary fibres", Nat.Phot. 13, 547 (2019)

[3] A.Ermolov et al, "Supercontinuum generation in the vacuum ultraviolet through dispersive-wave and soliton-plasma interaction in a noble-gas filled hollow core photonic crystal fibre" PRA, 92, 033821 (2015)

[4] H.Bromberger et al "Angle-resolved photoemission spectroscopy with 9 eV photon-energy pulses generated in a gas filled hollow core photonic crystal fibre" Appl.Phys.Lett. 107, 091101 (2015)

[5] M.Krebs et al "Towards isolated attosecond pulses at megahertz repetition rates" Nat.Phot., &, 555 (2013)

[6] Perucchi et al, Rev. Sci. Instrum. 84, 022702 (2013)

[7] Forst et al, THPC84, IPAC2011

[8] S.Gerber et al "Three dimensional charge density wave order in $YBa_2Cu_3O_{6.67}$ at high magnetic fields" Science, 350, 949 (2015)

[9] J.Yang et al, Nat.Comm. 7, 11232 (2016), S.P.Weathersby et al, Rev,Sci.Inst, 86, 073702 (2015)

[10] U.Weierstall et al "Injector for scattering measurements on fully solvated biospecies", Rev.Sci.Inst. 83, 035108 (2012) DOI:10.1063/1.3693040

[11] G.Galinis et al "Micrometer-thickness liquid sheet jets flowing in vacuum", Rev.Sci.Inst. 88, 083117 (2017), DOI: 10.1063/1.4990130

[12] J.D.Koralek et al "Generation and characterisation of ultrathin free-flowing liquid sheets", Nat.Comm. 9, 1353 (2018) DOI:10.1038/s41467-018-03696-w

[13] A.Sanchez-Gonzalez et al, "Accurate prediction of X-ray pulse properties from a free-electron laser using machine learning", Nat.Comm. 8, 15461 (2017)

Appendix 1: An outline of a technical solution

To consider the various technical options for a UK XFEL facility requires a dedicated conceptual design phase, beyond the scope of the science case. Nevertheless it is important to consider some of the ways in which a UK XFEL could be optimised to meet the ambitious requirements of the science. This section details preliminary work to outline technical solutions for different scenarios, each of which would feature world-leading capabilities, customised to the needs of the UK.

Introduction

Section 9.3 sets out the different options for UK FEL science, including option A – to build a unique UK XFEL optimised for new capability and option B – to build a UK XFEL providing capacity well beyond 10 years. This section details two different technical solutions for option A: *Concept outline 1*, which would be a fully superconducting accelerator with maximum capability, including up to MHz repetition rate at all photon energies; and *Concept outline 2*, a hybrid superconducting/normal conducting accelerator, expected to be somewhat less expensive by operating at kHz repetition rate for hard x-rays but otherwise featuring a full complement of capabilities. A technical solution for option B – *Concept outline 3* – is also described: this would be the least expensive option, with reduced repetition rate and possibly lower photon energy reach, but it would be a world competitive facility with capabilities optimised for UK science. The rationale behind the technology choices is also described.

Key parameters for facility design

As shown in **Figure 1**, some of the most significant factors that influence the facility design are repetition rate, photon energy, and energy per pulse:

- **Repetition rate is a driving factor behind the choice of accelerator technology.** As described in **Section 2.3**, the majority of existing XFELs use normal conducting linacs, which deliver pulses at ~100 Hz, however advanced designs and reduced gradient may enable higher (~1 kHz) repetition rates in a future facility. Superconducting linacs deliver significantly higher repetition rates, e.g. the European XFEL utilises superconducting linacs to deliver 27,000 pulses per second in a pulse train structure, while superconducting linac facilities presently under construction (LCLS-II, SHINE) will deliver a continuous train of pulses at ~1 MHz. For even higher repetition rates, Energy Recovery Linacs (ERLs) may reach ~100 MHz by transferring energy from used bunches to subsequent bunches. Very advanced concepts such as plasma acceleration are not yet considered to be mature enough to be on the critical path.

- **Photon energy and energy per pulse strongly affect the required electron beam energy.** Typically, facilities producing extreme ultra-violet (EUV) light have electron beam energy of 1-1.5 GeV (e.g. FLASH, FERMI). Soft x-ray (SX) output (up to a few keV) requires electron beam energy of 2-3 GeV, hard x-rays (HX) up to ~15 keV can be produced with an electron beam energy of 6-8 GeV, while there are proposals to extend the photon energy reach of European XFEL to 100 keV, utilising its very high electron beam energy (17.5 GeV). UK XFEL could utilise novel short period undulators (e.g. superconducting) to access higher photon energies for a given electron beam energy, together with advanced low-emittance photoinjectors to provide suitable electron beam quality. All else being equal, the energy per pulse strongly scales with the electron beam energy.

Figure 1 shows the clear diagonal trade-off between repetition rate and photon energy in the science requirements as highlighted in **Section 9.1**, relative to the facility design considerations. It is clear that a high electron beam energy (~10 GeV) facility is needed to deliver the required photon energies. The requirement for high pulse energy at high photon energy is also a key driver that directs the design to high electron beam energy. There are two options to meet the majority of the repetition rate requirements – either a fully superconducting linac to deliver MHz pulses across all photon energies,

or a hybrid approach – partially superconducting to deliver MHz pulses at lower photon energies, with an advanced normal conducting linac to provide kHz bunches for the higher photon energies.

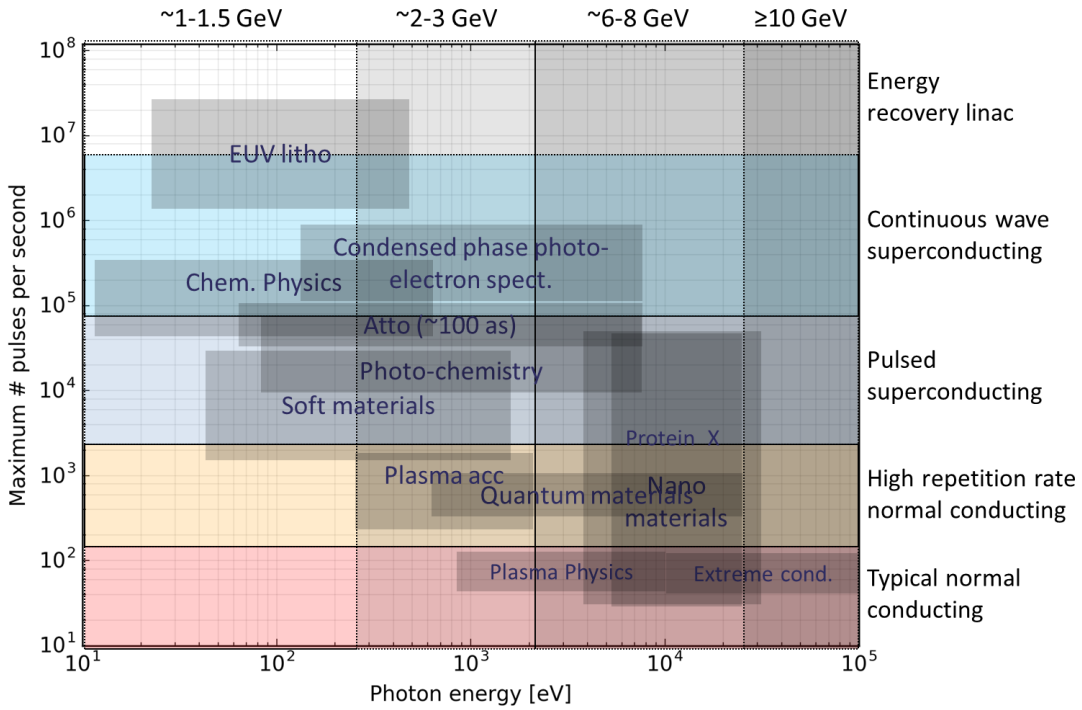

Figure 1: How the repetition rate and photon energy requirements of the science case map onto the choice of accelerator technology (right labels) and approximate electron beam energy (top labels).

Other key features

While the parameters already described provide the basis of the technical solutions, there are numerous additional features that could be incorporated to provide a UK XFEL with unique capability. As described in **Section 2.4**, some of the most promising features for world-leading capability matched to UK needs are:

- High repetition rate laser seeding
- High spectral purity x-rays
- Attosecond pulses across all photon energies
- Combining X-rays with other advanced capability
- High average power for EUV/gammas

All these features could be incorporated into *Concept outlines 1 and 2*, and some could feature in *Concept outline 3*, as described below.

Concept outline 1: Superconducting accelerator

Concept outline 1 is a high energy (~10 GeV) superconducting accelerator operating with MHz repetition rate, as shown in **Figure 2**. By combining high energy and high repetition rate, it covers the full repetition rate-photon energy parameter space required by the science case. High electron energy and advanced (e.g. superconducting) undulators provide access to very high energy per pulse up to very hard x-ray. Fast kickers can be used to distribute bunches between different FEL lines, with the ability to deliver lower repetition rates where required. The linear (i.e. single-pass) layout shown in **Figure 2** would be broadly similar to LCLS-II HE and SHINE, however a recirculating option (i.e. a shorter linac used e.g. 2-3 times) could also be considered to reduce cost.

High repetition rate seeding would be incorporated to as high a photon energy as possible. Beyond this, other high spectral purity techniques would be used such as HB-SASE, and oscillator FELs including

XFELO are an option due to MHz repetition rates. Techniques for attosecond pulse could be incorporated at all photon energies. End-stations would be equipped with the most advanced lasers, THz radiation sources and electron beams, for use in combination with the x-rays.

A feature under consideration for both *Concept outlines 1 and 2* is to have a second photo-injector towards the end of the main linac. While it is not essential in this case, it offers the opportunity to provide lower energy electron beams to serve the soft and hard x-ray undulator lines independently – or in combination for multi-colour experiments with widely separated photon energies. Soft x-rays with high pulse energy could be generated from the 10 GeV beam if required. A second injector also provides the option of upgrading this region to even higher repetition rate by introducing an energy recovery linac, which could support a high average power EUV FEL and a high brightness gamma ray source.

Concept outline 1: Superconducting accelerator

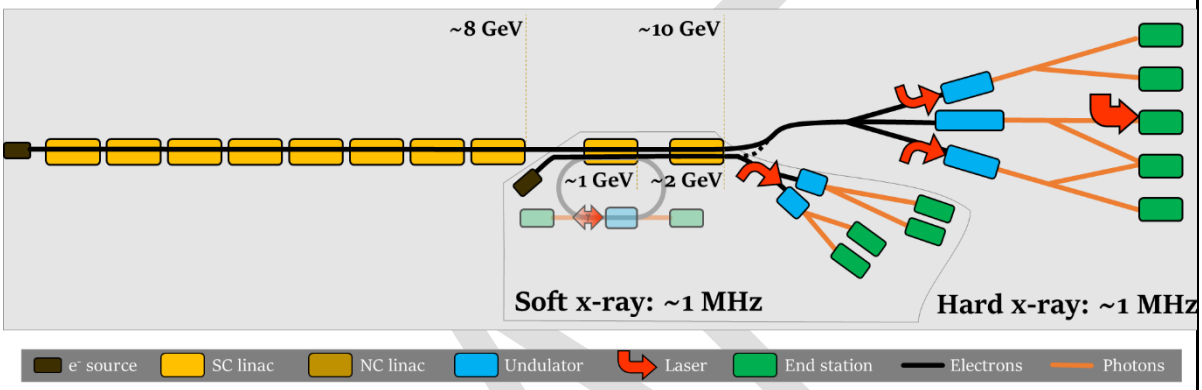

Figure 2: UK XFEL Concept outline 1: superconducting accelerator. The above schematic shows the layout for a ~10 GeV superconducting accelerator facility proposed to meet the science requirements.

The plot to the right shows how such a technical solution would cover the repetition rate-photon energy requirements of the science case.

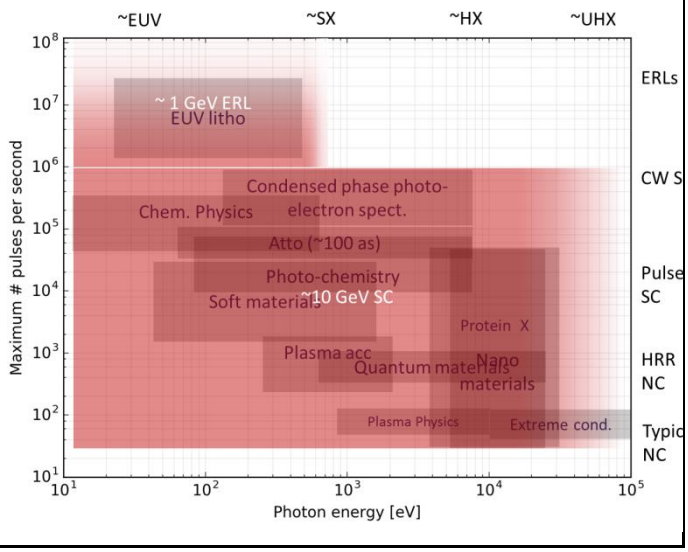

Concept outline 2: Hybrid accelerator

Concept outline 2 is a high energy (~10 GeV) hybrid of two accelerator types as shown in **Figure 3**. It features a ~2 GeV superconducting linac, operating to provide MHz repetition rate up to a few keV photon energy. This is coupled to an ~8 GeV advanced normal conducting linac, to provide kHz repetition rate for up to very hard x-ray photon energies.

Concept outline 2: Hybrid accelerator

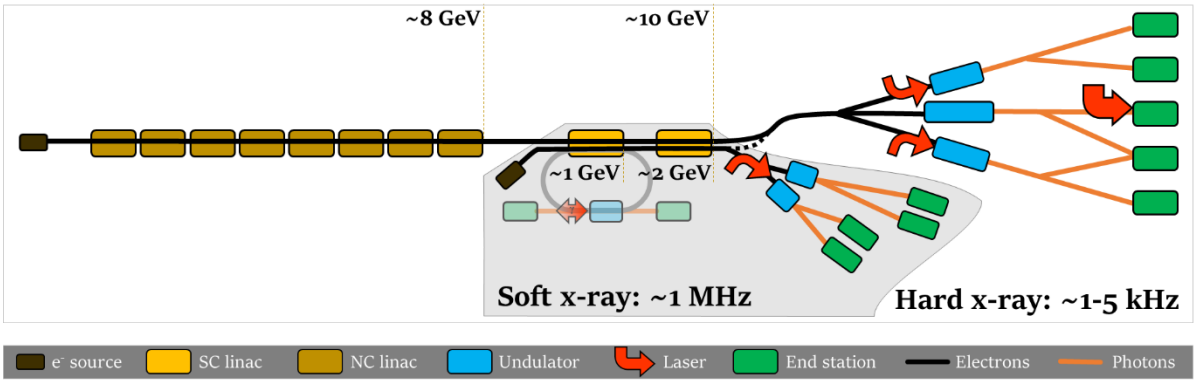

Figure 3: Concept outline 2: hybrid accelerator. The above schematic shows the layout for a ~10 GeV hybrid accelerator facility proposed to meet the science requirements. The plot to the right shows how such a technical solution would cover the repetition rate-photon energy requirements of the science case. The plots below show the trade-off between repetition rate and gradient (left) and corresponding linac length for an 8 GeV NC linac (right), with estimated peak field limits imposed at lower repetition rates.

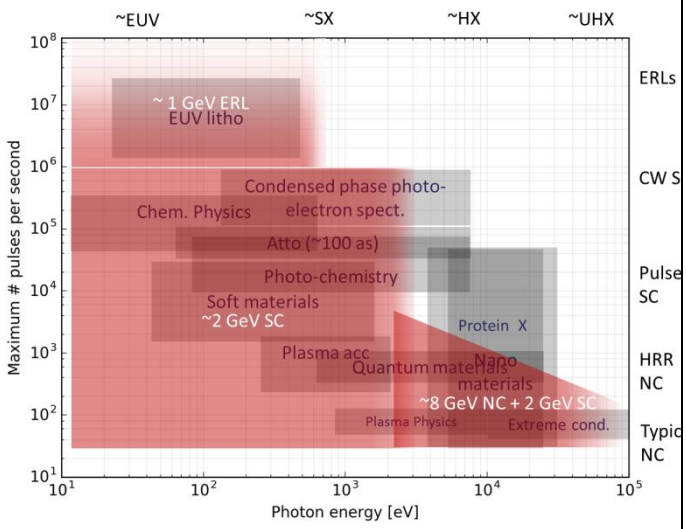

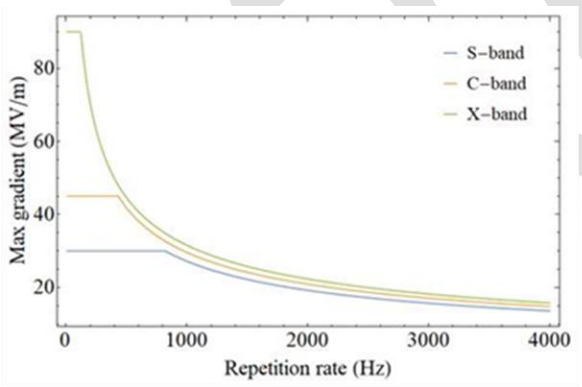

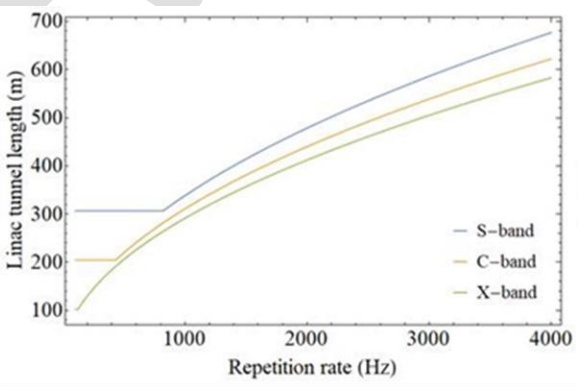

Operating in this way provides a more targeted approach to covering the repetition rate-photon energy requirements of the science case, as shown in **Figure 3**. While it cannot deliver MHz repetition rates at high energy as per *Concept outline 1*, the hybrid option would likely be more flexible for trading off gradient against repetition rate (as shown in **Figure 3**), meaning it could more efficiently target the very high photon energies required by some areas of the science, albeit at low repetition rate. Preliminary work is ongoing around a baseline of 8 GeV at 1 kHz for the normal conducting section, potentially scaling up to 5 kHz at lower gradient, or to higher energy at lower repetition rate. Again, advanced undulators would be used for maximum reach in terms of photon energy/pulse energy, and fast kickers would distribute bunches between different FEL lines.

Two electron injectors would be essential in this case: an ultra-low emittance, low repetition rate injector for hard x-rays, together with a high-repetition rate injector for soft x-rays. This would also provide opportunity for multi-colour experiments with widely separated photon energies. Soft x-rays with high pulse energy could be generated from the 10 GeV beam if required, albeit at lower repetition rate. A second injector again provides the option of upgrading this region to an energy recovery linac to support a high average power EUV FEL and a high brightness gamma ray source. Alternatively, recirculation around the superconducting section would be a promising future upgrade to extend MHz repetition rates towards hard x-ray.

As for *Concept outline 1,* high repetition rate seeding, attosecond pulse generation, and high spectral purity techniques could be incorporated, although the use of oscillator FELs would be limited to photon energies where MHz is available (i.e. up to a few keV). An oscillator FEL could potentially be used to seed to higher photon energy. Again, end-stations would be equipped with the most advanced lasers, THz radiation sources and electron beams, for use in combination with the x-rays.

Concept outline 3: Normal conducting accelerator

Concept outline 3 is a proposed technical solution for option B of **Section 9.3** – to build a UK XFEL providing capacity well beyond 10 years. It is less ambitious than *Concept outlines 1 and 2.* It could include still some novel features and combinations of capabilities that would make it a world competitive facility, but not the full array envisioned under option A.

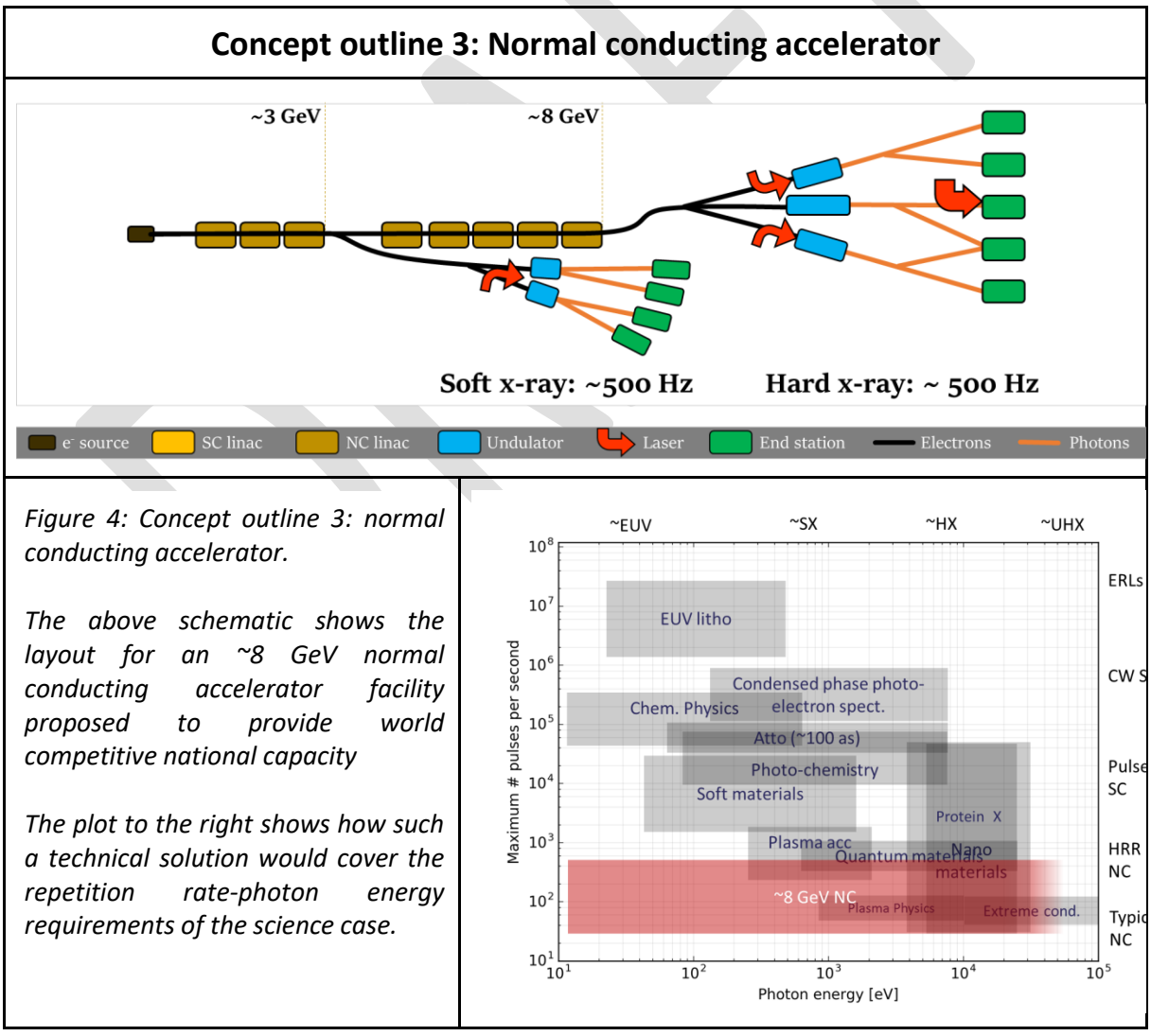

Figure 4: Concept outline 3: normal conducting accelerator.

The above schematic shows the layout for an ~8 GeV normal conducting accelerator facility proposed to provide world competitive national capacity

The plot to the right shows how such a technical solution would cover the repetition rate-photon energy requirements of the science case.

As shown in **Figure 4**, it features a fully normal conducting accelerator, operating with a repetition rate of approximately 500 Hz. This is lower than the normal conducting section of *Concept outline 2* but higher than the present generation of normal conducting XFELs. An electron beam energy of ~8 GeV would be internationally competitive, and advanced undulators could be employed to extend the photon energy reach beyond comparable existing machines. Trading off gradient against repetition rate could potentially be employed to increase to kHz repetition rate at lower photon energies. This is not shown in **Figure 4** but in any case the coverage of the repetition rate-photon energy parameter space is limited compared to *Concept outlines 1 and 2.* An extraction line at ~3 GeV could serve the lower photon energy undulator lines, or soft x-rays with higher pulse energy could be generated from the 8 GeV beam.

Seeding, attosecond pulses and high spectral purity methods could be incorporated, though oscillator FELs would not be an option. End-stations could be equipped with the most advanced lasers, THz radiation sources and electron beams, for use in combination with the x-rays.

Appendix 2: Complementarity of techniques

A2.1 Cryo-Electron Microscopy (Cryo-EM), Tomography (cryo-ET), and Diffraction (cryo-ED)

Cryo-EM, with the recent resolution revolution, is trending toward becoming a major method for macromolecular structural studies. An active R&D area includes time-resolved studies with samples trapped by freeze-quench methods at the ms and longer timeframe. Current challenges in cryo-EM include a) the development of new approaches towards cryo-EM sample preparation, reaction triggering, and delivery in order to b) improve efficiency and reduce the time required from pure proteins to structures, and c) the ability to assign structures to functional states during a dynamic process. Cryo-ET provides structural detail within context, such as whole cells, albeit without as high a resolution. Cryo-ED yields atomic resolution models from sub-micron size crystals and time-resolved methods are a very active R&D area. These all complement macromolecular crystallography (MX), currently the major technique in structural biology. Time-resolved serial MX data collected at physiological temperatures at XFELs probe fs and longer, whereas studies at microfocus synchrotron sources probe reactions from ~ns - µs and longer. Together, these complementary approaches share R&D efforts in sample delivery, reaction triggering strategies, and data analysis algorithms

For decades macromolecular crystallography (MX) has been the main technique in structural biology.[1-5] An unavoidable issue of MX is the need to obtain well-ordered crystals, which remains a trial and error process. Although often automated and using nL volumes per condition, crystallization trials can consume large amounts of samples and take significant time to optimize. In addition, the crystallisation process requires a homogenous macromolecular conformation, which poses challenges for large, dynamic and transient complexes that play key roles in mediating many biological processes.

The 2017 Nobel Prize in Chemistry was awarded to Dubochet, Frank, and Henderson "for developing cryo-electron microscopy for the high-resolution structure determination of biomolecules in solution." This reinforces the recent revolutionary advances in cryo-EM.[6-14] These include microscope instrumentation, detector developments and image processing algorithms. An advantage of cryo-EM is that it only needs a relatively small amount of sample at a significantly lower (100-1000x) concentration compared to MX. Consequently, structural determination by cryo-EM is an attainable goal for many large proteins and complexes that are difficult to produce, purify or crystallize. The method allows fast structural determination for many proteins, as demonstrated by the recent structures of COVID-19 spike protein, which were resolved within weeks of genes being sequenced (see also section 8.5).[15] Furthermore, since each particle is imaged individually, and can be sorted out *in silico* according to their conformation, even dynamic proteins and complexes can now be imaged and their structures determined, provided that their different structural classes are sufficiently differentiated. Stunning cryo-EM results are published frequently in *Science* (13 published in 2020 through 31 March 2020) and *Nature* (14 published in 2020 through 31 March 2020), as well as other high profile journals; a selected subset are listed here.[15-30]

The principal structural methods that use frozen-hydrated samples and a transmission electron microscope apply to macromolecular samples in pure states in solution (cryo-EM) or submicron crystals (cryo-ED) to heterogenous samples in complex environments such as whole cells (cryo-ET) (Figure A2.1).[31-37] Current cryo-EM single particle analysis methods focus on biomolecules ranging from ~50 kilo-Daltons (kD) to several Mega-Daltons, covering the majority of macromolecules complexes as well as viruses.[35, 38-43] Indeed, recent examples demonstrate that even haemoglobin (64 kD) can be studied by cryo-EM and 10 of the 4641 atomic models released by the PDB (29 March 2020) are to better than 2 Å resolution.[34, 35, 38, 41, 44-46] Cryo-ET provides structural information *in situ* and with the extraordinarily valuable context of whole cells.[6, 10, 47-54] The technique is very likely to unravel new biology as we start to observe links between different macromolecular complexes inside the cell, track how different macromolecular complexes change in response to environment stimuli

and complexes associate and dissociate. However, samples must be less than 500 microns thick and often require cryo-focused ion beam milling, a laborious and time consuming process. Similarly, cyro-ED requires submicron size crystals to reduce or eliminate multiple diffraction events from the sample, but it can provide truly atomic resolution results.[31, 32, 37, 55-59] To date all cryo-ED structure have been solved by molecular replacement, with the exception of the very high resolution data set of a prion peptide that enabled direct methods to calculate phases.[37] Analogous to cryogenic X-ray crystallography, cryo-ED data are collected with continuous-rotation methods. In comparison to X-rays however, electrons interact much more strongly with matter and thereby yield high- resolution diffraction from much smaller samples. The requirement to use submicron size samples also makes cryo-ED synergistic with SFX and serial MX methods at XFELs and synchrotrons.

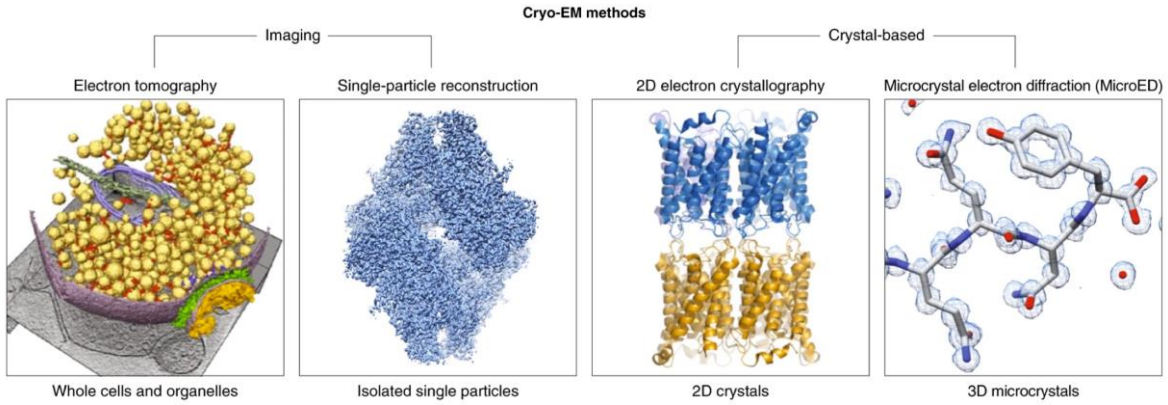

Figure A2.1. The diverse imaging-based and diffraction-based techniques used in cryo-EM can provide structural information from a wide range of samples. Images acquired with the different techniques are shown here, depicting the synaptosome (electron tomography), a 2.2 Å reconstruction of β-galactosidase (single-particle reconstruction), a 1.9 Å structure of aquaporin-0 (2D electron crystallography) and a 1.0 Å structure of the NNQQNY Sup35 prion fragment (MicroED). From Nannenga & Gonen (2019) Nature Methods 16: 369–379.

To achieve the highest resolution in single partial imaging by cryo-EM requires optimum samples and sufficient microscope time. Rapidly improving technologies and high end instruments are becoming more widespread, which in aggregate are producing many new results on a daily basis.[7] All of the 4641 cryo-EM models released by the PDB give an average 5.92 Å resolution; however, for those 485 models released in 2020 as of 29 March the average is 3.9 Å resolution. Fortunately, the trend is to higher resolution. Thus, cryo-EM is becoming the leading methodology for most structural biology projects, including structural studies to characterise ligand and/or inhibitor binding. Cryo-EM methods complement MX, wherein the latter often provides atomic resolution to well beyond 2 Å resolution and sometimes even with direct correlations with spectroscopic data from the same samples. Although time-resolved MX studies at physiological conditions with XFELs is a major use case, time-resolved cryo-EM is also very actively perused by several research groups.[60-63] For instance, the Frank group has recently published freeze-quench cryo-EM studies of the ribosome initiation of translation with time points at 20, 80, 200 and 600 ms, wherein the rapid formation of the 70S initiation complex transitions into 70S elongation-competent complex.[64]

In addition to resolving multiple conformations and composition heterogeneity within a single sample, cryo-EM is well suited to study dynamic systems, at the milliseconds to seconds time frame dictated by freeze-quench methods, within which many macromolecular assembling, co-factor binding, conformational changes and signalling events, take place. However, in order to track a dynamic process, precise and well controlled sample preparation, triggering and delivery systems are required to capture different functional states or distributions of functional states during a dynamic biological process. Despite these clear advantages and capabilities, there are a number of challenges and limitations that hinder cryo-EM to reach its full potential:

1) Instrumentation Capacity

A significant problem for cryo-EM is the limited access and long waits to use extraordinarily expensive microscopes. In the last few years, the UKRI and Wellcome Trust as well as individual universities/institutes have invested significantly in high end instrumentations. This includes establishing the national electron bio-imaging centre (eBIC) at Diamond Light Source, a successful model that is now widely adapted in many other countries. However, these instruments are expensive to purchase, maintain and require expertise to operate; they are thus best placed in centres or institutions with sufficient user groups. To best utilise these high end instruments and to allow more scientists to have access to cryo-EM, samples need to be screened first, which should be assessed locally. There is currently limited access to screening instruments across the whole UK structural biology community. Fortunately, there are a number of current efforts and approaches to address this; for instance, the development of 100 keV instrument that aims to democratise cryo-EM.[65, 66]

2) Sample Preparation and Delivery

Current methods in cryo-EM sample and grids preparation dated back to 1980s. Although blotting works for many samples, it is becoming increasingly a major bottleneck as the numbers of samples and their complexity increases. The difficulty is that many macromolecular complexes dissociate, aggregate, denature or simply do not go into the holes of the cryo-EM grids. A further complication is the lack of rapid and easy quality assessment early in the process, which now happens after the samples have been imaged using a cryo-EM instrument and analysed computationally. The lack of robust and reliable specimen preparations, the inability to assess sample quality prior to cryo-EM imaging, hinder the overall efficiency of structural determinations by cryo-EM. This is one area that requires urgent development. Given that sample delivery is a major area of development required for successful XFEL experiments as detailed in section 7, there is significant synergy with the sample delivery systems developed for serial methods at XFELs.

3) Cryo-ET Development

One of the most exciting but least developed areas is the ability to image and recognise macromolecules to high resolution *in situ*. Electron cryo-tomography reconstructs a three-dimensional image from a series of tilted images, which limits resolution to about 15-20 Å. Furthermore, the limited penetration power of electrons in the available microscopes (100-300 keV, limiting to ~ 200 nM) requires many of the biological samples to be thinned first, currently through focused-ion beam milling.[52] The resolution limitation can be overcome and 3-4 Å resolution has been achieved through sub-tomographic averaging in some cases;[67, 68] but this is not always possible, due to the small numbers and small sizes of the objects within the biological specimen. There remains a significant technical challenge to develop methodologies to improve the resolution, to increase penetration power and develop new ways to obtain thinner specimens, and to enable particles to be identified in tomograms.

References

[1] Maveyraud, L., and Mourey, L. (2020) Protein X-ray Crystallography and Drug Discovery, *Molecules 25* doi: 10.3390/molecules25051030

[2] Haas, D. J. (2020) The early history of cryo-cooling for macromolecular crystallography, *IUCrJ 7*, 148-157 doi: 10.1107/S2052252519016993

[3] Chapman, H. N. (2019) X-Ray Free-Electron Lasers for the Structure and Dynamics of Macromolecules, *Annu Rev Biochem 88*, 35-58 doi: 10.1146/annurev-biochem-013118-110744

[4] Grimes, J. M., Hall, D. R., Ashton, A. W., Evans, G., Owen, R. L., Wagner, A., et al, Stuart, D. I. (2018) Where is crystallography going?, *Acta Crystallogr D Struct Biol 74*, 152-166 doi: 10.1107/S2059798317016709

[5] Owen, R. L., Juanhuix, J., and Fuchs, M. (2016) Current advances in synchrotron radiation instrumentation for MX experiments, *Arch Biochem Biophys 602*, 21-31 doi: 10.1016/j.abb.2016.03.021

[6] Benjin, X., and Ling, L. (2020) Developments, applications, and prospects of cryo-electron microscopy, *Protein Sci 29*, 872-882 doi: 10.1002/pro.3805

[7] Callaway, E. (2020) Revolutionary cryo-EM is taking over structural biology, *Nature 578*, 201 doi: 10.1038/d41586-020-00341-9

[8] Subramaniam, S. (2019) The cryo-EM revolution: fueling the next phase, *IUCrJ 6*, 1-2 doi: 10.1107/S2052252519000277

[9] Lyumkis, D. (2019) Challenges and opportunities in cryo-EM single-particle analysis, *J Biol Chem 294*, 5181-5197 doi: 10.1074/jbc.REV118.005602

[10] Cheng, Y. (2018) Single-particle cryo-EM-How did it get here and where will it go, *Science 361*, 876-880 doi: 10.1126/science.aat4346

[11] (2016) Method of the Year 2015, *Nature Methods 13*, 1-1 doi: 10.1038/nmeth.3730

[12] Elmlund, D., and Elmlund, H. (2015) Cryogenic electron microscopy and single-particle analysis, *Annu Rev Biochem 84*, 499-517 doi: 10.1146/annurev-biochem-060614-034226

[13] Cheng, Y. (2015) Single-Particle Cryo-EM at Crystallographic Resolution, *Cell 161*, 450-457 doi: 10.1016/j.cell.2015.03.049

[14] Ourmazd, A. (2019) Cryo-EM, XFELs and the structure conundrum in structural biology, *Nature Methods* doi: 10.1038/s41592-019-0587-4

[15] Walls, A. C., Park, Y. J., Tortorici, M. A., Wall, A., McGuire, A. T., and Veesler, D. (2020) Structure, Function, and Antigenicity of the SARS-CoV-2 Spike Glycoprotein, *Cell* doi: 10.1016/j.cell.2020.02.058

[16] Coscia, F., Taler-Vercic, A., Chang, V. T., Sinn, L., O'Reilly, F. J., Izore, T., et al, Lowe, J. (2020) The structure of human thyroglobulin, *Nature 578*, 627-630 doi: 10.1038/s41586-020-1995-4

[17] Huang, W., Masureel, M., Qu, Q., Janetzko, J., Inoue, A., Kato, H. E., et al, Kobilka, B. K. (2020) Structure of the neurotensin receptor 1 in complex with beta-arrestin 1, *Nature* doi: 10.1038/s41586-020-1953-1

[18] Ma, J., You, X., Sun, S., Wang, X., Qin, S., and Sui, S. F. (2020) Structural basis of energy transfer in Porphyridium purpureum phycobilisome, *Nature 579*, 146-151 doi: 10.1038/s41586-020-2020-7

[19] Staus, D. P., Hu, H., Robertson, M. J., Kleinhenz, A. L. W., Wingler, L. M., Capel, W. D., et al, Skiniotis, G. (2020) Structure of the M2 muscarinic receptor-beta-arrestin complex in a lipid nanodisc, *Nature 579*, 297-302 doi: 10.1038/s41586-020-1954-0

[20] Wagner, F. R., Dienemann, C., Wang, H., Stutzer, A., Tegunov, D., Urlaub, H., and Cramer, P. (2020) Structure of SWI/SNF chromatin remodeller RSC bound to a nucleosome, *Nature 579*, 448-451 doi: 10.1038/s41586-020-2088-0

[21] Zhang, W., Tarutani, A., Newell, K. L., Murzin, A. G., Matsubara, T., Falcon, B., et al, Scheres, S. H. W. (2020) Novel tau filament fold in corticobasal degeneration, *Nature* doi: 10.1038/s41586-020-2043-0

[22] Abbas, Y. M., Wu, D., Bueler, S. A., Robinson, C. V., and Rubinstein, J. L. (2020) Structure of V-ATPase from the mammalian brain, *Science 367*, 1240-1246 doi: 10.1126/science.aaz2924

[23] Cook, N. J., Li, W., Berta, D., Badaoui, M., Ballandras-Colas, A., Nans, A., et al, Cherepanov, P. (2020) Structural basis of second-generation HIV integrase inhibitor action and viral resistance, *Science 367*, 806-810 doi: 10.1126/science.aay4919

[24] He, S., Wu, Z., Tian, Y., Yu, Z., Yu, J., Wang, X., et al, Xu, Y. (2020) Structure of nucleosome-bound human BAF complex, *Science 367*, 875-881 doi: 10.1126/science.aaz9761

[25] Hoffman, D. P., Shtengel, G., Xu, C. S., Campbell, K. R., Freeman, M., Wang, L., et al, Hess, H. F. (2020) Correlative three-dimensional super-resolution and block-face electron microscopy of whole vitreously frozen cells, *Science 367* doi: 10.1126/science.aaz5357

[26] Kang, G., Taguchi, A. T., Stubbe, J., and Drennan, C. L. (2020) Structure of a trapped radical transfer pathway within a ribonucleotide reductase holocomplex, *Science* doi: 10.1126/science.aba6794

[27] Qiao, A., Han, S., Li, X., Li, Z., Zhao, P., Dai, A., et al, Wu, B. (2020) Structural basis of Gs and Gi recognition by the human glucagon receptor, *Science 367*, 1346-1352 doi: 10.1126/science.aaz5346

[28] Wrapp, D., Wang, N., Corbett, K. S., Goldsmith, J. A., Hsieh, C. L., Abiona, O., et al, McLellan, J. S. (2020) Cryo-EM structure of the 2019-nCoV spike in the prefusion conformation, *Science 367*, 1260-1263 doi: 10.1126/science.abb2507

[29] Yan, R., Zhang, Y., Li, Y., Xia, L., Guo, Y., and Zhou, Q. (2020) Structural basis for the recognition of SARS-CoV-2 by full-length human ACE2, *Science 367*, 1444-1448 doi: 10.1126/science.abb2762

[30] Schommers, P., Gruell, H., Abernathy, M. E., Tran, M. K., Dingens, A. S., Gristick, H. B., et al, Klein, F. (2020) Restriction of HIV-1 Escape by a Highly Broad and Potent Neutralizing Antibody, *Cell 180*, 471-489 e422 doi: 10.1016/j.cell.2020.01.010

[31] Nannenga, B. L., and Gonen, T. (2019) The cryo-EM method microcrystal electron diffraction (MicroED), *Nat Methods 16*, 369-379 doi: 10.1038/s41592-019-0395-x

[32] Nannenga, B. L., and Gonen, T. (2016) MicroED opens a new era for biological structure determination, *Curr Opin Struct Biol 40*, 128-135 doi: 10.1016/j.sbi.2016.09.007

[33] Fernandez-Busnadiego, R., Schrod, N., Kochovski, Z., Asano, S., Vanhecke, D., Baumeister, W., and Lucic, V. (2011) Insights into the molecular organization of the neuron by cryo-electron tomography, *J Electron Microsc (Tokyo) 60 Suppl 1*, S137-148 doi: 10.1093/jmicro/dfr018

[34] Bartesaghi, A., Aguerrebere, C., Falconieri, V., Banerjee, S., Earl, L. A., Zhu, X., et al, Subramaniam, S. (2018) Atomic Resolution Cryo-EM Structure of beta-Galactosidase, *Structure 26*, 848-856 e843 doi: 10.1016/j.str.2018.04.004
[35] Bartesaghi, A., Merk, A., Banerjee, S., Matthies, D., Wu, X., Milne, J. L., and Subramaniam, S. (2015) 2.2 A resolution cryo-EM structure of beta-galactosidase in complex with a cell-permeant inhibitor, *Science 348*, 1147-1151 doi: 10.1126/science.aab1576
[36] Gonen, T., Cheng, Y., Sliz, P., Hiroaki, Y., Fujiyoshi, Y., Harrison, S. C., and Walz, T. (2005) Lipid-protein interactions in double-layered two-dimensional AQP0 crystals, *Nature 438*, 633-638 doi: 10.1038/nature04321
[37] Sawaya, M. R., Rodriguez, J., Cascio, D., Collazo, M. J., Shi, D., Reyes, F. E., et al, Eisenberg, D. S. (2016) Ab initio structure determination from prion nanocrystals at atomic resolution by MicroED, *Proc Natl Acad Sci U S A 113*, 11232-11236 doi: 10.1073/pnas.1606287113
[38] Pena, A., Sweeney, A., Cook, A. D., Topf, M., and Moores, C. A. (2020) Structure of Microtubule-Trapped Human Kinesin-5 and Its Mechanism of Inhibition Revealed Using Cryoelectron Microscopy, *Structure* doi: 10.1016/j.str.2020.01.013
[39] Yan, R., Zhang, Y., Li, Y., Xia, L., Guo, Y., and Zhou, Q. (2020) Structural basis for the recognition of the SARS-CoV-2 by full-length human ACE2, *Science* doi: 10.1126/science.abb2762
[40] Yuan, S., Wang, J., Zhu, D., Wang, N., Gao, Q., Chen, W., et al, Wang, X. (2018) Cryo-EM structure of a herpesvirus capsid at 3.1 A, *Science 360* doi: 10.1126/science.aao7283
[41] Zivanov, J., Nakane, T., Forsberg, B. O., Kimanius, D., Hagen, W. J., Lindahl, E., and Scheres, S. H. (2018) New tools for automated high-resolution cryo-EM structure determination in RELION-3, *Elife 7* doi: 10.7554/eLife.42166
[42] Herzik, M. A., Jr., Wu, M., and Lander, G. C. (2019) High-resolution structure determination of sub-100 kDa complexes using conventional cryo-EM, *Nat Commun 10*, 1032 doi: 10.1038/s41467-019-08991-8
[43] Shen, L., Huang, Z., Chang, S., Wang, W., Wang, J., Kuang, T., et al, Zhang, X. (2019) Structure of a C2S2M2N2-type PSII-LHCII supercomplex from the green alga Chlamydomonas reinhardtii, *Proc Natl Acad Sci U S A 116*, 21246-21255 doi: 10.1073/pnas.1912462116
[44] Merk, A., Bartesaghi, A., Banerjee, S., Falconieri, V., Rao, P., Davis, M. I., et al, Subramaniam, S. (2016) Breaking Cryo-EM Resolution Barriers to Facilitate Drug Discovery, *Cell 165*, 1698-1707 doi: 10.1016/j.cell.2016.05.040
[45] Tan, Y. Z., Aiyer, S., Mietzsch, M., Hull, J. A., McKenna, R., Grieger, J., et al, Lyumkis, D. (2018) Sub-2 A Ewald curvature corrected structure of an AAV2 capsid variant, *Nat Commun 9*, 3628 doi: 10.1038/s41467-018-06076-6
[46] Weis, F., Beckers, M., von der Hocht, I., and Sachse, C. (2019) Elucidation of the viral disassembly switch of tobacco mosaic virus, *EMBO Rep 20*, e48451 doi: 10.15252/embr.201948451
[47] Do, M., Isaacson, S. A., McDermott, G., Le Gros, M. A., and Larabell, C. A. (2015) Imaging and characterizing cells using tomography, *Arch Biochem Biophys 581*, 111-121 doi: 10.1016/j.abb.2015.01.011
[48] Schur, F. K. (2019) Toward high-resolution in situ structural biology with cryo-electron tomography and subtomogram averaging, *Curr Opin Struct Biol 58*, 1-9 doi: 10.1016/j.sbi.2019.03.018
[49] Lucic, V., Rigort, A., and Baumeister, W. (2013) Cryo-electron tomography: the challenge of doing structural biology in situ, *J Cell Biol 202*, 407-419 doi: 10.1083/jcb.201304193
[50] Burt, A., Cassidy, C. K., Ames, P., Bacia-Verloop, M., Baulard, M., Huard, K., et al, Gutsche, I. (2020) Complete structure of the chemosensory array core signalling unit in an E. coli minicell strain, *Nat Commun 11*, 743 doi: 10.1038/s41467-020-14350-9
[51] Turonova, B., Hagen, W. J. H., Obr, M., Mosalaganti, S., Beugelink, J. W., Zimmerli, C. E., et al, Beck, M. (2020) Benchmarking tomographic acquisition schemes for high-resolution structural biology, *Nat Commun 11*, 876 doi: 10.1038/s41467-020-14535-2
[52] Schaffer, M., Pfeffer, S., Mahamid, J., Kleindiek, S., Laugks, T., Albert, S., et al, Plitzko, J. M. (2019) A cryo-FIB lift-out technique enables molecular-resolution cryo-ET within native Caenorhabditis elegans tissue, *Nat Methods 16*, 757-762 doi: 10.1038/s41592-019-0497-5
[53] Beck, M., and Baumeister, W. (2016) Cryo-Electron Tomography: Can it Reveal the Molecular Sociology of Cells in Atomic Detail?, *Trends Cell Biol 26*, 825-837 doi: 10.1016/j.tcb.2016.08.006
[54] Strack, R. (2020) Structures in situ, *Nature Methods 17*, 21-21 doi: 10.1038/s41592-019-0704-4
[55] Wolff, A. M., Young, I. D., Sierra, R. G., Brewster, A. S., Martynowycz, M. W., Nango, E., et al, Thompson, M. C. (2020) Comparing serial X-ray crystallography and microcrystal electron diffraction (MicroED) as methods for routine structure determination from small macromolecular crystals, *IUCrJ 7*, 306-323 doi: doi:10.1107/S205225252000072X
[56] Martynowycz, M. W., Zhao, W., Hattne, J., Jensen, G. J., and Gonen, T. (2019) Qualitative Analyses of Polishing and Precoating FIB Milled Crystals for MicroED, *Structure 27*, 1594-1600 e1592 doi: 10.1016/j.str.2019.07.004
[57] Shi, D., Nannenga, B. L., de la Cruz, M. J., Liu, J., Sawtelle, S., Calero, G., et al, Gonen, T. (2016) The collection of MicroED data for macromolecular crystallography, *Nat Protoc 11*, 895-904 doi: 10.1038/nprot.2016.046
[58] Shi, D., Nannenga, B. L., Iadanza, M. G., and Gonen, T. (2013) Three-dimensional electron crystallography of protein microcrystals, *Elife 2*, e01345 doi: 10.7554/eLife.01345
[59] Martynowycz, M. W., Zhao, W., Hattne, J., Jensen, G. J., and Gonen, T. (2019) Collection of Continuous Rotation MicroED Data from Ion Beam-Milled Crystals of Any Size, *Structure 27*, 545-548 e542 doi: 10.1016/j.str.2018.12.003
[60] Schmidli, C., Albiez, S., Rima, L., Righetto, R., Mohammed, I., Oliva, P., et al, Braun, T. (2019) Microfluidic protein isolation and sample preparation for high-resolution cryo-EM, *Proc Natl Acad Sci U S A 116*, 15007-15012 doi: 10.1073/pnas.1907214116
[61] Kontziampasis, D., Klebl, D. P., Iadanza, M. G., Scarff, C. A., Kopf, F., Sobott, F., et al, White, H. D. (2019) A cryo-EM grid preparation device for time-resolved structural studies, *IUCrJ 6* doi: doi:10.1107/S2052252519011345
[62] Kaledhonkar, S., Fu, Z., White, H., and Frank, J. (2018) Time-Resolved Cryo-electron Microscopy Using a Microfluidic Chip, *Methods Mol Biol 1764*, 59-71 doi: 10.1007/978-1-4939-7759-8_4

[63] Frank, J. (2017) Time-resolved cryo-electron microscopy: Recent progress, *J Struct Biol 200*, 303-306 doi: 10.1016/j.jsb.2017.06.005
[64] Kaledhonkar, S., Fu, Z., Caban, K., Li, W., Chen, B., Sun, M., et al, Frank, J. (2019) Late steps in bacterial translation initiation visualized using time-resolved cryo-EM, *Nature 570*, 400-404 doi: 10.1038/s41586-019-1249-5
[65] Hand, E. (2020) 'We need a people's cryo-EM.' Scientists hope to bring revolutionary microscope to the masses, American Association for the Advancement of Science, Sciencemag.org, https://www.sciencemag.org/news/2020/01/we-need-people-s-cryo-em-scientists-hope-bring-revolutionary-microscope-masses#, access date (30 March 2020)
[66] Naydenova, K., McMullan, G., Peet, M. J., Lee, Y., Edwards, P. C., Chen, S., et al, Russo, C. J. (2019) CryoEM at 100 keV: a demonstration and prospects, *IUCrJ 6*, 1086-1098 doi: doi:10.1107/S2052252519012612
[67] Schur, F. K., Obr, M., Hagen, W. J., Wan, W., Jakobi, A. J., Kirkpatrick, J. M., et al, Briggs, J. A. (2016) An atomic model of HIV-1 capsid-SP1 reveals structures regulating assembly and maturation, *Science 353*, 506-508 doi: 10.1126/science.aaf9620
[68] Himes, B. A., and Zhang, P. (2018) emClarity: software for high-resolution cryo-electron tomography and subtomogram averaging, *Nat Methods 15*, 955-961 doi: 10.1038/s41592-018-0167-z

A2.2 Ultrafast Electron Diffraction (UED)

Ultrafast electron diffraction (UED) with a relativistic electron gun is an emerging method in structural dynamics. We discuss the synergy with an XFEL facility and point to unique scientific possibilities if a UED apparatus were synchronised with the XFEL.

The use of monoenergetic electron beams for atomic scale structure determination by diffraction has a long history stretching back to the Nobel Prize winning work of Thompson, Davisson and Germer in 1926. Electron diffraction is a natural complement to X-ray diffraction as it has different sensitivities and characteristics. Electrons have 10^4-10^6 higher scattering cross-sections than X-rays making them more suitable for thin or diffuse samples. In 1930, Mark and Wierl realised that diffraction patterns for the molecule CCl_4 in the gas phase could be acquired in a fraction of the time required for X-rays[1]. A few short years later, the structure of 146 molecules in the gas phase had been determined[2] and structural determination of gas phase molecules using electron diffraction became an important technique that remains in use[1]. Electrons scatter from both the electrons and the nuclei in the target, in contrast to X-rays that scatter only from the electrons, making electron diffraction more sensitive to low Z atoms. In principle, it can be used to detect H atoms, which are effectively invisible to X-rays. The possibility to use diffraction of ultrafast electron pulses to image structural dynamics has therefore caused substantial interest in the chemical dynamics and materials communities in recent decades. Not unexpectedly, the impact has been greatest for probing dynamics in gas phase molecules and thin films of crystalline material. Early work by Zeweil[3] and Miller[4] and others on ultrafast electron diffraction (UED) demonstrated what is possible. There is a strong consensus that UED is, along with time-resolved X-ray diffraction, a powerful route to access structural dynamics in molecules undergoing chemical reactions[5] and in crystalline materials undergoing phase changes[6] .

Despite this promise, there are severe limits to temporal resolution set by space-charge repulsion between electrons in an electron bunch. Unless the number of electrons in the bunch is kept unrealistically low, the time-resolution becomes badly degraded (although single electron "attosecond" experiments are possible when sampling periodic dynamics[7]). This has limited the temporal resolution in most UED experiments to picoseconds, despite efforts to design optimal electron optics. A big improvement is gained by using relativistic electron guns that rapidly accelerate the electron bunch to >1 MeV. In this case, relativistic Lorentz contraction reduces the effective space-charge by an enormous factor so allowing simultaneously very short pulses (< 100 fs) and high bunch charges that enable good signal to noise measurements. A UED facility based upon a relativistic electron gun operating at 2-4 MeV with ~100 fs pulses has been established at SLAC[8,9] and this has been running as a user facility alongside LCLS for the last 18 months. The SLAC facility has achieved significant scientific impact in this short time with measurements in photochemistry [10] [11] and condensed matter physics[12] among prominent recent results. The high scattering cross-section and small de Broglie wavelength of the electrons is likely to enable time-resolved pair-distribution function retrieval in liquids in the future.

A relativistic UED instrument of the type operating at SLAC, or the REGAE system being developed at DESY, is arguably two orders of magnitude cheaper than a hard X-ray FEL and far more compact. It can be synchronised with external pump lasers to enable a wide range of pump-probe studies. It can deliver a range of structural dynamics information in gas phase, thin films and perhaps in liquid samples (providing the liquid thickness is maintained at ~100 nm or less) with temporal resolution <100 fs. Although the present SLAC gun is operating at 180 Hz higher repetition rate upgrades are foreseen to reach >1 kHz repetition rate. The pulse duration at SLAC has recently been reduced, *e.g.* using THz driven electron beam compression, to around 35 fs in development experiments and so higher temporal resolution is expected to be achievable.

The complementarity with XFELs is best understood by considering the limitations, as well as the strengths, of UED. First and foremost, the penetration length, due to the inherent high scattering cross-section, is much less than hard X-rays and so precludes the study of bulk material properties,

buried structures and 3D biological samples. The temporal resolution is currently two orders of magnitude worse than that achieved with eSASE modes of an XFEL and is only likely to see modest improvements in the foreseeable future. Moreover, whilst electron diffraction can retrieve crystalline structures there is no method equivalent to X-ray CDI that permits the retrieval of irregular structures, limiting the application mainly to macroscopically crystalline samples and gas phase molecules. Likewise, there is no equivalent to inelastic scattering currently stimulating powerful new notions in X-ray scattering measurement (see discussion of coherent mixed scattering and quantum imaging see section 3.2). Finally, the argument has been advanced that new high-flux x-ray photon sources can achieve higher spatial resolution than UED during realistic exposure times, due to significantly lower noise in the large momentum-transfer data where UED suffers from much stronger quenching than X-ray scattering[13] . Ultimately, the greatest strength of electron scattering is as a structural technique and we will still need the power of X-ray spectroscopy, XES, RIXS and XPS, plus the emerging non-linear techniques, to address the electronic state dynamics that accompany, and drive, structural changes. A state-of-the-art relativistic UED facility would be far less versatile and scientifically pervasive than an X-ray FEL but would still likely find an enthusiastic user base.

In view of this it is reasonable to propose the development of a UED facility alongside a UK XFEL to complement the capabilities and increase capacity for users who are addressing questions of structural dynamics that the more limited temporal resolution of UED can deliver. This model of co-location has been effective at SLAC and has led to significant extra scientific productivity and reach for that laboratory. We do not, however, advocate merely co-location of UED and XFEL capability. Instead we would consider developing a more synergistic model where an end-station for time-resolved X-ray diffraction and X-ray spectroscopy can also be equipped with a UED gun that delivers electrons close to collinearly with the X-ray beam. In this way some common installations and equipment can be shared and the end station can maintain productivity even when X-rays are not available. Sharing of the pump beam capabilities, including a wide spectral range of advanced femtosecond laser and THz sources, which will be established at a UK XFEL can thus be used with significant scientific benefit for UED studies.

Further there is then the possibility to interrogate the dynamics of the same systems via multiple channels, e.g. XES, UED and time-resolved X-ray diffraction, thus exploiting the strengths of each method in an integrative methodology. Additionally, this configuration will open-up new scientific possibilities where an electron or an X-ray pulse is used as a pump and the other synchronised, but controllably delayed, X-ray or electron pulse is used as a probe. One possible scientific application is touched on in the Chemical Dynamics section 6.2 where the possibility for research into fast radiolysis processes will be enabled by such a configuration. The chemical and physical effects of an electron ionisation can thus be probed by X-ray spectroscopy and allied X-ray methods. We would foresee a wide range of other scientific possibilities with this dual XFEL/UED capability.

References

[1] I. Hargittai and M. Hargittai, "Stereochemical Applications of Gas-Phase Electron Diffraction : Part A The Electron Diffraction Technique", VCH Publishers, 1988, ISBN 0-89573-337-4

[2] L. O. Browckway, "Electron Diffraction by Gas Molecules", Rev. Mod. Phys., 8, 231 (1936)

[3] J. C. Williamson and A. H. Zewail, "Ultrafast Electron Diffraction. 4. Molecular Structures and Coherent Dynamics", J. Phys. Chem., 98, 2766 (1994)

[4] B. J. Siwick et al, "An atomic level view of melting using femtosecond electron diffraction", Science, 302, 1382 (2003)

[5] A. A. Ischenko et al, "Capturing chemistry in action with electrons: Realization of atomically resolved reaction dynamics", Chemical Reviews, 117, 11066 (2017)

[6] T. Ishikawa *et al.*, "Direct observation of collective modes coupled to molecular orbital-driven charge transfer", Science, 350, 6267 (2015)

[7] Y. Morimoto and P. Baum, "Diffraction and microscopy with attosecond electron pulse trains", Nature Physics, 14, 252 (2017)

[8] J. Yang et al, Nat. Comm. 7, 11232 (2016)

[9] S. P. Weathersby et al, Rev. Sci. Inst, 86, 073702 (2015)

[10] J. Yang et al, "Imaging CF_3I conical intersection and photodissociation dynamics with ultrafast electron diffraction", Science, 361, 64 (2018)

[11] T. J. A. Wolf et al, "The photochemical ring-opening of 1,3 cyclohexadiene imaged by ultrafast electron diffraction", Nat. Chem. 11, 504 (2019) DOI:10.1036/s41557-019-0252-7

[12] E. J. Sie et al, "An ultrafast symmetry switch in a Weyl semimetal", Nature, 565, 61 (2019) DOI: 10.1038/s41586-018-0809-4

[13] Lingyu Ma and Peter M. Weber, in press 2020

Appendix 3: Complementary Technologies

A3.1 Complementary Pulsed X-ray Technologies

Two nascent compact pulse X-ray source technologies based upon electron pre-bunching and radiation either in an undulator or via inverse Compton scattering are discussed. These hold promise of short X-ray pulses, albeit at much lower peak powers and repetition rates than a full scale XFEL. These ideas are being developed at UCLA and University of Arizona where demonstration systems are being built. If these demonstrations are successful, we recognise synergies with a UK XFEL in providing additional X-ray pulse pumping/probing capability and the possibility of use as sources for hard X-ray seeding in a future enhancement of the XFEL.

Only a multi-GeV facility can cover the full range of FEL user requirements, in particular the requirement for high photon flux and mJ pulse energies. This is because the FEL is a device for converting electron beam kinetic energy into photon beam energy, and while it may be possible to produce HXR photons with significantly lower beam energies there are two fundamental factors which compound one another to limit the flux. First, to obtain the required wavelength with a low energy beam the undulator period must be very short. Technologies are available, or under development, to achieve this, but the efficiency of the FEL, i.e. the fraction of electron beam power converted to photon beam power, scales with undulator period so will always be low. Second, the electron beam power is itself proportional to the beam energy. Taken together these two factors prohibit the production of high photon flux and mJ pulse energies from a low energy facility. To obtain FEL pulses appropriate for high energy density science multi-GeV electron beams are essential.

However, proposals are under development for compact, university scale, accelerator-based HXR sources. Such sources can be seen as complementary, offering pulse energies only a few percent of that available from a full scale facility, but which may be appropriate for some science applications, as discussed below. By co-locating such sources at a large facility they could provide additional pump-probe capability and potentially be used as HXR seed sources.

The table shows the main parameters of two well developed proposals. The first is from UCLA[1] (UC-XFEL). It features high gradient cryogenically cooled accelerating sections and a short period cryogenically cooled undulator. The electron bunch is modulated with a laser and converted into a train of microbunches – by doing so the beam quality in each low charge microbunch can be conserved, and the peak current in each microbunch is high enough that FEL saturation is reached in a few metres. The micro-modulated beam is less susceptible to wakefield degradation in the undulator than a conventional bunch, allowing a very small gap of 2mm so that the undulator period can be made very short while maintaining sufficient on-axis field. For this reason 8 keV photons can be produced with a beam energy of only 1.6 GeV. The pulse energy is around 12 uJ. The second proposal is by Arizona State University[2] (CXFEL), with funding secured for construction and experimental verification. Beam tests are now ongoing. The method is to generate a prebunched electron beam by translating the transverse diffraction pattern of the electron beam incident on a nano-patterned silicon crystal into a longitudinal modulation. The photons are then emitted through coherent Inverse Compton Scattering off an incident laser, demonstrating good temporal coherence with a pulse energy of 0.13uJ. This source could potentially be used as a direct HXR seed for an FEL amplifier driven by a multi-GeV beam because the peak power is sufficient to dominate the noise from the SASE process.

Table A3.1. Performance parameters (simulated) of the UCLA and U.Arizona compact light source projects

	UC-XFEL [1]	**CXFEL** [2]
Beam Energy	1.6 GeV	35 MeV
Photon Energy	7.8 keV	8 keV
Peak Power	8 GW	2 MW
Pulse Energy	12 uJ	0.13uJ
Bandwidth	0.1 %	0.01 %
Repetition Rate	100 Hz	1 kHz
Facility Length	40 m	10 m

A3.2 Plasma and Laser Wakefield Acceleration

Plasma and laser wakefields are novel concepts for electron acceleration that are likely to have considerable technology impact in the future. Although the technology remains insufficiently mature for the foreseeable future to replace the conventional linear accelerator in the UK XFEL we see strong synergies with UK XFEL. These are in: incorporation of laser wakefield capability at some end-stations, and for a plasma wakefield accelerator test end-station integrated into the facility design.

Plasma wakefield accelerators utilize the huge electric fields generated within plasma waves driven by intense laser pulses or particle beams. These fields are of order 100 GV m^{-1}, or around one thousand times greater than those possible with conventional radio-frequency (RF) technology. In addition to being extremely compact, plasma accelerators generate electron bunches with several highly desirable properties. These include: few-femtosecond bunch duration; multi-kA peak current; sub-micron normalized transverse emittance, with prospects for reaching emittances in the nanometre range; and, for laser-driven or hybrid plasma accelerators, tight synchronization with an ultrafast laser system. To date, plasma accelerators have accelerated electrons to tens of GeV energies in accelerator stages only a few tens of centimetres long [3,4,5,6,7]. The electron bunches they produce have been used to generate radiation from 100 eV to 1 MeV in magnetic undulators[8,9], via betatron oscillations in the plasma accelerator[10,11], and by Compton scattering[12,13,14]. They have also been used to generate positron beams[15], positron-electron plasmas,[16] and pions[17], and have been employed in fundamental physics tests[18,19].

The UK is a world leader in the development of both laser-driven and electron-driven plasma wakefield acceleration (laser wakefield accelerators (LWFA) and plasma wakefield accelerators (PWFA) respectively). This work is coordinated by the Plasma Wakefield Accelerator Steering Committee (PWASC, http://pwasc.org.uk/), which represents UK universities, ASTeC, the CLF, and the two Accelerator Institutes. In 2019, the PWASC summarized the rapid developments in plasma wakefield accelerators, and published a roadmap[20] for research and development to 2040. The potential of plasma wakefield accelerators, and the applications they enable, has proved a major driver for significant investments, such as: the £81.2M Extreme Photonics Application Centre (EPAC) at RAL; the Compact Linear Accelerator for Research and Applications (CLARA) at Daresbury Laboratory; and university-centred initiatives, including the Scottish Centre for the Application of Plasma-based Accelerators (SCAPA), and upgrades to several university-based systems across the UK. The importance of novel accelerator science has also been recognized by STFC, which selected the UK Novel Accelerator project as a “priority project”.

The repetition rate, energy gain and bunch properties of plasma accelerators continue to improve at a rapid pace,[21] and the number of applications they enable continues to grow. Current laser technology is limiting the repetition rate of laser-driven, GeV-scale plasma accelerators to around 10 Hz, but a variety of approaches for increasing the repetition rate of LWFAs is being pursued. One approach is the development of more efficient, higher-repetition rate lasers, such as the CLF’s DiPOLE technology. A complementary approach is the use of different methods for driving the plasma wave; for example, in the multi-pulse approach,[22,23] the drive energy is delivered over many plasma periods, which allows the use of novel lasers, such as thin-disk lasers, that can deliver picosecond-duration, joule-class laser pulses with high wall-plug efficiency and at multi-kHz repetition rates.

To improve the quality of the electron bunches, potentially transformative prospects are being pursued through projects such as the STFC PWFA-FEL, H2020 EuPRAXIA and NeXource. One prospect, the use of plasma photocathodes (“Trojan Horse”), offers the potential to improve the stability, energy spread[24], emittance and brightness[25] by orders of magnitude, and reached LCLS-level emittances in the first proof-of-concept[23]. If optimized, these electron beams could become orders of magnitude brighter than even those used in state-of-the-art hard x-ray facilities today. It is worth noting that laser-plasma accelerators and hybrid plasma wakefield accelerators[26] offer intrinsic time-synchronization, for example, for pump-probe experiments.

Although very promising, this new accelerator technology is not yet at a point that would allow a coherent x-ray light source facility to be planned around it. The levels of energy spread, emittance and shot-to-shot stability, although improving, remain inferior to conventional linac technology by a significant factor. Moreover, the requirement, for laser wakefield accelerators, of relativistic intensity laser pulses, is limiting realistic repetition rates to around 10 Hz at the current time. In contrast the "first generation XFELS" operate at ~ 100 Hz and the "second generation" at 1 – 1000 kHz. As reflected in this Science Case there is a demand for these higher repetition rates across the majority of the proposed applications. While the quality and repetition rate of beams from plasma accelerators obtained experimentally are currently far below those from conventional linac technology prospects for improving both could add unique opportunities for the UK XFEL in future upgrades.

Synergies between plasma wakefield acceleration and XFEL output and performance are strong. Consequently, it appears opportune to integrate laser- and electron-beam driven plasma wakefield acceleration capabilities and capacities into the design of a future, cutting-edge XFEL machine, although significant R&D would be required. Auxiliary compact betatron[10,9] or inverse Compton scattering-based secondary light sources[12,13] (e.g. for poly-x-ray beam illumination), with tight synchronization to ultra-fast visible lasers, could complement these features, as discussed in Sections 3 and 4. Plasma wakefield accelerators and laser-driven plasmas and are already employed in XFELs, such as the Matter at Extreme Conditions station at LCLS and the HIBEF beamline at the European XFEL. Attempts to drive FELs directly with LWFAs are being pursued by several groups worldwide. Furthermore, in view of the superior emittance and brightness offered, programmes have been initiated at Daresbury Laboratory and SLAC (for example, via the STFC PWFA-FEL project), and at DESY, to integrate plasma accelerators into existing and future (X)FELs.

Using PWFA at the UK XFEL facility would enable additional capabilities, including the use of plasma stages to boost the bunch energy (by a factor of two to five), and the use of plasma photocathodes as compact electron brightness afterburners (up to 100,000 times). Such an approach would open pathways to higher photon energies at reduced electron energies and/or sub-femtosecond, higher brilliance photon pulses, and intrinsically synchronized pump-probe multi-colour experiments. Such hard-x-ray flashes may even allow imaging of electronic motion inside atoms and molecules on their natural timescales.

Plasma wakefield accelerators are compact and highly flexible, and could also be implemented after the FEL undulator stages, to provide energy and brightness afterburners, and exploitation of novel XFEL in compact undulators instead of wasting the electrons in (conventional or plasma[27]) beam dumps. Such dedicated research stations could also be used for related applications, such as high-field science[18,19]. Bringing together researchers with expertise in conventional accelerators, plasma accelerators, and XFELs is likely to promote advances at the interface of these disciplines, such as the development of novel laser and XFEL diagnostics.

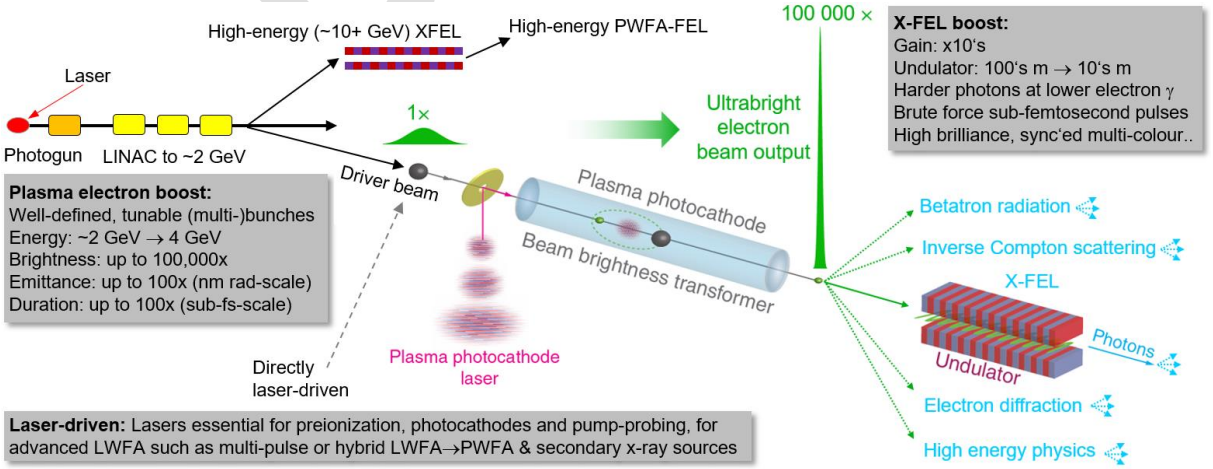

Figure A3.1. Schematic diagram of the capabilities enabled by combining XFEL beamlines and plasma accelerators

A3.3 High Harmonic Sources

High order harmonic generation (HHG) driven by high power ultrashort pulse optical lasers is a standard technique for generating short wavelength coherent radiation in the 10 – 500 eV photon energy range. It was, until the recent eSASE demonstration, the only way to generate attosecond pulses and remains the workhorse for attosecond science. Although pulse energies are low it is a compact and versatile method that naturally offers itself for incorporation into XFEL pump-probe experiments.

Both high harmonic generation (HHG) based attosecond sources and X-ray free electron lasers (XFELs) are now established methods for generating light of unique characteristics. Both are sources of short wavelength (VUV to X-ray) ultrashort light pulses with durations in the range from 100 fs to < 0.5 fs (500 attoseconds). This is having an impact through the rich scientific applications so far achieved. In the scientific sphere both have proved extraordinary in enabling things not possible before. Both are unique tools that are finding growing applications in science, technology and medicine. For HHG sources the brightness in the spectral range from 10 - 100 eV has proved sufficient to enable a wide range of applications e.g. in time resolved photoelectron spectroscopy, coherent diffraction imaging and time resolved absorption spectroscopy in a wide variety of settings including: surface science, photochemical reaction dynamics, time resolved band structure imaging, nanostructure and biological structure imaging.

A significant number of facility scale beamlines have been developed at institutions around the world and some made available to a wider user base (e.g. Artemis in the UK, various LaserLab Europe facilities, the nascent ELI facilities) and also now a number of commercialisations are being made available. The importance is reflected in a significant level of public investment in these facilities amounting to hundreds of millions of Euros globally. There has been a steady stream of applications and it is clear that this capability is firmly established in the repertoire of ultrafast probing methods available to science and technology. HHG has been widely applied as a short pulse (femtosecond domain) source of coherent X-rays for imaging and time-resolved spectroscopy applications [28] [29] [30].

The unique selling point of HHG sources has however been the potential to do something hitherto no other source could – to provide sub-femtosecond time domain pulses for directly measuring and controlling electronic dynamics in matter. This latter possibility termed *attosecond science* has generated a great deal of excitement and effort over the past two decades. This is not surprising as HHG is an enabling tool to probe the most fundamental events of electronic dynamics in matter. There have been remarkable developments and insights obtained over these years from laboratories all around the world. The first unambiguous confirmation of the production of attosecond pulses (a pulse train) in HHG was carried out using a side-band modulation (RABBIT) method by Agostini's group at Saclay . [31] The sideband method has now been widely used with considerable success in characterising ionisation (phase) delays at the attosecond level in atoms and molecules with work progressing in a number of groups around the world. The first demonstration of isolated attosecond pulses was, however, made in Garching using the streaking idea. Isolated pulses are an essential measurement tool for the most general implementation of attosecond science [32] [33] [34] [35] [36] [37]. More recently attention has also turned to attosecond electron control concepts in condensed phase systems[38] [39], new concepts in ultrafast field metrology [40] and applications towards photochemistry[41] [42]. The field continues to flourish and expand backed by accompanying technical work pushing HHG attosecond sources deeper into the soft X-ray range.

A large-scale European investment to establish the ELI-ALP (Attosecond) facility in Szeged, Hungary illustrates the maturity of the technology and the confidence for impact. This facility will concentrate on delivering XUV attosecond capability (up to 100 eV) with (for HHG sources) unprecedented brightness. Pulse energies of 100's nJ are likely in the lower photon energy range of operation, below 30 eV with pulse energies approaching the microjoule range have been demonstrated using high power drive lasers. Potentially this is an excellent complement to the soft-X-ray ESASE capabilities being developed at XFELs such as Fermi, Flash and LCLS which we anticipate also being an integral part

of any UK XFEL. HHG is now reaching into the soft X-ray range[43], but above 100 eV the demonstrated efficiency of HHG falls rather rapidly[44] (see figure 3.3.1). This is due to scaling limits placed on efficiency when the required longer wavelength lasers are used[45], so that pJ pulses are likely to remain the norm in the soft X-ray range. In contrast ESASE which so far has shown exceptional brightness between 500-1000 eV (>20 microJ pulses across this range with no fall off with photon number)[46]. SXR HHG research will still continue to be an important area for the time being and even in the long term, especially where perfect synchronisation to optical fields is required and for exploratory and complementary studies in collaboration with XFELs. Future ESASE developments are likely to extend this range down towards 100 eV and upwards into the hard X-ray range. Although currently ESASE pulses are somewhat longer than the best HHG based sources (by around a factor 5) we should anticipate continued improvement in pulse duration especially as harder X-rays are developed. Current HHG sources, nor none currently predicted, can compete with the ESASE FEL attosecond pulse brightness in the X-ray range.

Nevertheless high repetition rate drive lasers based on OPCPA and fibre laser technology are now making an impact even on attosecond generation[47]. These are pushing towards the MHz repetition rate with moderate pulse energies sufficient for reaching the XUV via HHG. We can therefore expect significant improvements in average flux performance in the XUV. Therefore, we anticipate XFEL based sources to be dominant in attosecond applications above 100 eV photon energy, whilst HHG based systems will continue to be competitive and probably the source of choice up to around 100 eV. For non-linear X-ray interactions, diffract-and-destroy and other single shot measurement schemes and probing hot plasmas XFELs will dominate across the XUV – X-ray range.

An alternative route to HHG, based upon the relativistic acceleration of particles at surfaces, has excited substantial interest over the last decades [48]. Development at various laser facilities has proceeded to improve the performance and to establish attosecond capability [49] [50]. These sources promise to be high brightness with significant energy conversion efficiency from the laser pulse to the HHG. Currently proven performance is limited to the soft X-ray range. Moreover, a relativistic laser intensity (> 10^{18} Wcm^{-2}) is required which limits the repetition rate to around 10 Hz at current laser technology. Efforts to develop these sources continue, at facilities such as ELI-ALP and through laser development programmes, and so in the longer term they may prove more competitive although they cannot form the basis of a facility plan at the current time.

Importantly the availability of XUV pump sources based on HHG alongside higher photon energy XFEL based eSASE sources at a facility endstation is an exciting and so far untapped opportunity that should add considerable additional attosecond and ultrafast measurement capability. It is thus likely that there will be substantial synergy with HHG sources at future XFEL facilities, especially as techniques for synchronization and time stamping improve to the sub-femtosecond range. We would plan to make such capability an integral part of the facility at some end-stations as the incremental cost of setting this up beyond the already installed high-repetition rate femtosecond lasers is on the order of just £100k.

References

[1] J. B. Rosenzweig et al, "*An Ultra-Compact X-Ray Free-Electron Laser*", arXiv:2003.06083, 13 March 2020

[2] W. S. Graves et al, "*ASU Compact XFEL*", Proceedings of FEL2017, p225, TUB03, doi:10.18429/JACoW-FEL2017-TUB03

[3] M.J. Hogan, C.D. Barnes, et al., "Multi-GeV energy gain in a plasma-wakefield accelerator", Phys Rev Lett **95**, 054802, (2005) DOI: 10.1103/PhysRevLett.95.054802

[4] W.P. Leemans, E. Esarey, et al., "GeV electron beams from a centimetre-scale accelerator", Nat Phys **2**, 696 (2006) DOI: 10.1038/nphys418

[5] I. Blumenfeld, C. Joshi, et al. "Energy doubling of 42 GeV electrons in a metre-scale plasma wakefield accelerator", Nature 445, 741 (2007) DOI: 10.1038/nature05538

[6] S. Kneip et al., "Near-GeV acceleration of electrons by a nonlinear plasma wave driven by a self-guided laser pulse", Phys Rev Lett **103**, 035002 (2009) DOI: 10.1103/PhysRevLett.103.035002

[7] A.J. Gonsalves et al., "Petawatt laser guiding and electron beam acceleration to 8 GeV in a laser-heated capillary discharge waveguide", Phys Rev Lett 122, 084801 (2019) DOI: 10.1103/PhysRevLett.122.084801

[8] H.-P. Schlenvoigt, D.A. Jaroszynski, et al., "A compact synchrotron radiation source driven by a laser-plasma

wakefield accelerator", Nat Phys **4**, 130 (2008) DOI: 10.1038/nphys811

[9] M. Fuchs, S. Karsch, F. Gruener, et al., "Laser-driven soft-X-ray undulator source", Nat Phys **5**, 826 (2009) DOI: 10.1038/nphys1404

[10] S. Kneip, Z. Najmudin, et al., "Bright spatially coherent synchrotron X-rays from a table-top source", Nat Phys **6**, 980 (2010) Doi: 10.1038/nphys1789

[11] S. Cipiccia, D.A. Jaroszynski, et al., "Gamma-rays from harmonically resonant betatron oscillations in a plasma wake", Nat Phys **7**, 867 (2011) DOI: 10.1038/nphys2090

[12] N.D. Powers, D.P. Umstadter, et al., "Quasi-monoenergetic and tunable X-rays from a laser-driven Compton light source", Nature Photonics **8**, 28-31 (2014) DOI: 10.1038/nphoton.2013.314

[13] K. Khrennikov, L. Veisz, S. Karsch, et al., "Tunable all-optical quasimonochromatic Thomson X-ray source in the nonlinear regime", Phys Rev Lett **114**, 195003 (2015) DOI: 10.1103/PhysRevLett.114.195003

[14] H.-E. Tsai, M. C. Downer, et al., "Compact tunable Compton x-ray source from laser-plasma accelerator and plasma mirror", Phys. Plasmas **22**, 023106 (2015) DOI: 10.1063/1.4907655

[15] G. Sarri et al., "Table-top laser-based source of femtosecond, collimated, ultrarelativistic positron beams", Phys Rev Lett **110**, 255002 (2013) DOI: 10.1103/PhysRevLett.110.255002

[16] G. Sarri et al., "Generation of neutral and high-density electron-positron pair plasmas in the laboratory", Nature Communications **6**, 6747 (2015) DOI: 10.1038/ncomms7747

[17] W. Schumaker et al., "Making pions with laser light", New J Phys **20**, 073008 (2018) DOI: 10.1088/1367-2630/aace0c

[18] G. Sarri et al., "Experimental signatures of the quantum nature of radiation reaction in the field of an ultraintense laser", Physical Review X **8**, 031004 (2018) DOI: 10.1103/PhysRevX.8.031004

[19] J.M. Cole, S.P.D. Mangles, et al., "Experimental evidence of radiation reaction in the collision of a high-intensity laser pulse with a laser-wakefield accelerated electron beam", , Physical Review X **8**, 011020 (2018) DOI: 10.1103/PhysRevX.8.011020

[20] B. Hidding et al., "Plasma Wakefield Accelerator Research 2019 - 2040: A community-driven UK roadmap compiled by the Plasma Wakefield Accelerator Steering Committee (PWASC)," arXiv:1904.09205 [physics.acc-ph]

[21] S.M. Hooker, "Developments in laser-driven plasma accelerators", Nature Photonics **7**, 775-782 (2013) DOI: 10.1038/nphoton.2013.234

[22] J. Cowley et al., "Excitation and control of plasma wakefields by multiple laser pulses", Phys Rev Lett **119**, 044802 (2017) DOI: 10.1103/PhysRevLett.119.044802

[23] S.M. Hooker et al. "Multi-pulse laser wakefield acceleration; a new route to efficient, high-repetition-rate plasma accelerators and high flux radiation sources", J. Phys. B: At. Mol. Opt. Phys. 47 234003 (2014) DOI: 10.1088/0953-4075/47/23/234003

[24] G.G. Manahan, A. Habib, P. Scherkl, et al., "Single-stage plasma-based correlated energy spread compensation for ultrahigh 6D brightness electron beams", Nature Communications **8**, 1 (2017) DOI: 10.1038/ncomms15705

[25] A. Deng, O.S. Karger, T. Heinemann, et al., "Generation and acceleration of electron bunches from a plasma photocathode", Nat Phys **15**, 1156-1160 (2019) DOI: 10.1038/s41567-019-0610-9

[26] M.F. Gilljohann, H. Ding, A. Döpp, et al., "Direct observation of plasma waves and dynamics induced by laser-accelerated electron beams", Physical Review X **9**, 011046 (2019) DOI: 10.1103/PhysRevX.9.011046

[27] S. Chou et al., "Collective deceleration of laser-driven electron bunches", Phys Rev Lett **117**, 144801 (2016) DOI: 10.1103/PhysRevLett.117.144801

[28] M.Kovacev et al, "Extreme ultraviolet Fourier-transform spectroscopy with high order harmonics", Phys.Rev.Lett., **95**, 223903 (2005)

[29] E. Gagnon et al, "Soft X-ray driven femtosecond molecular dynamics", Science, **317,** 1374 (2007)

[30] P.Wernet et al, "Real-time evolution of the valence electronic structure in a dissociating molecule", Phys.Rev.Lett., **103**, 013001 (2009)

[31] P.M.Paul et al, "Observation of a train of attosecond pulses from high harmonic generation", Science 292, 1689 (2001)

[32] M.Hentschel et al, "Attosecond metrology", Nature 414, 509 (2001)

[33] R.Kienberger et al, "Steering attosecond electron wavepackets with light", Science 297, 1144 (2002)

[34] A.Baltuska et al, "Attosecond control of electronic processes by intense light fields", Nature 421, 611 (2003)

[35] R.Kienberger et al, "Atomic transient recorder", Nature 427, 817 (2004)

[36] E.Goulielmakis et al, "Direct measurement of light waves", Science 305, 1267 (2004),

[37] E.Goulielmakis et al, "Single cycle nonlinear optics", Science 320, 1614 (2008)

[38] S.Ghirmire et al, "Observation of high-order harmonic generation in a bulk crystal", Nature Physics **7** , 138 (2011)

[39] M.Schultze et al, "Attosecond band-gap dynamics in silicon", Science **346**, 1348 (2014)

[40] S.Keiber et al, "Electro-optic sampling of near infrared waveforms", Nature Photonics **10**, 159 (2016)

[41] F.Calegari et al, "Ultrafast electron dynamics in phenylalanine intiated by attosecond pulses", Science 346, 336 (2014), Science 10.1126/science.aah6114

[42] A.A.Attar et al, "Femtosecond x-ray spectroscopy of an electrocyclic ring opening reaction", Science 356, 54-59 (2017)

[43] T.Popmintchev et al, "Bright coherent ultrahigh harmonics in the keV X-ray regime from IR femtosecond lasers" Science, 336, 1287 (2012) DOI:10.1126/science.1218497

[44] S.M.Teichmann et al, "0.5 keV soft X-ray attosecond continuua", Nat.Comm. 7, 11493 (2016) DOI:10.1038/ncomms11493

[45] A.S.Johnson et al, "High flux soft X-ray harmonic generation from ionization-shaped few-cycle pulses", Sci.Adv. 4, eaar3761 (2018) DOI:10.1126/sciadv.aar3761

[46] J.Duris et al, "Tunable isolated attosecond X-ray pulses with gigawatt peak power from a free-electron laser", Nature Photonics, 14, 30 (2020) DOI:10.1038/s41566-019-0549-5

[47] M.Krebs et al, "Towards isolated attosecond pulses at megahertz repetition rates", Nature Photonics, (2013), DOI: 10.1038/nphoton.2013.131

[48] Y.Nomura et al, Attosecond phase locking of harmonics emitted from laser produced plasmas, Nature Physics, 5, 124 (2009)

[49] A.Borot et al, Attosecond control of collective motions in plasmas, Nat.Phys, 8, 416 (2012)

[50] J.Wheeler et al, Attosecond lighthouses from plasma mirrors, Nat.Phot. 6, 829 (2012)

Appendix 4: Community engagement and authorship

Workshops and community engagement events

Table A4.1: Workshops and numbers attending

Jul 16th	*Launch Meeting (Royal Society)*	*[72]*
Oct 2nd	*Matter at Extreme Conditions (Edinburgh)*	*[27]*
Nov 5th	*Life Sciences (Crick)*	*[160]*
Nov 13th	*Frontiers in Physical Sciences (Imperial)*	*[102]*
Nov 27th	*Quantum Materials & Nanotechnology (Southampton)*	*[40]*
Dec 4th	*X-ray FEL Applications (Warwick)*	*[29]*
Dec 11th	*Chemical Dynamics & Energy (Newcastle)*	*[50]*

A website was established dedicated to community engagement with presentations from workshops and opportunity to input:

https://www.clf.stfc.ac.uk/Pages/UK-XFEL-Scientific-Case-Consultations.aspx

A number of discussion meetings were organised for the science and technical teams were arranged to facilitate the development of machine specification and construction of the science case.

Meeting of Science and Technical teams September 27th Kings College London

Meeting of full Science team January 15th-16th Coseners House, Abingdon

Authorship team of 1st draft of Science Case

Initial	Surname	Affiliation	Project role
M.	Altarreli	MPSD	Science advisor
F.	Alves Lima	Eu XFEL	Science advisor
M.	Attallah	University of Birmingham	Industry advisor
S.	Bartlett	Diamond Light Source	Science advisor
J.	Baxter	Imperial College London	Science advisor
U.	Bergmann	SLAC	Science advisor
T.	Blackburn	Chalmers University, Sweden	Science advisor
R.	Boll	Eu XFEL	Science advisor
S.	Bonetti	University of Stockholm	Science advisor
M.	Borghesi	Queens University Belfast	Science team
C.	Bressler	Eu XFEL	Science advisor
B.	Brocklesby	University of Southampton	Science advisor
C.	Brown	AWE	Science advisor
P.H.	Bucksbaum	University of Stanford	Science advisor
T.	Burge	Central Laser Facility, Rutherford Appleton Lab	Technical Author
A.D.	Burnett	University of Leeds	Science team
C.R.A	Catlow	University College London	Science advisor
R.	Chantrell	University of York	Science advisor
J.	Clarke	ASTEC, Daresbury Laboratory	Technical team
A.	Cohen	SLAC/LCLS	Science advisor
J.	Collier	Central Laser Facility, Rutherford Appleton Lab	Project Champion

A.	Collins	Daresbury Laboratory	Graphic Designer
A.	Comley	AWE	Science team
L.	Cowie	Daresbury Laboratory	Technical team
J.	Cryan	SLAC/University of Stanford	Science advisor
G.	Dakovski	SLAC	Science advisor
M.P.	Dean	Brookhaven National Laboratory	Science advisor
S.	Dhesi	Diamond Light Source	Science advisor
S.	Diaz-Moreno	Diamond Light Source	Science team
P.	Dowding	Infineum	Industry advisor
D.	Dunning	ASTEC, Daresbury Laboratory	Technical Team
D.	Dye	Imperial College London	Science team
J.	Dyke	University of Southampton	Science advisor
D.	Eakins	University of Oxford	Science advisor
G.	Evans	Diamond Light Source	Science advisor
M.	Foerst	Max Planck Institute for Structural Dynamics, Hamburg	Science advisor
L.J.	Frasinski	Imperial College London	Science advisor
J.	Green	Central Laser Facility, Rutherford Appleton Lab	Physical Sciences Hub
J.	Greenwood	Queens University Belfast	Science team
G.	Gregori	University of Oxford	Science advisor
M.	Guehr	University of Potsdam	Science advisor
F.	Habib	University of Strathclyde	Science advisor
D.	Hall	Diamond Light Source	Science advisor
S.	Hasnain	University of Liverpool	Science advisor
T.	Heinzl	University of Plymouth	Science advisor
B.	Hidding	University of Strathclyde	Science advisor
A.	Higginbotham	University of York	Science team
S.	Hooker	University of Oxford	Science advisor
N.	Huse	University of Hamburg, Germany	Science advisor
O.	Johnansson	University of Edinburgh	Science advisor
D.	Keen	ISIS/ University of Oxford	Science advisor
A.	Kirrander	University of Edinburgh	Science team
P.	Kolorenc	Charles University Prague	Science advisor
A.	Mancuso	SPB/SFX Instrument, Eu XFEL	Science advisor
S.	Mangles	Imperial College London	Science advisor
J.P.	Marangos	Imperial College London	Science team/ Lead
M.	Marklund	Chalmers University, Sweden	Science advisor
P.	Martin	AWE	Industry advisor
S.	Matthews	Imperial College London	Science advisor
S.	Mc Williams	University of Edinburgh	Science advisor
M.	McCoustra	Heriot Watt	Science advisor
P.	McKenna	University of Strathclyde	Science advisor
M.I.	McMahon	University of Edinburgh	Science team
B.W.J.	McNeil	University of Strathclyde	Technical team
C.	Milne	Paul Scherrer Institute, Switzerland	Science advisor
R.S.	Minns	University of Southampton	Science team
H.	Mueller-Werkmeister	University of Potsdam	Science advisor
S.	Mukamel	University of California, Irvine	Science advisor

J.	Naismith	RFI / University of Oxford	Science advisor
K.	Nelson	Massachussetts Institute of Technology	Science advisor
M.C.	Newton	University of Southampton	Science team
A.	Orville	Diamond Light Source	Science team
A.	Ourmazd	University of Wisconsin-Milwaukee	Science advisor
R.	Owen	Diamond Light Source	Science advisor
T.	Penfold	University of Newcastle	Science team
F.	Perakis	University of Stockholm	Science advisor
P.	Radaelli	University of Oxford	Science advisor
A.	Randewich	AWE	Industry advisor
A.	Regoutz	University College London	Science team
D.	Riley	Queens University Belfast	Science advisor
I.	Robinson	University College London	Science team
A.	Robinson	Central Laser Facility, Rutherford Appleton Lab	Science advisor
J.	Rodenberg	University of Sheffield	Science advisor
N.	Rohringer	University of Hamburg, Germany	Science advisor
K.	Rossnagel	University of Kiel, DESY	Science advisor
M.	Ruberti	Imperial College London	Science advisor
D.	Rugg	Rolls Royce	Science team/Industry advisor
C.	Russo	MRC-LMB, Cambridge	Science advisor
C.	Sanders	Central Laser Facility, Rutherford Appleton Lab	Science advisor
M.	Scheck	University of West Scotland	Science advisor
P.	Scherkl	University of Strathclyde	Science advisor
C.J.	Schofield	University of Oxford	Science advisor
S.L.M	Schroeder	University of Leeds	Science team
E.	Snell	SUNY Buffalo, BioXFEL	Science advisor
TJ.T	Spencer	UK NNL	Industry advisor
E.	Springate	Central Laser Facility, Rutherford Appleton Lab	Science advisor
D.	Stuart	Diamond Light Source	Science advisor
N.	Thompson	ASTEC, Daresbury Laboratory	Technical team
G.	Thornton	University College London	Science advisor
J.	van Thor	Imperial College London	Scince team
S.M.	Vinko	University of Oxford	Science team
J.	von Zanthier	University of Erlangen, Germany	Science advisor
S.	Wall	ICFO, Barcelona	Science team
M.	Walsh	Diamond Light Source	Science advisor
J.S.	Wark	University of Oxford	Science team
M.R.	Warren	Diamond Light Source	Science advisor
P.	Weber	Brown University, USA	Science advisor
J.	Weinstein	University of Sheffield	Science team
P.W.	Williams	ASTEC, Daresbury Laboratory	Technical team
P.	Withers	Henry Royce Institute/ University of Manchester	Industry advisor
J.	Yano	Lawrence Berkeley National Laboratory	Science advisor
A.	Zair	Kings College London	Science team
X.	Zhang	Imperial College London	Science team